BIOPHYSICAL STUDIES OF AROMATIC β-AMINO ACID TETHERED HETEROGENEOUS PEPTIDE OLIGOMERS AND ANALOGUES OF IXORAPEPTIDES

A THESIS TO BE SUBMITTED TO THE

UNIVERSITY OF PUNE

FOR THE DEGREE OF

DOCTOR OF PHILOSOPHY

(IN CHEMISTRY)

By

GOWRI PRIYA SAKALA

Research Supervisor
Dr. G. J. SANJAYAN

DIVISION OF ORGANIC CHEMISTRY
NATIONAL CHEMICAL LABORATORY
PUNE 411008
INDIA

JUNE 2013

DECLARATION

I hereby declare that the thesis entitled ***"Biophysical Studies of Aromatic β-amino acid Tethered Heterogeneous Peptide Oligomers and Analogues of Ixorapeptides."*** submitted for the Degree of Doctor of Philosophy in Chemistry to the University of Pune, has not been submitted by me to any other university or institution. This work has been carried out at Division of Organic Chemistry, National Chemical Laboratory, Pune under the supervision of Dr. G. J. Sanjayan (Research guide).

Date:
Division of Organic Chemistry
National Chemical Laboratory
Pune

Gowri Priya Sakala
(Research student)

राष्ट्रीय रासायनिक प्रयोगशाला
(वैज्ञानिक तथा औद्योगिक अनुसंधान परिषद)
डॉ. होमी भाभा रोड, पुणे - 411 008. भारत
NATIONAL CHEMICAL LABORATORY
(Council of Scientific & Industrial Research)
Dr. Homi Bhabha Road, Pune - 411008. India

CERTIFICATE

Certified that the work incorporated in the thesis entitled "***Biophysical studies of Aromatic β-amino acid Tethered Heterogeneous Peptide Oligomers and Analogues of Ixorapeptides.***" submitted by Ms. Gowri Priya Sakala for the degree of Doctor of Philosophy was carried out by the candidate under my supervision in Organic Chemistry Division, National Chemical Laboratory, Pune, India. Materials obtained from other sources have been duly acknowledged in the thesis.

Date:
Place: Pune

Dr. G. J. Sanjayan
(Research Guide)

Communications Channels ☎ +91 20 25902000 +91 20 25893300 +91 20 25893400 Fax +91 20 25902601 (Director) +91 20 25902660 (Admin.) +91 20 25902639 (Business Development) URL : www.ncl-india.o

Dedicated to my family

Acknowledgement

*Firstly I would like to thank my beloved parents (**Shri. Ramesh Babu** & **Smt. Leelavathi**) and brother (**Dr. Nitin Krishna Srinivas**) in bringing me up to this stage and for encouraging me to pursue my career. Without their support, my ambition to pursue research in NCL can be hardly realized.*

*I would like to express my sincere gratitude to my research supervisor **Dr. G. J. Sanjayan** for the guidance, motivation, encouragement, and timely advices given by him during the course of my research. His expertise, understanding and patience helped me in shaping my interest and ideas. His tireless enthusiasm was always a source of inspiration for me. I revere his lessons on independent thinking, perfection, softs kills and many more.*

*I owe my gratitude to **Dr. Ganesh Pandey**, Head of the Organic Chemistry Division, **Dr. P. K. Tripathi**, Acting chair and **Dr. Sourav Pal**, Director, for rendering all laboratory facilities in the institute to carry out my research work smoothly.*

*I acknowledge my sincere thanks to **Dr. P. R. Rajamohanan** and **Amol Kotmale** for their help in carrying out the 2D NMR studies which is highly requisite for the completion of my thesis work. I thank **Jima**, **Hilda**, **Snehal** and **Shrikant** from NMR facility in helping me for the NMR analyses.*

*I am deeply indebted to **Dr. Vedavati. G. Puranik**, **Mr. Rupesh Gawade** and **Debamitra** for helping me to get the solid state conformation of compounds. They helped me to understand many interesting concepts in crystallography.*

*I thank **Dr. Sourav Pal**, **Mrs. Deepti Mishra, Dr. Lalitha** and **Achintya** for their judicious help in doing the ab-initio molecular modeling studies.*

*My warm and sincere thanks to **Mrs. Santhakumari**, **Swamy** and **Sanjeev** for helping me to do the mass analyses.*

*I am also grateful to **Dr. Chaitanya Athale**, **Sayali Joshi** and **Kunalika** for helping me to do the biological studies at IISER, Pune.*

*I take this opportunity to express my heartfelt gratitude to my teachers **Nagaraju Sir**, **Dr. Sudhakar Babu**, **Dr. Chandraiah Chowdary**, **Dr. Ramana**, **Dr. Jayaprakash**, **Dr. Chakravarthy** who helped me to learn the basics of Chemistry. They encouraged me extending their full support which made me*

ambitious in life. Among all my chemistry teachers, I am deeply indebted to my beloved teacher ***Dr. C. V. Rajeswari****, who is more like a friend and philosopher rather than a teacher, for her encouragement in each and every aspect of my life.*

I would like to thank my senior labmates ***Dr. Panchami****,* ***Dr. Sreenivas****,* ***Dr. Pranjal****,* ***Dr. Amol****,* ***Dr. Pinak****, for their valuable help and guidance. I also thank my labmates* ***Ramesh****,* ***Sangram****,* ***Roshna****,* ***Vijayadas****,* ***Vijay****,* ***Ganesh****,* ***Sachin Baravkar****,* ***Sanjeev****,* ***Shivakumar****,* ***M. Suresh*** *and* ***Krishnaprasad*** *for their cheerful company at the work place. No words will be sufficient to thank* ***Arup Roy****,* ***R. Suresh*** *and* ***Tukaram*** *as they extended their help more than labmates.*

I express heartfelt thanks to friends ***Radhika****,* ***Mallikarjun Reddy****,* ***Dr. Marivel****,* ***Neelima****,* ***Uma****,* ***Padma****, who always encouraged and helped me in pursuing my career.*

My special thanks to friends ***Reetika****,* ***Seema****,* ***Liton shil****,* ***Yogitha****,* ***Dr. Madhuri****,* ***Dr. Jayanti****,* ***Dr. Priyanka****,* ***Pragati****,* ***Tanaya*** *for their advices and help to cheer me.*

I would like to thank the seniors ***Dr. Manaswini****,* ***Dr. Rajender Reddy****,* ***Dr. Induvadana****,* ***Dr. Mythri****,* ***Dr. Geetali****,* ***Dr. Meera*** *in NCL for their advices.*

I would also like to thank the friends ***Manisha Kapoor****,* ***Mun Mun****,* ***Jhumur****,* ***Priyanka Sharma****,* ***Anjali****,* ***Subha****,for making my stay happier at Golden Jubilee Hostel.*

I would also like to thank friends ***Sreenivas****,* ***Pranaya****,* ***Harshali****,* ***Richa Sardessai****,* ***Namrata****,* ***Sujith****,* ***Asif****,* ***Anand****,* ***Shantivardhan reddy****,* ***Trinath****,* ***Sachin****,* ***Bhaskar****,* ***Krishanu****,* ***Debashish Dey****,* ***Narasimha Reddy****,* ***Yadagiri****,* ***Chandrababu Naidu****,* ***Nagendra****, at NCL.*

I thank CSIR, New Delhi, for financial support.

Finally I would like to thank all those who have contributed to the successful realization of this dissertation and I express my apology that I could not mention personally one by one.

This chain of my gratitude will be completed only if I would thank the Almighty. My deepest and sincere gratitude for inspiring and guiding this humble being.

Gowri Priya

Table of Contents

Chapter 1

Heterogeneous α/β hybrid peptide oligomers devoid of inter-residual hydrogen bonding

Section B

Conformational features of α/β/α hybrid peptides –A direct comparison between carboxamide oligomer and sulfonamide oligomer

Section C

Consequences of introduction of ^{S}Ant in Pro-Gly, Gly-Pro and Ant-Ant-Pro sequences

Section B

Synthesis of analogues of Ixorapeptide I-their biological evaluation.

Abbreviations

A

Å	Ångström
AA	Amino acid
Ac	Acetyl
AcOH	Acetic acid
Aib	Amino isobutyric acid
Ant	Anthranilic acid

B

Boc	tert- Butyloxycarbonyl
Bn	Benzyl

C

$CDCl_3$	Chloroform-d
COSY	Correlated spectroscopy
CD	Circular dichroism
Cbz	Carboxybenzyl

D

d	doublet (NMR)
δ	Chemical shift (NMR)
DCC	*N, N'*-dicyclohexyl-carbodimide
DCM	Dichloromethane
DMF	Dimethyl formamide
DIPEA	Diisopropyl ethylamine
DMSO	Dimethylsulfoxide
4-DMAP	4-dimethyl aminopyridine

E

EDC.HCl	N'-ethylcarbodiimide hydrochloride
ESI	Electron spray ionization
Et_3N	Triethyl amine

G

Gly	Glycine

H

H-bond	Hydrogen bond
HMBC	Hetero Multiple Bond Correlation
HBTU	O-benzotriazol-1-yl-N,N, N',N'-tetramethyluronium hexafluorophosphate
HOBt	1-hydroxybenzotriazole
HSQC	Hetero Nuclear Single Quantum Coherence
Hz	Hertz

L

LCMS	Liquid chromatography–mass spectrometry

M

MALDI	Matrix-Assisted Laser Desorption Ionization
m	Multiplet (NMR)
MS	Mass Spectrometry
Me	Methyl

N

NOESY	Nuclear Overhauser and Exchange Spectroscopy

P

Pro	Proline
Pd/C	palladium 10 % on activated carbon

Q

q	Quartet
quin	Quintet

S

s	Singlet (NMR)
sext	Sextet
^{S}Ant	2-aminobenzenesulfonic acid
$SnCl_2$	Stannous chloride
SEM	Scanning Electron Microscopy

T

TFA	Trifluroacetic acid
TFE	Trifluoro ethanol
THF	Tetrahydrofuran
TBDMS	tert-Butyldimethysilyl
t	Triplet (NMR)

ABSTRACT

Name of the Candidate	**S. Gowri Priya**
Name of the Research Guide	**Dr. G. J. Sanjayan**
Title of the Ph. D. thesis	**Biophysical Studies of Aromatic β-amino acid Tethered Heterogeneous Peptide Oligomers and Analogues of Ixorapeptides**

Chapter 1: This chapter deals with the design, synthesis and the conformational studies of the well ordered Pro-Atc hybrid oligomers comprising of Pro-2Atc and Pro-3Atc dipeptide building blocks, wherein the isosteric modification on the backbone was successfully achieved to elucidate that the class of Pro-Atc oligomers display a robust helical architecture without any inter-residual hydrogen bonding, distinctly owing to the conformational rigidity of the amino acids chosen.

The conformational features of the oligomers were clearly evident from the crystal structures of the tetrapeptides which revealed a folded conformation devoid of inter-residual hydrogen bonding, maintaining the intra-residual 6-membered hydrogen bonding. The isosteric replacement does not effect the backbone conformation by and large (Fig. 1).

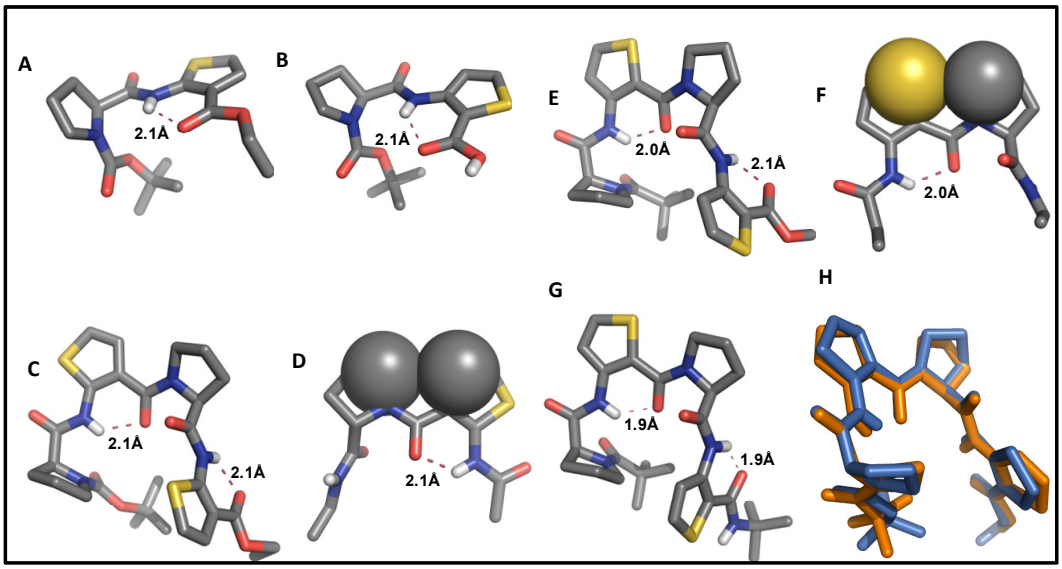

Fig. 1: Crystal structures of the peptides **1a** (A), **2b** (B), **3a** (C), **4d** (E), and **4f** (G), comparison of the isosteric dipeptide segments of **3a** (D) and **4d** (F) and the overlaid crystal structures of **3a** and **4d** (H). All hydrogens, except the polar ones, have been deleted for clarity.

The conformational features of the oligomers were also supported by the *ab-initio* molecular modeling studies revealing a right handed helical conformation for the octapeptides (Fig. 2).

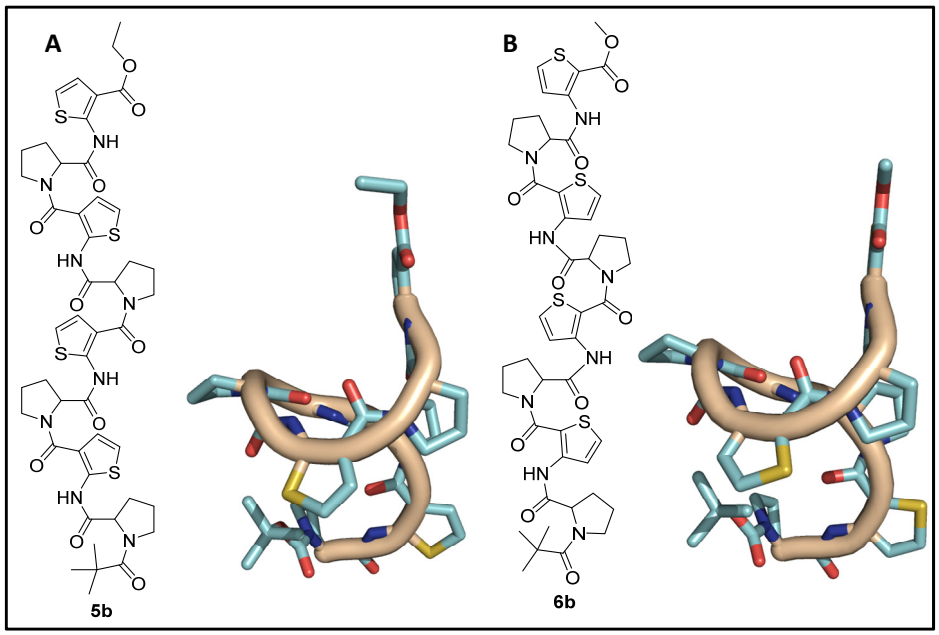

Fig. 2: **(A)** Molecular structure and cartoon representation of the octapeptide **5b** and (B) Molecular structure and cartoon representation of the octapeptide **6b**.

[Helical folding in heterogeneous foldamers without inter-residual backbone hydrogen-bonding: **Priya, G.**; Kotmale, A. S.; Gawade, R. L.; Mishra, D.; Pal, S.; Puranik, V. G.; Rajamohanan, P. R.; Sanjayan, G. J., *Chem. Commun*. **2012**, *48*, 8922-8924.]

Chapter 2: This chapter describes the conformational modulation attained by the peptide sequences due to incorporating of orthanilic acid (^{S}Ant) on their backbone.

Section A of this chapter deals with the study of the conformational bias observed due to the introduction of ^{S}Ant in peptide sequences. The investigation of the conformational features of the peptides, wherein ^{S}Ant is incorporated, clearly reveals the existence of 11-membered hydrogen bonding which is apparent from the crystal structures of the peptides. The C11 turn observed is profoundly robust which is clearly reflected in all the solid-state conformations of the designed peptides (Fig. 3), even after considerable modulation of amino acid residues at the termini.

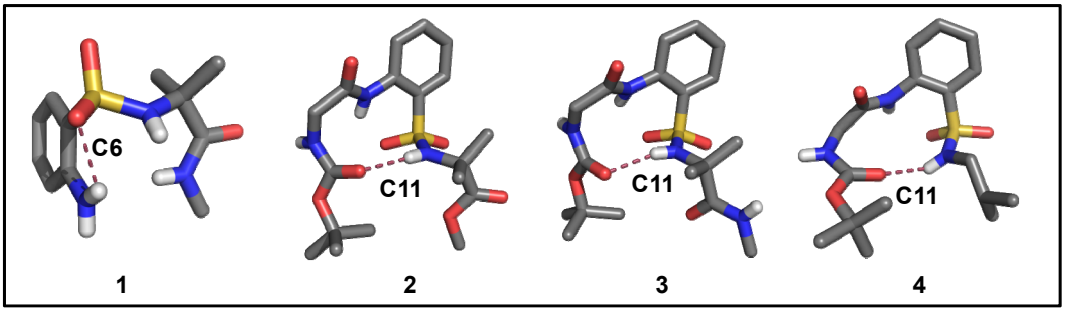

Fig. 3: PyMOL-rendered crystal structures of peptides **1-4** featuring C6 and C11 H-bonding patterns. All the hydrogens, other than the polar ones, have been deleted for clarity.

[Orthanilic acid promoted reverse turn formation in peptides: Kale, S. S.; **Priya. G**.; Kotmale, A. S.; Gawade, R. L.; Puranik, V. G.; Rajamohanan, P. R.; Sanjayan, G. J. *Chem. Commun*. **2012**, *49*, 2222-2224.]

Section B describes the conformational preferences adopted by α/β/α hybrid foldamers featuring carboxamide and sulfonamide building blocks. The designed sequences feature a conformationally rigid amino acid residue (Aib) and a conformationally flexible amino acid residue (Gly) sandwiching the aromatic β-amino acid building blocks Ant and ^{S}Ant. This study provides a clear comparison between the conformational preferences of carboxamide and sulfonamide oligomers. The carboxamide oligomers with an intra-residual 6-membered H-bond reveal an unfolded architecture, while the sulfonamide oligomers with inter-residual 11- and 14-membered H-bonds reveal a characteristic folded conformation, which is evident in the solid-state crystal structures of the peptides.

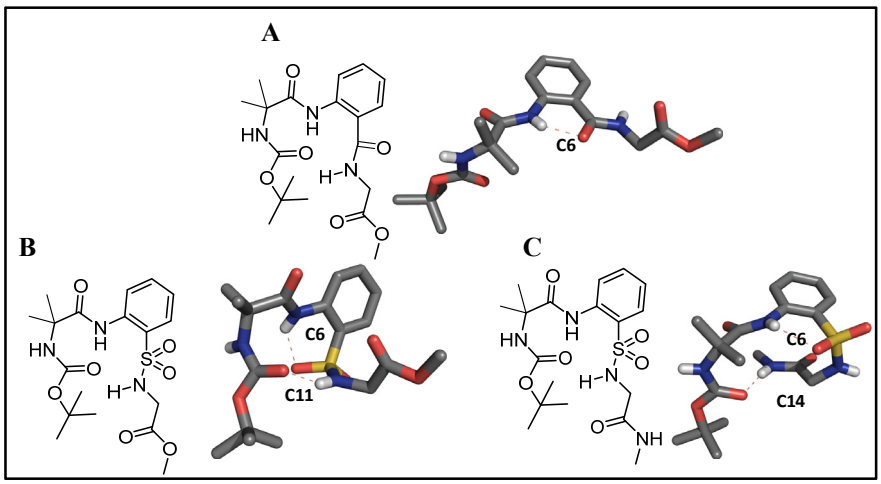

Fig. 4: Molecular and crystal structure of carboxamide oligomer (A); Molecular and crystal structures of sulfonamide oligomers (B and C).

This study proved that ^{S}Ant translates its rigidity to the peptides into which it is introduced irrespective of the surrounding residues. The conformation of the hexapeptide featuring sulfonamide was derived from MD simulation studies based on the nOe constraints obtained from the solution-state NMR studies, which revealed a helical conformation (Fig. 5).

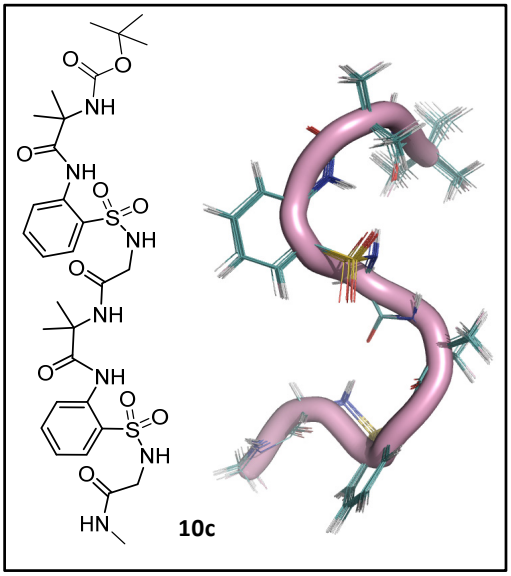

Fig. 5: Molecular structure of (Aib-^{S}Ant-Gly)$_2$ oligomer. Cartoon representation of the optimized structure of **10c**, revealing a helical conformation.

[Deciphering the conformational preference of Orthanilic acid- a case study in αβα-hybrid sequence: **Priya, G.**; Kotmale, A. S.; Gawade, R. L.; Puranik, V. G.; Rajamohanan, P. R.; Sanjayan, G. J. (*manuscript under preparation*)]

Section C describes the conformational consequences observed by hybridizing peptide sequences of known conformations by introducing or substituting one of the residues of the sequence with ^{S}Ant. Orthanilic acid was inserted between Pro and Gly as well as Gly and Pro residues to study the conformational consequences. The solid-state crystal structures of the designed peptides clearly revealed C11 H-bonding in the Pro-^{S}Ant-Gly sequence and C10 H-bonding in the representative sequence of Gly-^{S}Ant-Pro hybrid oligomer. The conformations of the peptides were well established both in the solid and solution states. It is clearly evident from the crystal structures that ^{S}Ant does not interfere with the secondary structural preferences of the peptides much and maintains the rigidity of the peptide without disturbing it.

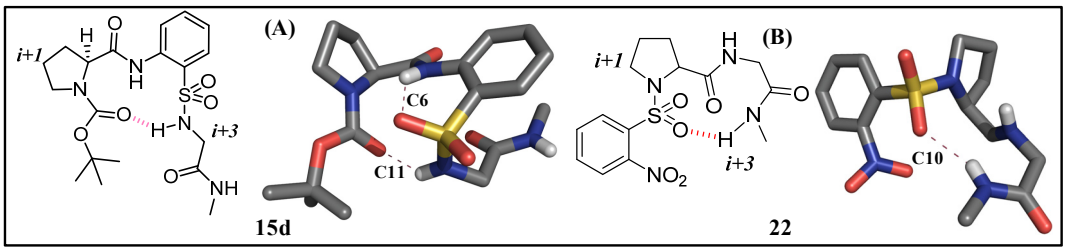

Fig. 6: Molecular and PyMOL-rendered crystal structures of **15d** (A) and **22** (B) showing robust C11 and C10 H-bonding patterns.

The conformation of the hexapeptide (Pro-^{S}Ant-Gly)$_2$ **16b** was derived from MD simulation studies as it couldn't be crystallized. The solution-state nOe based derived structure clearly revealed a helical conformation with two C11 H-bonded ring networks (Fig. 7).

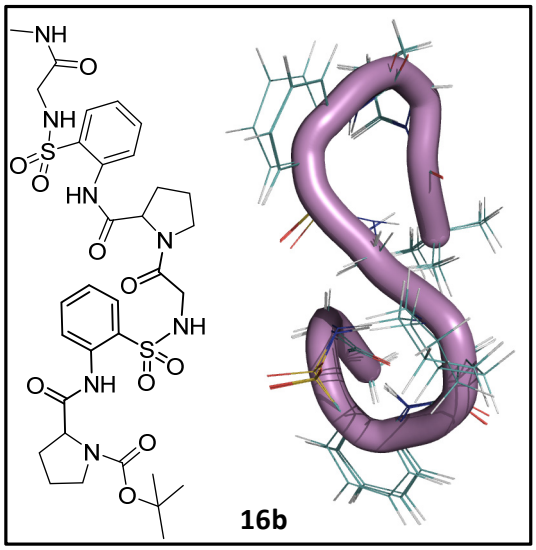

Fig. 7: Molecular structure of (Pro-^{S}Ant-Gly)$_2$ oligomer and cartoon representation of the optimized structure of **16b**, revealing a helical conformation.

[Consequences observed by interchanging the residues around a turn inducing building block: **Priya, G.**; Kotmale, A. S.; Gawade, R. L.; Puranik, V. G.; Rajamohanan, P. R.; Sanjayan, G. J. (*manuscript under preparation*)]

It was observed that Ant-Ant-Pro peptide exists in a doubly folded conformation, wherein one of the Ant residues was substituted by ^{S}Ant residue to study the conformational consequences observed in the peptides sequences. The crystal structures obtained in this study clearly showed that the substitution of Ant by SAnt effects the overall conformation of the peptide.

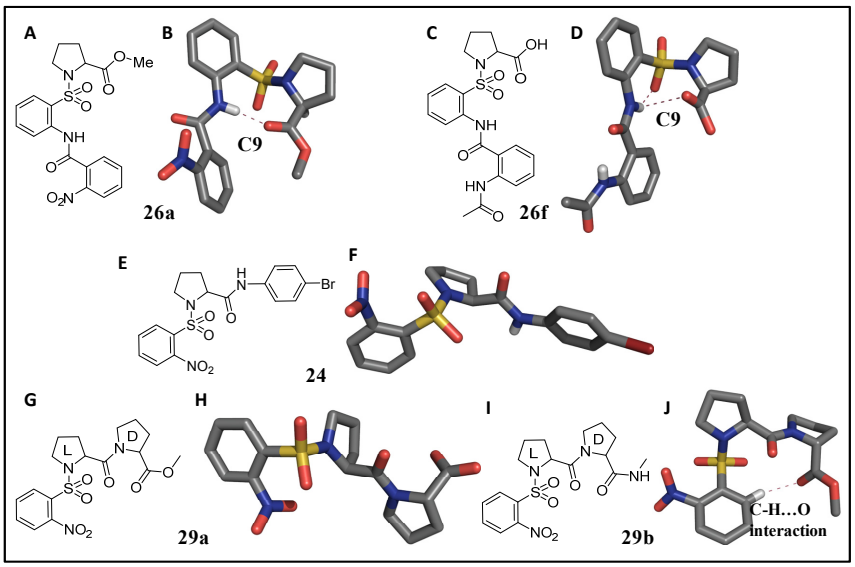

Fig. 7: Molecular and crystal structures of **24** (A, B), **26a** (C, D), **26f** (E, F), **29a** (G, H), and **29b** (I, J), respectively. All hydrogens, other than the polar ones have been deleted for clarity in the crystal structures

Since the peptide **26g** and **27e** couldn't be crystallized, their conformations were established using MD simulation studies which revealed the consequences of introduction of SAnt into the peptide sequences.

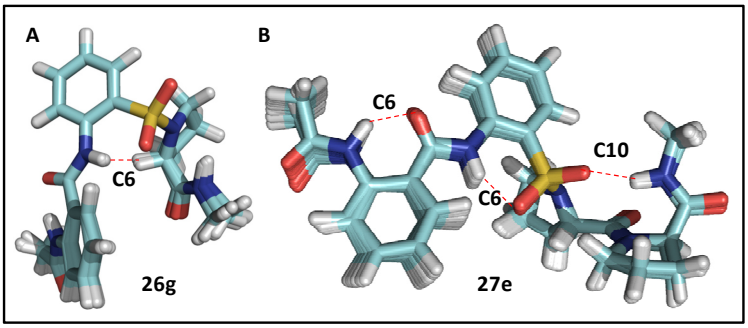

Fig. 8: Overlay of the 20 minimum energy conformations derived from the MD studies of **26g** (left) and **27e** (right).

Chapter 3: This chapter describes the synthesis and biological evaluation of structural analogues of peptide-based antimitotic agents.

Section A describes the synthesis of Pro-Atc dipeptide-based analogues as antimitotic agents. As mentioned in Chapter I, the Pro-Atc oligomers adopt a well defined folded conformation devoid of inter-residual hydrogen bonds. To probe the application of such folded systems, we designed few analogues with D-amino acid residues and variety of side chains that can provide sufficient hydrophobicity and proteolytic resistance in the biological systems (Fig 8).

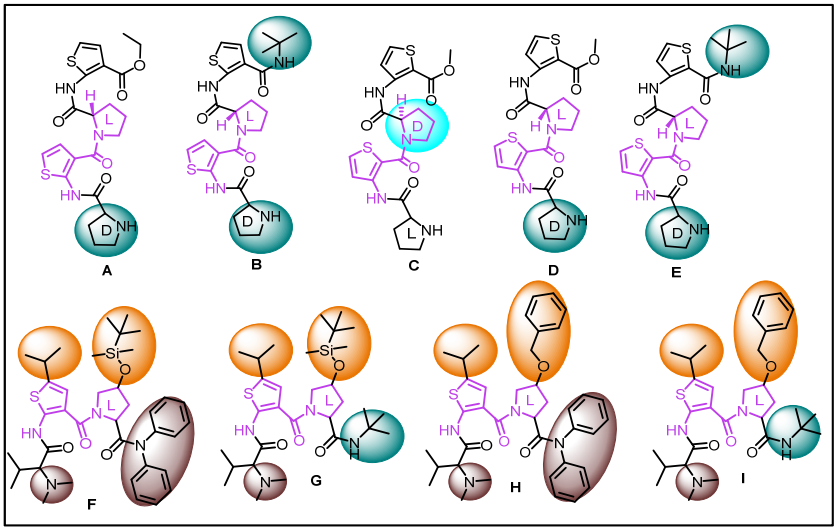

Fig. 9: Pro-Atc dipeptide based analogues featuring modifications highlighted.

Section B includes the synthesis of analogues of Ixorapeptides wherein N and C termini modifications, side chain modifications as well as backbone modifications have been incorporated to increase the potency of binding to tubulin protein (Fig. 9). Preliminary studies to biologically evaluate the tubulin binding phenomenon of the synthesized analogues was also attempted which revealed that the compound **J** is enough potent to bind to the tubulin protein inferring the biological application of the analogues synthesised.

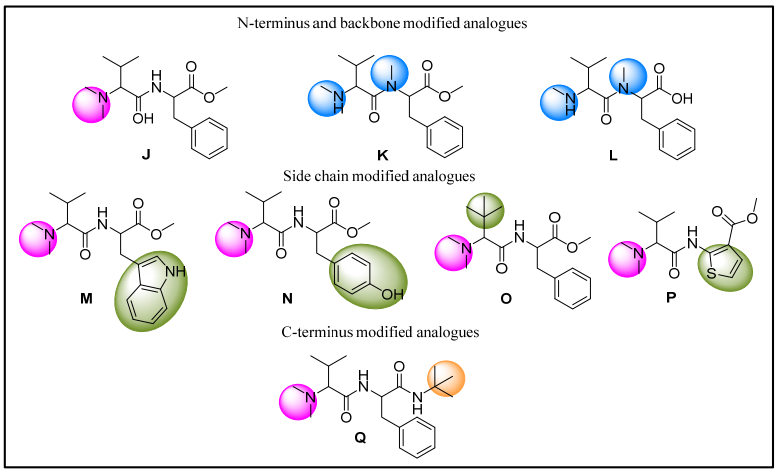

Fig. 10: Structures of the designed synthetic analogues of Ixorapeptide I. the modifications attempted are highlighted.

[Novel analogues of Ixora peptide I as anti-cancer agents: **Priya, G.**; Kunalika,; Chaitanya, A; Sanjayan, G. J. (*manuscript under preparation*).]

General Remarks

- Unless otherwise stated, all the chemicals and reagents were obtained commercially.
- Required dry solvents and reagents were prepared using the standard procedures.
- All the reactions were monitored by thin layer chromatography (TLC) on precoated silica gel plates (kieselgel $60F_{254}$, Merck) with UV, I_2 or ninhydrin solution as the developing reagents in the concerned cases.
- Column chromatographic purifications were done with 100-200 Mesh Silica gel or with Flash silica gel (230-400) mesh in special cases.
- Melting points were determined on a Buchi Melting Point B-540 and are uncorrected.
- IR spectra were recorded in nujol or $CHCl_3$ using Shimadzu FTIR-8400 spectrophotometer.
- NMR spectra were recorded on Ac 200 MHz, AV 400 MHz or DRX-500 MHz Bruker NMR spectrometers. All chemical shifts are reported in δ ppm downfield to TMS and peak multiplicities as singlet (s), doublet (d), quartet (q), broad (br), broad singlet (bs) and multiplet (m).
- Elemental analyses were performed on a Elmentar-Vario- EL.
- Electron Scattered Ionization (ESI) Mass Spectrometric measurements were done with API QSTAR Pulsar mass Spectrometer and MALDI-TOF mass spectrometric measurements were done on Voyager-DE STR mass spectrometer.
- Quantum chemical calculations were performed employing the Guassian 03 program package (Guassian, Inc., Wallingford, CT 06492, USA).
- Single crystal X-ray data were collected on a *Bruker SMART APEX* CCD Area diffractometer.

List of Publications

(1) Helical folding in heterogeneous foldamers without inter-residual backbone hydrogen-bonding: **Priya, G.**; Kotmale, A. S.; Gawade, R. L.; Mishra, D.; Pal, S.; Puranik, V. G.; Rajamohanan, P. R.; Sanjayan, G. J. *Chem. Commun.* **2012***, 48,* 8922-8924.

(2) Orthanilic acid-Promoted *Reverse-Turn* Formation in Peptides: Kale, S. S.; **Priya, G.**; Kotmale, A. S.; Gawade, R. L.; Puranik, V. G.; Rajamohanan, P. R.; Sanjayan, G. J. *Chem. Commun.* **2013,** *49*, 2222-2224.

(3) Foldamers: They're Not Just for Biomedical Applications Anymore: Prabhakaran, P**.; Priya, G.**; Sanjayan, G. J., *Angew. Chem. Int. Ed.* **2012***, 51,* 4006-4008.

(4) Multifaceted Folding in a Foldamer Featuring Highly Cooperative Folds: Ramesh, V. V. E.; **Priya, G.**; Gonnade, R. G.; Rajamohanan, P. R.; Hofmann, H.-J. r.; Sanjayan, G. J. *Chem. Commun*. **2012**, *48*, 11205-11207.

(5) Expanding the structural repertoire of β/α Ant-Pro (anthranilic acid-proline) oligomers into γ/α 2-Amb-Pro (2-aminomethyl benzoic acid-proline) oligomers: Ramesh, V. V. E.; **Priya, G.**; Rajamohanan, P. R.; Hofmann, H.-J.; Sanjayan, G. J. *Tetrahedron* **2012***, 68, 4399-4405.*

(6) Deciphering the conformational preference of Orthanilic acid- a case study in αβα-hybrid sequence: **Priya, G.**; Kotmale, A. S.; Gawade, R. L.; Puranik, V. G.; Rajamohanan, P. R.; Sanjayan, G. J. (*manuscript under preparation*)

(7) Consequences observed by interchanging the residues around a turn inducing building block: **Priya, G.**; Kotmale, A. S.; Gawade, R. L.; Puranik, V. G.; Rajamohanan, P. R.; Sanjayan, G. J. (*manuscript under preparation*).

(8) Novel analogues of Ixora peptide I as anti-cancer agents: **Priya, G.**; Kunalika,; Chaitanya, A; Sanjayan, G. J. (*manuscript under preparation*).

Chapter 1

Heterogeneous α/β hybrid peptide oligomers devoid of inter-residual hydrogen bonding

Heterogeneous α/β hybrid peptide oligomers devoid of inter-residual hydrogen bonding

1.1 Introduction

Natural bio-polymers such as DNA, RNA, proteins and many other bio-machineries are astoundingly complex in their structure and function. Among all the bio-polymers, proteins/polypeptides are considered to be vital and unique bio-molecular building blocks for life. They are very well recognized to be the fundamental components involved in myriad of cell metabolic activities.[1] These bio-polymers assume diverse roles in the biological scenario: providing structural components within and outside the cell (being the components of cytoskeleton and extra cellular matrix); as intra and inter cellular messengers (as hormones and kinases); in small molecule transportation (in calcium and oxygen binding); for energy transduction (in synthesis of ATP); as bio-catalysts (enzymes) and several other crucial phenomena. Most of these functions accomplish successfully as the proteins/polypeptides adopt a specific compact conformation essential to carry out the activities, in the three dimensional space. The polypeptides perform these activities being in their quaternary or tertiary structural conformations which are the assemblies of well defined and organized secondary structural units that make use of several non-covalent interactions like hydrogen bonding, Van der Waals forces, π-π stacking, steric effects etc.[2] to exist, while these secondary structural entities arise from the simpler long chain amino acids constituting the primary structure of a protein.[3] This hierarchical structural architecture of protein is shown in Fig 1.1.

To understand the complex protein structure or conformation, it is necessary to understand the secondary structural architecture involved in it. The regular secondary structure of a protein mainly comprises of helices, sheets, turns and loops.[4] Thus, unravelling how a one dimensional pattern of α-amino acids encode into a specific and compact three-dimensional conformation remains an essential topic of research in chemistry as well as biology since this structural feature is responsible for various biological effects. The mysterious relationship between the biological processes and the conformation of a protein has inspired

the chemists to build up synthetic molecules 'that can fold'- ***foldamers*** to unveil the mechanism involved in such processes. This might be helpful in disclosing the sequence-to-structure relation- ship in proteins. Pursuing and understanding such relationships is significant because it would be of great help in designing and building synthetic bio-machineries. This is known as *de novo* peptide/protein design. Hence, this area of research has drawn much attention in the recent years.

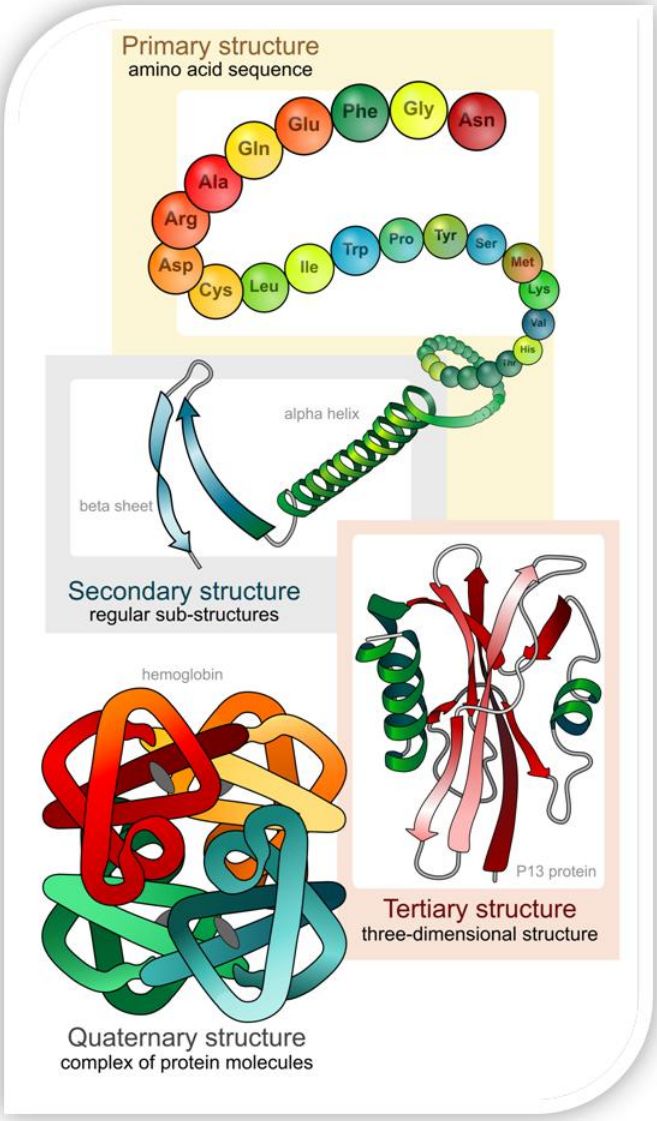

Fig. 1.1: The hierarchical structure of protein. Cartoon representation of primary, secondary, tertiary and quaternary structures shown sequentially from top to bottom.

1.2 Foldamers

As defined by Gellman, foldamer is ***'any oligomer with a strong tendency to adopt a specific compact conformation'***.[5] Foldamers are unnatural oligomers that adopt well defined conformations akin to the natural polymers.[6] These are also known to assume distinct conformational preferences being at the interface of covalent (molecular) and non-covalent (supramolecular) interactions. In general, the geometries of these molecules are controlled by several parameters such as backbone conformational preferences,[7] backbone inter-chromophoric interactions (aromatic-aromatic interactions),[8] side chain interactions, solvophobic interactions,[9] metal ion coordination[10] and H-bonding interactions. These molecules with such features may find applications as novel bio-mimetic receptors, catalysts, energy capturing and storing devices, delivery and transport systems for synthetic drugs and membrane-impermeable bio-molecules as they possess well defined and pre-organised conformational features. Thus, fully predictable foldamers are currently the object of interest that can be highly versatile building blocks in designing hierarchically integrated large architectures.

Among all the secondary structural architectures of proteins, ***helices*** need a special mention for the reason that they possess applications as antibacterial agents, inhibitors, agonists, antagonists, transporters, ability to stably insert across lipid bi-layers and can participate in protein-protein interactions.[11] The helices are unique in adopting a specific folded conformation which provides a precise spatial orientation of side chains and back bone that comprise the *"active-site"*. Creation of synthetic peptide oligomers can refine our ability to understand the folding propensities of these flexible molecules into specific shapes. The foldamer chemistry which relies on predictable conformations of large oligomers provides new strategies in mimicking the biomoleculer functions. In this context, in order to mimic the natural helices both structurally and functionally, many synthetic oligomers have been reported wherein unnatural, constrained building blocks including β, γ, δ, ε amino acids, vinylogous amino-acids, peptoids, aminoxy acids, oligo pyrrolidines, pyridine/pyrimidines etc., and their combination as hybrid sequences have been used to develop a variety of secondary structures.

Accordingly, there is an urge for the design of novel helical architectures that can be of medicinal and pharmacological interest in future.

1.3 Classification of Foldamers

Foldamers are classified[12] into different types based on the nature of backbone *viz*. biotic and abiotic, aliphatic and aromatic, peptidic and non-peptidic etc. Based on the subunits involved in the backbone, they are generally classified into homogeneous and heterogeneous foldamers.

1.3.1 Homogeneous foldamers

This class of foldamers possesses the features analogous to the parent polypeptides or proteins. Hence, they are also termed as *peptidomimetic foldamers*. This strategy includes the modifications of amino acid side chains, introduction of constraints to increase the overall rigidity and development of templates and scaffolds that increase the stability of the secondary structure achieved. Homogeneous foldamers were achieved by using a variety of building blocks from α-amino acid family (1,2 diamino ethanes, peptoids,[13] azapeptides,[14] azatides,[15] oxazolidinones,[16] pyrrolinones etc.) β-amino acid family (cyclic β-amino acids,[17] aminoxy acids,[18] anthralinamides,[7a,b] sulfonamides, sulfinamides, sulfoximines,[19] hydrazino peptides,[20] ureas[21] etc.), γ-amino acid family[22, 23] (vinylogous amino acids, vinylogous sulfonyl peptides, carbamates, γ-amino acids etc.), and δ-amino acid family[24] (δ-amino acids, carbopeptides etc.). In addition, backbone modifications in these cases include isosteric or isoelectronic replacement of the subunits and introduction of additional fragments in order to achieve efficient building blocks. The structures of all these building blocks are shown clearly in Fig. 1.2.

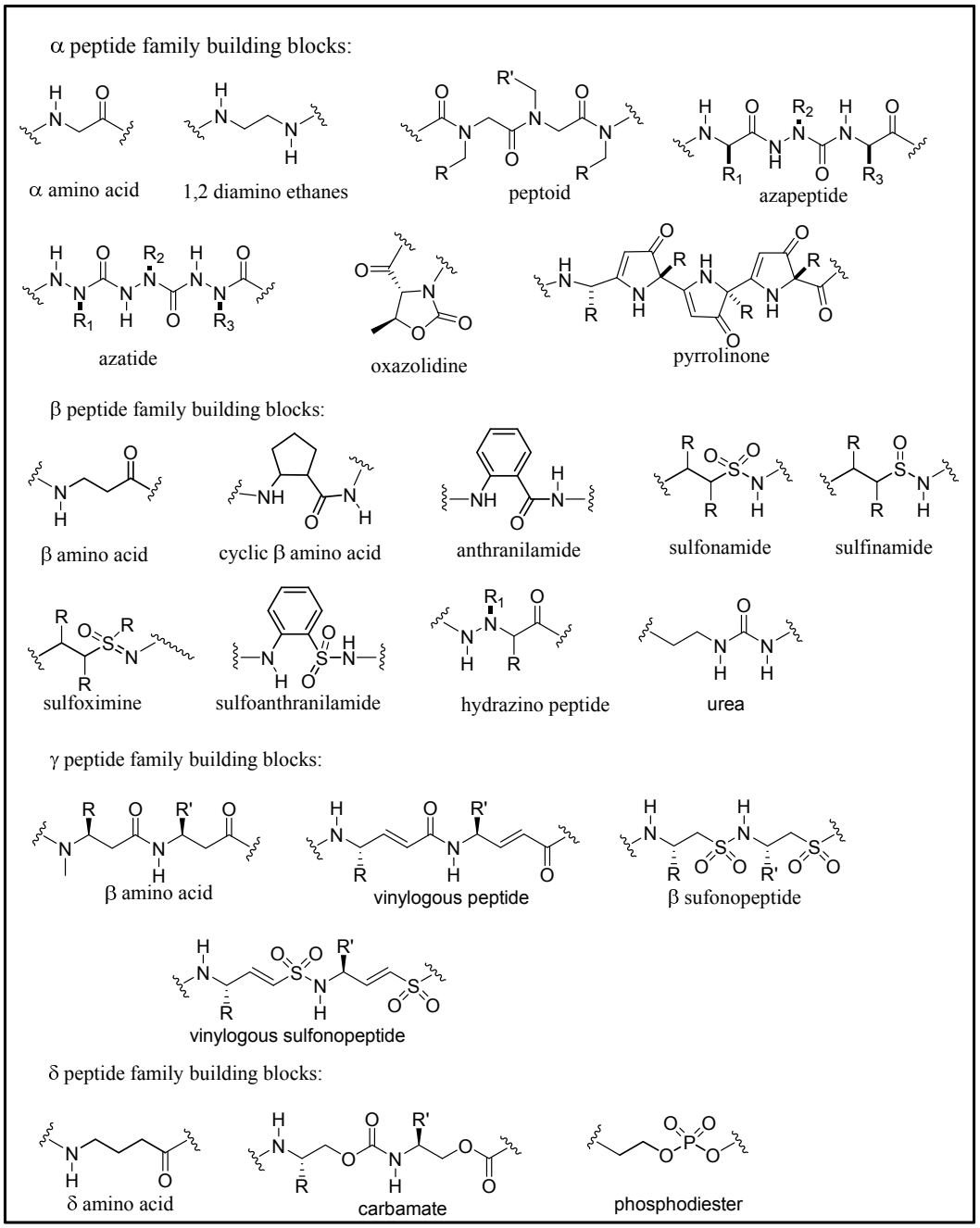

Fig. 1.2: Selected building blocks used in the synthesis of homogeneous biotic foldamers.[25]

The oligomers reported in literature using the building blocks mentioned above feature variety of secondary structural architectures that are proved to be useful in different fields (Fig 1.3).[26]

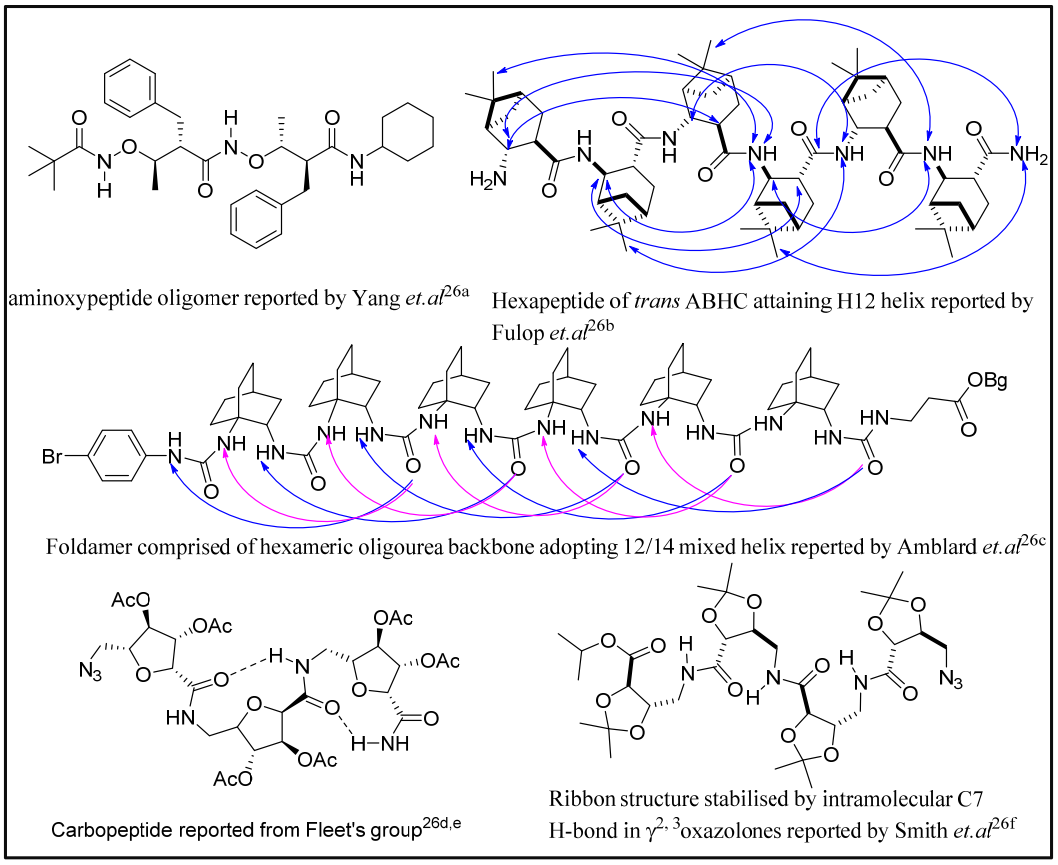

Fig. 1.3: Selected examples of homogeneous foldamers which use diverse building blocks to adopt specific secondary structural architectures.

In addition to the above mentioned building blocks, several aromatic building blocks have been used to develop aromatic amide foldamers as shown in Fig.1.4.[27] The first example of aromatic amide oligomers was reported by Hamilton's group using anthralinamide oligomers that adopt a sheet-like conformation.[7a,b] Although different from natural α-amino acids that possess a chiral atom, aromatic monomers do not possess any chiral centre: However, helical structures can be achieved by simply inserting one or more chiral groups at the ends or in the middle of the backbones. These building blocks rely to a larger extent on the intramolecular pre-organized H-bonding patterns of the monomeric building blocks. Owing to the pre-organised intramolecular hydrogen bonding in the backbone subunits, these oligomers adopt specific secondary structures such as helices, extended helices, zigzag structures, V-styled structures, sheets etc. This class of foldamers (Fig 1.5) proved its application in molecular design to target

biomacromolecules, cell membranes, molecular recognition and self assembly and promoting macrocyclization etc.[28]

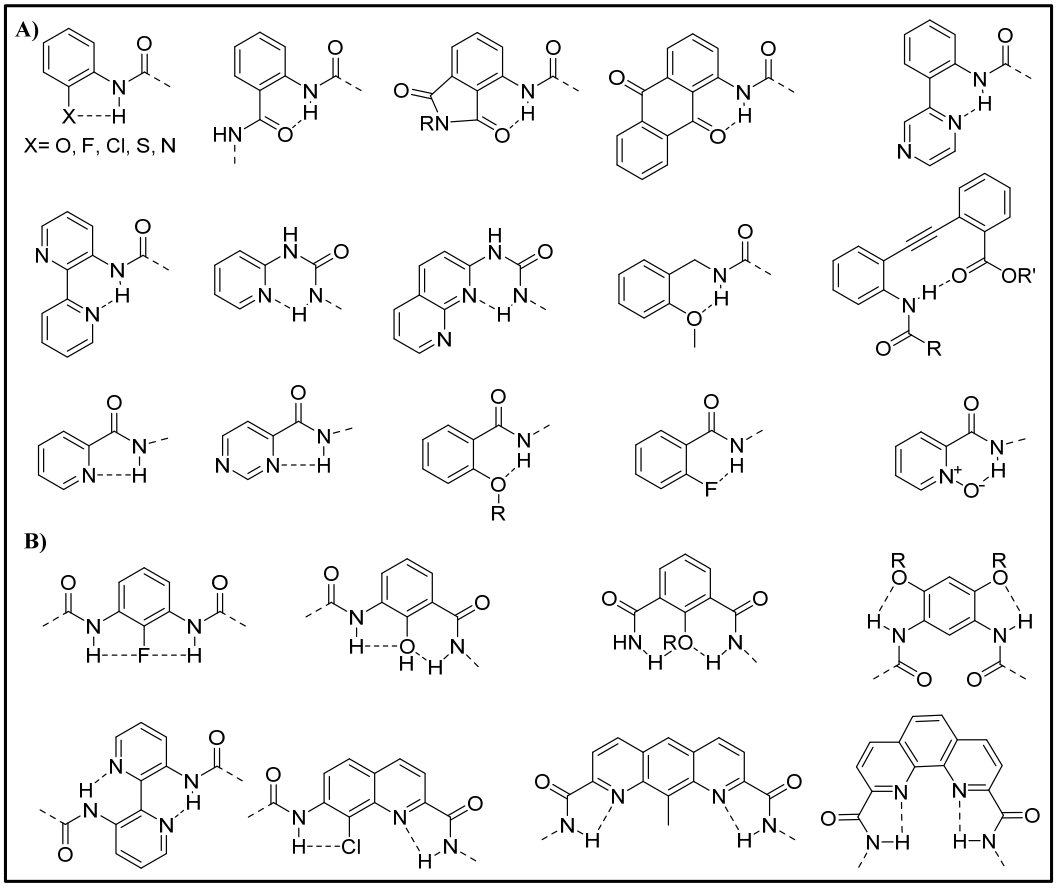

Fig. 1.4: Selected aromatic amide building blocks.[27] A) Building blocks with pre-organized H-bonding codes. B) Building blocks with bifurcated H-bonding codes.

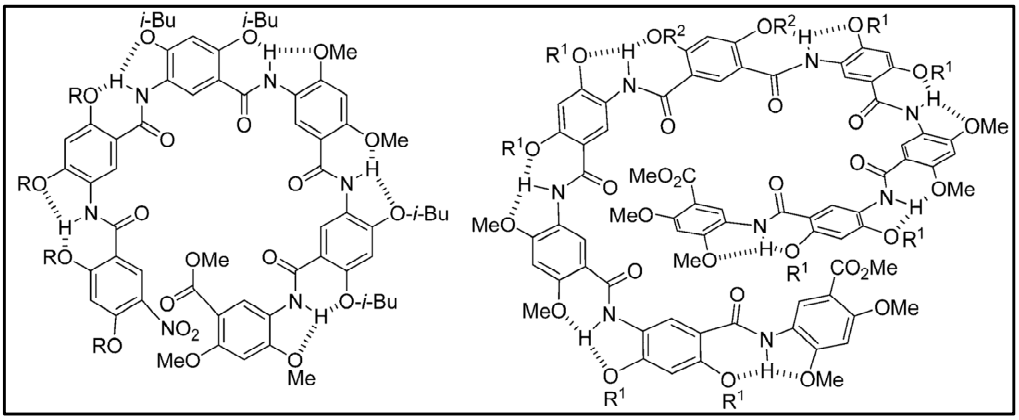

Fig. 1.5: Selected examples of homogeneous aromatic amide foldamers adopting helical structures.[28]

1.3.2 Heterogeneous foldamers

In recent years, the study of the heterogeneous foldamers is emerging as a significant area of research owing to their advantages over the homogeneous counter parts. This approach allows numerous combinations of subunits like αβ, ααβ, αββ, αβγ, βγ, ββγ, etc in developing novel secondary architectures. Each of the heterogeneous backbone offers a distinct way to project the side chains in space, thus increasing the diversity. The launch of β-peptides into the foldamer chemistry paved fascinating avenues to increase the synthetic peptide sequences in leaps and bounds which possess applications in various fields of science. The *β*-peptides being stable against proteolytic, hydrolytic, and metabolizing enzymes, are much favoured building blocks in the design strategies.[29] Selected examples of the building blocks with imposed rigidity are shown below in Fig 1.6.

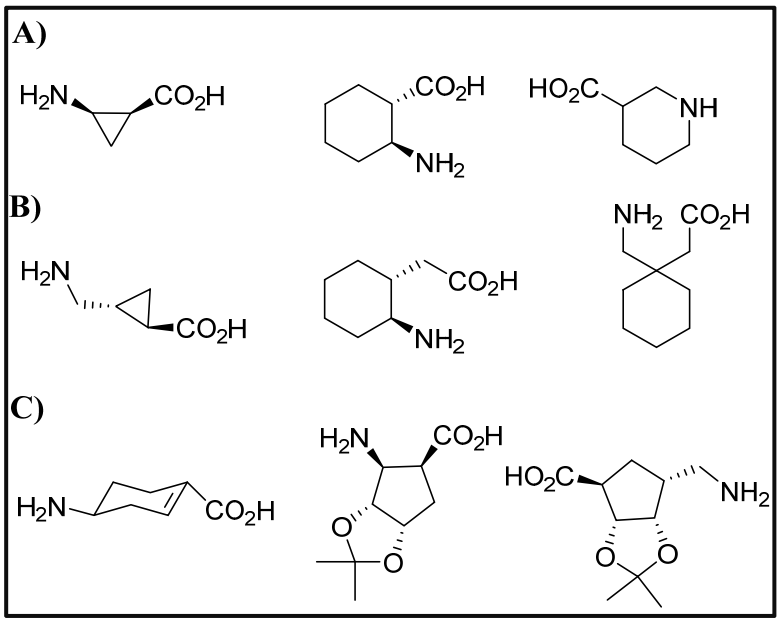

Fig 1.6: Few selected examples of monomeric building blocks: A) Constrained β-amino acids, B) Constrained γ-amino acids, C) constrained δ-amino acids.

1.3.2.1 *αβ*-hybrid foldamers

The helices generated from α-amino acids are *α*-helices, 3_{10}-helices and *π*-helices, typically. The insertion of a β-amino acid subunit into these helices exponentially increases the range of potential foldamers providing wide scope for the development of novel unseen architectures with desired applications. Reiser's group reported this hybrid strategy in case of *cis*-β-aminocyclopropanecarboxylic

acid and L-alanine that exhibited helical conformation.[30] Similarly, Gellman's group reported a hybrid foldamer comprising of (*S*, *S*)-*trans*-ACPC units and L-*α*-amino acids which displayed a mixed helix with 11-membered and 14/15-membered and 18- membered hydrogen bonding patterns as shown in Fig 1.7.[31]

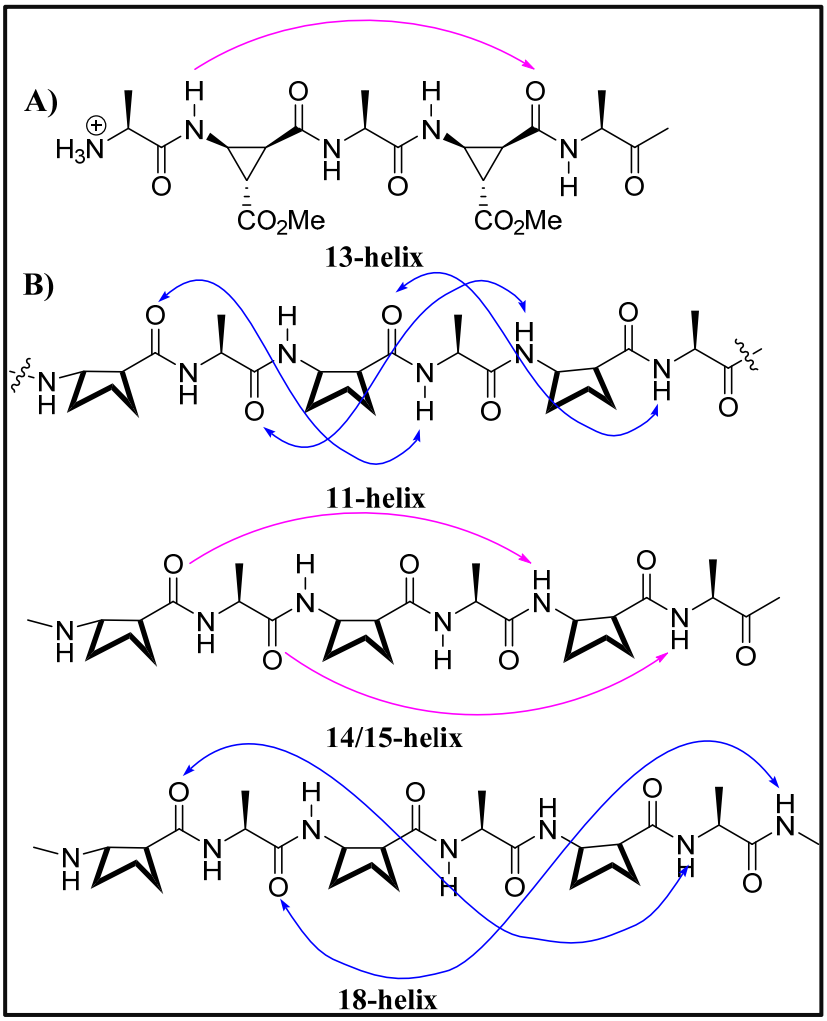

Fig. 1.7: αβ-hybrid foldamers reported by A) Reiser's group,[30] B) Gellman's group,[31]

Later, it was proved that the incorporation of Aib instead of Ala enhanced stability of the helix. Recently, Balaram's group reported that insertion of β-amino acid into a polypeptide sequence: Boc-Leu-Phe-Val-Aib-βPhe-Leu-Phe-Val-OMe, does not effect the overall conformation of the peptide.[32] Chandrasekhar *et.al.* reported that alternating L-ala and *cis*-β-furanoid sugar amino acid and its *vice versa* in the oligomeric state adopted a left handed 11 helix and 14/15 helix, respectively, in solution state.[33]

1.3.2.2 ααβ, βαα, αββ, βαβ- hybrid foldamers

The study of hybrid foldamers has been extended by varying the ratios of *α* and β subunits on the foldamer backbone also. The conformational preferences of Foldamers comprising of 1:1, 1:2 and 2:1 ratios of *α* and β-amino acids have been reported by Gellman's group which show *i-i+3* C=O…H-N hydrogen bonds in the crystallized peptides (Fig 1.8 A and B).[34] Very recently, Arora *et. al.* reported an oligomer (Fig 1.8 C) comprising of αααβ repeats adopting 13- and 14-membered H-bonding patterns where in a hydrogen bond surrogate (HBS)- the replacement of N-terminus *i-i+4* intramolecular hydrogen bond by a covalent bond was done.[35]

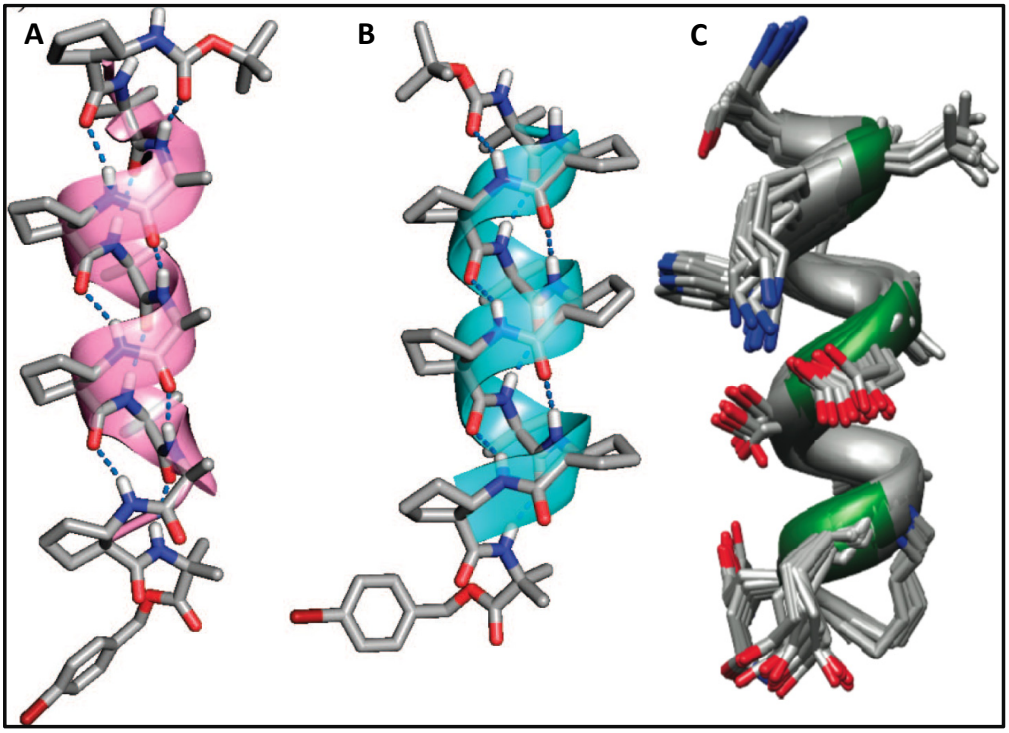

Fig. 1.8: Crystal structures overlaid by cartoons of ββα and αββ hybrid foldamers reported by Gellman *et.al* (A and B)[34] and nOe based structure of αααβ hybrid foldamer reported by Arora *et.al*. (C).[35]

Balaram's group reported an undecapeptide: Boc-Val-Ala-Phe-β^{3}hVal-β^{3}h-Phe-Aib-Val-Ala-Phe-Aib-OMe that forms a helix with 13-membered hydrogen bonding at the C-terminus and 15- as well as 14- membered hydrogen bonded rings in the αββ, ααβ and βαα segment region respectively.[36] A recent report from Sanjayan's group showed a direct comparison of carboxamide and sulphonamide foldamers with repeating αβα residues which develop helical conformation both in solid and solution states. They report that the carboxamide

sequence retains the native C6 hydrogen bonding which is the characteristic feature of anthranilamides, but the sulphonamide sequence adopts a C11 hydrogen bonded helix.[37]

1.3.2.3 αγ-hybrid foldamers

Gabapentin (Gpn), a conformationally restricted $\gamma^{3,3}$- amino acid, the higher homologue of α, α disubstituted aminoisobutyric acid, is considerably used as constrained building block in the construction of αγ- hybrid foldamers. In a specific sequence: Boc-Leu-Gpn-Leu-Aib-OMe, reported by Balaram *et.al,* a mixed C10/C11 hydrogen bonding pattern was observed for the αγα motif. The same group reported a hybrid αγαγ peptide that adopted two successive C12 H-bonding repeats in a helical conformation, while its positional isomer γαγα peptide adopted a conformation stabilised by C9 and C7 hydrogen bonding networks.[38] Later, Gellman's group developed constrained chiral γ-amino acid building blocks to synthesize a hybrid αγ foldamer featuring 1:1 ratio of the chiral γ-amino acid building block and Gpn, wherein the tetrameric sequence γαγα and the hexameric sequence αγαγαγ are shown to preferentially exist in C12 hydrogen bonded helical conformation.[39] Sanjayan *et. al.* reported a novel αγ-hybrid peptide comprised of proline (Pro) and 3-amino-5-bromo-2-methoxy benzoic acid (Amb) that features a repeated γ-turn.[40] The same group reported a ααγ hybrid peptide oligomer with Aib, Pro and 3-amino-4, 6-dimethoxybenzoic acid subunits which showed a C10 H-bonding pattern (β-turn) in its oligomers.[41] Sharma *et. al* reported an oligomer featuring mixed C10/C12 H-bonding pattern in a αγ hybrid helix which was supported by MD simulation studies.[42] They also used ε-amino acids to develop novel heterogeneous foldamers as shown in the Fig 1.9.[43]

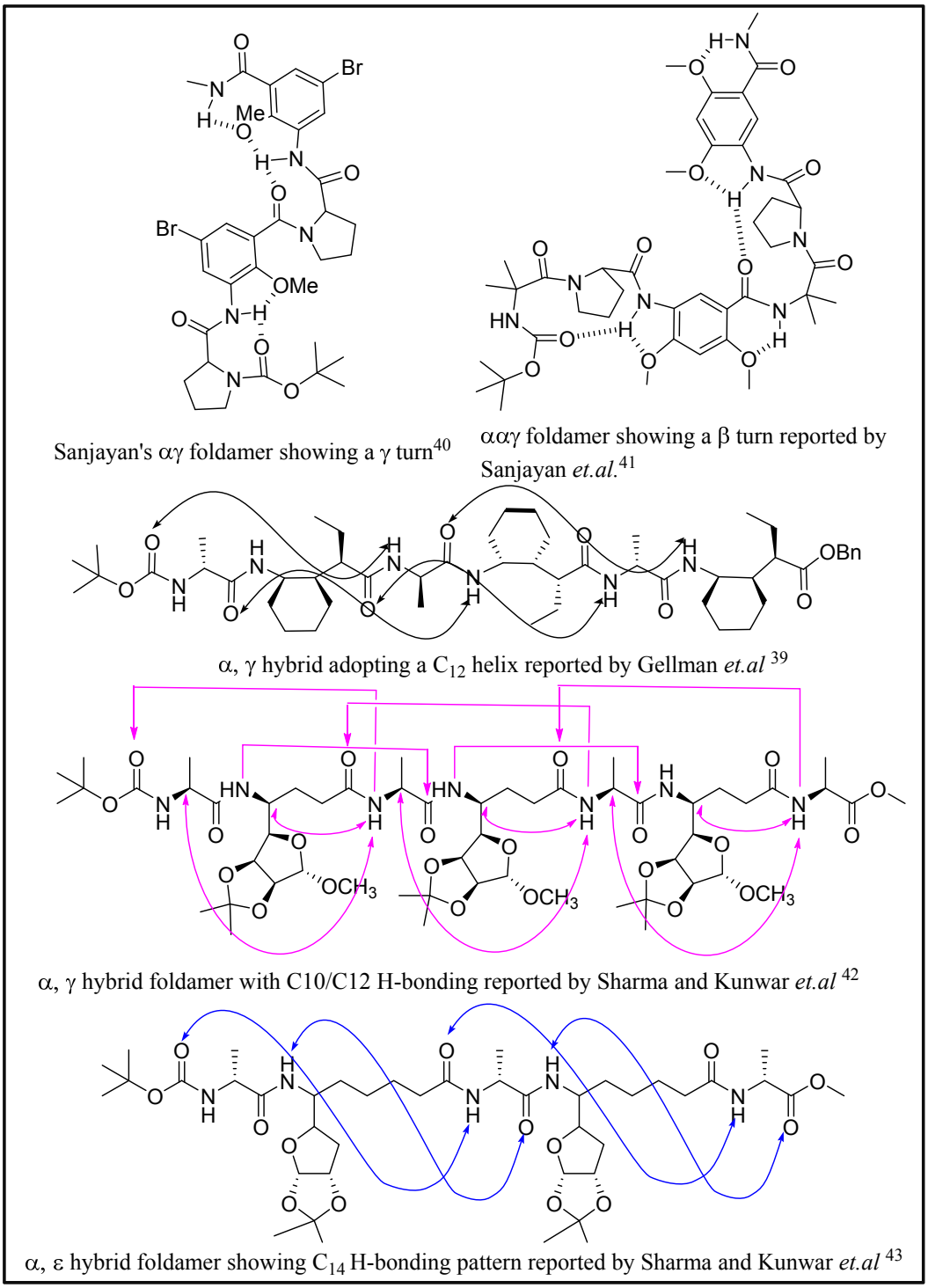

Fig 1.9: αγ and αε hybrid oligomers adopting various hydrogen bonding patterns.

1.3.2.4 βγ-hybrid foldamers

The βγ-hybrid peptide segment attained considerable interest because of the fact that the number of atoms in βγ-dipeptide subunit is similar to that in a α-tripeptide (from its N- to C-terminus). It is reported that βγ-hybrid peptide with β^3 and γ^4 residues i.e., β-Caa and γ-Caa (C-linked carbo-β- and γ-amino acids of D-xylose) adopt a mixed H11/13 helix by Sharma *et.al*.[42, 44] Gellman's group did a detailed comparison of β/γ helix and α-helix and concluded that both possess a rise-per-turn of 5.4 Å and similar radii (2.5 vs 2.3 Å) which suggested that the β/γ helices may be promising scaffolds for the functional mimicry of natural α-helices (Fig 1.10).[45]

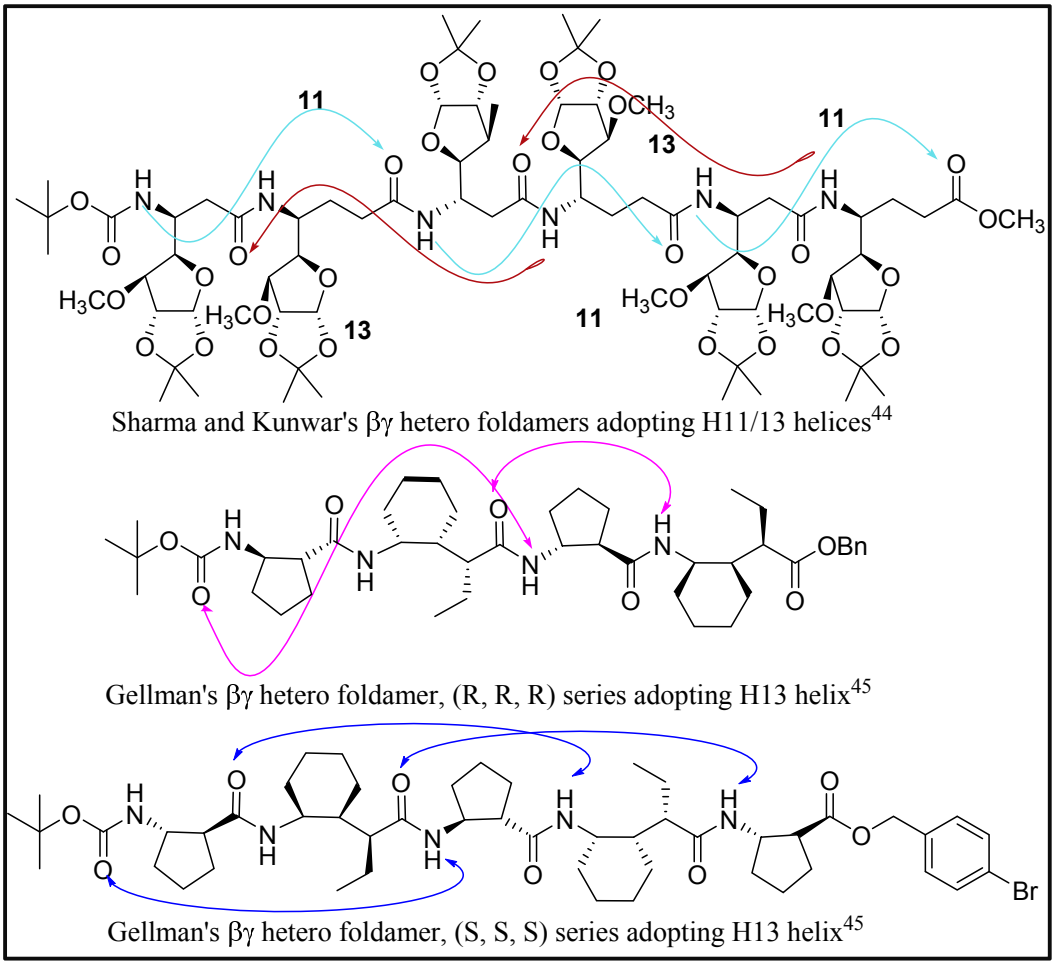

Sharma and Kunwar's βγ hetero foldamers adopting H11/13 helices[44]

Gellman's βγ hetero foldamer, (R, R, R) series adopting H13 helix[45]

Gellman's βγ hetero foldamer, (S, S, S) series adopting H13 helix[45]

Fig 1.10: βγ-hetero foldamers featuring secondary structures similar to that of α-helices.

1.3.2.5 αβγ-hybrid foldamers

Gellman *et.al.* reported a αβγ-hybrid peptide recently with αγααβα repeating units which is considerably more stable than the α-helix formed by analogous 14-mer α-peptide using solid phase synthesis.[46] The high stability of the hybrid peptide is attributed to the appropriately pre-organised β and γ residues.

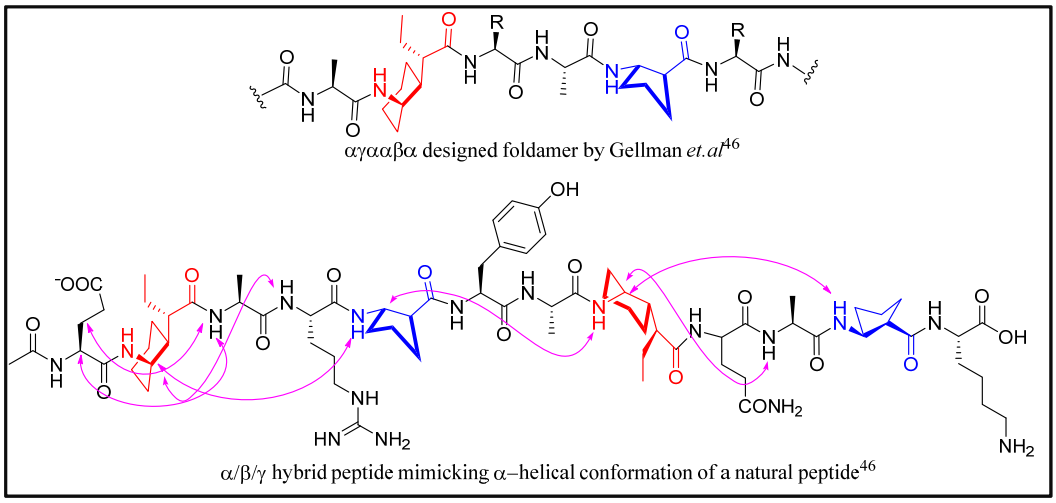

Fig 1.11: αβγ hybrid foldamer mimicking the natural α-helical peptide.[46]

1.4 Foldamer design

The design strategy of foldamers aims to develop synthetic systems with pre-organised folding patterns since the type of fold a peptide molecule adopts is much significant and is influenced by several factors mentioned below.

1.4.1 Factors influencing a helical fold

Majority of the protein biological domains known are α-helices although both α-helices and β-sheets satisfy the structural requirement to perform the metabolic tasks involved in the biological systems. This is due to the fact that the helical conformation has the ability to stabilize itself using the intra-molecular hydrogen bonding independently, whilst the β-strand requires additional intermolecular association with another β-strand to fold precisely. Thus, helical conformation is the energetically preferred conformation for a protein which relies on the appropriate fold/turn that the amino acids develop on the backbone.[47] In general, the folding in a peptide molecule is due to the influencing factors such as

local conformational preference, intramolecular hydrogen bonding, with/without inter-residual hydrogen bonding, solvophobic effects, hindered oligomer backbones, steric effects, π-π interactions, hydrophobicity of the residues used in foldamer design etc. Diverse class of foldamers with striking conformational features have been reported in the literature till date which can adopt helical conformation based on the factors mentioned above. Few selected examples that adopt helical folding are discussed below.

1.4.2 Folding in aromatic oligoamides using spacer

Li *et. al.* reported hydrogen bonding-induced aromatic oligobenzamide foldamers which develop a helical conformation with the two peripheral benzene units stacking with each other and are capable receptors that can efficiently bind saccharides in chloroform.[48] Gong and co-workers reported aromatic amide oligomers comprised of 4-amino-2,3-dimethoxybenzamide residues. Molecular modelling studies of the respective oligomers stated that the 15-mer was not long enough to exist in a helical conformation and thus existed in a crescent shaped conformation while the higher oligomer, 21-mer exhibited a helical conformation (Fig 1.12).[49]

Huc, Lehn and co-workers designed oligomers which consisted of 2,6 diamino pyridine and 2,6 pryidine-dicarbonyl segments that exhibited a helical folded conformation.[50] In dilute solutions, these oligomers are reported to adopt a single folded strand while in concentrated solution they formed a double helix. Huc and co-workers prepared oligomers containing quinoline derived δ-amino acids which exhibit a helical conformation extending to more than three turns, five segments formed two helical turns which correspond to the highest curvature reached by helical aromatic oligoamides.[51] The same group reported oligomers which were synthesised by linking quinoline amide helical segments to 2,5-dimethoxyterephthalic acid and pyridine spacers. The crystal structures of these molecules clearly show that they exist in helical conformations.[52]

Parquett and co-workers designed oligomers comprised of alternating pyridine 2,6 dicaboxamides and *meta*-(phenylazo)azobenzene sub-units. The solid state conformation of these molecules clearly suggests a two turn helical

conformation even though the benzene rings linking to two azo groups bear no amide units to form intramolecular hydrogen bonding.[53] Sanjayan *et. al.* reported an oligomer from iterative coupling of chiral BINOL diacid and 2,6-diaminopyridine which gave rise to a chiral helix even though the intramolecular stacking is relatively weak due to herring bone conformation of BINOL moiety (Fig 1.12).[54]

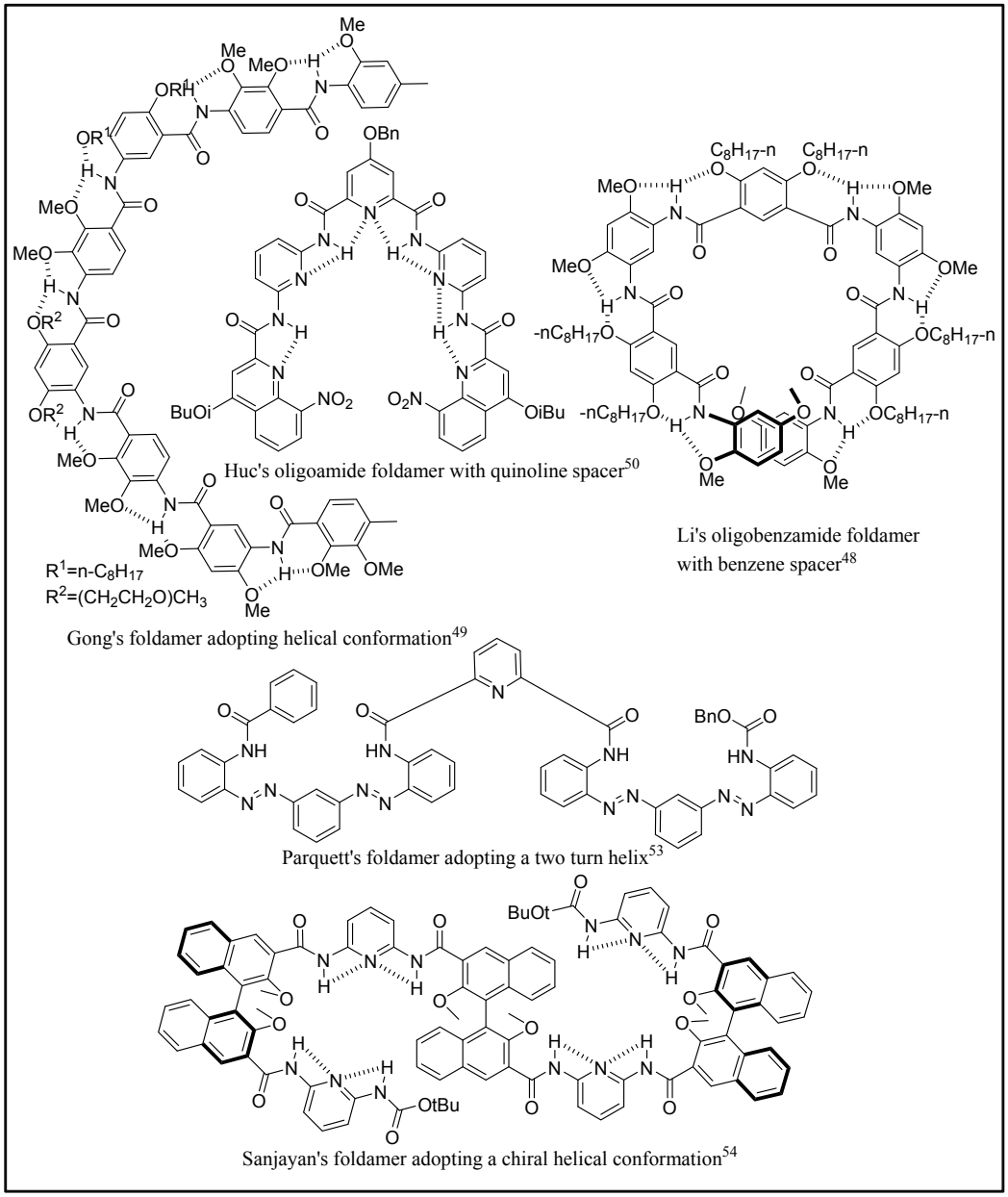

Fig 1.12: Aromatic foldamers adopting folded conformation.

1.4.3 Binding-induced folding

Jeong *et. al.* reported a new class of foldamers comprising oligoindoles that adopt a helical architecture stabilized by hydrogen bonding interactions with chlorine atom. This was confirmed by the solution state 2D NMR studies which clearly revealed the diagnostic stacking of the indole rings. The absence of chloride ion couldn't show the diagnostic nOe interactions which supports the induced folding pattern of the oligomer.[55] The same group reported oligomers comprised of indolocarbazole building blocks that possess extended π-surfaces relative to the corresponding biindole-based subunits. The sulphate ion complex of the respective indolocarbazole oligomer was formed by a total of eight hydrogen bonds, each oxygen of sulphate ion forming two hydrogen bonds which was clearly found in the crystal structures of the compounds shown in Fig 1.13 (A and B).[56] Gale *et.al.* reported, fluorine-directed assembly of isophthalamide cleft into a double helix. Single crystal X-ray diffraction analysis of the foldamer revealed a helical wrapping of oligomer around the two F^- ions which were held by two N-H…F^- hydrogen bonds, although the helical complex was stabilised by the π-π interactions between the terminal nitro aromatic arms of the cleft (Fig 1.13 C).[57] Zhao, Li and co-workers reported that alternating naphthalene and benzene-linked oligomers adopted a helical conformation on binding to benzene 1,3,5 tricarboxylate anion in solution state. *meta*-Substituted benzamides were also shown to adopt helical conformation upon binding with mono, di and tri carboxylate anions into a helical conformation *via* 1:1 ratio complexation. Hydrogen bonding complementarity towards the tricarboxylate anion in these examples was imperative for the helicity observed.[58]

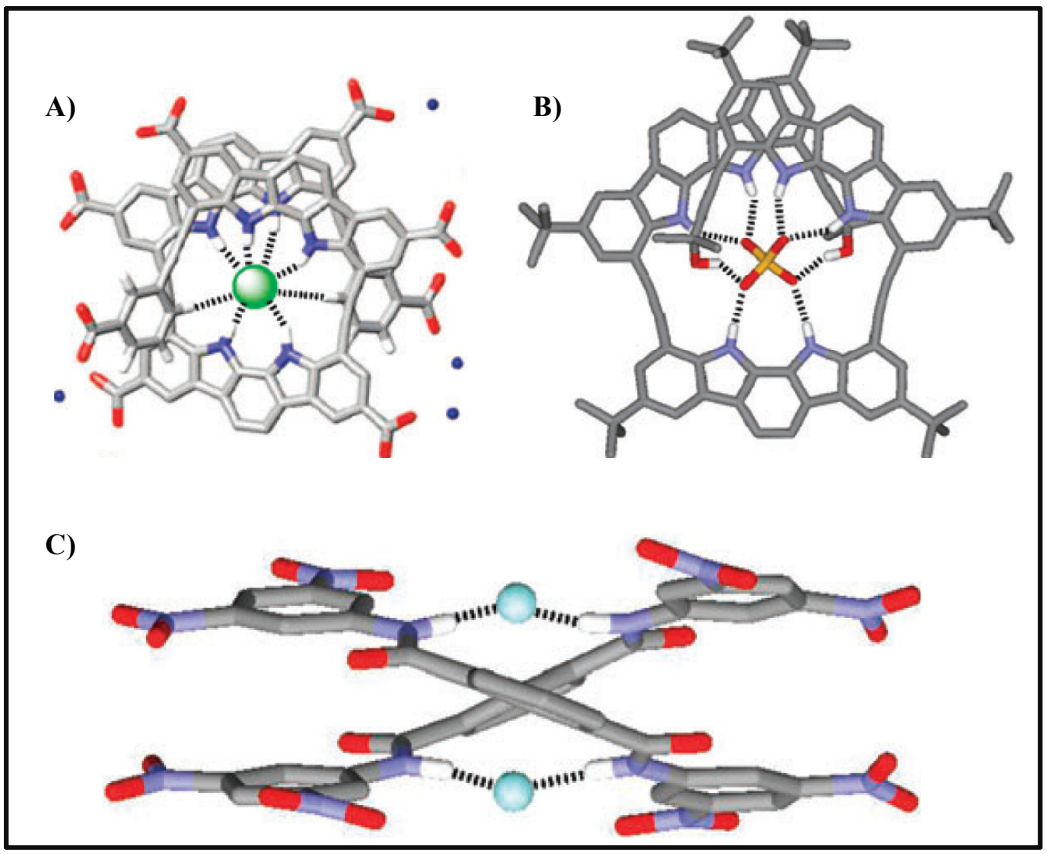

Fig 1.13: Crystal structures of A) oligoindoles forming a helix in presence of Cl^- ions.[55] B) oligoindolocarbazoles adopting a helical conformation using $SO4^{-2}$ ions.[56] C) helical wrapping of isophthalamide foldamer in the presence of F^- ions.[57]

1.4.4 Folding based on solvophobic effects

Hydrophobic effect plays a vital role in a variety of processes such as membrane formation, protein folding, protein-protein interactions, ligand receptor binding, drug formulation and several other processes where non-polar groups interact with water in biological systems. This concept can be extended to create mesoscopic foldamers with folding motifs resembling the natural ones as shown in Fig 1.14. In this regard, a report from Moore's group showed that *meta*-phenylacetylene oligomer favors a compact helical conformation in polar solvents such as acetonitrile. On the contrary, it exhibits a random coil conformation in chloroform.[59] Iverson *et.al* reported a class of foldamers which are termed as *aedamers* (named for *a*romatic *e*lectron *d*onor-*a*cceptor folda*mer*), comprised of electron rich 1,5 dialkoxynaphthalene (Dan) and electron deficient 1,4,5,8 naphthalenetetracarboxylicacid diimide (Ndi) building blocks. In this case,

Dan:Ndi complexation was observed to be favourable compared to Dan:Dan or Ndi:Ndi self association in water.[60]

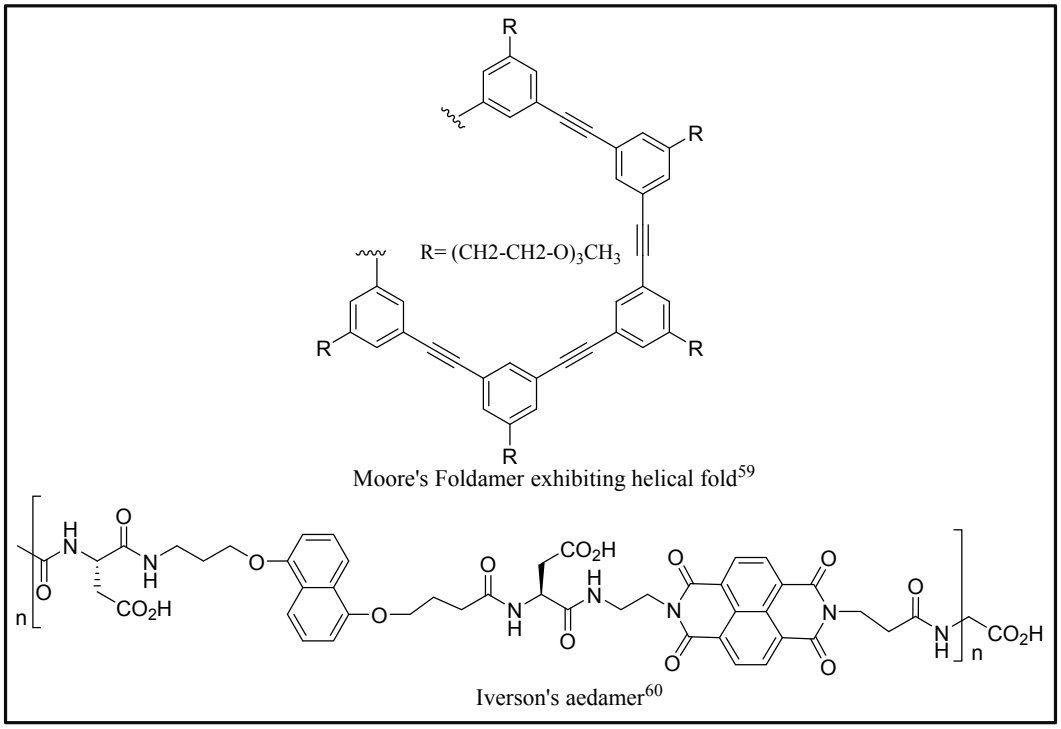

Fig 1.14: Synthetic oligomers adopting folded conformation due to solvophobic effects.

1.4.5 Effect of π-π stacking and C-H….O interaction on folding

π-π stacking interactions, being non-directional, are often considered to be the complementary interactions in stabilizing the secondary structures of the foldamer molecules. These interactions reported in a foldamer consisting of naphthalene diimides (Ndi) and porphyrin subunits form S-shaped folded architecture. *meta* phenylene oligomers with an inserted pyridine ring adopt a stable folded conformation making use of the π-π stacking interactions (Fig 1.15 A).[61]

C-H…O interactions are considered to be weaker interactions compared to that of N-H…O and O-H…O interactions. But, there are instances where they do play a major role in adopting a conformational bias. Balaram *et. al.* reported a decapeptide: Boc-Leu-Aib-Val-Ala-Leu-Aib-^{D}Ala-^{D}Leu-Aib-OMe which gets stabilized using an unusual C-H…O interaction at the C-terminus leading to the polypeptide chain reversal (Fig 1.15 B).[62]

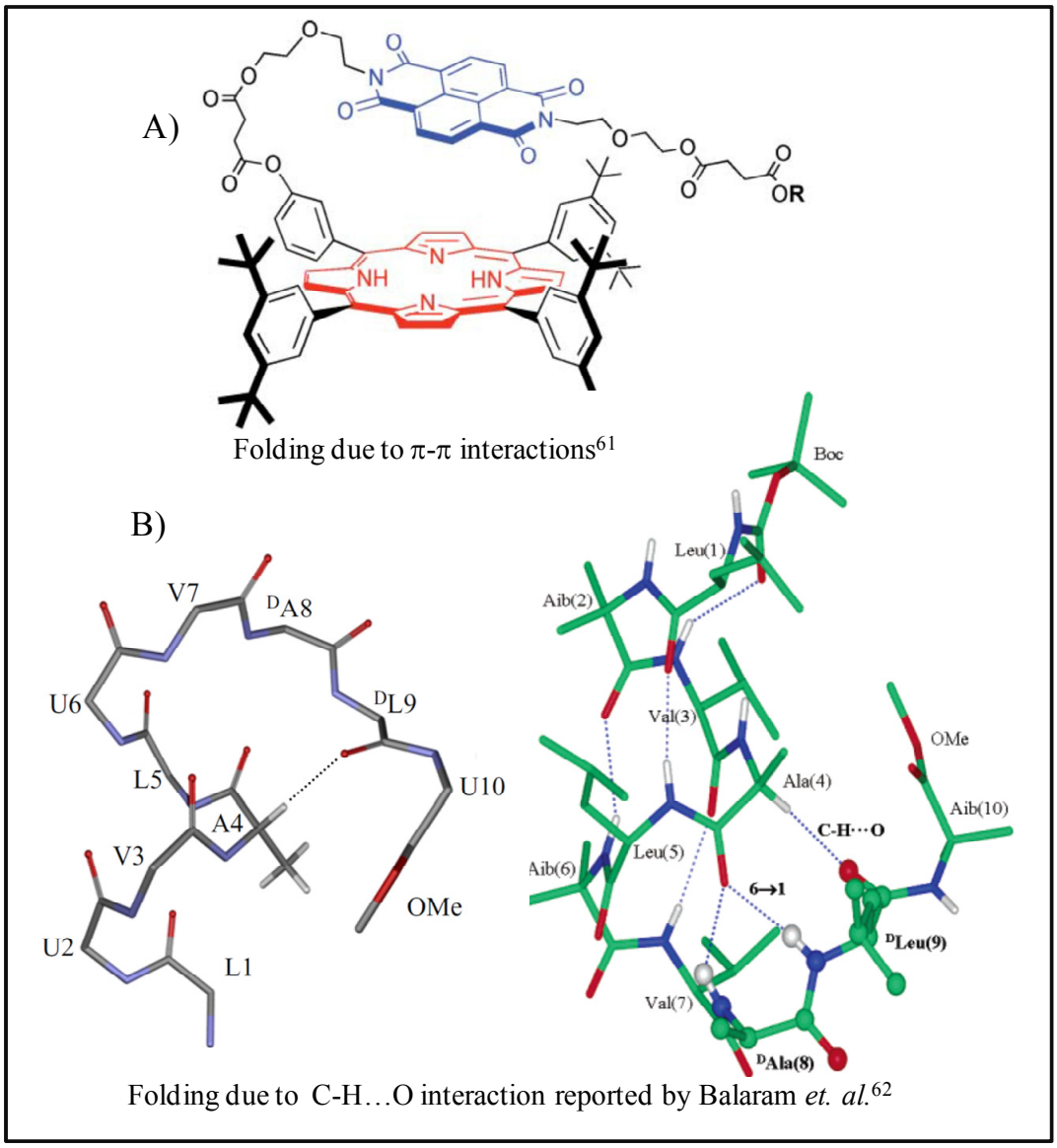

Fig 1.15: Peptide oligomers adopting folds due to A) π-π interactions,[61] and B) C-H…O interactions.[62]

1.4.6 Folding devoid of inter-residual hydrogen bonds

There are few classes of oligomers which adopt stable helical conformations without any inter-residual hydrogen bonds owing to the rigidity of the individual building blocks employed in the construction. Polyprolines, peptoids, oligoprolines, oxazolidines, diketopiperazines[63] and tertiary amide building blocks fall into this category which relies on their backbone rigidity to stabilize the helical conformation. Generally, the helices obtained from α or β-amino acids feature inter-residual hydrogen bonding, also C=O…H-N is needed

for the oligomer to get folded. Intuitively, conversion of the secondary amide nitrogen to tertiary alkyl amide, would destroy the secondary structure since it lacks the hydrogen bonding donor.

Polyprolines, naturally existing oligomers, are one of such examples that adopt a helical conformation despite of the fact that proline is a seconadary amine and its oligomers are tertiary amides which cannot participate in intramolecular hydrogen bonding (Fig 1.16). For α-helices, the φ and ψ values lie between -63^0 and -42^0 in the Ramachandran plot. However, for the left handed popyproline helix type II where all the amides are *trans* φ and ψ values lie near to -75^0 and 145^0. For polyproline helix type I where the amide bonds are *cis* φ and ψ values lie near to -70^0 and 160^0 . The triple helix architecture of collagen contains three polyproline type II helices interwined together.[64] The reason why polyproline helices are stable, being devoid of intramolecular hydrogen bonding is still ambiguous.

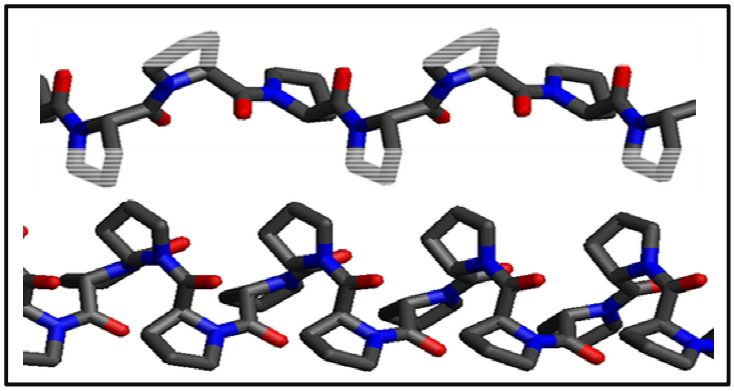

Fig 1.16: Polyproline helices type II (top) and type I (bottom).

Peptoids, N-substituted glycine derivatives have similar features as that of polyproline helices. Peptoid oligomers adopt a helical conformation based on the preferences of side-chain-backbone steric repulsions and dipole-dipole repulsions between main chain amide carbonyl electrons. Their backbone is achiral in nature and the chirality to the secondary structure can be induced by the side chains alone. These peptoid oligomers have proved their applications as antimicrobial agents, as lung surfactant mimic, amylin mimics, protein-protein interaction inhibitors etc. Appella *et.al* and Kodadek *et.al* reported peptoid oligomers that act as protein-protein interation inhibitors.[65] Recently, Blackwell *et.al* reported a

robust peptoid helix generated *via* the incorporation of α-chiral aromatic N-1-naphthylethyl side chains.[66]

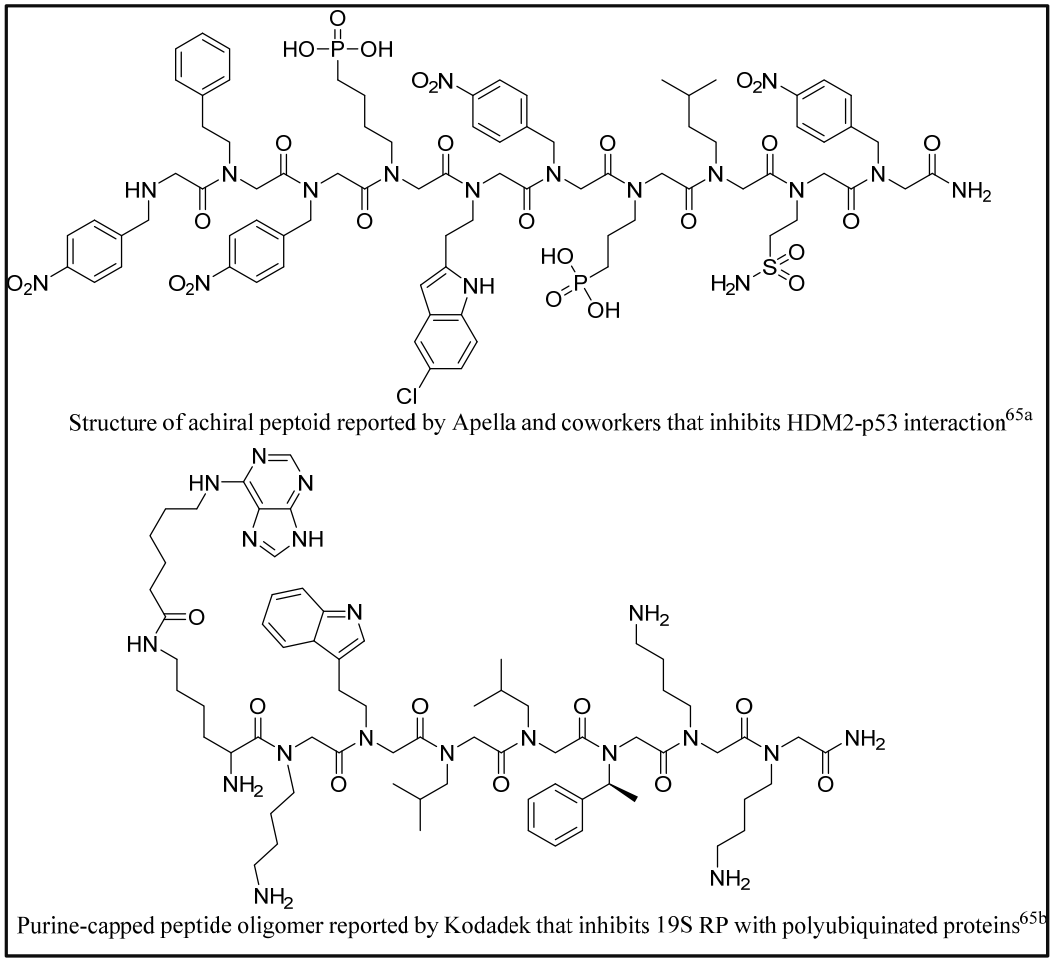

Fig 1.17: Peptoid oligomers that exhibit biological activity.[65]

Tertiary aromatic amide oligomers are another class of foldamers which exhibit bent conformation without any inter-residual hydrogen bonding. This bent conformation is attributed to the preferred *cis* conformation of the tertiary amides of aromatic acids and aliphatic secondary amines.[67]

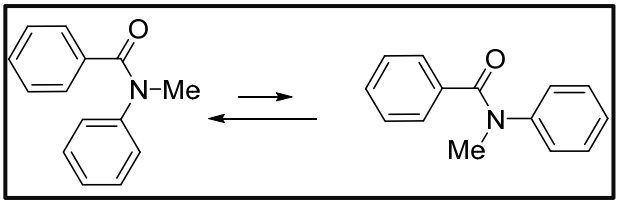

Fig 1.18: *cis-trans* equilibrium of aliphatic aromatic amides.

Oxazolidine (Oxd) oligomers are a class of foldamers that adopt helical conformation stabilized by intramolecular C-H…O=C hydrogen bonds. Homo oligomers of (4S, 5R)-5-methyl-2-oxo-1, 3-oxazolidine-4-carboxylate adopt a helical conformation. Tomasini *et.al.* reported Gly-L-Oxd oligomers where they observed that the conformationally free Gly residue reduced the folding bias of the oligomer. Thus, they extended their work by incorporating L-Ala and Aib residues in combination with D-oxd. The crystal structure analysis of the oligomers clearly revealed the β-bent spiral ribbon conformation attributed to the rigid oxazolidine moiety that often tends to remain in *trans* conformation. It comprised of C=O…H-$^{\alpha}$C and 1 ← 4 C=O…H-N intramolecular hydrogen bonding interactions on the back bone (Fig 1.19 A and B).[68]

A report from Gellman's group showed that the oligomers constructed from 2, 2-disubstituted-pyrrolidine-4-carboxylic acid adopted characteristic secondary structure. This feature of the oligomers was supported by CD studies and *ab-initio* molecular modeling studies as well (Fig 1.19 C).[69] Recently, Alezra *et. al.* reported small α/γ foldamer with alternating α, α disubstituted isobutyric acid and cyclic γ-amino acid residues that are able to adopt an extended structure in solution which was supported by molecular modeling studies (Fig 1.19 D). These oligomers also exhibited the secondary structural features without making use of any inter-residual hydrogen bonds.[70]

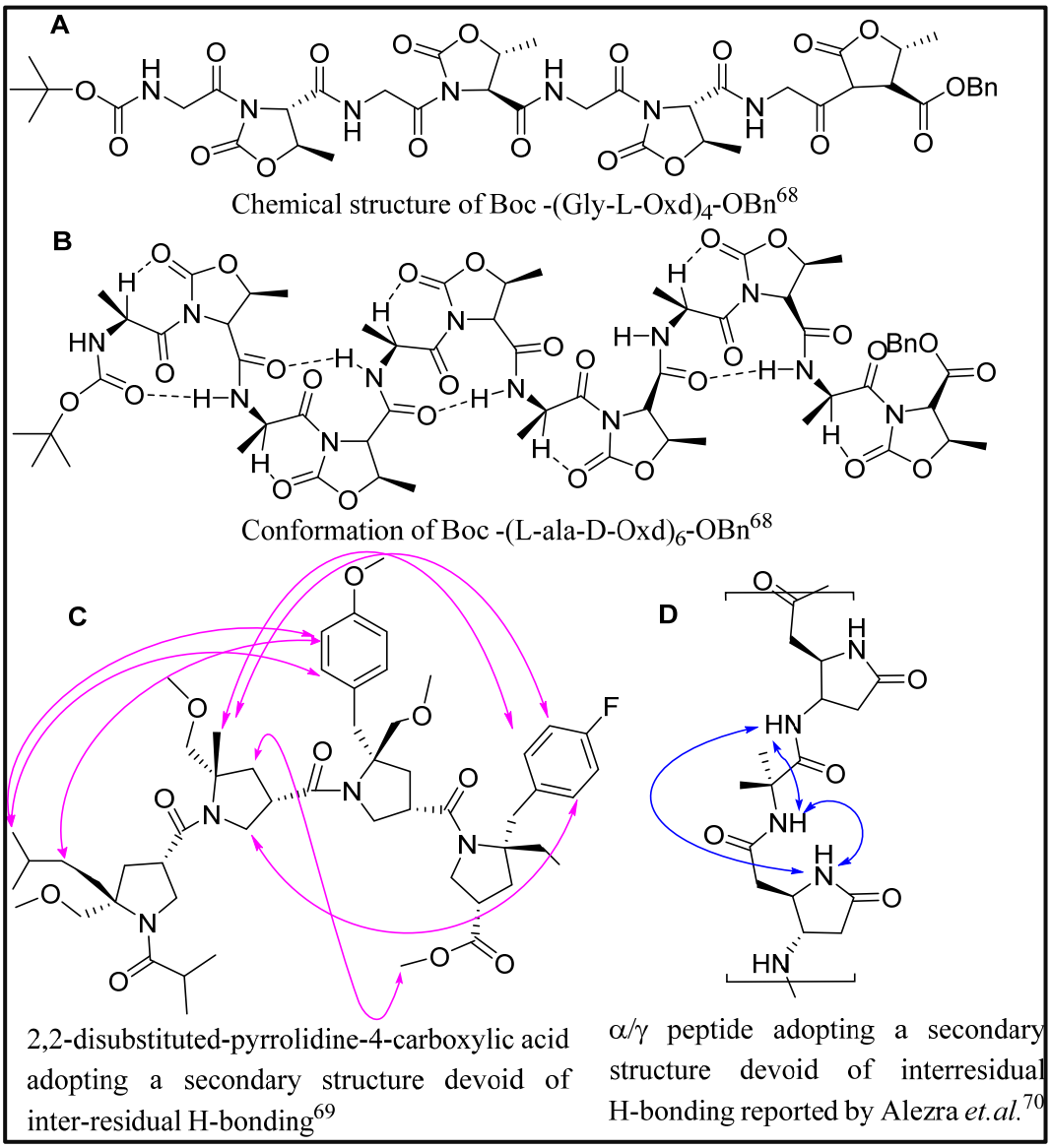

Fig 1.19: Foldamers that exist in folded conformations devoid of inter-residual hydrogen bonding pattern. The strong nOe signals obtained in 2D NMR are shown through arrows.

1.5 Applications of Heterogeneous Foldamers

Relatively, the design of foldamers is quiet straightforward and uncomplicated to conceptualize, mimicking the naturally occurring peptide sequences. Employing repetitive sequences of a combination of building blocks would generate synthetic peptide of a desired conformational feature. Thus, tailoring the hydrophobic or polar amino acids with β-amino acids (giving rise to heterogeneous foldamers), which are known to be stable structurally and

biologically would aid in developing sequences of specific utility. Due to the dynamic nature of the foldamer molecules, they are well suited to execute various applications in variety of mechanisms. Few such applications have been discussed under appropriate headings below.

1.5.1 Biomedical applications

Several foldamers were developed as inhibitors of protein-protein interactions. Degrado's group pioneered the application of aromatic amide foldamers as antimicrobial agents.[71] Gellman's group developed certain foldamers comprising of nine α/β subunits that can bind to anti-apoptotic proteins such as Bcl-x_L in nanomolar range.[72] Recently, Huc and coworkers designed a foldamer to investigate the interactions of longer foldamer sequences with DNA by attaching biotin to oligomer cationic quinoline helix of over three turns. They identified DNA aptamers that have strong affinity for the designed foldamer and establish a specific interaction between multi-turn quinoline helices and G-quadruplex DNA.[73]

1.5.2 Molecular recognition

Foldamers are proven to be ideal receptors when there exists a driving force for binding a guest molecule. The length of the foldamer molecules can be easily tuned and side-chains can be modified readily with discrete functionalities. This criterion was employed to the maximum extent in the design strategy of oligomers to find applications as molecular receptors. Li and coworkers utilized the foldamer backbones to develop tweezer receptors. A foldamer derived bis-porphyrin was found to complex C_{60} and C_{70} derivatives. This concept was further extended to design a huge foldamer with six appended zinc porphyrin rings having C60 molecules in a domino pattern resulting in a propeller-shaped structure of the 1:6 complex molecule.[74] Huc *et. al.* developed a quinoline foldamer with pyridine-pyridazine-pyridine segment at the centre which forces the quinoline helical segment to orient in a fashion that substantially increases the helical diameter and enables to entrap tartaric acid molecule in solution as well as solid state.[75] Lehn and coworkers reported a helical foldamer that can complex a cyanurate in chloroform in 1:2 ratio through six intermolecular hydrogen bonds.[76]

1.5.3 Heterogeneous foldamers as catalysts

The application of foldamers as catalysts is relatively new concept. Recently, Gellman and Hilvert research groups reported the utility of a foldamer as catalyst in retro-aldol reaction wherein the lysine side chains of the corresponding building block were of major utility.[77] Smith *et. al* reported the application of thio urea as a catalyst which comprises of a heterogeneous backbone with β-turn like structure, in Mukaiyama-Mannich reaction resulting in high enantioselectivity.[78]

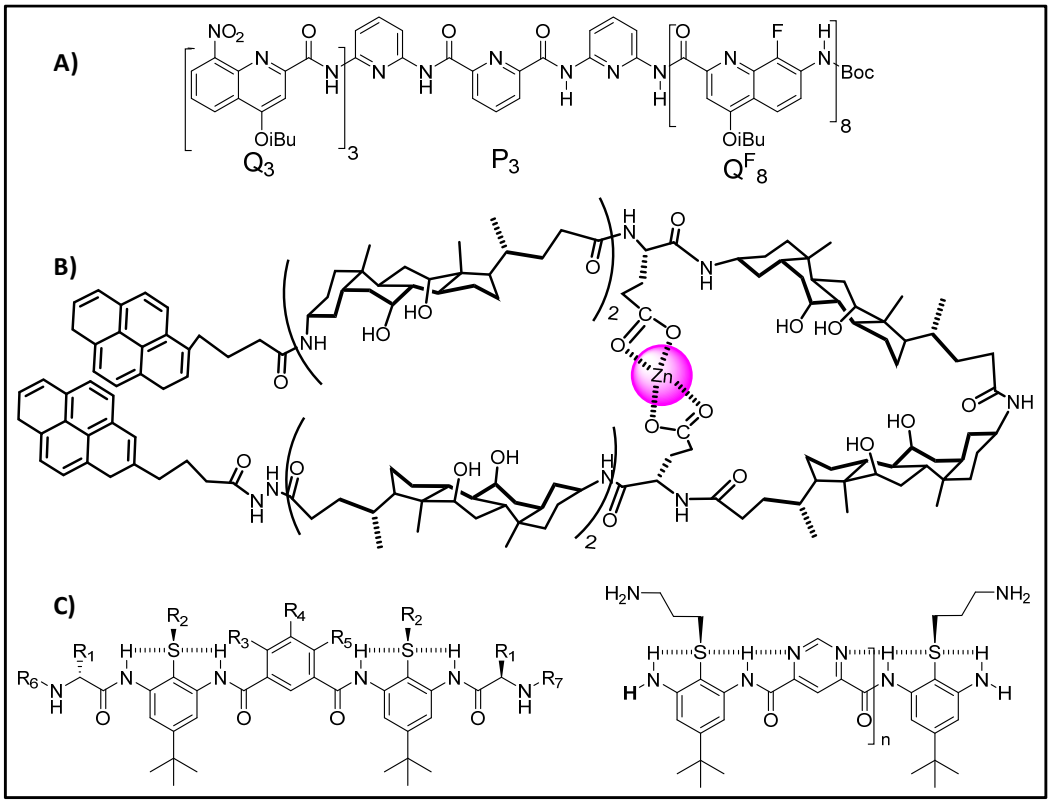

Fig 1.20: A) Huc's aromatic foldamer encapsulating 1,10 decanediol.[75b] B) A cholate-glutamic acid hybrid foldamer as a sensor for Zn ions.[79] C) Degrado's antibacterial foldamer (left)[71a] and antibacterial foldamer reported by Tew's group (right).[71b]

1.6 Objective and Design strategy

The basic endeavour of this work was the design, synthesis and investigation of the conformational features of the helical architectures achieved based on diverse non-covalent interactions that include steric effects and hydrogen bonding preferences. In an earlier study from our laboratory, Pro-Ant oligomers were shown to adopt right-handed helical conformation featuring 9-membered hydrogen bonding repeats. The robust feature of this class of oligomers was studied by modulating the chirality of the amino acids both at the N- and C-termini of the Ant-Pro (turn segment) dipeptide building block.[80] Further, modifications were attempted by incorporating a sulfonamide group by replacing the carboxamide group which additionally supported the unique feature of the oligomeric sequence.[81]

Extending our studies to investigate this structural feature, in the present study described here, we undertook investigation of the role of steric effects in the structural bias observed in case of Pro-Ant, by substituting the aromatic six-membered ring β-amino acid Ant (anthranilic acid) with aromatic five-membered ring β-amino acids, 2-Atc and 3-Atc (2- amino thiophene carboxylic acid and 3-amino thiophene carboxylic acid, respectively) which are structural isomers as novel building blocks to achieve isosteric replacement on the oligomeric backbones. The oligomers featuring, isosteric replacement on the backbone were designed in such a way that, in the Pro-2Atc sequence, steric effect would be offered by a carbon atom while in Pro-3Atc sequence, the steric effect would be offered by a hetero atom i.e., sulphur atom. Our basic objective was to study whether this isosteric replacement would retain the C9 turn as observed in case of Pro-Ant oligomers or would lead to some novel conformational preference in the resulting oligomeris (Fig 1.21).

Oligomeric sequences upto octamers were designed with respect to both Pro-2Atc and Pro-3Atc building blocks starting from dipeptide building blocks in each of the cases (Fig 1.22) to study and investigate the conformational preferences and the role of steric effect on the helical conformation of the peptides.

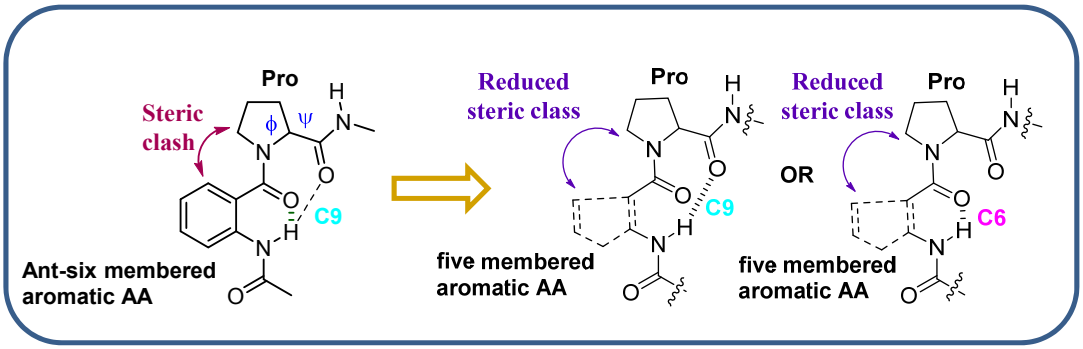

Fig 1.21: Design strategy employed in constructing the oligomers mentioned in the present study.

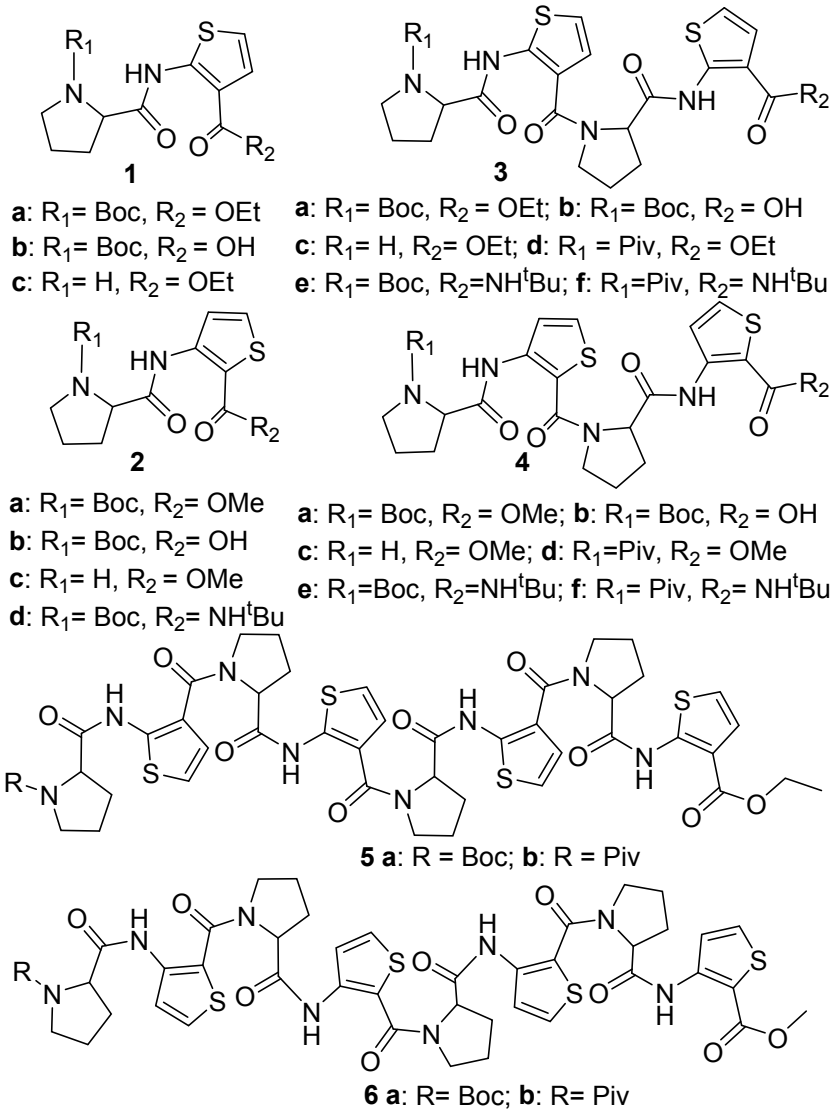

Fig 1.22: Structures of the oligomers designed to study the role of steric effect in the present study.

1.7 Synthesis

Heterogeneous α/β-hybrid oligomers featuring proline (Pro) and amino thiophene carboxylic acid (2-Atc and 3-Atc) building blocks were synthesised using the strategies mentioned in scheme 1.1 and scheme 1.2. The dipeptide building blocks **1** and **2** were synthesised using mixed anhydride method. Further, the tetra peptides **3** and **4** were synthesised employing the segment doubling strategy by coupling the acids **1b**, **2b** with the amines **1c**, **2c,** respectively, following standard conditions. Similarly, the octapeptides **5** and **6** were achieved by coupling the acids **3b** and **4b** with the amines **3c** and **4c** using EDC.HCl and HBTU as coupling agents, respectively.

1.7.1 Synthesis of oligomers 3 and 5

Scheme 1.1

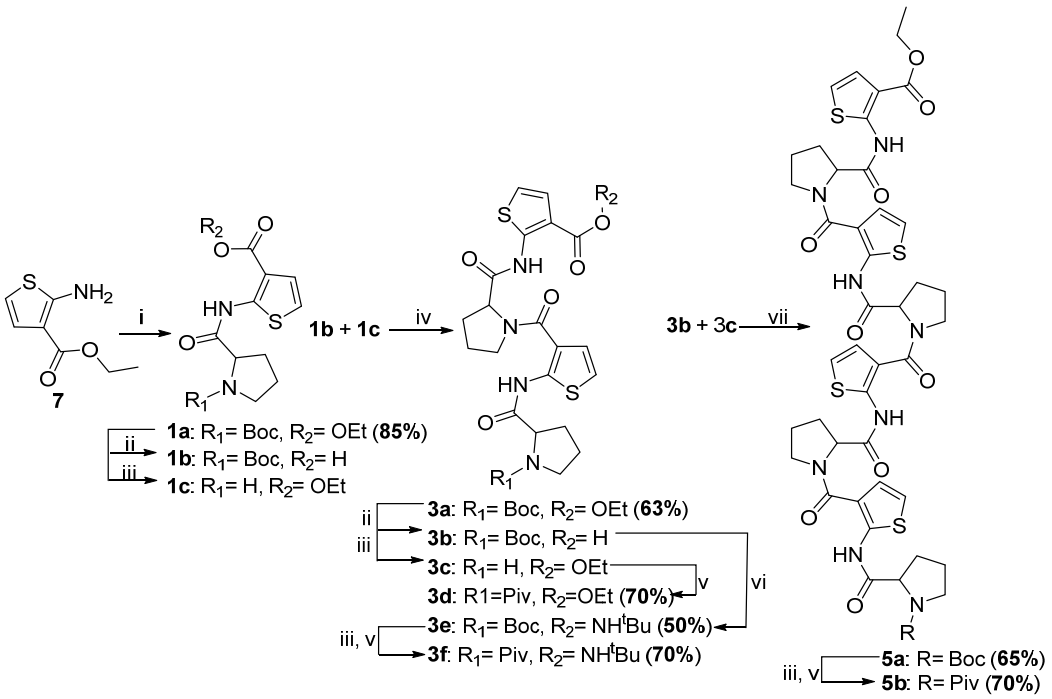

Scheme 1.1: Reagents and conditions: (i) Boc ^{L}Pro-OH, ethyl chloroformate, Et_3N, THF, 80 °C, 48 h; (ii) aq. LiOH, MeOH, rt, 4 h; (iii) TFA:DCM (1:1), rt, 2 h; (iv) DCC, HOBt, Et_3N, DCM, rt, 12 h; (v) Piv-Cl, Et_3N, DCM, rt, 4 h; (vi) $^{t}BuNH_2$, Et_3N, EDC.HCl, CH_3CN; (vii) HBTU, HOBt, Et_3N, CH_3CN, rt, 12 h.

1.7.2 Synthesis of oligomers 4 and 6

Scheme 1.2

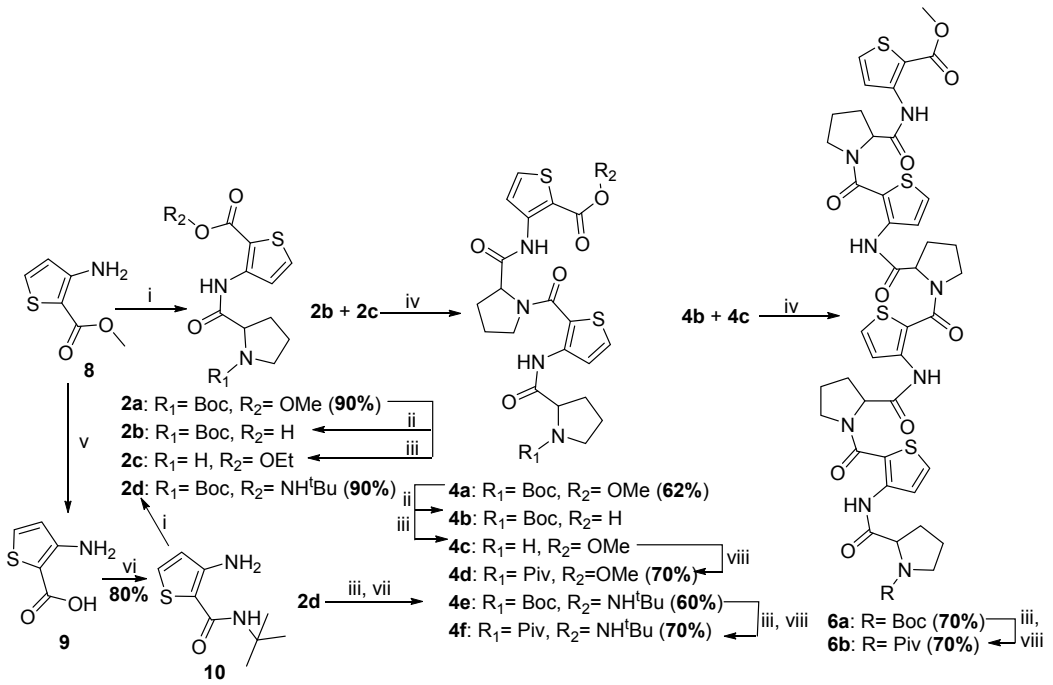

Scheme 1.2: Reagents and conditions: (i) Boc ^{L}Pro-OH, ethyl chloroformate, Et_3N, DCM, 80 °C, 48 h; (ii) aq. LiOH, MeOH, rt, 4h; (iii) TFA:DCM (1:1), rt, 2 h; (iv) DCC, HOBt, Et_3N, DCM, rt, 12 h; (v) 2N NaOH, 60 °C, 5 h; (vi) $^{t}BuNH_2$, EDC.HCl, Et_3N, CH_3CN, rt, 12 h; (vii) **2b**, DCC, HOBt, Et_3N, DCM, rt, 12 h; (viii) Piv-Cl, Et_3N, DCM, rt, 4 h.

The N-terminus pivolyl analogues **3d**, **3f**, **4d**, **4f**, **5b**, **6b** were synthesized to arrest the rotameric conformers formed because of the N-terminus ^{t}Boc group attached to the Pro residue of the respective oligomers in a single conformation.[82] Later, the C-terminus amide analogues **3e** and **10** were also synthesized using the conditions mentioned above. The synthesis of **4e** was not straight forward as that was observed for **3e**. It was obtained by coupling of **3b** with $^{t}BuNH_2$ using EDC.HCl as coupling agent. The oligomer **4e** was synthesized starting from compound **10** which was prepared by coupling $^{t}BuNH_2$ with the amino acid **9**.

1.8 Conformational studies

The conformational features of the synthesized sequences were established by the solid state single crystal X-ray diffraction studies as well as extensive solution state 2D NMR experiments in case of the tetrapeptides. In case of

octapeptides, as all the efforts for crystallization went in vain, *ab-initio* molecular modeling studies were taken up to establish the conformations.

1.8.1 Single crystal X-ray diffraction studies

Intense efforts to crystallize the oligomers resulted in the crystals of **1a**, **2b**, **3a**, **4b** and **4f** (Fig 1.22).[83] The crystal structures clearly confirm that the five membered ring β-aromatic acids 2-Atc and 3-Atc clearly maintain the intra-residual six membered ring hydrogen bonding (d_{av} N-H…O 2.07Å and d_{av} N-O 2.71 Å) regardless of whether they are proceeded or succeeded by proline residue.

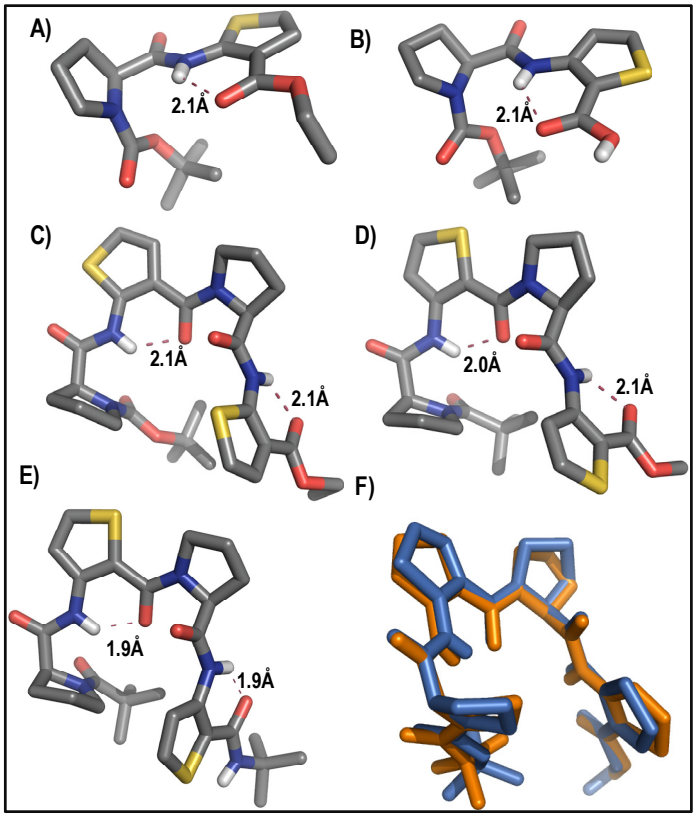

Fig 1.22: Crystal structures of the compounds **1a** (A), **2b** (B), **3a** (C), **4d** (D), **4f** (E). Overlay of the crystal structures **3a**, **4d** (F). All hydrogens, except the polar ones have been deleted for clarity.

It is evident from the solid state crystal structures of **3a**, **4d**, **4f** that these oligomers exist in a folded conformation. The excellent resemblance of both the oligomers **3a** and **4d** is evident from their overlaid crystal structures (RMSD=0.133) (Fig 1.22 F). It is also noteworthy that the C-terminus amidation as seen in **4f** (Fig 1.22 E) features exactly the similar backbone conformation compared to that of its ester analogue **4d** (Fig 1.22 D), suggesting that the

backbone is robust and insensitive to structural perturbations either it may be the isosteric replacement on the back bone or by altering the hydrogen bond code at the C-terminus.

1.8.1.1 Effect of isosteric replacement on the backbone

A close observation of the crystal structures of **3a** and **4d** revealed that in the central dipeptide segment, the Pro residue succeeded by 2-Atc and 3-Atc, respectively maintains nearly a *coplanar* arrangement although the terminal dipeptide segments maintain anti-periplanar arrangement. This structural feature endowed the peptides **3a** and **4d** a characteristic folded conformation whose backbones are almost similar.

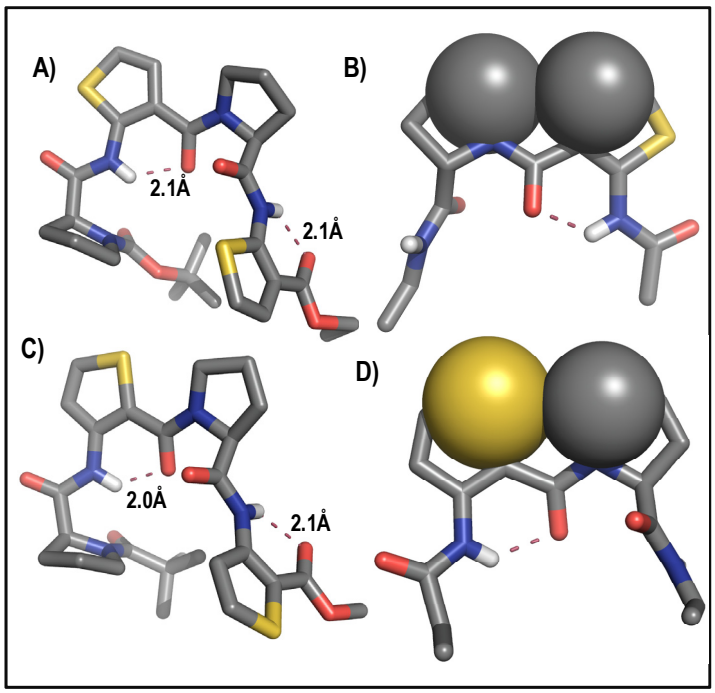

Fig 1.23: Crystal structures of compounds **3a** (A) and **4d** (C) respectively. Comparison of isosteric dipeptide segments of **3a** (B) and **4d** (D). All hydrogens except the polar ones have been deleted for clarity.

It is noteworthy that the oligomers **3a** and **4d** possess close similarity in the folded conformation attained, although they possess regio-isomeric isosteres as building blocks. While **4d** endows a sulfur atom (van der Waal's radii: 1.8Å) on the five membered aromatic ring in closer vicinity to the preceding Pro residue (Fig 1.23 B), its region-isomer **3a** has an isosteric carbon atom (van der Waal's radii: 1.7Å) at a similar position (Fig 1.23 D). This explains their closer

conformational resemblance, which also implies that isosteric replacements do not affect, by and large the backbone conformation.

1.8.2 NMR Studies

In an effort to gain insight into the conformational features of the oligomers in the solution state, NMR studies were undertaken - the results of which suggested the characteristic folding observed in the solid state conformation prevails in the solution state as well. All oligomers were readily soluble in all the non-polar organic solvents (>> 100 mmol in $CDCl_3$) at ambient temperature suggesting that the polar hydrogen bonding groups are strongly solvent shielded, preventing the formation of polymeric aggregates.[84] The oligomers **3d** and **4d** exhibited sharp well dispersed signals rendering their conformational analysis easy though **5a** and **6a** showed considerable signal overlapping presumably owing to the repetitive residues with which the oligomers are made of. The signal assignment was done unambiguously employing the 2-dimensional NMR experiments. Analysis of the crystal structures of **3a** and **4d** suggest that the most characteristic nOes to support a folded solution state conformation. As seen in the crystal structures, the diagnostic long range inter-residual coupling would be between the termini since they would be in close proximity when fully folded. Some of the characteristic nOes are the ones observed between the far distant groups such as Piv *vs* 2-Atc in **3d** and Piv *vs* 3-Atc in **4d**, in addition to several other inter-residual nOes.

The characteristic nOes observed in the case of **3d** are clearly represented with arrows in Fig 1.24. The long range inter-residual dipolar couplings observed in case of **3d** are: NH1 *vs* C2H and C5H; NH2 *vs* C12H, C14H and C15H; NH2 *vs* C22H; tBu *vs* C19H; C9H *vs* C12H. Similarly, the characteristic nOes observed in case of **4d** are represented by arrows as shown in Fig 1.25. The long range inter-residual dipolar couplings evident from the solution-state NMR studies are: tBu *vs* NH1, NH2 and C15H; NH1 *vs* C3H and C15H; NH2 *vs* C15H. This strongly supports the prevalence of a similar folded conformation in solution state, as that observed in the solid state.

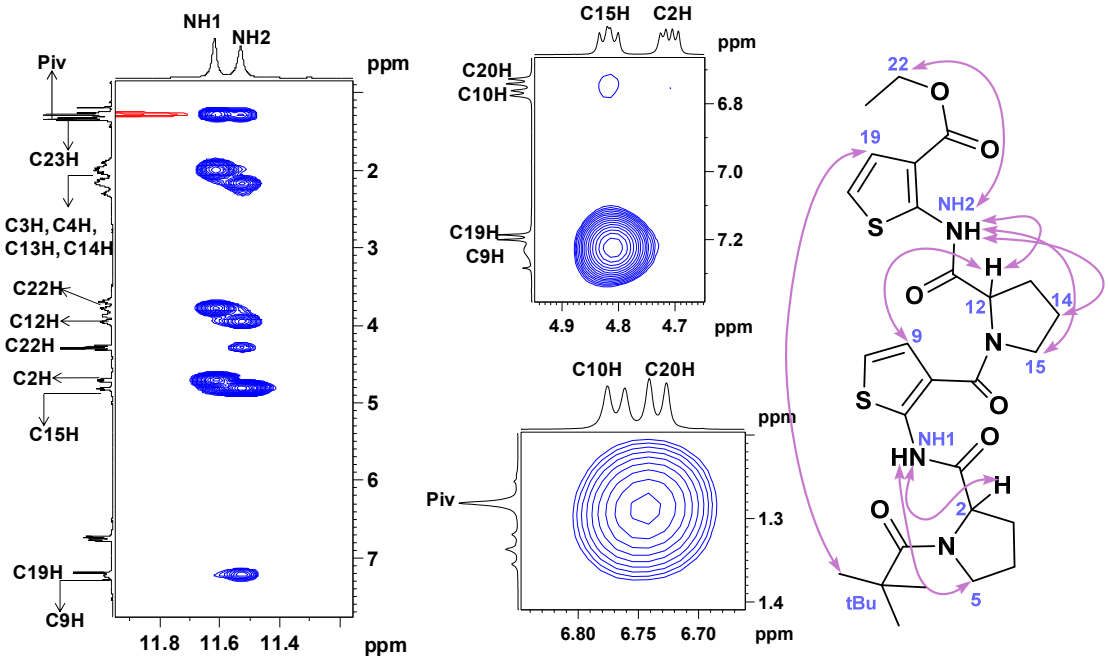

Fig 1.24: Selected 2D excerpts of **3d** (left). Selected 2D NOESY excerpts of **3d** (right).

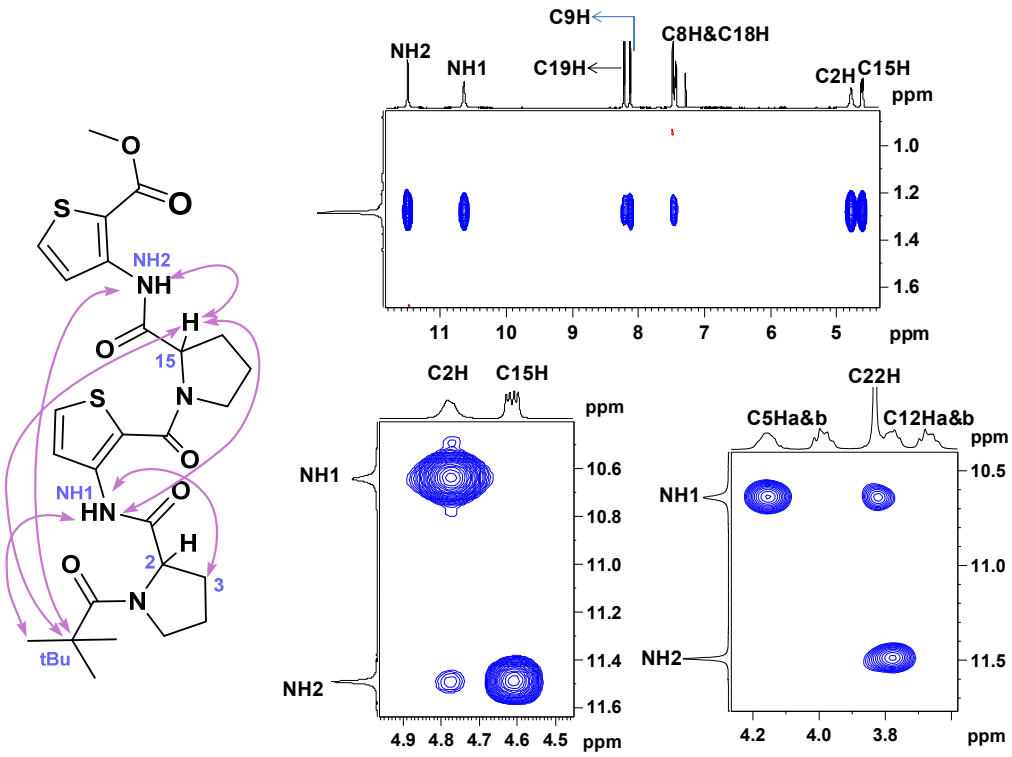

Fig 1.25: Structure of **4d** (left). Selected 2D NOESY excerpts of **4d** (right).

The involvement of strong intra-residual six membered ring hydrogen bonding was also substantiated by DMSO-d_6 titration studies (Fig 1.26) of **3f**, **4f**, **5a**, **5b**, **6a**, **6b** oligomers ($\Delta\delta$ (NH) = 0.32 ppm) and variable temperature studies of **3f**, **5b**, **6b** (Fig 1.27) and **5a**, **6a** (Fig 1.28) (263-323 °K; $\Delta\delta/\Delta T$ < -2 ppb K^{-1}).

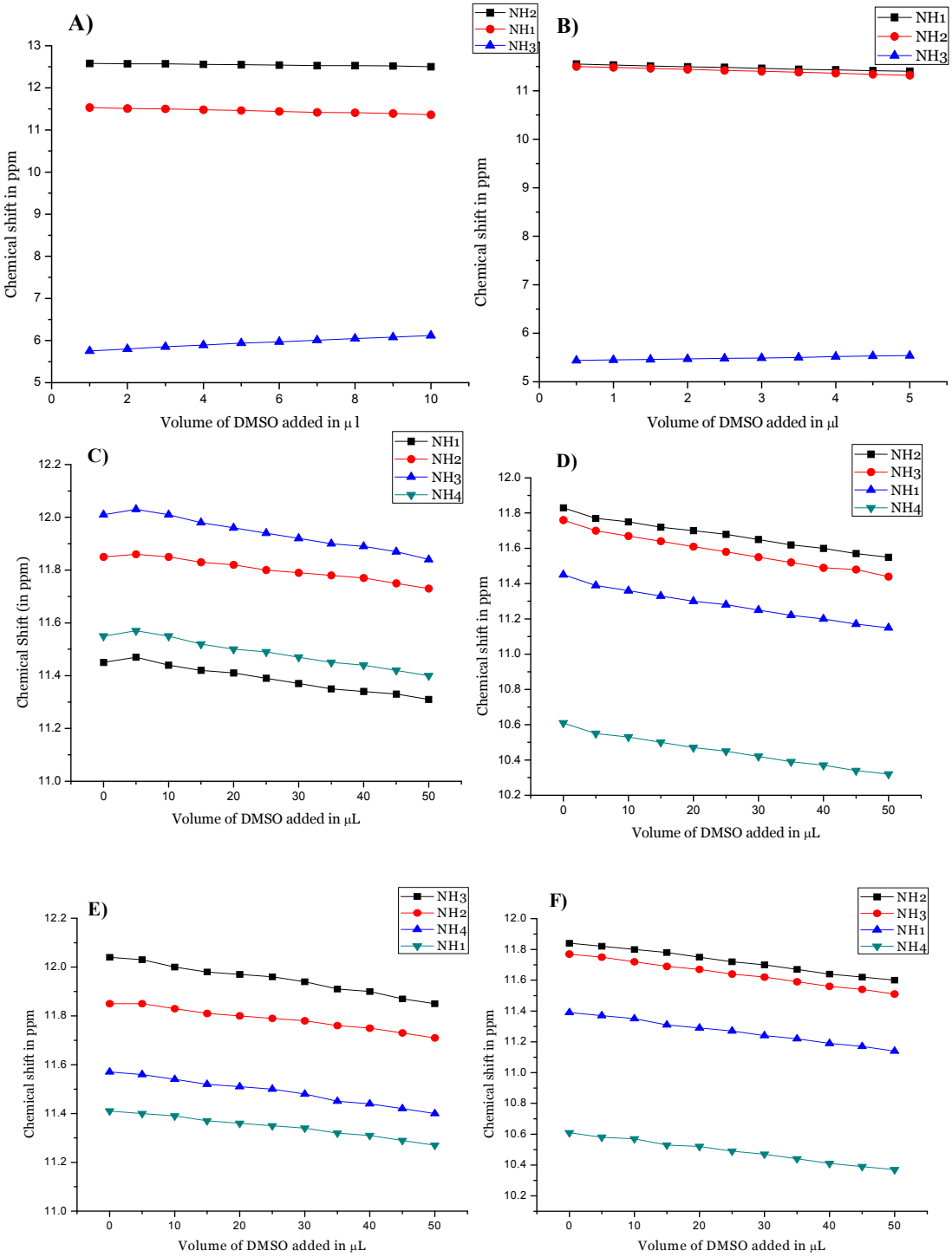

Fig 1.26: Plots representing DMSO-d_6 titration study of **3f** (A), **4f** (B), **5a** (C), **6a** (D), **5b** (E) and **6b** (F).

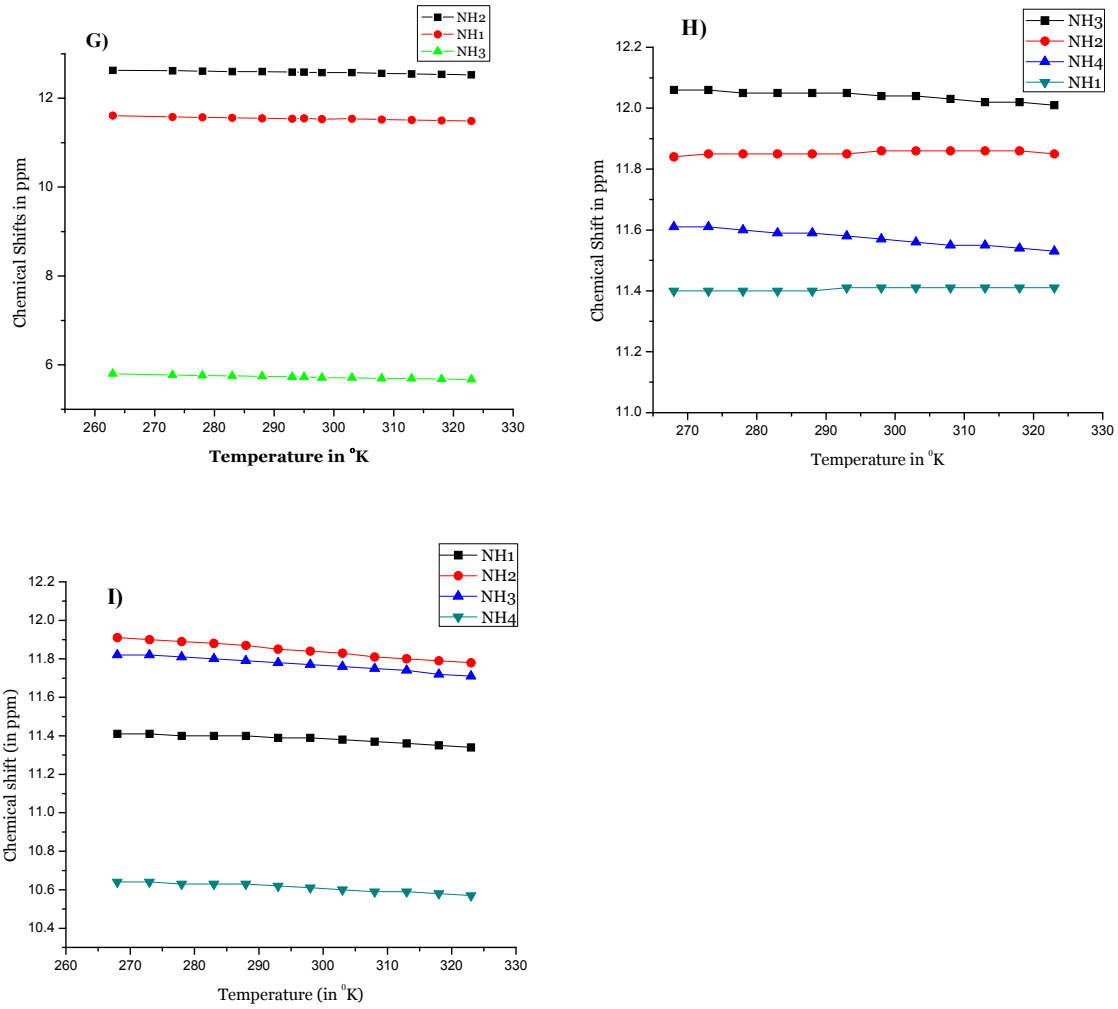

Fig 1.27: Plots representing variable temperature study of **3f** (G), **5b** (H), and **6b** (I).

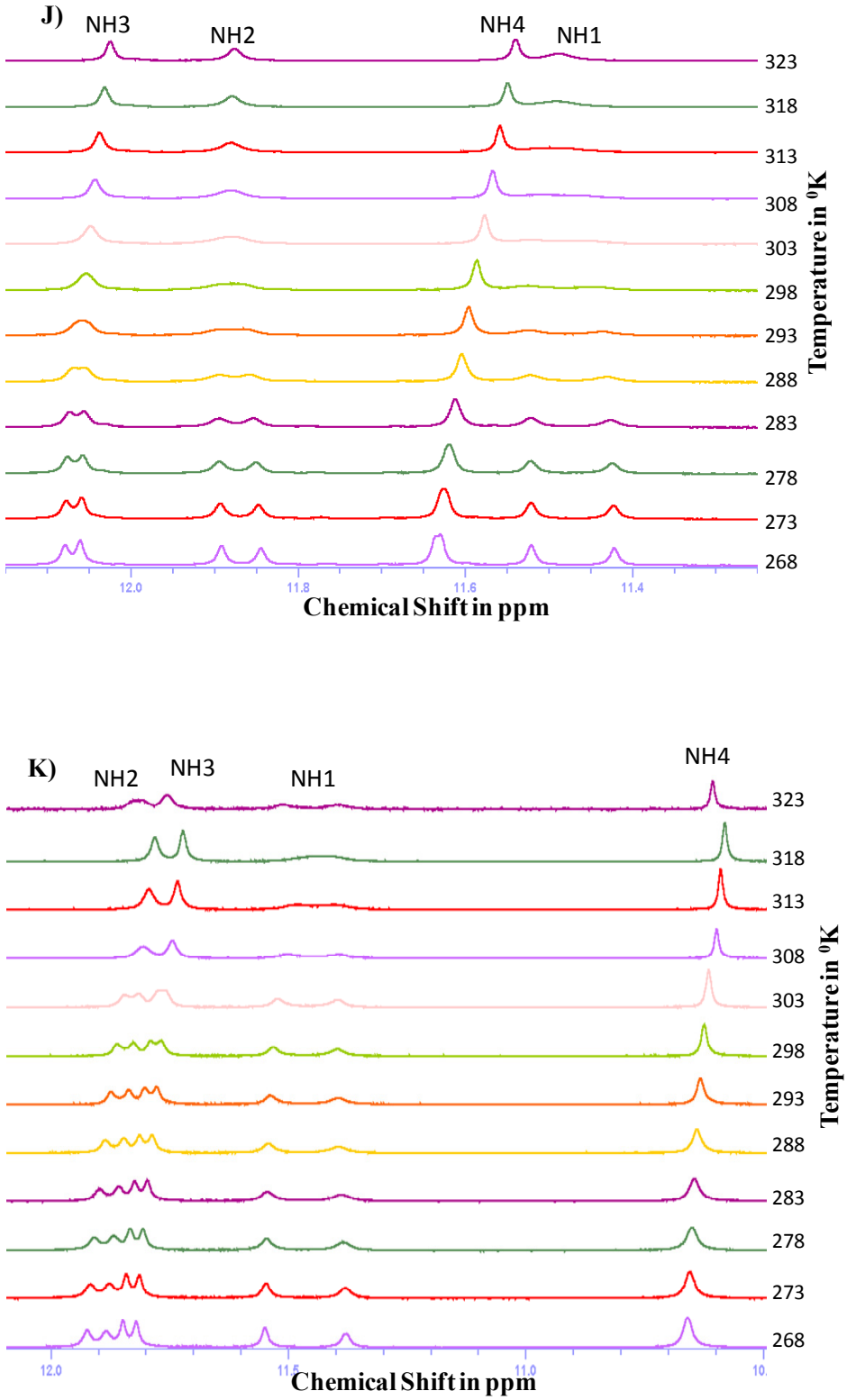

Fig 1.28: Stacked plots representing variable temperature study of **5a** (J) and **6a** (K).

1.8.3 Circular Dichroism (CD) Studies:

Circular dichroism (CD) studies are useful to establish the characteristic secondary structural features of a oligopeptide. The CD spectra of compounds **3a**, **4a**, **5a**, **6a**, **5b** and **6b** were recorded using 0.2 mmol solutions in trifluoro ethanol. Although the curves do not show the exact characteristic pattern of a helical secondary structure, the curves obtained for the octapeptides **5a** and **6b** show a minima at 210 nm which might be attributed to the helical folding pattern of this class of foldamers, without any inter-residual hydrogen bonding observed in the respective oligomers.

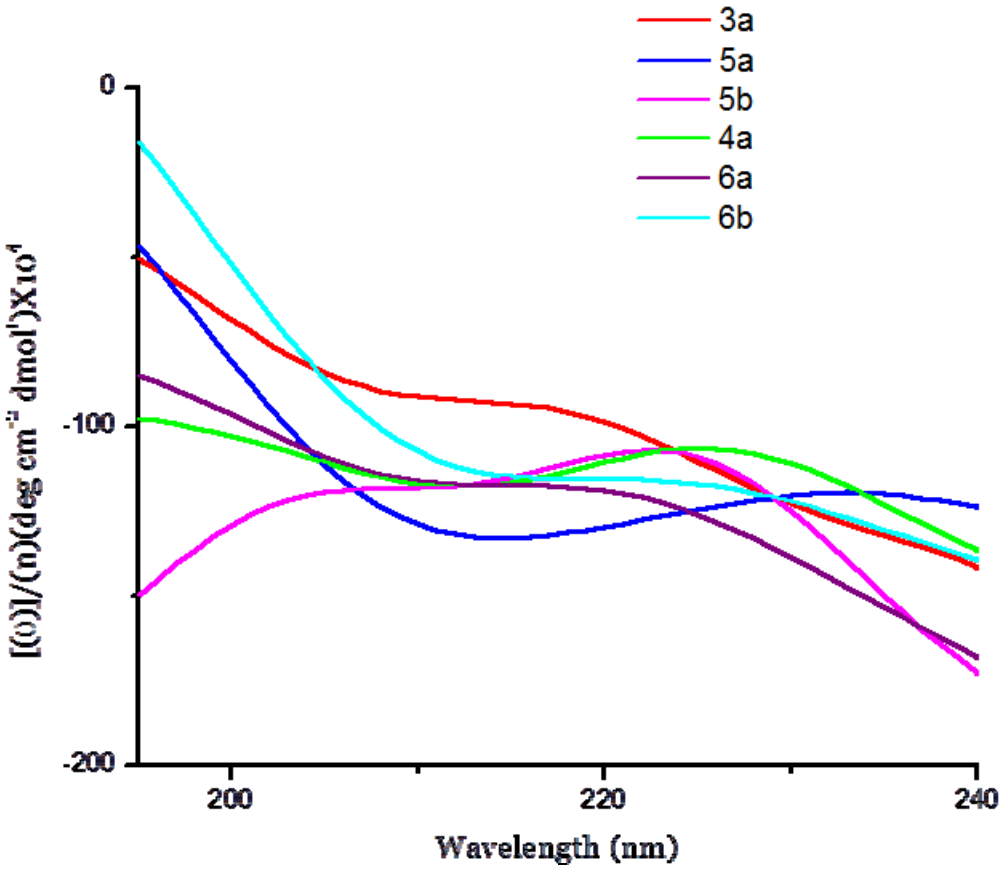

Fig 1.29: Circular dichroism (CD) spectra of tetrapeptides (**3a** and **4a**) and octapeptides (**5a**, **5b**, **6a** and **6b**) [0.2mmol solution in trifluoro ethanol].

1.8.4 *ab-initio* molecular modeling studies

The larger oligomers **5a**, **6a**, **5b** and **6b** were resistant to crystal formation and their conformational analysis by NMR experiments was also too difficult owing to the poor signal dispersion. However, insight into their conformational characteristics, particularly their right handed helically folded architecture could be obtained by computational *ab-initio* molecular modeling studies at HF/6-31G**++ level using Guassian03 software package.[85] This was also confirmed by the overlay of crystal structures with their respective *ab-initio* structures for the tetrapeptides **3a** and **4d** (Fig 1.29). The good agreement between *ab-initio* molecular modeling studies and experimental data of **3a** (RMSD = 0.46) and **4d** (RMSD = 1.34) presumably, owing to high conformational rigidity of the foldamer backbone, confirms the reliability of *ab-initio* MO theory in prediction of the foldamer conformation.

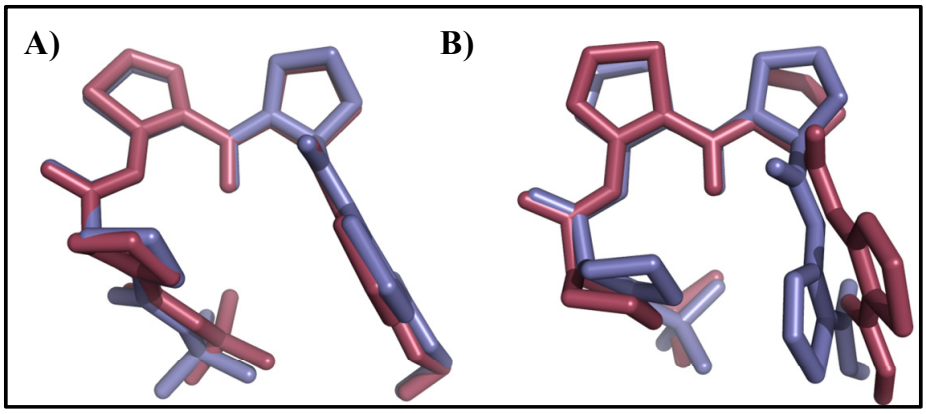

Fig 1.30: Overlaid structures of the crystal and optimized structures of **3d** and **4d**.

1.8.4.1 Details of the quantum chemical calculations

Table 1.1: Backbone Torsion Angles (in degrees)[a] for **3a** according to the HF/6-31G**++.

Pro1		Atc1			Pro2		Atc2		
ϕ	ψ	ϕ	θ	ψ	ϕ	ψ	ϕ	θ	ψ
-86.10	-5.76	179.21	-1.10	-157.37	-58.07	145.04	-178.99	1.39	178.46
-84.75	-12.27	173.33	-1.14	152.75	-61.57	148.15	-179.7	0.22	179.0

[a]First row includes data of the crystal **3a**, second row includes the data of the model **3a** obtained from HF/6-31G**++. E_T(HF/6-31G**++) = -2579.3011 a.u.

Table 1.2: Backbone Torsion Angles (in degrees)[a] for **4d** according to the HF/6-31G**++.

Pro1		Atc1			Pro2		Atc2		
ϕ	ψ	ϕ	θ	ψ	ϕ	ψ	ϕ	θ	ψ
-83.35	-3.67	158.12	1.43	-165.69	-56.45	144.51	-170.90	0.35	176.34
-75.02	-24.65	179.2	-2.96	167.55	-62.62	140.20	-176.28	-0.32	179.30

[a]First row includes the data of the crystal **4d** , second row includes the data of the model **4a** obtained using HF/6-31G**++. E_T(HF/6-31G**++) = -2465.3680 a.u

Table 1.3. Backbone Torsion Angles (in degrees) for **5a** according to the HF/6-31G**++

Pro1		Atc1			Pro2		Atc2		
ϕ	ψ	ϕ	θ	ψ	ϕ	ψ	ϕ	θ	ψ
-87.51	-7.62	173.92	-0.10	-151.79	-61.82	151.71	-178.97	0.16	-168.04
Pro3		Atc3			Pro4		Atc4		
ϕ	ψ	ϕ	θ	ψ	ϕ	ψ	ϕ	θ	ψ
-64.86	134.06	164.49	-2.64	-153.33	-62.01	142.16	178.62	-0.38	-179.19

The data of the model **5a** obtained using HF/6-31G**++. E_T(HF/6-31G**++) = -4660.7033 a.u.

Table 1.4. Backbone Torsion Angles (in degrees) for **6a** according to the HF/6-31G**++

Pro1		Atc1			Pro2		Atc2		
ϕ	ψ	ϕ	θ	ψ	ϕ	ψ	ϕ	θ	ψ
-88.33	-6.90	169.72	2.97	-159.85	-64.69	151.69	-179.92	2.24	-174.66
Pro3		Atc3			Pro4		Atc4		
ϕ	ψ	ϕ	θ	ψ	ϕ	ψ	ϕ	θ	ψ
-66.95	143.77	137.12	1.74	-158.57	-64.08	143.77	-178.37	0.06	179.75

The data of the model **6a** obtained using HF/6-31G**++. E_T(HF/6-31G**++) = -4621.6695 a.u.

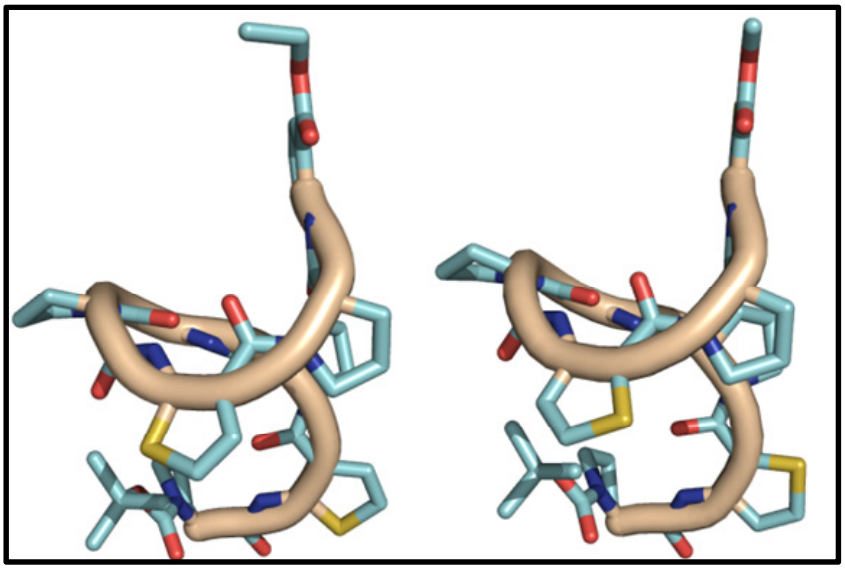

Fig 1.31: Cartoon representations of the minimum energy conformations of octapeptides **5a** (left) and **6a** (right) obtained at HF/6-31G**++ level.

1.9 Conclusion

In summary, we could develop synthetic oligomers that do not form inter-residual backbone hydrogen bonding, yet adopt preferentially a folded conformation. Conformational ordering observed in this class of oligomers is apparently due to the combined conformational restrictions exerted by the conformationally rigid individual amino acid residues with which the oligomers are made of. It is intriguing that the robust heterogeneous backbone maintains its conformational integrity even though substantial isosteric replacements have been carried on the backbone as evident from the results of crystal structure, NMR studies and *ab-initio* modeling studies. The folding characteristics observed in the oligomers containing 1:1 ratio of Pto and Atc building blocks might provide insights in exploring the biological applications of such folded systems and mimicking several naturally occurring peptides.

1.10 Experimental Section

Crystal Data:

Data for the compounds **1a**, **2b**, **3a** and **4d** were collected on SMART APEX CCD Single Crystal X-ray diffractometer using Mo-Kα radiation (λ = 0.7107 Å) to a maximum θ range of 25.00°. Crystal to detector distance 6.05 cm, 512 x 512 pixels / frame, Oscillation / frame -0.3º, maximum detector swing angle = –30.0º, beam center = (260.2, 252.5), in plane spot width = 1.24, SAINT integration with different exposure time per frame and SADABS correction applied.

Data for the compound **4f** was collected on SMART APEX-II CCD using Mo-Kα radiation (λ = 0.7107 Å) to a maximum θ range of 25.00°. Crystal to detector distance 5.00 cm, 512 x 512 pixels / frame, Oscillation / frame -0.5º, maximum detector swing angle = –30.0º, beam center = (260.2, 252.5), in plane spot width = 1.24, SAINT integration with different exposure time per frame and SADABS correction applied. [86]

All the structures were solved by direct methods using SHELXTL. All the data were corrected for Lorentzian, polarisation and absorption effects. SHELX-97 (ShelxTL) was used for structure solution and full matrix least squares refinement on F^2. Hydrogen atoms were included in the refinement as per the riding model. The refinements were carried out using SHELXL-97.

Crystal data for 1a:

Single crystals of the compound **1a** were grown by slow evaporation of the solution a mixture of pet. ether and ethyl acetate. Pale yellow plate-like crystal of approximate size 0.42 x 0.17 x 0.04 mm^3, was used for data collection. Multi-run data acquisition. Total scans = 5, total frames = 2809, exposure / frame = 20.0 sec / frame, θ range = 1.75 to 25.50º, completeness to θ of 25.50º is 100.0 %. $C_{17}H_{24}N_2O_5S$, M = 368.44. Crystals belong to Tetragonal, space group $P4_32_12$, a = 9.2214(4), b = 9.2214 (4), c = 46.482(2) Å, V = 3952.6(3) $Å^3$, Z = 8, D_c = 1.238 g /cc, μ (Mo–Kα) = 0.191 mm^{-1}, 44585, reflections measured, 3674 unique [I>2σ(I)], R value 0.0454, wR2 = = 0.1193. Largest diff. peak and hole 0.159 and -0.173 e. $Å^{-3}$.

Crystal data for 2b:

Single crystals of the compound **2b** were grown by slow evaporation of a solution of ethyl acetate. Colorless plate-like crystal of approximate size 0.29 x 0.20 x 0.04 mm^3, was used for data collection. Multi-run data acquisition. Total scans = 5, total frames = 1271, exposure / frame = 20.0 sec / frame, θ range = 2.06 to 25º, completeness to θ of 25º is 100.0 %. $C_{15}H_{20}N_2O_5S$, M = 340.39. Crystals belong to Orthorhombic, space group $P2_12_12_1$, a = 7.8940(7) Å b = 10.9470(9) Å, c = 19.7800(2) Å, V = 1709.3(2) $Å^3$, Z = 4, D_c = 1.323 g/cc, μ (Mo–Kα) = 0.215 mm^{-1}, 7939, reflections measured, 3001 unique [I>2σ(I)], R value 0.0436, wR2 = 0.0826. Largest diff. peak and hole 0.223 and -0.217 e.$Å^{-3}$.

Crystal data for 3a:

Single crystals of the compound **3a** were grown by slow evaporation of the solution a mixture of pet. ether and ethyl acetate. Colorless needle-like crystal of approximate size 0.14 x 0.04 x 0.04 mm^3, was used for data collection. Multi-run data acquisition. Total scans = 5, total frames = 1271, exposure / frame = 20.0 sec / frame, θ range = 2.18 to 25.00°, completeness to θ of 24.00º is 100.0 %. $C_{27}H_{34}N_4O_7S_2$, M = 590.70. Crystals belong to Orthorhombic, space group $P2_12_12_1$, a = 11.077(1) Å, b = 16.0203(2) Å, c = 17.3250(2) Å, V = 3074.4(6) $Å^3$, Z = 4, D_c = 1.276 g /cc, μ (Mo–Kα) = 0.221 mm^{-1}, 15654, reflections measured, 5415 unique [I>2σ(I)], R value 0.0586, wR2 = = 0.1467. Largest diff. peak and hole 0.345 and -0.275 e.$Å^{-3}$.

Crystal data for 4d:

Single crystals of the compound **4d** were grown by slow evaporation of the solution of methanol. Colorless plate-like crystal of approximate size 0.45 x 0.15 x 0.13 mm^3, was used for data collection. Multi-run data acquisition. Total scans = 5, total frames = 1271, exposure / frame = 20.0 sec / frame, θ range = 2.09 to 25.00°, completeness to θ of 25.00º is 99.8 %. $C_{26}H_{32}N_4O_6S_2$, M = 560.68. Crystals belong to Monoclinic space group $P2_1$, a = 7.3385(4) Å, b = 38.880(2)Å, c = 9.7776(6) Å, V = 2780.7(3) $Å^3$, Z = 4, D_c = 1.339 g /cc, μ (Mo–Kα) = 0.238 mm^{-1}, 14101, reflections measured, 9614 unique [I>2σ(I)], R value 0.0424, wR2 = = 0.0961. Largest diff. peak and hole 0.216 and -0.161 e.$Å^{-3}$. It has been observed that two molecules, with a slight different conformation at the C-terminus, are

packed in the unit cell of the molecule (Fig1.31).

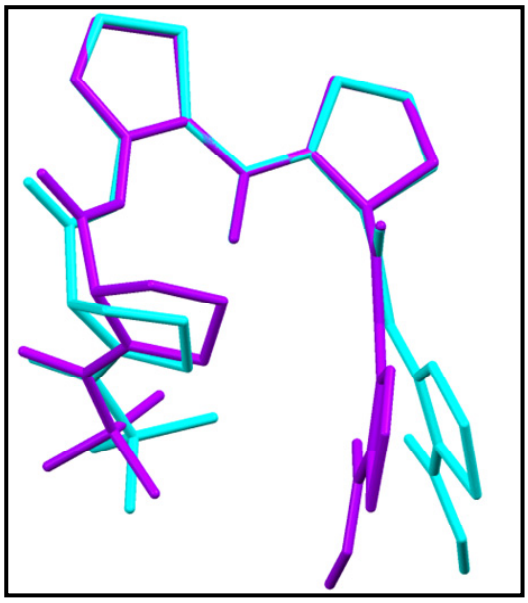

Fig 1.32: Overlay of the two molecules present in the unit cell of **4d**.

Crystal data for 4f:

Single crystals of compound **4f** were grown by slow evaporation of the solution of methanol. Colorless plate-like crystal of approximate size 0.45 x 0.31 x 0.14 mm^3, was used for data collection. Multi-run data acquisition. Total scans = 5, total frames = 669, exposure / frame = 20.0 sec / frame, θ range = 1.59 to 25.00°, completeness to θ of 25.00º is 100.0 %. $C_{29}H_{35}N_5O_5S_2$, M = 601.77. Crystals belong to Orthorhombic, space group $P2_12_12_1$, a = 9.3121(9) Å, b = 17.9909(2) Å, c = 18.1542(2) Å, V = 3041.4(5) $Å^3$, Z = 4, D_c = 1.314 g /cc, μ (Mo–Kα) = 0.221 mm^{-1}, 13111, reflections measured, 5244 unique [I>2σ(I)], R value 0.0317, wR2 = = 0.0766. Largest diff. peak and hole 0.164 and -0.177 e.$Å^{-3}$.

General Method for the preparation of dipeptides 1a and 2a:

To a solution of Boc ^{L}Proline (0.2 g, 0.9 mmol, 1 equiv) in THF at 0 °C, ethyl chloroformate (0.11 g, 1.0 mmol, 1.2 equiv), Et_3N (0.14 mL, 1.0 mmol, 1.2 equiv) were added followed by the addition of amino esters **7** (0.15 g, 0.8 mmol, 1 equiv) (the amino ester **7** was prepared according to the reported protocol[87]) in case of **1a** and **8** (0.17 g, 1.02 mmol, 1.1 equiv) in case of **2a**, respectively, and stirred for 30 min at 0 °C. Then, the reaction mixture was refluxed for 48 h at 80 °C. Later, the reaction mixture was filtered and the solvent was stripped off under reduced pressure. The residue was taken into DCM and the organic layer was washed sequentially with sat. $KHSO_4$, brine, sat. $NaHCO_3$ and water. The organic layer was dried over anhydrous Na_2SO_4 and evaporated under reduced pressure to get the crude products which were purified by column chromatography.

tert-butyl 2-((3-(ethoxycarbonyl)thiophen-2-yl)carbamoyl)pyrrolidine-1-carboxylate 1a:

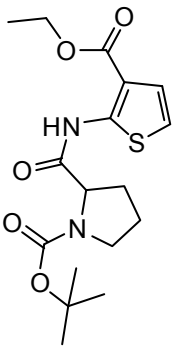

1a

Compound **1a** was isolated as a yellow solid (0.3 g, 85%); m.p: 66-69 °C; $[\alpha]^{26}_{D}$: -120° (*c* = 1, $CHCl_3$); IR ($CHCl_3$) ν (cm^{-1}): 3276, 3019, 2982, 2400, 1685, 1550, 1498, 1478, 1238, 1215, 1034, 927, 747, 702, 668. ^{1}H NMR (400 MHz, $CDCl_3$) δ: $11.54_{rotamer}$(0.45H), $11.38_{rotamer}$(0.55H), 7.20-7.17 (d, *J* = 5.4 Hz, 1H), 6.73-6.71 (d, *J* = 4.5 Hz, 1H), $4.53_{rotamer}$ (0.45H), $4.50_{rotamer}$ (0.55H), 4.36-4.25 (q, *J* = 7.1 Hz, 2H), 3.61-3.45 (m, 2H), 2.24-2.14 (m, 4H), 1.95-1.88 (t, *J* = 6.8 Hz, 3H), $1.48_{rotamer}$ (4H), $1.33_{rotamer}$ (5H); ^{13}C NMR (100 MHz, $CDCl_3$) δ: 170.4, 169.9, 164.9, 123.8, 115.9, 113.3, 80.5, 61.3, 60.6, 46.7, 31.2, 29.6, 28.2, 24.4, 23.8, 14.2; ESI-MS: 369.3233 $(M+H)^+$, 391.3003 $(M+Na)^+$, 407.2976 $(M+K)^+$; Elemental analysis calculated for $C_{17}H_{24}N_2O_5S$: C, 55.42; H, 6.65; N, 8.56; S, 8.70; Found: C, 55.6; H, 6.65; N, 8.56; S, 8.76.

tert-butyl-2-((3-(methoxycarbonyl)thiophen-2-yl)carbamoyl)pyrrolidine-1-carboxylate 2a:

Compound **2a** was isolated as a white solid (0.3 g, 90%); m.p: 67-70 °C; $[\alpha]^{26}_{D}$: -138° (*c* = 1, $CHCl_3$); IR ($CHCl_3$) ν (cm^{-1}): 3308, 3015, 1684, 1570, 1388, 1282, 1216, 1160, 1095, 755; ^{1}H NMR (400 MHz, $CDCl_3$) δ: $10.75_{rotamer}$ (0.45H), $10.62_{rotamer}$ (0.55H), 8.15-8.12 (d, *J* = 5.6 Hz, 1H), 7.47 (bs, 1H), $4.44_{rotamer}$

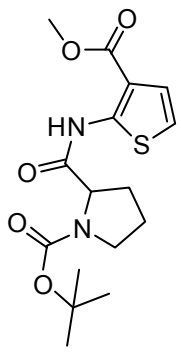

2a

(0.45H), 4.30$_{rotamer}$ (0.55H), 4.16-4.06 (q, ethyl acetate), 3.87 (s, 3H), 3.64-3.58 (m, 2H), 2.20-2.17 (m, 2H), 2.04 (s, ethyl acetate), 1.93 (m,2H), 1.49$_{rotamer}$ (4H), 1.33$_{rotamer}$ (5H); ^{13}C NMR (100 MHz, $CDCl_3$) δ: 171.0, 170.4, 164.1, 154.1, 143.8, 131.6, 122.0, 110.7, 80.4, 61.9, 61.3, 51.9, 46.8, 31.3, 30.0, 28.1 23.1, 14.0; ESI-MS: 355.3549 $(M+H)^+$, 377.3449 $(M+Na)^+$, 393.2878 $(M+K)^+$; Elemental analysis calculated for $C_{16}H_{22}N_2O_5S$: C, 54.22; H, 6.26; N, 7.90; S, 9.05; Found: C, 55.56; H, 6.50, N, 6.85; S, 10.66.

General method for ester hydrolysis:

To the solutions of esters **1a**, **2a**, **3a** and **4a** (10 mmol, 1 equiv) in methanol, $LiOH{\cdot}H_2O$ (40 mmol, 4 equiv) was added in water (12 mL) at 0 °C and the reaction mixture was stirred for 12 h. After the complete consumption of the starting material, the solvent was evaporated under reduced pressure and the residue was treated with sat. $KHSO_4$ solution, followed by extraction with DCM (2 X 25 mL). The corresponding acid derivatives **1b**, **2b**, **3b** and **4b**, respectively, obtained after evaporation of the solvent were carried forward for the next reaction without any purification.

3-(1-(tert-butoxycarbonyl)-pyrrolidine-2-carboxamido)thiophene-2-carboxylic acid 2b:

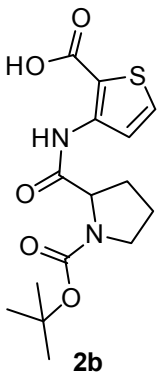

2b

Compound **2b** was isolated as a yellow solid; mp: 155-158 °C; $[\alpha]^{26}_D$: -110° (*c* = 1, $CHCl_3$); IR ($CHCl_3$) ν (cm^{-1}): 3684, 3303, 3018, 2980, 2621, 2401, 1681, 1566, 1409, 1216, 1161, 769, 667; ^{1}H NMR (400 MHz, $CDCl_3$) δ: 10.72$_{rotamer}$ (0.45H), 10.68$_{rotamer}$ (0.55H), 8.17-8.16 (d, *J* = 4.9 Hz, 1H), 7.57-7.50 (m, 1H), 4.64$_{rotamer}$ (0.55H), 4.35$_{rotamer}$ (0.45H), 3.64-3.47 (m, 2H), 2.32-2.24 (m, 1H), 2.18 (bs, 1H), 1.96 (bs, 2H), 1.49$_{rotamer}$ (5H), 1.33$_{rotamer}$ (4H); ^{13}C NMR (100 MHz, $CDCl_3$) δ: 170.9, 170.4, 167.8, 167.2, 155.2, 154.2, 145.0, 144.5, 132.8, 122.2, 110.7, 110.2, 80.9, 62.0, 61.1, 47.2, 46.8, 31.3, 30.4, 28.3, 24.3, 23.7; ESI-MS: 341.0 $(M+H)^+$, 362.54 $(M+Na-1)^+$, 363.87 $(M+Na+1)^+$, 364.94 $(M+Na+2)^+$, Elemental analysis calculated for $C_{15}H_{20}N_2O_5S$: C, 52.93; H, 5.92; N, 8.23; S, 9.42; Found: C, 53.65; H, 6.21, N, 7.99; S, 10.50.

General method for Boc deprotection:

The solutions of Boc-peptides **1a**, **2a**, **3a**, **4a**, **5a** and **6a** (3 mmol) were subjected to deprotection using DCM/TFA (1:1, 5 mL) at 0°C. After completion of the reaction (~2 h), the solvent was stripped off, the residue was taken into DCM (30 mL), washed with sat. $NaHCO_3$ solution (3x10 mL) and the product was repeatedly extracted. The organic layer was dried over anhydrous Na_2SO_4. The residues **1c**, **2c**, **3c**, **4c**, **5b** and **6b**, respectively, obtained after evaporation of the solvent were carried forward for the next step without any purification**.**

tert-butyl-2((3-(2-((3-(ethoxycarbonyl)thiophen-2-yl)carbamoyl)pyrrolidine-1-carbonyl) thiophen-2-yl)carbamoyl)pyrrolidine-1-carboxylate 3a:

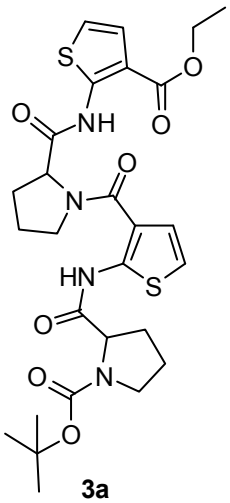

3a

The acid **1b** (0.18 g, 0.5 mmol, 1 equiv) was coupled with the amine **1c** (0.14 g, 0.5 mmol, 1 equiv) using DCC (0.12 g, 0.5 mmol, 1.1 eqiv) and HOBt (0.01 g, 0.1 mmol, 0.2 equiv) in DCM . Work up, as that described for **1a** followed by column chromatographic purification yielded compound **3a** as a white solid (0.2 g, 63%); mp: 86-90 °C; $[\alpha]^{26}_{D}$: -190° (*c* = 1, $CHCl_3$); IR ($CHCl_3$) ν (cm^{-1}): 3272, 3019, 1681, 1551, 1399, 1215, 702, 668; ^{1}H NMR (400 MHz, $CDCl_3$) δ: 11.73 (s, 1H), 11.60 (s, 1H), 7.27-7.25 (bs, 1H), 7.21-7.18 (d, *J* = 5.8 Hz, 1H), 6.82-6.80 (m, 1H), 6.75-6.73 (d, *J* = 5.7 Hz, 1H), 4.97-4.91 (m, 1H), 4.51-4.48 (m, 1H), 4.34-4.24 (q, *J* = 6.9 Hz, 2H), 4.04-3.87 (m, 2H), 3.53-3.33 (m, 2H), 2.37-1.85 (m, 8H), $1.49_{rotamer}$ (4H), 1.40-1.33 (m, 3H), $1.29_{rotamer}$ (5H); ^{13}C NMR (100 MHz, $CDCl_3$) δ: 170.5, 169.9, 168.9, 166.6, 165.1, 155.0, 153.7, 148.0, 147.2, 123.7, 123.2, 115.9, 115.2, 113.4, 96.0, 80.2, 80.1, 79.4, 61.1, 60.5, 57.4, 50.0, 46.9, 46.5, 36.5, 31.2, 29.8, 28.3, 25.7, 25.1, 24.2, 23.7, 14.2; ESI-MS: 613.4067 $(M+Na)^+$; Elemental analysis calculated for $C_{27}H_{34}N_4O_7S_2$: C, 54.90; H, 5.80; N, 9.48; S, 10.86; Found: C, 52.54; H, 5.42; N, 10.01; S, 10.66.

tert-butyl-2-((2-(2-((2-(methoxycarbonyl)thiophen-3-l)carbamoyl)pyrrolidine -1-carbonyl) thiophen-3-yl)carbamoyl)pyrrolidine-1-carboxylate 4a:

The acid **2b** (0.28 g, 0.8 mmol, 1 equiv) was coupled with the amine **2c** (0.21 g, 0.8 mmol, 1 equiv) using DCC (0.19 g, 0.9 mmol, 1.1 eqiv) and HOBt (0.02 g, 0.1

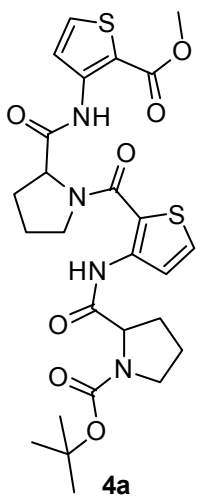

4a

mmol, 0.2 equiv) in DCM . Work up, as that described for **1a** followed by column chromatographic purification yielded compound **4a** as white solid (0.3 g, 62%); mp: 140-143 °C; $[\alpha]^{26}_{D}$: -120° (*c* = 1, $CHCl_3$); IR ($CHCl_3$) ν (cm^{-1}): 3309, 3019, 1557, 1422, 1446, 1403, 1355, 1283, 1246, 1215, 755, 668, 649; ^{1}H NMR (500 MHz, $CDCl_3$) δ: 11.65-11.58 (m, 1H), 10.67 (s, 1H), 8.22-8.20 (m, 1H), 8.13-8.10 (m, 1H), 7.48-7.43 (m, 2H), $4.90_{rotamer}$ (0.4H), $4.83_{rotamer}$ (0.6H), $4.39_{rotamer}$ (0.5H), $4.23_{rotamer}$ (0.5H), 4.15 (bs, 1H), 4.0-3.97 (m, 1H), 3.82-3.80 (m, 3H), $3.60_{rotamer}$ (0.5H), 3.48-3.42 (m, 1H), $3.32_{rotamer}$ (0.5H), 2.24 (bs, 4H), 2.11 (bs,2H), $2.04_{rotamer}$ (0.55H), 1.94-1.89 (m, 0.45H) 1.79-1.74 (m, 1H), $1.47_{rotamer}$ (4H), $1.28_{rotamer}$ (5H); ^{13}C NMR (125 MHz, $CDCl_3$) δ: 171.1, 170.6, 169.4, 164.7. 164.3, 154.8, 153.9. 144.8, 144.0, 131.4, 129.0, 128.7, 122.1, 112.1, 111.9, 110.9, 79.9, 62.7, 61.9, 61.3, 51.8, 48.9, 46.5, 31.3, 30.4, 28.3, 28.1, 24.1, 23.6; ESI-MS: 599.7709 $(M+Na)^{+}$; Elemental analysis calculated for $C_{26}H_{32}N_4O_7S_2$: C, 54.15; H, 5.59; N, 9.72; S, 11.12; Found: C, 55.2; H, 5.3; N, 9.1; S, 10.8.

tert-butyl-2-((3-(2-((3-(2-((3-(2-((3-(ethoxycarbonyl)thiophen-2-yl)carbamoyl) pyrrolidine-1-carbonyl)thiophen-2-yl)carbamoyl)pyrrolidine-1-arbonyl)thiophen-2-yl)carbamoyl)pyrrolidine-1-carbonyl)thiophen-2-yl)carbamoyl)pyrrolidine-1-carboxylate 5a:

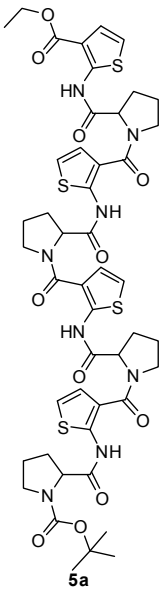

5a

The acid **3b** (0.19 g, 0.3 mmol, 1 equiv) was coupled with the amine **3c** (0.16 g, 0.3 mmol, 1 equiv) using HBTU (0.15 g, 0.4 mmol, 1.2 eqiv), DIPEA (0.08 mL, 0.5 mmol, 1.5 equiv) and HOBt (0.02 g, 0.1 mmol, 0.2 equiv) in dry CH_3CN. Work up, as that described for **1a** followed by column chromatographic purification yielded compound **5a** as white solid (0.21 g, 60%); mp: 180-184 °C; $[\alpha]^{26}_{D}$: -272° (*c* =1, $CHCl_3$); IR ($CHCl_3$) ν (cm^{-1}): 3270, 3019, 2400, 1685, 1676, 1596, 1545, 1492, 1432, 1400, 1356, 1215, 1034, 927, 755, 668; ^{1}H NMR (400 MHz, $CDCl_3$) δ: 12.07 (s, 1H), 11.88, (bs, 1H), 11.61 (s, 1H), $11.54_{rotamer}$ (0.5H), $11.46_{rotamer}$ (0.5H), 7.39 (bs, 1H), 7.34-7.29 (m, 3H), 7.25-7.22 (d,

J = 5.8 Hz, 1H), 6.86-6.84 (d, *J* = 5.8 Hz, 2H), 6.80-6.77 (d, *J* = 5.7 Hz, 1H), 5.01-4.90 (m, 1H), 4.82-4.75 (m, 2H), 4.52-4.48 (m, 1H), 4.39-4.28 (q, *J* = 7.1 Hz, 2H), 4.04-3.90 (m, 4H), 3.80-3.70 (m, 2H), 3.59-3.34 (m, 2H), 2.41-1.98 (m, 10H), 1.89 (bs, 6H), $1.50_{rotamer}$ (4H), 1.38 (t, *J* = 7.1 Hz, 3H), $1.31_{rotamer}$ (5H); ^{13}C NMR (100 MHz, $CDCl_3$) δ: 171.0, 169.1, 166.5, 165.4, 153.8, 148.1, 147.3, 146.8, 123.8, 123.2, 116.0, 115.7, 115.5, 113.4, 80.1, 61.4, 61.0, 60.6, 60.2, 50.1, 49.9, 47.0, 46.6, 38.5, 31.1, 28.9, 28.2, 28.0, 25.7, 25.6, 23.7, 20.9, 20.4, 14.2, 14.1; MALDI-TOF: 1056.4635 $(M+Na-1)^+$, 1057.4781 $(M+Na)^+$, 1058.4454 $(M+Na+1)^+$, 1059.5731 $(M+Na+2)^+$, 1072.4297 $(M+K-1)^+$, 1073.4417 $(M+K)^+$, 1074.4271 $(M+K+1)^+$, 1075.3999 $(M+K+2)^+$; Elemental analysis calculated for $C_{47}H_{54}N_8O_{11}S_4$: C, 54.53; H, 5.26; N, 10.82; S, 12.39; Found: C, 56.6; H, 6.3; N, 10.5; S, 12.8.

tert-butyl-2-((2-(2-((2-(2-((2-(2-((2-(2-((2-(methoxycarbonyl)thiophen-3-yl) carbamoyl)pyrrolidine-1-carbonyl)thiophen-3-yl)carbamoyl)pyrrolidine-1-carbonyl)thiophen-3-yl)carbamoyl)pyrrolidine-1-carbonyl)thiophen-3-yl)carbamoyl)pyrro-lidine-1-carboxylate 6a:

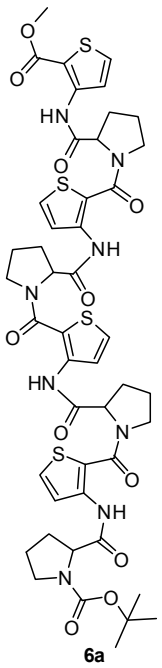

6a

The acid **4b** (0.12 g, 0.2 mmol, 1 equiv) was coupled with the amine **4c** (0.14 g, 0.2 mmol, 1 equiv) using DCC (0.05 g, 0.2 mmol, 1.1 eqiv), HOBt (0.007 g, 0.05 mmol, 0.2 equiv) in dry DCM. Work up, as that described for **1a** followed by column chromatographic purification yielded compound **6a** as white solid (0.17 g, 65%); mp: 155-158 °C; $[\alpha]^{26}_D$: -154° (*c* = 1, $CHCl_3$); IR ($CHCl_3$) ν (cm^{-1}): 3610, 3445, 3308, 3131, 3018, 2934, 2858, 1694, 1682, 1574, 1567, 1557, 1435, 1446, 1403, 1366, 1283, 1246, 1215, 1435, 1446, 1403, 1366, 1283, 1246, 1215, 1062, 1025, 969, 889, 844, 771, 667, 648; ^{1}H NMR (400 MHz, $CDCl_3$) δ: $11.84_{rotamer}$ (0.5H), $11.80_{rotamer}$ (0.5H), $11.76_{rotamer}$ (0.5H), $11.74_{rotamer}$ (0.5H), $11.51_{rotamer}$ (0.5H), $11.38_{rotamer}$ (0.5H), 10.60 (s, 1H), 8.23-8.22 (d, *J* = 5.2 Hz, 1H), 8.14-8.09 (m, 2H), 8.04 (bs, 2H), 7.49-7.47 (m, 2H), 7.44-7.43 (m, 2H), $4.82_{rotamer}$ (0.5H), $4.77_{rotamer}$ (0.5H), 4.70-4.65 (m, 1H), 4.55-4.50 (m, 1H), $4.34_{rotamer}$ (0.5H), $4.17_{rotamer}$ (1.5H), 4.04-3.97, (m, 3H), 3.83 (s, 3H), 3.79 (bs, 1H), 3.72 (bs, 1H), $3.59_{rotamer}$ (0.5H),

$3.52_{rotamer}$ (0.5H), $3.46_{rotamer}$ (0.5H), $3.33_{rotamer}$ (0.5H), 2.25-1.89 (m, 15H), 1.77-1.72 (m, 1H), $1.43_{rotamer}$ (4H), $1.27_{rotamer}$ (5H); ^{13}C NMR (100 MHz, $CDCl_3$) δ: 170.9, 169.4, 164.6, 164.3, 154.8, 153.9, 144.9, 144.2, 131.6, 129.1, 122.1, 121.7, 112.5, 111.9, 110.6, 110.4, 96.0. 79.9, 62.9, 61.8, 61.3. 51.9, 48.9, 48.6, 46.9, 46.5, 31.3, 30.4, 29.04, 28.3, 28.1, 25.4, 24.0, 23.6; MALDI-TOF: 1042.8814 $(M+Na-1)^+$, 1043.8922 $(M+Na)^+$, 1044.8918 $(M+Na+1)^+$, 1058.8540 $(M+K-1)^+$, 1059 $(M+K)^+$; Elemental analysis calculated for $C_{46}H_{52}N_8O_{11}S_4$: C, 54.96; H, 5.21; N, 11.15; S, 12.76; Found: C, 55.5; H, 5.8; N, 10.9; S, 12.8.

tert-butyl-2-((3-(2-((3-(tert-butylcarbamoyl)thiophen-2-yl)carbamoyl) pyrrolidine-1-carbonyl)thiophen-2-yl)carbamoyl)pyrrolidine-1-carboxylate 4e:

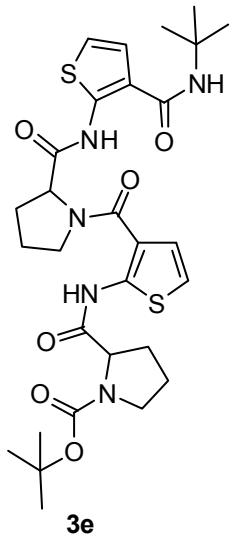

3e

The acid **3b** (0.18 g, 0.33 mmol, 1equiv) was coupled with $^tBuNH_2$ (0.1 mL, 1.01 mmol, using HBTU (0.19 g, 0.5 mmol, 1.5 equiv) and DIPEA (0.11 mL, 0.6 mmol, 2 equiv). Work up, as that described for **1a** followed by column chromatographic purification yielded compound **4e** (0.1 g, 50%) as brownish yellow solid; mp: 83-86 °C; $[\alpha]^{26}_D$: -142° (*c* = 1, $CHCl_3$); IR ($CHCl_3$) ν (cm^{-1}): 3368, 2976, 1682, 1548, 1453, 1313, 1216, 1161, 917, 853, 759, 694, 663; ^{1}H NMR (200 MHz, $CDCl_3$) δ: $11.69_{rotamer}$ (0.4H), 11.63 (s, 1H), 11.58, $_{rotamer}$ (0.6H), 8.20-8.17 (d, *J* = 5.6 Hz, 1H), 8.12-8.10 (m, 1H), 7.48-7.43 (m, 1H), 7.27-7.24 (d, *J* = 5.4 Hz, 1H), 5.44, (s, 1H), 4.90-4.82 (m, 1H), 4.41-4.36 (m, 1H), 4.28-4.18 (m, 1H), 4.04-3.96 (m, 1H), 3.66-3.23 (m, 2H), 2.23-1.62 (m, 8H), $1.47_{rotamer}$ (4H), 1.34 (s, 9H), $1.28_{rotamer}$ (5H); ^{13}C NMR (100 MHz, $CDCl_3$) δ: 169.4, 166.5, 164.7, 146.4, 145.7, 123.7, 120.7, 115.9, 115.3, 80.1, 60.9, 51.5, 50.6, 49.9, 46.7, 38.4, 28.6, 28.0, 24.3; MALDI-TOF: 639.7768 $(M+Na-1)^+$, 640.7768 $(M+Na)^+$, 641.7773 $(M+Na+1)^+$, 655.7349 $(M+K-1)^+$, 656.7327 $(M+K)^+$, 657.7293 $(M+Na+1)^+$; Elemental analysis calculated for $C_{29}H_{39}N_5O_6S_2$: C, 54.96; H, 5.21; N, 11.15; S, 12.76; Found: C, 55.5; H, 5.8; N, 10.9; S, 12.8.

3-amino-N-(tert-butyl)thiophene-2-carboxamide 10:

The amino ester **8** (0.1 g, 0.5 mmol, 1 equiv) was subjected to hydrolysis

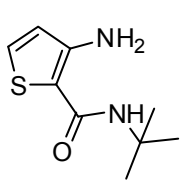

10

using 5N NaOH (4 mL) by heating the reaction mixture at 60 °C for 12 h. Later, the solvent was evaporated under reduced pressure, the residue obtained was taken into DCM, washed with sat $KHSO_4$ solution (2x10 mL), The organic layer was dried over Na_2SO_4, and evaporated, which gave the free amino acid **9** as a yellow solid. This amino acid **9** (0.09 g, 0.58 mmol, 1 equiv) was coupled with $^{t}BuNH_2$ (0.3 mL, 2.92 mmol, 5 equiv) using HBTU (0.33 g, 0.87 mmol, 1.5 equiv) and DIPEA (0.2 mL, 1.16 mmol, 2 equiv).Work up, as that described for **1a** followed by column chromatographic purification yielded compound **10** as a pasty mass (0.1 g, 80%); ^{1}H NMR (200 MHz, $CDCl_3$) δ: 7.07-7.04 (d, *J* = 5.3Hz, 1H), 6.54-6.52 (d, *J* = 5.3 Hz, 1H), 5.26 (bs, 1H), 1.42 (s, 9H); ^{13}C NMR (50 MHz, $CDCl_3$) δ: 164.6, 152.0, 125.7, 121.4, 104.0, 51.4, 29.1; ESI-MS: 221.2014 $(M+Na)^{+}$; Elemental analysis calculated for $C_9H_{14}N_2OS$: C, 54.52; H, 7.12; N, 14.13; S, 16.17; Found: C, 53.5; H, 7.8; N, 15.9; S, 16.8.

tert-butyl-2-((2-(tert-butylcarbamoyl)thiophen-3-yl)carbamoyl)pyrrolidine-1-carboxylate 2d:

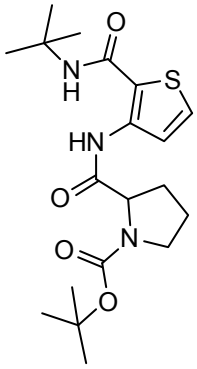

2d

To a solution of Boc ^{L}Proline (0.47 g, 2.22 mmol, 1.1 equiv) in THF at 0 °C, ethyl chloroformate (0.2 mL, 2.42 mmol, 1.2 equiv), Et_3N (0.33 mL, 2.42 mmol, 1.2 equiv) were added followed by the addition of **10** (0.4 g, 2.02 mmol, 1 equiv) and stirred for 30 min at 0 °C. Then the reaction mixture was refluxed for 48 h at 80 °C. Later, the reaction mixture was filtered and the solvent was stripped off under reduced pressure. The residue was taken into DCM and the organic layer was washed sequentially with sat. $KHSO_4$, brine, sat. $NaHCO_3$ and water. The organic layer was dried over anhydrous Na_2SO_4 and evaporated under reduced pressure to get the crude product which after purification by column chromatography gave **2d** as a brownish yellow solid; mp: 53-55 °C; $[\alpha]^{26}_{D}$: +2° (*c* = 1, $CHCl_3$); IR ($CHCl_3$) ν (cm^{-1}): 3681, 3483, 3423, 3352, 3012, 2967, 2400, 1629, 1535, 1475, 1364, 1306, 1218, 1096, 1082, 772, 669; ^{1}H NMR (200 MHz, $CDCl_3$) δ: $11.50_{rotamer}$ (0.4H), $11.42_{rotamer}$ (0.6H), 8.15-8.13 (d, *J* = 5.3 Hz, 1H), 7.24-7.20 (m, 1H), 5.46 (bs, 1H), 4.45-$4.40_{rotamer}$ (0.5H), 4.28-$4.22_{rotamer}$(0.5H), 3.68-3.42 (m, 2H), 2.25-1.83 (m, 4H), $1.49_{rotamer}$ (4H), $1.42_{rotamer}$ (5H); ^{13}C NMR (50 MHz, $CDCl_3$) δ:

176.4, 175.1, 170.9, 170.4, 163.2, 154.7, 153.9, 142.2, 125.8, 125.4, 122.7, 113.7, 113.6, 79.8, 61.6, 61.1, 58.7, 52.0, 46.7, 46.4, 46.0, 31.2, 30.5, 28.6, 28.0, 24.0, 23.5, 23.4; ESI-MS: 418.7926 $(M+Na)^+$; Elemental analysis calculated for $C_{19}H_{29}N_3O_4S$: C, 57.70; H, 7.39; N, 10.62; S, 8.11; Found: C, 59.6; H, 8.4; N, 11.2; S, 7.9.

tert-butyl-2-((2-(2-((2-(tert-butylcarbamoyl)thiophen-3-yl)carbamoyl)pyrrolidine-1-carbonyl)thiophen-3-yl)carbamoyl)pyrrolidine-1-carboxylate 4e:

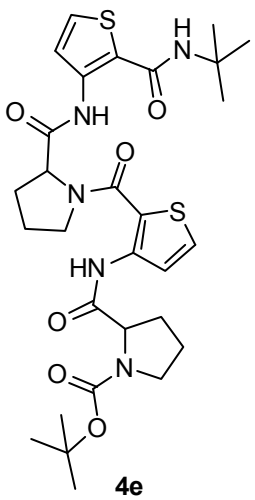

4e

Compound **2d** was subjected to Boc deprotection following the similar procedure mentioned to obtain **2c**. The free amine obtained was coupled with **2b** (0.31 g, 0.93 mmol, 1.1 equiv) using DCC (0.19 g, 0.93 mmol, 1.1 equiv) and HOBt (0.02 g, 1.69 mmol, 0.2 equiv) in dry DCM. Later, the reaction mixture was dilute dwith DCM and washed sequentially with sat. $KHSO_4$, brine, sat. $NaHCO_3$ and water. The organic layer was dried over anhydrous Na_2SO_4 and evaporated under reduced pressure to get the crude product which was purified by column chromatography yielded **4e** as a white solid (0.31 g, 60%), mp: 116-119 °C; $[\alpha]^{26}_D$: -140° (*c* = 1, $CHCl_3$); IR ($CHCl_3$) ν (cm^{-1}): 3246, 3019, 2979, 1686, 1560, 1403, 1289, 1215, 1092, 890; ^{1}H NMR (400 MHz, $CDCl_3$) δ: $11.65_{rotamer}$ (0.4H), 11.59, (s, 1H), $11.56_{rotamer}$ (0.6H), 8.17-8.16 (d, *J* = 5.3 Hz) 8.09-8.08 (m, 1H), 7.45-7.39 (dd, *J* = 4.5Hz, 1H), 7.24-7.22 (d, *J* = 5.3 Hz, 1H), 5.44 (s, 1H), $4.88_{rotamer}$ (0.5H), $4.80_{rotamer}$ (0.5H), $4.36_{rotamer}$ (0.5H), $4.19_{rotamer}$ (1.5H), 3.96 (bs, 1H), $3.58_{rotamer}$ (0.5H), 3.48-3.45 (m, 1H), $3.29_{rotamer}$ (0.5H), 2.22-2.18 (bs, 4H), 2.10-2.07 (m, 2H), 1.90-1.87 (m, 1H), 1.76 (bs, 1H), $1.45_{rotamer}$ (4H), 1.32 (s, 9H), $1.26_{rotamer}$ (5H); ^{13}C NMR (50 MHz, $CDCl_3$) δ: 171.0, 170.5, 169.3, 164.5, 163.4, 154.8, 153.9, 144.5, 142.5, 128.8, 125.8, 122.9, 121.9, 113.7, 112.6, 112.3, 79.9, 62.6, 61.8, 61.3, 52.1, 48.8, 46.8, 46.5. 31.2, 28.7, 28.0, 24.0, 23.6; ESI-MS: 640.6573 $(M+Na)^+$; Elemental analysis calculated for $C_{29}H_{39}N_5O_6S_2$: C, 56.38; H, 6.36; N, 11.34; S, 10.38; Found: C, 57.1; H, 6.9; N, 11.1; S, 10.1.

General Method for Pivolyl protection:

To the solutions of amines **3c**, **4c**, and the amines obtained from the Boc

deprotection of **3e**, **4e**, **5a**, and **6a** (10 mmol, 1equiv) in DCM, Piv-Cl (12 mmol, 1.2 equiv) and Et_3N (15 mmol, 1.5 equiv) were added at 0 °C, and the reaction mixture was stirred for 12 h. After the complete consumption of the starting material, the reaction mixture was diluted with DCM and washed sequentially with sat. $KHSO_4$ solution, brine, sat. $NaHCO_3$ solution and water, the organic layer was dried over Na_2SO_4. Later, the solvent was evaporated and the residues obtained were purified by column chromatography to yield the products **3d**, **4d**, **3f**, **4f**, **5b** and **6b**, respectively.

ethyl-2-(1-(2-(1-pivaloylpyrrolidine-2-carboxamido)thiophene-3-carbonyl) pyrrolidine-2-carboxamido)thiophene-3-carboxylate 3d:

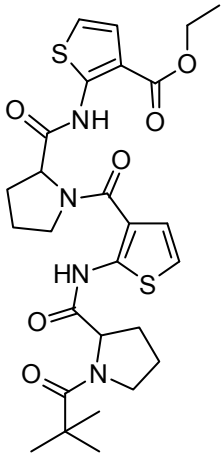

3d

Compound **3d** was isolated as a yellow solid (0.20 g, 70%), mp: 168-172 °C; $[\alpha]^{26}_D$: -102° (*c* = 1, $CHCl_3$); IR ($CHCl_3$) ν (cm^{-1}): 3018, 1671, 1616, 1542, 1405, 1290, 1215, 1089, 1033, 922, 853, 756, 668; ^1H NMR (400 MHz, $CDCl_3$) δ: 11.63 (s, 1H), 11.54 (s, 1H), 7.24 (bs, 1H), 7.21-7.20 (d, *J* = 5.8 Hz, 1H), 6.79-6.77, (d, *J* = 6.2 Hz, 1H), 6.75-6.74 (d, *J* = 5.8 Hz, 1H), 4.84-4.81 (m 1H), 4.74-4.70 (m, 1H), 4.33-4.27 (q, *J* = 7Hz, 2H), 4.0-3.94 (m, 1H), 3.90-3.85 (m,1H), 3.82-3.77 (m,1H), 3.73-3.67 (m, 1H), 2.36-2.29 (m,1H), 2.21-2.09 (m, 3H), 2.07-1.95 (m, 3H), 1.93-1.87 (m, 1H), 1.36-1.33 (t, *J* = 7Hz, 3H), 1.29 (s, 9H); ^{13}C NMR (100 MHz, $CDCl_3$) δ: 177.8, 169.7, 169.1, 165.1, 148.0, 147.5, 123.7, 122.9, 115.9, 115.5, 115.0, 62.7, 60.5, 49.9, 48.2, 39.0, 28.4, 27.2, 25.6, 14.2; ESI-MS: 575.4474 $(M+H)^+$, 597.4312 $(M+Na)^+$; Elemental analysis calculated for $C_{27}H_{34}N_4O_6S_2$: C, 56.43; H, 5.96; N, 9.75; S, 11.16; Found: C, 55.93; H, 5.91; N, 10.70; S, 10.1.

methyl-3-(1-(3-(1-pivaloylpyrrolidine-2-carboxamido)thiophene-2-carbonyl) pyrrolidine-2-carboxamido)thiophene-2-carboxylate 4d:

Compound **4d** was isolated as a white solid (0.20 g, 70%), mp: 156-158 °C; $[\alpha]^{26}_D$: -128° (*c* = 1, $CHCl_3$); IR ($CHCl_3$) ν (cm^{-1}): 3309, 3017, 1680, 1572, 1445, 1361, 1282, 1246, 1215, 1088, 754, 667, 649; ^1H NMR (400 MHz, $CDCl_3$) δ: 11.48 (s, 1H), 10.63 (s, 1H), 8.21-8.20 (d, *J* = 5.5 Hz, 1H), 8.12-8.10 (d, *J* = 5.5 Hz, 1H),7.47-7.46 (d, *J* = 5.5 Hz, 1H), 7.43-7.42 (d, *J* = 5.5 Hz, 1H), 4.77 (bs,

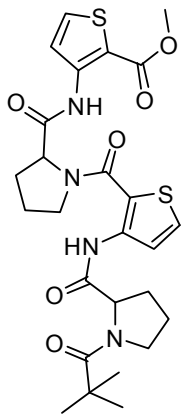

4d

1H), 4.61-4.58 (dd, *J* = 8.7 Hz, 1H), 4.15-4.12 (m, 1H), 4.00-3.96 (m, 1H), 3.82 (s, 3H), 3.77-3.74 (m, 1H), 3.68-3.63 (m, 1H), 2.23 (bs, 3H), 2.11-2.07 (m, 2H), 2.03-1.94 (m, 2H), 1.85-1.80 (m, 1H), 1.27 (s, 9H); ^{13}C NMR (100 MHz, $CDCl_3$) δ: 177.6, 170.4, 169.4, 164.6, 164.4, 145.0, 144.0, 131.5, 128.7, 122.4, 122.1, 111.7, 63.6, 62.9, 51.9, 48.8, 48.2, 39.0, 28.6, 27.3, 25.5; ESI-MS: 583.5084 $(M+Na)^+$; Elemental analysis calculated for $C_{26}H_{32}N_4O_6S_2$: C, 55.70; H, 5.75; N, 9.99; S, 11.44; Found: C, 54.8; H, 5.5; N, 10.10; S, 10.9.

N-(3-(tert-butylcarbamoyl)thiophen-2-yl)-1-(2-(1-pivaloylpyrrolidine-2-carbox-amido)thiophene-3-carbonyl)pyrrolidine-2-carboxamide 3f:

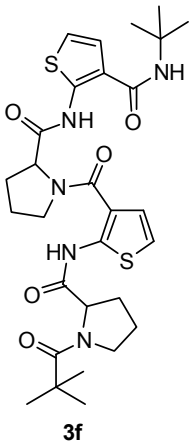

3f

Compound **3f** was isolated as a yellow solid (0.20 g, 70%), mp: 106-109 °C; $[\alpha]^{26}_D$: -102° (*c* = 1, $CHCl_3$); IR ($CHCl_3$) ν (cm^{-1}): 3019, 1674, 1626, 1547, 1485, 1405, 1361, 1215, 758, 668; ^{1}H NMR (400 MHz, $CDCl_3$) δ: 12.59 (s, 1H), 11.54 (s, 1H), 7.33 (bs, 1H), 6.87-6.86 (d, *J* = 5.8 Hz, 1H), 6.76-6.75 (d, *J* = 4.6 Hz, 2H), 5.73 (s, 1H), 4.84-4.82 (m, 1H), 4.73-4.71 (m, 1H), 4.04-4.01 (m, 1H), 3.89-3.84 (m, 1H), 3.81-3.77 (m, 1H), 3.72-3.67 (m, 1H), 3.50-3.46 (q, ethyl acetate), 2.37-2.32 (m, 1H), 2.17-2.10 (m, 3H), 2.07-2.01 (m, 1H), 2.0-1.94 (m, 2H), 1.91-1.87 (m, 1H), 1.41 (s, 9H), 1.30 (s. 9H), 1.24-1.23 (ethyl acetate); ^{13}C NMR (100 MHz, $CDCl_3$) δ: 178.0, 169.7, 169.4, 166.5, 164.8, 147.1, 146.1, 123.4, 120.5, 116.2, 115.6, 115.3, 65.8, 62.8, 61.3, 51.7, 50.0, 48.3, 39.1, 28.9, 27.4, 25.7, 15.2; ESI-MS: 603.11 $(M+H)^+$, 624.04 $(M+Na)^+$; Elemental analysis calculated for $C_{29}H_{39}N_5O_5S_2$: C, 57.88; H, 6.53; N, 11.64; S, 10.66; Found: C, 58.2; H, 7.1; N, 10.30; S, 9.8.

N-(2-(tert-butylcarbamoyl)thiophen-3-yl)-1-(3-(1-pivaloylpyrrolidine-2-carbox-amido)thiophene-2-carbonyl)pyrrolidine-2-carboxamide 4f:

Compound **4f** was isolated as a white solid (0.20 g, 70%), mp: 118-120 °C; $[\alpha]^{26}_D$: 158° (*c* = 1, $CHCl_3$); IR ($CHCl_3$) ν (cm^{-1}): 3019, 2400, 1685, 1628, 1559, 1423, 1404, 1365, 1289, 1215, 11.51 (s, 1H), 8.18-8.17 (d, *J* = 5.5 Hz, 1H), 8.13-8.11 (d, *J* = 5.5 Hz, 1H), 7.40-7.39 (d, *J* = 5.3 Hz, 1H), 7.25-7.24 (d, *J* = 5.5 Hz, 1H), 5.45

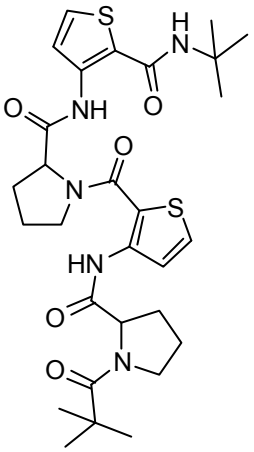

4f

(s, 1H), 4.74 (bs, 1H), 4.61-4.58 (dd, *J* = 8.5 Hz, 1H), 4.19-4.18 (m, 1H), 4.00-3.94 (m, 1H), 3.78-3.72 (m, 1H), 3.66-3.61 (m, 1H), 2.29-2.15 (m, 3H), 2.09-2.04 (m, 2H), 2.01—1.90 (m, 2H), 1.85-1.75 (m, 1H), 1.36 (s, 9H), 1.27 (s, 9H); ^{13}C NMR (100 MHz, $CDCl_3$) δ: 177.6, 170.3, 169.5, 164.4, 163.5, 144.7, 142.7, 128.4, 125.7, 123.0, 122.3, 113.5, 112.1, 63.6, 62.9, 52.1, 48.8, 48.2, 39.0, 28.8, 27.4, 25.5; ESI-MS: 601.84 $(M)^+$, 603.11 $(M+2H)^+$, 624.11 $(M+Na)^+$; Elemental analysis calculated for $C_{29}H_{39}N_5O_5S_2$: C, 57.88; H, 6.53; N, 11.64; S, 10.66; Found: C, 58.1; H, 6.5; N, 11.30; S, 9.91.

ethyl-2-(1-(2-(1-(2-(1-(2-(1-pivaloylpyrrolidine-2-carboxamido)thiophene-3-carbonyl)pyrrolidine-2-carboxamido)thiophene-3-carbonyl)pyrrolidine-2-carboxamido)thiophene-3-carbonyl)pyrrolidine-2-carboxamido)thiophene-3-carboxylate 5b:

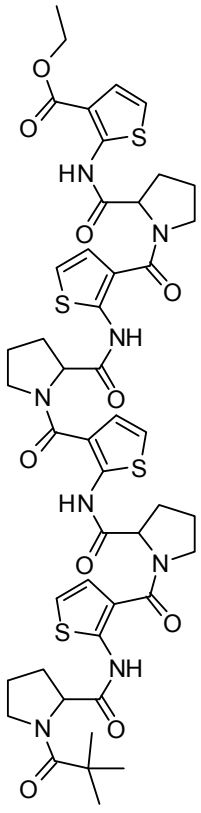

5b

Compound **5b** was isolated as a white solid (0.20 g, 70%), mp: 170-174 °C; $[\alpha]^{26}_D$: -266° (*c* = 1, $CHCl_3$); IR ($CHCl_3$) ν (cm^{-1}): 3439, 3263, 3114, 3015, 2982, 2447, 1674, 1600, 1489, 1435, 1403, 1357, 1179, 1097, 1033, 912, 876, 852, 833, 754, 699, 666; ^{1}H NMR (400 MHz, $CDCl_3$) δ: 12.04 (s, 1H), 11.86 (s, 1H), 11.57 (s, 1H), 11.42 (s, 1H), 7.31-7.27 (m, 3H), 7.22-7.20 (d, *J* = 5.5 Hz, 1H), 6.83-6.81 (d, *J* = 5.8 Hz, 2H), 6.79-6.78 (d, *J* = 5.5 Hz, 1H), 6.77-6.75 (d, *J* = 5.8 Hz, 1H), 4.83-4.8 (t, *J* = 7.3 Hz, 1H), 4.77-4.74 (m, 1H), 4.72-4.68 (m, 1H), 4.67-4.64 (dd, *J* = 8.4 Hz, 3.9Hz, 1H), 4.33-4.20 (q, *J* = 7 Hz, 2H), 4.14-4.09 (q, ethyl acetate), 4.01-3.94 (m, 1H), 3.91-3.85 (m, 4H), 3.76-3.71 (m, 3H), 2.34-2.25 (m, 3H), 2.18-1.95 (m, 10H), 1.92-1.84 (m, 3H), 1.36-1.33 (t, *J* = 7.2 Hz, 3H), 1.29 (s, 9H); ^{13}C NMR (100 MHz, $CDCl_3$) δ: 177.6, 169.6, 168.9, 166.4, 165.3, 148.0, 147.1, 147.0, 146.6, 123.7, 123.6, 123.1, 116.0 115.5, 115.3, 115.2, 62.7, 60.6, 50.0, 48.3, 38.9, 28.8, 28.3, 27.2, 25.6, 14.1; MALDI-TOF: 1018.7148 $(M)^+$, 1019.7191 $(M+H)^+$, 1020.7153 $(M+2H)^+$, 1043.7069 $(M+Na-1)^+$, 1041.7144 $(M+Na)^+$, 1042.7101 $(M+Na+1)^+$, 1043.7061

$(M+Na+2)^+$, 1056.6581 $(M+K-1)^+$, 1057.6554 $(M+K)^+$, 1058.6558 $(M+K+1)^+$, 1059.6614 $(M+K+2)^+$; Elemental analysis calculated for $C_{47}H_{54}N_8O_{10}S_4$: C, 55.38; H, 5.34; N, 10.99; S, 12.58; Found: C, 56.5; H, 5.8; N, 10.80; S, 12.60.

methyl-3-(1-(3-(1-(3-(1-(3-(1-pivaloylpyrrolidine-2-carboxamido)thiophene-2-carbonyl)pyrrolidine-2-carboxamido)thiophene-2-carbonyl)pyrrolidine-2-carboxamido)thiophene-2-carbonyl)pyrrolidine-2-carboxamido)thiophene-2-carboxylate 6b:

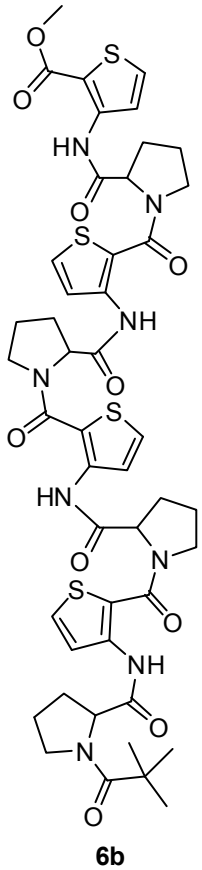

6b

Compound **6b** was isolated as a white solid (0.20 g, 70%), mp: 170-174 °C; $[\alpha]^{26}_D$: -158° (*c* = 1, $CHCl_3$); IR ($CHCl_3$) ν (cm^{-1}): 3243, 3131, 3019, 2400, 1681, 1563, 1557, 1444, 1404, 1360, 1283, 1246, 1215, 1096, 668, 648; ^1H NMR (400 MHz, $CDCl_3$) δ: 11.83 (s, 1H), 11.76 (s, 1H), 11.38 (s, 1H), 10.60 (s, 1H), 8.23-8.22 (d, *J* = 5.5 Hz, 1H), 8.14-8.12 (d, *J* = 5.5 Hz, 1H), 8.10-8.08 (d, *J* = 5.5 Hz, 1H), 8.06-8.04 (d, *J* = 5.3 Hz, 1H), 7.49-7.48 (d, *J* = 5.3 Hz, 2H), 7.44-7.43 (d, *J* = 5 Hz, 2H), 4.69 (bs, 2H), 4.55-4.52 (dd, *J* = 8.3 Hz, 3.8 Hz, 2H), 4.17 (bs, 1H), 4.14-4.08 (q, ethyl acetate), 4.04-3.94 (m, 3H), 3.83 (s, 3H), 3.80-3.75 (m, 2H), 3.73-3.70 (m, 1H), 3.67-3.61 (m, 1H), 2.27-2.16 (m, 6H), 2.13-2.01 (m, 6H), 1.95-1.89 (m, 4H), 1.80-1.77 (m, 1H), 1.24 (s, 9H); ^{13}C NMR (100 MHz, $CDCl_3$) δ: 177.6, 170.3, 169.6, 169.4, 164.5, 164.5, 164.3, 144.9, 144.5, 144.1, 131.9, 129.2, 129.0, 122.1, 121.7, 112.3, 112.1, 111.8, 110.5, 63.6, 62.9, 60.3, 51.9, 48.8, 48.3, 38.9, 29.6, 29.0, 27.3, 25.5; MALDI-TOF: 1018.7148 $(M)^+$, 1019.7191 $(M+H)^+$, 1020.7153 $(M+2H)^+$, 1026.9773 $(M+Na-1)^+$, 1027.1059 $(M+Na)^+$, 1028.7229 $(M+Na+1)^+$, 1029.7169 $(M+Na+2)^+$, 1042.6831 $(M+K-1)^+$, 1043.6793 $(M+K)^+$, 1044.6777 (M+K+1) Elemental analysis calculated for $C_{47}H_{54}N_8O_{10}S_4$: C, 54.96; H, 5.21; N, 11.15; S, 12.76; Found: C, 56.2; H, 6.1; N, 10.6; S, 11.9.

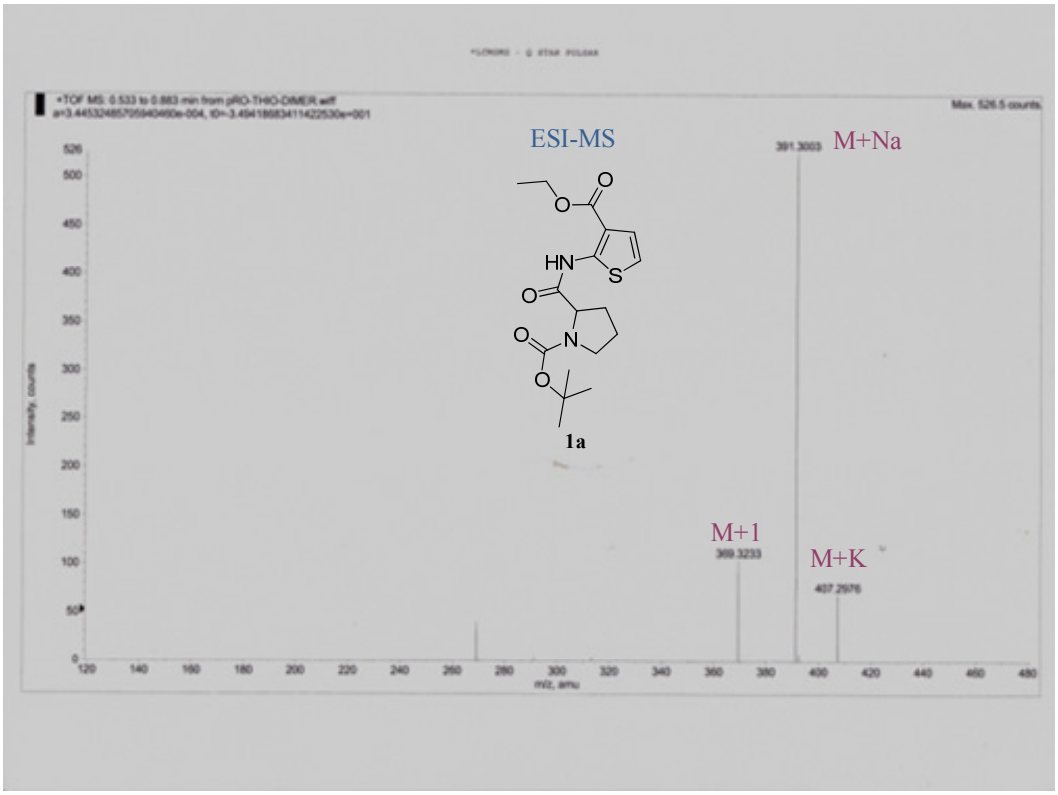
ESI-MS
391.3003 M+Na
M+1
389.3233
M+K
407.2976
1a

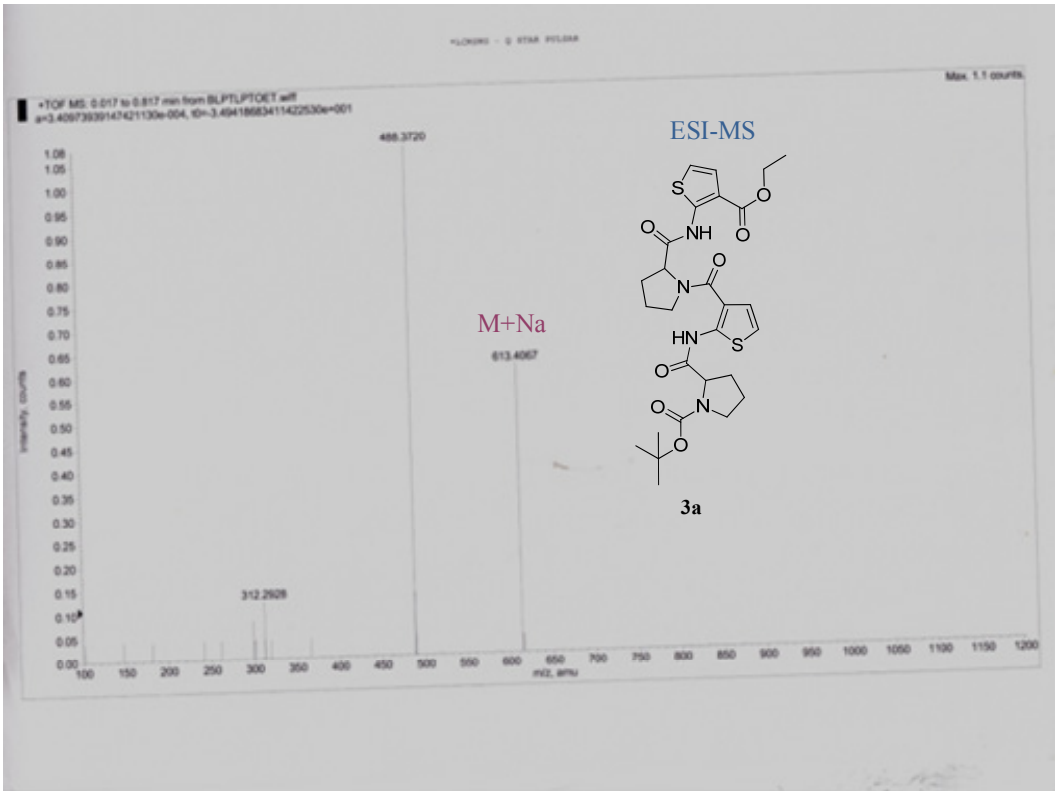
ESI-MS
488.3720
M+Na
613.4067
312.2928
3a

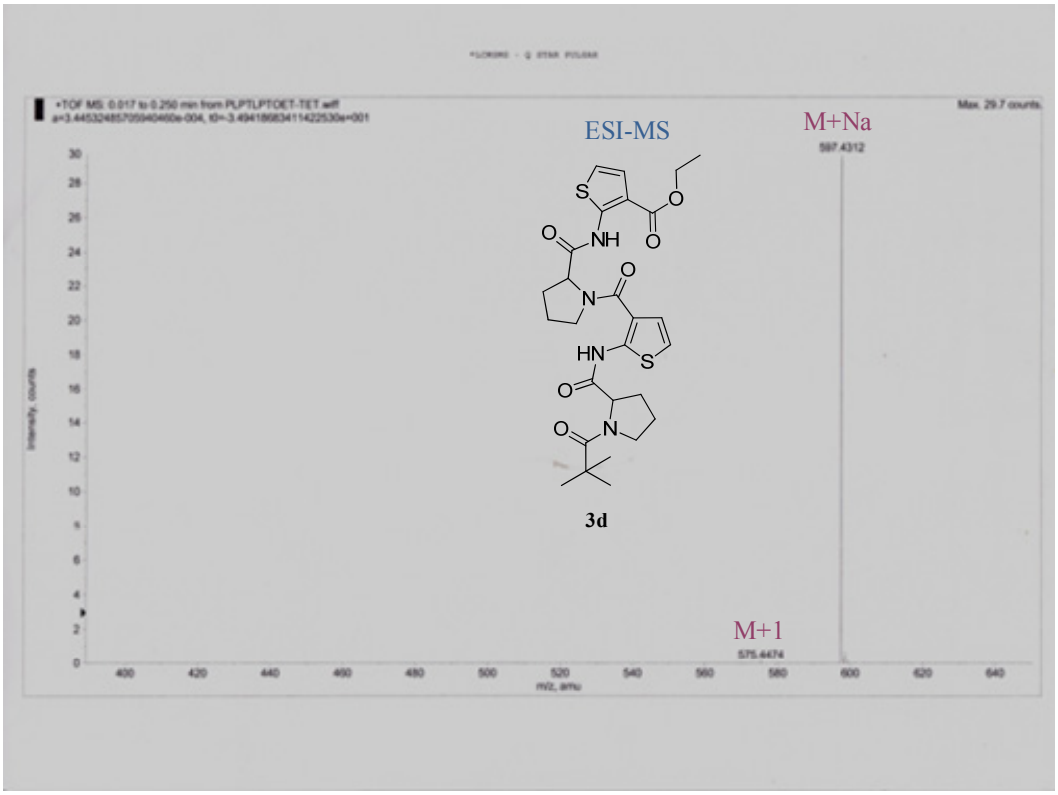
ESI-MS
M+Na
587.4312
M+1
575.4474
3d

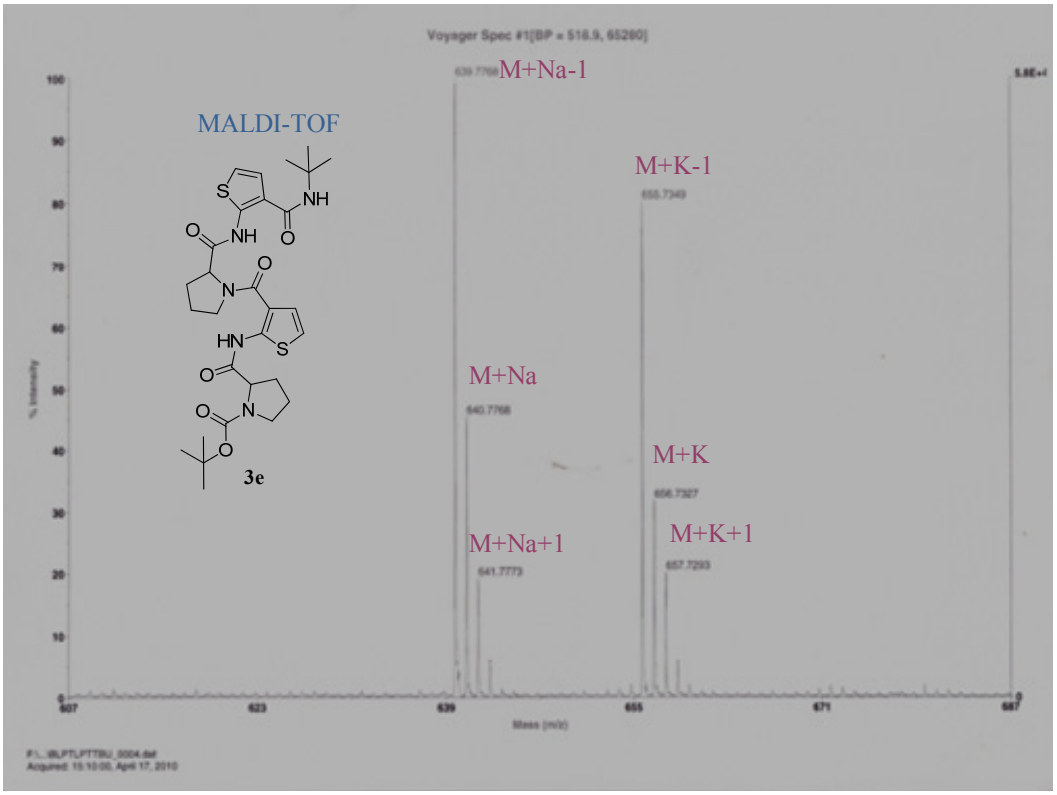
MALDI-TOF
M+Na-1
M+K-1
M+Na
M+K
M+Na+1
M+K+1
3e

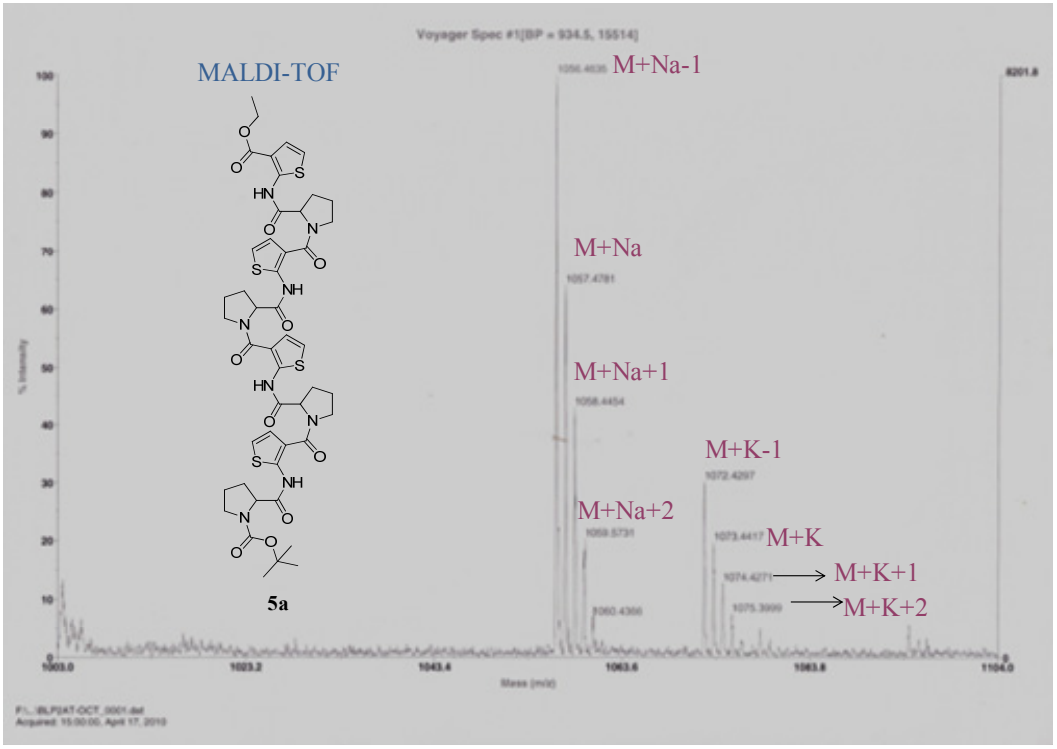
MALDI-TOF
5a
M+Na-1
M+Na
M+Na+1
M+K-1
M+Na+2
M+K
M+K+1
M+K+2

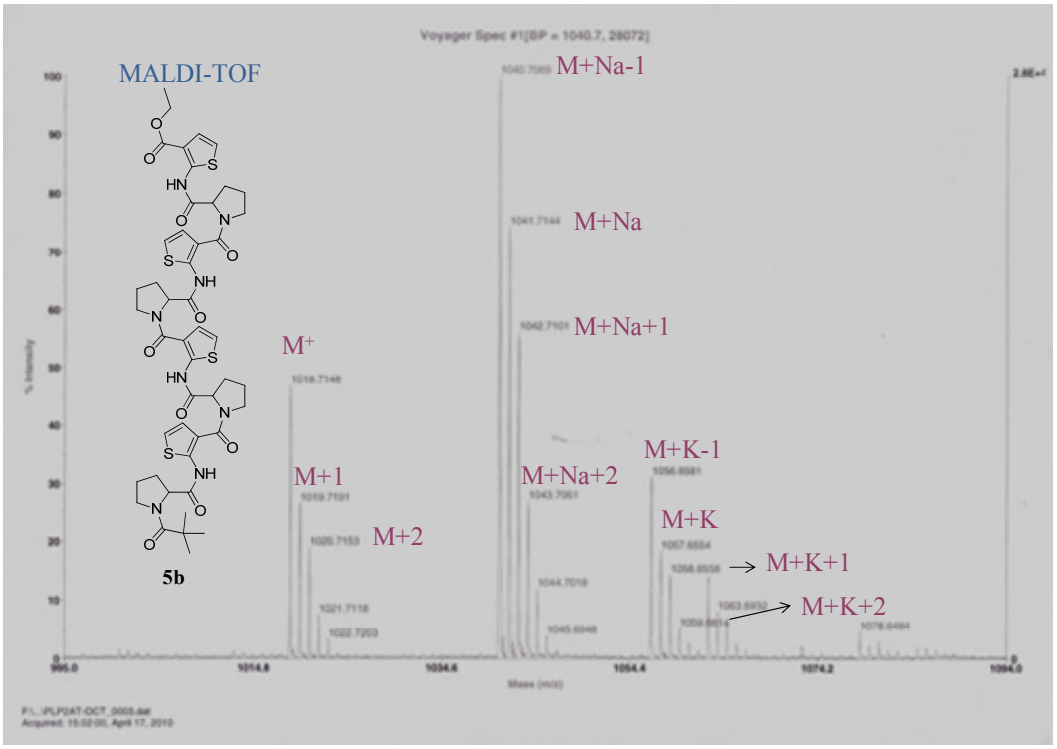
MALDI-TOF
5b
M+Na-1
M+Na
M+Na+1
M+
M+1
M+2
M+Na+2
M+K-1
M+K
M+K+1
M+K+2

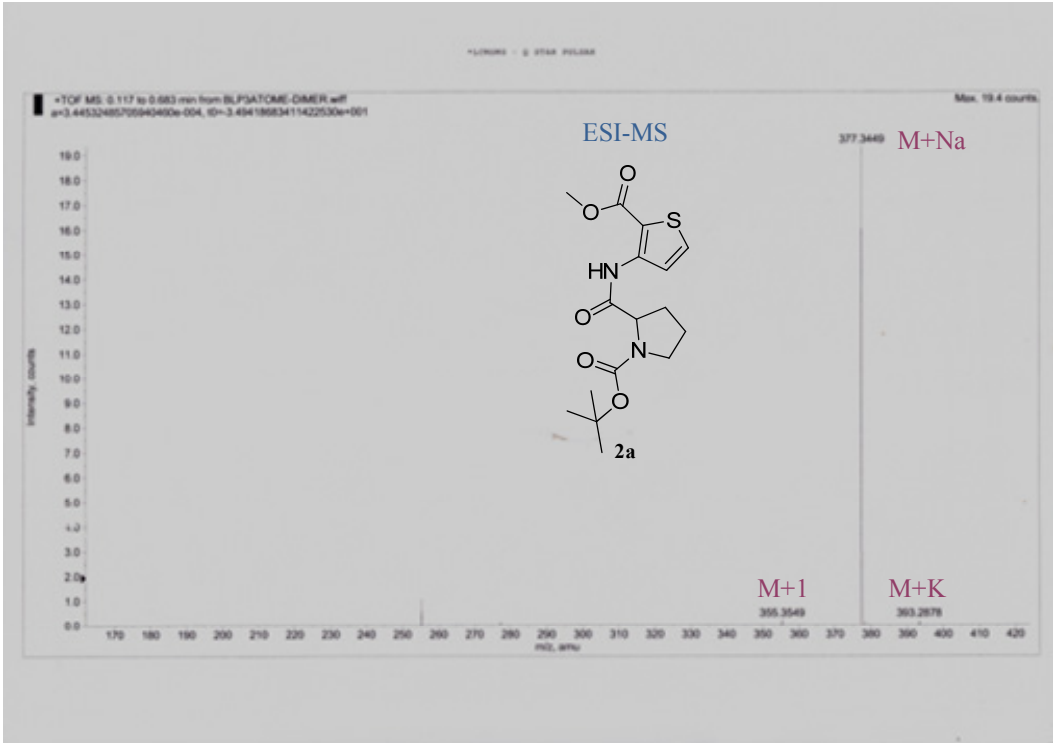
ESI-MS
377.3449 M+Na
M+1
355.3549
M+K
363.2878
2a

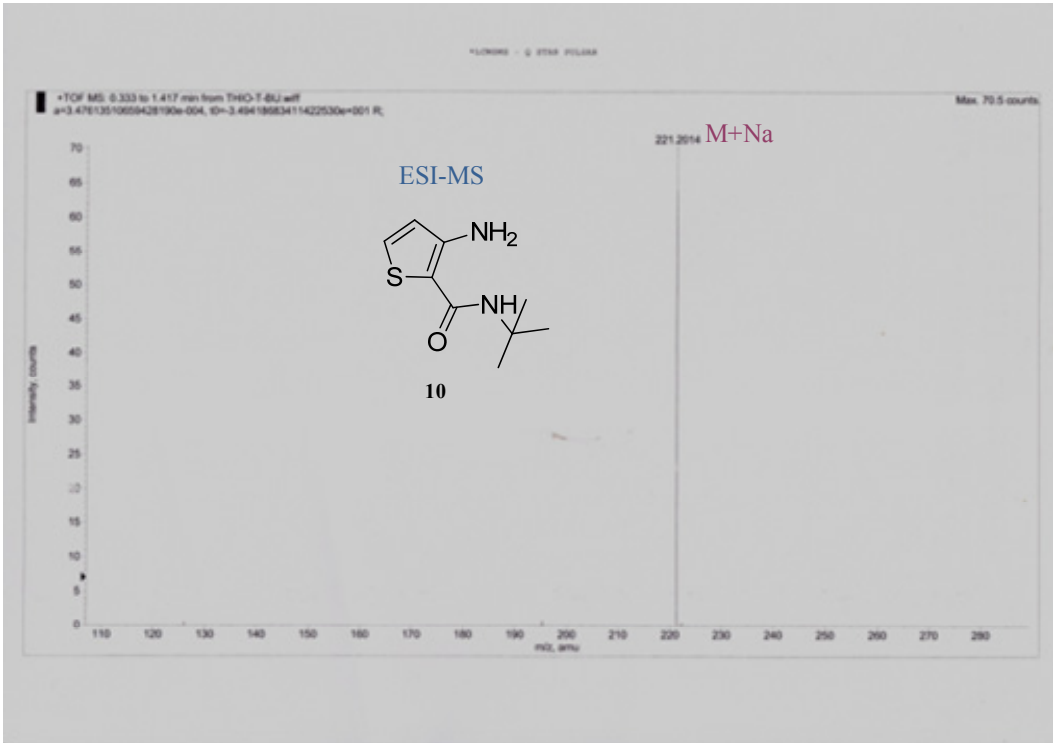
ESI-MS
221.2014 M+Na
10

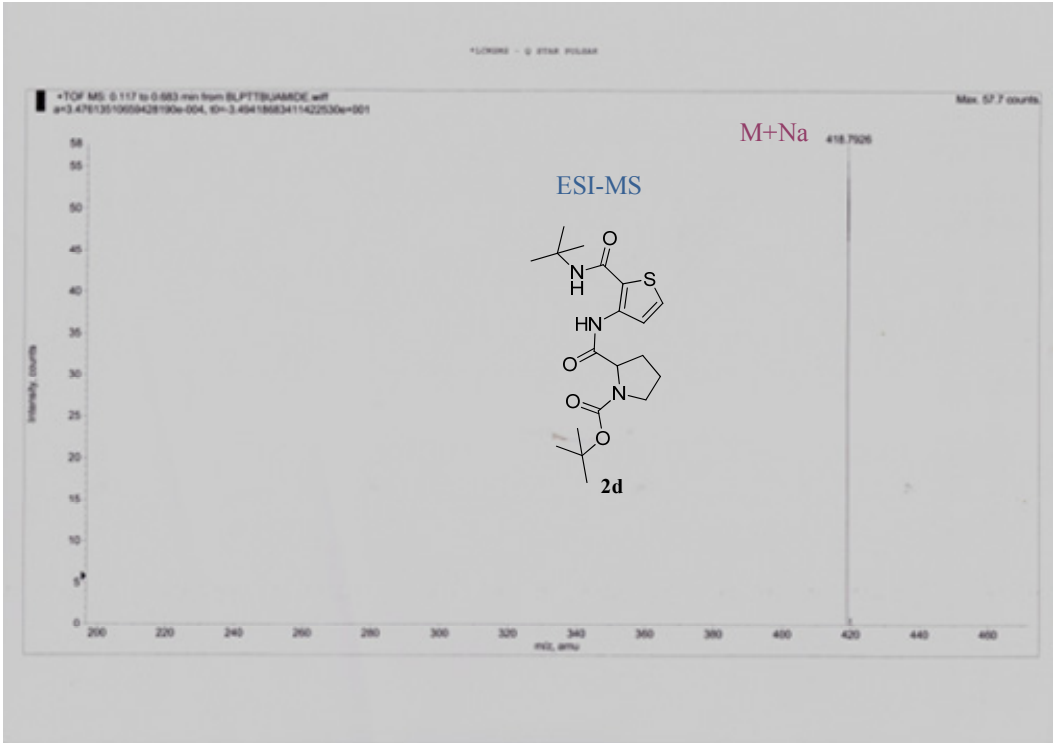
M+Na
418.7926
ESI-MS
2d

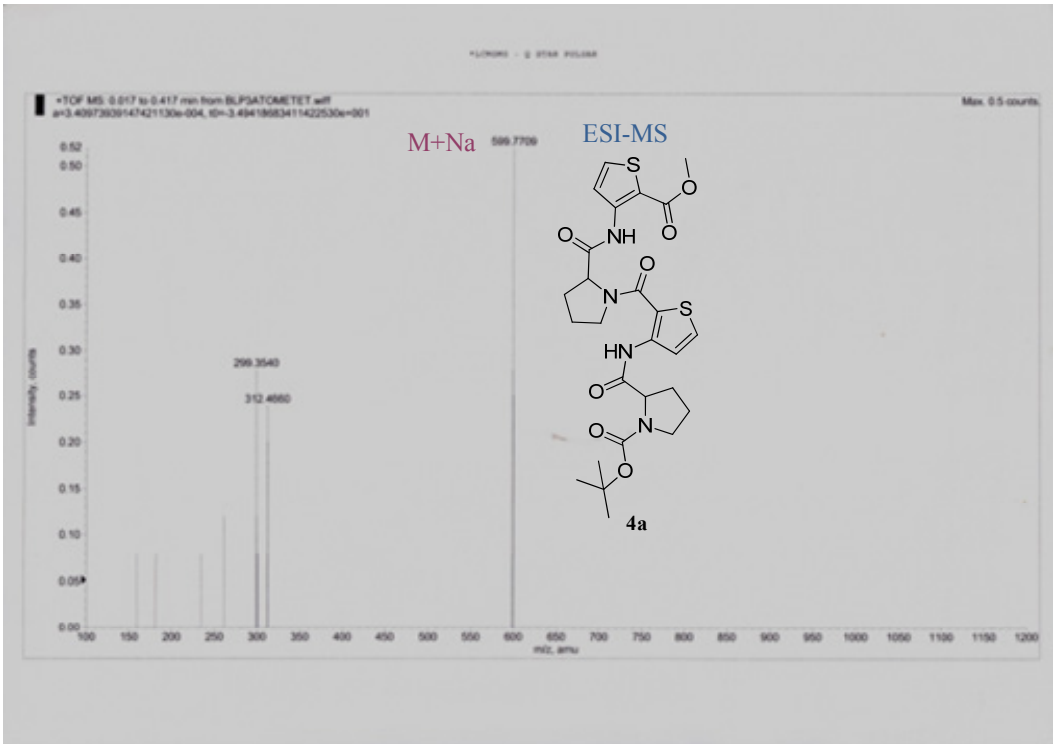
M+Na
599.7709
ESI-MS
299.3540
312.4660
4a

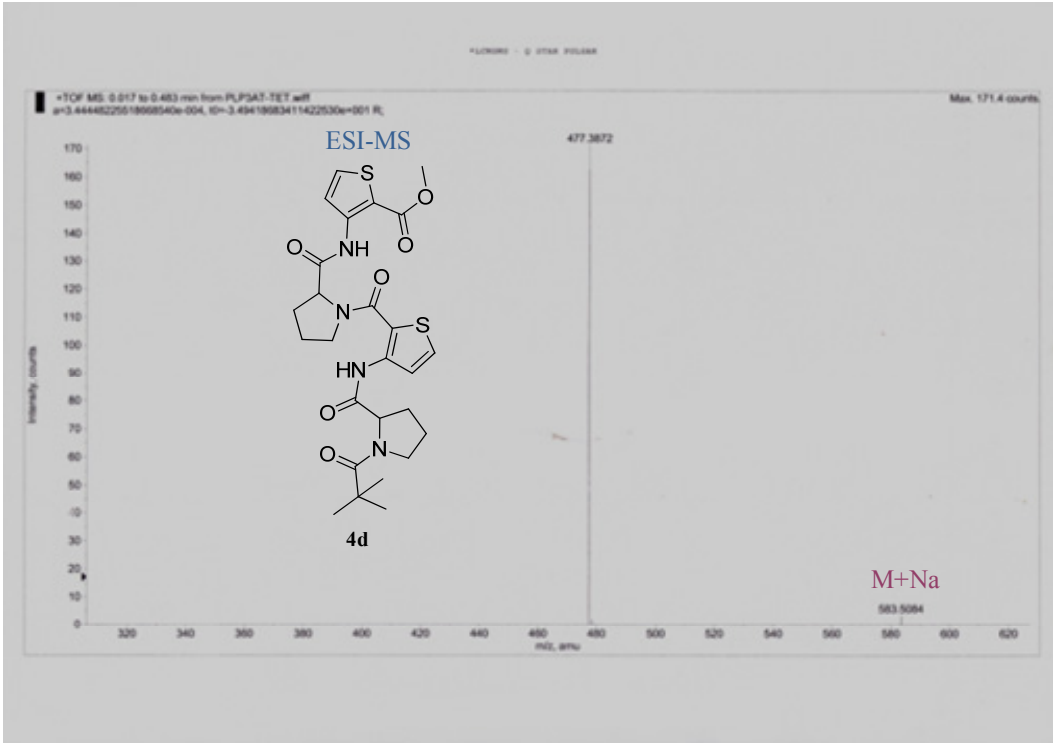
ESI-MS
477.3872
M+Na
583.5084
4d

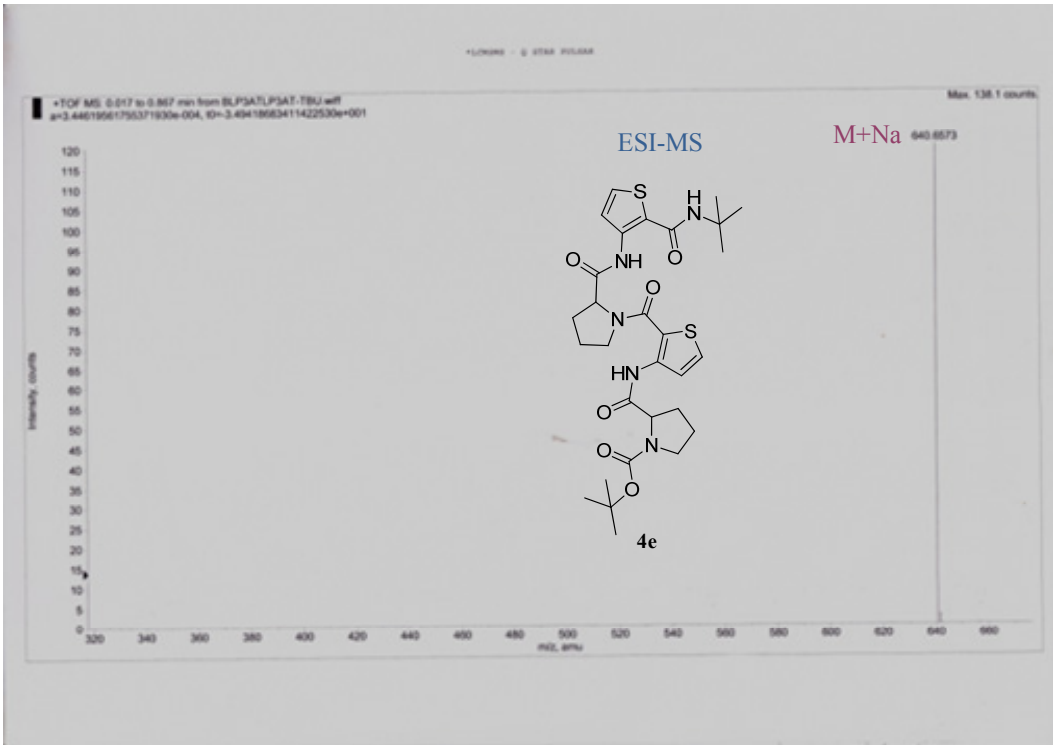
ESI-MS
M+Na
640.6573
4e

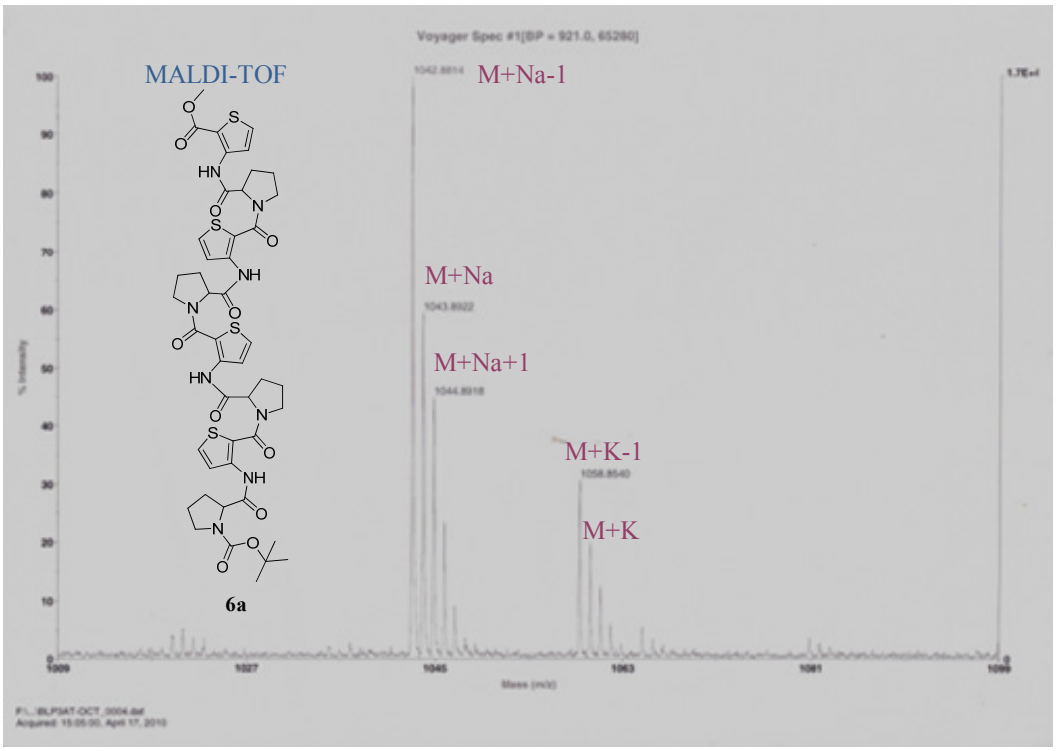
MALDI-TOF
6a
M+Na-1
M+Na
M+Na+1
M+K-1
M+K

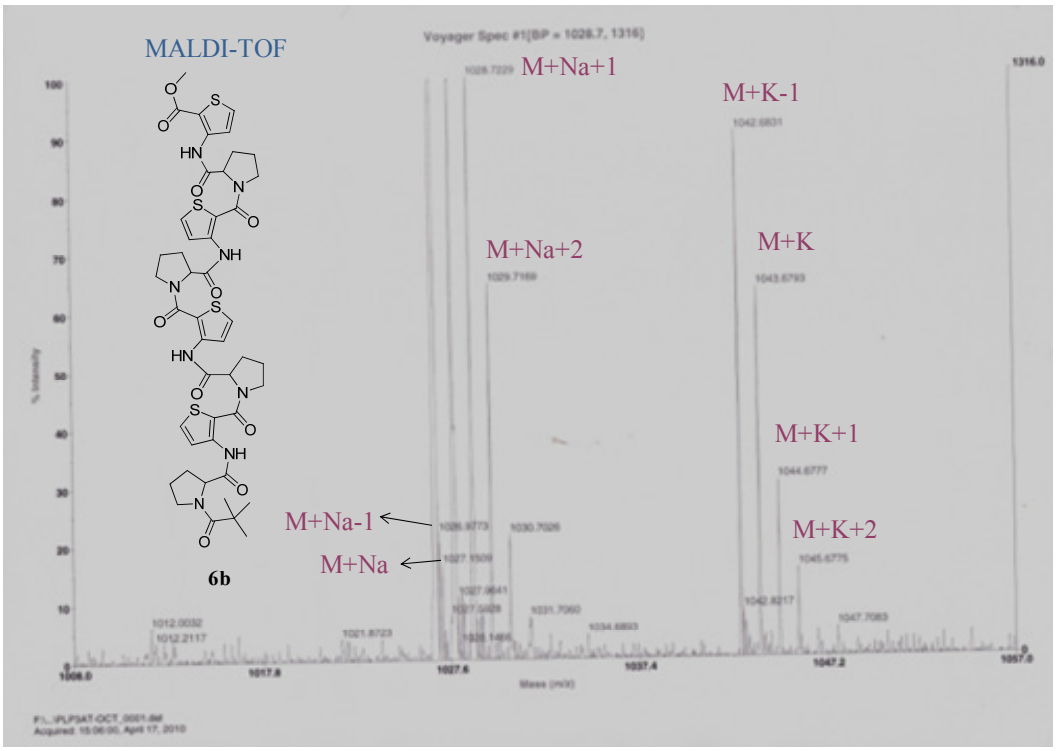
MALDI-TOF
6b
M+Na+1
M+K-1
M+Na+2
M+K
M+K+1
M+K+2
M+Na-1
M+Na

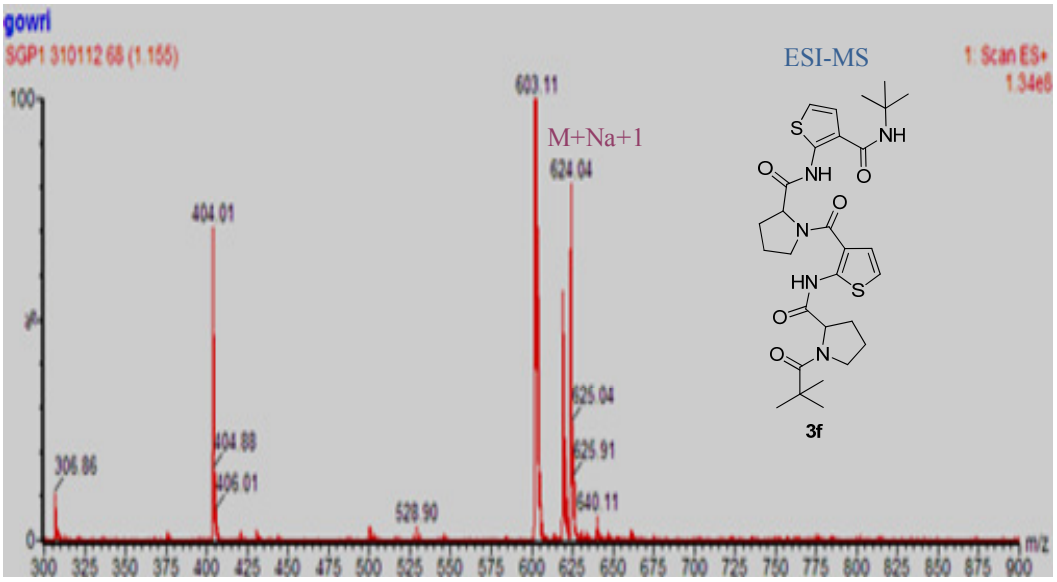
gowri
SGP1 310112 68 (1.155)
1: Scan ES+
1.34e8
ESI-MS
M+Na+1
603.11
624.04
404.01
625.04
404.88
625.91
406.01
640.11
306.86
528.90
3f
m/z

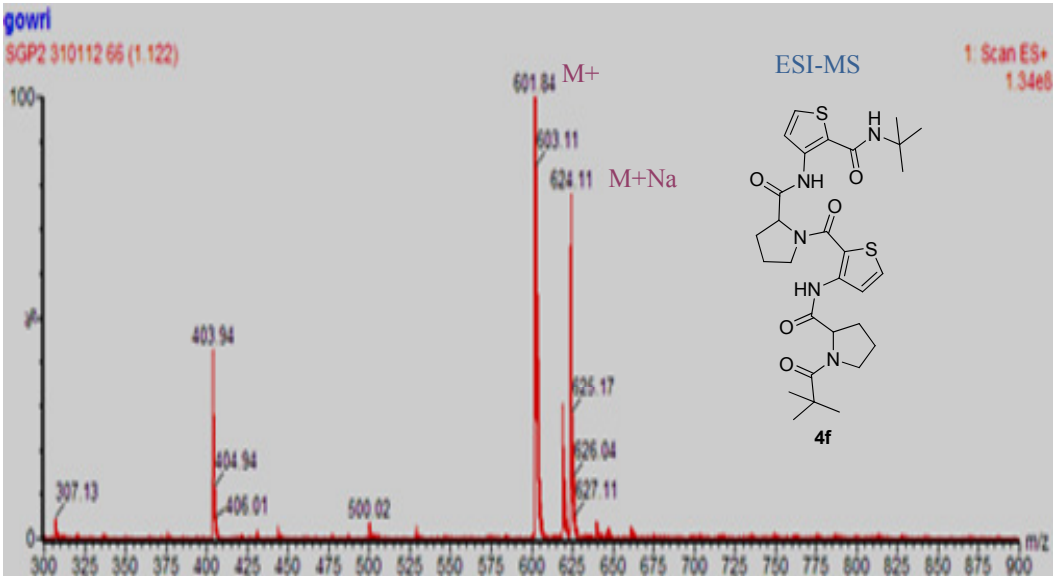
gowri
SGP2 310112 66 (1.122)
1: Scan ES+
1.34e8
ESI-MS
601.84 M+
603.11
624.11 M+Na
403.94
625.17
404.94
626.04
406.01
627.11
307.13
500.02
4f
m/z

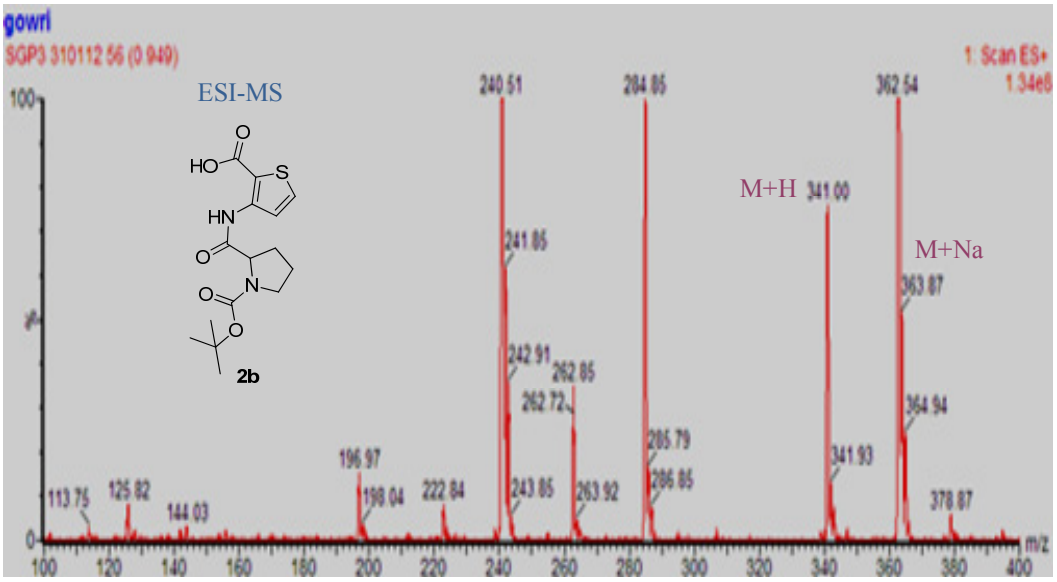
gowri
SGP3 310112 56 (0.949)
1: Scan ES+
1.34e8
ESI-MS
2b
M+H
M+Na
240.51
284.85
362.54
341.00
241.85
363.87
242.91
262.85
262.72
364.94
285.79
341.93
196.97
286.85
198.04
222.84
243.85
263.92
378.87
113.75
125.82
144.03
m/z

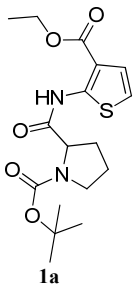

1a

NOTE: Signal broadening and / or multiple set of signals seen are due to rotamer formation at the N-terminus (N-^{t}BOC Pro effect: *Chem. Eur. J.* **2008**, 14, 6192).

^{1}H NMR(200MHz, $CDCl_3$)

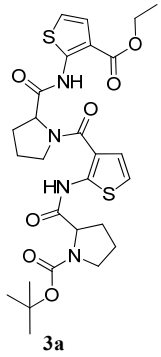

3a

NOTE: Signal broadening and / or multiple set of signals seen are due to rotamer formation at the N-terminus (N-^{t}BOC Pro effect: *Chem. Eur. J.* **2008**, 14, 6192).

^{1}H NMR(400MHz, $CDCl_3$)

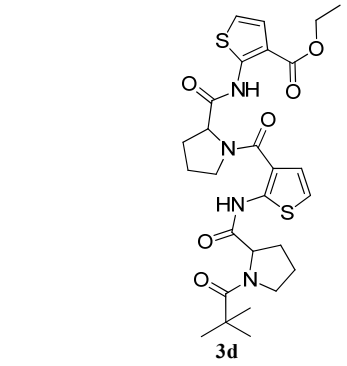

3d

^{1}H NMR(400MHz, $CDCl_3$)

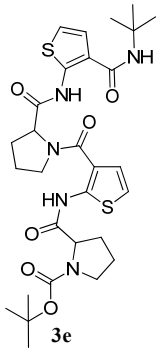

3e

NOTE: Signal broadening and / or multiple set of signals seen are due to rotamer formation at the N-terminus (N-^{t}BOC Pro effect: *Chem. Eur. J.* **2008**, 14, 6192)

^{1}H NMR(200MHz, $CDCl_3$)

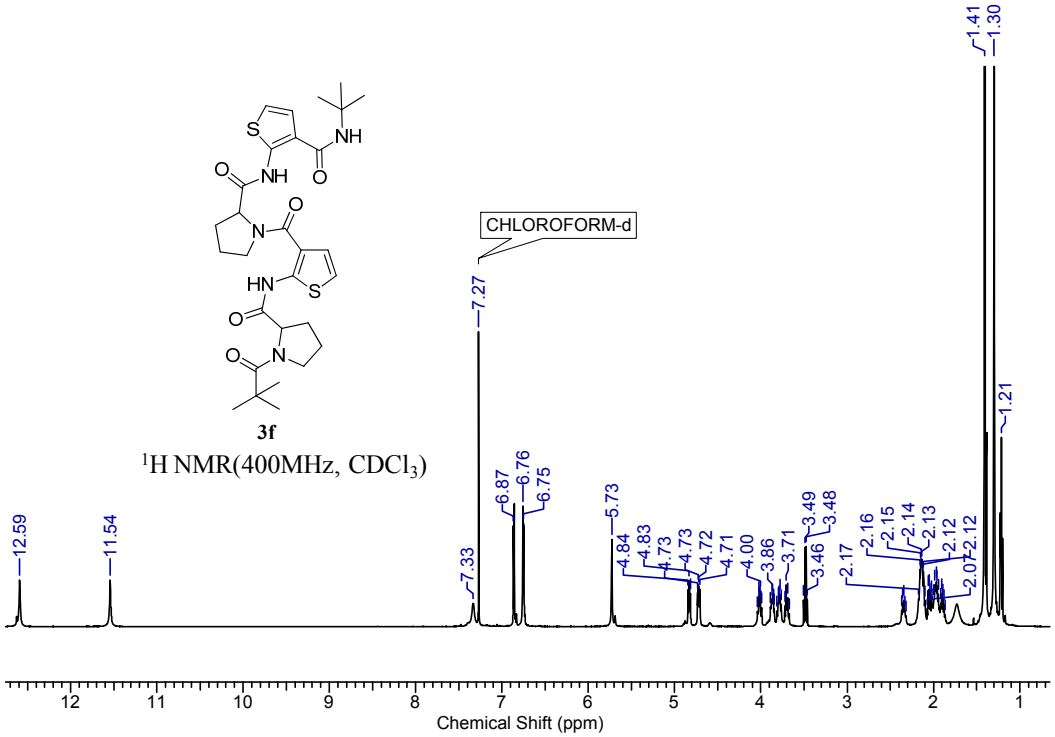

3f

^{1}H NMR(400MHz, $CDCl_3$)

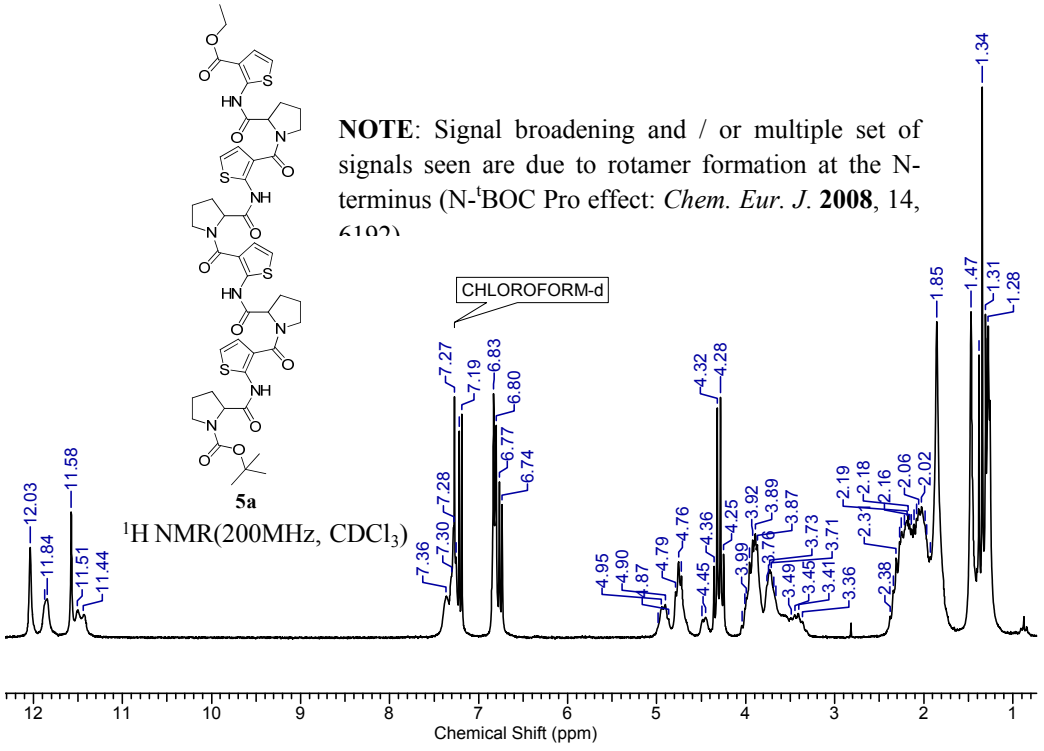

5a

^{1}H NMR(200MHz, $CDCl_3$)

NOTE: Signal broadening and / or multiple set of signals seen are due to rotamer formation at the N-terminus (N-^{t}BOC Pro effect: *Chem. Eur. J.* **2008**, 14, 6192)

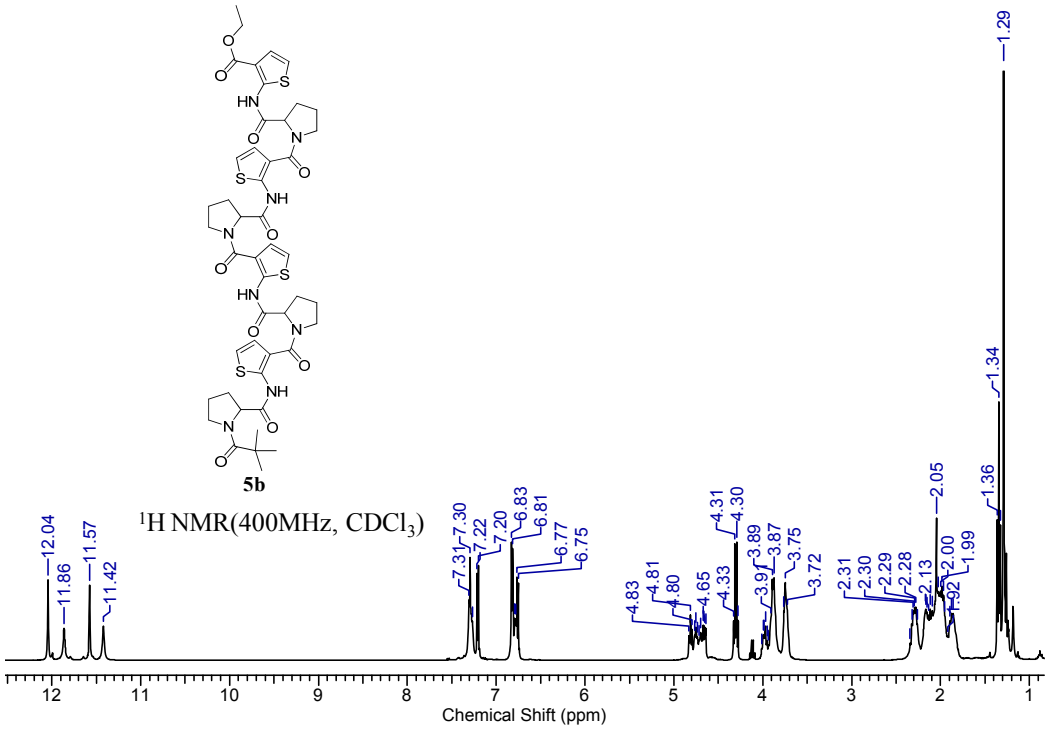

NOTE: Signal broadening and / or multiple set of signals seen are due to rotamer formation at the N-terminus (N-^{t}BOC Pro effect: *Chem. Eur. J.* **2008**, 14, 6192).

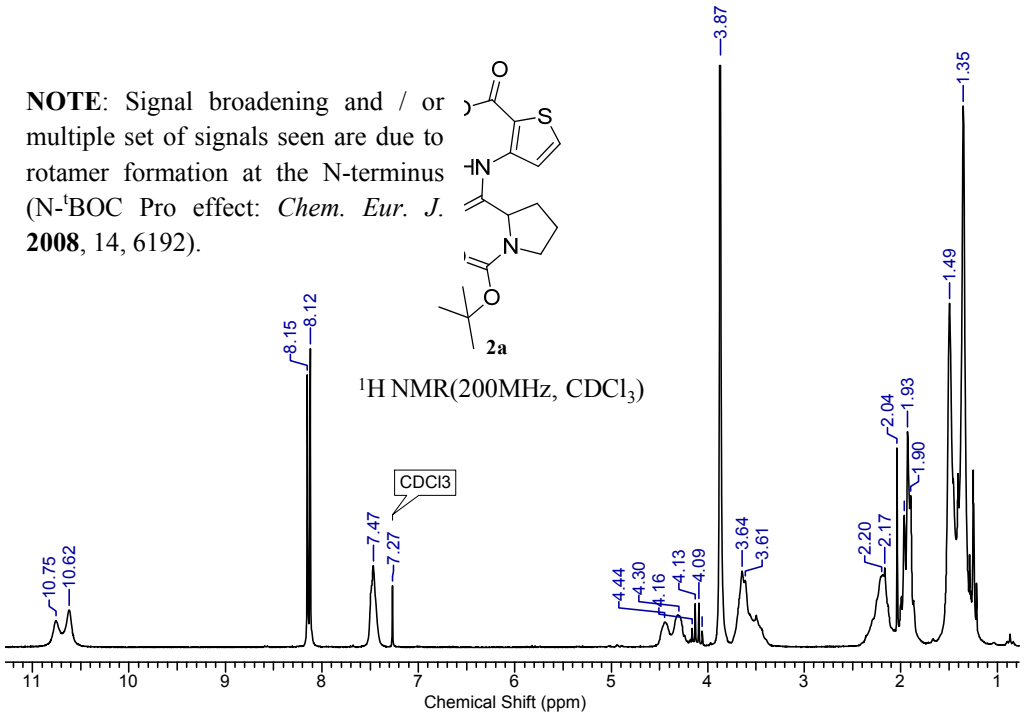

NOTE: Signal broadening and / or multiple set of signals seen are due to rotamer formation at the N-terminus (N-^{t}BOC Pro effect: *Chem. Eur. J.* **2008**, 14, 6192).

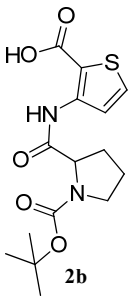

2b

^{1}H NMR(500MHz, $CDCl_3$)

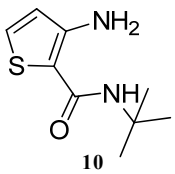

10

^{1}H NMR(200MHz, $CDCl_3$)

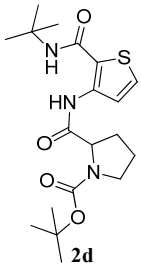

2d

NOTE: Signal broadening and / or multiple set of signals seen are due to rotamer formation at the N-terminus (N-^{t}BOC Pro effect: *Chem. Eur. J.* **2008**, 14, 6192).

^{1}H NMR(200MHz, $CDCl_3$)

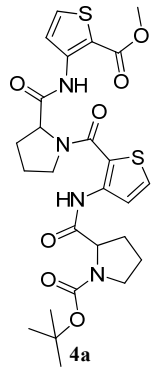

4a

NOTE: Signal broadening and / or multiple set of signals seen are due to rotamer formation at the N-terminus (N-^{t}BOC Pro effect: *Chem. Eur. J.* **2008**, 14, 6192).

^{1}H NMR(400MHz, $CDCl_3$)

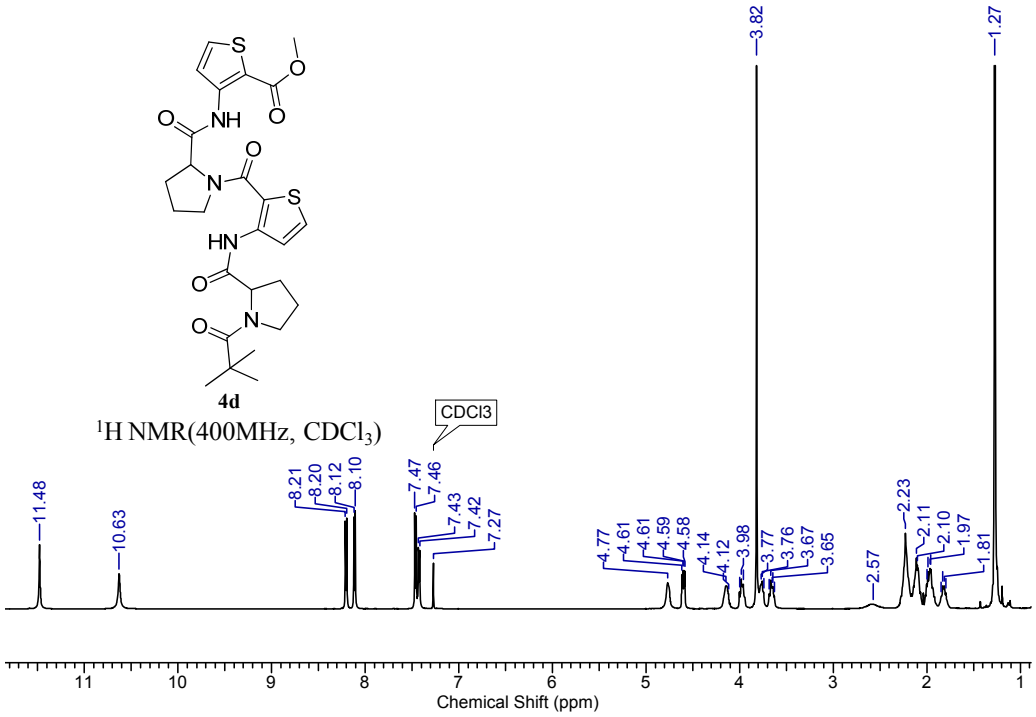

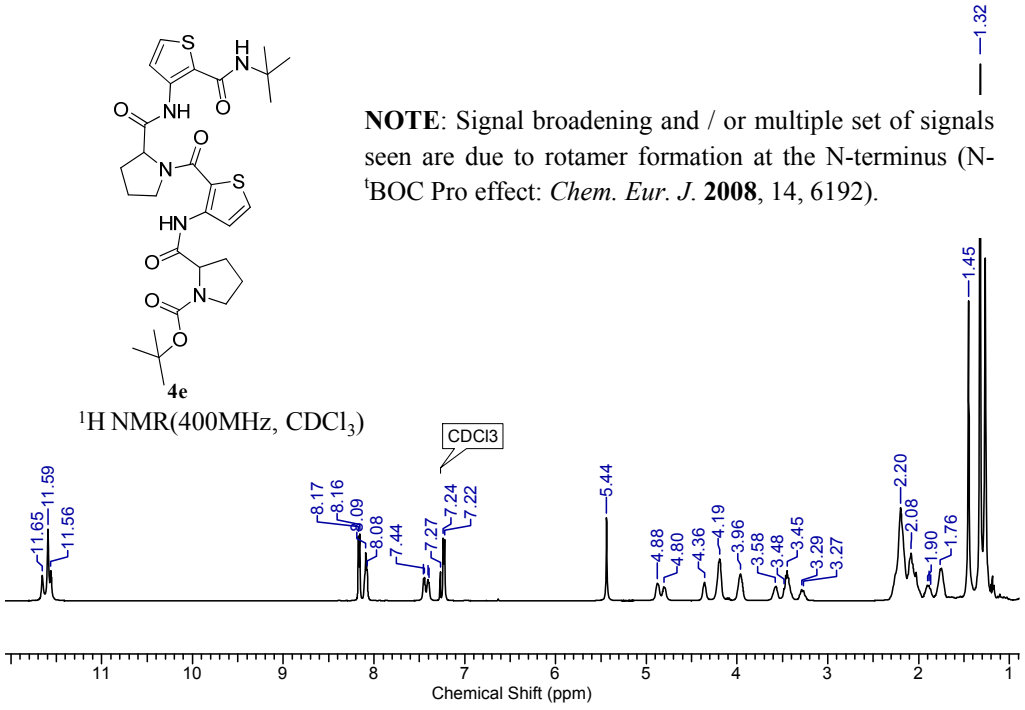

NOTE: Signal broadening and / or multiple set of signals seen are due to rotamer formation at the N-terminus (N-^{t}BOC Pro effect: *Chem. Eur. J.* **2008**, 14, 6192).

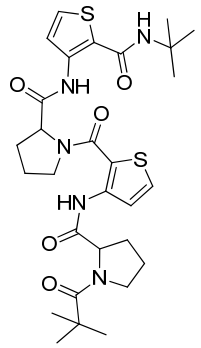

4f

^{1}H NMR(400MHz, $CDCl_3$)

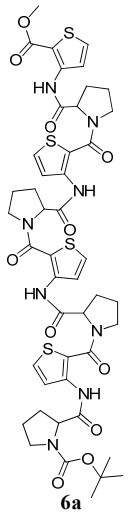

6a

NOTE: Signal broadening and / or multiple set of signals seen are due to rotamer formation at the N-terminus (N-^{t}BOC Pro effect: *Chem. Eur. J.* **2008**, 14, 6192).

^{1}H NMR(400MHz, $CDCl_3$)

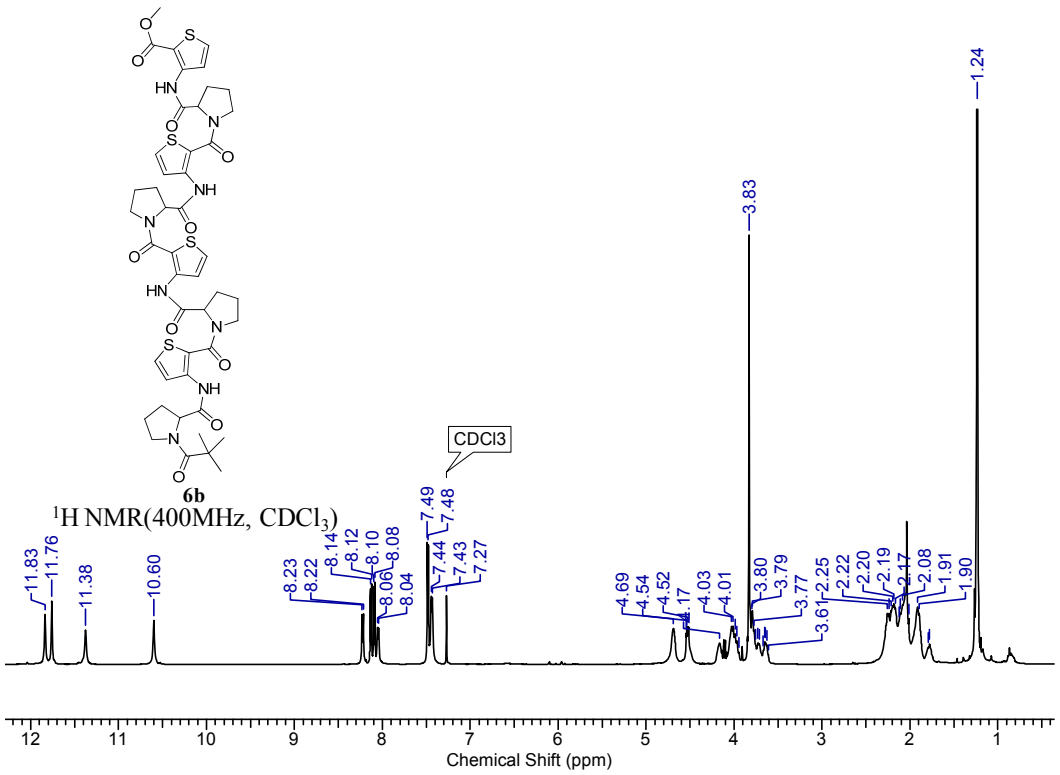
6b
^{1}H NMR(400MHz, $CDCl_3$)
CDCl3
11.83
11.76
11.38
10.60
8.23
8.22
8.14
8.12
8.10
8.08
8.06
8.04
7.49
7.48
7.44
7.43
7.27
4.69
4.54
4.52
4.17
4.03
4.01
3.83
3.80
3.79
3.77
3.61
2.25
2.22
2.20
2.19
2.17
2.08
1.91
1.90
1.24
12
11
10
9
8
7
6
5
4
3
2
1
Chemical Shift (ppm)

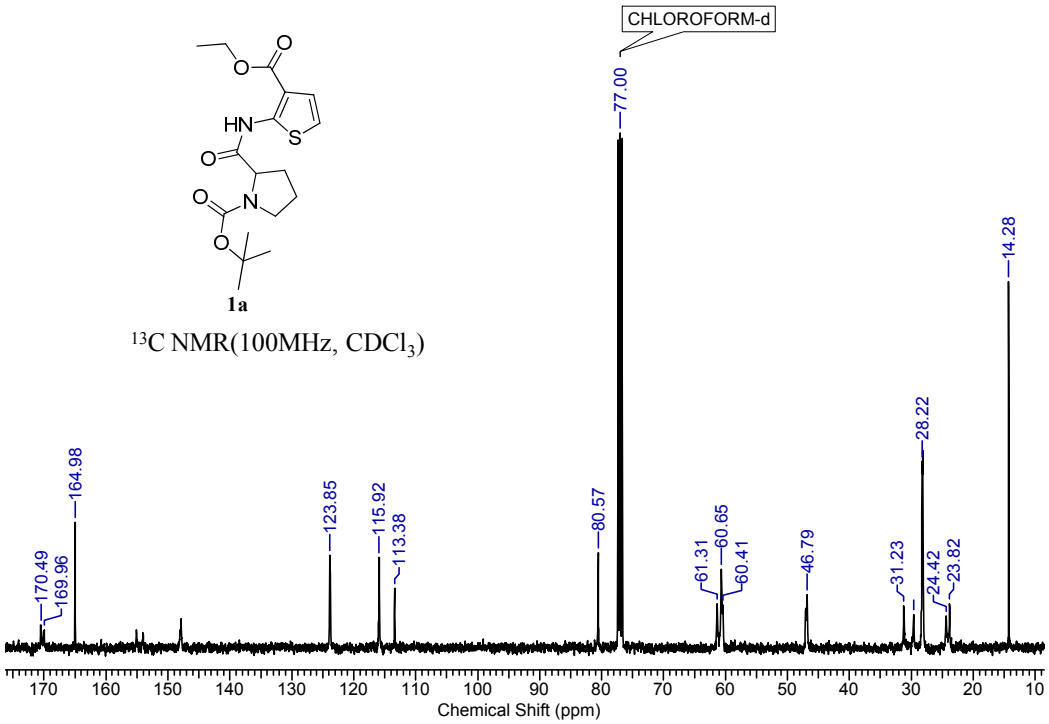

1a

^{13}C NMR(100MHz, $CDCl_3$)

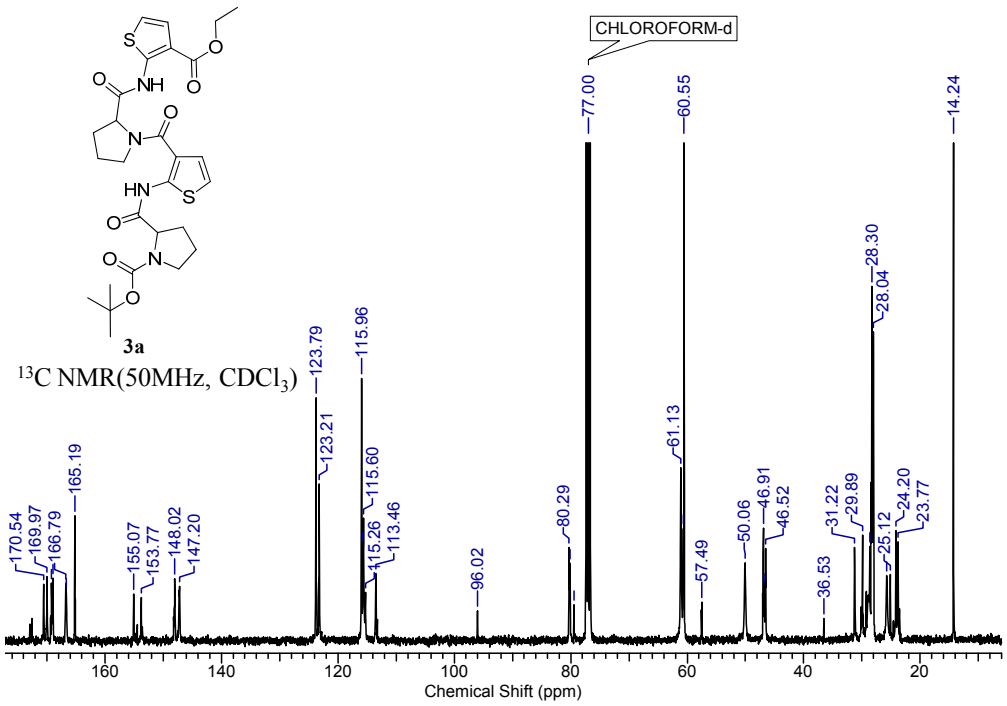

3a

^{13}C NMR(50MHz, $CDCl_3$)

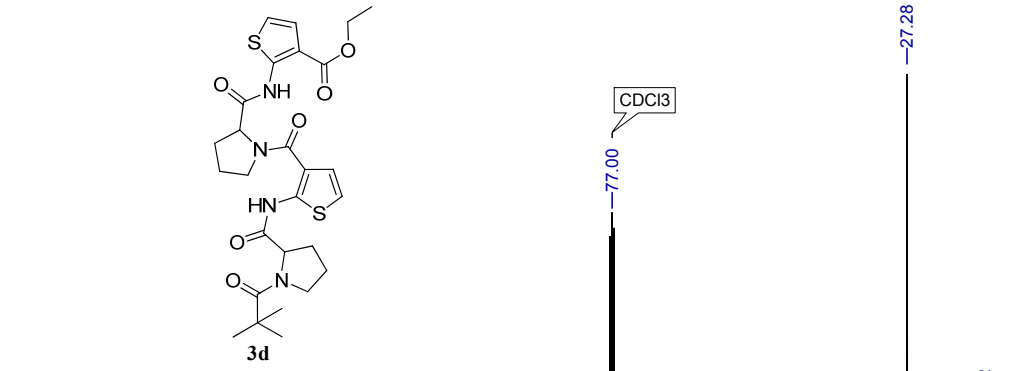

3d

^{13}C NMR(100MHz, $CDCl_3$)

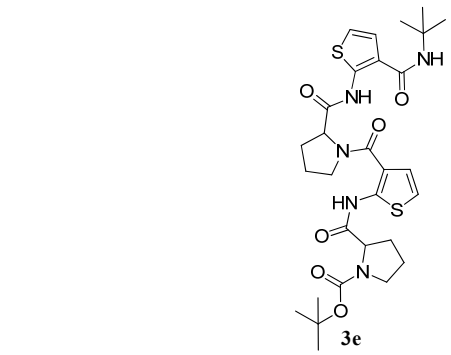

3e

^{13}C NMR (50MHz, $CDCl_3$)

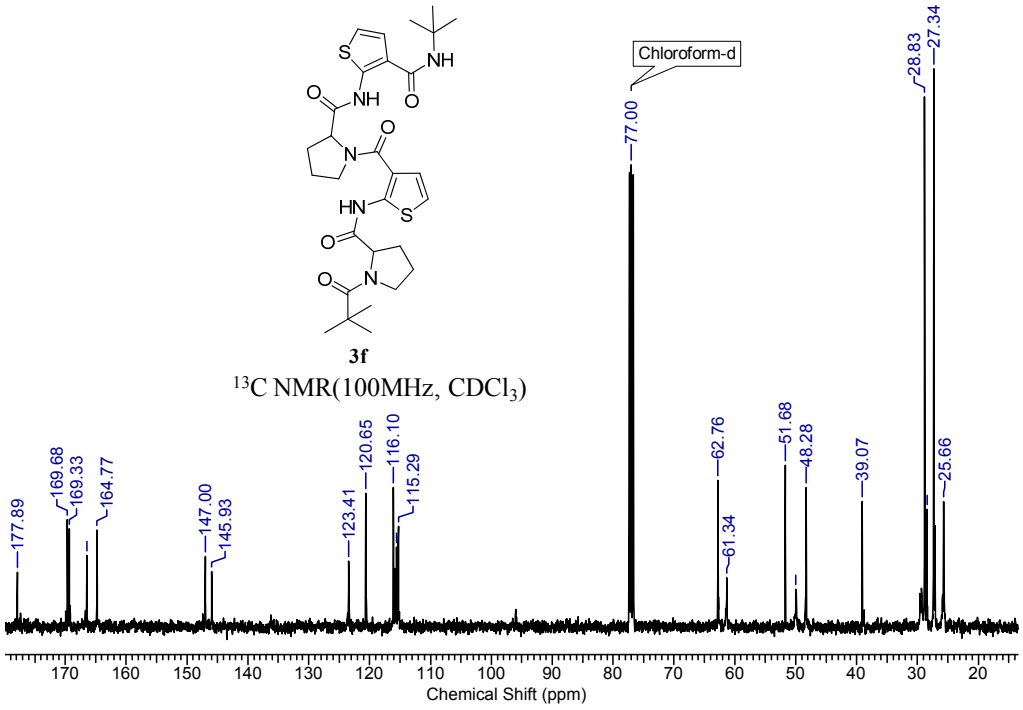

3f

^{13}C NMR(100MHz, $CDCl_3$)

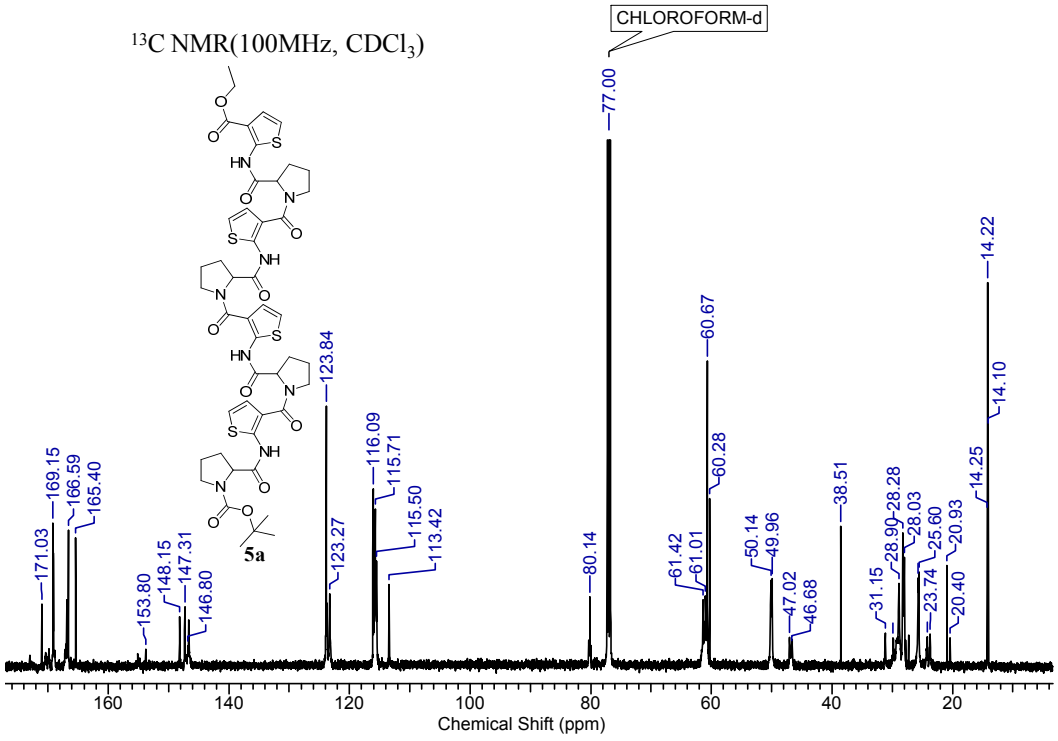

5a

^{13}C NMR(100MHz, $CDCl_3$)

^{13}C NMR(50MHz, $CDCl_3$)

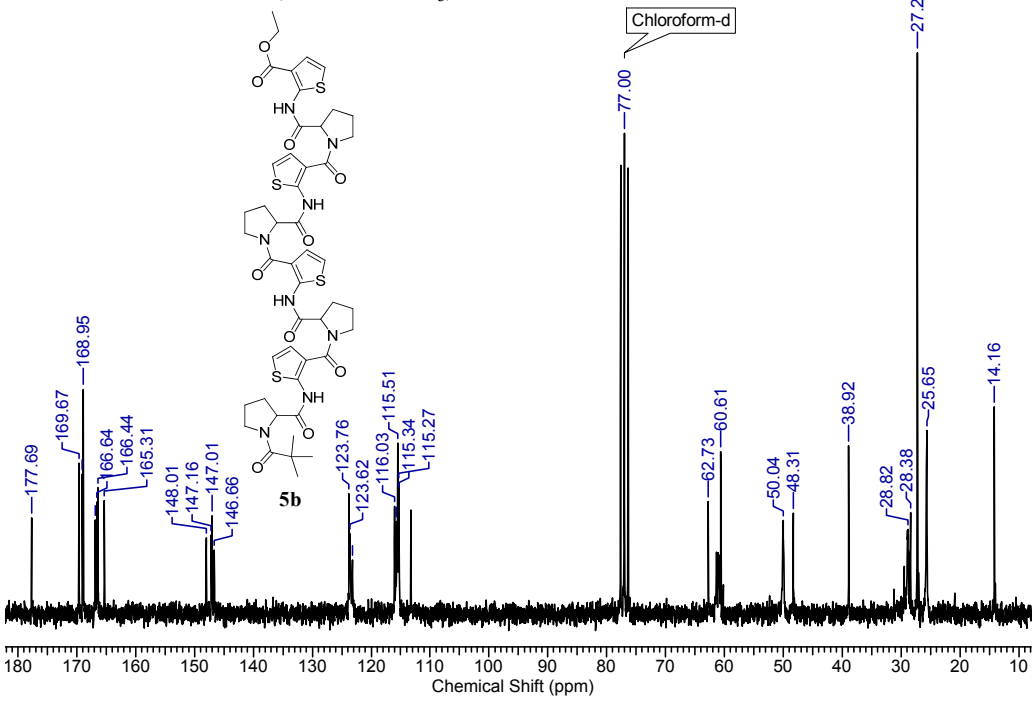

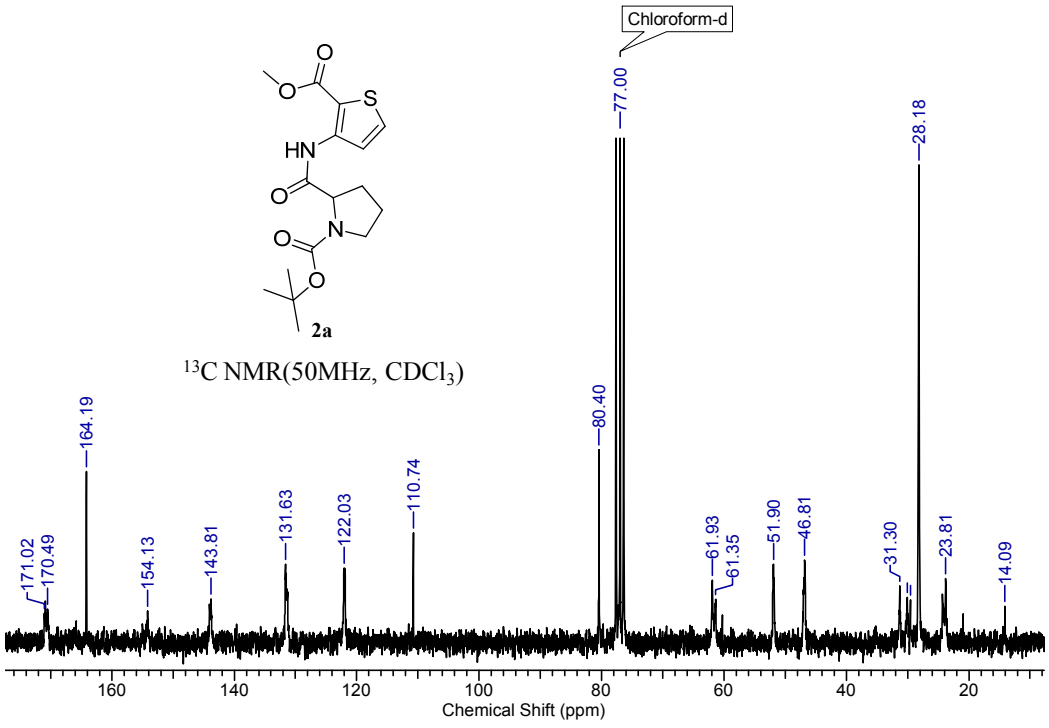

^{13}C NMR(50MHz, $CDCl_3$)

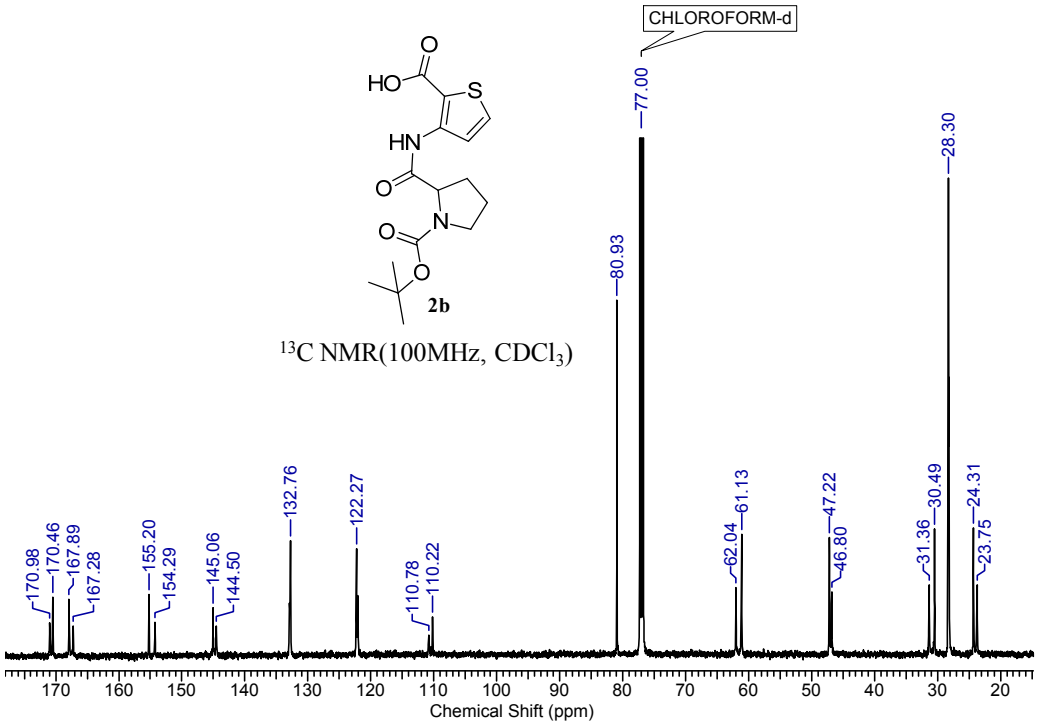

2b

^{13}C NMR(100MHz, $CDCl_3$)

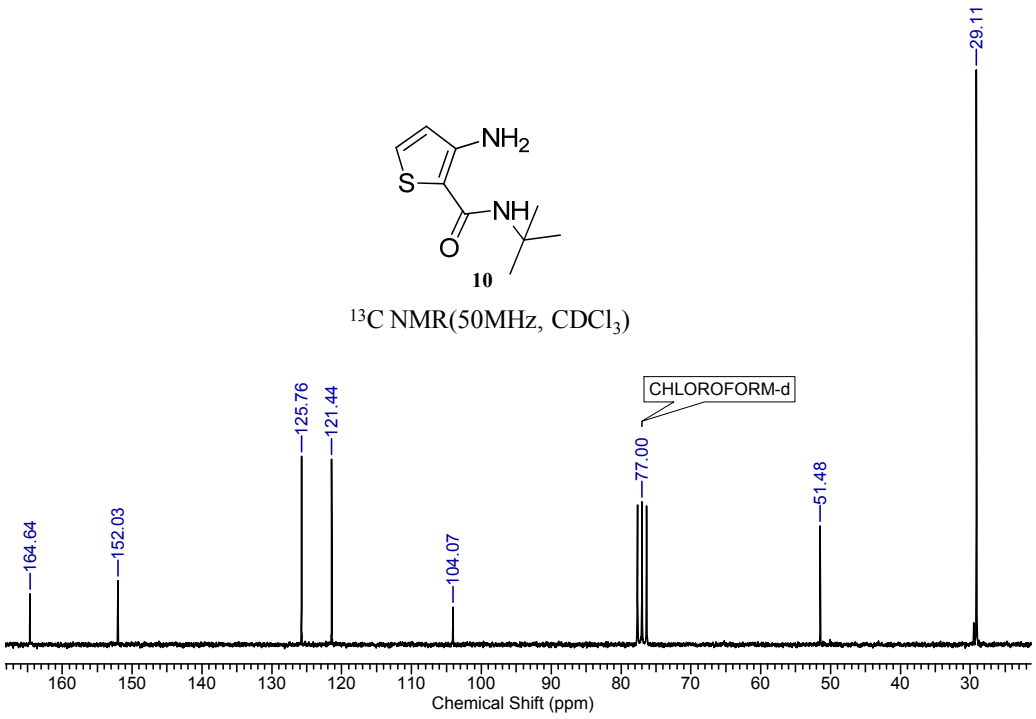

10

^{13}C NMR(50MHz, $CDCl_3$)

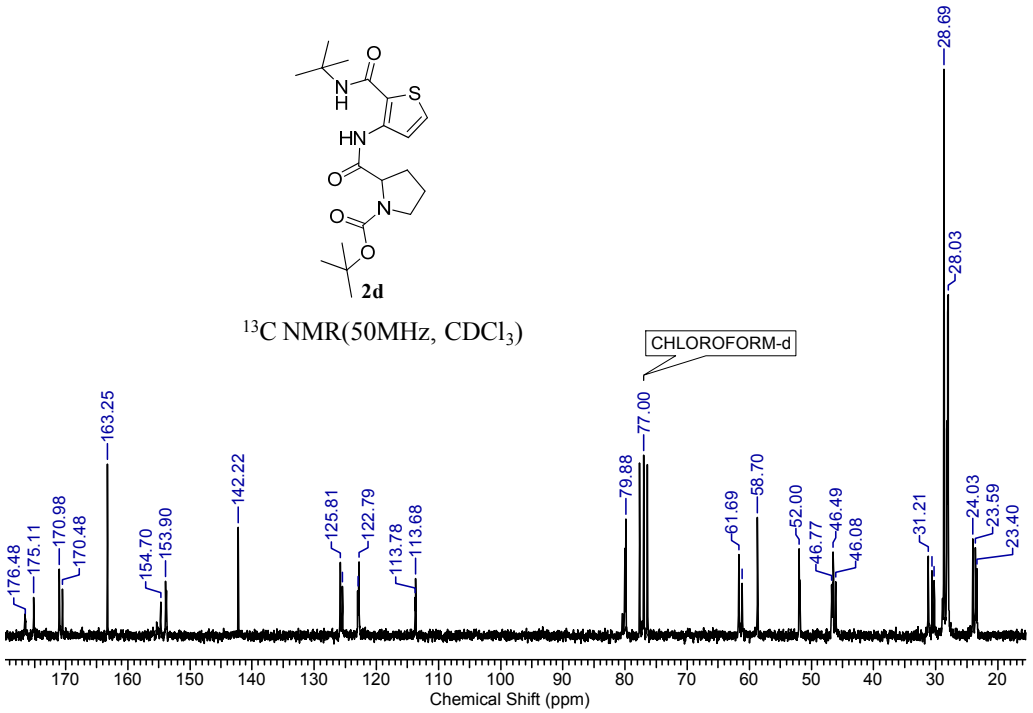
2d
^{13}C NMR(50MHz, CDCl$_3$)
CHLOROFORM-d
28.69
28.03
163.25
142.22
125.81
122.79
113.78
113.68
79.88
77.00
61.69
58.70
52.00
46.77
46.49
46.08
31.21
24.03
23.59
23.40
176.48
175.11
170.98
170.48
154.70
153.90
Chemical Shift (ppm)

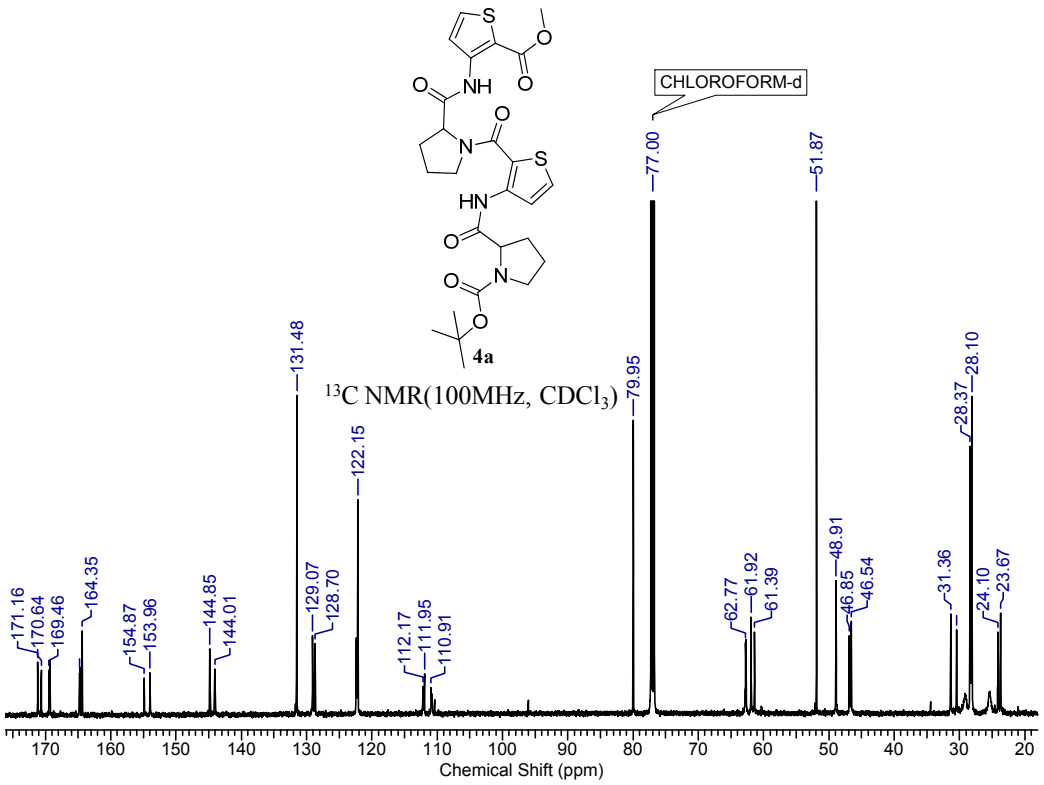
4a
^{13}C NMR(100MHz, CDCl$_3$)
CHLOROFORM-d
131.48
122.15
79.95
77.00
51.87
48.91
46.85
46.54
28.37
28.10
24.10
23.67
31.36
62.77
61.92
61.39
129.07
128.70
112.17
111.95
110.91
171.16
170.64
169.46
164.35
154.87
153.96
144.85
144.01
Chemical Shift (ppm)

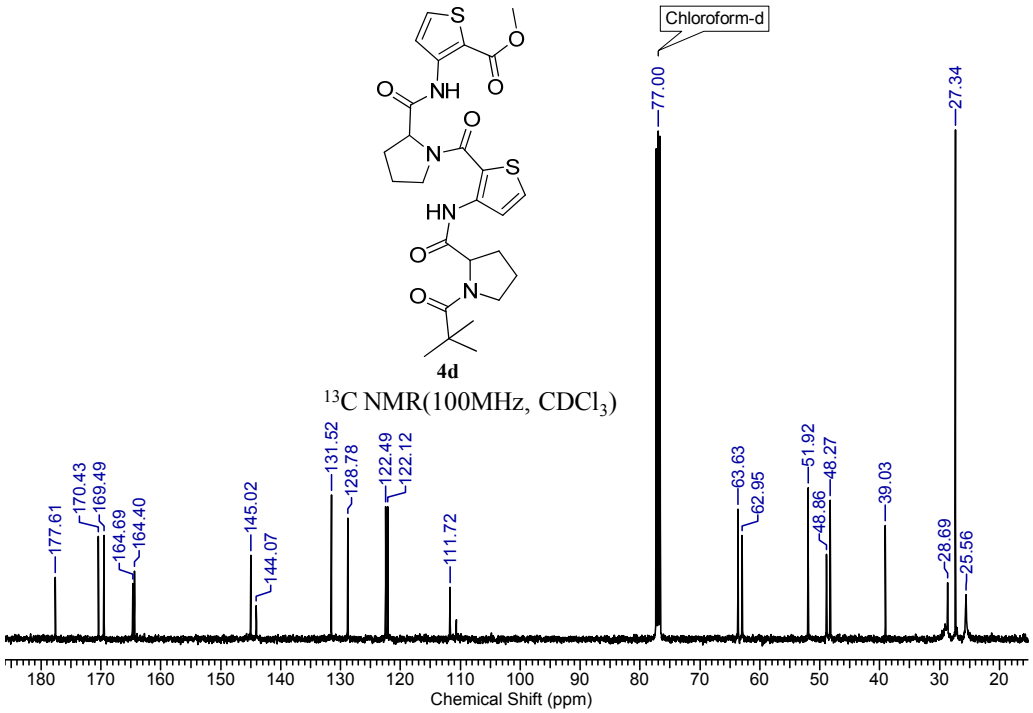

4d

^{13}C NMR(100MHz, $CDCl_3$)

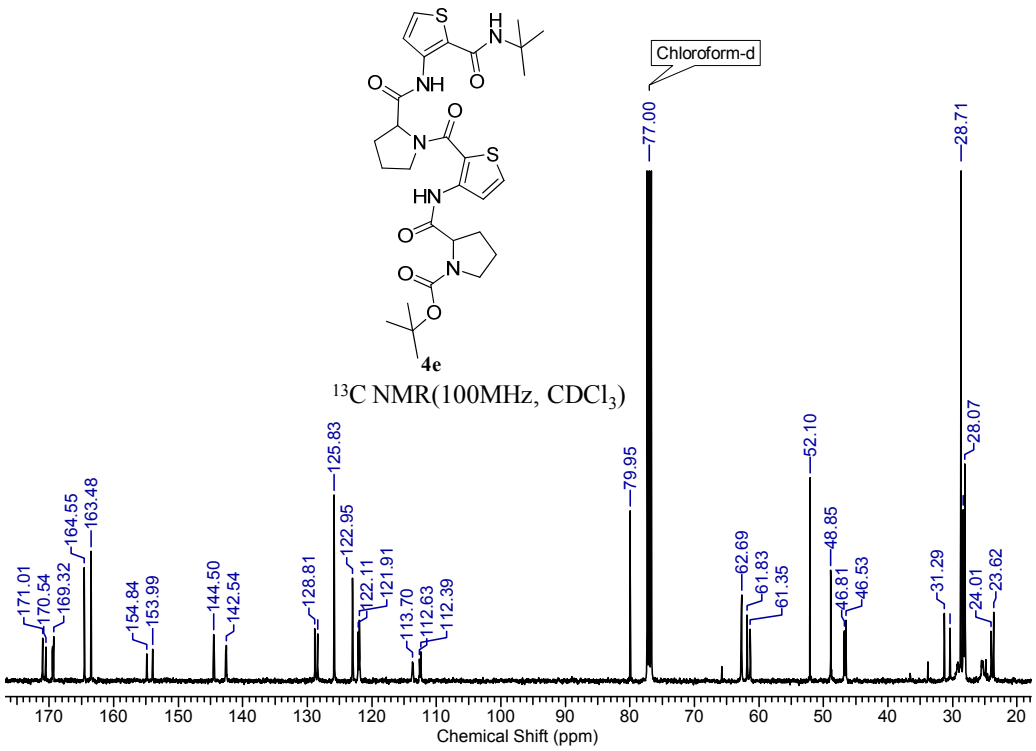

4e

^{13}C NMR(100MHz, $CDCl_3$)

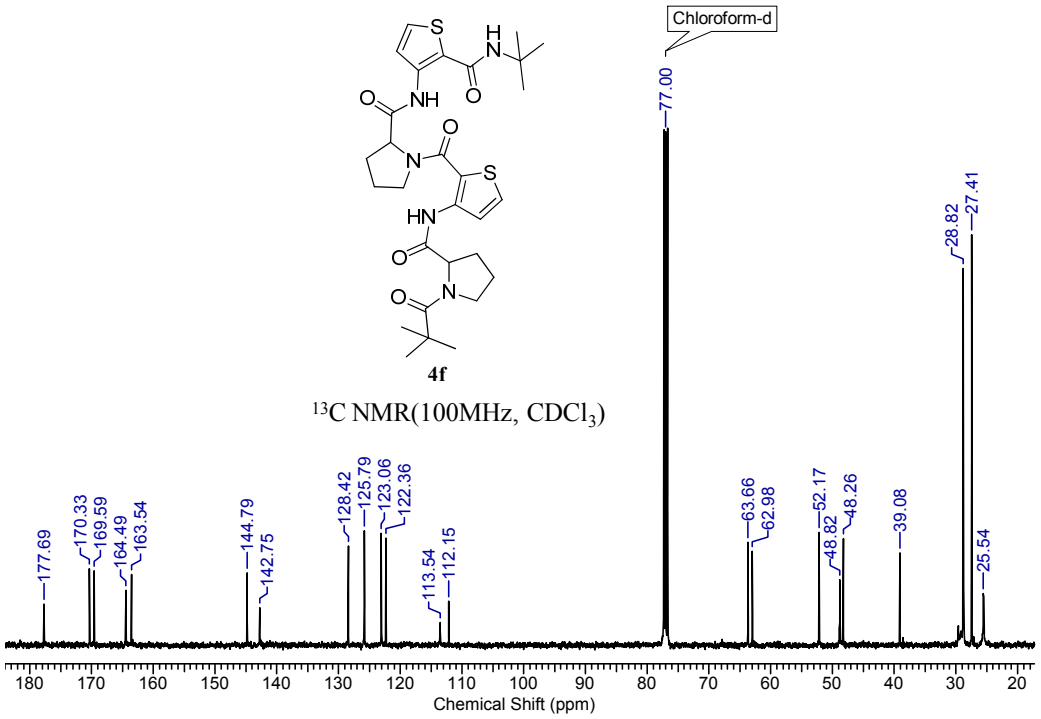

4f

^{13}C NMR(100MHz, $CDCl_3$)

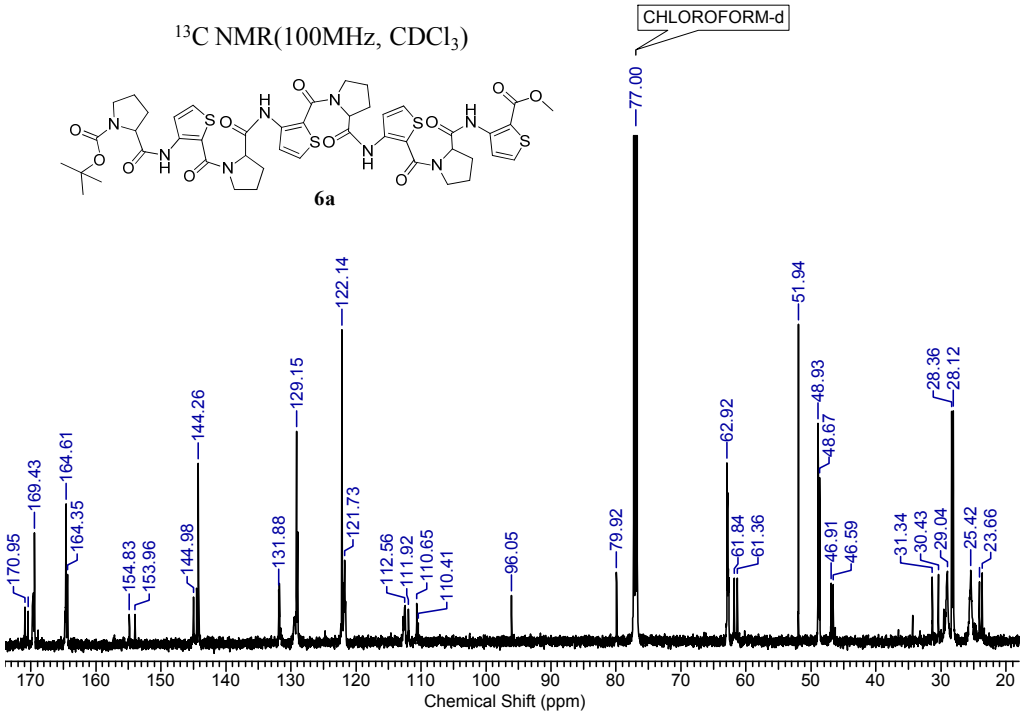

6a

^{13}C NMR(100MHz, $CDCl_3$)

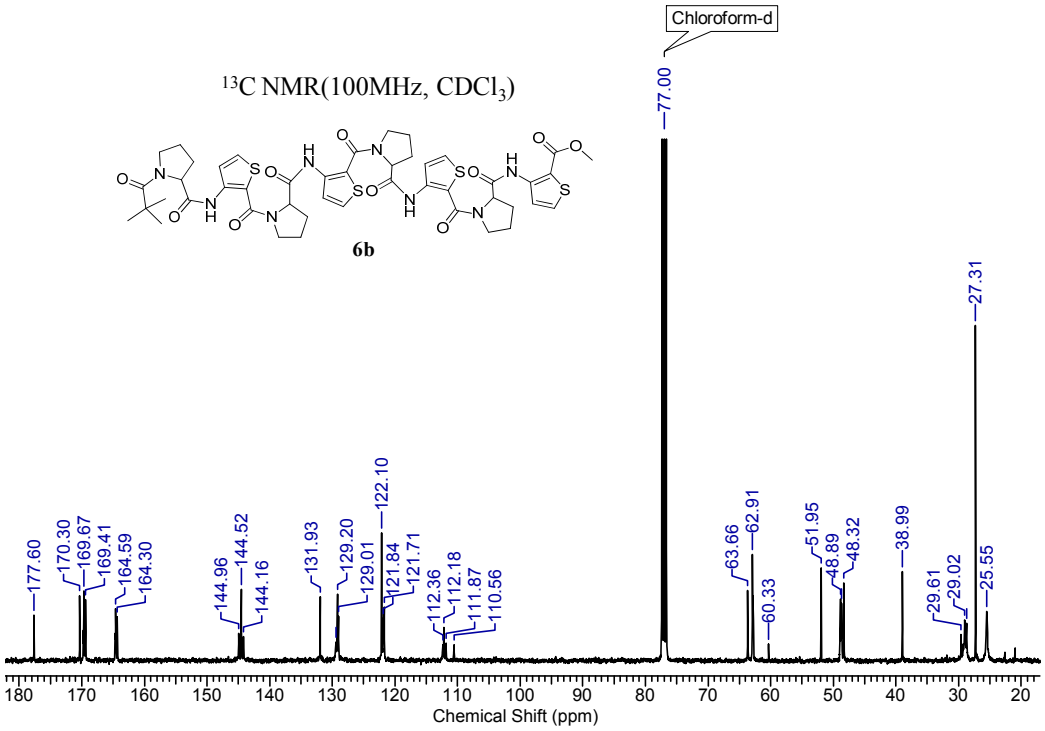
^{13}C NMR(100MHz, $CDCl_3$)
Chloroform-d
77.00
6b
177.60
170.30
169.67
169.41
164.59
164.30
144.96
144.52
144.16
131.93
129.20
129.01
122.10
121.84
121.71
112.36
112.18
111.87
110.56
63.66
62.91
60.33
51.95
48.89
48.32
38.99
29.61
29.02
27.31
25.55
180 170 160 150 140 130 120 110 100 90 80 70 60 50 40 30 20
Chemical Shift (ppm)

Table 1.5. Titration study of tetrapeptide 3f in $CDCl_3$ (10 mmol) with DMSO-d_6 (volume of DMSO-d_6 added at each addition = 5 µl)

Volume of DMSO-d6 added (in µL)	Chemical Shift (in ppm)		
	δNH1	δNH2	δNH3
0	11.54	12.59	5.70
5	11.53	12.58	5.75
10	11.51	12.57	5.80
15	11.50	12.57	5.85
20	11.48	12.56	5.89
25	11.46	12.55	5.94
30	11.44	12.54	5.97
35	11.42	12.53	6.01
40	11.41	12.53	6.05
45	11.39	12.52	6.08
50	11.36	12.50	6.12

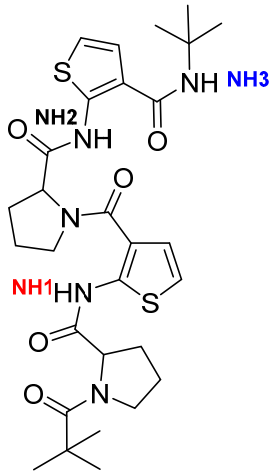

3f

Table 1.6. Titration study of tetrapeptide 4f in $CDCl_3$ (10 mmol) with DMSO-d_6 (volume of DMSO-d_6 added at each addition = 5 µl)

Volume of DMSO-d6 added (in µL)	Chemical Shift (in ppm)		
	δNH1	δNH2	δNH3
0	11.57	11.52	5.43
5	11.55	11.50	5.44
10	11.53	11.48	5.45
15	11.51	11.46	5.46
20	11.49	11.44	5.47
25	11.48	11.42	5.48
30	11.46	11.40	5.49
35	11.44	11.38	5.50
40	11.43	11.36	5.52
45	11.41	11.34	5.53
50	11.40	11.32	5.54

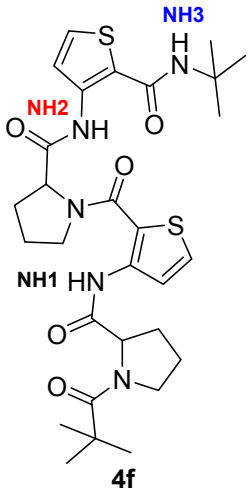

4f

Table 1.7. Titration study of octapeptide 5a (10 mmol, 400 MHz, $CDCl_3$) with DMSO-d_6 (volume of DMSO-d_6 added at each addition = 5 µl)

Volume of DMSO-d6 added (in µL)	Chemical Shift (in ppm)			
	δNH1	δNH2	δNH3	δNH4
0	11.45	11.85	12.01	11.55
5	11.47	11.86	12.03	11.57
10	11.44	11.85	12.01	11.55
15	11.42	11.83	11.98	11.52
20	11.41	11.82	11.96	11.50
25	11.39	11.80	11.94	11.49
30	11.37	11.79	11.92	11.47
35	11.35	11.78	11.90	11.45
40	11.34	11.77	11.89	11.44
45	11.33	11.75	11.87	11.42
50	11.31	11.73	11.84	11.40

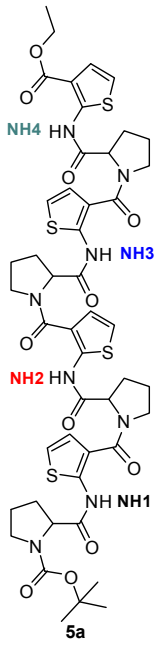

5a

Table 1.8. Titration study of octapeptide 5b (10 mmol, 400 MHz, $CDCl_3$) with DMSO-d_6 (volume of DMSO-d_6 added at each addition = 5 µl)

Volume of DMSO-d6 added (in µL)	Chemical Shift (in ppm)			
	δNH1	δNH2	δNH3	δNH4
0	11.41	11.85	12.04	11.57
5	11.40	11.85	12.03	11.56
10	11.39	11.83	12.00	11.54
15	11.37	11.81	11.98	11.52
20	11.36	11.80	11.97	11.51
25	11.35	11.79	11.96	11.50
30	11.34	11.78	11.94	11.48
35	11.32	11.76	11.91	11.45
40	11.31	11.75	11.90	11.44
45	11.29	11.73	11.87	11.42
50	11.27	11.71	11.85	11.40

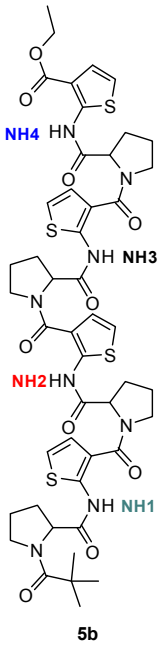

5b

Table 1.9. Titration study of octapeptide 6a (10 mmol, 400 MHz, $CDCl_3$) with DMSO-d_6 (volume of DMSO-d_6 added at each addition = 5 µl)

Volume of DMSO-d6 added (in µL)	Chemical Shift (in ppm)			
	δNH1	δNH2	δNH3	δNH4
0	11.45	11.83	11.76	10.61
5	11.39	11.77	11.70	10.55
10	11.36	11.75	11.67	10.53
15	11.33	11.72	11.64	10.50
20	11.30	11.70	11.61	10.47
25	11.28	11.68	11.58	10.45
30	11.25	11.65	11.55	10.42
35	11.22	11.62	11.52	10.39
40	11.20	11.60	11.49	10.37
45	11.17	11.57	11.48	10.34
50	11.15	11.55	11.44	10.32

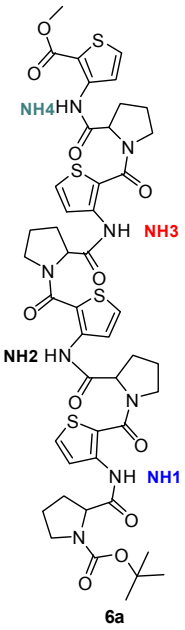

6a

Table 1.10. Titration study of octapeptide 6b (10 mmol, 400 MHz, $CDCl_3$) with DMSO-d_6 (volume of DMSO-d_6 added at each addition = 5 µl)

Volume of DMSO-d6 added (in µL)	Chemical Shift (in ppm)			
	δNH1	δNH2	δNH3	δNH4
0	11.39	11.84	11.77	10.61
5	11.37	11.82	11.75	10.58
10	11.35	11.80	11.72	10.57
15	11.31	11.78	11.69	10.53
20	11.29	11.75	11.67	10.52
25	11.27	11.72	11.64	10.49
30	11.24	11.70	11.62	10.47
35	11.22	11.67	11.59	10.44
40	11.19	11.64	11.56	10.41
45	11.17	11.62	11.54	10.39
50	11.14	11.60	11.51	10.37

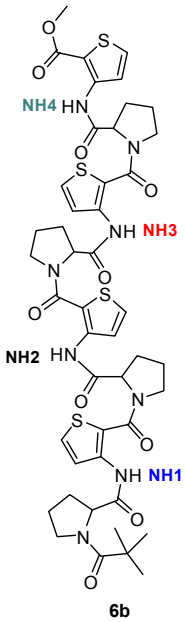

6b

Table 1.11. Variable temperature study of tetrapeptide 3f (10 mmol, 400 MHz, $CDCl_3$)

Temperature (in K)	Chemical shift (in ppm)		
	δNH1	δNH2	δNH3
263	11.61	12.63	5.80
273	11.58	12.62	5.77
278	11.57	12.61	5.76
283	11.56	12.60	5.75
288	11.55	12.60	5.74
293	11.54	12.59	5.73
295	11.55	12.59	5.73
298	11.53	12.58	5.71
303	11.54	12.58	5.71
308	11.52	12.56	5.69
313	11.51	12.55	5.69
318	11.50	12.54	5.68
323	11.49	12.53	5.67

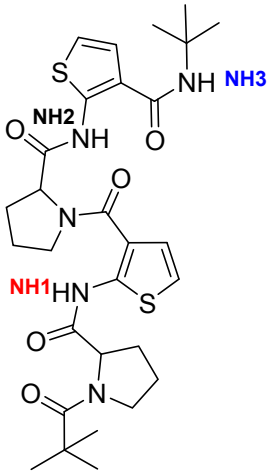

3f

Table 1.12. Variable temperature study of octapeptide 5b (10 mmol, 400 MHz, $CDCl_3$)

Temperature (in K)	Chemical shift (in ppm)			
	δNH1	δNH2	δNH3	δNH4
268	11.40	11.84	12.06	11.61
273	11.40	11.85	12.06	11.61
278	11.40	11.85	12.05	11.60
283	11.40	11.85	12.05	11.59
288	11.40	11.85	12.05	11.59
293	11.41	11.85	12.05	11.58
298	11.41	11.85	12.04	11.57
303	11.41	11.86	12.04	11.56
308	11.41	11.86	12.03	11.55
313	11.41	11.86	12.02	11.55
318	11.41	11.86	12.02	11.54
323	11.41	11.85	12.01	11.53

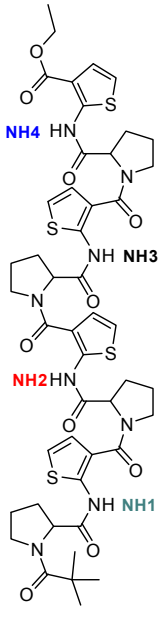

5b

Table 1.13. Variable temperature study of octapeptide 6b (10 mmol, 400 MHz, CDCl3)

Temperature (in K)	δNH1	δNH2	δNH3	δNH4
268	11.41	11.91	11.82	10.64
273	11.41	11.90	11.82	10.64
278	11.40	11.89	11.81	10.63
283	11.40	11.88	11.80	10.63
288	11.40	11.87	11.79	10.63
293	11.39	11.85	11.78	10.62
298	11.39	11.84	11.77	10.61
303	11.38	11.83	11.76	10.60
308	11.37	11.81	11.75	10.59
313	11.36	11.80	11.74	10.59
318	11.35	11.79	11.72	10.58
323	11.34	11.78	11.71	10.57

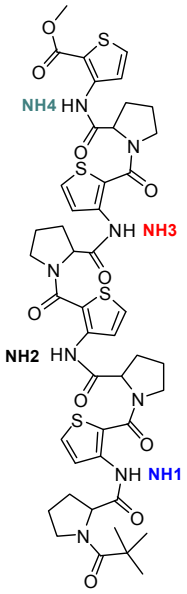

6b

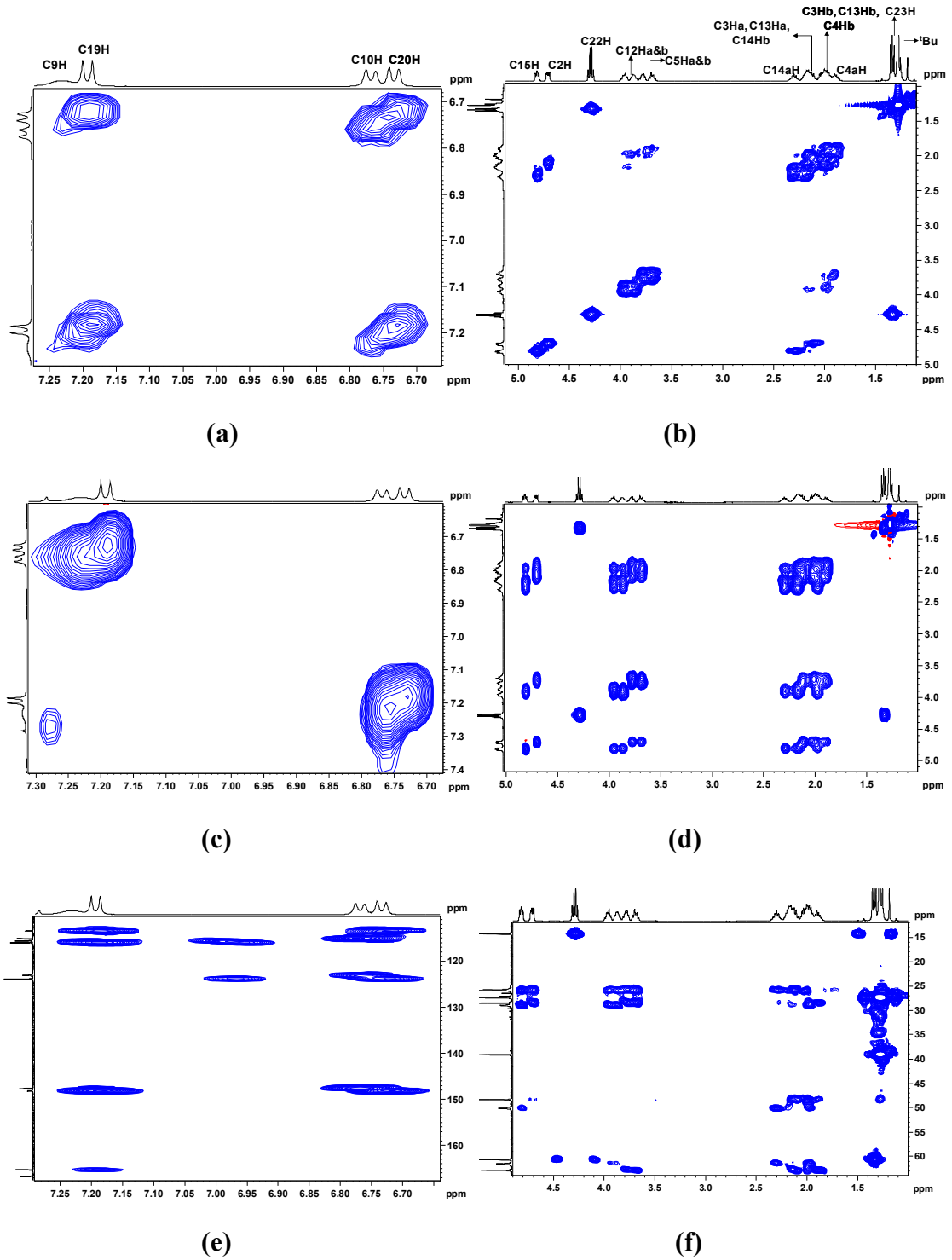

Fig 1.33: Partial COSY (a), (b); TOCSY, (c), (d); and HMBC (e), (f) spectra of **3d** (400 MHz, $CDCl_3$). For better view, aromatic and aliphatic regions are shown separately.

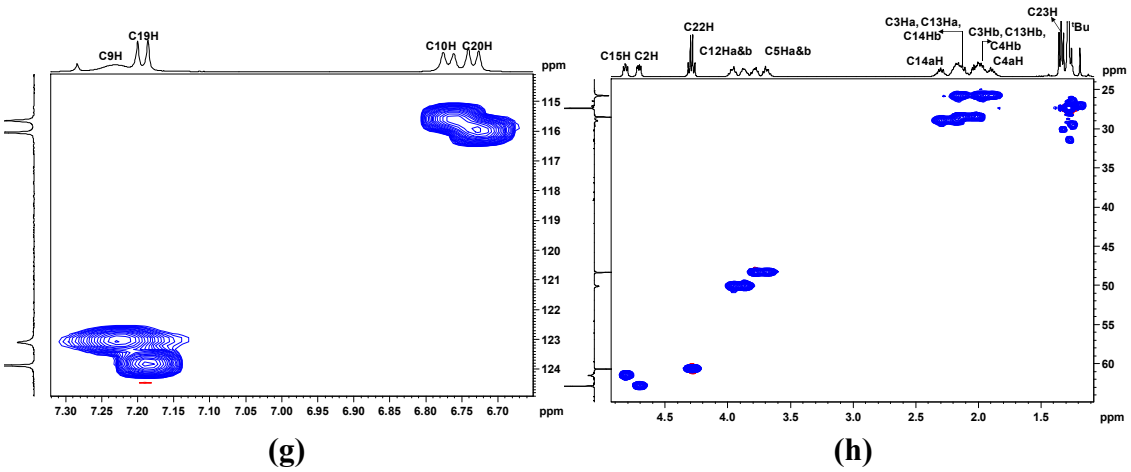

Fig 1.34: Partial HSQC (g), (h) spectra of **3d** (400 MHz, $CDCl_3$). For better view, aromatic and aliphatic regions are shown separately.

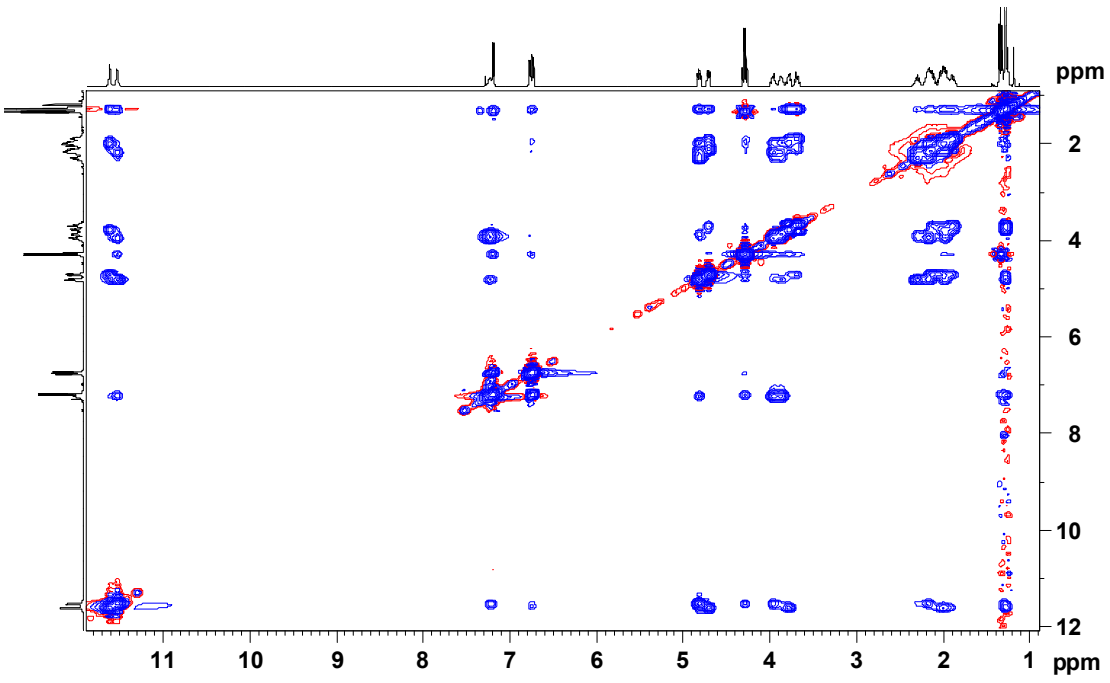

Fig 1.35: Full 2D NOESY spectrum of **3d** (400 MHz, $CDCl_3$).

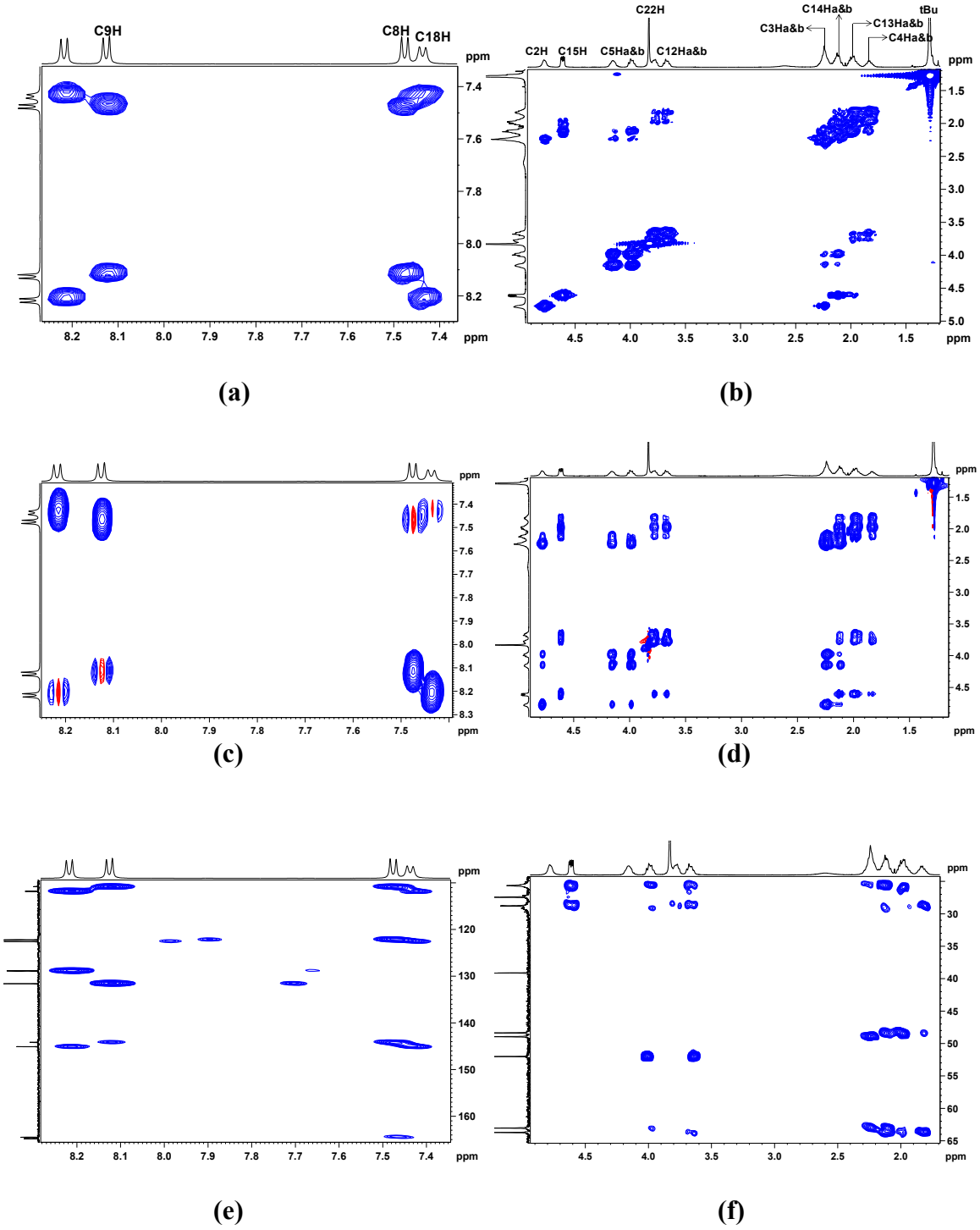

Fig 1.36: Partial COSY (a), (b); TOCSY (c), (d) and HMBC (e), (f) spectra of **4d** (400 MHz, $CDCl_3$). For better view, aromatic and aliphatic regions are shown separately.

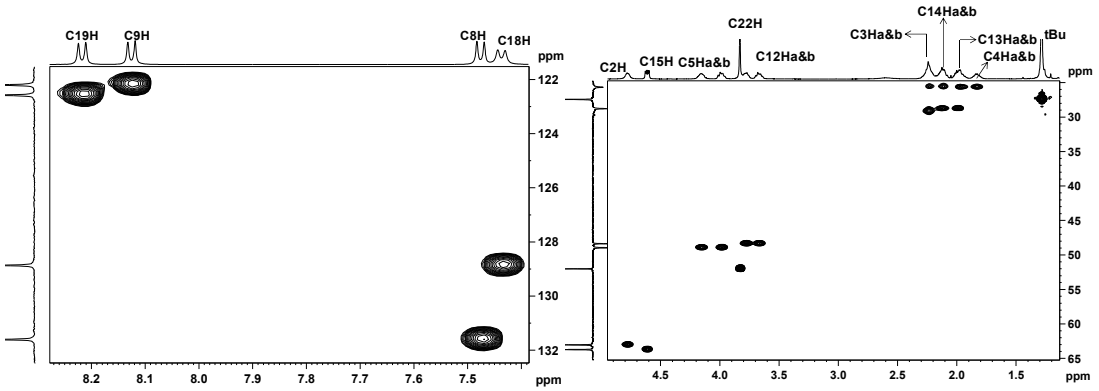

(g) **(h)**

Fig 1.37: Partial HSQC (g), (h) spectra of **4d** (400 MHz, $CDCl_3$). For better view, aromatic and aliphatic regions are shown separately.

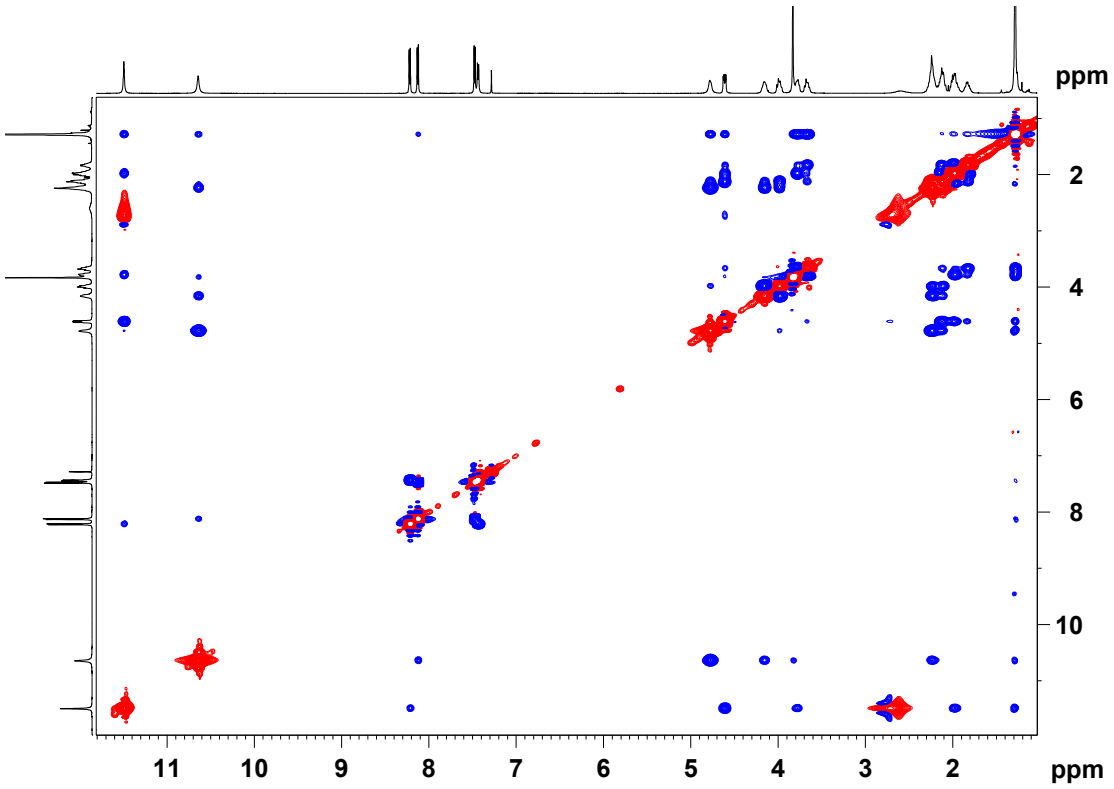

Fig 1.38: Full 2D NOESY spectrum of **4d** (400 MHz, $CDCl_3$).

1.11 References and Notes

(1) (a) Eisenberg, D. *Annu. Rev. Biochem*. **1984**, *53*, 595. (b) Saudek, V.; Atkinson, A.; Pelton, J. T. *Biochemistry*. **1991**, *30*, 7369. (c) Hendrick, J. P.; Hartl, F-U. *Annu. Rev. Biochem*. **1993**, *62*, 349.

(2) Karshikoff, A. Non-covalent interactions in proteins, Imperial College Press, United Kingdom, **2006**.

(3) LinderstrØm-Lang, K. U. "Proteins and Enzymes," Lane Medical Lectures, Stanford University Publications, University Series, Medical Sciences, Stanford University Press, **1952**, *6*.

(4) (a) Bajaj, M.; Blundell, T. *Annu. Rev. Biophys. Bioeng.* **1984**, *13*, 453. (b) Meiler, J.; Baker, D. *Proc. Natl. Acad. Sci.* **2003**, *100*, 12105.

(5) Gellman, S. H. *Acc. Chem. Res.* **1998,** *31*, 173.

(6) (a) Cheng, R. P.; Gellman, S. H.; DeGrado, W. F. *Chem. Rev.* **2001**, *101*, 3219. (b) Seebach, D.; Matthews, J. L. *Chem. Commun*. **1997**, 2015. (c) Cubberley, M. S.; Iverson, B. L. *Curr. Opin. Chem. Biol.* **2001**, *5*, 650. (d) Hill, D. J.; Mio, M. J.; Prince, R. B.; Hughes, T. S.; Moore, J. S. *Chem. Rev.* **2001**, *101*, 3893. (e) Cheng, R. P. *Curr. Opin. Chem. Biol.* **2004**, *14*, 512.

(7) (a) Hamuro, Y.; Geib, S. J.; Hamilton, A. D. *Angew. Chem. Int. Ed*. **1994**, *33*, 446. (b) Hamuro, Y.; Geib, S. J.; Hamilton, A. D. *J. Am. Chem. Soc*. **1996**, *118*, 7529. (c) Berl, V.; Huc, I.; Khoury, R. G.; Krische, M. J.; Lehn, J.-M. *Nature.* **2000**, *407*, 720. (d) Hu, Z.-Q.; Hu, H.-Y.; Chen, C.-F. *J. Org. Chem*. **2006**, *71*, 1131. (e) Gan, Q.; Bao, C.; Kauffmann, B.; Grelard, A.; Xiang, J.; Liu, S.; Huc, I.; Jiang, H. *Angew. Chem. Int. Ed*. **2008**, *47*, 1715. (e) Zhang, B.; Yuan, T.; Jiang, H.; Lei, M. *J. Phys. Chem. B* **2009**, *113*, 10934. (f) Gan, Q.; Li, F.; Li, G.; Kauffmann, B.; Xiang, J.; Huc, I.; Jiang, H. *Chem. Commun*. **2010**, *46*, 297. (g) Ong, W. Q.; Zhao, H.; Du, Z.; Yeh, J. Z. Y.; Ren, C.; Tan, L. Z. W.; Zhang, K.;
Zeng, H. *Chem. Commun*. **2011**, *47*, 6416.

(8) (a) Hu, Z.-Q.; Hu, H.-Y.; Chen, C.-F. *J. Am. Chem. Soc*. **2006**, *71*, 1131. (b) Ohkita, M.; Lehn, J.-M.; Baum, G.; Fenske, D. *Chem. Eur. J*. **1999**, *5*, 3471. (c) Schmitt, J.-L.; Stadler, A.-M.; Kyritsakas, N.; Lehn, J.-M. *Helv. Chim. Acta*. **2003**, *86*, 1598. (d) Gong, B.; Zeng, H.; Zhu, J.; Yua, L.; Han, Y.; Cheng, S.; Furukawa, M.; Parra, R. D.; Kovalevsky, A. Y.; Mills, J. L.;

Skrzypczac-Jankun, E.; Martinovic, S.; Smith, R. D. ; Zheng, C.; Szyperski, T.; Zeng, X. C. *Proc. Natl. Acad. Sci.* USA **2002**, *99*, 11583.

(9) (a) Muller, N.; *Acc. Chem. Res.* **1990**, *23*, 23. (b) Privalov, P. L.; Gill, S. *J. Pure Appl. Chem.* **1989**, *61*, 1097. (c) Kauzmann, W. *In Advances in protein chemistry*; Anfinsen, C. B. Jr.; Anson, M. L. ; Bailey, K.; Edsall, J. T.; *Eds., Academic Press*, New York, London, **1959**, *6*, 1. (d) Abraham, M. H.; *J. Am. Chem. Soc*. **1982**, *104*, 2085. (e) Shinoda, K. *J. Phys. Chem.* **1977**, *81*, 1300. (f) Cramer, R. D. *J. Am. Chem. Soc*. **1977**, *99*, 5408. (g) Frank, H. S.; Evans, M. W.; *J. Chem. Phys.* **1945**, *13*, 507. (h) Butler, J. A. V.; Reid, W. S. *J. Chem. Soc*. **1936**, 1171.

(10) (a) Juwarker, H.; Suk, J.-m.; Jeong, K.-S. *Chem. Soc. Rev.* **2009**, *38*, 3316. (b) Kubik, S. *Chem. Soc. Rev.* **2009**, *38*, 585.

(11) (a) Beevers, A. J.; Dixon, A. M. *Chem. Soc. Rev.* **2010**, *39*, 2146. (b) Imamura, Y.; Watanabe, N.; Umezawa, N.; Iwatsubo, T.; Kato, N.; Tomita, T.; Higuchi, T. *J. Am. Chem. Soc.* **2009,** *131*, 7353. (c) Boyle, A. L.; Woolfson, D. N. *Chem. Soc. Rev.* **2011,** *40*, 4295. (d) Haase, H. S.; Peterson-Kaufman, K. J.; Lan Levengood, S. K.; Checco, J. W.; Murphy, W. L.; Gellman, S. H. *J. Am. Chem. Soc.* **2012,** *134*, 7652. (e) Lee, E. F.; Sadowsky, J. D.; Smith, B. J.; Czabotar, P. E.; Peterson-Kaufman, K. J.; Colman, P. M.; Gellman, S. H.; Fairlie, W. D. *.Angew. Chem. Int. Ed.* **2009,** *48*, 4318.

(12) (a) Roy, A.; Prabhakaran, P.; Baruah, P. K.; Sanjayan, G. J. *Chem. Commun.* **2011**, *47*, 11593. (b) Martinek, T. A.; Fulop, F. *Chem. Soc. Rev.* **2012**, *41*, 687. (c) Horne, W. S.; Gellman, S. H. *Acc. Chem. Res.* **2008,** *41*, 1399.

(13) (a) Fowler, S. A.; Blackwell, H. E., *Org. Biomol. Chem.* **2009**, *7*, 1508. (b) Crapster, J. A.; Stringer, J. R.; Guzei, I. A.; Blackwell, H. E. *Pept. Sci.* **2011,** *96*, 604. (b) Wetzler, M.; Barron, A. E. *Pept. Sci.* **2011,** *96*, 556. (c) Olsen, C. A. *Pept. Sci.* **2011,** *96*, 561.

(14) (a) Le Grel, P.; Salaun, A.; Potel, M.; Le Grel, B.; Lassagne, F. *J. Org. Chem.* **2006**, *71*, 5638. (b) Simo, C.; Salaun, A.; Arnarez, C.; Delemotte, L.; Haegy, A.; Kachmar, A.; Laurent, A. D.; Thomas, J.; Jamart-Gregoire, B.; Le Grel, P.; Hocquet, A. *Themochem.* **2008**, *869*, 41. (c) Salaun, A.; Potel, M.; Roisnel, T.; Gall, P.; Le Grel, P. *J. Org. Chem.*, **2005**, *70*, 6499. (d)

Hetényi, A.; Tóth, G. K.; Somlai, C.; Vass, E.; Martinek, T. A.; Fülöp, F. *Chem. Eur. J.* **2009,** *15*, 10736.

(15) (a) Han, H.; Janda, K. D. *J. Am. Chem. Soc.* **1996**, *118*, 2539. (b) Gante, J.; Krug, M.; Lauterbach, G.; Weitzel, R.; Hiller, W. *J. Pept. Sci.* **1995**, *2*, 201. (c) Reynolds, C. H.; Hormann, R. E. *J. Am. Chem. Soc.* **1996**, *118*, 9395. (d) Andre, F.; Boussard, D.; Bayeul, D.; Didierjean, C.; Aubry, A.; Marraud, M. *J. Pept. Res.* **1997**, *49*, 556-562.

(16) (a) Lucarini, S.; Tomasini. C. *J. Org. Chem.* **2001**, *66*, 727. (b) Luppi, G.; Soffre, C.; Tomasini, C. *Tetrahedron: Asymm.* **2004**, *15*, 1645. (c) Tomasini, C.; Angelici, G.; Castellucci, N. *Eur. J. Org. Chem*. **2011**, 3648.

(17) (a) Hetényi, A.; Mándity, I. M.; Martinek, T. A.; Tóth, G. K.; Fülöp, F. *J. Am. Chem. Soc.* **2004**, *127*, 547. (b) Fernandes, C.; Faure, S.; Pereira, E.; Théry, V.; Declerck, V. r.; Guillot, R. g.; Aitken, D. J. *Org. Lett.* **2010,** *12*, 3606. (c) Appella, D. H.; Christianson, L. A.; Karle, I. L.; Powell, D. R.; Gellman, S. H. *J. Am. Chem. Soc.* **1996,** *118*, 13071. (d) Sharma, G. V. M.; Subash, V.; Narsimulu, K.; Sankar, A. R.; Kunwar, A. C. *Angew. Chem.* **2006,** *118*, 8387. (e) Berlicki, Ł.; Pilsl, L.; Wéber, E.; Mándity, I. M.; Cabrele, C.; Martinek, T. A.; Fülöp, F.; Reiser, O. *Angew. Chem. Int. Ed.* **2012,** *51*, 2208.

(18) (a) Sharma, G. V. M.; Manohar, V.; Dutta, S. K.; Subash, V.; Kunwar, A. C. *J. Org. Chem.* **2008**, *73*, 3689. (b) Chen, F.; Zhu, N.-Y.; Yang, D. *J. Am. Chem. Soc.* **2004,** *126*, 15980. (c) Yang, D.; Zhang, D.-W.; Hao, Y.; Wu, Y.-D.; Luo, S.-W.; Zhu, N.-Y. *Angew. Chem. Int. Ed.* **2004,** *43*, 6719. (d) Yang, D.; Qu, J.; Li, W.; Wang, D.-P.; Ren, Y.; Wu, Y.-D. *J. Am. Chem. Soc.* **2003,** *125*, 14452. (e) Zhang, Y.-H.; Song, K.; Zhu, N.-Y.; Yang, D. *Chem. Eur. J.* **2010,** *16*, 577.

(19) (a) Gennari, C.; Salom, B.; Potenza, D.; Williams, A. *Angew. Chem. Int. Ed.* **1994**, *33*, 2067. (b) Moree, W. J.; van der Marel, G. A.; Liskamp, R. J. *J. Org. Chem.* **1995,** *60*, 5157. (c) Gude, M.; Piarulli, U.; Potenza, D.; Salom, B.; Gennari, C. *Tetrahedron Lett.* **1996,** *37*, 8589. (d) Monnee, M. C. F.; Marijne, M. F.; Brouwer, A. J.; Liskamp, R. M. J. *Tetrahedron Lett.* **2000,** *41*, 7991. (e) Gennari, C.; Salom, B.; Potenza, D.; Longari, C.; Fioravanzo, E.; Carugo, O.; Sardone, N. *Chem. Eur. J.* **1996**, *2*, 644. (f) Vijayadas, K. N.;

Davis, H. C.; Kotmale, A. S.; Gawade, R. L.; Puranik, V. G.; Rajamohanan, P. R.; Sanjayan, G. J. *Chem. Commun.* **2012**, *48*, 9747. (g) Bindal, R. D.; Golab, J. T.; Katzenellenbogen, J. A. *J. Am. Chem.Soc.* **1990**, *112*, 7861. (h) Radkiewicz, J. L.; McAllister, M. A.; Goldstein, E.; Houk, K. N. *J. Org. Chem.* **1998**, *63*, 1419. (i) Gennari, C.; Gude, M.; Potenza, D.; Piarulli, U. *Chem. Eur. J.* **1998**, *4*, 1924. (j) Liskamp, R. M. J.; Rijkers, D. T. S.; Kruijtzer, J. A. W.; Kemmink, J. *Chem.Bio.Chem*, **2011**, *12*, 1626. (k) Turcotte, S.; Gervais, S. H. B.; Lubell, W. D. *Org. Lett*. **2012**, *14*, 1318. (l) Baldauf, C.; Gunther, R.; Hofmann, H.-J. *Thermochem.* **2004**, *675*, 19. (m) Bolm, C.; Moll, G.; Kahmann, J. D. *Chem. Eur. J.* **2001**, *7*, 1118.

(20) (a) Gunther, R.; Hofmann, H.-J. *J. Am. Chem. Soc.* **2001**, *123*, 247. Patch, J. A.; Barron, A. E. *Curr. Opin. Chem. Biol.* **2002,** *6*, 872. (b) Salaün, A.; Potel, M.; Roisnel, T.; Gall, P.; Le Grel, P. *J. Org. Chem.* **2005,** *70*, 6499.

(21) (a) Claudon, P.; Violette, A.; Lamour, K.; Decossas, M.; Fournel, S.; Heurtault, B.; Godet, J.; Mély, Y.; Jamart-Grégoire, B.; Averlant-Petit, M.-C.; Briand, J.-P.; Duportail, G.; Monteil, H.; Guichard, G. *Angew. Chem. Int. Ed.* **2010,** *49*, 333. (b) Fischer, L.; Claudon, P.; Pendem, N.; Miclet, E.; Didierjean, C.; Ennifar, E.; Guichard, G. *Angew. Chem. Int. Ed.* **2010,** *49*, 1067. (c) Violette, A.; Averlant-Petit, M. C.; Semetey, V.; Hemmerlin, C.; Casimir, R.; Graff, R.; Marraud, M.; Briand, J.-P.; Rognan, D.; Guichard, G. *J. Am. Chem. Soc.* **2005,** *127*, 2156. (d) Mousseau, J. J.; Xing, L.; Tang, N.; Cuccia, L. A. *Chem. Eur. J.*, **2009**, *15*, 10030.

(22) (a) Brenner, M.; Seebach, D. *Helv. Chim. Acta* **2001**, *84*, 1181. (b) Seebach, D.; Brenner, M.; Rueping, M.; Schweizer, W. B.; Jaun, B. *Chem. Commun.* **2001**, 207. (c) Machetti, F.; Ferrali, A.; Menchi, G.; Occhiato, E. G.; Guarna, A. *Org. Lett.* **2000**, *2*, 3987.

(23) Vasudev, P. G.; Chatterjee, S.; Shamala, N.; Balaram, P. *Chem. Rev.* **2010**, *111*, 657. (a) Chatterjee, S.; Vasudev, P. G.; Raghothama, S.; Ramakrishnan, C.; Shamala, N.; Balaram, P. *J. Am. Chem. Soc.* **2009**, *131*, 5956. (b) Chatterjee, S.; Vasudev, P. G.; Raghothama, S.; Shamala, N.; Balaram, P. *Biopolymers.* **2008**, *90*, 759. (c) Vasudev, P. G.; Chatterjee, S.; Ananda, K.;

Shamala, N.; Balaram, P. *Angew. Chem. Int. Ed.* **2008**, *47*, 6430. (d) Chatterjee, S.; Vasudev, P. G.; Ananda, K.; Raghothama, S.; Shamala, N.; Balaram, P. *J. Org. Chem.* **2008**, *73*, 6595.

(24) (a) Smith, M. D.; Long, D. D.; Martı´n, A.; Marquess, D. G.; Claridge, T. D. W.; Fleet, G. W. J. *Tetrahedron Lett.* **1999**, *40*, 2191.(b) Smith, M. D.; Claridge, T. D. W.; Tranter, G. E.; Sansom, M. S. P.; Fleet, G. W. J. *Chem. Commun.* **1998**, 2041. (c) Brittain, D. E. A.; Watterson, M. P.; Claridge, T. D. W.; Smith, M. D.; Fleet, G. W. J. *J. Chem. Soc., Perkin Trans. 1* **2000**, 3655. (d) Claridge, T. D. W.; Long, D. D.; Hungerford, N. L.; Aplin, R. T.; Smith, M. D.; Marquess, D. G.; Fleet, G. W. J. *Tetrahedron Lett.* **1999**, *40*, 2199. (e) Chakraborty, T. K.; Jayaprakash, S.; Srinivasu, P.; Chary, M. G.; Diwan, P. V.; Nagaraj, R.; Sankar, A. R.; Kunwar, A. C. *Tetrahedron Lett.* **2000**, *41*, 8167. (f) Schrey, A.; Vescovi, A.; Knoll, A.; Rickert, C.; Koert, U. *Angew. Chem. Int. Ed.* **2000**, *39*, 900. (g) Fleet, G. W. J.; Johnson, S. W.; Jones, J. H. J. *Pept. Sci.,* **2006**, *12*, 559. (h) Chakraborty, T. K.; Reddy, V. R.; Sudhakar, G.; Kumar, S. U.; Reddy, T. J.; Kuran, S. K.; Kunwar, A. C.; Mathur, A.; Sharma, R. ; Gupta, N.; Prasad, S. *Tetrahedron*, **2004**, *60*, 8329. (i) Fuchs, E. -F.; Lehmann, J. *Chem. Ber.*, **1975**, *108*, 2254.

(25) Hill, D. J.; Mio, M. J.; Prince, R. B.; Hughes, T. S.; Moore, J. S. *Chem. Rev.* **2001**, *101*, 3893.

(26) (a) Zhang, Y.-H.; Song, K.; Zhu, N.-Y.; Yang, D. *Chem. Eur. J.* **2010**, *16*, 577. (b) Hetenyi, A.; Szakonyi, Z.; Mandity, I. M.; Szolnoki, E.; Toth, G. K.; Martinek, T. A.; Fulop, F. *Chem. Commun.* **2009,** 2, 177. (c) Legrand, B.; André, C.; Wenger, E.; Didierjean, C.; Averlant-Petit, M. C.; Martinez, J.; Calmes, M.; Amblard, M. *Angew. Chem. Int. Ed.* **2012**, *51*, 11267. (d) Long, D. D.; Smith, M. D.; Marquess, D. G.; Claridge, T. D. W.; Fleet, G. W. J. *Tetrahedron Lett.,* **1998**, *39*, 9293. (e) Watterson, M. P.; Pickering, L.; Smith, M. D.; Hudson, S. J.; Marsh, P. R.; Mordaunt, J. E.; Watkin, D. J.; Newman, C. J.; Fleet, G. W. J. *Tetrahedron: Asymm.* **1999**, *10*, 1855. (f) Kothari, A.; Qureshi, M. K. N.; Beck, E. M.; Smith, M. D. *Chem. Commun.* **2007,** 27, 2814.

(27) Zhang, D.-W.; Zhao, X.; Hou, J.-L.; Li, Z.-T. *Chem. Rev.* **2012**, *112*, 5271.

(28) (a) Zhu, J.; Parra, R. D.; Zeng, H.; Skrzypczak-Jankun, E.; Zeng, X. C.; Gong, B. *J. Am. Chem. Soc*. **2000**, *122*, 4219. (b) (a) Qin, B.; Chen, X.; Fang, X.; Shu, Y.; Yip, Y. K.; Yan, Y.; Pan, S.; Ong, W. Q.; Ren, C.; Su, H.; Zeng, H. *Org. Lett*. **2008**, *10*, 5127.

(29) Seebach, D.; Gardiner, J. *Acc. Chem. Res.* **2008**, *41*, 1366.

(30) (a) De Pol, S.; Zorn, C.; Klein, C. D.; Zerbe, O.; Reiser, O. *Angew. Chem. Int. Ed.* **2004**, *43*, 511. (b) Gnad, F. ; Reiser, O. *Chem. Rev*. **2003**, *103*, 1603.

(31) (a) Hayen, A.; Schmitt, M. A.; Ngassa, F. N.; Thomasson, K. A.; Gellman, S. H. *Angew. Chem.* **2004**, *116*, 511. (b) Schmitt, M. A.; Weisblum, B.; Gellman, S. H. *J. Am. Chem. Soc.* **2004,** *126*, 6848. (c) Berlicki, Ł.; Pilsl, L.; Wéber, E.; Mándity, I. M.; Cabrele, C.; Martinek, T. A.; Fülöp, F.; Reiser, O. *Angew. Chem. Int. Ed.* **2012,** *51*, 2208.

(32) (a) Ananda, K.; Vasudev, P. G.; Sengupta, A.; Poopathi Raja, K. M.; Shamala, N.; Balaram, P. *J. Am. Chem. Soc.* **2005**, *127*, 16668.

(33) Jagadeesh, B.; Prabhakar, A.; Sarma, G. D.; Chandrasekhar, S.; Chandrashekar, G.; Reddy, M. S.; Jagannadh, B. *Chem. Commun.* **2007**, 4, 371.

(34) (a) Choi, S. H.; Guzei, I. A.; Spencer, L. C.; Gellman, S. H. *J. Am. Chem. Soc.* **2008**, *130*, 6544. (b) Guo, L.; Chi, Y.; Almeida, A. M.; Guzei, I. A.; Parker, B. K.; Gellman, S. H. *J. Am. Chem. Soc.* **2009**, *131*, 16018. (c) Guo, L.; Zhang, W.; Guzei, I. A.; Spencer, L. C.; Gellman, S. H. *Tetrahedron.* **2012**, *68*, 4413.

(35) (a) Patgiri, A.; Joy, S. T.; Arora, P. S. *J. Am. Chem. Soc.* **2012**, *134*, 11495. (b) Henchey, L. K.; Porter, J. R.; Ghosh, I.; Arora, P. S. *Chem. Bio. Chem*. **2010**, *11*, 2104. (c) Mahon, A. B.; Arora, P. S. *Chem. Commun*. **2012**, *48*, 1416.

(36) (a) Roy, R. S. ; Karle, I. L.; Raghothama, S.; Balaram, P. *Proc. Natl. Acad.*

Sci. U. S. A., **2004**, *101*, 16478. (b) Schmitt, M. A.; Choi, S. H.; Guzei, I. A.; Gellman, S. H. *J. Am. Chem. Soc.* **2006**, *128*, 4538.

(37) Ramesh, V. V. E.; Kale, S. S.; Kotmale, A. S.; Gawade, R. L.; Puranik, V. G.; Rajamohanan, P. R.; Sanjayan, G. J. *Org. Lett.* **2013**, *15*, 1504**.**

(38) (a) Balaram, P.; *Angew. Chem., Int. Ed.* **2008**, *47*, 6430. (b) Chatterjee, S.; Vasudev, P. G.; Ananda, V; Raghothama, V; Shamala, N.; Balaram, P. *J. Org. Chem*. **2008**, *73*, 6595.

(39) Guo, L.; Chi, Y. G.; Almeida, A. M.; Guzei, I. A.; Parker, B. K.; Gellman, S. H. *J. Am. Chem. Soc.* **2009**, *131*, 16018.

(40) Baruah, P. K.; Sreedevi, N. K.; Gonnade, R.; Ravindranathan, S.; Damodaran, K.; Hofmann, H.-J.; Sanjayan, G. J. *J. Org. Chem.* **2006**, *72*, 636.

(41) Srinivas, D.; Gonnade, R.; Ravindranathan, S.; Sanjayan, G. J. *J. Org. Chem*. **2007**, *72*, 7022.

(42) Sharma, G. V. M.; Jadhav, V. B.; Ramakrishna, K. V. S.; Jayaprakash, P.; Narsimulu, K.; Subash, V.; Kunwar, A. C. *J. Am. Chem. Soc.* **2006**, *128*, 14657.

(43) Schramm, P.; Sharma, G. V. M.; Hofmann, H. J. *Biopolymers.* **2010**, *93*, 279.

(44) Baldauf, C.; Gunther, R.; Hofmann, H.-J. *J. Org. Chem.* **2006**, *71*, 1200–1208.

(45) Guo, L.; Almeida, A. M.; Zhang, W.; Reidenbach, A. G.; Choi, S. H.; Guzei, I. A.; Gellman, S. H. *J. Am. Chem. Soc.* **2010**, *132*, 7868.

(46) Sawada, T.; Gellman, S. H. *J. Am. Chem. Soc.* **2011**, *133*, 7336.

(47) Popot, J. L.; Engelman, D. M. *Annu. Rev. Biochem.* **2000**, *69*, 881.

(48) Yi, H.-P.; Shao, X.-B.; Hou, J.-L.; Li, C.; Jiang, X.-K.; Li, Z.-T. *New J. Chem.* **2005**, *29*, 1213.

(49) (a) Gong, B. *Acc. Chem. Res.* **2008**, *41*, 1376. (b) (b) Gong, B.; Zeng, H.; Zhu, J.; Yua, L.; Han, Y.; Cheng, S.; Furukawa, M.; Parra, R. D.; Kovalevsky, A. Y.; Mills, J. L.; Skrzypczak-Jankun, E.; Martinovic, S.; Smith, R. D.; Zheng, C.; Szyperski, T.; Zeng, X. C. *Proc. Natl. Acad. Sci. U. S. A*. **2002**, *99*, 11583.

(50) (a) Berl, V.; Huc, I.; Khoury, R. G.; Krische, M. J.; Lehn, J.-M. *Nature*. **2000**, *407*, 720. (b) Yan, Y.; Qin, B.; Ren, C.; Chen, X.; Yip, Y. K.; Ye, R.; Zhang, D.; Su, H.; Zeng, H. *J. Am. Chem. Soc*. **2010**, *132*, 5869. (c) Ong, W. Q.; Zhao, H.; Du, Z.; Yeh, J. Z. Y.; Ren, C.; Tan, L. Z. W.; Zhang, K.; Zeng, H. *Chem. Commun.* **2011**, *47*, 6416. (d) Berl, V.; Huc, I.; Khoury, R. G.; Lehn, J.-M. *Chem. Eur. J*. **2001**, *7*, 2798.

(51) Maurizot, V.; Dolain, C.; Leydet, Y.; Leger, J.-M.; Guionneau, P.; Huc, I. *J. Am. Chem. Soc.* **2004**, *126*, 10049.

(52) Maurizot, V.; Dolain, C.; Leydet, Y.; Le´ger, J.-M.; Guionneau, P.; Huc, I. *J. Am. Chem. Soc.* **2004**, *126*, 10049.

(53) (a) Tie, C.; Gallucci, J. C.; Parquette, J. R. *J. Am. Chem. Soc.* **2006**, *128*, 1162. (b) King, E. D.; Tao, P.; Sanan, T. T.; Hadad, C. M.; Parquette, J. R. *Org. Lett*. **2008**, *10*, 1671.

(54) Baruah, P. K.; Gonnade, R.; Rajamohanan, P. R.; Hofmann, H.-J.; Sanjayan, G. J. *J. Org. Chem*. **2007**, *72*, 5077.

(55) (a) Chang, K.-J.; Kang, B.-N.; Lee, M.-H.; Jeong, K.-S. *J. Am. Chem. Soc.* **2005**, *127*, 12214.(b) Kim, U.-I.; Suk, J.-m.; Naidu, V. R.; Jeong, K.-S. *Chem. Eur. J*. **2008**, *14*, 11406. (c) Naidu, V. R.; Kim, M. C.; Suk, J.-M.; Kim, H.-J.; Lee, M.; Sim, E.; Jeong, K.-S. *Org. Lett*. **2008**, *10*, 5373.

(56) (a) Suk, J. m.; Jeong, K.-S. *J. Am. Chem. Soc*. **2008**, *130*, 11868. (b) Kim, J. i.; Juwarker, H.; Liu, X.; Lah, M. S.; Jeong, K.-S. *Chem. Commun*. **2010**, *46*, 764.

(57) Coles, S. J.; Frey, J. G.; Gale, P. A.; Hursthouse, M. B.; Light, M. E.;

Navakhun, K.; Thomas, G. L. *Chem. Commun*. **2003**, 568.

(58) Xu, Y.-X. ; Wang, G.-T.; Zhao, X.; Jiang, X.-K.; Li, Z.-T. *J. Org. Chem*. **2009**, *74*, 7267.

(59) Nelson, J. C.; Saven, J. G.; Moore, J. S.; Wolyner, P. G. *Science.* **1997**, *277*, 1793.

(60) (a) Gabriel, G. J.; Sorey, S.; Iverson, B. L. *J. Am. Chem. Soc.* **2005**, *127*, 2637. (b) Bradford, V. J.; Iverson, B. L. *J. Am. Chem. Soc.* **2008,** *130*, 1517.

(61) (a) Salonen, L. M.; Ellermann, M.; Diederich, F. *Angew. Chem. Int. Ed.* **2011**, *50*, 4808. (b) Merican, Z.; Johnstone, K. D.; Gunter, M. J. *Org. Biomol. Chem.* **2008**, *6*, 2534. (c) Heemstra, J. M.; Moore, J. S. *Org. Lett.* **2004**, *6*, 659.

(62) (a) Aravinda, S.; Datta, S.; Shamala, N.; Balaram, P. *Angew. Chem. Int. Ed.* **2004**, *43*, 6728. (b) Aravinda, S.; Shamala, N.; Pramanik, A.; Das, C.; Balaram, P. *Biochem. Biophy. Res. Commun.* **2000,** *273*, 933. (c) Madan Babu, M.; Kumar Singh, S.; Balaram, P. *J. Mol. Biol.* **2002,** *322*, 871. (d) Aravinda, S.; Shamala, N.; Bandyopadhyay, A.; Balaram, P. *J. Am. Chem. Soc.* **2003,** *125*, 15065.

(63) Chanda, K.; Chou, C.-T.; Lai, J.-J.; Lin, S.-F.; Yellol, G.; Sun, C.-M. *Mol. Divers.* **2011**, *15*, 569.

(64) (a) Crisma, M.; Formaggio, F.; Moretto, A.; Toniolo, C.; *Biopolymers.* **2006**, *84*, 3. (b) Horng, J.-C.; Raines, R. T. *Prot. Sci.* 2006, *15*, 74. (c) Kay, B. K.; Williamson, M. P.; Sudol, M. *FASEB J.* **2000**, *14*, 231. (d) Shi, Z.; Chen, K.; Liu, Z.; Kallenbach, N. R. *Chem. Rev*. **2006**, *106*, 1877.

(65) (a) Hara, T.; Durell, S. R.; Myers, M. C.; Appella, D. H. *J. Am. Chem. Soc.* **2006**, *128*, 1995. (b) Xiao, X. S.; Yu, P.; Lim, H.-S.; Sikder, D.; Kodadek, T. *J. Comb. Chem.* **2007**, *9*, 592.

(66) (a) Fowler, S. A.; Blackwell, H. E. *Org. Biomol. Chem.* **2009**, *7*, 1508. (b) Gorske, B. C.; Bastian, B. L.; Geske, G. D.; Blackwell, H. E. *J. Am. Chem.*

Soc. **2007,** *129*, 8928. (c) Stringer, J. R.; Crapster, J. A.; Guzei, I. A.; Blackwell, H. E. *J. Am. Chem. Soc.* **2011,** *133*, 15559. (d) Laursen, J. S.; Engel-Andreasen, J.; Fristrup, P.; Harris, P.; Olsen, C. A. *J. Am. Chem. Soc.* **2013,** *135*, 2835. (e) Fowler, S. A.; Luechapanichkul, R.; Blackwell, H. E. *J. Org. Chem.* **2009,** *74*, 1440. (f) Crapster, J. A.; Stringer, J. R.; Guzei, I. A.; Blackwell, H. E. *Pept. Sci.* **2011,** *96*, 604.

(67) (a) Yang, D.; Qu, J.; Li, B.; Ng, F. F.; Wang, X. C.; Cheung, K. K.; Wang, D. P.; Wu, Y. D. *J. Am. Chem. Soc*. **1999**, *121*, 589. (b) Yang, D.; Qu, J.; Li, W.; Ren, Y.; Wang, D.-P.; Wu, Y. D. *J. Am. Chem. Soc*. **2003**, *125*, 14452. (c) Yang, D.; Zhang, Y. H.; Zhu, N. Y. *J. Am. Chem. Soc.* **2002**, *124*, 9966. (d) Yang, D.; Zhang, Y. H.; Li, B.; Zhang, D. W.; Chan, J. C. Y.; Zhu, N. Y.; Luo, S. W.; Wu, Y. D.; *J. Am. Chem. Soc.* **2004**, *126*, 6956. (d) Yang, D.; Zhang, D. W.; Hao, Y.; Wu, Y. D.; Luo, S. W.; Zhu, N. Y. *Angew. Chem. Int. Ed*. **2004**, *43*, 6719. (e) Chen, F.; Zhu, N. Y.; Yang, D. *J. Am. Chem. Soc*. **2004**, *126*, 15980. (f) Gunther, R.; Hoffmann, H.-J. *J. Am. Chem. Soc.* **2001**, *123*, 247. (g) Lelais, G.; Seebach, D. *Helv. Chim. Acta.* **2003**, *86*, 4152.

(68) Tomasini, C.; Luppi, G.; Monari, M. *J. Am. Chem. Soc.* **2006**, *128*, 2410.

(69) Huck, B. R.; Fisk, J. D.; Guzei, I. A.; Carlson, H. A.; Gellman, S. H. *J. Am. Chem. Soc.* **2003**, *125*, 9035.

(70) Bouillere, F.; Feytens, D.; Gori, D.; Guillot, R.; Kouklovsky, C.; Miclet, E.; Alezra, V. *Chem. Commun.* **2012**, *48*, 1982.

(71) (a) Tew, G. N.; Scott, R. W.; Klein, M. L.; DeGrado, W. F. *Acc. Chem. Res.* **2009**, *43*, 30. (b) Hamuro, Y.; Schneider, J. P.; DeGrado, W. F. *J. Am. Chem. Soc.* **1999,** *121*, 12200.

(72) Sadowsky, J. D.; Schmitt, M. A.; Lee, H. S.; Umezawa, N.; Wang, S.; Tomita, Y.; Gellman, S. H. *J. Am. Chem. Soc*. **2005**, *127*, 11966.

(73) Delauriere, L.; Dong, Z.; Laxmi-Reddy, K.; Godde, F.; Toulme, J.-J.; Huc, I. *Angew. Chem. Int. Ed*. **2012**, *51*, 473.

(74) (a) Hou, L.-L.; Yi, H.-P.; Shao, X.-B.; Li, C.; Wu, Z.-Q.; Jiang, X.-K.; Wu, L.-Z.; Tung, C.-H.; Li, Z.-T. *Angew. Chem. Int. Ed*. **2006**, *45*, 796. (b) Liu, H.; Wu, J.; Jiang, X.-K.; Li, Z.-T. *Tetrahedron Lett*. **2007**, *48*, 7327. (c) Feng, D.-J.; Wang, G.-T.; Wu, J.; Wang, R.-X.; Li, Z.-T. *Tetrahedron Lett*. **2007**, *48*, 6181. (d) Wu, Z.-Q.; Li, C.-Z.; Feng, D.-J.; Jiang, X.-K.; Li, Z.-T. *Tetrahedron.* **2006**, *62*, 11054. (e) Li, C.-Z.; Zhu, J.; Wu, Z.-Q.; Hou, J.-L.; Li, C.; Shao, X.-B.; Jiang, X.-K.; Li, Z.-T.; Gao, X.; Wang, Q.-R. *Tetrahedron*. **2006**, *62*, 6973. (f) Li, C.-Z.; Li, Z.-T.; Gao, X.; Wang, Q.-R. *Chin*. *J. Chem.* **2007**, *25*, 1417. (g) Xiao, Z.-Y.; Hou, J.-L.; Jiang, X.-K.; Li, Z.-T.; Ma, Z. *Tetrahedron.* **2009**, *65*, 10182.

(75) (a) Ferrand, Y.; Kendhale, A. M.; Kauffmann, B.; Grelard, A.; Marie, C.; Blot, V.; Pipelier, M.; Dubreuil, D.; Huc, I. *J. Am. Chem. Soc*. **2010**, *132*, 7858. (b) Bao, C. Y.; Gan, Q.; Kauffmann, B.; Jiang, H.; Huc, I. *Chem. Eur. J*. **2009**, *15*, 11530.

(76) (a) Berl, V.; Krische, M. J.; Huc, I.; Lehn, J.-M.; Schmutz, M. *Chem. Eur. J.* **2000**, *6*, 1938. (b) Chang, S.-K.; Van Engen, D.; Fan, E.; Hamilton, A. D. *J. Am. Chem. Soc*. **1991**, *113*, 7640.

(77) Müller, M. M.; Windsor, M. A.; Pomerantz, W. C.; Gellman, S. H.; Hilvert, D. *Angew. Chem. Int. Ed.* **2009**, *48*, 922.

(78) Jones, C. R.; Pantos, G. D.; Morrison, A. J.; Smith, M. D. *Angew. Chem. Int. Ed.* **2009**, *48*, 7391.

(79) Zhong, Z.; Zhao, Y. *Org. Lett*. **2007**, *9*, 2891.

(80) (a) Prabhakaran, P.; Kale, S. S.; Puranik, V. G.; Rajamohanan, P. R.; Chetina, O.; Howard, J. A. K.; Hofmann, H.-J.; Sanjayan, G. J. *J. Am. Chem. Soc.* **2008**, *130*, 17743. (b) Kale, S. S.; Kotmale, A. S.; Dutta, A. K.; Pal, S.; Rajamohanan, P. R.; Sanjayan, G. J. *Org. Biomol. Chem.* **2012,** *10*, 8426.

(81) Vijayadas, K. N.; Davis, H. C.; Kotmale, A. S.; Gawade, R. L.; Puranik, V. G.; Rajamohanan, P. R.; Sanjayan, G. J. *Chem. Commun.* **2012**, *48*, 9747.

(82) Chatterjee, B.; Saha, I.; Raghothama, S.; Aravinda, S.; Rai, R.; Shamala, N.; Balaram, P. *Chem. Eur. J.* **2008**, *14*, 6192.

(83) Crystallographic data for **1a**, **2b**, **3a**, **4d**, and **4f** have been deposited with the Cambridge Crystallographic Data Centre CCDC - 866203 (**1a**), 866201 (**2b**), 866204 (**3a**), 866205 (**4d**), and 866202 (**4f**).

(84) Mathias, J. P.; Simanek, E. E.; Whitesides, G. M. *J. Am. Chem. Soc.* **1994**, *116*, 4326. (b) Damodaran, K.; Sanjayan, G. J.; Rajamohanan, P. R.; Ganapathy, S.; Ganesh, K. N. *Org. Lett.* **2001**, *3*, 1921.

(85) (a) Gunther, R.; Hofmann, H.-J. *J. Am. Chem. Soc.* **2001**, *123*, 247. (b) Baldauf, C.; Gunther, R.; Hofmann, H.-J. *Angew. Chem. Int. Ed.* **2004**, *43*, 1594. (c) Baldauf, C.; Gunther, R.; Hofmann, H.-J. *J. Org. Chem.* **2004**, *69*, 6214.

(86) Bruker (2006). *APEX2*, *SAINT* and *SADABS*. Bruker AXS Inc., Madison, Wisconsin, USA.

(87) Gaschow, M.; Kuerschner, L.; Neumann, U.; Pietsch, M.; Laser, R.; Koglin, N.; Eger, K. *J. Med. Chem*. **1999**, *42*, 5437.

Chapter 2

Conformational Modulation of peptide sequences using orthanilic acid (^{S}Ant)

Section A: *Study of the conformational bias due to the introduction of orthanilic acid (^{S}Ant) in peptide sequences*

Section B: *Conformational features of α/β/α hybrid peptides –A direct comparison between carboxamide oligomer and sulfonamide oligomer*

Section C: *Consequences of introduction of ^{S}Ant in Pro-Gly, Gly-Pro and Ant-Ant-Pro sequences*

Study of the conformational bias due to the introduction of orthanilic acid (^{S}Ant) in peptide sequences

2.1 Introduction

The salient feature of proteins/polypeptides is their ability to adopt folded structures. The proteins, which occur naturally, are known to be the richest family of folded molecules.[1] As mentioned in chapter 1, numerous factors impinge on this folding propensity of the proteins/polypeptides.[2] This phenomenal folding of protein involves reversing of the polypeptide chain direction which is termed as a ***turn***. This structural entity is considered to be the nucleation site of protein folding. Precisely, this structural motif of the polypeptide chain where it reverses its overall direction is termed as a ***reverse turn***. Reverse turns are the hallmarked segments found in many peptide hormones, neurotransmitters etc, that provide recognition sites for initiation of complex immunological, endocrinological or metabolic reactions.[3a] These motifs induce certain ***conformational bias*** by establishing intra-molecular hydrogen bonds between the carbonyl oxygen and amide protons on the backbone of the peptide. These turns are classified based on the hydrogen bonding pattern and dihedral angles on the peptide backbone. [3b] At the level of hydrogen bonds, the nomenclature of these turns is similar to that of helices (Fig 2.1).

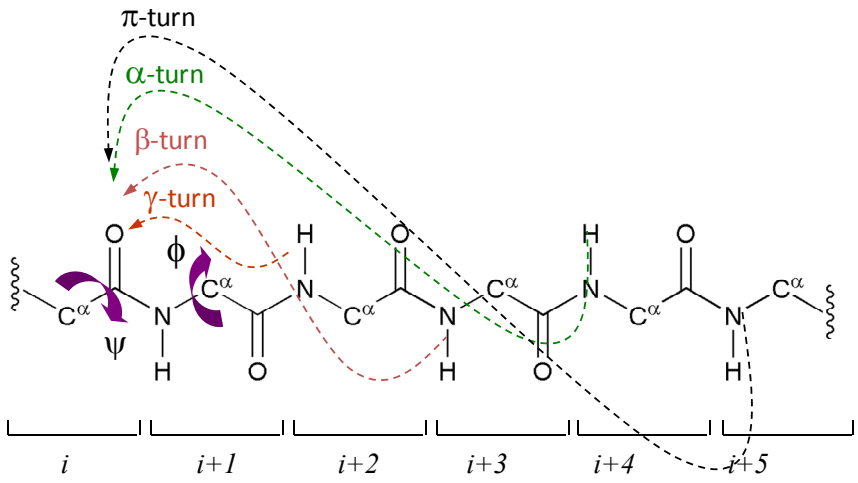

Fig 2.1: Plausible hydrogen bonding patterns on a peptide backbone (shown in dotted lines). The donor and acceptor residues separated by: five residues in α-turn ($i \rightarrow i+4$), four residues in β-turn ($i \rightarrow i+3$), three residues in γ-turn ($i \rightarrow i+2$) and six residues in π-turn ($i \rightarrow i+5$).

In general, this structural organization is involved in the binding processes i.e., found between the peptide ligands and receptors. It leads to the formation of mismatched pairs sometimes which is the root cause for most of the diseases. Several literature indicate that substituting the natural amino acids in peptides with synthetic, non-natural, rigid amino acid building blocks which have the ability to induce turns can act as drug molecules and solve the tribulations. These novel unnatural building blocks induce fold in the synthetic peptide molecules. Hence, the prospect of extending the folding phenomenon into the synthetic building blocks would be exceptionally helpful to develop synthetic peptide molecules with well-known conformational features. Even the hydrogen bonding propensities and the folding patterns involved in the natural proteins can be studied by designing and synthesizing synthetic turn mimetic sequences.[4] It is a known fact that the natural proteins due to their poor solubility, poor oral availability, poor conformational stability and high molecular weights, cannot be accessed as therapeutics and drugs. Owing to these drawbacks, there is a need for such synthetic systems. This provides a wide scope for the design of synthetic peptide molecules with rigid structural motifs/scaffolds which can serve as lead molecules to overcome the mentioned setbacks.[4]

Foldamer-based bio-mimicry can provide not only insights to understand the nature's mysteries but also allows inventing novel architectures comprising of non-natural/abiotic folding motifs that find applications in diverse fields.[5] The desired synthetic targets with pre-organized conformational bias can be achieved by inventing novel rigid building blocks/synthetic peptide mimics that are able to mimic the natural counterparts leading to more stable peptides.[6] Apart from conformational rigidity, which would have direct implications in modulating the receptor selectivity, proteolytic stability is another topic of concern in developing a synthetic peptide mimic which can be solved by introducing novel rigid amino acid units like β-amino acids in the designed systems.

2.1.1 β-amino acid building blocks

β-amino acids, the next higher homologues of α-amino acids provide considerable insight into designing synthetic peptides with improved proteolytic

and structural stability. As the β-amino acids are stable against proteolytic degradation, they are considered to be one of the key structural entities in drug design as well.[7] The oligomers derived from β-amino acids form stable secondary structures such as turns, loops, helices, sheets etc., and offer avenues for the structural exploration of diversely functionalized novel building blocks and to investigate their conformational preferences.[8] Recent years have witnessed the development of diversely functionalized β-amino acids with varying degrees of conformational freedom with respect to β-alanine - the only naturally occuring β-amino acid among the β-amino acid family. Amongst the huge repertoire of β-amino acids known in the literature, 2-aminocyclopropanecarboxylic acid (ACC),[9] 2-aminopentanecarboxylic acid (ACPC),[10] 2-aminocyclohexanecarboxylic acid (ACHC),[11] 2-aminobenzoic acid (anthranilic acid, Ant),[12] and (S)-aminobicyclo-[2.2.2]-octane-2-carboxylic acid[13] attain special status owing to their high backbone rigidity (Fig 2.2).

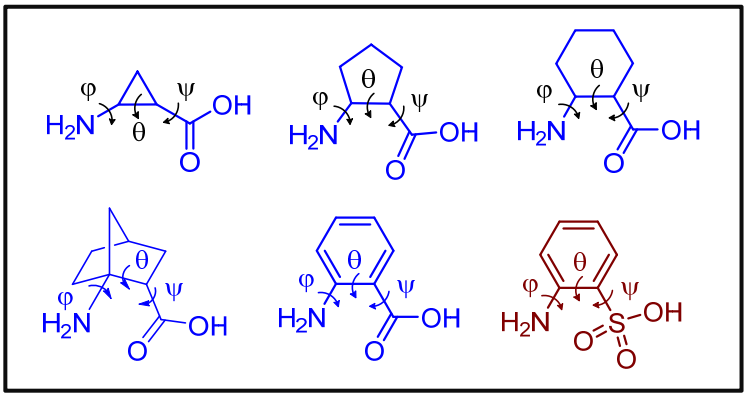

Fig 2.2: Few examples of rigid and constrained β-amino acid building blocks.

2.1.2 Orthanilic acid as a building block

In continuation of the ongoing research using anthranilic acid (Ant) in our laboratory, we undertook the conformational investigation of synthetic peptides using orthanilic acid (^{S}Ant) as a constrained β-amino acid. We chose ^{S}Ant as we were intrigued by its unusual features like (1) low rotation barrier about S-N bond in sulfonamide compared to C-N bond in carboxamide, (2) the sulfonamide bond is comparatively stable towards hydrolysis and can serve as an isostere for carboxamide, (3) the presence of an additional acceptor oxygen atom attached to sulfur increases the hydrogen bonding ability of sulfonamide, (4) the enhanced

acidity of sulfonamide NH increases the hydrogen bond donor capacity and (5) the dihedral angle ω being close to 90° maintains a twisted/tetrahedral conformation at the basic building block level itself.

Oligomers comprised of sulfonamides (β-sulfonopeptides),[14] sulfonamides, sulfoximines[15] have been reported in literature, though few in number. Gellman's group investigated the possibility of the characteristic hydrogen bonding between secondary sulfonamide and an α-amino acid residue (N-H…O=S) in a molecule containing sulfonamide linked to valine using NMR studies.[16] Hu and Chen reported that a sulfonamide incorporated sequence develops a V-shaped conformation featuring a three centered H-bonding involving the pyridine nitrogen, amide hydrogen and one of the sulfonyl oxygens in the hydrogen bonded network.[17] This was also supported by the solid-state crystal structure analysis. Sanjayan *et. al.* recently reported that (Pro-^{S}Ant-Aib)$_n$ oligomers adopt a specific helical conformation with characteristic repetitive 11-membered hydrogen bonded rings on their backbone (Fig 2.3).[18]

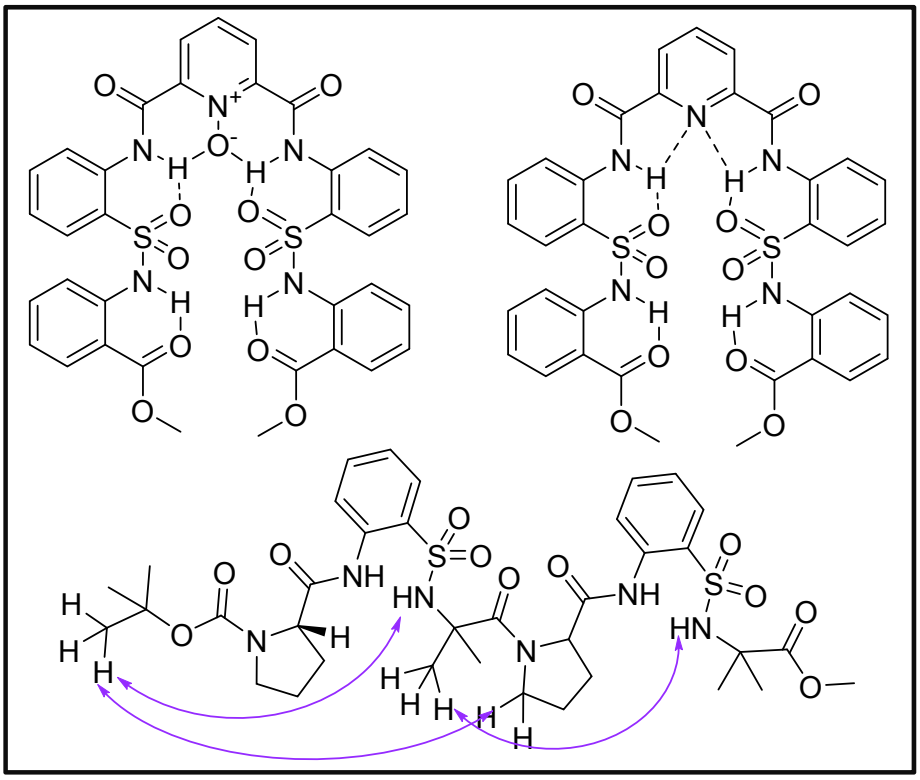

Fig 2.3: Sulfonamide oligomers adopting a folded conformation.

2.2 Design strategy

We designed peptide sequences wherein the aromatic β-amino acid, orthanilic acid was inserted between two amino acids in a fashion that it would form a sequence: Xaa-^{S}Ant-Yaa, to study the conformational preferences promoted by ^{S}Ant. Orthanilic acid with its amino and sulfonic acid groups attached to a rigid aromatic framework is characterized by well-defined torsional angles and constraints. The sulfonic acid group has a tetrahedral geometry which is in contrast to that of the planar carboxyl group found in the wide-range of amino acids.[19] Accordingly, we envisioned that the introduction of ^{S}Ant into the peptide sequences would not only cause rigidification of the backbone but also might result in a vivid conformational predisposition. Our efforts were also emboldened by the general observation that sulfonamides are ushering into prominence owing to their potential application in development of drug candidates to treat different kinds of ailments.[20]

An observation in our laboratory revealed that (Pro-^{S}Ant-Aib)$_n$ oligomers display a periodic 11-membered intra-molecular hydrogen bonded right handed helical conformation both in solid and solution states (Fig 2.4).[18] The significant feature of the designed peptide was that the conformationally rigid Pro and Aib residues surround the aromatic β-amino acid.

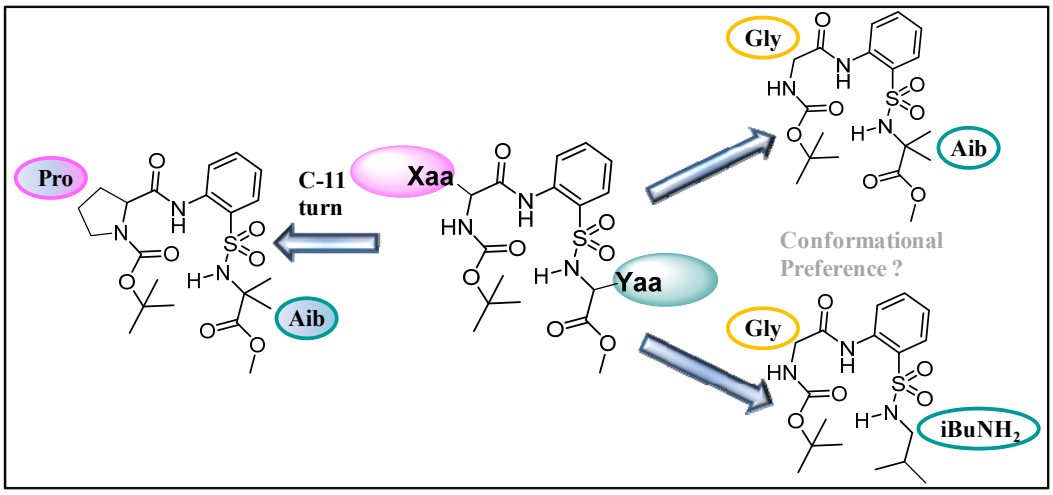

Fig 2.4: Design strategy employed to investigate orthanilic acid as a turn inducer.

To investigate the conformational bias developed by the peptide and the role of orthanilic acid in inducing a reverse turn, we designed the synthetic peptides as shown in Fig 2.5. The N-terminus Pro residue was substituted with a conformationally flexible Gly residue (as in peptides **2** and **3** shown in Fig 2.5). The C-terminus Aib was substituted by a flexible amine (as in peptide **4** shown in Fig 2.5). We also designed a peptide **1** (Fig 2.5) in which the N-terminus amino acid was completely removed in order to clearly understand the role of ^{S}Ant.

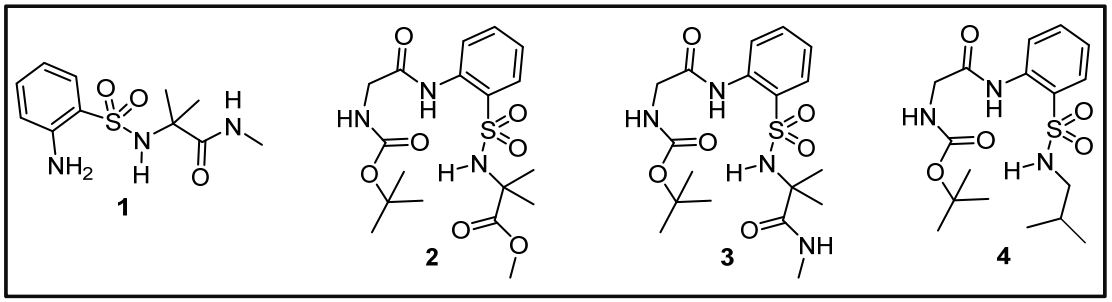

Fig 2.5: Designed peptide molecules to investigate the role of orthanilic acid as turn inducer.

2.3 Synthesis

Compound **1a** was synthesized using standard conditions by coupling 2-nitro benzene sulfonyl chloride with hydrochloride salt of methyl 2-amino 2-methyl propionate. Later, it was subjected to reduction using 10% Pd/C catalyst under hydrogen pressure at 60 psi to yield **1b**. Further, **1b** was amidated to obtain the target peptide **1** using methanolic CH_3NH_2. To achieve compound **2**, the amine **1b** was coupled with Boc-Gly-OH using ethyl chloroformate and Et_3N which was refluxed for 18 h at 80 °C. Then, it was subjected to C-terminus amidation using methanolic CH_3NH_2 to furnish the target peptide **3**. Compound **5** was synthesized following the similar procedure used to synthesize **1a**. Compound **5** was then subjected to reduction which gave the amine **6**. This amine **6** was coupled to Boc-Gly-OH following the same reaction conditions used to prepare the peptide **2** which resulted in the C-terminus modified peptide **4**.

2.3.1 Synthesis of the designed peptides

Scheme 2.1

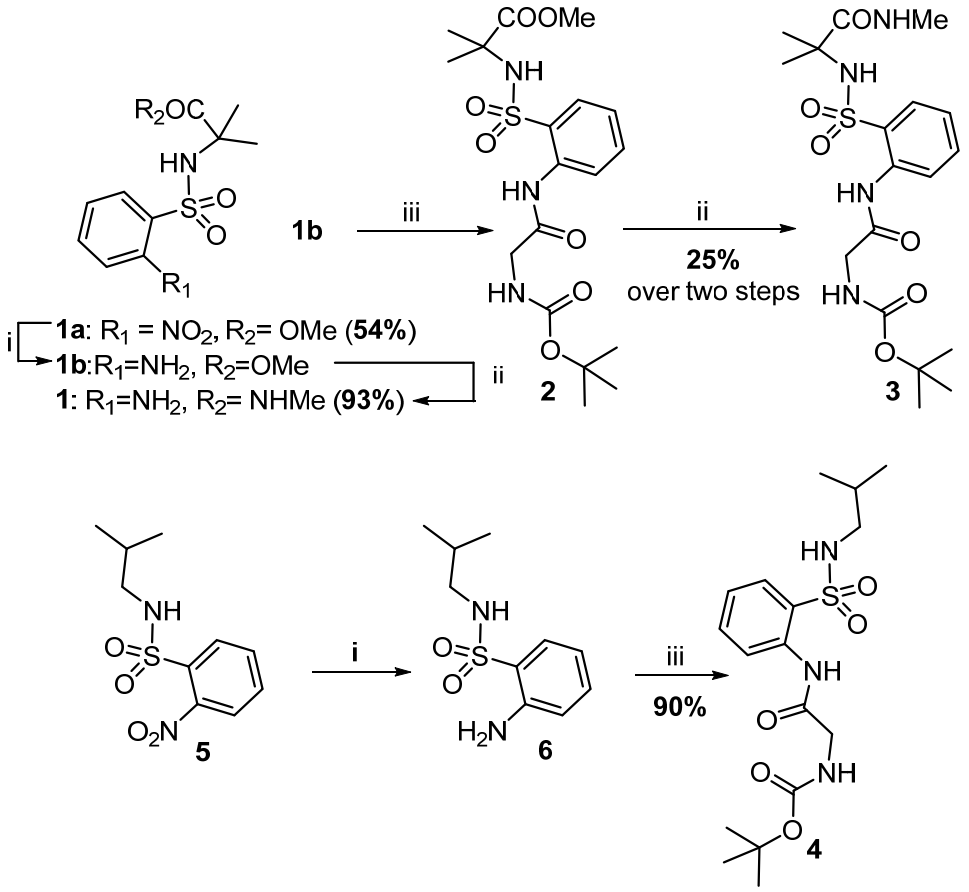

Scheme 2.1: Reagents and conditions: (i) H_2, Pd/C, MeOH, 60 psi, 5 h; (ii) methanolic CH_3NH_2, 5 h; (iii) Boc-Gly-OH, ethyl chloroformate, Et_3N, THF, reflux, 80 °C, 18 h.

2.4 Conformational Studies

The conformational analysis was performed using single crystal X-ray diffraction studies and 2D NMR techniques, the details of which are given below.

2.4.1 Single crystal X-ray diffraction studies

Extensive crystallization trials led to the formation of crystals of the peptides **1**, **2**, **3** and **4**. The crystal structures of **2**, **3** and **4** commonly display two types of intra-molecular hydrogen bonding patterns: one type involving the typical 6-membered hydrogen bonding (C6 H-bonding) and another type involving the unusual and strong 11-membered hydrogen bonding (Fig 2.6)

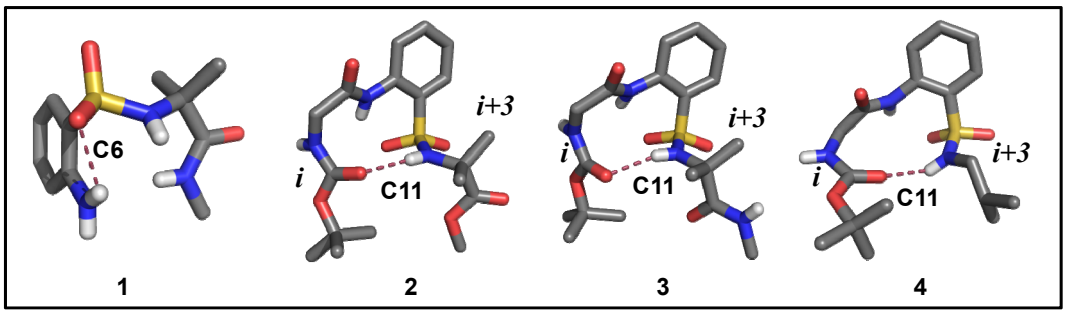

Fig 2.6: PyMOL-rendered crystal structures of peptides **1**-**4** featuring C6 and C11 hydrogen bonding patterns. All the hydrogens, other than the polar ones. have been deleted for clarity.

It is clearly evident from the crystal structures that the C6 H-bonding is intra-residual, formed within ^{S}Ant itself, while the C11 H-bonding is inter-residual interaction formed of four residues between -C=O of i^{th} residue and the sulfonamide -HN of $i+3^{rd}$ residue (as indicated in Fig 2.6) in backward direction (4 ← 1) as found in the classical β-turns. The hydrogen bonding distances [*d*(H…A)] of the C11 reverse turns in **2**-**4** were found to be ranging from 2.17 Å to 2.2 Å suggesting that the C11 H-bonded network is robust. The hydrogen bonding angle [Δ (D-H…A)] varies from 137^{0} (in compound **4**) to 169° (in compound **2**). The dihedral angle descriptors of ^{S}Ant, with its twisted conformation, are informative. Of particular note is the characteristic sulfonamide torsion (ω) of ^{S}Ant observed in **1**-**4** which is in the range of 77.2(2) to 93.5(3). It is noteworthy that in majority of the sulfonamide crystal structures reported in literature, the sulfonamide torsion (ω) is found to be ~90° (±30º) that is in stark contrast to the ω of planar carboxamides [180 (±30º)]. The restriction of the torsion (ω) of ^{S}Ant to ~90°, obviously imparted a twisted conformation to ^{S}Ant which is translated into the peptide backbones. Notably, the C-terminus amidation also did not significantly alter the H-bonding pattern in the peptide molecules which is clearly evident from the crystal structure of **3**. Finally, in order to understand the role of ^{S}Ant in folding, we synthesized the peptide **1** which is devoid of the N-terminus arm essential for the C11 H-bonding. The crystal structure of **1** clearly revealed a folded conformation even in the absence of any inter-residual H-bonding which clearly substantiates the pivotal role of ^{S}Ant with its twisted conformation in inducing fold in peptides. As in other cases, the usual intra-residual C6 hydrogen bonding was observed in peptide **1**. The torsional

angle and H-bonding parameters evidently provided insights into the conformational rigidity imparted by ^{S}Ant, leading to reverse turn conformation in peptides.

2.4.2 NMR Studies

The solution-state NMR studies firmly suggested that the solid-state conformation is prevalent in the solution-state as well. The characteristic inter-residual nOe interactions supportive of the folded conformation are the diagnostic long range inter-residual dipolar couplings between the N- and C-termini groups. Some of the selected nOes that support the reverse-turn conformation of **2** are ^{t}Boc (C16H) *vs*. NH3 and NH4, C16H *vs* C12H and NH2 *vs* NH3 (Fig 2.7).

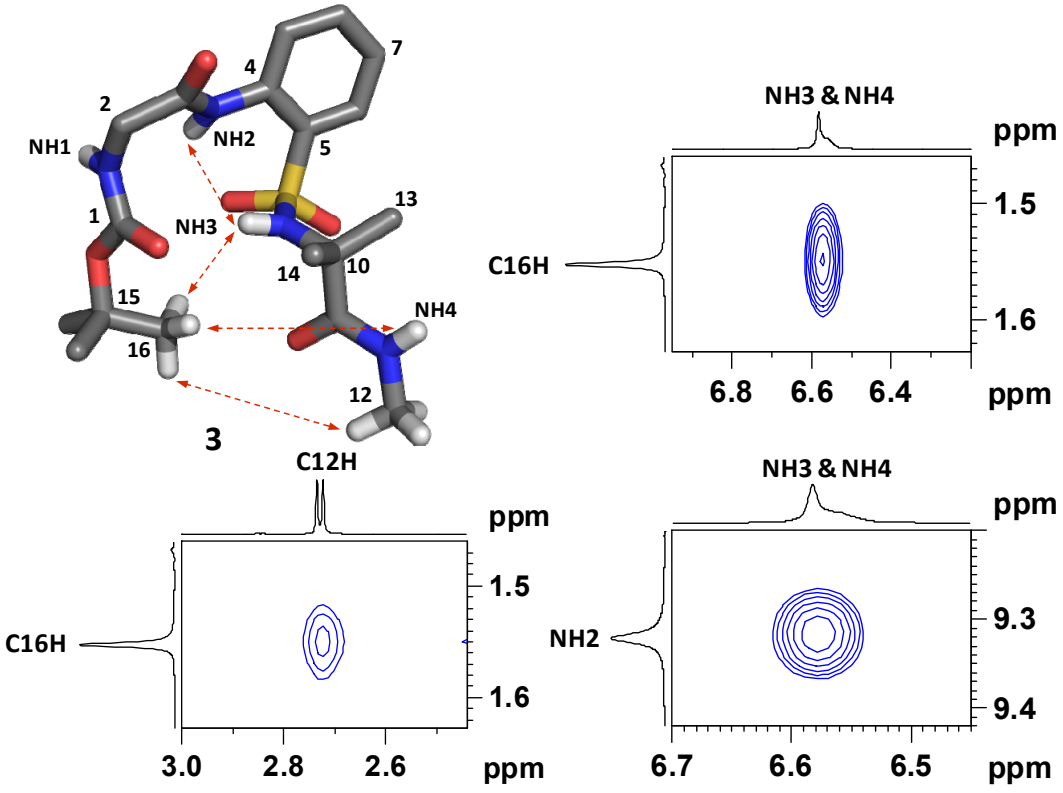

Fig 2.7: Crystal structure of **3** and selected 2D NOESY excerpts of peptide **3**. All the hydrogens, except the polar ones, have been deleted for clarity.

Similarly, in case of peptide **4**, the selected nOes that confirm the folded conformation are ^{t}Boc (C16H) *vs* NH3; C12H and C13H *vs* NH3; C10H *vs* NH3, C10H *vs* C8H; NH3 *vs* NH2; NH1 *vs* NH2; and C2H *vs* NH2 (Fig 2.8).

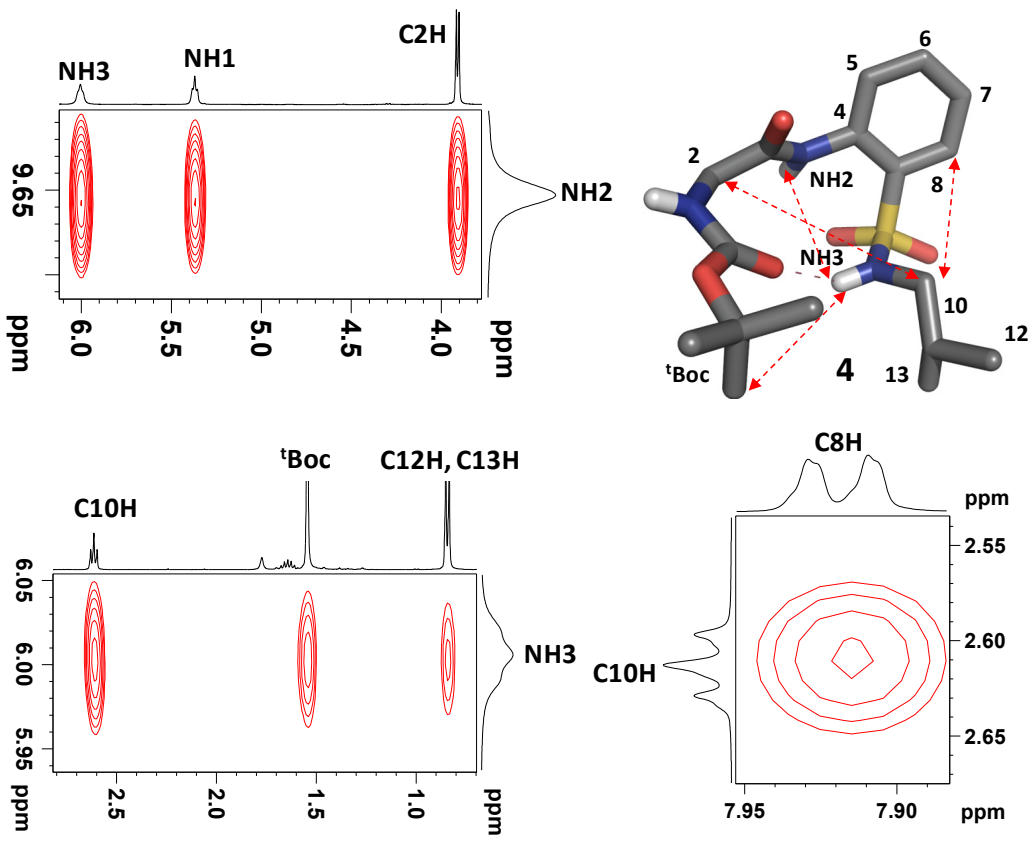

Fig 2.8: Crystal structure of and selected 2D NOESY excerpts of peptide **4** displaying reverse turn conformation. All the hydrogens, other than polar ones, have been deleted for clarity.

Further, the titration and variable temperature NMR studies supported the folded conformation of these peptides. The negligible chemical shift Δδ (NH) < 0.33, observed in the DMSO-d_6 titration experiments (Fig 2.9 A and B) strongly suggest the intra-molecular nature of the 11-membered hydrogen bonds observed in the compounds **2-4**. The results derived from the variable temperature experiments (Fig 2.9 C and D) indicate the temperature coefficient (263-323 °K), $\Delta\delta/\Delta T \sim 3.8$ ppb K^{-1} supporting the robustness of the hydrogen bonding pattern observed in the designed peptide sequences.

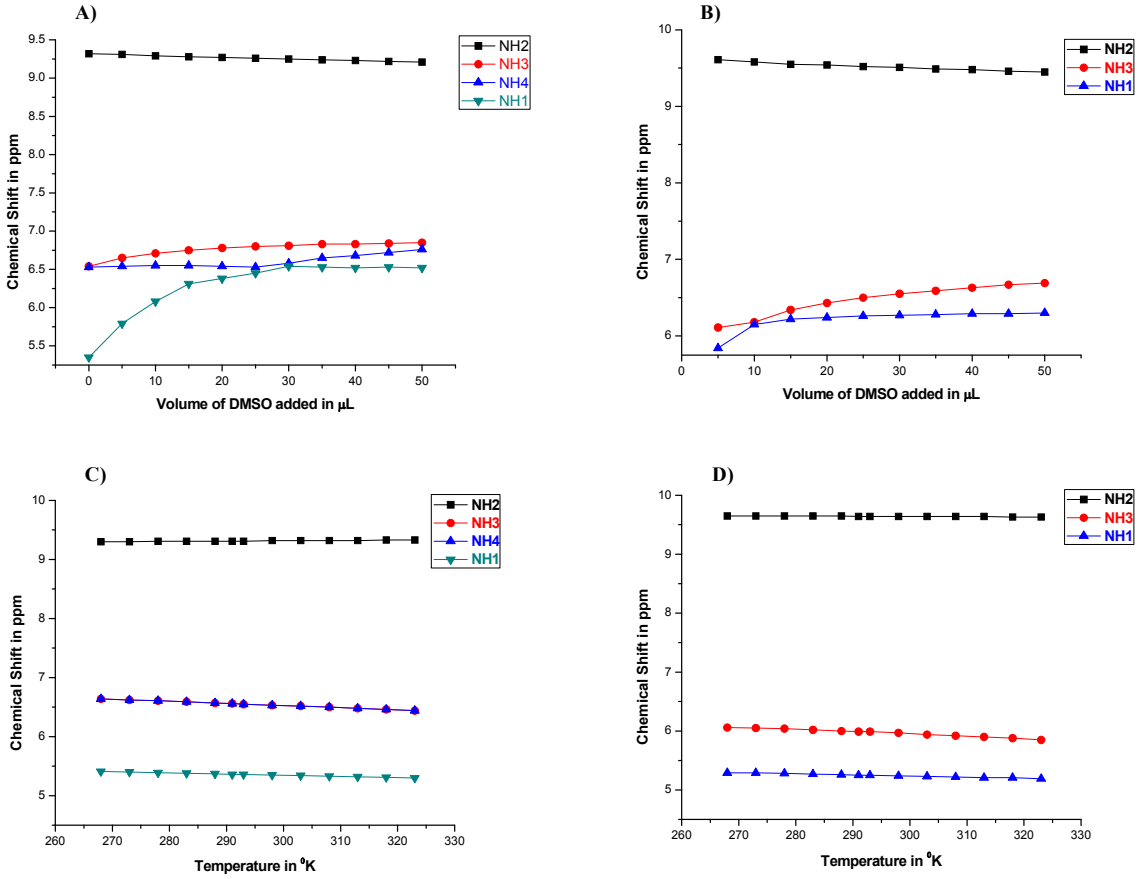

Fig 2.9: Plots representing DMSO-d_6 titration study of **3** (A), **4** (B) and variable temperature study of **3** (C), **4** (D).

2.5 Conclusion

In this part of work, we could demonstrate orthanilic acid as a strong reverse turn inducer when incorporated into peptide sequences of Xaa-^{S}Ant-Yaa. All the designed peptides feature an unusual 11-membered H-bonding formed in the backward direction analogous to that found in the native β-turns. The results signify the strong turn inducing tendency of ^{S}Ant that efficiently translates its rigidity into the peptide sequences. The various structural perturbations around the turn segment do not disturb the hydrogen bonding pattern suggesting that the conformation observed is robust in nature. The comparison of the crystal structures clearly proved that the torsional constraints of orthanilic acid are exclusively responsible for the turn formation in the designed peptides.

Conformational features of α/β/α hybrid peptides –A direct comparison between carboxamide oligomer and sulfonamide oligomer

2.6 Introduction

Construction of higher order tertiary and quaternary structures has been a long standing goal in the field of foldamers. The complex folding propensity of polypeptides is a reflection of the information embedded in a primary sequence, which is a prerequisite for the protein's function.[21] It is noteworthy that very few protein-like molecules with altered backbones are known in the literature, which makes it tempting to assume that the conformational preference of a protein is highly dependent on the poly-α-amino acid backbone. Thus, examination of peptide/protein structures by making synthetic analogous architectures with altered backbones would solve this entangled issue of understanding the protein folding and its function.[22] The pioneering work from Gellman's group in the field of foldamers, reported high resolution crystal structures of six novel hybrid foldamers featuring ααβ backbone repeats. These foldamers show a four helix bundle quaternary structure in the solid state.[23] Efforts have been taken up to study the sequence-structure relationships of proteins by modulating the side chains on the peptide backbone. The complementary approach i.e., modifying the polypeptide backbone retaining the original side chains can definitely bridge the gap between understanding local conformational preference and complex protein structure. This motivates a synthetic chemist to pursue the study of conformational preferences attained by backbone modified synthetic oligomers.

2.7 Objective of the present work

Literature reports indicate that $(\alpha\alpha\beta)_n$ and $(\beta\alpha\alpha)_n$ hybrid peptide oligomers adopt a C14 H-bonding,[25] while $(\alpha\beta\beta)_n$ hybrid peptides adopt C15 H-bonding[26] in their oligomers. But, the possible hydrogen bonding propensities in the class of αβα hybrid oligomers is not very well known in the literature. The aim of this piece of work was to study the conformational preferences adopted by αβα hybrid peptides. The present study also provides an insight into the study of hydrogen bonding propensities in the class of αβα hybrid oligomers. The significant feature

of αβα hybrid peptide sequence is that the aromatic unit is bridged with aliphatic units on either side making the backbone less flexible and more tunable.[24] Since, the aliphatic side chains are non-planar, the prediction of conformation would be trickier compared to that of aromatic oligomer built by aromatic sub-units only.

2.8 Design strategy

As mentioned in Section A of this chapter, orthanilic acid was observed to be a strong turn inducer in peptides due to its high conformational rigidity. Thus, we extended our efforts to understand the role of conformational ordering translated into the designed peptide sequences due to the insertion of orthanilic acid. We designed few αβα hybrid foldamers: Aib-Ant-Gly and Aib-^{S}Ant-Gly, featuring the combination of a rigid amino acid-Aib at the N-terminus and a flexible amino acid-Gly at the C-terminus, sandwiching the β-aromatic amino acids Ant and ^{S}Ant. This strategy can also provide a direct comparison between the conformational preferences adopted by the hybrid oligomers featuring carboxamide and sulfonamide. Oligomers upto hexapeptides were designed to study the conformational preferences of the αβα hybrid oligomers.

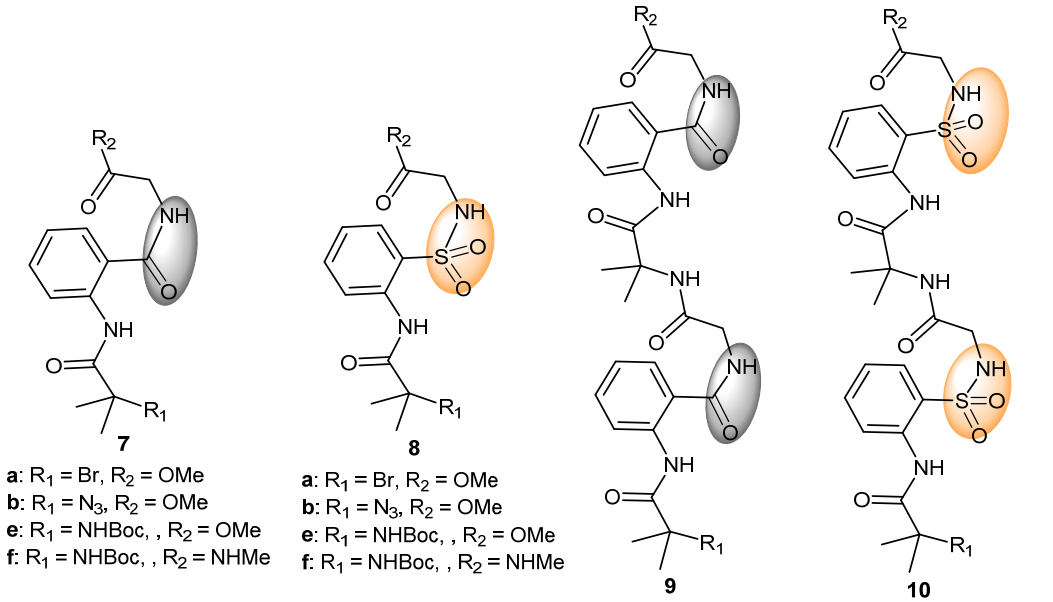

Fig 2.10: Designed oligomers to study the conformational features of αβα foldamer featuring carboxamide and sulfonamide groups on their backbones.

2.9 Synthesis

2.9.1 Synthesis of Aib-Ant-Gly oligomers

The nitro compound **11** was synthesized by coupling the hydrochloride salt of glycine methyl ester with 2-nitro benzoyl chloride which was further reduced using 10% Pd/C under H_2 pressure at 60 psi to yield the corresponding amine **12**. Amine **12** was then coupled with 2-bromo-2-methyl isopropyl bromide to give **7a**. Later, **7a** was heated to 80 °C in the presence of NaN_3 in DMF to give the azido compound **7b**. Then, the azide **7b** was subjected to reduction to form the corresponding amine which was *in situ* protected as Boc derivative **7e**. Further, **7e** was amidated using methanolic methyl amine to yield **7f**. The building blocks **7c** (carboxylic acid) and **7d** (amine) required for oligomer synthesis were obtained from **7b** by C-terminal hydrolysis and N-terminus azide reduction, respectively, coupling of **7c** and **7d** using EDC.HCl afforded **9a** which was treated with methanolic methyl amine to yield the C-terminus amidated derivative **9b** (Scheme 2.2).

Scheme 2.2

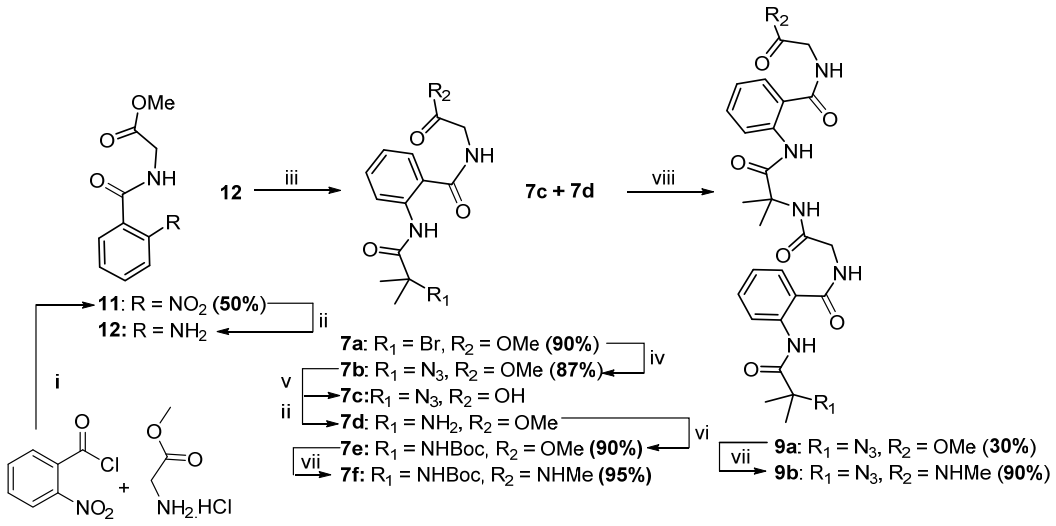

Scheme 2.2: Reagents and conditions: (i) DIPEA, DCM, rt, 12 h; (ii) Pd/C, MeOH, H_2, 60 psi, 12 h; (iii) 2-bromo-2-methyl isopropyl bromide, DIPEA, DCM, rt, 8 h; (iv) NaN_3, DMF, 80 °C, 12 h; (v) $LiOH.H_2O$, MeOH, rt, 12 h; (vi) $(Boc)_2O$, Et_3N, rt, 12 h; (vii) methanolic CH_3NH_2, MeOH, 12 h; (viii) EDC.HCl, Et_3N, DCM, rt, 72 h.

2.9.2 Synthesis of Aib-^{S}Ant-Gly oligomers

All the compounds **13**, **14**, **8a-f** and **10a** were synthesized using similar procedures used to prepare **11**, **12**, **7a-f** and **9a**, respectively, as shown in Scheme 2.3. The azide **10a** was subjected to reduction using 10% Pd/C under H_2 pressure at 60 psi, the resultant amine was trapped *in situ* as a Boc derivative, **10b** by reacting with Boc anhydride. Then, **10b** was treated with methanolic methyl amine to yield the amidated peptide **10c**.

Scheme 2.3

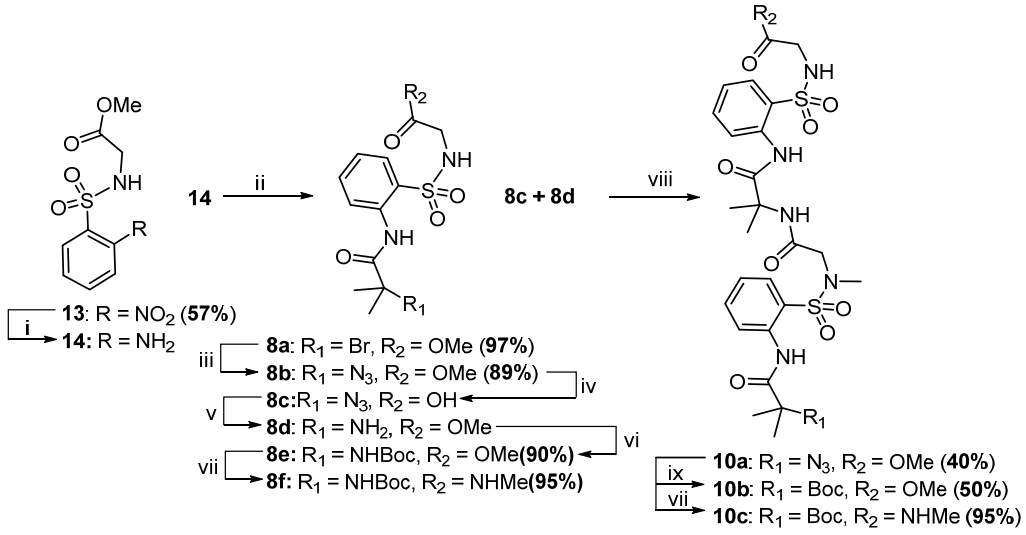

Scheme 2.3: Reagents and Conditions: (i) Pd/C, MeOH, H_2, 60 psi, 12 h; (ii) 2-bromo 2-methyl isopropyl bromide, DIPEA, DCM, rt, 8 h; (iii) NaN_3, DMF, 80°C, 12 h; (iv) $LiOH.H_2O$, MeOH, rt, 12 h; (v) Pd/C, MeOH; (vi) $(Boc)_2O$, Et_3N, rt, 12 h; (vii) methanolic CH_3NH_2, MeOH, 12 h; (viii) HBTU, DIPEA, CH_3CN, rt, 72 h; (ix) Pd/C, DIPEA, $(Boc)_2O$, MeOH, H_2, 60 psi, 48 h.

2.10 Conformational studies

The conformational features of the synthesized peptides were established by the solid-state single crystal X-ray diffraction studies as well as extensive solution-state 2D NMR experiments for the oligomers **7e**, **8e 8f** and **10c**. The efforts for crystallization weren't fruitful in case of hexapeptide **10c**. Hence, nOe based MD simulation studies were carried out to study the conformational pattern adopted by the oligomers.

2.10.1 Single crystal X-ray diffraction studies

Intense efforts for crystallization led to the crystals of tripeptide **7e** in the set of of Aib-Ant-Gly oligomers and the tripeptides **8e**, **8f** among the set of Aib-^{S}Ant-Pro oligomers. Crystal structure of **7e** (Fig 2.11 B) featuring a carboxamide clearly revealed that it does not exist in folded conformation although there is an intra-residual C6 H-bonding present on its backbone. The C-terminus amide **7f** showed strong tendency of self assembly which is apparent from the SEM analysis. In contrast, the crystal structures of **8e** and **8f**, featuring a sulfonamide clearly showed a characteristic fold featuring inter-residual C11 and C14 hydrogen bonding patterns, respectively.

It is noteworthy that the crystal lattice of **8e** comprises of two molecules, one of the structures shows the characteristic inter-residual C11 H-bonding in addition to the intra-residual C6 H-bonding (Fig 2.11 G), while the other shows a folded conformation devoid of C11 H-bonding retaining the intra-residual C6 H-bonding (Fig 2.11 F). These two molecules vary in the orientation of the C-terminus Gly residue wherein the -NH of sulfonamide frays from the -C=O of the Aib residue instead of participating in the hydrogen bonding, which is clearly evident from the overlaid structure of the molecules present in the crystal lattice (Fig 2.11 H). Intriguingly, the C-terminus amidated derivative **8f** showed a C14 H-bonding pattern in addition to the intra-residual C6 H-bonding (Fig 2.11 D). This pattern of H-bondings observed in the set of Aib-^{S}Ant-Gly tripeptides **8e** or **8f** might be due to the conformational flexibility of the Gly residue situated at the C-terminus of the synthetic peptide.

It is quite fascinating to note that the sequences featuring a sulfonamide apparently displayed a characteristic fold, featuring inter-residual C11 hydrogen bonding in addition to the intra-residual C6 H-bonding in their oligomeric sequences, owing to the structural pre-organization induced by the rigid aromatic β-amino acid, ^{S}Ant. The tripeptides **8e** and **8f** would be additional examples which profoundly suggest that ^{S}Ant is a strong reverse turn inducer as described in Section A of this chapter.

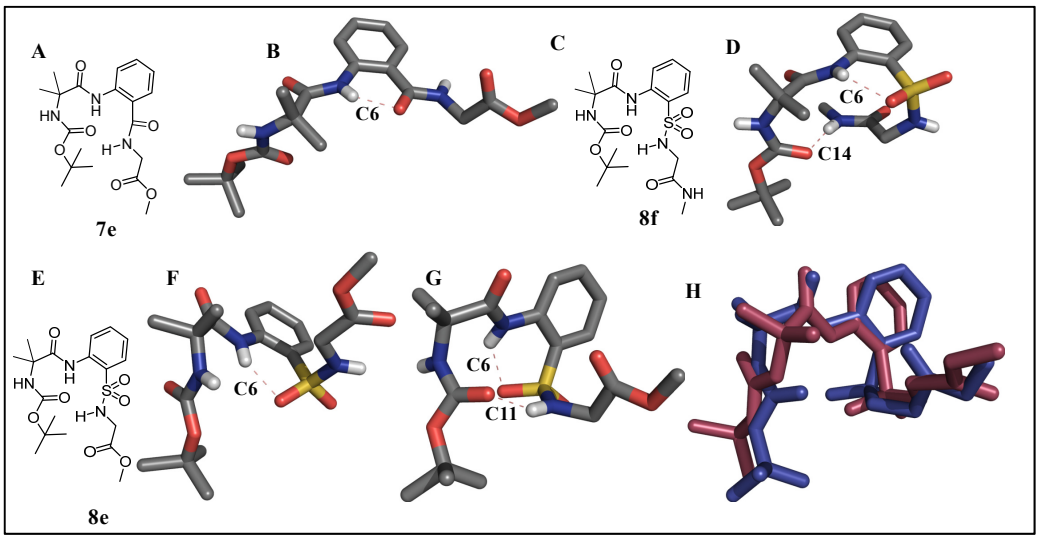

Fig 2.11: Molecular structures and crystal structures representing the characteristic H-bonding patterns in **7e** (A, B), **8f** (C, D) and **8e** (E-H). The two molecules present in the unit cell of **8e** (F and G) and their overlaid structure (H) are shown. All the hydrogens, except the polar ones, are deleted for clarity.

A closer look into the torsional angles in the crystal structures of **7e**, **8e** and **8f** reveals the significance of ^{S}Ant to induce fold. Among all the torsional parameters, ω of Ant and ^{S}Ant vary to a larger extent. In the carboxamide sequences, the ω of Ant is 174.2° (**7e**), while in the sulfonamide sequences, ω of ^{S}Ant varies from -64.6° (**8f**) to 68.7° (**8e**). This unambiguously explains the conformational divergence between the carboxamides (ω~180°) and sulfonamides (ω~90°). The intra-residual hydrogen bond distance [d(N-H…O=C)] in **7e** is 1.93 Å suggesting a strong C6 H-bonding, while the inter-residual hydrogen bond distances in **8e** is 2.24 Å and **8f** is 2.04 Å supporting the C11 and C14 H-bonding networks.

2.10.2 NMR studies

The conformation of the oligomers in solution-state was confirmed by extensive NMR studies which suggested an extended architecture for **7e** and a characteristic folded architecture for **8e** and **8f** with C11 and C14 H-bonding patterns, respectively. All the oligomers **7e**, **8e** and **8f** were readily soluble in non-polar organic solvents (>> 100 mmol in $CDCl_3$) at ambient temperature suggesting that all the polar hydrogen bonding groups are strongly solvent shielded, preventing the formation of polymeric aggregates. The oligomers **7e**, **8e**

and **8f** showed well dispersed signals rendering their conformational analysis easy. The signal assignment was done unambiguously using a combination of 2D COSY, HSQC, HMBC and NOESY experiments. The characteristic nOe's of **8e** and **8f** supported the folded conformation similar to that observed in solid-state.

In case of **7e**, no characteristic inter-residual nOes were observed in the solution-state which clearly supported the solid-state extended conformation. The characteristic nOes observed for **7e** which supported the solid-state conformation are NH2 *vs* ^{t}Boc; NH2 *vs* C13H, and C14H; NH3 *vs* C10H; C13H and C14H *vs* C9H that are shown in Fig 2.12. It was observed that the C-terminus amidated analogue **7f** was sparingly soluble in non-polar solvents (< 1 mmol in $CDCl_3$) suggesting strong aggregation, indicating that the polar hydrogen bonding groups are not solvent shielded.

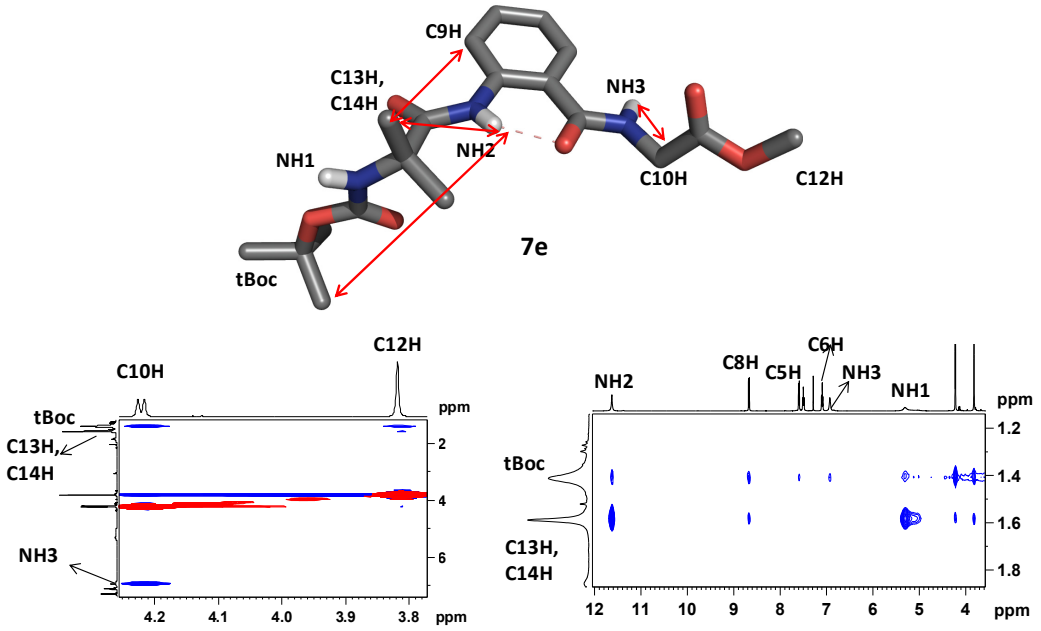

Fig 2.12: Crystal structure of **7e** (top). Selected 2D NOESY excerpts of **7e** (bottom). All hydrogens, except the polar ones, have been deleted for clarity in the crystal structure.

For **8e**, diagnostic inter-residual couplings were observed between the termini which clearly indicated their close proximity in the folded conformation. Some of the characteristic nOes observed between terminal residues are ^{t}Boc *vs* C10H and C12H; ^{t}Boc *vs* NH2; NH1 *vs* C13H and C14H; NH1 *vs* NH2 that are clearly shown in Fig 2.13. This confirms the prevalence of C11 H-bonded network

in the peptide **8e** in solution-state, although there are two molecules found in the soli-state crystal structure.

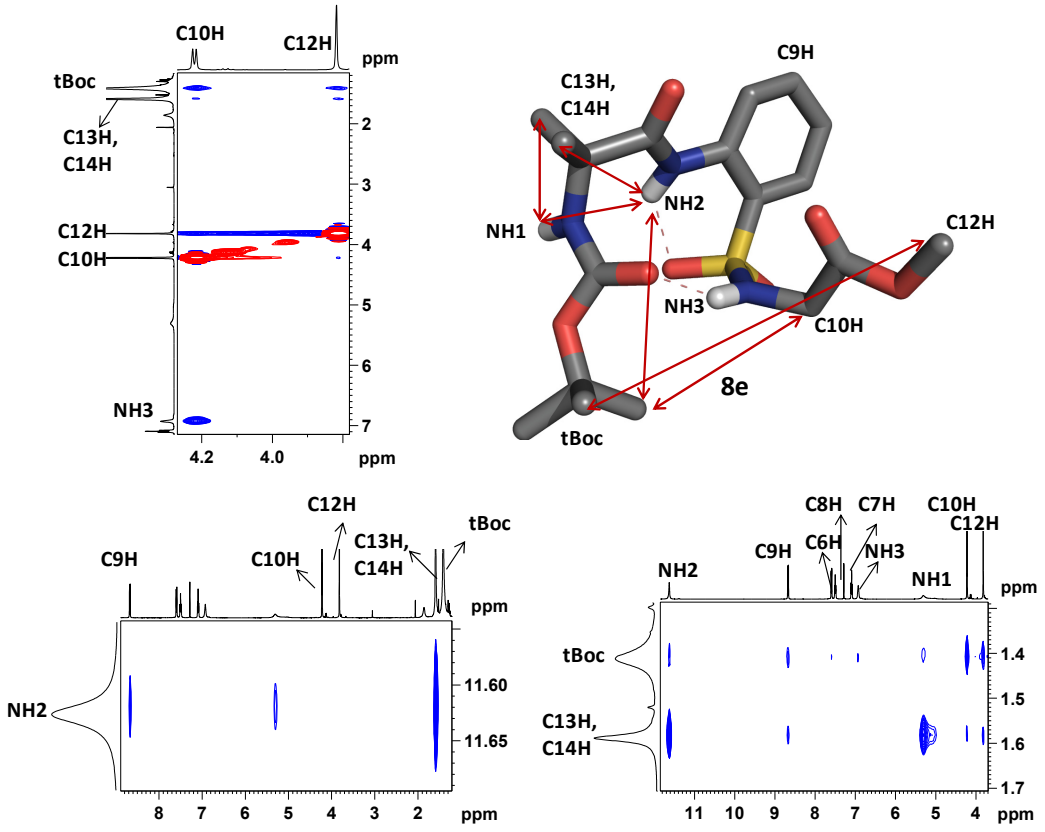

Fig 2.13: Crystal structure of **8e** and selected 2D NOESY excerpts in solution state. All hydrogens, except the polar ones have been deleted for clarity in the crystal structure.

In case of **8f**, the characteristic long range inter-residual couplings observed were C13H and C14H *vs* NH1; C13H and C14H *vs* NH2; ^{t}Boc *vs* NH1, ^{t}Bu *vs* C10H, ^{t}Bu *vs* C11H; C10H *vs* C9H that are clearly shown in Fig 2.14. Thus, the solution-state conformation clearly supported the solid-state conformation observed for **8f** featuring the inter-residual C14 hydrogen bonding in addition to the intra-residual C6 H-bonding present in the ^{S}Ant residue. This study clearly explains the significance of ^{S}Ant in turn formation in peptides.

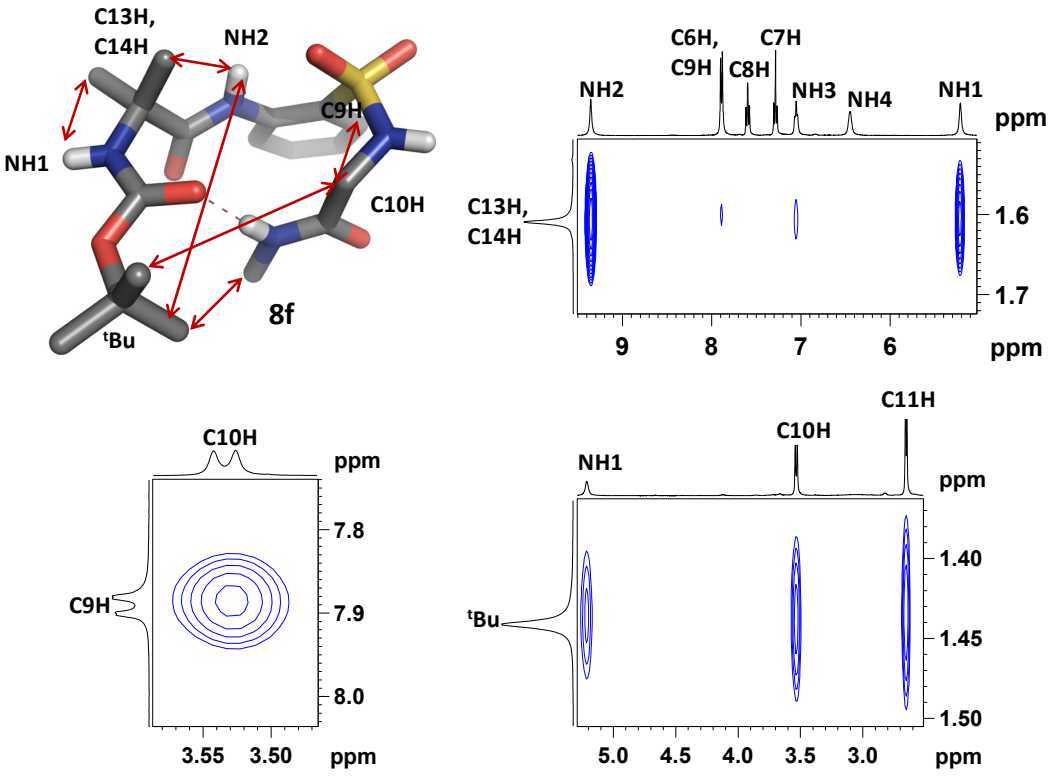

Fig 2.14: Crystal structure of **8f** (all hydrogens except the polar ones have been deleted for clarity) and selected 2D excerpts in solution state.

2.10.3 NMR derived structure of hexapeptide 10c

As the higher oligomers couldn't be crystallized, the conformational investigation of the hexapeptide (Aib-^{S}Ant-Gly)$_2$ **10c** was carried out using MD simulation studies. These studies revealed that the oligomer adopts two C11 H-bonded rings on the oligomeric backbone resulting in a helical conformation (Fig 2.15). Similarly, the conformations of the tripeptides **7e**, **8e** and **8f** were studied which revealed a similar conformational feature as observed in their solid-states, respectively. This was confirmed by the overlay of crystal structures with their respective NMR derived structures as shown in Fig 2.16. The good agreement between the NMR derived structures and experimental data of **7e**, **8e** and **8f** presumably, owing to high conformational preference induced by the β-amino acid-^{S}Ant, confirmed the reliability of MD-NMR derived structures in prediction of the foldamer conformation.

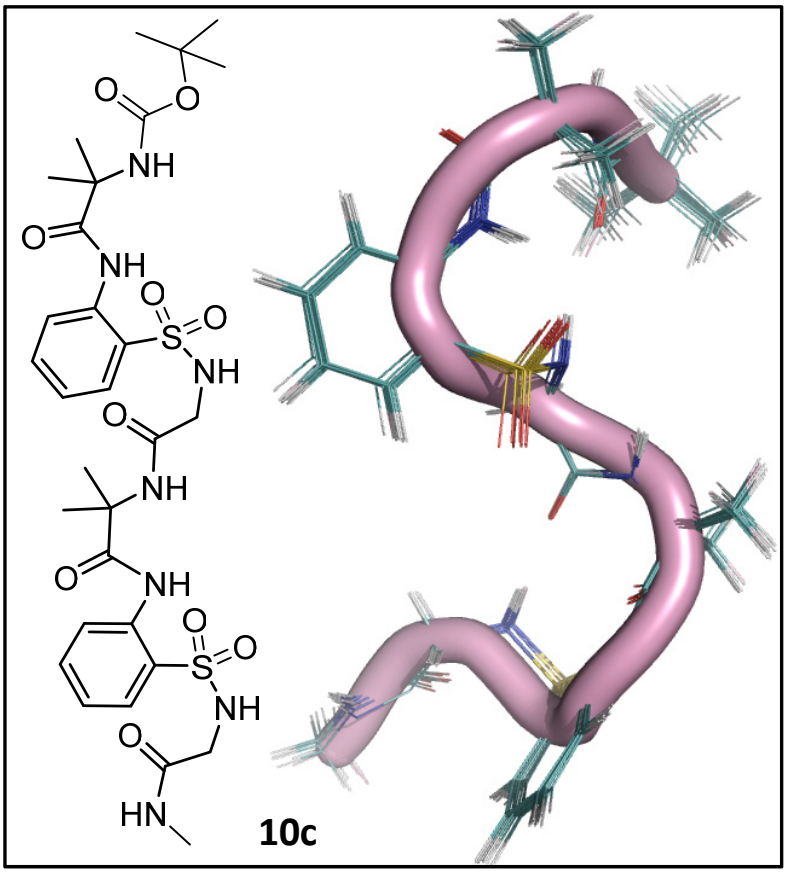

Fig 2.15: Molecular structure of hexapeptide **10c** (left). Cartoon representation of the overlaid 20 minimum energy conformations derived from the MD simulation studies revealing a helical conformation for **10c** (right).

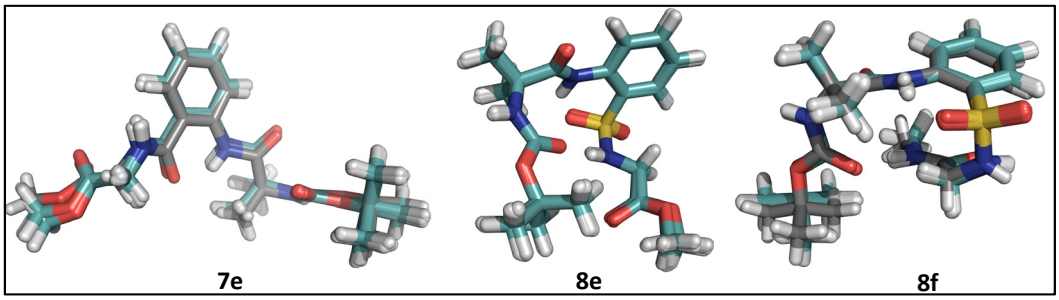

Fig 2.16: Minimum energy conformations derived from MD simulation studies of **7e**, **8e** and **8f** overlaid by their crystal structures, respectively.

The involvement of -NH protons in various H-bonding patterns observed in **7e** and, **8e**, **8f**, **10c,** respectively was substantiated by DMSO-d_6 titration studies (Fig 2.17). The negligible chemical shift values [$\Delta\delta$ (NH) = 0.23 ppb] of the amide protons involved in inter-residual C11 H-bonding clearly indicated the strength of H-bonding.

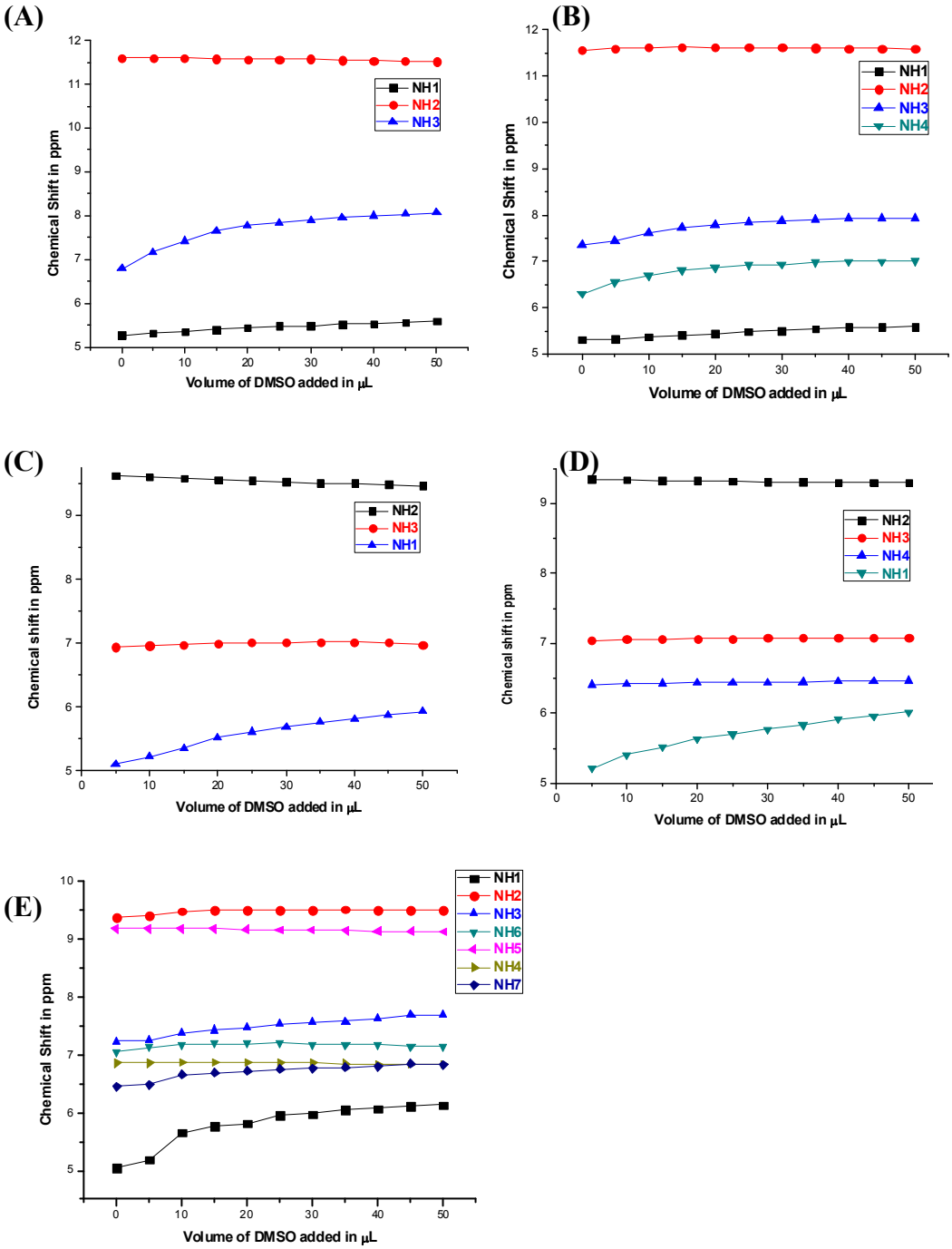

Fig 2.17: Plots representing DMSO-d_6 titration study of **7e** (A), 7**f** (B), **8e** (C), **8f** (D) and **10c** (E).

The variable temperature experiments (263-323 °K; $\Delta\delta/\Delta T < -1.5$ ppb K^{-1}) also supported the conformational patterns observed in the oligomers **7e**, **7f**, **8e** **8f**, **10c** (Fig 2.18 and Fig 2.19).

(F) **(H)**

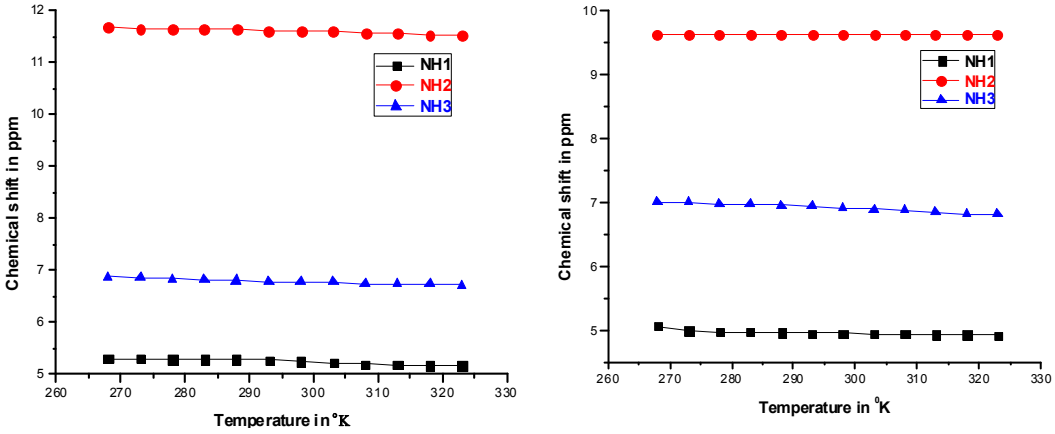

Fig 2.18: Plots representing variable temperature study of **7e** (F), **7f** (G) and **8e** (H).

(G)

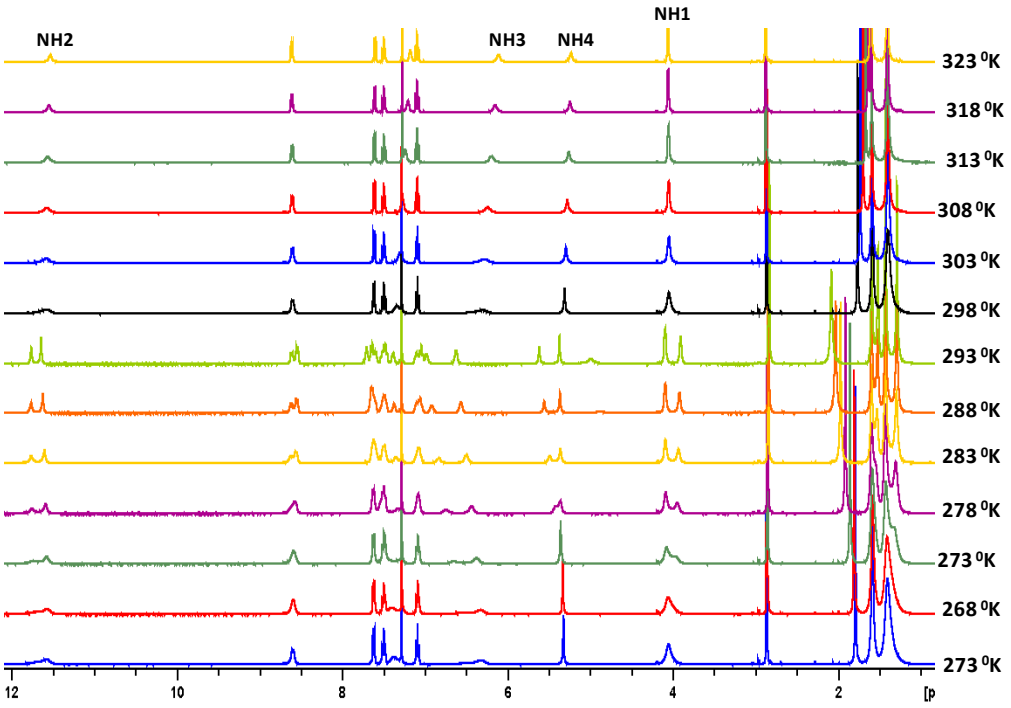

Fig 2.19: Stacked plot representing variable temperature study of **7f** (G).

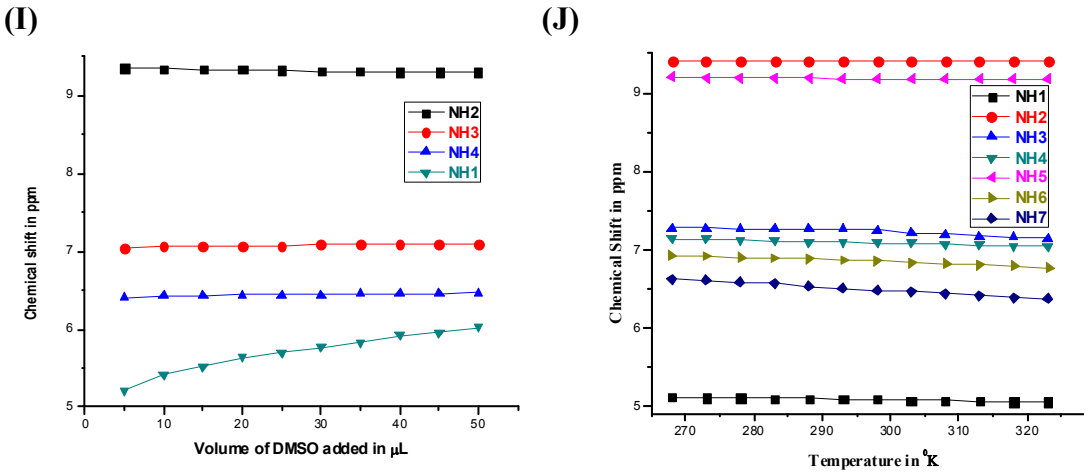

Fig 2.20: Plots representing variable temperature study of **8f** (I) and **10c** (J).

2.11 SEM analysis

Comparison of the microscopic images of the oligomers **7f** and **9b** revealed that they exist in a self-assembled fashion. As the length of the oligomer increases from tripeptide to hexapeptide, the self-assembling property of the respective oligomers increased which is clearly found in the images shown in Fig 2.21. This property of the Aib-Ant-Gly set of oligomers is reflected in the low solubility profile of these oligomers in organic solvents.

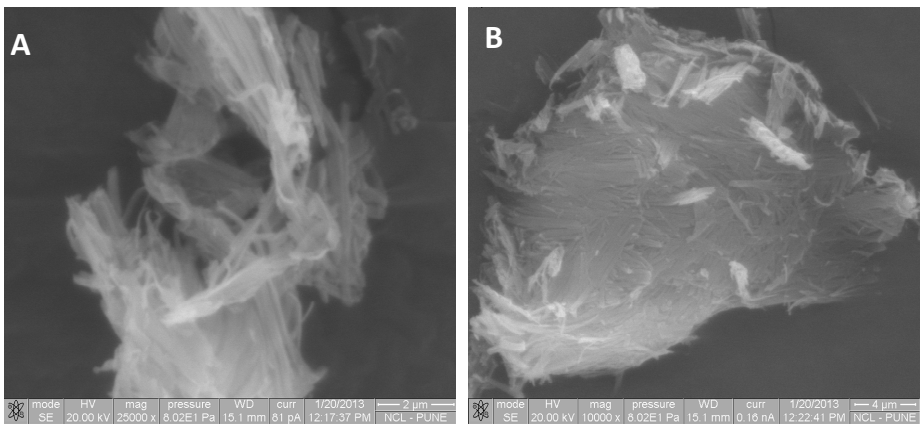

Fig 2.21: SEM images of the oligomers. (A) SEM image of the tripeptide **7f** and (B) SEM image of hexapeptide **9b**, deposited on carbon coated polymer film.

2.12 Conclusion

In summary, this study substantiates that the β-amino acid, ^{S}Ant is a turn inducer in peptide sequences irrespective of the neighbouring residues, in contrast to Ant, specifically in the class of αβα hybrid foldamers. We could successfully investigate the structure of the hexapeptide using MD-NMR-derived solution phase structure. Although, the shorter oligomers with ^{S}Ant as the central residue of the sequence exhibited a variety of conformational patterns, the higher oligomer exists in a helically folded conformation with C11 H-bonded repeats as revealed by the MD studies. A comparison of conformational preferences adopted by carboxamide and sulfonamide oligomers, where Ant and ^{S}Ant were sandwiched by α-amino acids was studied successfully. This study unequivocally proved the utility of ^{S}Ant as a turn inducer.

Consequences of introduction of ^{S}Ant in Pro-Gly, Gly-Pro and Ant-Ant-Pro sequences

2.13 Introduction

Pro-Gly and Gly-Pro amino acid segments in a peptide sequence differ in their conformation. According to the theoretical considerations, Gly-Pro sequence energetically favors an "extended conformation" with $\phi_{Gly} = 178°$, $\psi_{Gly} = 175°$ and $\phi_{Pro} = -75°$, $\psi_{Pro} = 79°$. On the other hand, the –Pro-Gly- sequence favors a folded conformation similar to type II β-turn as the minimum energy conformation.[27] It was observed previously in our laboratory that a synthetic peptide Ant-Ant-Pro sequence adopts a doubly folded conformation with strikingly dissimilar, closed H-bonded networks which are highly mutually dependent.[12b] Hybridizing these segments, by introducing orthanilic acid, may give rise to extremely rigid conformations leading to novel folded architectures in their oligomeric states.

2.14 Design strategy

As discussed in previous sections of this chapter, we found ^{S}Ant to be a strong turn inducer. In continuance with the search of novel hybrid foldamer architectures, we designed hybrid sequences Pro-^{S}Ant-Gly and Gly-^{S}Ant-Pro to study the consequences of inserting an unnatural β-amino sulfonic acid at the central position of Pro-Gly and Gly-Pro segments, which in turn may give an insight into the study of conformational features adopted by interchanging residues (N-terminus residue to C-terminus and *vice versa*) around a turn inducing amino acid in the respective oligomers. This concept of interchanging residues on a foldameric backbone will be helpful in constructing foldamers with diverse side chains (Fig 2.22).

Furthermore, hybrid peptide sequences: Ac-Ant-^{S}Ant-^{L}Pro-NHMe and Ac-Ant-^{S}Ant-^{L}Pro-^{D}Pro-NHMe were designed to study the conformational consequences at the cost of substituting one of the Ant residues by ^{S}Ant and by introducing ^{D}Pro residue at the C-terminus of a Ant-Ant-Pro synthetic peptide featuring two highly mutually dependent, yet dissimilar, hydrogen bonded networks in a cumulative fashion to stabilize the folded architecture (Fig 2.23).[12b]

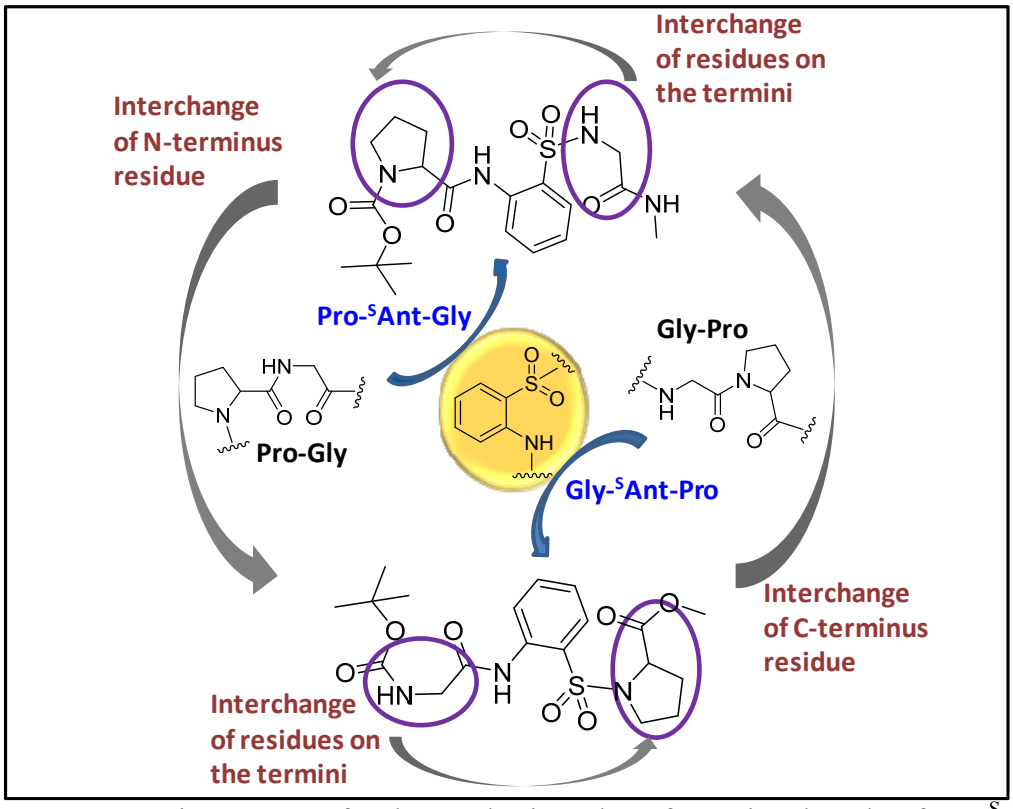

Fig 2.22: Design strategy for the synthesis and conformational study of Pro-^{S}Ant-Gly and Gly-^{S}Ant-Pro hybrid foldameric building blocks.

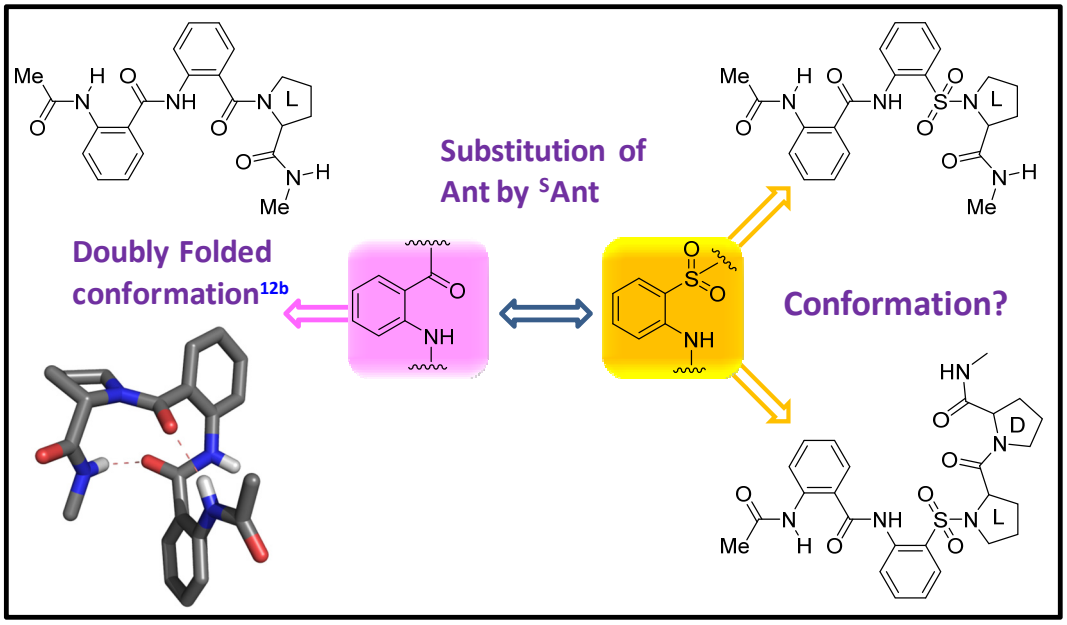

Fig 2.23: Conformational study of Ac-Ant-Ant-Pro-NHMe and Ac-Ant-^{S}Ant-^{L}Pro-^{D}Pro building blocks.

2.15 Synthesis

2.15.1 Synthesis of hexapeptide 16

Amine **14** was coupled to Boc-proline using ethyl chloro formate in THF by heating to 80 °C for 48 h to give the tripeptide **15a**. This tripeptide **15a** was subjected to Boc deprotection using TFA and ester hydrolysis using $LiOH.H_2O$ to give the amine **15b** and acid **15c** respectively. The C-terminus of **15c** was amidated to give **15d** using methanolic CH_3NH_2. Later, amine **15b** and acid **15c** were coupled using EDC.HCl to obtain the target hexapeptide **16a** (Scheme 2.4). The C-terminus amide derivative **16b** was prepared using the same protocol as used to synthesize **15d**.

Scheme 2.4

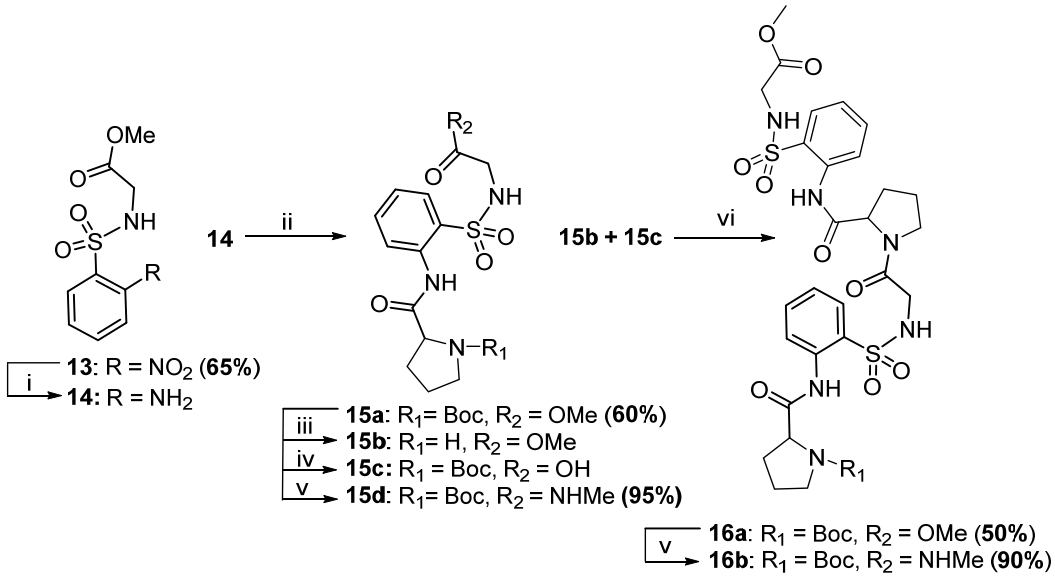

Scheme 2.4: Reagents and conditions: (i) Pd/C, MeOH, H_2, 60 psi, 12 h; (ii) Boc-Pro-OH, ethyl chloroformate Et_3N, THF, 80 °C, 48 h; (iii) TFA, DCM (1:1); (iv) $LiOH.H_2O$, MeOH; (v) methanolic CH_3NH_2, MeOH, 12 h; (vi) EDC.HCl, HOBt, Et_3N, DCM, rt, 12 h.

2.15.2 Synthesis of hexapeptide 20

Nitro compound **17** was synthesized following the reported procedure. It was reduced to amine **18** using 10% Pd/C under H_2 pressure at 60 psi. This amine, **18** was coupled to 2-bromo acetyl bromide to obtain **19a** which was further converted to the azido compound **19b** by heating **19a** in DMF in the presence of NaN_3 at 50 °C for 3 h. This azide **19b** was reduced to amine which was trapped as Boc derivative using Boc anhydride in the presence of 10% Pd/C under H_2 pressure at 60 psi. The amine **19d** and acid **19e** were coupled using EDC.HCl to obtain the target hexapeptide **20a** in moderate yields. The C-terminus amide derivative **20b** was also prepared following the similar protocol as **15d** was synthesized. Another derivative **22** with a nitro group at the N-terminus was synthesized by coupling **21** with 2-nitro benzene sulfonyl chloride using Et_3N as a base (Scheme 2.5).

Scheme 2.5

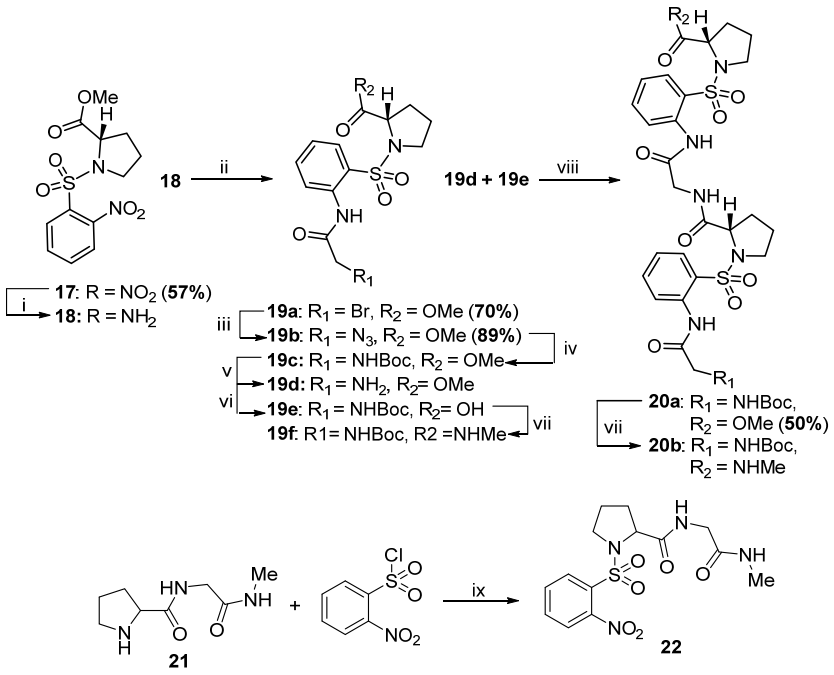

Scheme 2.5: Reagents and conditions: (i) Pd/C, MeOH, H_2, 60 psi, 12 h; (ii) bromo acetyl bromide, DIPEA, DCM, rt, 8 h; (iii) NaN_3, DMF, 50 °C, 12 h; (iv) $(Boc)_2O$, Pd/C, MeOH, H_2, 60 psi, 8 h; (v) TFA : DCM (1:1), (vi) aq. $LiOH.H_2O$, MeOH, rt, 12 h; (vii) methanolic CH_3NH_2, MeOH, 12 h; (viii) EDC.HCl, HOBt, Et_3N, DCM, rt, 12 h; (ix) Et_3N, DCM, rt, 5 h.

2.15.3 Synthesis of Ac-Ant-SAnt-Pro-NHMe

Compounds **17** and **24** were synthesized following the reported procedures[18] by coupling 2-nitro benzene sulfonyl chloride with **23a** and **23b**. The nitro compound **17** was subjected to reduction using 10% Pd/C in MeOH under H_2 pressure at 60 psi to obtain the amine **18** while **24** was reduced using $SnCl_2$. $2H_2O$ in MeOH under heating condition at 80 °C to obtain the amine **25**. These amines **18** and **25** were then coupled with 2-nitro benzoyl chloride to give **26a** and **26d**, respectively. Later, compound **26a** was subjected to hydrolysis using $LiOH.H_2O$ to give the acid **26b**. The C-terminus of **26a** was amidated using methanolic CH_3NH_2 to yield **26c**. The nitro compound **26a** was reduced using 10% Pd/C as catalyst in MeOH under H_2 pressure at 60 psi while the nitro group of **26c** was reduced using $SnCl_2$. H_2O in MeOH which was heated to 80 °C for 12 h to give the respective amines. The amines obtained were subjected to N-acetylation without further purification using Ac_2O in the presence of Et_3N and DMAP to obtain the designed compounds **26e**, **26g** and **26h** (Scheme 2.6).

Scheme 2.6

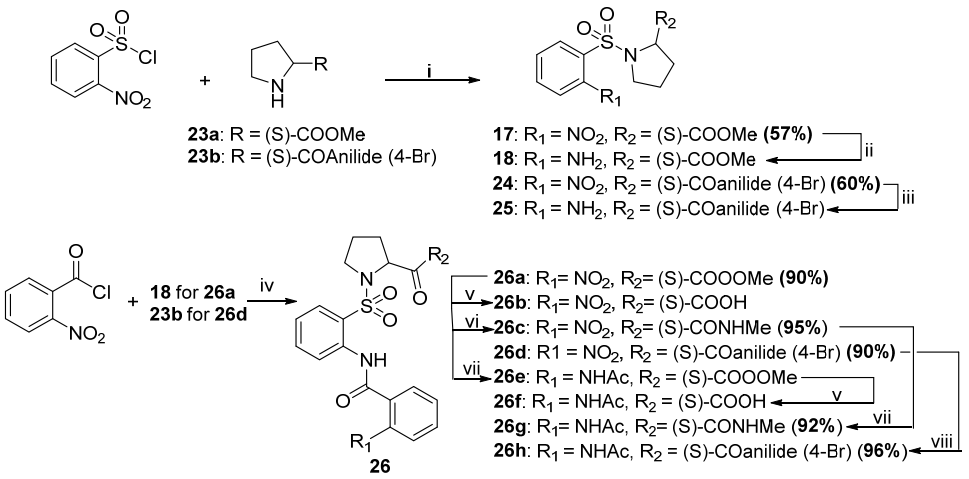

Scheme 2.6: Reagents and conditions: (i) Et_3N, DCM, rt, 12 h; (ii) 10% Pd/C, MeOH, H_2, 60 psi; (iii) $SnCl_2$. $2H_2O$, MeOH, reflux, 80 °C; (iv) Py, DCM, rt, 5 h; (v) $LiOH.H_2O$, MeOH, rt, 5 h; (vi) methanolic CH_3NH_2, rt, 8 h; (vii) (a) 10% Pd/C, MeOH, H_2, 60 psi; (b) Ac_2O, Et_3N, DMAP, DCM, rt, 6 h; (viii) (a) $SnCl_2$. $2H_2O$, MeOH, reflux, 80 °C; (b) Ac_2O, Et_3N, DMAP, DCM, rt, 6 h.

2.15.4 Synthesis of Ac-Ant-SAnt-^{L}Pro-^{D}Pro-NHMe

The acid **26b** (Scheme 2.6) was coupled with **23c** and **23d** separately to yield the derivatives **27a** and **27c**, respectively. It is noteworthy that the compound **27a** showed two conformations in the solution state which is clearly observed in the ^{1}H NMR spectrum of the compound showing two sets of signals (experimental section). To overcome this problem, **27a** was subjected to C-terminus amidation to obtain **27b**. The C-terminus amide derivative **27b** showed a single set of signals in ^{1}H NMR. Later, the nitro groups of **27a** and **27d** were subjected to reduction using 10% Pd/C and $SnCl_2.2H_2O$ under standard conditions. The amines obtained, without further purification, were then subjected to N-acetylation to yield **27d** and **27f** (Scheme 2.7).

The amines **28a** and **28b** were coupled with 2-nitro benzene sulfonyl chloride to yield the compounds **29a** and **29b**, respectively. The ester **29a** was subjected to C-terminus amidation to yield **29c** using methanolic CH_3NH_2 in MeOH (Scheme 2.7).

Scheme 2.7

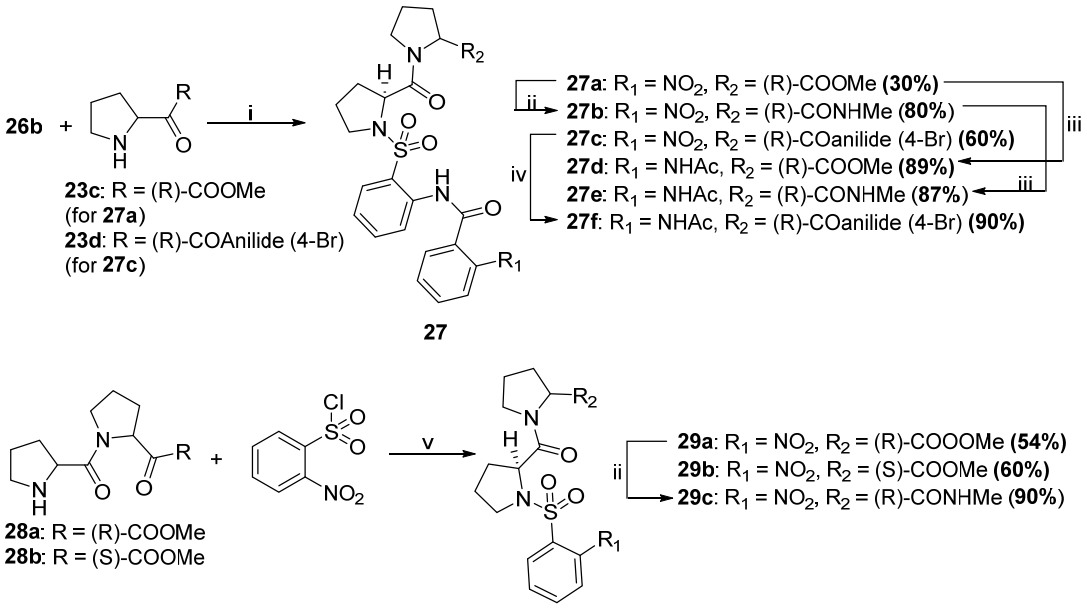

Scheme 2.7: Reagents and conditions: (i) HBTU, HOBt, Et_3N, CH_3CN, rt, 5 h; (ii) methanolic CH_3NH_2; (iii) (a) 10% Pd/C, MeOH, H_2, 60 psi; (b) Py, Ac_2O, DMAP, DCM, rt, 6 h; (iv) (a) $SnCl_2$. $2H_2O$, MeOH, reflux, 80 °C; (b) Ac_2O, Et_3N, DMAP, DCM, rt, 6 h; (v) Et_3N, DCM, rt, 5 h.

2.16 Conformational studies

The conformational features of the synthesized peptides were established by solid-state single crystal X-ray diffraction studies as well as extensive solution state 2D NMR experiments.

2.16.1 Single crystal X-ray diffraction studies

Extensive efforts for the crystallization led to the crystals of **15d** and **22**. The crystal structure of **15d** clearly revealed a C11 H-bonded ring, extended β-turn, where the hydrogen bond exists between the -C=O of i^{th} residue and –NH of $i+3^{th}$ residue (Fig 2.24 A). Neither the tripeptide **19f** nor the hexapeptide **20b** resulted in crystal formation even after extensive trials to study the conformational preference of Gly-^{S}Ant-Pro hybrid foldamers. Interestingly, the crystal of **22** revealed a C10 H-bonded conformation, characteristic β-turn, (Fig 2.24 B) which represented the turn forming segment of the hexapeptide **20b**: Boc Gly-^{S}*Ant-Pro-Gly*-^{S}Ant-Pro-Gly-NHMe. It is noteworthy that the oxygen of the $–SO_2$ group in **22** participates in the H-bonded network with the -NH of the C-terminus amide. It is worth mentioning that ω of ^{S}Ant in **15d** and **22** are 53.8° and -66.6°, respectively, which is responsible for the characteristic fold observed in the peptides.

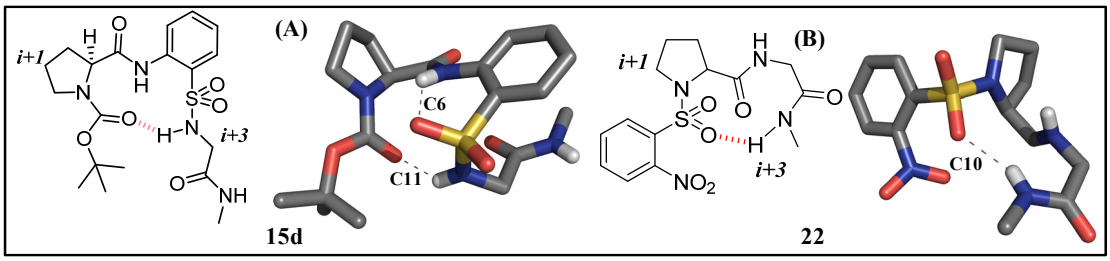

Fig 2.24: (A) Molecular structure and crystal structure of **15a**; (B) molecular structure and crystal structure of **22**. All the hydrogens, except the polar ones, have been deleted for clarity in the crystal structures.

In the case of Ac-Ant-^{S}Ant-Pro-NHMe and Ac-Ant-^{S}Ant-^{L}Pro-^{D}Pro-NHMe oligomerics, intense efforts for crystallization led to the crystals of **24**, **26a**, **26f**, **29a** and **29b**. The crystal structure of **24** (Fig 2.25 B) revealed that the residues ^{S}Ant and Pro orient themselves in different planes. The crystal structures of **26a** and **26f** (Fig 2.25 D and F) wherein Ant residue has been introduced at the

N-terminus clearly showed the formation of a C9 turn. It is noteworthy that acetylation of N-terminus of the Ant ring doesn't affect the conformation of the peptide, which is clearly evident from the crystal structure of **26f** (Fig 2.25 F). All the efforts to crystallize the compounds **26g** and **27e** went in vain.

To study the effect of ^{S}Ant on the conformational bias of ^{L}Pro-^{L}Pro and ^{L}Pro-^{D}Pro dipeptide segments,[29] the compounds **29a** and **29b** were crystallized. The crystal structure of **29a** and **29b** (Fig 2.25 H and J) clearly showed that ^{S}Ant does not affect the conformation of ^{L}Pro-^{L}Pro and ^{L}Pro-^{D}Pro dipeptides. The crystal structure of **29b** (Fig 2.25 J) revealed a folded conformation featuring a C-H…O interaction due to the ^{L}Pro-^{D}Pro fold in the molecule.

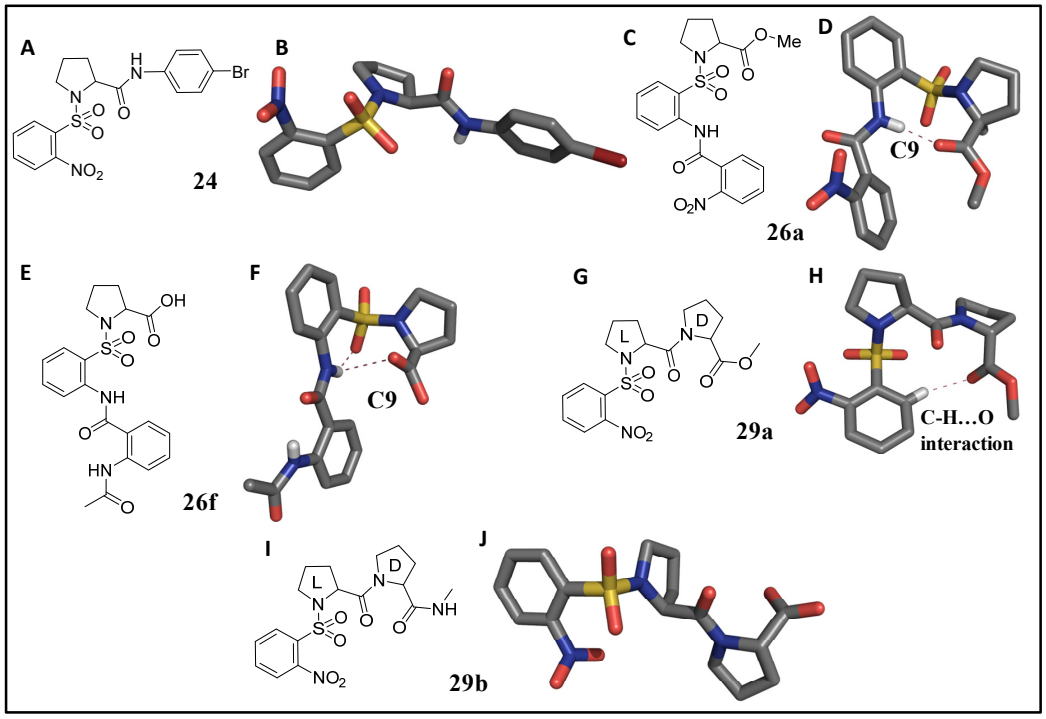

Fig 2.25: Molecular and crystal structures of **24** (A, B), **26a** (C, D), **26f** (E, F), **29a** (G, H), and **29b** (I, J), respectively. All hydrogens, other than the polar ones have been deleted for clarity in the crystal structures

2.16.2 NMR Studies

Conformations of the peptides in solution-state were investigated by extensive NMR studies revealing a folded architecture for **15d** and **22** with the characteristic C11 and C10 H-bonding patterns, respectively. Both the synthetic peptides **15d** and **22** were readily soluble in non-polar organic solvents (>> 100 mmol in $CDCl_3$) at ambient temperature suggesting that all the polar hydrogen bonding groups are strongly solvent shielded. Both **15d** and **22** showed sharp well dispersed signals rendering their conformational analysis easy. The signal assignment was done unambiguously using 2D COSY, HSQC, HMBC and NOESY experiments. Analysis of the 2D NOESY spectra of **15d** and **22** suggested the characteristic nOes supporting the folded conformation as observed in the solid-state.

The characteristic long range inter-residual couplings observed in the solution-state conformation of **15d** are ^{t}Boc *vs* C2H, NH2 and NH3; NH1 *vs* C5H; C10H *vs* C14H (Fig 2.26). This strongly supports the conformation of the peptide observed in the solid-state.

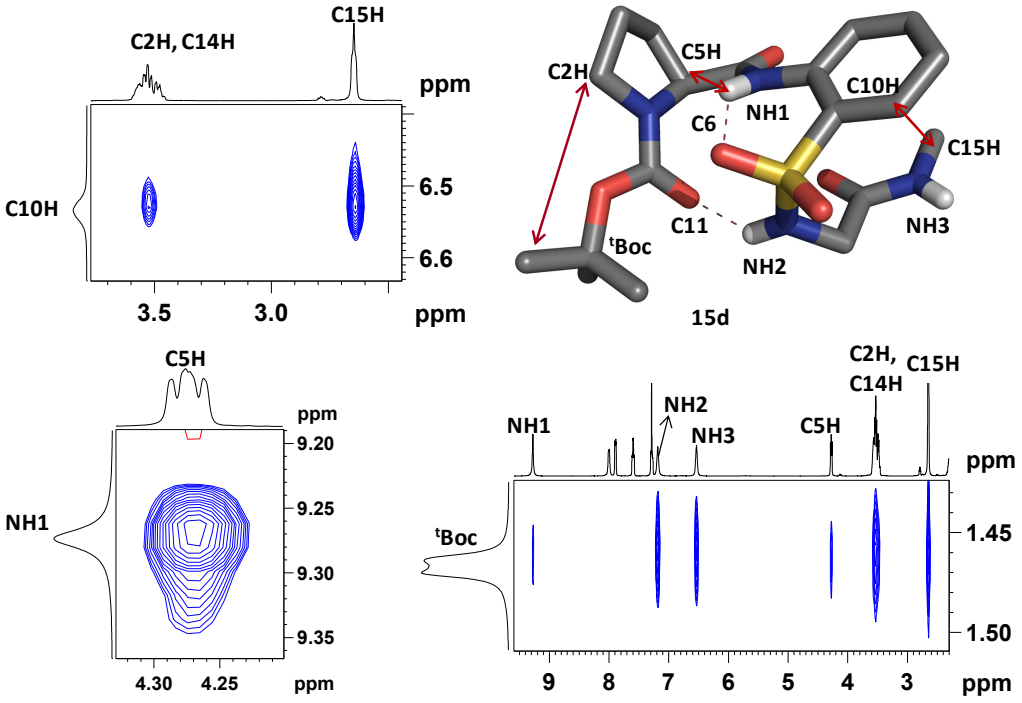

Fig 2.26: Crystal structure of **15d** and selected 2D NOESY excerpts in solution-state. All hydrogens, except the polar ones, have been deleted for clarity.

For **22**, the characteristic long range inter-residual couplings observed were C2 *vs* NH1and NH2; C7H *vs* NH2; C9H *vs* C7H; NH2 *vs* C6H and C5H (Fig 2.27).

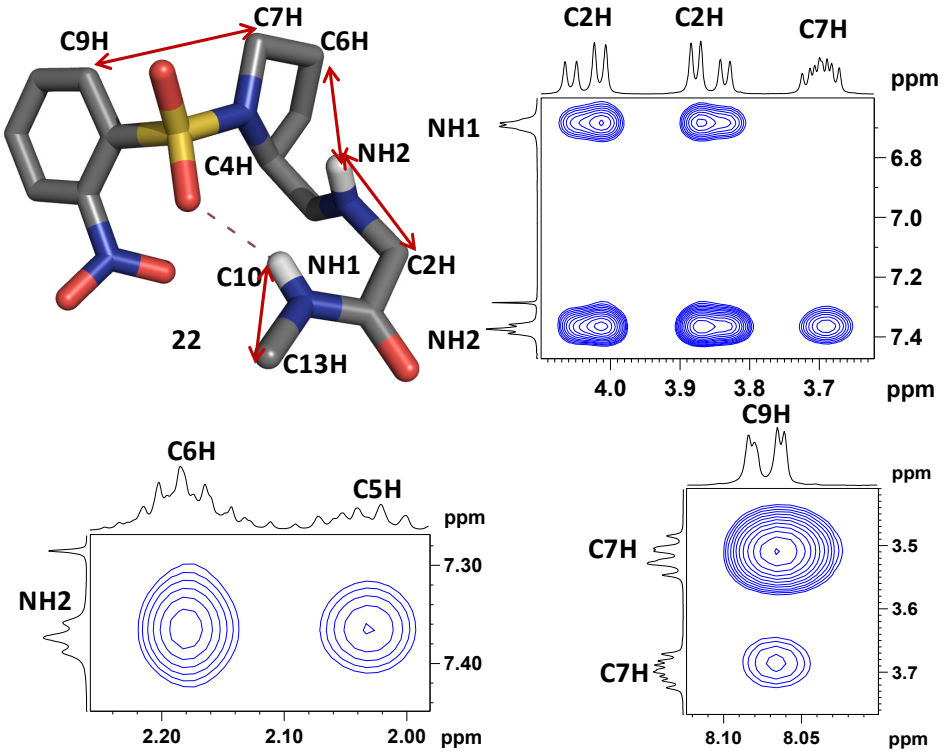

Fig 2.27: Crystal structure of **22** and selected 2D NOESY excerpts in solution-state. All hydrogens, except the polar ones, have been deleted for clarity in the crystal structures.

2.16.3 NMR derived structure of 16b

As the higher oligomers were resistant to crystallization after several trials of crystallization, the conformations of the hexapeptide **16b** was studied using NMR derived MD simulation studies. These studies strongly suggested that the oligomer **16b** adopts two C11 H-bonded rings on the backbone revealing a helical conformation for **16b** (Fig 2.28).

Similarly, the conformational investigation of the short peptides **15d** and **22** were carried out using MD studies that revealed similar conformational features observed in the solid-state. This was confirmed by the overlay of crystal structures with the respective NMR derived structures for both **15d** and **22** (Fig 2.29). The good agreement between the NMR derived structures and the solid-

state crystal structure with RMSD<0.2 confirmed the consistency of MD-NMR derived structures of the foldamers.

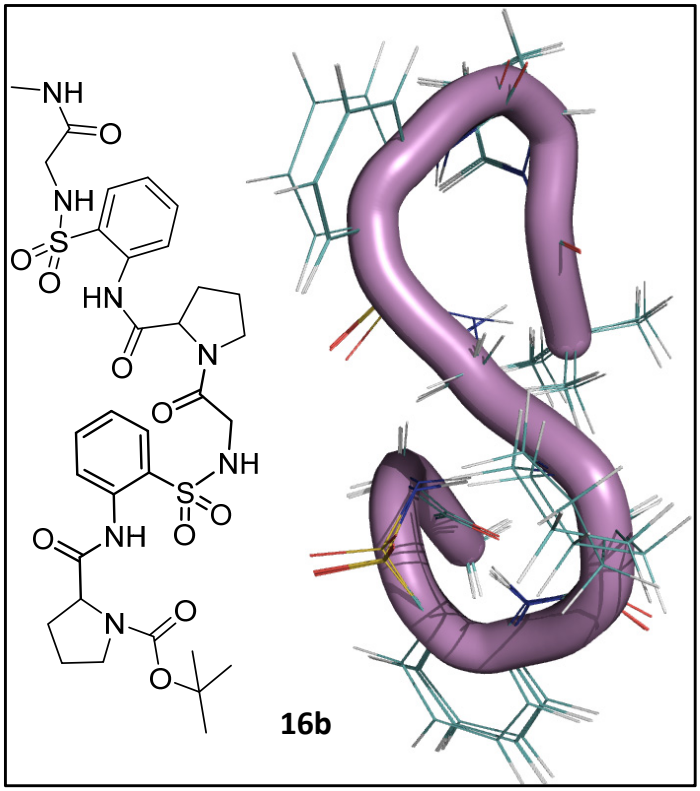

Fig 2.28: Molecular structure of hexapeptide **16b** (left). Overlaid structure of cartoon and 20 minimum energy conformations derived from the MD simulation studies revealing a helical conformation for **16b** (right).

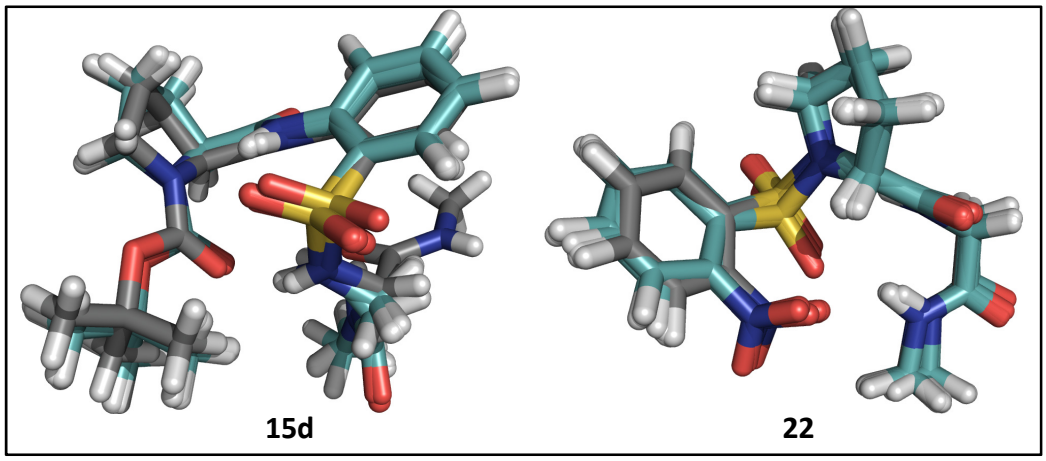

Fig 2.29: Overlay of 20 minimum energy conformations derived from the MD studies with the crystal structures of **15d** (left) and **22** (right).

The compounds **26g** and **27e** couldn't be crystallized. Their conformations in solution-state were studied using MD simulation studies. These studies revealed the existence of intra-residual C6 and inter-residual C7 H-bonding patterns in solution-state for **26g** (Fig 2.30 A). The conformational feature observed for **26g** was clearly different from that observed in **26a** (Fig 2.25 D), which clearly showed a C9 H-bonding pattern featuring a nitro group at the N-terminus and ester functionality at the C-terminus. The terminal modifications on the peptide **29a** played a considerable role in the overall conformational pattern of the molecule. The diverse conformational feature of **26g** is due to swapping of a carboxamide with a sulfonamide which was clearly evident from the solution-state structure of the hybrid peptide.

Furthermore, the conformational features suggested by the MD simulation studies for **27e** revealed intra-residual C6 and inter-residual C10 H-bonding patterns in solution-state. The intra-residual C6 H-bonding was observed in the Ant ring present at the N-terminus and the C10 H-bonding pattern was observed at the C-terminus between $-SO_2$ group of ^{S}Ant and –NH of the C-terminus amide in addition to the intra-residual C6 H-bond present in ^{S}Ant (Fig 2.30 B). This study clearly showed that the introduction of a ^{D}Pro residue at the C-terminus of a doubly folded peptide strongly influences the conformation. The consequences of swapping carboxamide by sulphonamide as well as introduction of ^{D}Pro residue at the C-terminus of **29a** were reflected in the solution-state derived structure of **27e**.

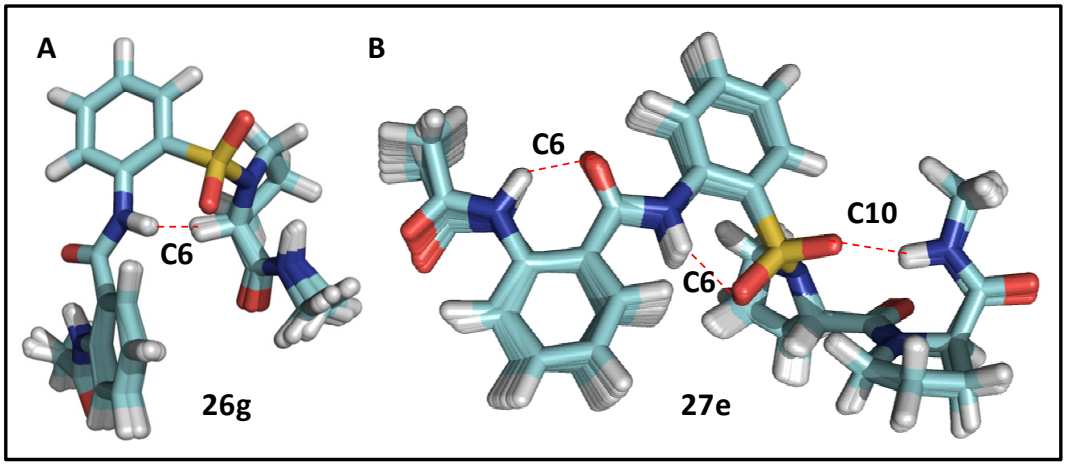

Fig 2.30: Overlay of the 20 minimum energy conformations derived from the MD studies of **26g** (left) and **27e** (right).

The hydrogen bonding pattern observed in **15d**, **22**, **16b**, **26g, 27e** was substantiated by DMSO-d_6 titration studies also (Fig 2.31). The negligible shift in the chemical shift values [$\Delta\delta$ (NH) = 0.3 ppb] of the amide protons revealed that they are strongly solvent shielded and are involved in strong intramolecular hydrogen bonded networks.

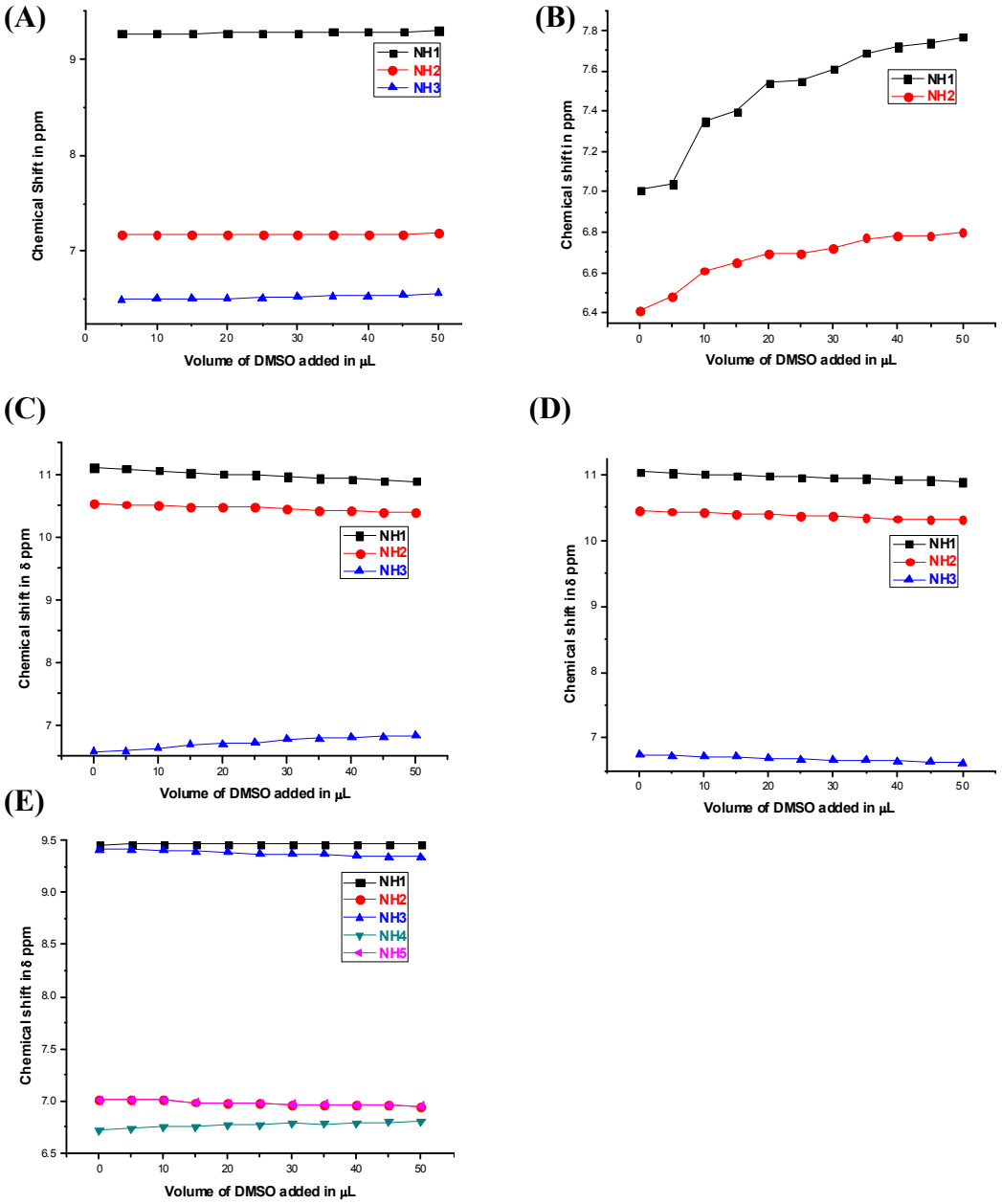

Fig 2.31: Plots representing DMSO-d_6 titration study of **15d** (A), **22** (B), **26g** (C), **27e** (D) and **16b** (E).

The variable temperature experiments also substantiated the conformational patterns observed in the oligomers **15d**, **22**, **26g**, **27e**, and **16b** (263-323 °K; $\Delta\delta/\Delta T < -2.5$ ppb K^{-1}) as shown in Fig 2.32 and Fig 2.33.

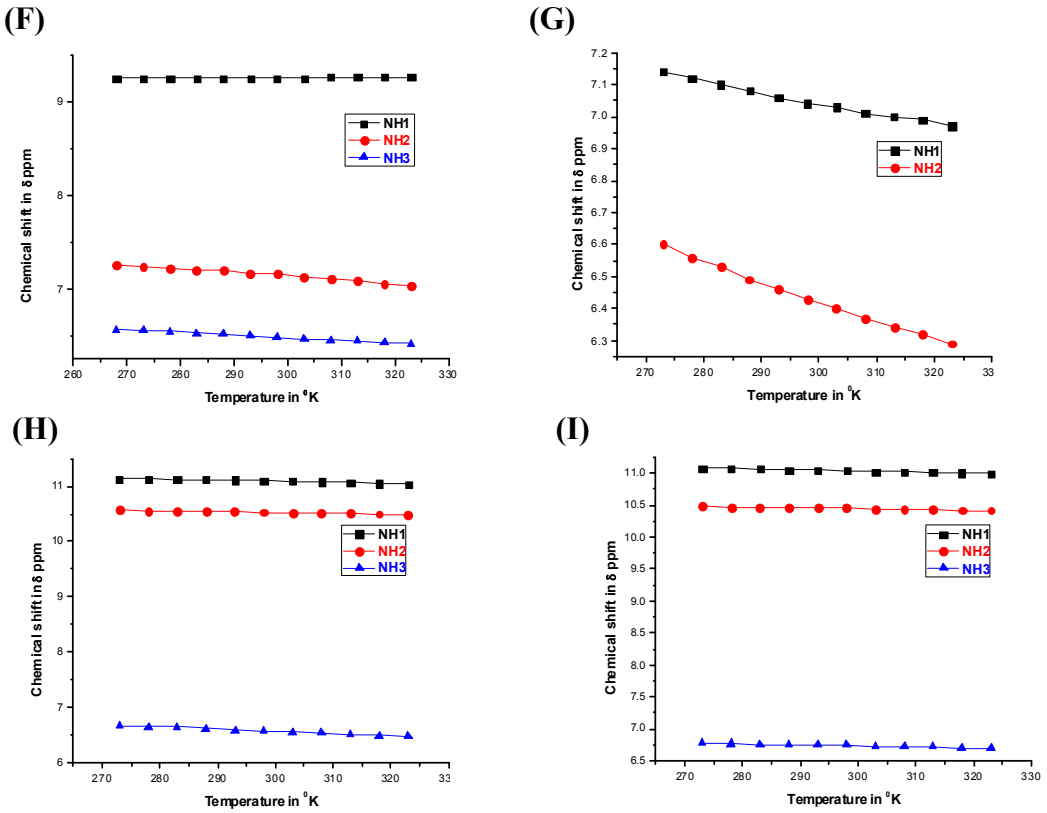

Fig 2.32: Plots representing variable temperature study of **15d** (F), **22** (G) **26g** (H), and **27e** (I).

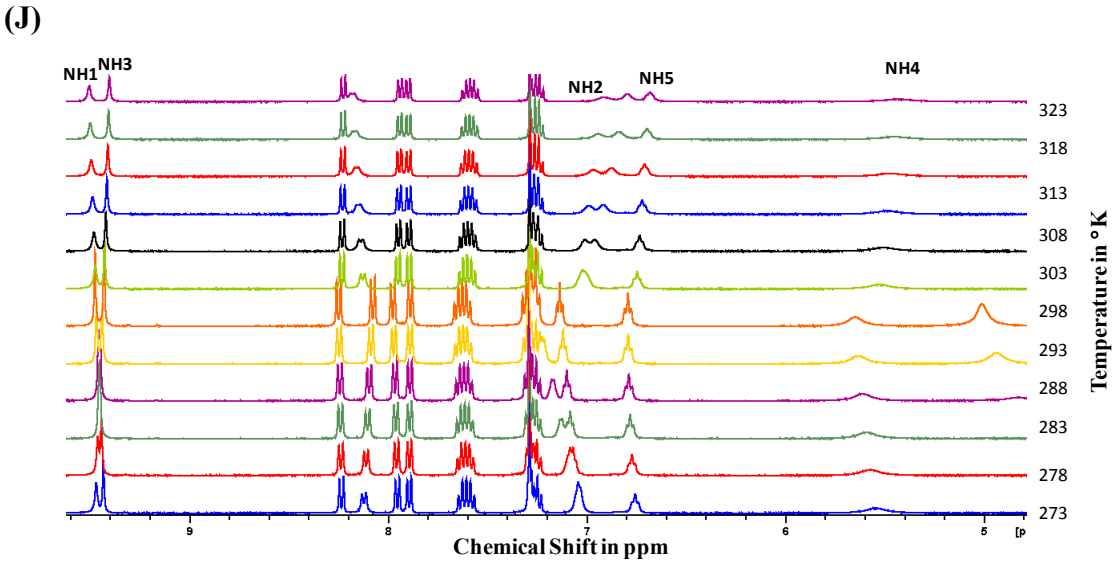

Fig 2.33: Stacked plot representing variable temperature study of **16b** (J).

2.17 Circular Dichroism studies

CD spectra of **15d** and **16b** showed maxima at about 194 nm, zero-crossing at about 206 nm and strong minima at about 240 nm which supported helical conformation of the oligomers Circular dichroism studies suggested that oligomers **15d** and **16b** showed typical signature of right-handed helical structure. The CD spectrum clearly showed that the helical tendency of the hybrid sequences increase with the length of the oligomers.

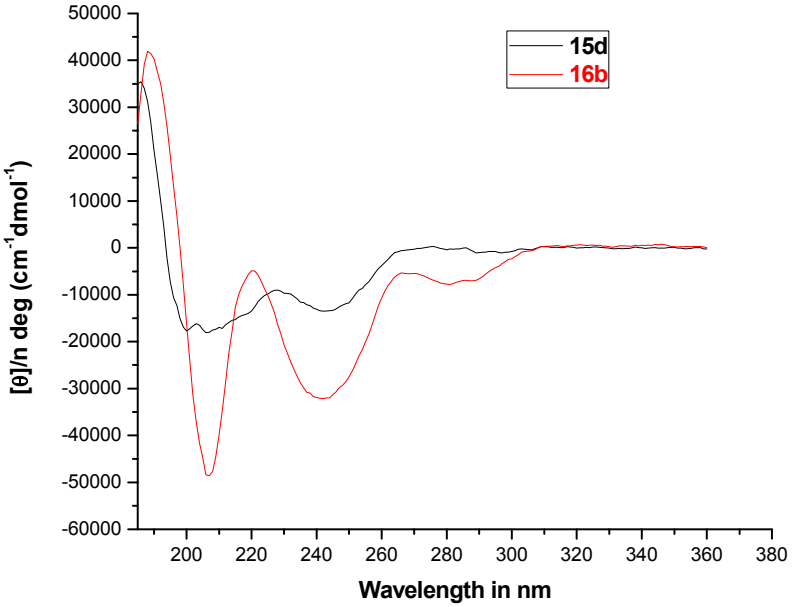

Fig 2.34: CD absorption spectra of **15d** and **16b** in TFE. All the spectra were recorded at 298 °K with a concentration of 0.2mM.

2.18 Conclusion

In summary, orthanilic acid was found to be exceptionally strong reverse turn inducer in peptide sequences. The consequences observed in the conformational preferences of peptides, by inserting ^{S}Ant into the peptides such as Pro-Gly, Gly-Pro and Ant-Ant-Pro were studied. Our findings might increase the possibility of designing rigid peptide systems using unusual amino acids. The designed hybrid peptides may find potential biological applications as peptidomimetic drugs since they comprise of unnatural β-amino acid residues which are not susceptible to enzymatic hydrolysis.

2.19 Experimental Section (Section A)

Crystal data for 1:

Single crystals of **1** were grown by slow evaporation of the solution in chloroform and pet ether. Colorless needle like crystal of approximate size 0.44 x 0.28 x 0.055 mm^3, was used for data collection. Multi-run data acquisition. Total scans = 4, total frames = 1559, exposure / frame = 10.0 sec / frame, θ range = 1.76 to 25.00°, completeness to θ of 25.00 º is 99.9 %. $C_{11}H_{17}N_3O_3S$, *MW* = 271.34, crystals belong to monoclinic, space group P21/c, *a* = 12.6119(3) Å, *b* = 7.6788(1) Å, *c* = 15.0308(3) Å, V = 1337.34(5) $Å^3$, *Z* = 4, D_c = 1.348 g/cc, (Mo–K_α) = 0.247 mm^{-1}, 9599 reflections measured, 2351 unique, [I>2σ(I)] R1 = 0.0372, wR2 = 0.0969, largest diff. peak and hole 0.296 and -0.404 e.$Å^{-3}$.

Crystal data for 2:

Single crystals of **2** were grown by slow evaporation of the solution in diethyl ether. Colorless rectangular like crystal of approximate size 0.39 x 0.21 x 0.09 mm^3, was used for data collection. Multi-run data acquisition. Total scans = 3, total frames = 626, exposure / frame = 10.0 sec / frame, θ range = 2.18 to 25.00°, completeness to θ of 25.00 º is 99.9%. $C_{18}H_{27}N_3O_7S$, *MW* = 429.49, crystals belong to orthorhombic, space group Pna21, *a* = 14.8435 (6), *b* = 9.8421 (4), *c* = 29.388 (1) Å, V = 4293.3 (3) $Å^3$, *Z* = 8, D_c = 1.329 g/cc, (Mo–K_α) = 0.194 mm^{-1}, 17432 reflections measured, 5881 unique, [I>2σ(I)] R1 = 0.0350, wR2 = 0.0884, largest diff. peak and hole 0.535 and -0.506 e.$Å^{-3}$. Flack parameter [0.49(8)].

Crystal data for 3:

Single crystals of **3** were grown by slow evaporation of the solution in DCM/ ether. Colorless needle like crystal of approximate size 0.36 x 0.18 x 0.07 mm^3, was used for data collection. Multi-run data acquisition. Total scans = 4, total frames = 1378, exposure / frame = 10.0 sec / frame, θ range = 2.42 to 25.00°, completeness to θ of 25.00 º is 99.8 %. $C_{18}H_{28}N_4O_6S$, *MW* = 428.50, crystals belong to monoclinic, space group P21/c, *a* = 17.3832(5), *b* = 8.5835(2), *c* = 15.0137(4) Å, V = 2165.69 (10) $Å^3$, *Z* = 4, D_c = 1.314 g/cc, (Mo–K_α) = 0.190 mm^-

[1], 16473 reflections measured, 3807 unique, [I>2σ(I)] R1 = 0.0315, wR2 = 0.0822, largest diff. peak and hole 0.419 and -0.422 e.Å^{-3}.

Crystal data for 4:

Single crystals of **4** were grown by slow evaporation of the solution in diethyl ether/pet ether. Colorless rectangular like crystal of approximate size 0.42 x 0.10 x 0.05 mm^3, was used for data collection. Multi-run data acquisition. Total scans = 7, total frames = 2288, exposure / frame = 20.0 sec / frame, θ range = 2.24 to 25.00°, completeness to θ of 25.00 º is 99.7 %.$C_{17}H_{27}N_3O_5S$, *MW* = 385.48, crystals belong to orthorhombic, space group Fdd2, *a* = 29.2950 (3), *b* = 46.5380 (5), *c* = 5.7943 (1) Å, V = 7899.55 (18) Å^3, *Z* = 16, D_c = 1.296 g/cc, (Mo–K_α) = 0.196 mm^{-1}, 24244 reflections measured, 3477 unique, [I>2σ(I)] R1 = 0.0748, wR2 = 0.1906, Largest diff. peak and hole 0.692 and -0.432 e.Å^{-3}. Flack parameter [-0.12(7)]. DFIX restraint was applied to disordered methyl groups so that the C-C distance is similar in the iso-butyl group. Restrain for C24 and C24'disordered atoms was applied so that they are not connected to each other.

Methyl 2-methyl-2-(2-nitrophenylsulfonamido) propanoate 1a:

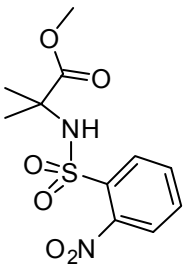

1a

To a solution of 2-nitrobenzenesulfonylchloride (2.6 g, 11.7 mmol) in dry DCM (30 mL) was added 2-aminoisobutylmethyl ester hydrochloride (2.0 g, 13.0 mmol) at 0 ^oC followed by the addition of Et_3N (4.94 mL, 35.5 mmol). The reaction mixture was allowed to attain room temperature and was further stirred for 12 h. Later, the reaction mixture was washed sequentially with sat. $NaHCO_3$, water, dil. HCl and brine solutions. The organic layer was dried over anhydrous Na_2SO_4 and evaporated under reduced pressure to get the crude product which on purification by column chromatography (eluent: pet ether/ethyl acetate: 50:50, R*f*: 0.45) yielded **1a** (1.92 g, 54%); mp: 114-115 ^oC; IR ($CHCl_3$) ν (cm^{-1}) 3401, 3019, 1737, 1635, 1543, 1411, 1351, 1216, 1048, 769; ^{1}H NMR (400 MHz, $CDCl_3$) δ: 8.11-8.09 (d, *J* = 8 Hz, 1H), 7.90-7.88 (d, *J* = 8 Hz, 1H), 7.77-7.70 (m, 2H), 6.18 (s, 1H), 3.64 (s, 3H), 1.57 (s, 6H); ^{13}C NMR (100 MHz, $CDCl_3$) δ: 173.7, 147.5, 136.2, 133.3, 132.9, 130.1, 125.3, 60.1, 52.9, 26.3; LCMS: 325.04 $(M+Na)^+$; Anal. Calcd for $C_{11}H_{14}N_2O_6S$: C, 43.70; H, 4.67; N, 9.27; Found: C, 43.34.; H, 4.90.; N, 9.43.

General procedure for reduction of nitro compounds 1a and 5 to respective amines 1b and 6

To the solutions of **1a** and **5** (0.5 g, 1.59 mmol) in methanol (15 mL), 10% Pd/C (0.06 g) was added. Then, the reaction mixture was subjected to shaking in parr shaker at 60 psi for 12 h. Later, the catalyst was filtered through celite and the solvent was removed under reduced pressure to get the products **1b** and **6**, which were carried forward to the next reaction without any purification.

2-(2-aminophenylsulfonamido)-N, 2-dimethylpropanamide 1:

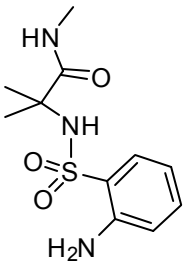

1

Compound **1b** was dissolved in MeOH (2 mL) followed by addition of methanolic methyl amine solution (2 mL) at 0 ^{o}C. Progress of the reaction was monitored by TLC and after completion of reaction (48 h), the solvent was stripped off and crude product was purified by column chromatography (eluent: pet ether/ethyl acetate: 50:50, R*f*: 0.4) to yield **1** (0.04 g, 90%); mp: 136-138 ^{o}C. IR ($CHCl_3$) ν (cm^{-1}) 3685, 3448, 3365, 3020, 2400, 1671, 1524, 1416, 1329, 1216, 1155, 1020, 928, 851, 770, 668. ^{1}H NMR (500 MHz, $CDCl_3$) δ: 7.72-7.70- (dd, *J* = 8.2 Hz, 1.5 Hz, 1H), 7.35-7.33 (t, *J* = 7 Hz, 2H), 6.85-6.83 (d, *J* = 7.3 Hz, 1H), 6.80-6.78 (d, *J* = 8.2 Hz, 1H), 5.66 (s, 1H), 4.86 (s, 2H), 2.75-2.74 (d, *J* = 4.9 Hz, 3H), 1.38 (s, 6H); ^{13}C NMR (100 MHz, $CDCl_3$) δ: 174.5, 144.6, 134.3, 129.2, 124.2, 118.4, 117.9, 60.1, 28.5, 25.6; HRMS: $C_{11}H_{18}O_3N_3S$, Calcd: 272.1063 Found: 272.1064.

Methyl-2-(2-(2-((tert-butoxycarbonyl)amino)acetamido)phenylsulfonamido)-2-methylpropanoate 2:

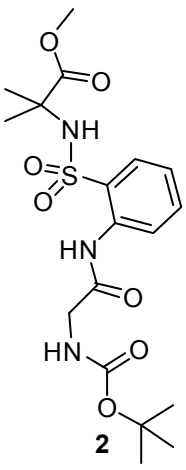

2

To a two necked round-bottomed flask containing Boc-Glycine (0.11 g, 0.66 mmol) in 10 mL dry THF, dry Et_3N (0.13 mL, 0.99 mmol) was added under N_2 atmosphere. The resultant solution was cooled to 0°C. Subsequently, ethyl chloroformate (0.07 mL, 0.79 mmol) was added drop wise. The solution was stirred at 0 ^{o}C for 1 h, amine **1b** (0.18 g, 0.66 mmol) in 10 mL dry THF was added, the reaction mixture was allowed to stir for 2 h at room temperature, and then refluxed for 48 h. Later, the reaction mixture was cooled to room temperature and filtered. The solvent

was removed under reduced pressure to get the crude product, which was dissolved in DCM (10 mL) and washed with sat. $NaHCO_3$ followed by brine. The organic layer was dried over anhydrous Na_2SO_4 and evaporated under reduced pressure to get the crude product which was further purified by column chromatography (eluent: pet ether/ethyl acetate: 50:50, R*f*: 0.5) to furnish **2** (0.19 g, 70%) as a white solid; mp: 149-152 ^oC. IR ($CHCl_3$) ν (cm^{-1}) 3684, 3447, 3237, 3020, 2400, 1736, 1700, 1584, 1523, 1497, 1439, 1331, 1215, 1161, 1024, 929, 851, 762, 669, 481. ^1H NMR (400 MHz, $CDCl_3$) δ: 9.55 (s, 1H), 8.1-8.08 (d, *J* = 8Hz, 1H), 7.88-7.86 (dd, *J* = 7.9 Hz, 1.3 Hz, 1H), 7.58-7.54 (t, *J* = 7Hz, 1H), 7.26-7.22 (t, *J* = 7.3 Hz, 1H), 6.54 (s, 1H), 5.31-5.29 (m, 1H), 3.96-3.94 (d, *J* = 6 Hz, 2H), 3.49 (s, 3H), 1.57 (s, 9H), 1.40 (s, 6H); ^{13}C NMR (100 MHz, $CDCl_3$) δ: 173.8, 167.9, 157.9, 134.4, 133.3, 131.6, 128.7, 124.5, 82.1, 58.4, 52.6, 45.7, 28.5, 25.6; HRMS: $C_{18}H_{28}O_7N_3S$, Calcd: 430.1642 Found: 430.1637.

tert-butyl-(2-((2-(N-(2-methyl-1-(methylamino)-1-oxopropan-2-yl)sulfamoyl)ph-enyl)amino)-2-oxoethyl)carbamate 3:

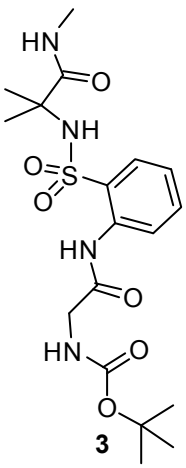

3

Compound **2** was dissolved in MeOH (2 mL) followed by the addition of methanolic methyl amine solution (2 mL) at 0 ^oC. The reaction was monitored by TLC and after completion of reaction (48 h), the solvent was stripped off and the crude product was purified by column chromatography (eluent: pet ether/ethyl acetate: 50:50, R*f*: 0.3) to yield **3** (0.09 g, 50%); mp: 170-172 ^oC. IR ($CHCl_3$) ν (cm^{-1}) 3683, 3582, 3447, 3020, 2400, 1696, 1520, 1426, 1370, 1284, 1215, 1022, 760, 669; ^1H NMR (400 MHz, $CDCl_3$) δ: 9.31 (s, 1H), 7.98-7.96 (d, *J* = 8 Hz, 1H), 7.93-7.90 (dd, *J* = 8 Hz, 1.3 Hz, 1H), 7.62-7.58 (t, *J* = 7 Hz, 1H), 7.31-7.29 (t, *J* = 7.3 Hz, 1H), 6.57 (s, 2H), 5.48-5.45 (m, 1H), 3.93-3.91 (d, *J* = 5.8 Hz, 2H), 2.72-2.71 (d, *J* = 4.8 Hz, 3H), 1.54 (s, 9H) 1.31 (s, 6H); ^{13}C NMR (100 MHz, $CDCl_3$) δ: 174.2, 168.0, 158.1, 133.6, 132.8, 129, 125.6, 125.3, 82.2, 60.3, 45.7, 28.4, 26.5, 25.5; HRMS: $C_{18}H_{29}O_6N_4S$, Calcd: 429.1802 Found: 430.1797.

N-isobutyl-2-nitrobenzenesulfonamide 5:

Compound **5** was synthesized following the procedure used to synthesize **1a** to couple 2-nitrosulfonyl chloride and isobutyl amine. Yield (87%); mp: 78-79 ^oC;

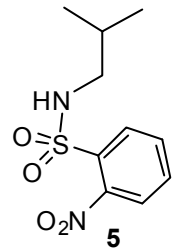

5

IR ($CHCl_3$) ν (cm^{-1}) 3621, 3393, 3019, 1596, 1542, 1362, 1216, 1170, 1124, 1046, 758; ^1H NMR (500 MHz, $CDCl_3$) δ: 8.14-8.12 (d, *J* = 9 Hz, 1H), 7.87-7.85 (d, *J* = 9 Hz, 1H), 7.17-7.13 (m, 2H), 5.33-5.30 (t, *J* = 6.6 Hz, 1H), 2.92-2.89 (t, *J* = 6.6 Hz, 2H), 1.83-1.75 (septet, *J* = 6.7 Hz, 1H), 0.92 (s, 3H), 0.90 (s, 3H); ^{13}C NMR (125 MHz, $CDCl_3$) δ: 148.1, 133.8, 133.5, 132.8, 131.1, 125.4, 51.2, 28.5, 19.8; HRMS: $C_{10}H_{15}N_2O_4S$ Calcd: 259.0747; Found: 259.0741.

tert-butyl-(2-((2-(N-isobutylsulfamoyl)phenyl)amino)-2-oxoethyl)carbamate 4:

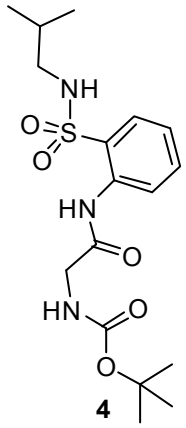

4

Compound **4** was synthesized following the procedure mentioned to prepare **1a** using amine **6**. Yield (90%); mp: 127-129 ^oC; IR ($CHCl_3$) ν (cm^{-1}) 3684, 3447, 3336, 3265, 3020, 2933, 2874, 2400, 1700, 1584, 1523, 1442, 1328, 1215, 1072, 930, 852, 752, 591, 487; ^1H NMR (400 MHz, $CDCl_3$) δ: 9.63 (s, 1H), 8.11-8.09 (d, *J* = 8.3 Hz, 1H), 7.91-7.89 (d, *J* = 8 Hz, 1H), 7.58-7.55 (m, 1H), 7.25-7.23 (d, *J* = 7.8 Hz, 1H), 5.99 (bs, 1H), 3.90-3.89 (d, *J* = 6 Hz, 2H), 2.61-2.58 (t, *J* = 6.4 Hz, 2H), 1.69-1.58 (m, 1H), 1.53 (s, 9H), 0.84-0.82 (d, *J* = 6.8 Hz, 6H); ^{13}C NMR (100 MHz, $CDCl_3$) δ: 168.0, 157.9, 134.1, 133.3, 129.4, 124.4, 82.0, 50.1, 45.8, 28.5, 19.7; HRMS: $C_{17}H_{28}O_5N_3S$, Calcd: 386.1744 Found: 386.1741.

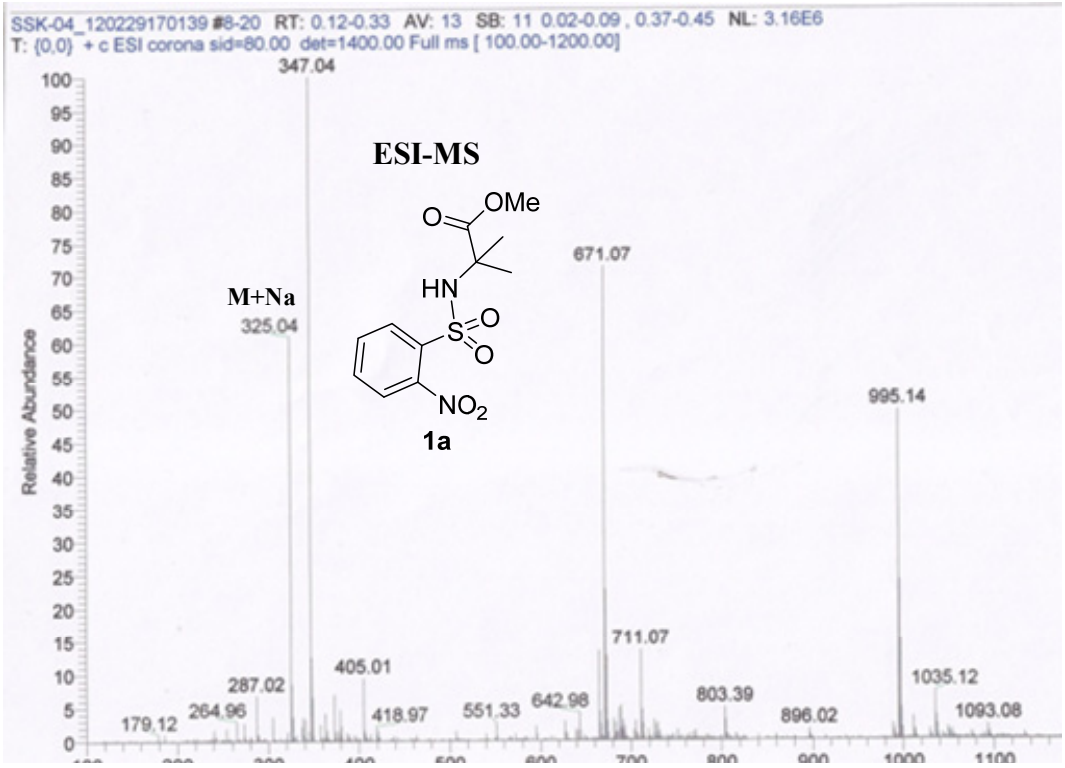
SSK-04_120229170139 #8-20 RT: 0.12-0.33 AV: 13 SB: 11 0.02-0.09 , 0.37-0.45 NL: 3.16E6
T: {0,0} + c ESI corona sid=80.00 det=1400.00 Full ms [100.00-1200.00]
ESI-MS
M+Na
325.04
347.04
671.07
995.14
711.07
405.01
287.02
1035.12
803.39
1093.08
179.12
264.96
418.97
551.33
642.98
896.02
Relative Abundance
OMe
HN
S
O
NO2
1a

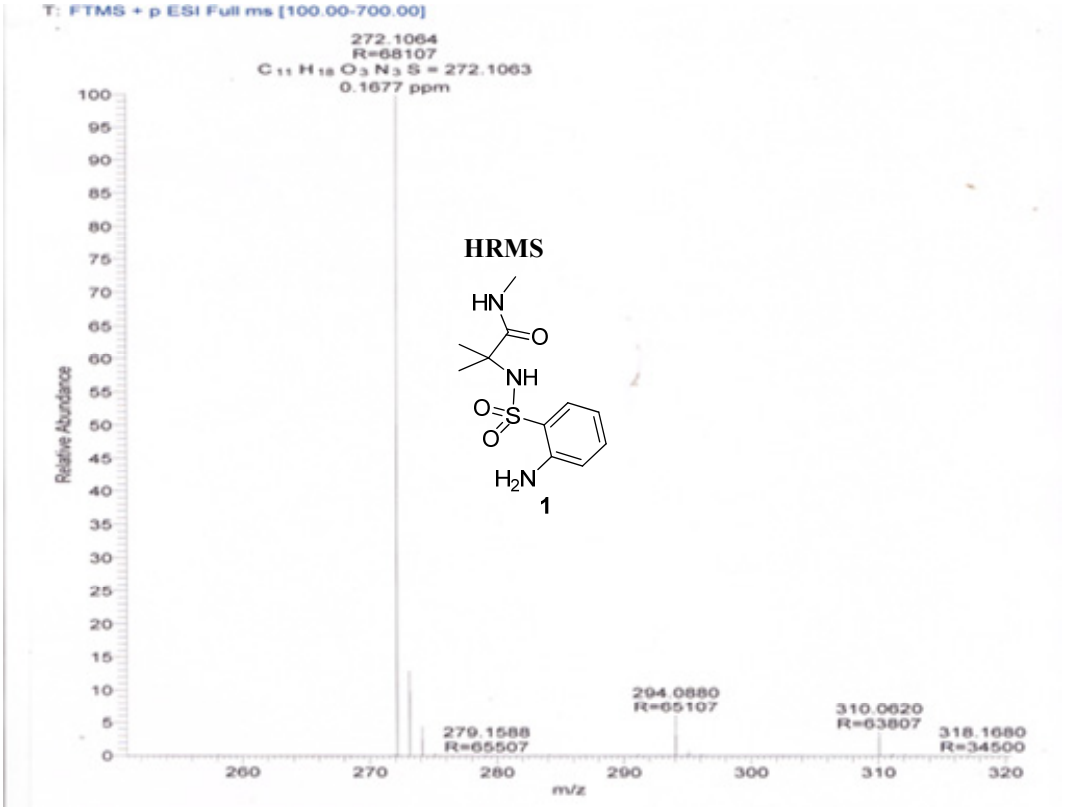
T: FTMS + p ESI Full ms [100.00-700.00]
272.1064
R=68107
C11 H18 O3 N3 S = 272.1063
0.1677 ppm
HRMS
294.0880
R=65107
310.0620
R=63807
279.1588
R=65507
318.1680
R=34500
Relative Abundance
m/z
HN
NH
O
S
H2N
1

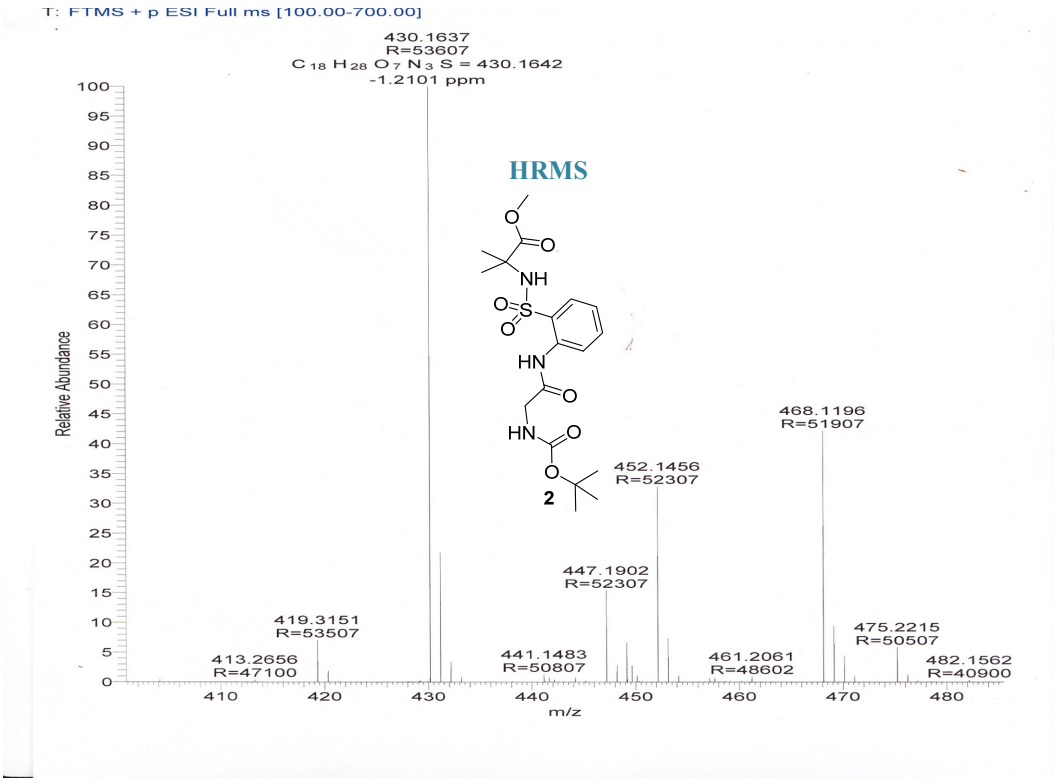
T: FTMS + p ESI Full ms [100.00-700.00]
430.1637
R=53607
C 18 H 28 O 7 N 3 S = 430.1642
-1.2101 ppm
HRMS
2
452.1456
R=52307
468.1196
R=51907
447.1902
R=52307
419.3151
R=53507
413.2656
R=47100
441.1483
R=50807
461.2061
R=48602
475.2215
R=50507
482.1562
R=40900
Relative Abundance
m/z

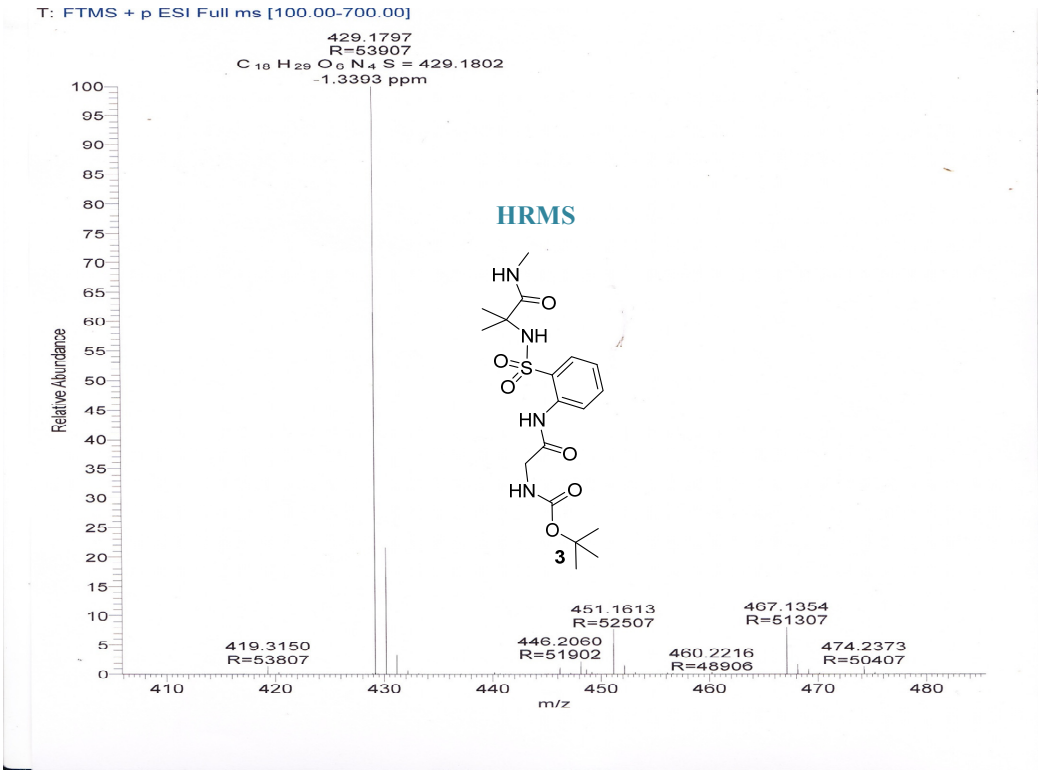
T: FTMS + p ESI Full ms [100.00-700.00]
429.1797
R=53907
C 18 H 29 O 6 N 4 S = 429.1802
-1.3393 ppm
HRMS
3
451.1613
R=52507
467.1354
R=51307
419.3150
R=53807
446.2060
R=51902
460.2216
R=48906
474.2373
R=50407
Relative Abundance
m/z

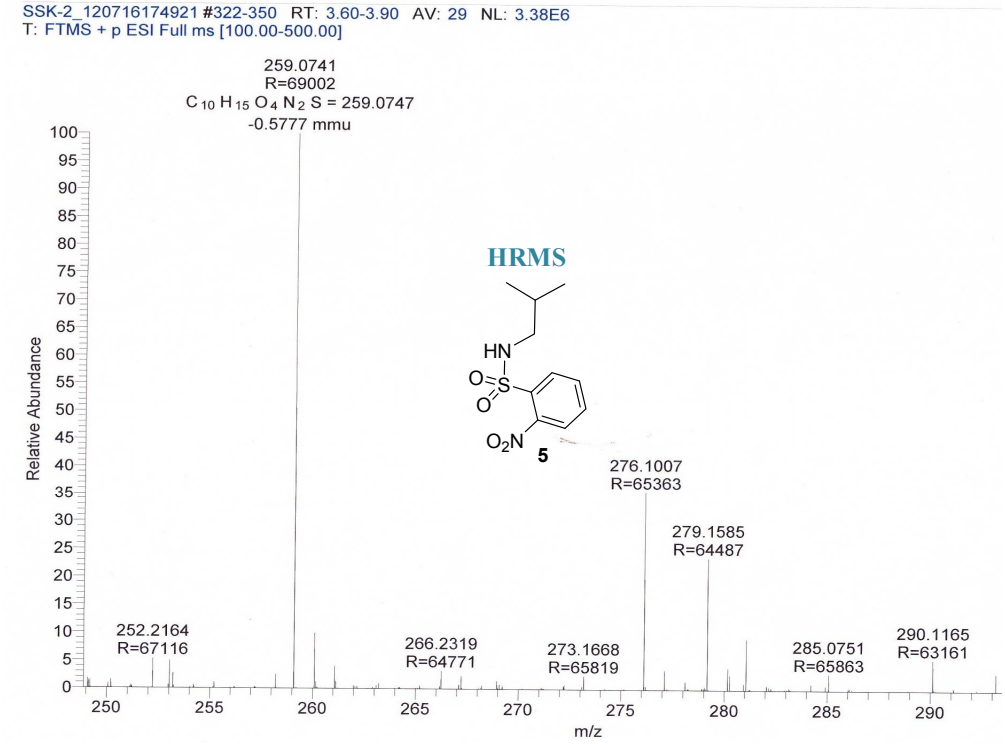
SSK-2_120716174921 #322-350 RT: 3.60-3.90 AV: 29 NL: 3.38E6
T: FTMS + p ESI Full ms [100.00-500.00]
259.0741
R=69002
C 10 H 15 O 4 N 2 S = 259.0747
-0.5777 mmu
HRMS
5
276.1007
R=65363
279.1585
R=64487
252.2164
R=67116
266.2319
R=64771
273.1668
R=65819
285.0751
R=65863
290.1165
R=63161
Relative Abundance
m/z

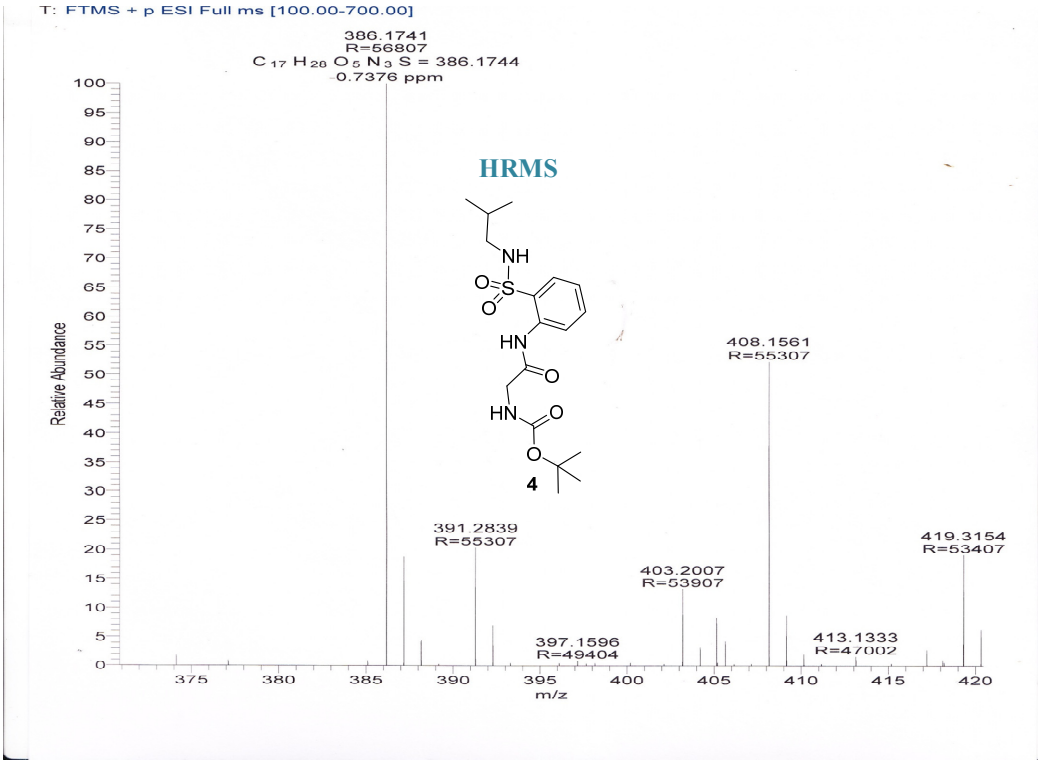
T: FTMS + p ESI Full ms [100.00-700.00]
386.1741
R=56807
C 17 H 28 O 5 N 3 S = 386.1744
-0.7376 ppm
HRMS
4
408.1561
R=55307
391.2839
R=55307
419.3154
R=53407
403.2007
R=53907
397.1596
R=49404
413.1333
R=47002
Relative Abundance
m/z

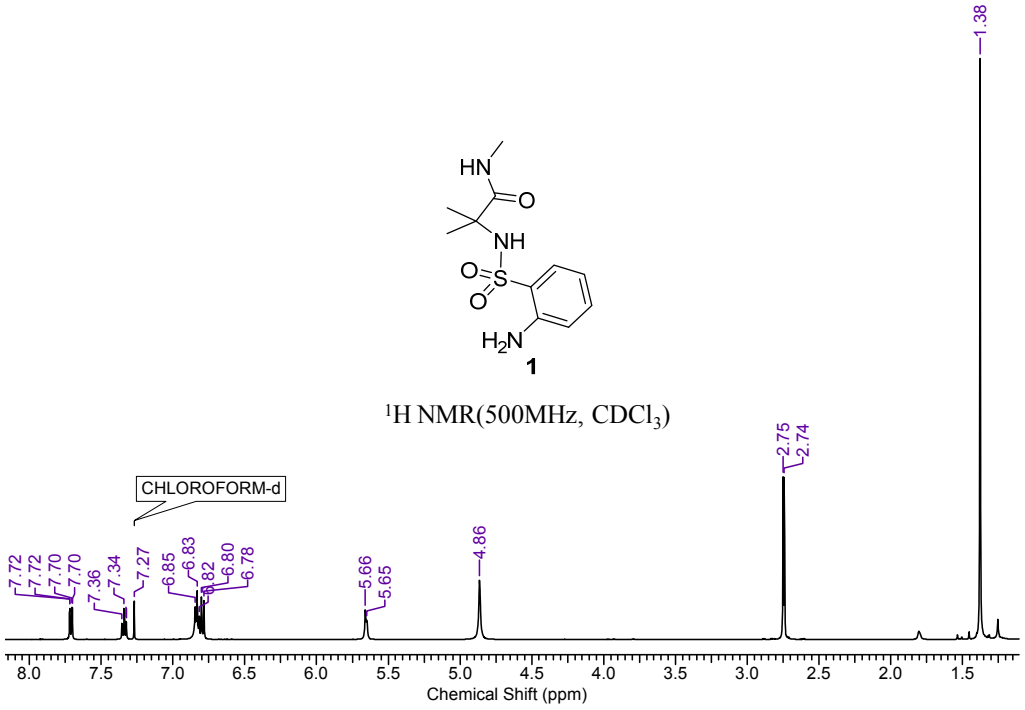
HN
O
NH
O=S=O
H2N
1
1H NMR(500MHz, CDCl3)
CHLOROFORM-d
7.72
7.72
7.70
7.70
7.36
7.34
7.27
6.85
6.83
6.82
6.80
6.78
5.66
5.65
4.86
2.75
2.74
1.38
8.0
7.5
7.0
6.5
6.0
5.5
5.0
4.5
4.0
3.5
3.0
2.5
2.0
1.5
Chemical Shift (ppm)

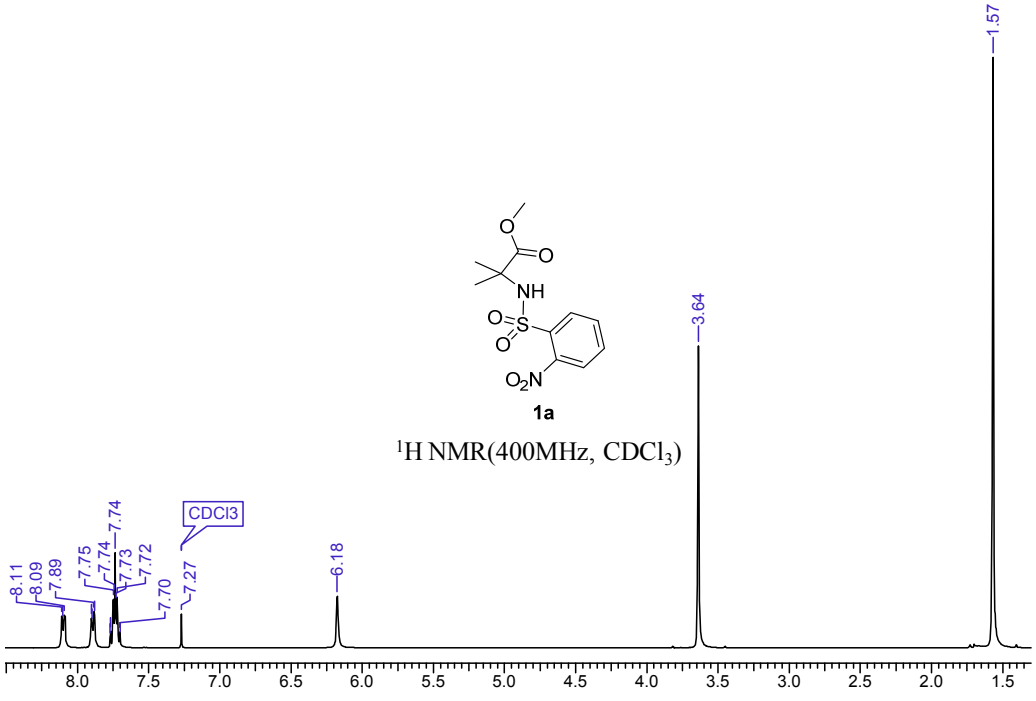
O
O
NH
O=S=O
O2N
1a
1H NMR(400MHz, CDCl3)
CDCl3
8.11
8.09
7.89
7.75
7.74
7.74
7.73
7.72
7.70
7.27
6.18
3.64
1.57
8.0
7.5
7.0
6.5
6.0
5.5
5.0
4.5
4.0
3.5
3.0
2.5
2.0
1.5

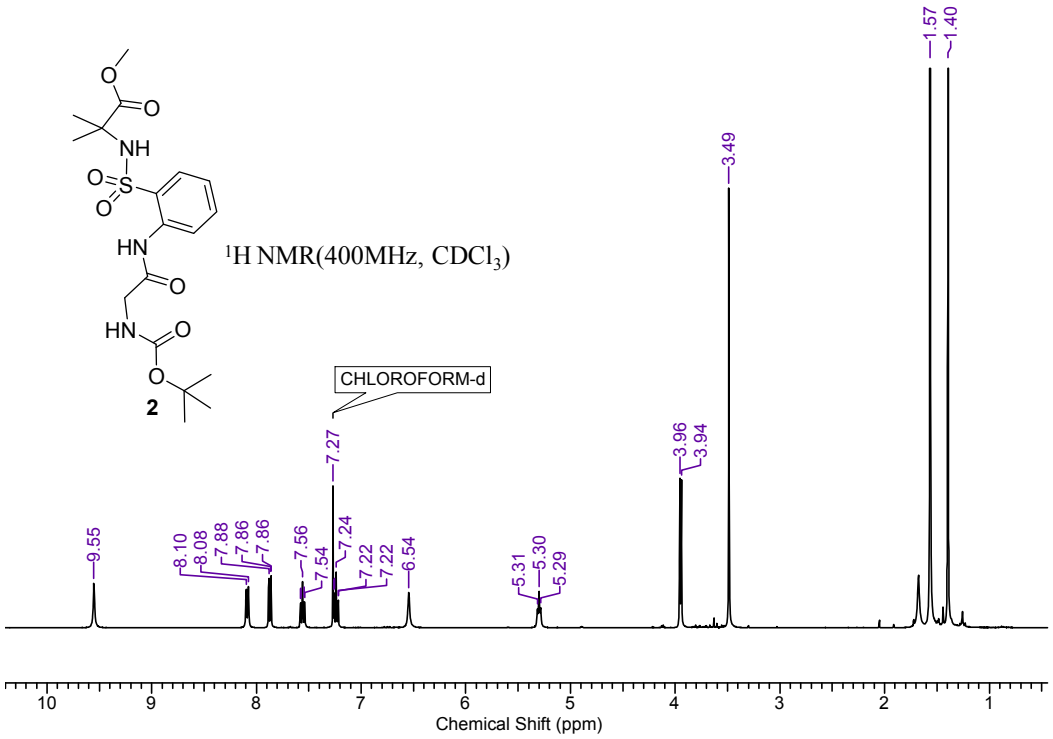
2
^{1}H NMR(400MHz, $CDCl_3$)
CHLOROFORM-d
9.55
8.10
8.08
7.88
7.86
7.86
7.56
7.54
7.27
7.24
7.22
7.22
6.54
5.31
5.30
5.29
3.96
3.94
3.49
1.57
1.40
Chemical Shift (ppm)

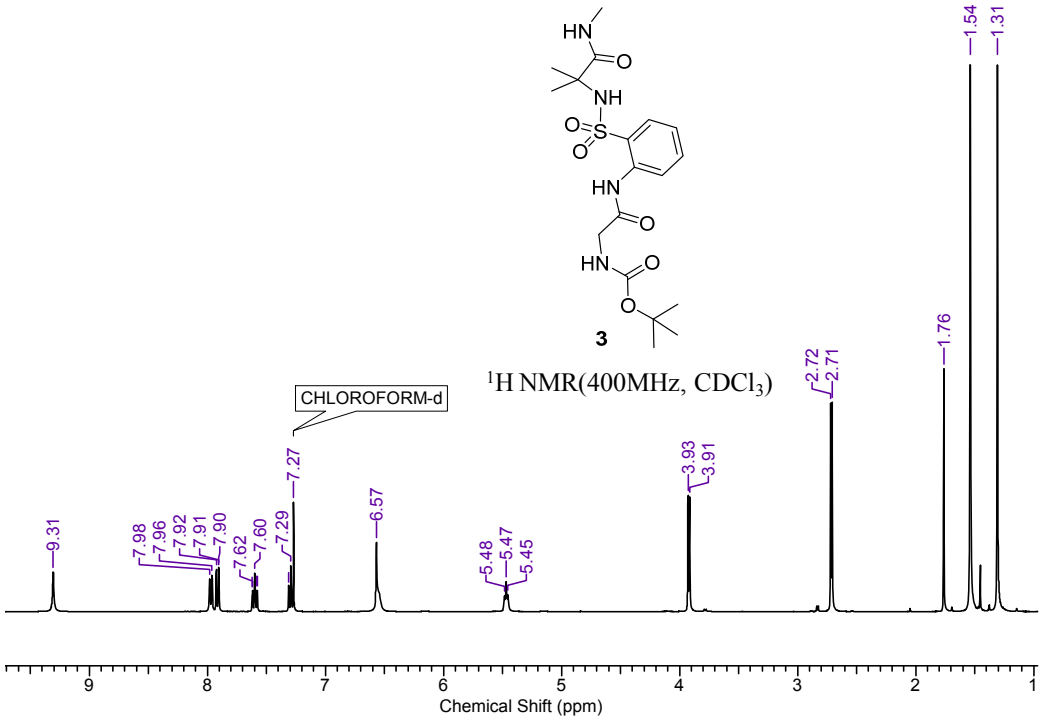
3
^{1}H NMR(400MHz, $CDCl_3$)
CHLOROFORM-d
9.31
7.98
7.96
7.92
7.91
7.90
7.62
7.60
7.29
7.27
6.57
5.48
5.47
5.45
3.93
3.91
2.72
2.71
1.76
1.54
1.31
Chemical Shift (ppm)

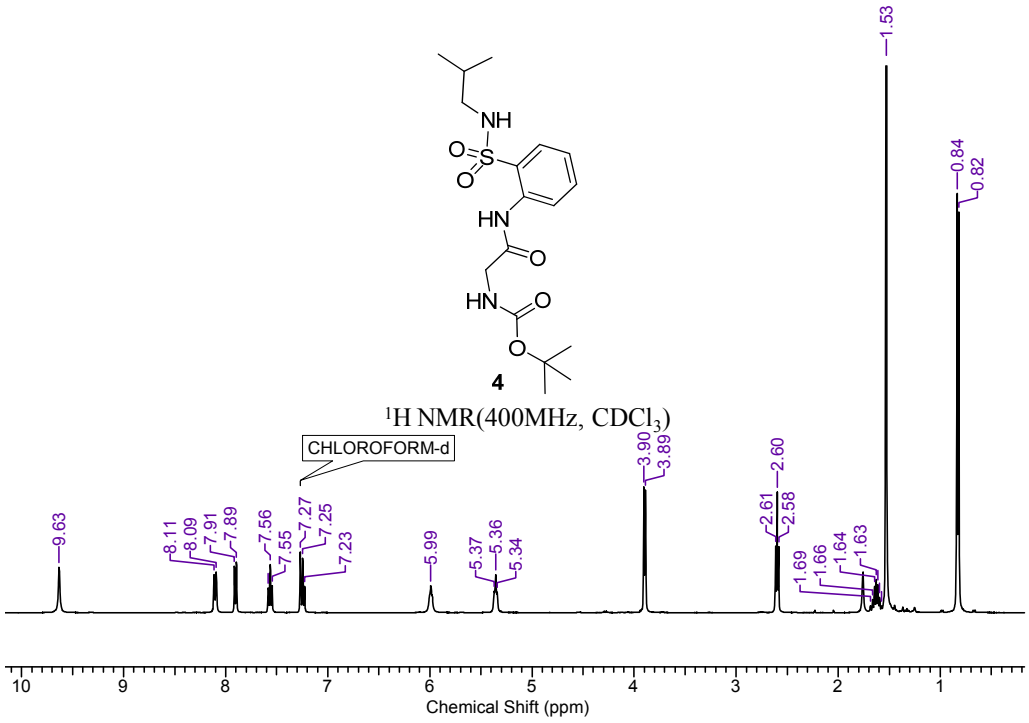
NH
O
S
O
HN
O
HN
O
O
4
^{1}H NMR(400MHz, CDCl$_3$)
CHLOROFORM-d
9.63
8.11
8.09
7.91
7.89
7.56
7.55
7.27
7.25
7.23
5.99
5.37
5.36
5.34
3.90
3.89
2.61
2.60
2.58
1.69
1.66
1.64
1.63
1.53
0.84
0.82
10
9
8
7
6
5
4
3
2
1
Chemical Shift (ppm)

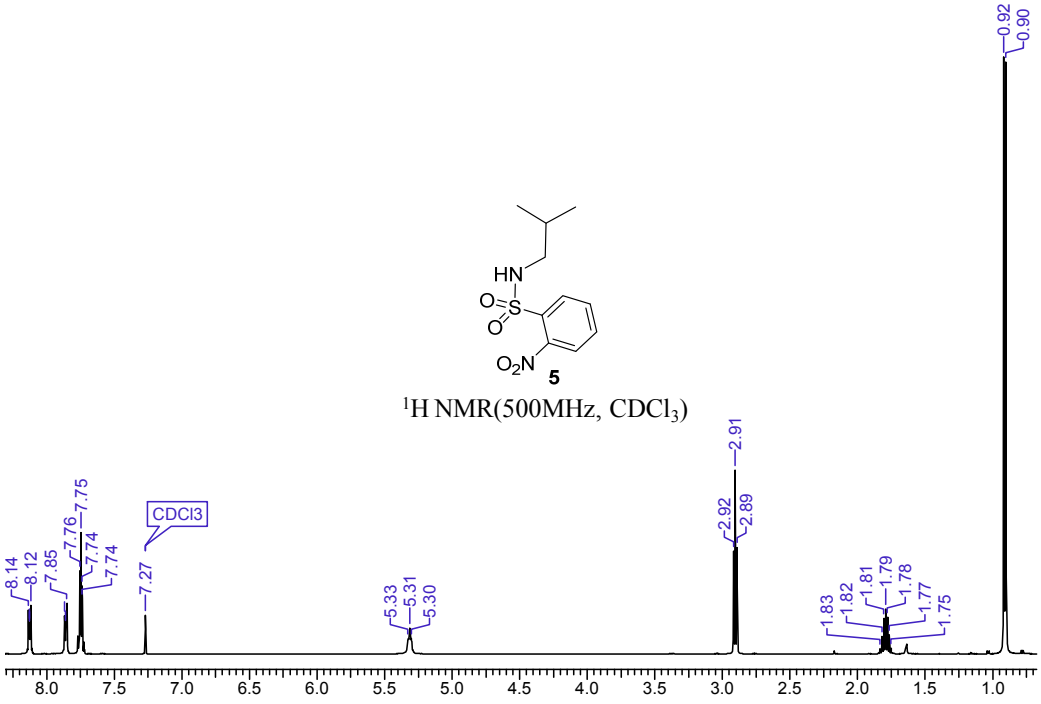
HN
O
S
O
O$_2$N
5
^{1}H NMR(500MHz, CDCl$_3$)
8.14
8.12
7.85
7.76
7.75
7.74
7.74
CDCl3
7.27
5.33
5.31
5.30
2.91
2.92
2.89
1.83
1.82
1.81
1.79
1.78
1.77
1.75
0.92
0.90
8.0
7.5
7.0
6.5
6.0
5.5
5.0
4.5
4.0
3.5
3.0
2.5
2.0
1.5
1.0

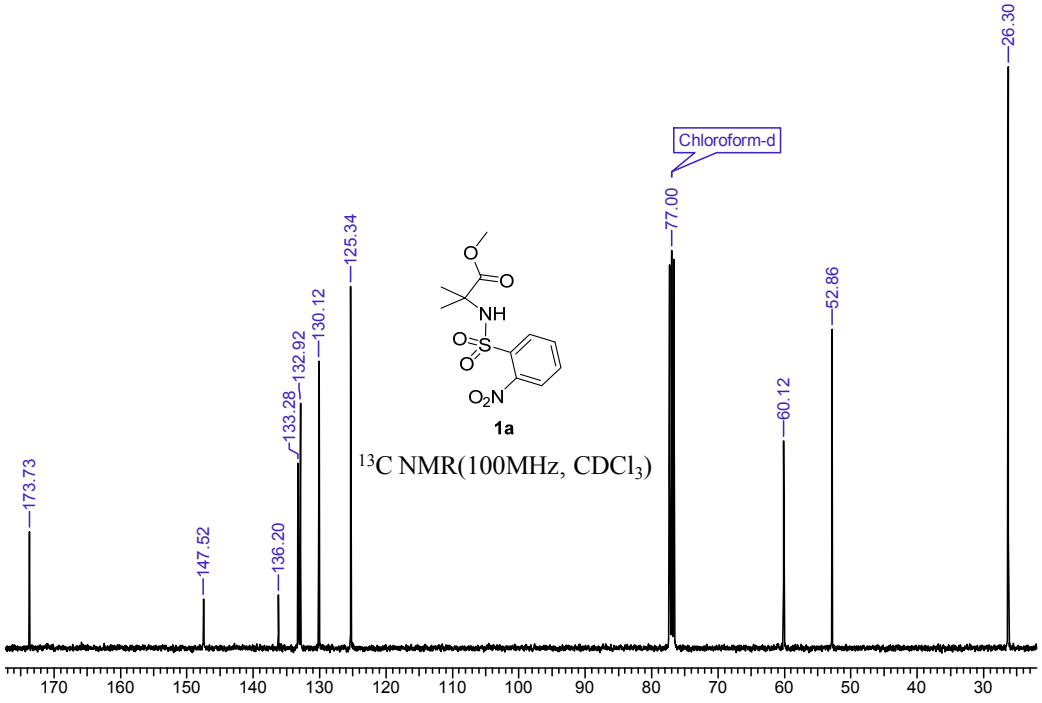
26.30
Chloroform-d
77.00
125.34
52.86
130.12
132.92
133.28
60.12
173.73
147.52
136.20
O
O
NH
O
S
O
O2N
1a
13C NMR(100MHz, CDCl3)
170
160
150
140
130
120
110
100
90
80
70
60
50
40
30

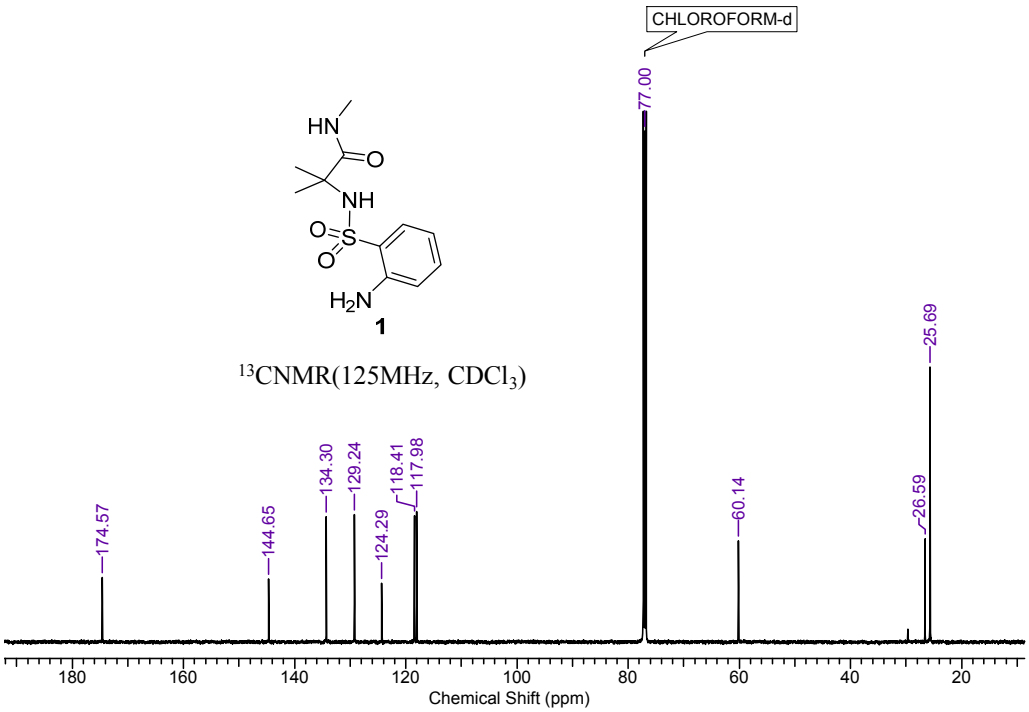
CHLOROFORM-d
77.00
25.69
HN
O
NH
O
S
O
H2N
1
13CNMR(125MHz, CDCl3)
134.30
129.24
118.41
117.98
174.57
144.65
124.29
60.14
26.59
180
160
140
120
100
80
60
40
20
Chemical Shift (ppm)

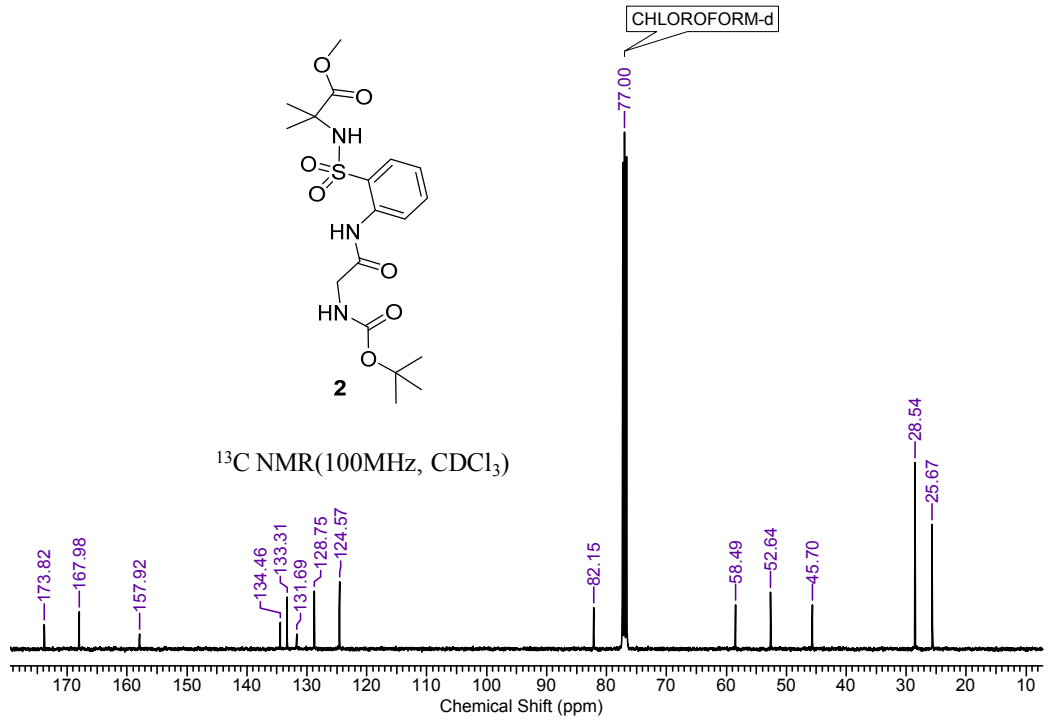

2

^{13}C NMR(100MHz, $CDCl_3$)

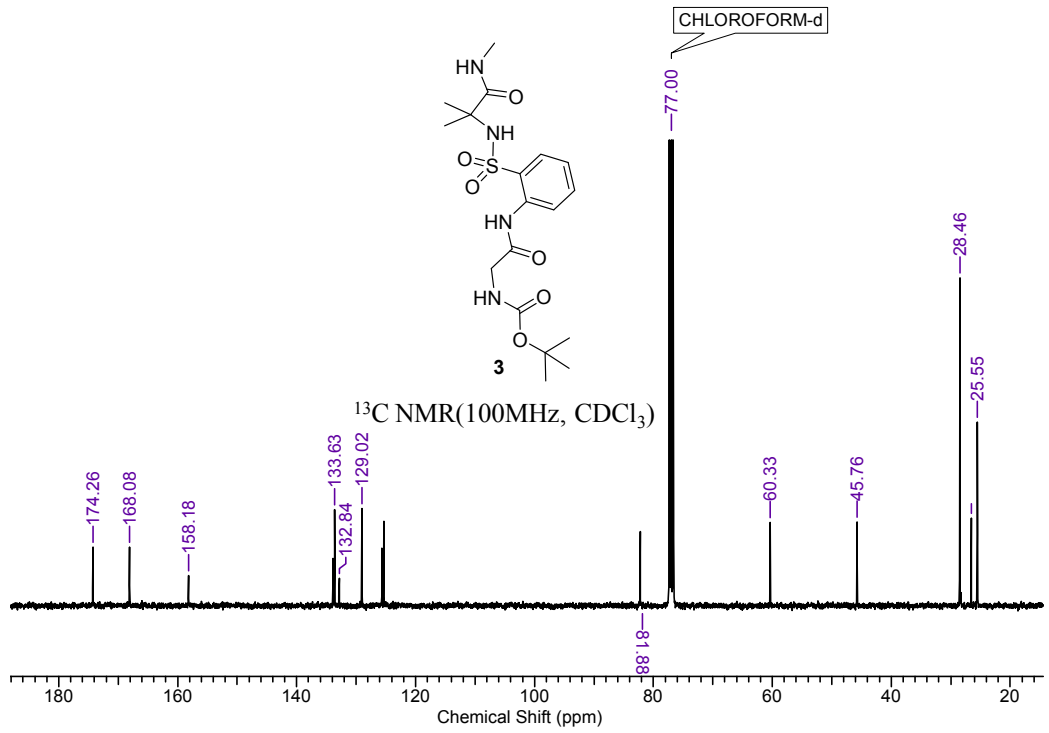

3

^{13}C NMR(100MHz, $CDCl_3$)

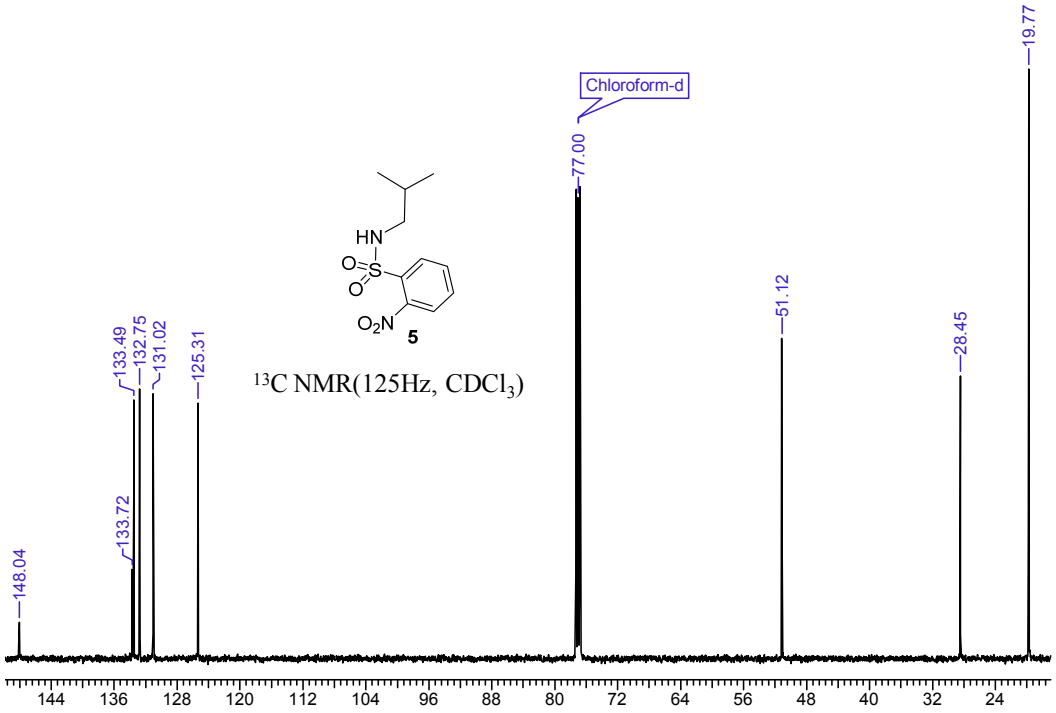
Chloroform-d
148.04
133.72
133.49
132.75
131.02
125.31
77.00
51.12
28.45
19.77
HN
O
S
O
O2N
5
13C NMR(125Hz, CDCl3)
144 136 128 120 112 104 96 88 80 72 64 56 48 40 32 24

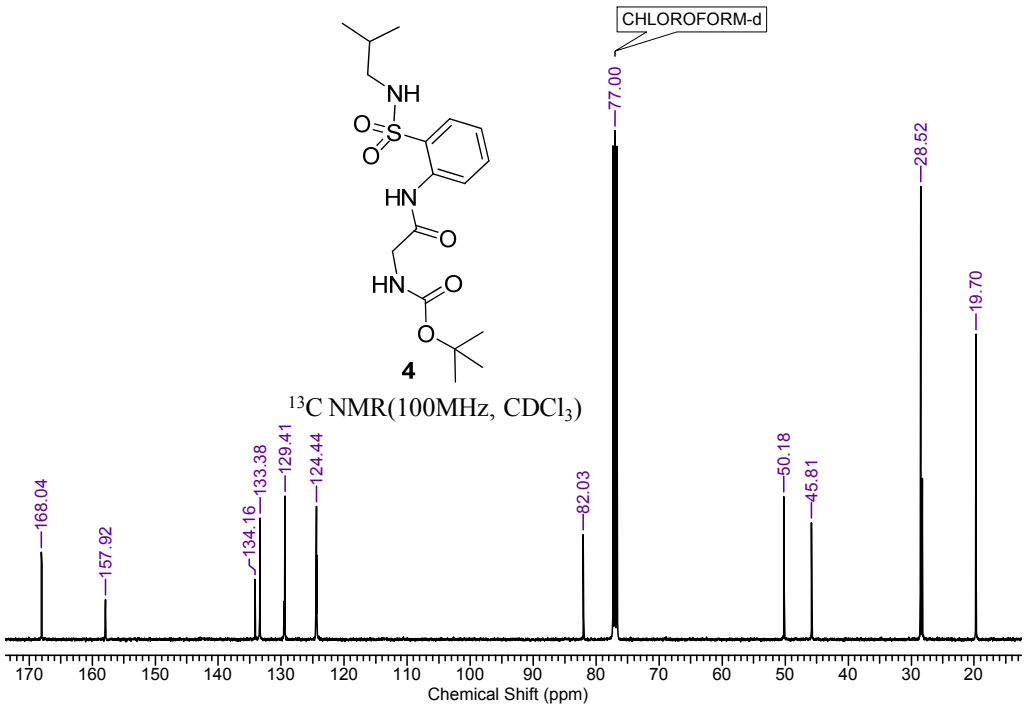
CHLOROFORM-d
168.04
157.92
134.16
133.38
129.41
124.44
82.03
77.00
50.18
45.81
28.52
19.70
NH
O
S
O
HN
O
HN
O
O
4
13C NMR(100MHz, CDCl3)
170 160 150 140 130 120 110 100 90 80 70 60 50 40 30 20
Chemical Shift (ppm)

Table 2.1. Titration study of 3 in $CDCl_3$ (20 mmol) with DMSO-d_6 (volume of DMSO-d_6 added at each addition = 5 µl)

S.No	V DMSO-d_6 (in µL)	Chemical Shift δ (ppm)			
		NH1	NH2	NH3	NH4
1	0	5.35	9.32	6.54	6.53
2	5	5.79	9.31	6.65	6.54
3	10	6.08	9.29	6.71	6.55
4	15	6.31	9.28	6.75	6.55
5	20	6.38	9.27	6.78	6.54
6	25	6.45	9.26	6.80	6.54
7	30	6.54	9.25	6.81	6.58
8	35	6.53	9.24	6.83	6.65
9	40	6.52	9.23	6.83	6.68
10	45	6.53	9.22	6.84	6.72
11	50	6.52	9.21	6.85	6.76

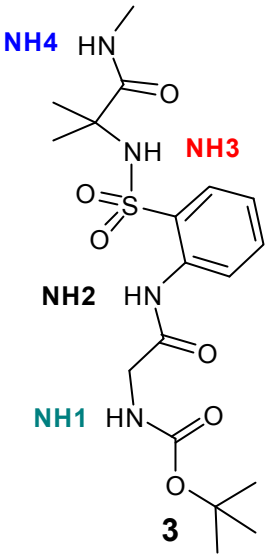

Table 2.2. Titration study of 4 in $CDCl_3$ (20 mmol) with DMSO-d_6 (volume of DMSO-d_6 added at each addition = 5 µl)

S.No	V DMSO-d_6 (in µL)	Chemical Shift δ (ppm)		
		NH1	NH2	NH3
1	0	5.24	9.64	5.97
2	5	5.84	9.61	6.11
3	10	6.15	9.58	6.18
4	15	6.34	9.55	6.22
5	20	6.43	9.54	6.24
6	25	6.50	9.52	6.26
7	30	6.55	9.51	6.27
8	35	6.59	9.49	6.28
9	40	6.63	9.48	6.29
10	45	6.67	9.46	6.29
11	50	6.69	9.45	6.30

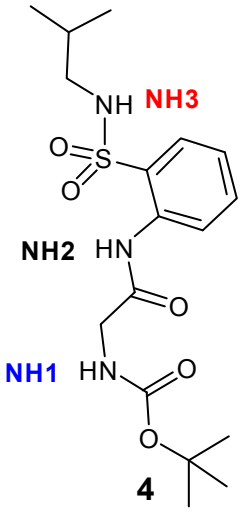

Table 2.3. Variable temperature study of 3 (20 mmol, 400 MHz, $CDCl_3$)

S.No	Temperature (in K)	Chemical Shift δ (ppm)		
		NH1	NH2/NH3	NH4
1	268	9.30	6.64	5.41
2	273	9.30	6.62	5.40
3	278	9.31	6.61	5.39
4	283	9.31	6.59	5.38
5	288	9.31	6.57	5.37
6	291	9.31	6.56	5.36
7	293	9.31	6.55	5.36
8	298	9.32	6.53	5.35
9	303	9.32	6.52	5.34
10	308	9.32	6.50	5.33
11	313	9.32	6.48	5.32
12	318	9.33	6.46	5.31
13	323	9.33	6.44	5.30

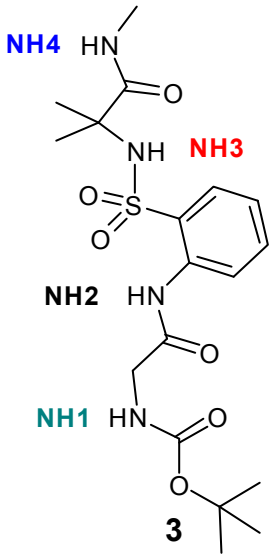

3

Table 2.4. Variable temperature study of 4 (20 mmol, 400 MHz, $CDCl_3$)

S. No	Temperature (in K)	Chemical Shift δ (ppm)		
		NH1	NH2	NH3
1	268	5.29	9.65	6.06
2	273	5.29	9.65	6.05
3	278	5.28	9.65	6.04
4	283	5.27	9.65	6.02
5	288	5.26	9.65	6.00
6	291	5.25	9.64	5.99
7	293	5.25	9.64	5.99
8	298	5.24	9.64	5.97
9	303	5.23	9.64	5.94
10	308	5.22	9.64	5.92
11	313	5.21	9.64	5.90
12	318	5.21	9.63	5.88
13	323	5.19	9.63	5.85

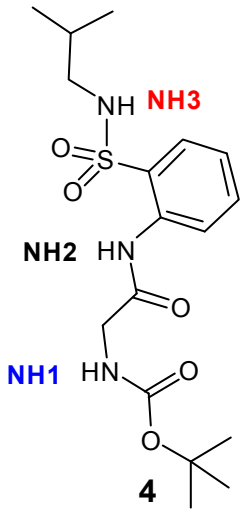

4

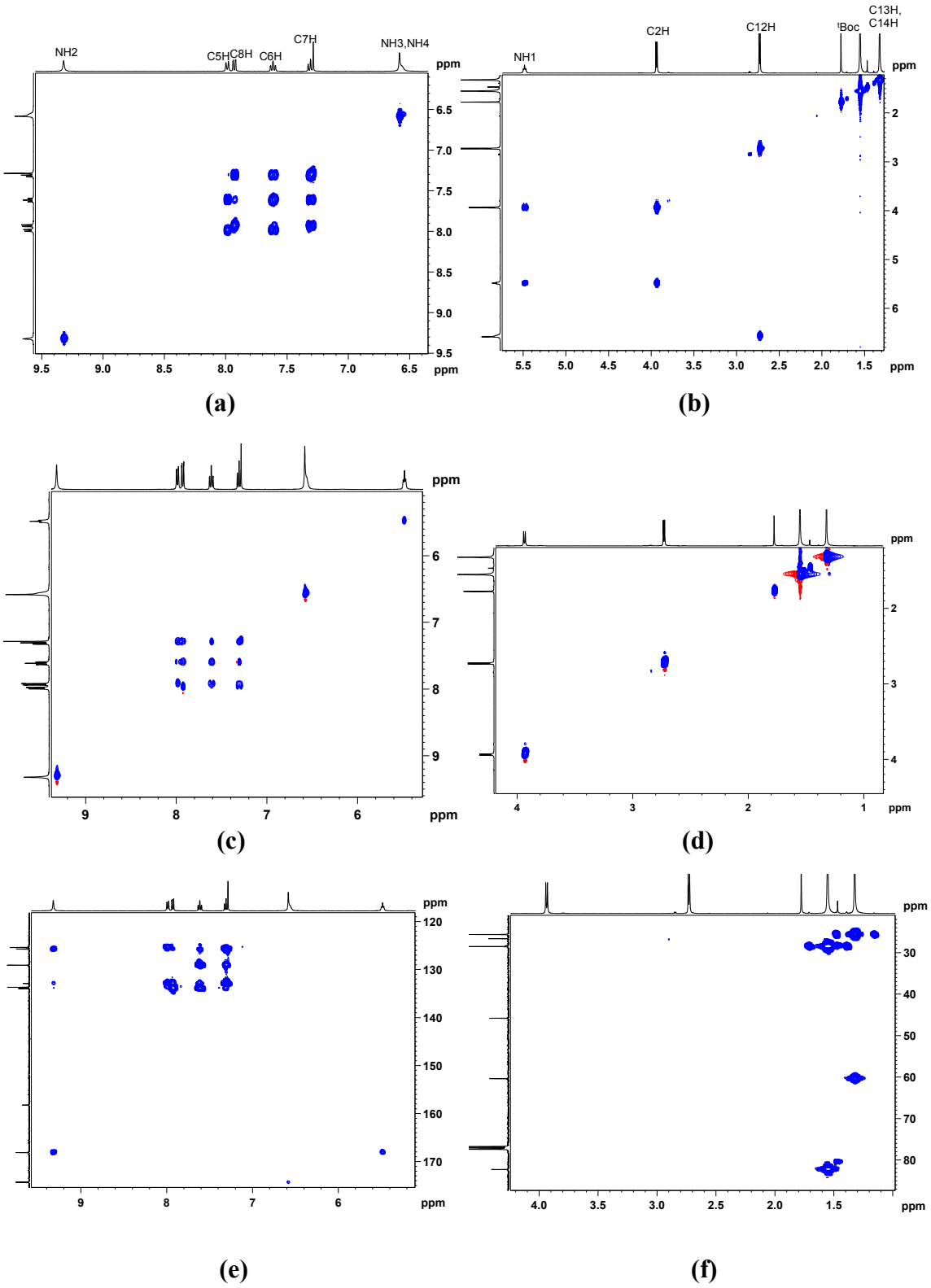

Fig 2.35: Partial COSY (a), (b); TOCSY, (c), (d); and HMBC (e), (f) spectra of **3** (500 MHz, $CDCl_3$). For better view, aromatic and aliphatic regions are shown separately.

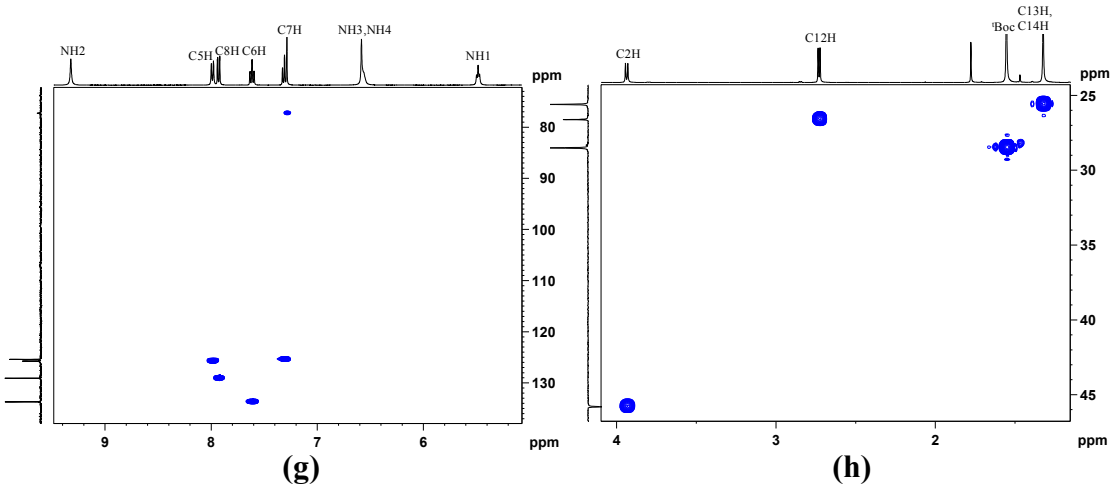

Fig 2.36: Partial HSQC (g), (h) spectra of **3** (500 MHz, $CDCl_3$). For better view, aromatic and aliphatic regions are shown separately.

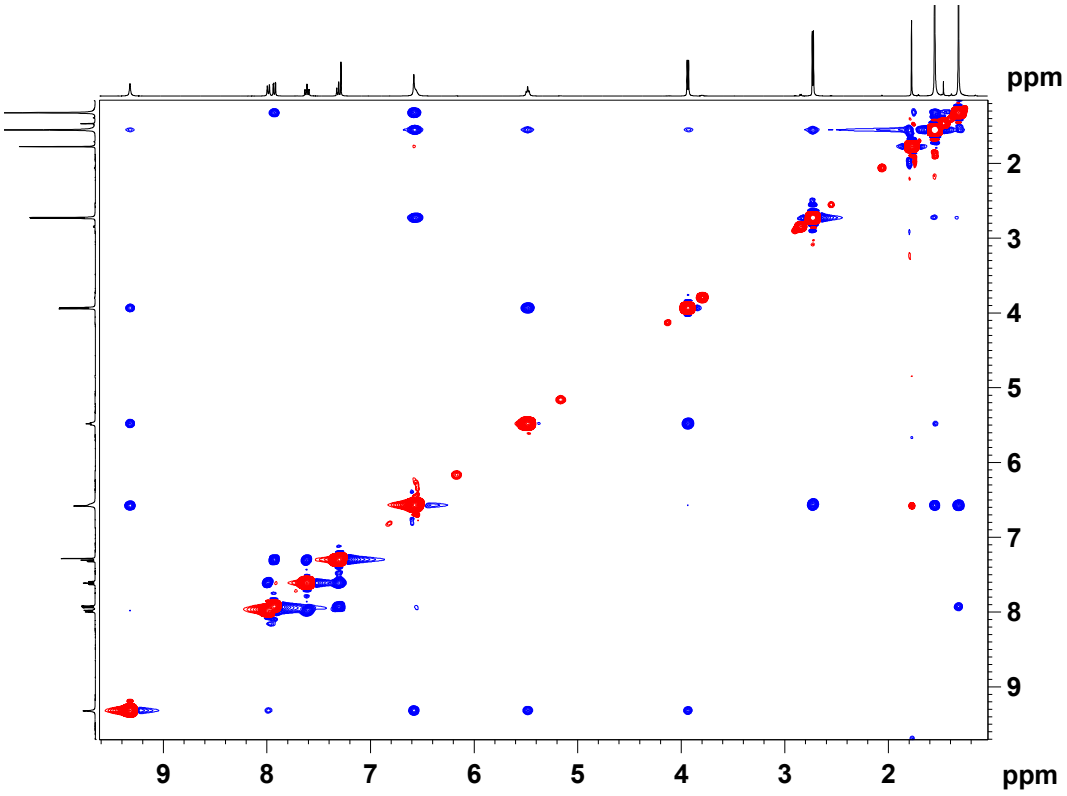

Fig 2.37: Full 2D NOESY spectrum of **3** (500 MHz, $CDCl_3$).

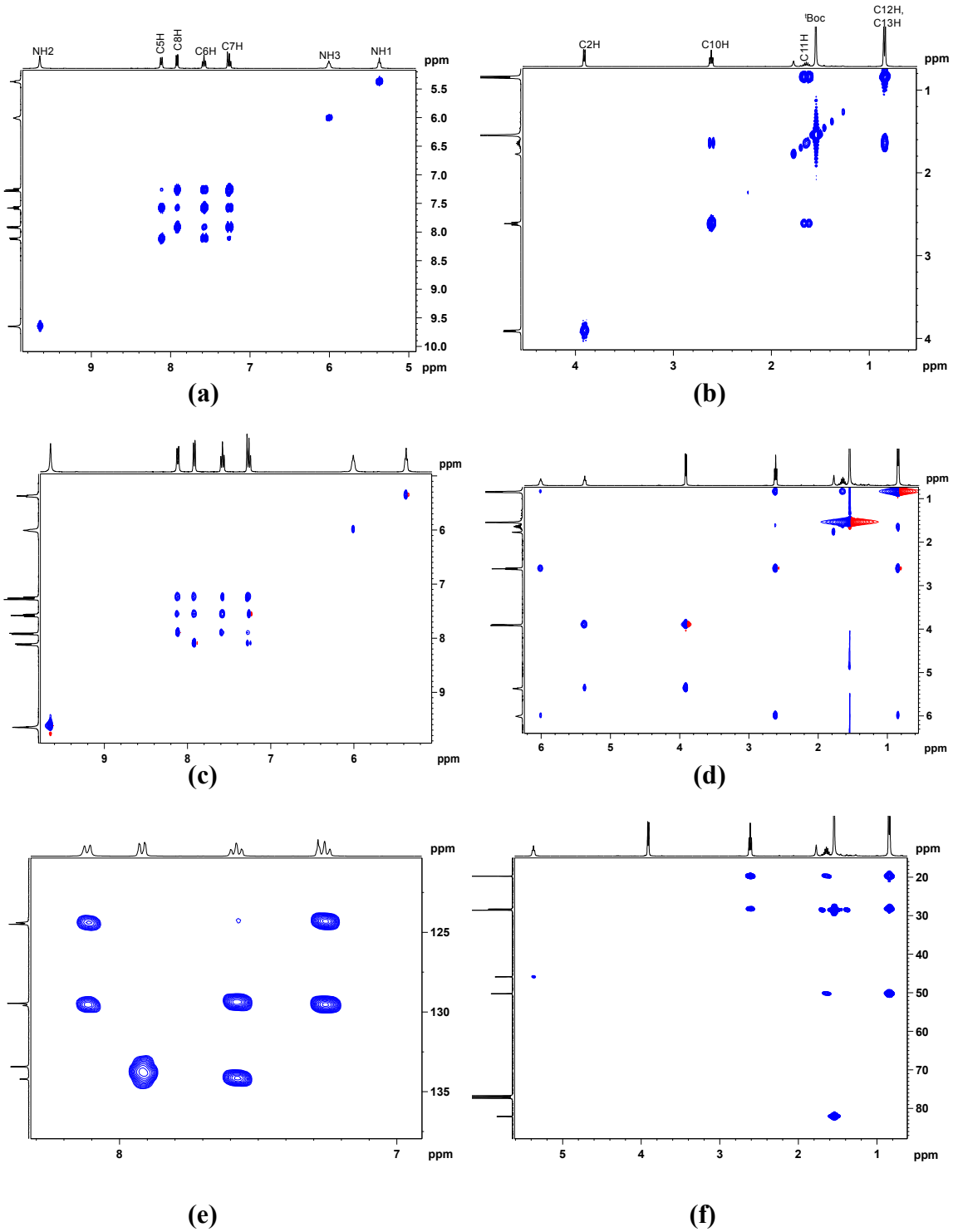

Fig 2.38: Partial COSY (a), (b); TOCSY, (c), (d); and HMBC (e), (f) spectra of **4** (500 MHz, $CDCl_3$). For better view, aromatic and aliphatic regions are shown separately.

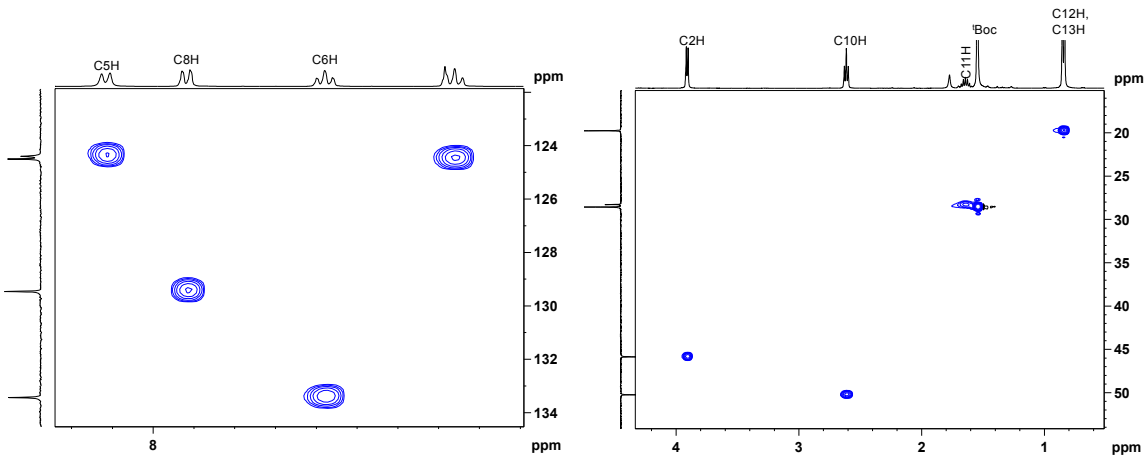

(g) **(h)**

Fig 2.39: Partial HSQC (g), (h) spectra of **4** (500 MHz, $CDCl_3$). For better view, aromatic and aliphatic regions are shown separately.

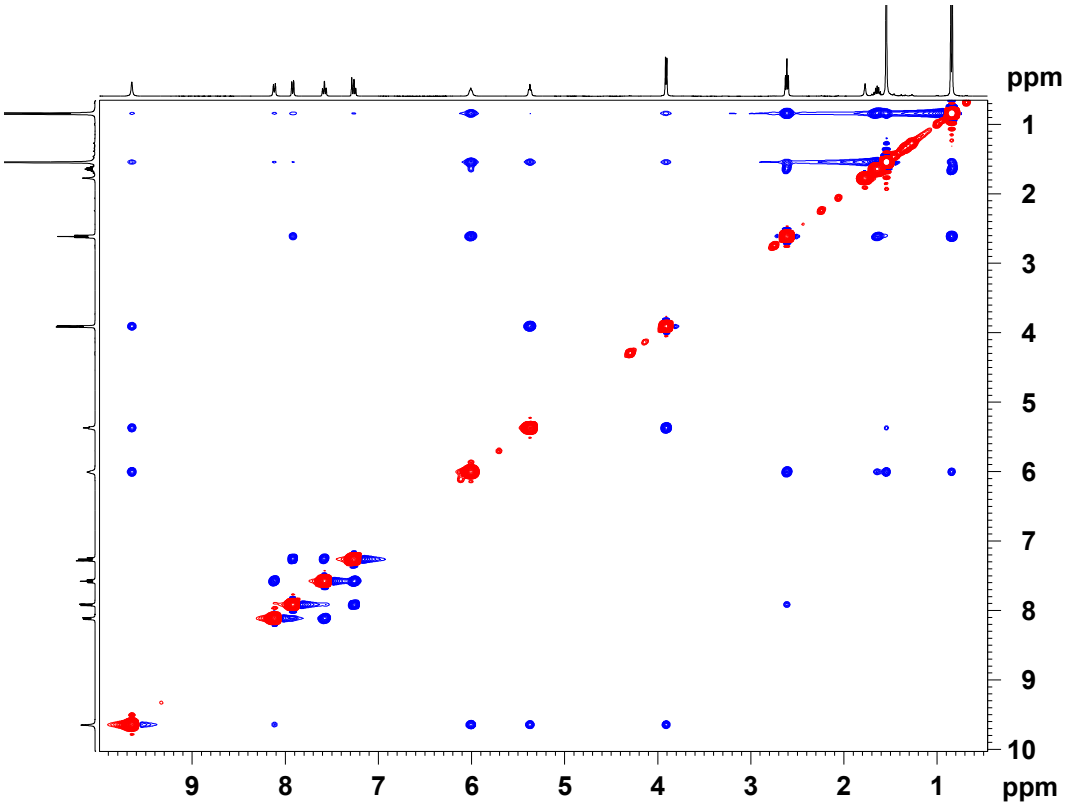

Fig 2.40: Full 2D NOESY spectrum of **4** (500 MHz, $CDCl_3$).

2.20 Experimental Section (Section B)

Crystal data for 7e:

Single crystals of **7e** were grown by slow evaporation of its solution in chloroform and ethyl acetate. Colorless rectangular like crystal of approximate size 0.46 x 0.29 x 0.25 mm^3, was used for data collection. Multirun data acquisition. Total scans = 4, total frames = 1271, Oscillation / frame -0.3º, exposure / frame = 15.0 sec / frame, θ range = 1.88 to 25.00°, completeness to θ of 25.00 º is 100.0 %. $C_{19}H_{27}N_3O_6$, *MW* = 393.44, Crystals belong to Monoclinic, space group P21/c, *a* = 8.8470(1), *b* = 20.2084(3), *c* = 11.8819(2) Å, V = 2078.28(5) $Å^3$, *Z* = 2, D_c = 1.257 g/cc, (Mo–K_α) = 0.094 mm^{-1}, 16080 reflections measured, 3657 unique [I>2σ(I)], R1 = 0.0401, wR2 = 0.1012, Largest diff. peak and hole 0.316 and -0.318 e.$Å^{-3}$.

Crystal data for 8e:

Single crystals of **8e** were grown by slow evaporation of its solution in ethyl acetate and DCM. Colorless cube like crystal of approximate size 0.31 x 0.12 x 0.07 mm^3, was used for data collection. Multi-run data acquisition. Total scans = 4, total frames = 1271, Oscillation / frame -0.3º, exposure / frame = 15.0 sec / frame, θ range = 2.23 to 25.00°, completeness to θ of 25.00 º is 99.9 %. $C_{18}H_{27}N_3O_7S$, *MW* = 429.49, Crystals belong to Triclinic, space group P-1, *a* = 10.0269(3), *b* = 11.0127(3), *c* = 19.1212(5) Å, V = 2072.5(1) $Å^3$, *Z* = 4, D_c = 1.376 g/cc, (Mo–K_α) = 0.201 mm^{-1}, 30705 reflections measured, 7277 unique [I>2σ(I)], R1 = 0.036, wR2 = 0.0829, Largest diff. peak and hole 0.576 and -0.519 e.$Å^{-3}$.

Two molecules with different conformations were present in the unit cell of **8e**. One of the molecules showed intra-residual C6 H-bonding and while the other molecule revealed inter-residual C11 H-bonding. The overlay of these two molecules is shown in Fig 2.31.

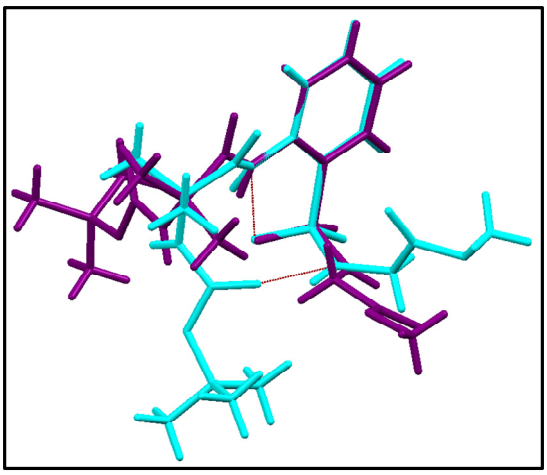

Fig 2.41: Overlay of the two crystals present in the unit cell of **8e**. The crystal in cyan features C11 H-bonding and the crystal in purple features C6 H-bonding.

Crystal data for 8f:

Single crystals of **8f** were grown by slow evaporation of its solution in ethyl acetate, Colorless needle like crystal of approximate size 0.42 x 0.25 x 0.12 mm^3, was used for data collection. Multi-run data acquisition. Total scans = 4, total frames = 1271, Oscillation / frame -0.3º, exposure / frame = 15.0 sec / frame, θ range = 2.23 to 25.00°, completeness to θ of 25.00 º is 100%. $C_{18}H_{28}N_4O_6S$, *MW* = 428.5, Crystals belong to Monoclinic, space group P21/c, *a* = 15.5747(6), *b* = 9.4947(3), *c* = 15.4473(6) Å, V = 2141.33(14) $Å^3$, *Z* = 4, D_c = 1.329 g/cc, (Mo–K_α) = 0.192 mm^{-1}, 16008 reflections measured, 3775 unique [I>2σ(I)], R1 = 0.0532, wR2 = 0.1145, Largest diff. peak and hole 0.286 and -0.347 e.$Å^{-3}$.

Methyl (2-nitrobenzoyl)glycinate 11:

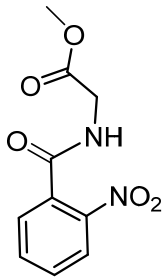

11

To the hydrochloride salt of glycine methyl ester in dry DCM (10 mL), DIPEA (1.04 mL, 6 mmol) was added and stirred at 0 °C for 15 min. Then, 2-nitrobenzoylchloride (0.5 g, 4 mmol) was added to the reaction mixture. The reaction mixture was allowed to attain room temperature and was further stirred for 12 h. Later, the reaction mixture was washed sequentially with sat. $NaHCO_3$, water, dil. HCl and brine solutions. The organic layer was dried over anhydrous Na_2SO_4 and evaporated under reduced pressure to get the crude product which on purification by column chromatography (eluent: pet ether/ethyl acetate: 50:50, R*f*: 0.45) yielded **11** (0.54 g, 57%); mp: 91-93 °C; IR ($CHCl_3$) ν (cm^{-1}): 3683, 3417,

3020, 2400, 1747, 1673, 1533, 1439, 1372, 1350, 1216, 979, 769, 668, 491; ^{1}H NMR (200 MHz, $CDCl_3$) δ: 8.08-8.03 (d, *J* = 6.9 Hz, 1H), 7.73-7.54 (m, 3H), 6.64 (bs, 1H), 4.25-4.23 (d, *J* = 5.2 Hz, 2H), 3.79 (s, 3H); ^{13}C NMR (50 MHz, $CDCl_3$) δ: 169.9, 146.35, 133.7, 132, 130.69, 128.7, 124.4, 52.5, 41.6; HRMS: $C_{10}H_{11}O_5N_2$, Calcd: 239.0662 Found: 239.0665; $C_{10}H_{10}O_5N_2Na$, Calcd: 261.0482 Found: 239.0484.

General procedure for reduction of nitro compounds 11 and 13 to respective amines 12 and 14:

To the solutions of **11** and **13** (0.35 g, 1.47 mmol) in methanol (15 mL), 10% Pd/C (0.06 g) was added. The reaction mixture was subjected to shaking in parr shaker at 60 psi for 12 h. The catalyst was filtered through celite and the solvent was evaporated to get products **12** and **14**, respectively, which were carried forward to the next reaction without purification.

Methyl (2-(2-bromo-2-methyl propanamido)benzoyl)glycinate 7a:

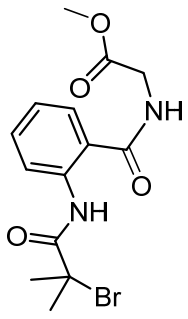

7a

To the solution of amine **12** (0.3g, 1.4 mmol) in dry DCM at 0 ^{o}C, 2-bromo-2-methylpropanoyl bromide (0.21 mL, 1.76 mmol) was added followed by the addition of Et_3N (0.3 mL, 2.2 mmol). Then, the reaction mixture was stirred for 12 h after attaining room temperature. Later, the reaction mixture was washed with saturated $NaHCO_3$, water and brine solution. The organic layer was dried over anhydrous Na_2SO_4 and evaporated under reduced pressure to get the crude product which on purification by column chromatography (eluent: pet ether/ethyl acetate: 70:30, R*f*: 0.5) yielded **7a** (0.43 g, 82%); IR ($CHCl_3$) ν (cm^{-1}): 3683, 3434, 3268, 3019, 2400, 1746, 1652, 1602, 1588, 1519, 1440, 1372, 1298, 1216, 1109, 928, 771, 668, 489; ^{1}H NMR (200 MHz, $CDCl_3$) δ: 11.81 (s, 1H), 8.62-8.57 (d, *J* = 5.1 Hz, 1H), 7.62-7.58 (dd, *J* = 7.8 Hz, 1.5 Hz, 1H), 7.56-7.47 (t, *J* = 6.1 Hz, 1H), 7.17-7.09 (td, *J* = 7.6 Hz, 1.2 Hz, 1H), 6.89 (bs, 1H), 4.26-4.23 (d, *J* = 5.1 Hz, 1H), 4.17-4.07 (q, ethyl acetate), 3.81 (s, 3H), 2.05 (s, 6H), 1.29-1.22 (t, ethyl acetate). ^{13}C NMR (50 MHz, $CDCl_3$) δ: 170.6, 170, 168.7, 132, 139.3, 132.9, 126.8, 123.2, 121.3, 119.9, 60.1, 52.5, 41.6, 31.7; HRMS: $C_{14}H_{18}O_4N_2$, Calcd: 357.0444 Found: 357.0450

Methyl (2-(2-azido-2-methylpropanamido)benzoyl)glycinate 7b:

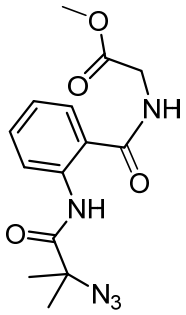

7b

A solution of compound **7a** (0.46g, 1.2 mmol) in dry DMF was heated at 80 ^{o}C in the presence of NaN_3 (0.23g, 3.6 mmol) for 8h. Later, the reaction mixture was taken into ethyl acetate and washed with water and brine solution. The organic layer was then dried over anhydrous Na_2SO_4 and evaporated under reduced pressure to get the crude product which on purification by column chromatography (eluent: petether/ethyl acetate: 70:30, R*f*: 0.5) yielded **7b** (0.41 g, 90%); IR ($CHCl_3$) ν (cm^{-1}): 3683, 3434, 3279, 3020, 2400, 2117, 1746, 1673, 1601, 1586, 1519, 1446, 1372, 1217, 928, 769, 482; ^{1}H NMR (500 MHz, $CDCl_3$) δ: 11.65 (s, 1H), 8.57-8.56 (d, *J* = 8.5 Hz, 1H), 7.59-7.57 (dd, *J* = 7.9 Hz, 1.2 Hz, 1H), 7.48-7.45 (t, *J* = 7.6 Hz, 1H), 7.11-7.08 (t, *J* = 7.6 Hz, 1H), 7.02 (bs, 1H), 4.22-4.21 (d, *J* = 5.1 Hz, 2H), 3.78 (s, 3H), 1,58 (s, 6H); ^{13}C NMR (125 MHz, $CDCl_3$) δ: 171.4, 170.7, 168.8, 138.8, 132.7, 126.8, 123.2, 121.3, 120.3, 64.6, 60.3, 52.4, 41.5, 24.5; HRMS: $C_{14}H_{18}O_4N_5$, Calcd: 320.1353 Found: 320.1351. $C_{14}H_{17}O_4N_5Na$, Calcd: 342.1173 Found: 342.1169.

General procedure for the reduction of azido compounds 7b and 8b and their Boc protection resulting in 7e and 8e:

To the solutions of **7b** and **8b** (0.35 g, 1.47 mmol) in methanol (15 mL), 10% Pd/C (0.06 g) was added and subjected to shaking in parr shaker at 60 psi for 12 h to yield amines **7d** and **8d**, respectively. These amines were trapped *in situ* as Boc derivatives by adding $(Boc)_2O$ (0.179g, 0.82 mmol) to the reaction mixture. Later, the catalyst was filtered through celite and the solvent was evaporated and the crude product was subjected to column chromatography (eluent: petether/ethyl acetate: 70:30, R*f*: 0.5) to yield **7e** and **8e**, respectively.

Methyl-(2-(2-((tert-butoxycarbonyl)amino)-2-methylpropanamido)benzoyl)

glyci-nate 7e:

Compound **7e** was prepared according to the above mentioned procedure; mp: 158-161 ^{o}C; IR ($CHCl_3$) ν(cm^{-1}): 3685, 3438, 3020, 2400, 1719, 1649, 1601, 1587, 1519, 1440, 1370, 1218, 1075, 1016, 929, 771, 667; ^{1}H NMR (500 MHz,

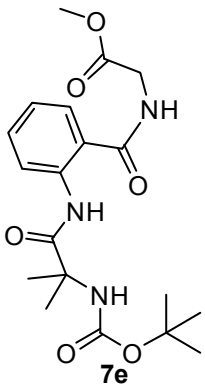

7e

$CDCl_3$) δ: 11.61 (s, 1H), 8.66-8.65 (d, *J* = 8.5 Hz, 1H), 7.59-7.57 (d, *J* = 7.6 Hz, 1H), 7.5-7.47 (t, *J* = 7.9 Hz, 1H), 7.09-7.06 (t, *J* = 7.6 Hz, 1H), 6.91 (bs, 1H), 5.3 (bs, 1H), 4.21-4.2 (d, *J* = 4.9 Hz, 2H), 3.8 (s, 3H), 1.57 (s, 6H), 1.4 (s, 9H); ^{13}C NMR (125 MHz, $CDCl_3$) δ: 173.8, 170.1, 168.7, 154.3, 140, 133.3, 126.8, 122.6, 121.2, 119.2, 52.5, 41.5, 28.2, 25.4; HRMS: $C_{19}H_{28}O_6N_3$, Calcd: 394.1973 Found: 394.1969; $C_{19}H_{27}O_6N_3Na$, Calcd: 416.1973 Found: 416.1788.

General procedure for the C-terminus amidation 7e, 9a, 8e and 10b compounds to their respective amides 7f, 9b, 8f, 10c:

The compounds **7e**, **9a**, **8e** and **10b** were dissolved in MeOH (2 mL) followed by addition of methanolic methyl amine solution (2 mL) at 0 ^oC. The reaction was monitored by TLC. After completion, solvent was stripped off and the crude product was purified by column chromatography which yielded **7f**, **9b**, **8f** and **10c**, respectively.

tert-butyl(2-methyl-1-((2-((2-(methylamino)-2-oxoethyl)carbamoyl)phenyl) amino)-1-oxopropan-2-yl)carbamate 7f:

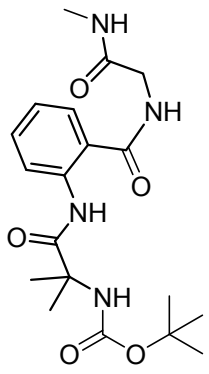

7f

Compound **7f** was isolated as a white solid with 95% yield ; mp: 153-155 ^oC; IR ($CHCl_3$) ν (cm^{-1}): 3684, 3566, 3449, 3315, 3020, 2400, 1687, 1601, 1521, 1446, 1367, 1217, 1078, 1029, 928, 771, 669, 627, 478; ^1H NMR (500 MHz, $CDCl_3$) δ: 11.57 (s, 1H), 8.56 (bs, 1H), 7.63-7.61 (d, *J* = 7.6 Hz, 1H), 7.48-7.45 (t, *J* = 7.3 Hz, 1H), 7.06-7.04 (t, *J* = 7.3 Hz, 1H), 6.54 (bs, 1H), 5.39 (bs, 1H), 4.04 (bs, 2H), 2.82-2.18 (d, *J* = 4.6 Hz, 3H), 1.56 (s, 6H), 1.39 (s, 9H); ^{13}C NMR (125 MHz, $CDCl_3$) δ: 173.8, 169, 154.6, 139.6, 132.9, 127.2, 122.8, 43.2, 28.2, 26.3; HRMS: $C_{19}H_{29}O_5N_4$, Calcd: 393.2132 Found: 393.2130; $C_{19}H_{28}O_5N_4Na$, Calcd: 415.1952 Found: 415.1949.

General method for ester hydrolysis:

To the solutions of esters **7b** and **8b** (10 mmol, 1 equiv) in methanol,

$LiOH{\cdot}H_2O$ (40 mmol, 4 equiv) was added by dissolving it in water (12 mL) at 0 °C. After complete consumption of starting material, the solvent was evaporated under reduced pressure. The residue was treated with sat. $KHSO_4$ solution and then extracted into DCM (2 X 25 mL). The acid derivatives **7c** and **8c**, respectively, obtained after evaporation of the solvent were used for the next reaction without purification.

Methyl-(2-(2-(2-(2-(2-azido-2-methylpropanamido)benzamido)acetamido)-2-methylpropanamido)benzoyl)glycinate 9a:

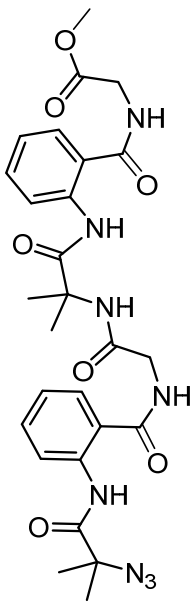

9a

The acid **7c** (0.13 g, 0.4 mmol) was coupled with the amine **7d** (0.12 g, 0.4 mmol) using EDC. HCl (0.1 g, 0.5 mmol), Et_3N (0.18 mL, 1.3 mmol) and HOBt (0.01 g, 0.08 mmol) in dry DCM at 0 °C, the reaction mixture was allowed to attain room temperature and stirred for 72h. Then, the reaction mixture was washed sequentially with sat. $NaHCO_3$, water, sat. $KHSO_4$ solutions. The organic layer was dried over anhydrous Na_2SO_4 and evaporated under reduced pressure to get the crude product which on purification by column chromatography (eluent: pet ether/ethyl acetate: 20:80, R*f*: 0.4) yielded **9a** (0.06 g, 30%); IR ($CHCl_3$) ν (cm^{-1}): 3683, 3317, 3019, 2400, 2116, 1745, 1676, 1600, 1586, 1520, 1445, 1371, 1218, 928, 771, 626, 515; ^1H NMR (500 MHz, $CDCl_3$) δ: 11.74 (s, 1H), 11.55 (s, 1H), 8.58-8.53 (t, *J* = 7.9 Hz, 1H), 7.68-7.66 (t, *J* = 7.9 Hz, 1H), 7.6-7.58 (dd, *J* = 7.9 Hz, 1.2 Hz, 1H), 7.49-7.44 (q, *J* = 7.6 Hz, 2H), 7.29 (bs, 1H), 7.1-7.05 (quin, *J* = 7.3 Hz, 14.9 Hz, 2H), 6.93 (bs, 1H), 4.18-4.17 (d, *J* = 5.1 Hz, 2H), 3.97-3.96 (d, *J* = 4.8 Hz, 2H), 3.68 (s, 3H), 1.63 (s, 6H), 1.61 (s, 6H); ^{13}C NMR (125 MHz, $CDCl_3$) δ: 172.7, 171.4, 169.9, 169.4, 168.8, 168.6, 139.5, 138.9, 133.1, 132.8, 127.1, 123.5, 122.9, 121.5, 121.3, 120.5, 119.3, 64.7, 58.2, 43.8, 41.6, 25.1, 24.6; HRMS: $C_{27}H_{33}O_7N_8$, Calcd: 581.2467 Found: 581.2465; $C_{27}H_{33}O_7N_8Na$, Calcd: 603.2286 Found: 603.2280.

2-(2-azido-2-methylpropanamido)-N-(2-((2-methyl-1-((2-((2-(methylamino)-2-oxoethyl)carbamoyl)phenyl)amino)-1-oxopropan-2-yl)amino)-2-oxoethyl) benzamide 9b:

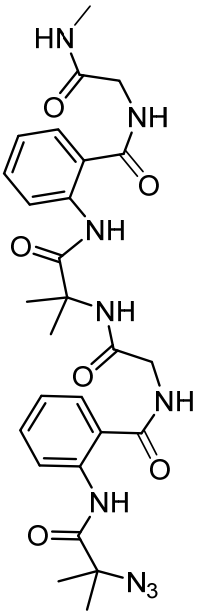

9b

Compound **9b** was isolated as a white solid in 90% yield (eluent: ethyl acetate: R*f*: 0.3); mp: 56-58 ^{o}C; IR ($CHCl_3$) ν (cm^{-1}): 3684, 3328, 3020, 2400, 2116, 1672, 1600, 1586, 1520, 1444, 1216, 1018, 928, 770, 668, 626; ^{1}H NMR (500 MHz, $CDCl_3$) δ: 11.69 (s, 1H), 11.64 (s, 1H), 8.5-8.49 (d, *J* = 8.2 Hz, 1H), 8.46-8.44 (d, *J* = 8.2 Hz, 1H), 7.94 (m, 1H), 7.7-7.68 (dd, *J* = 7.9 Hz, 1.2 Hz, 1H), 7.56 (bs, 1H), 7.53-7.52 (d, *J* = 7 Hz, 1H), 7.48-7.45 (t, *J* = 7.3 Hz, 1H), 7.42-7.38 (t, *J* = 7.6 Hz, 1H), 7.32 (bs, 1H), 7.11-7.08 (t, *J* = 7.9 Hz, 1H), 7.01-6.98 (t, *J* = 7.6 Hz, 1H), 6.63 (bs, 1H), 4.16-4.15 (d, *J* = 5.1 Hz, 2H), 3.68-3.67 (d, *J* = 4.8 Hz, 2H), 2.7-2.69 (d, *J* = 4.5 Hz, 3H), 1.6 (m, 12H); ^{13}C NMR (125 MHz, $CDCl_3$) δ: 172.9, 171.5, 169.3, 169.1, 169, 139.3, 138.6, 132.9, 132.7, 127.6, 123.7, 123, 121.6, 121.3, 121, 119.5, 64.8, 58.1, 44.2, 42.9, 26.2, 25.1, 24.6; HRMS: $C_{27}H_{34}O_6N_9$, Calcd: 580.2627 Found: 580.2626; $C_{27}H_{33}O_6N_9Na$, Calcd: 602.2446 Found: 602.2440.

Methyl ((2-nitrophenyl)sulfonyl)glycinate 13:

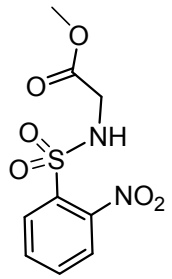

13

To the hydrochloride salt of glycine methyl ester in dry DCM (10 mL), Et_3N (0.57 mL, 4 mmol) was added and stirred at 0 ^{o}C for 15 min. Then, 2-nitrobenzoylchloride (0.3 g, 1.3 mmol) was added to the reaction mixture. The reaction mixture was allowed to attain room temperature and was further stirred for 12 h. Later, the reaction mixture was washed sequentially with sat. $NaHCO_3$, water, dil. HCl and brine solutions. The organic layer was dried over anhydrous Na_2SO_4 and evaporated under reduced pressure to get the crude product which on purification by column chromatography (eluent: pet ether/ethyl acetate: 60:40, R*f*: 0.5) yielded **13** (0.18 g, 50%); mp: 108-110 ^{o}C; IR ($CHCl_3$) ν (cm^{-1}): 3685, 3617, 3363, 3019, 2400, 1749, 1543, 1440, 161, 1218, 1171, 1046,

771, 668, 588; ^{1}H NMR (400 MHz, $CDCl_3$) δ: 8.11-8.08 (m, 1H), 7.95-7.92 (m, 1H), 7.76-7.74 (m, 2H), 6.08-6.05 (t, *J* = 5.1 Hz, 1H), 4.03-4.01 (d, *J* = 5.8 Hz, 2H), 3.61 (s, 3H); ^{13}C NMR (100 MHz, $CDCl_3$) δ: 169, 133.7, 132.9, 130.5, 125.6, 52.5, 44.7; HRMS: $C_9H_{10}O_6N_2NaS$, Calcd: 297.0152 Found: 297.0149.

Methyl ((2-(2-bromo-2-methylpropanamido)phenyl)sulfonyl)glycinate 8a:

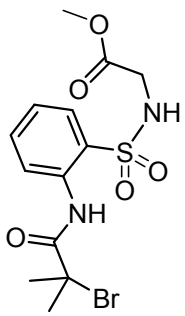

8a

To the solution of amine **14** (0.17g, 0.7 mmol) in dry DCM at 0 ^{o}C, 2-bromo-2-methylpropanoyl bromide (0.09 mL, 0.7 mmol) was added followed by the addition of Et_3N (0.12 mL, 0.8 mmol) and the reaction mixture was stirred for 8 h after attaining room temperature. Later, the reaction mixture was washed with sat. $NaHCO_3$, water and brine solutions. The organic layer was dried over anhydrous Na_2SO_4 and evaporated under reduced pressure to get the crude product which on purification by column chromatography (eluent: pet ether/ethyl acetate: 70:30, R*f*: 0.5) yielded **8a** (0.26 g, 97%); IR ($CHCl_3$) ν (cm^{-1}): 3331, 3022, 1745, 1700, 1586, 1528, 1438, 1332, 1218, 1154, 1113, 850, 771, 497; ^{1}H NMR (400 MHz, $CDCl_3$) δ: 9.98 (s, 1H), 8.37-8.35 (d, *J* = 8.3 Hz, 1H), 7.95-7.93 (d, *J* = 8 Hz, 1H), 7.67-7.63 (t, *J* = 7.8 Hz, 1H), 7.31-7.29 (d, *J* = 6.3 Hz, 1H), 5.55-5.52 (t, *J* = 5.3 Hz, 1H), 4.18-4.13(q, ethyl acetate), 3.81-3.8 (d, *J* = 5.5 Hz, 2H), 3.63 (s, 3H), 2.11 (s, 6H); ^{13}C NMR (100 MHz, $CDCl_3$) δ: 170.1, 168.5, 135.6, 134.3, 129.4, 126.8, 124.3, 123.2, 60.5, 60.4, 52.7, 43.8, 31.5, 21, 14.1; HRMS: $C_{13}H_{17}O_5N_2BrNaS$, Calcd: 416.9913 Found: 416.9909.

Methyl-((2-(2-azido-2-methylpropanamido)phenyl)sulfonyl)glycinate 8b:

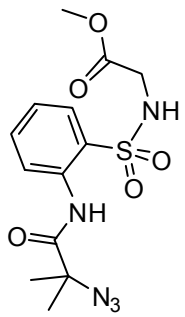

8b

A solution of compound **8a** (0.36g, 0.9 mmol) and NaN_3 (0.18g, 2.9 mmol) in dry DMF was heated at 80 ^{o}C for 8h. Later, the reaction mixture was taken into ethyl acetate and washed with water, brine solution. The organic layer was then dried over anhydrous Na_2SO_4 and evaporated under reduced pressure to get the crude product which on purification by column chromatography (eluent: petether/ethyl acetate: 70:30, R*f*: 0.5) yielded **8b** (0.29 g, 89%); IR ($CHCl_3$) ν (cm^{-1}): 3330, 3020, 2119, 1749, 1697, 1584, 1523, 1439, 1344, 1217, 1127, 771, 668, 460; ^{1}H NMR (400 MHz, $CDCl_3$)

δ: 10.02 (s, 1H), 8.41-8.39 (d, *J* = 8 Hz, 1H), 7.94-7.92 (dd, *J* = 7.8 Hz, 1.5 Hz, 1H), 7.64-7.60 (t, *J* = 7 Hz, 1H), 7.30-7.25 (m, 1H), 5.5 (s, 1H), 3.8 (s, 2H), 3.63 (s, 3H), 1.68 (s, 6H); ^{13}C NMR (100 MHz, $CDCl_3$) δ: 171, 168.7, 135.4, 134.3, 129.4, 127.1, 124.2, 123, 64.7, 52.7, 43.7, 24.3; HRMS: $C_{13}H_{17}O_5N_5NaS$, Calcd: 378.0843 Found: 378.0842.

Methyl-((2-(2-((tert-butoxycarbonyl)amino)-2-methylpropanamido)phenyl) sulfonyl)glycinate 8e:

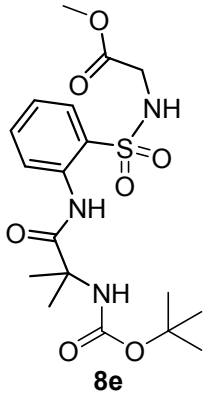

8e

Compound **8e** was synthesised according to the above mentioned procedure; mp: 110-113 ^{o}C; IR ($CHCl_3$) ν (cm^{-1}): 3356, 3020, 2400, 1698, 1583, 1514, 1439, 1336, 1218, 1128, 929, 771, 666, 476; ^{1}H NMR (500 MHz, $CDCl_3$) δ: 9.64 (s, 1H), 8.04-8.02 (d, *J* = 7.9 Hz, 1H), 7.86-7.85 (dd, *J* = 7.9 Hz, 1.2 Hz, 1H), 7.58-7.55 (t, *J* = 7.9 Hz, 1H), 7.22-7.19 (t, *J* = 7.9 Hz, 1H), 7.22-7.19 (t, *J* = 7.9 Hz, 1H), 6.93 (bs, 1H), 4.97 (s, 1H), 3.71-3.7 (d, *J* = 6.1 Hz, 2H), 3.47 (s, 3H), 1.6 (s, 6H), 1.5 (s, 9H); ^{13}C NMR (125 MHz, $CDCl_3$) δ: 172.8, 168.4, 156.1, 135.3, 133.4, 128.9, 124.1, 81.6, 57.7, 52.3, 44.1, 28.5, 25.5; HRMS: $C_{18}H_{27}O_7N_3NaS$, Calcd: 452.1462 Found: 452.1458.

tert-butyl-(2-methyl-1-((2-(N-(2-(methylamino)-2-oxoethyl)sulfamoyl)phenyl-amino)-1-oxopropan-2-yl)carbamate 8f:

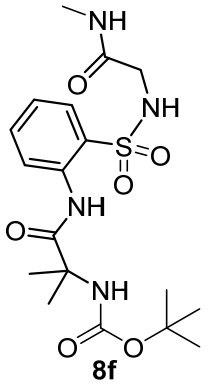

8f

Compound **8f** was isolated following to the above mentioned procedure (eluent: pet ether/ethyl acetate: 30:70, R*f*: 0.4) with 95% yield; mp: 143-146 ^{o}C; IR ($CHCl_3$) ν (cm^{-1}): 3683, 3620, 3439, 3376, 3217, 3020, 2400, 1682, 1582, 1503, 1337, 1217, 1159, 771, 669, 505; ^{1}H NMR (400 MHz, $CDCl_3$) δ: 9.28 (s, 1H), 7.83-7.81 (dd, *J* = 9 Hz, 1H), 7.54-7.50 (t, *J* = 8.2 Hz, 1H), 7.23-7.19 (t, *J* = 8 Hz, 1H), 6.99-6.96 (t, *J* = 6.2 Hz, 1H), 6.37 (bs, 1H), 5.14 (bs, 1H), 3.47-3.45 (d, *J* = 6.5 Hz, 2H), 2.58-2.57 (d, *J* = 4.8 Hz, 3H), 1.53 (s, 6H), 1.37 (s, 9H); ^{13}C NMR (100 MHz, $CDCl_3$) δ: 173.2, 168.2, 156.2, 134.8, 133.8, 129.7, 129.2, 125.1, 81.5, 57.3, 45.5, 28.3, 25.4; HRMS: $C_{18}H_{28}O_6N_4NaS$, Calcd: 451.1622 Found: 451.1617.

Methyl-((2-(2-(2-((2-(2-azido-2-methylpropanamido) phenyl) sulfonamido) acetamido)-2-methylpropanamido)phenyl)sulfonyl)glycinate 10a:

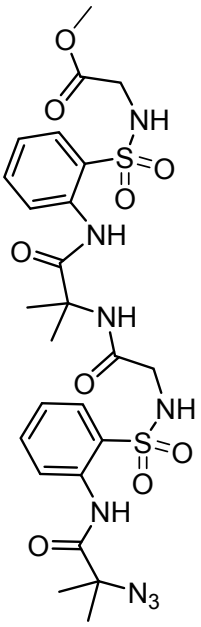

10a

The acid **8c** (0.07 g, 0.2 mmol) was coupled with the amine **8b** (0.07 g, 0.2 mmol) using HBTU (0.1 g, 0.2 mmol), Et_3N (0.05 mL, 0.3 mmol) and HOBt (0.006 g, 0.04 mmol) in dry CH_3CN at 0 °C. The reaction mixture was allowed to attain room temperature and stirred for 72h. Later, the solvent in the reaction mixture was stripped off under reduced pressure, the residue obtained was taken into ethyl acetate and washed sequentially with sat. $NaHCO_3$, water, sat. $KHSO_4$ and brine solutions. Then, the organic layer was dried over anhydrous Na_2SO_4 and evaporated under reduced pressure to get the crude product which on purification by column chromatography (eluent: pet ether/ethyl acetate: 20:80, R*f*: 0.4) yielded **10a** (0.06 g, 40%); mp: 101-103 ^oC ; IR ($CHCl_3$) ν (cm^{-1}): 3683, 3618, 3363, 3019, 2400, 2119, 1745, 1696, 1583, 1520, 1438, 1335, 1217, 1156, 928, 770, 668; ^1H NMR (400 MHz, $CDCl_3$) δ: 9.99 (s, 1H), 9.30 (s, 1H), 8.37-8.35 (d, *J* = 8.2 Hz, 1H), 8-7.98 (d, *J* = 8.2 Hz, 1H), 7.88-7.86 (d, *J* = 7.7 Hz, 1H), 7.72-7.7 (d, *J* = 7.7 Hz, 1H), 7.57-7.53 (t, *J* = 7.5 Hz, 1H), 7.51-7.47 (t, *J* = 7.5 Hz, 1H), 7.22-7.19 (t, *J* = 7.7 Hz, 1H), 7.14-7.11 (t, *J* = 7.7 Hz, 3.72 (s, 2H), 3.59 (s, 2H), 3.42 (s, 3H), 1.57 (s, 6H), 1.5 (s, 6H); ^{13}C NMR (100 MHz, $CDCl_3$) δ: 171.5, 171.3, 170.6, 168.4, 165.7, 135.5, 134.5, 133.7, 129.5, 128.8, 128.5, 127.1, 124.7, 124.6, 124.2, 123.2, 64.7, 60.3, 58.3, 52.4, 46.5, 44, 38.5, 25.1, 24.4; HRMS: $C_{25}H_{33}O_9N_8S$, Calcd: 653.1806 Found: 653.1804; $C_{25}H_{33}O_9N_8NaS$, Calcd: 675.1626 Found: 675.1613.

Methyl-((2-(2-(2-((2-(2-((tert-butoxycarbonyl)amino)-2-methylpropanamido) phe-nyl)sulfonamido)acetamido)ethylpropanamido)phenyl)sulfonyl)glycinate 10b:

The azide **10a** was reduced and protected *in situ* as Boc derivative following the above mentioned procedure which yielded compound **10b** (0.15g, 50%); mp:

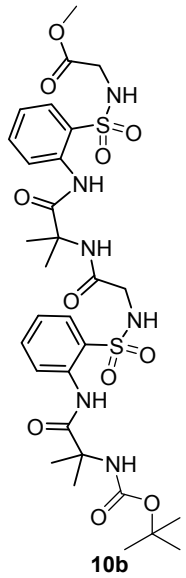

10b

101-103 °C IR ($CHCl_3$) ν (cm^{-1}): 3364, 3019, 2400, 1695, 1583, 1522, 1438, 1335, 1217, 1045, 929, 771, 669, 479; ^{1}H NMR (500 MHz, $CDCl_3$) δ: 10.1 (s, 1H), 9.56 (s, 1H), 8.67-8.66 (d, *J* = 8.2 Hz, 1H), 8.09-8.07 (d, *J* = 7.9 Hz, 1H), 7.83-7.81 (dd, *J* = 7.9 Hz, 1.5 Hz, 1H), 7.58-7.54 (m, 2H), 7.22-7.19 (m, 2H), 7.13-7.1 (m, 1H), 7.02-6.99 (m, 1H), 3.72-3.71 (m, 2H), 3.47-3.46 (m, 2H), 3.41 (s, 3H); ^{13}C NMR (100 MHz, $CDCl_3$) δ: 173.7, 169.1, 168.6, 154.6, 150.5, 138, 135.2, 133.5, 129, 128.9, 124.6, 124.1, 86, 58.1, 52.2, 49.7, 44.1, 28.2, 27.6, 25.3, 25.1; HRMS: $C_{30}H_{43}O_{11}N_6S_2$, Calcd: 727.2426 Found: 727.2430.

tert-butyl-(2-methyl-1-((2-(N-(2-((2-methyl-1-((2-(N-(2-(methylamino)2-oxoethyl)sulfamoyl)phenyl)amino)-1-oxopropan-2-yl)amino)2-oxoethyl) sulfamoyl)phenyl) amino)-1-oxopropan-2-yl)carbamate 10c:

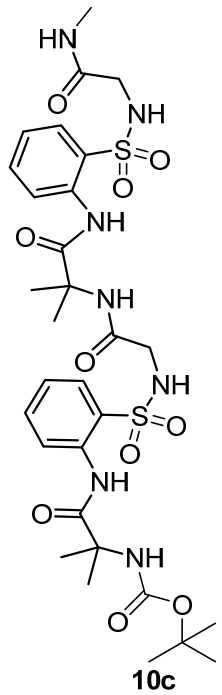

10c

Compound **10c** was isolated as a white solid using the above mentioned protocol (eluent: pet ether /ethyl acetate: 30:70, R*f*: 0.4) quantitatively; mp: 168-171 °C; IR ($CHCl_3$) ν (cm^{-1}): 3685, 3624, 3373, 3019, 2400, 1668, 1582, 1519, 1424, 1336, 1218, 1045, 929, 771, 668, 626; ^{1}H NMR (500 MHz, $CDCl_3$) δ: 9.39 (s, 1H), 9.17 (s, 1H), 7.93-7.91 (d, *J* = 7.9 Hz, 2H), 7.86-7.84 (dd, *J* = 7.9 Hz, 1.2 Hz, 1H), 7.66-7.62 (t, *J* = 8.5 Hz, 1H), 7.6-7.56 (t, *J* =8.2 Hz, 1H), 7.34-7.31(t, *J* = 7.3 Hz, 1H), 7.25-7.24 (d, *J* = 7 Hz, 2H), 7.07 (bs, 1H), 6.87-6.84 (t, *J* = 6.4 Hz, 1H), 6.48 (bs, 1H), 5.08 (bs, 1H), 3.64-3.63 (d, *J* = 6.1 Hz, 2H), 3.46-3.45 (d, *J* = 6.7 Hz, 2H), 2.68-2.67 (d, *J* = 4.8 Hz, 3H), 1.61 (s, 6H), 1.54 (s, 6H), 1.49 (s, 9H); ^{13}C NMR (100 MHz, $CDCl_3$) δ: 173.1, 172, 170.8, 168.2, 156.4, 134.6, 134.2, 133.9, 129.8, 129.6, 129, 125.8, 124.9, 81.8, 57.9, 57.6, 46.1, 45.4, 28.5, 26.1, 25.5, 25; HRMS: $C_{30}H_{44}O_{10}N_7S_2$, Calcd: 726.2586 Found: 727.2590. $C_{30}H_{44}O_{10}N_7S_2$, Calcd: 748.2405 Found: 748.2397.

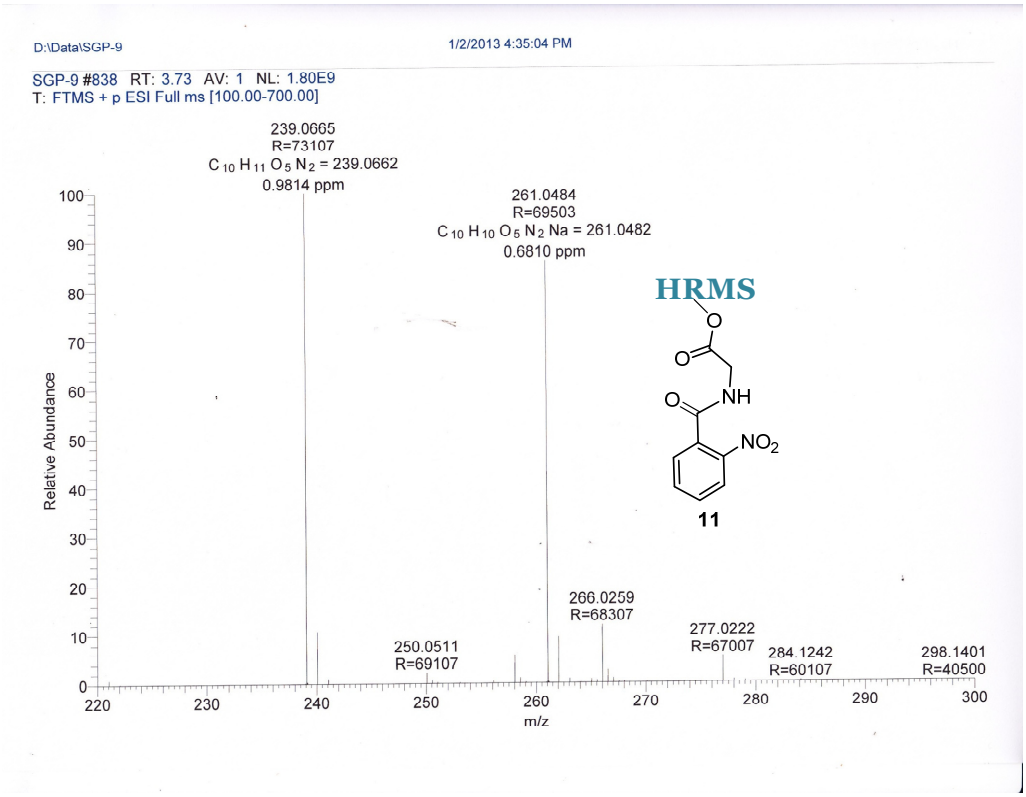
D:\Data\SGP-9
1/2/2013 4:35:04 PM
SGP-9 #838 RT: 3.73 AV: 1 NL: 1.80E9
T: FTMS + p ESI Full ms [100.00-700.00]
239.0665
R=73107
C 10 H 11 O 5 N 2 = 239.0662
0.9814 ppm
261.0484
R=69503
C 10 H 10 O 5 N 2 Na = 261.0482
0.6810 ppm
HRMS
11
266.0259
R=68307
277.0222
R=67007
250.0511
R=69107
284.1242
R=60107
298.1401
R=40500
Relative Abundance
m/z

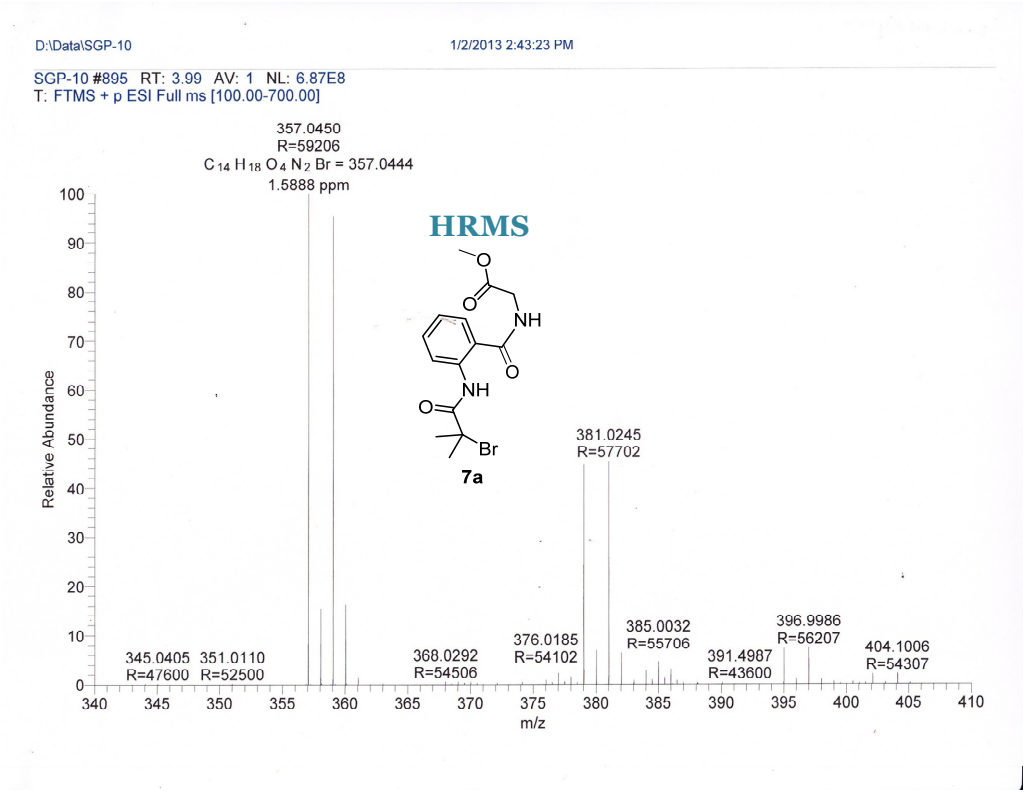
D:\Data\SGP-10
1/2/2013 2:43:23 PM
SGP-10 #895 RT: 3.99 AV: 1 NL: 6.87E8
T: FTMS + p ESI Full ms [100.00-700.00]
357.0450
R=59206
C 14 H 18 O 4 N 2 Br = 357.0444
1.5888 ppm
HRMS
7a
381.0245
R=57702
345.0405
R=47600
351.0110
R=52500
368.0292
R=54506
376.0185
R=54102
385.0032
R=55706
391.4987
R=43600
396.9986
R=56207
404.1006
R=54307
Relative Abundance
m/z

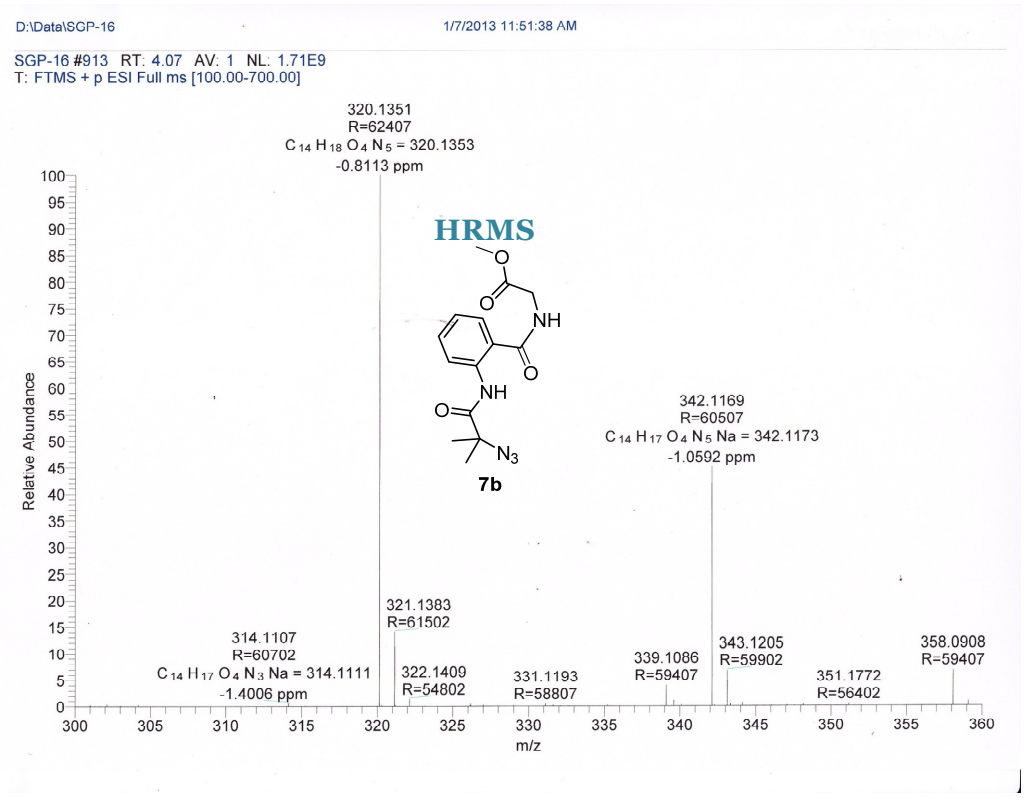
D:\Data\SGP-16
1/7/2013 11:51:38 AM
SGP-16 #913 RT: 4.07 AV: 1 NL: 1.71E9
T: FTMS + p ESI Full ms [100.00-700.00]
320.1351
R=62407
C14 H18 O4 N5 = 320.1353
-0.8113 ppm
HRMS
7b
342.1169
R=60507
C14 H17 O4 N5 Na = 342.1173
-1.0592 ppm
321.1383
R=61502
314.1107
R=60702
C14 H17 O4 N3 Na = 314.1111
-1.4006 ppm
322.1409
R=54802
331.1193
R=58807
339.1086
R=59407
343.1205
R=59902
351.1772
R=56402
358.0908
R=59407
Relative Abundance
m/z

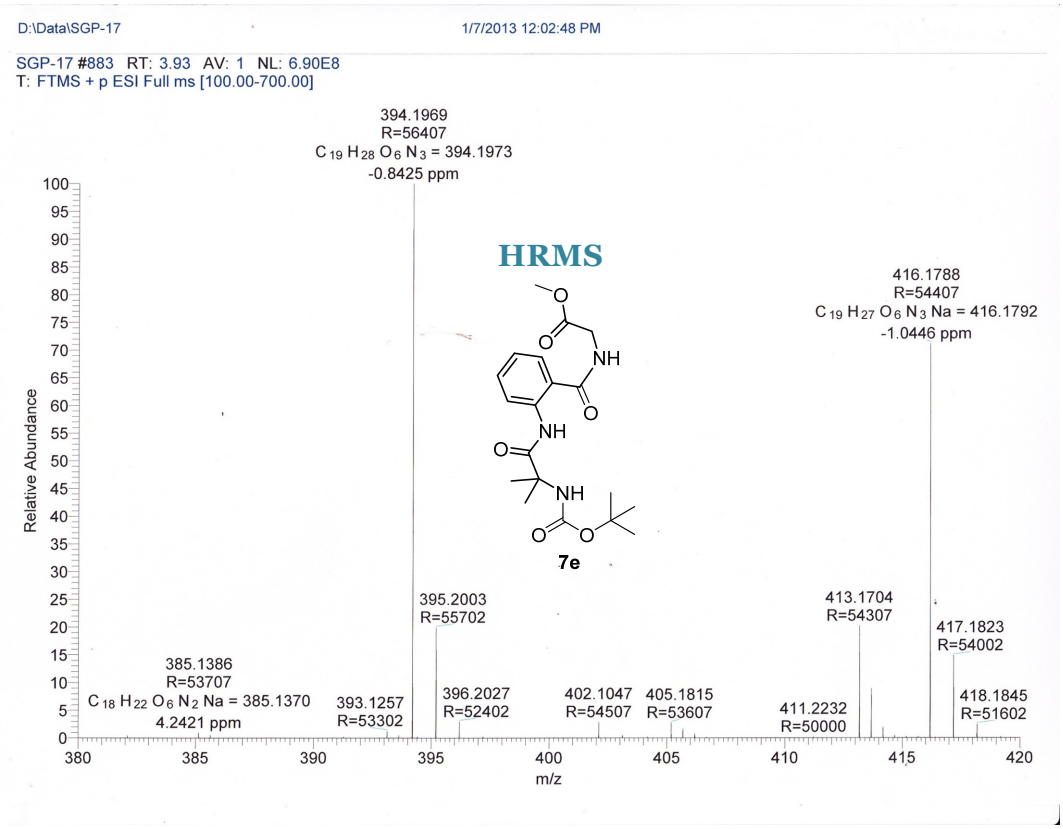
D:\Data\SGP-17
1/7/2013 12:02:48 PM
SGP-17 #883 RT: 3.93 AV: 1 NL: 6.90E8
T: FTMS + p ESI Full ms [100.00-700.00]
394.1969
R=56407
C19 H28 O6 N3 = 394.1973
-0.8425 ppm
HRMS
7e
416.1788
R=54407
C19 H27 O6 N3 Na = 416.1792
-1.0446 ppm
395.2003
R=55702
385.1386
R=53707
C18 H22 O6 N2 Na = 385.1370
4.2421 ppm
393.1257
R=53302
396.2027
R=52402
402.1047
R=54507
405.1815
R=53607
411.2232
R=50000
413.1704
R=54307
417.1823
R=54002
418.1845
R=51602
Relative Abundance
m/z

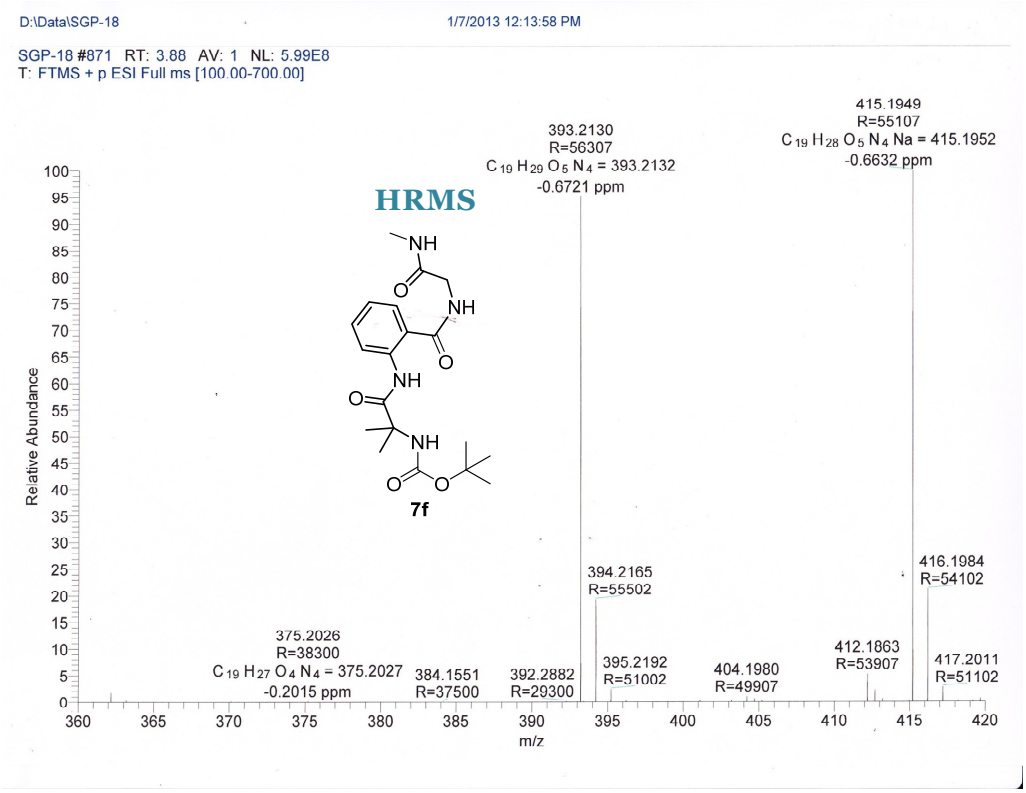
D:\Data\SGP-18
1/7/2013 12:13:58 PM
SGP-18 #871 RT: 3.88 AV: 1 NL: 5.99E8
T: FTMS + p ESI Full ms [100.00-700.00]
HRMS
7f
393.2130
R=56307
C19 H29 O5 N4 = 393.2132
-0.6721 ppm
415.1949
R=55107
C19 H28 O5 N4 Na = 415.1952
-0.6632 ppm
394.2165
R=55502
416.1984
R=54102
375.2026
R=38300
C19 H27 O4 N4 = 375.2027
-0.2015 ppm
384.1551
R=37500
392.2882
R=29300
395.2192
R=51002
404.1980
R=49907
412.1863
R=53907
417.2011
R=51102
Relative Abundance
m/z

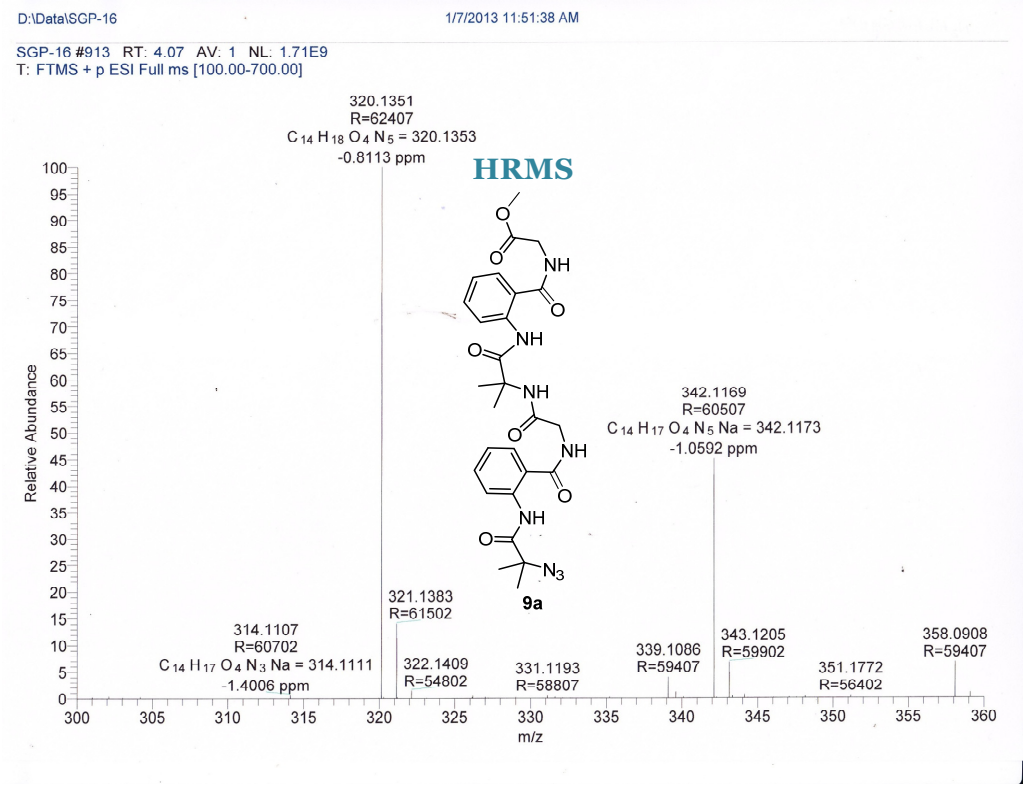
D:\Data\SGP-16
1/7/2013 11:51:38 AM
SGP-16 #913 RT: 4.07 AV: 1 NL: 1.71E9
T: FTMS + p ESI Full ms [100.00-700.00]
HRMS
9a
320.1351
R=62407
C14 H18 O4 N5 = 320.1353
-0.8113 ppm
342.1169
R=60507
C14 H17 O4 N5 Na = 342.1173
-1.0592 ppm
321.1383
R=61502
314.1107
R=60702
C14 H17 O4 N3 Na = 314.1111
-1.4006 ppm
322.1409
R=54802
331.1193
R=58807
339.1086
R=59407
343.1205
R=59902
351.1772
R=56402
358.0908
R=59407
Relative Abundance
m/z

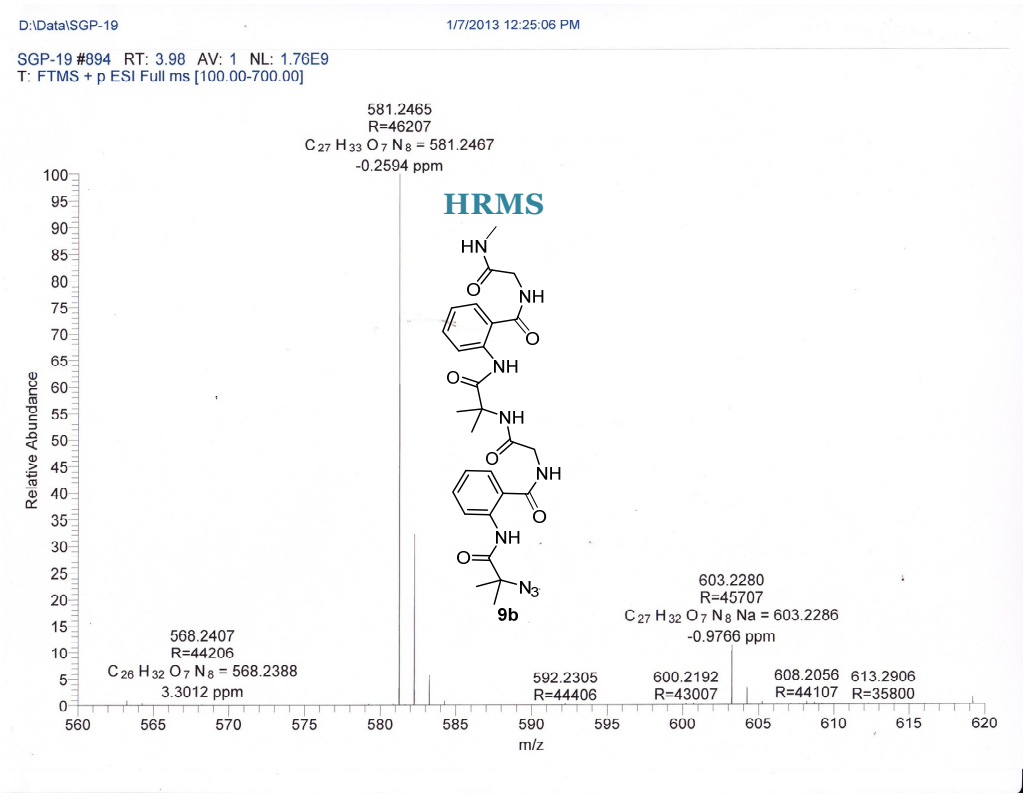
D:\Data\SGP-19
1/7/2013 12:25:06 PM
SGP-19 #894 RT: 3.98 AV: 1 NL: 1.76E9
T: FTMS + p ESI Full ms [100.00-700.00]
581.2465
R=46207
C27 H33 O7 N8 = 581.2467
-0.2594 ppm
HRMS
9b
603.2280
R=45707
C27 H32 O7 N8 Na = 603.2286
-0.9766 ppm
568.2407
R=44206
C26 H32 O7 N8 = 568.2388
3.3012 ppm
592.2305
R=44406
600.2192
R=43007
608.2056
R=44107
613.2906
R=35800
Relative Abundance
m/z

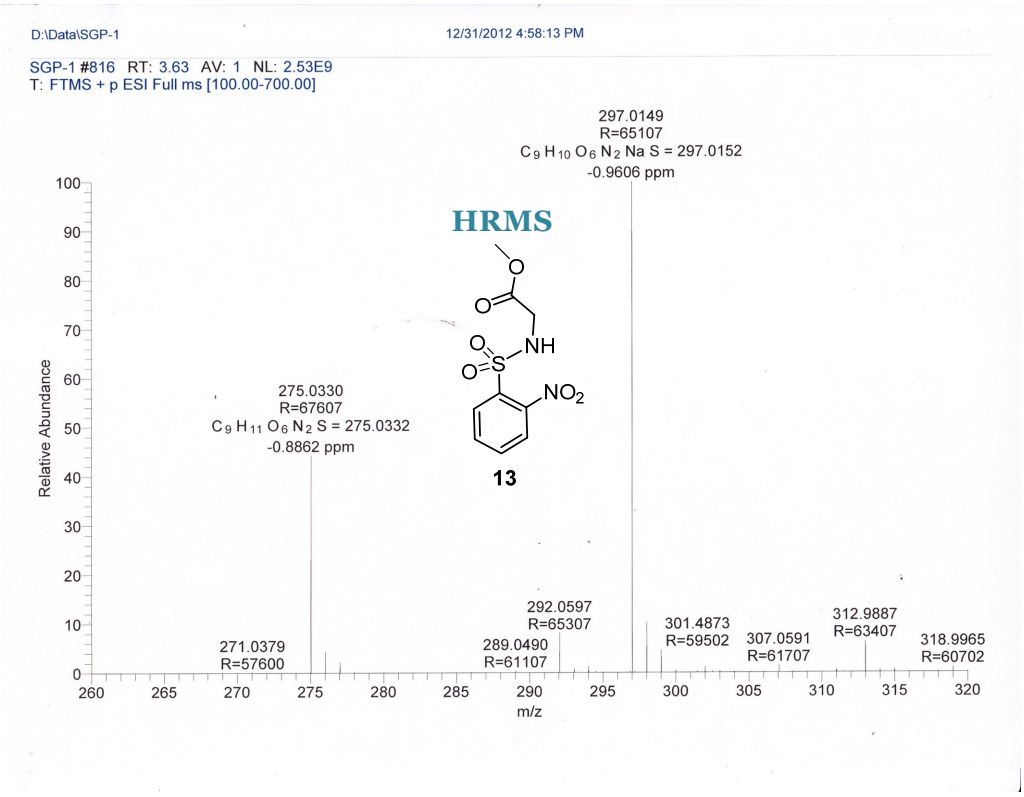
D:\Data\SGP-1
12/31/2012 4:58:13 PM
SGP-1 #816 RT: 3.63 AV: 1 NL: 2.53E9
T: FTMS + p ESI Full ms [100.00-700.00]
297.0149
R=65107
C9 H10 O6 N2 Na S = 297.0152
-0.9606 ppm
HRMS
13
275.0330
R=67607
C9 H11 O6 N2 S = 275.0332
-0.8862 ppm
271.0379
R=57600
289.0490
R=61107
292.0597
R=65307
301.4873
R=59502
307.0591
R=61707
312.9887
R=63407
318.9965
R=60702
Relative Abundance
m/z

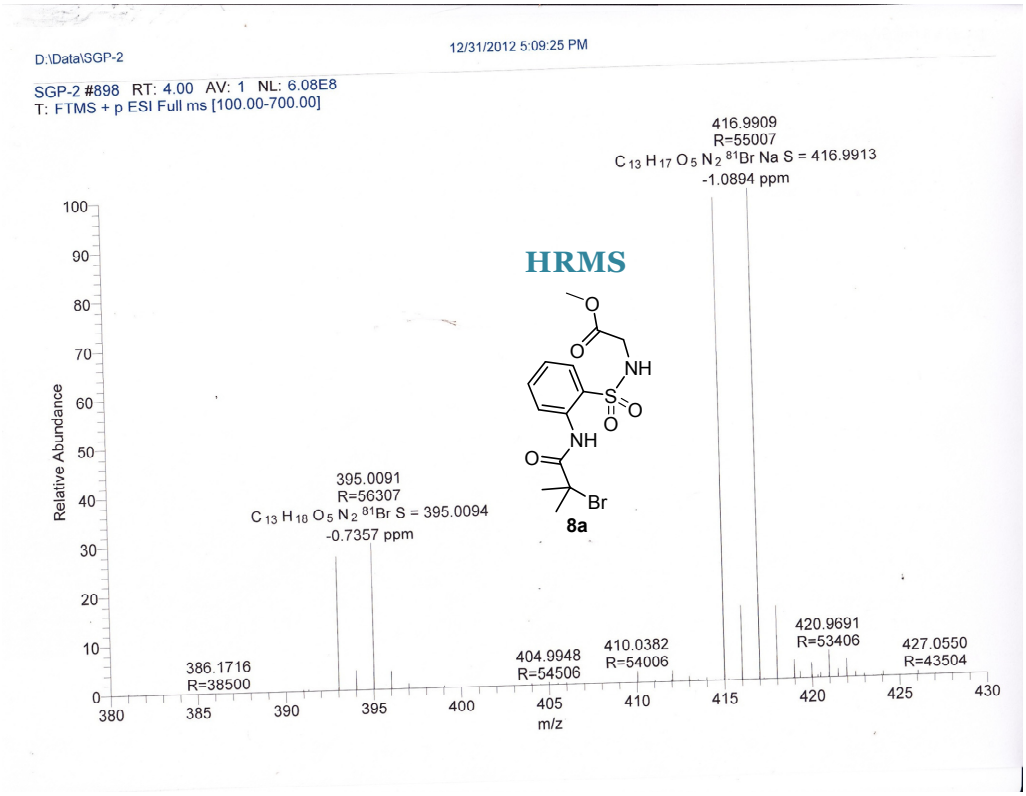
D:\Data\SGP-2
12/31/2012 5:09:25 PM
SGP-2 #898 RT: 4.00 AV: 1 NL: 6.08E8
T: FTMS + p ESI Full ms [100.00-700.00]
416.9909
R=55007
C 13 H 17 O 5 N 2 81Br Na S = 416.9913
-1.0894 ppm
HRMS
8a
395.0091
R=56307
C 13 H 10 O 5 N 2 81Br S = 395.0094
-0.7357 ppm
386.1716
R=38500
404.9948
R=54506
410.0382
R=54006
420.9691
R=53406
427.0550
R=43504
Relative Abundance
m/z

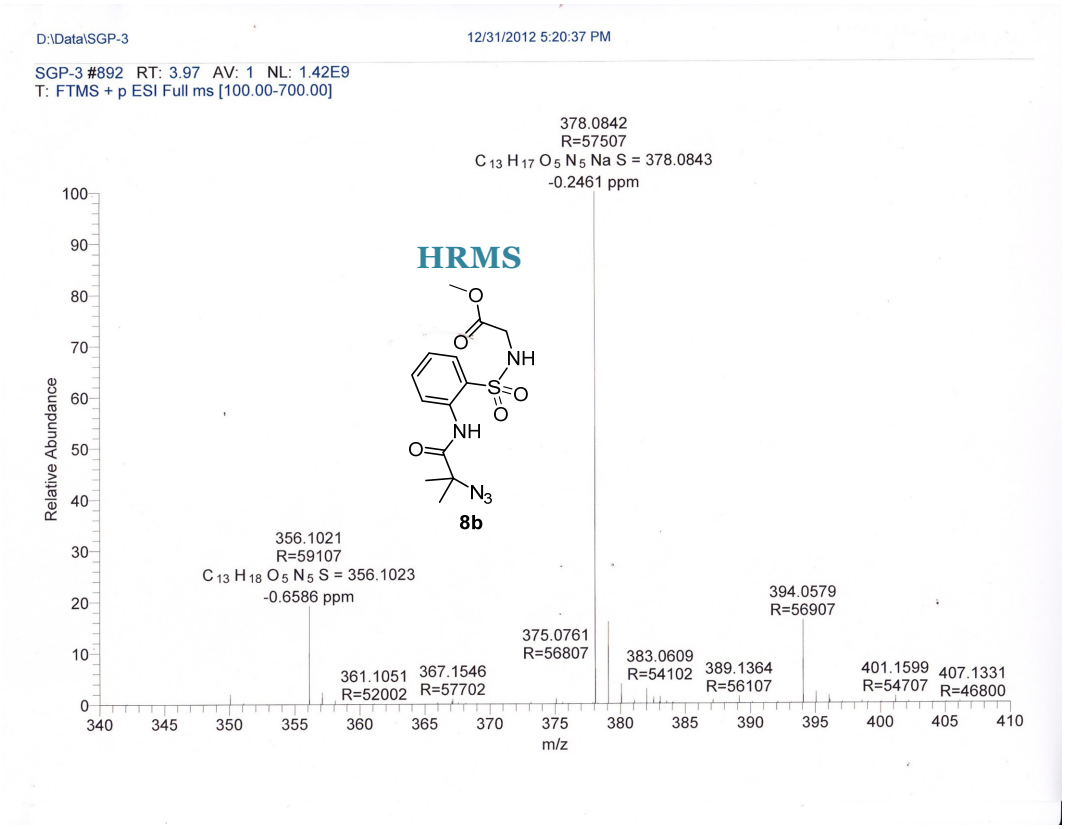
D:\Data\SGP-3
12/31/2012 5:20:37 PM
SGP-3 #892 RT: 3.97 AV: 1 NL: 1.42E9
T: FTMS + p ESI Full ms [100.00-700.00]
378.0842
R=57507
C 13 H 17 O 5 N 5 Na S = 378.0843
-0.2461 ppm
HRMS
8b
356.1021
R=59107
C 13 H 18 O 5 N 5 S = 356.1023
-0.6586 ppm
361.1051
R=52002
367.1546
R=57702
375.0761
R=56807
383.0609
R=54102
389.1364
R=56107
394.0579
R=56907
401.1599
R=54707
407.1331
R=46800
Relative Abundance
m/z

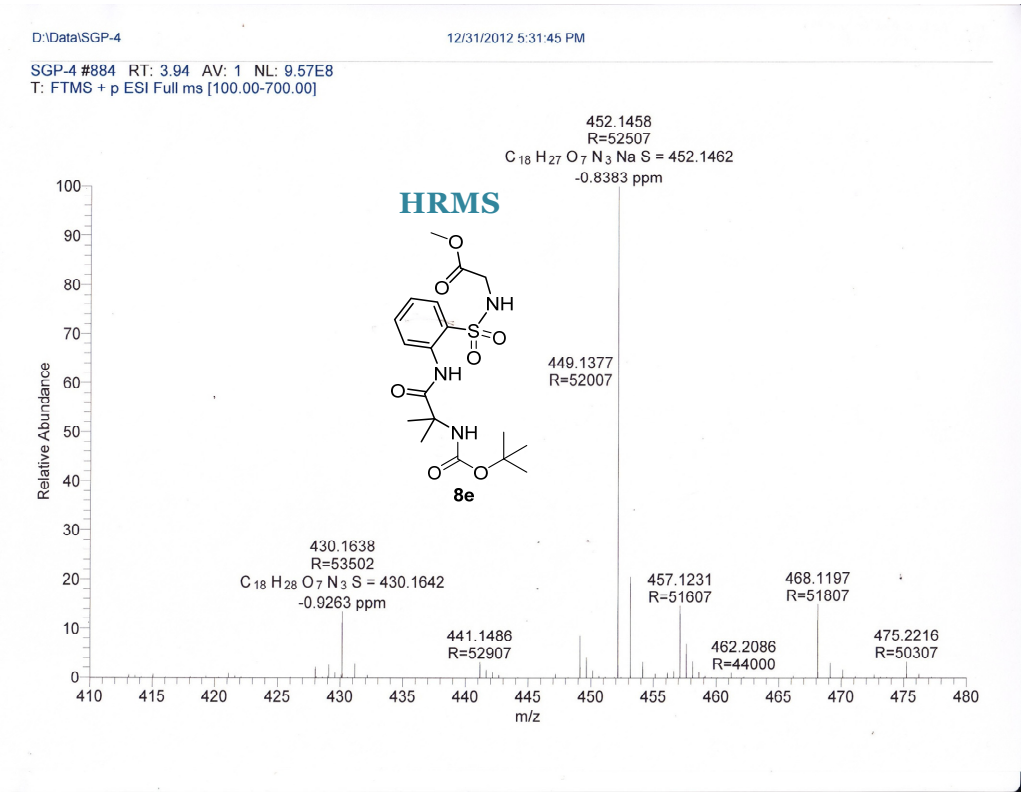
D:\Data\SGP-4
12/31/2012 5:31:45 PM
SGP-4 #884 RT: 3.94 AV: 1 NL: 9.57E8
T: FTMS + p ESI Full ms [100.00-700.00]
452.1458
R=52507
C 18 H 27 O 7 N 3 Na S = 452.1462
-0.8383 ppm
HRMS
449.1377
R=52007
430.1638
R=53502
C 18 H 28 O 7 N 3 S = 430.1642
-0.9263 ppm
457.1231
R=51607
468.1197
R=51807
441.1486
R=52907
462.2086
R=44000
475.2216
R=50307
8e
Relative Abundance
m/z

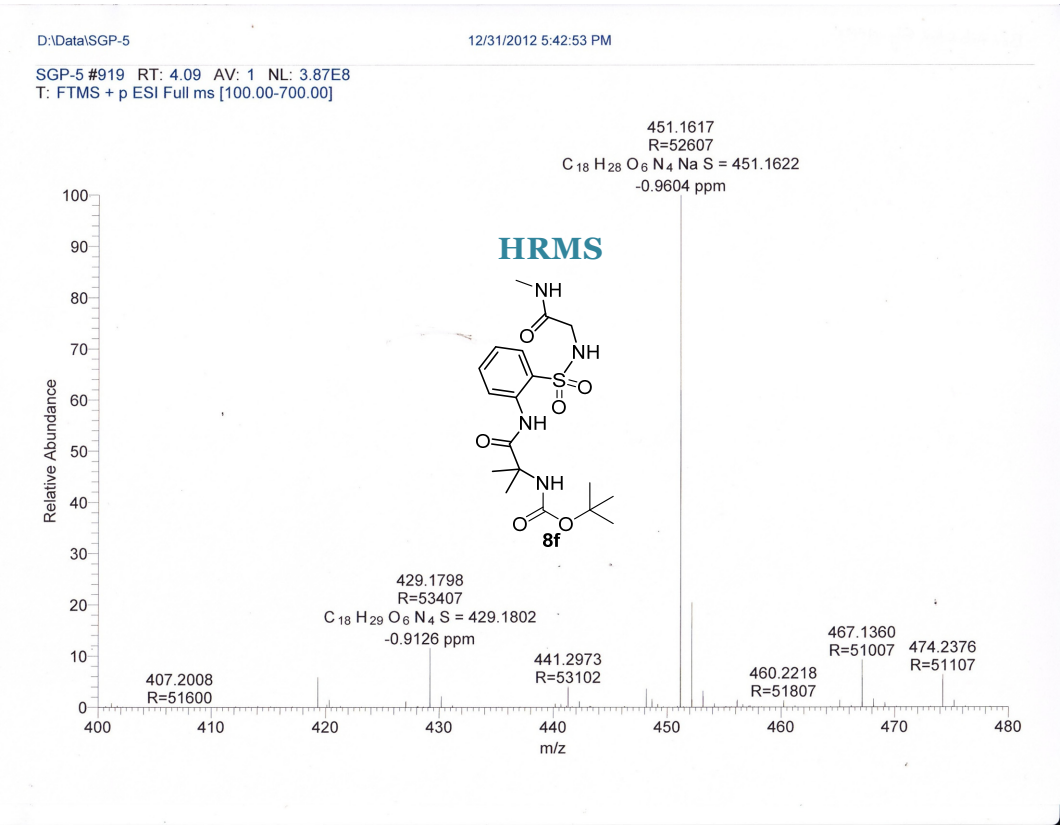
D:\Data\SGP-5
12/31/2012 5:42:53 PM
SGP-5 #919 RT: 4.09 AV: 1 NL: 3.87E8
T: FTMS + p ESI Full ms [100.00-700.00]
451.1617
R=52607
C 18 H 28 O 6 N 4 Na S = 451.1622
-0.9604 ppm
HRMS
429.1798
R=53407
C 18 H 29 O 6 N 4 S = 429.1802
-0.9126 ppm
441.2973
R=53102
467.1360
R=51007
474.2376
R=51107
407.2008
R=51600
460.2218
R=51807
8f
Relative Abundance
m/z

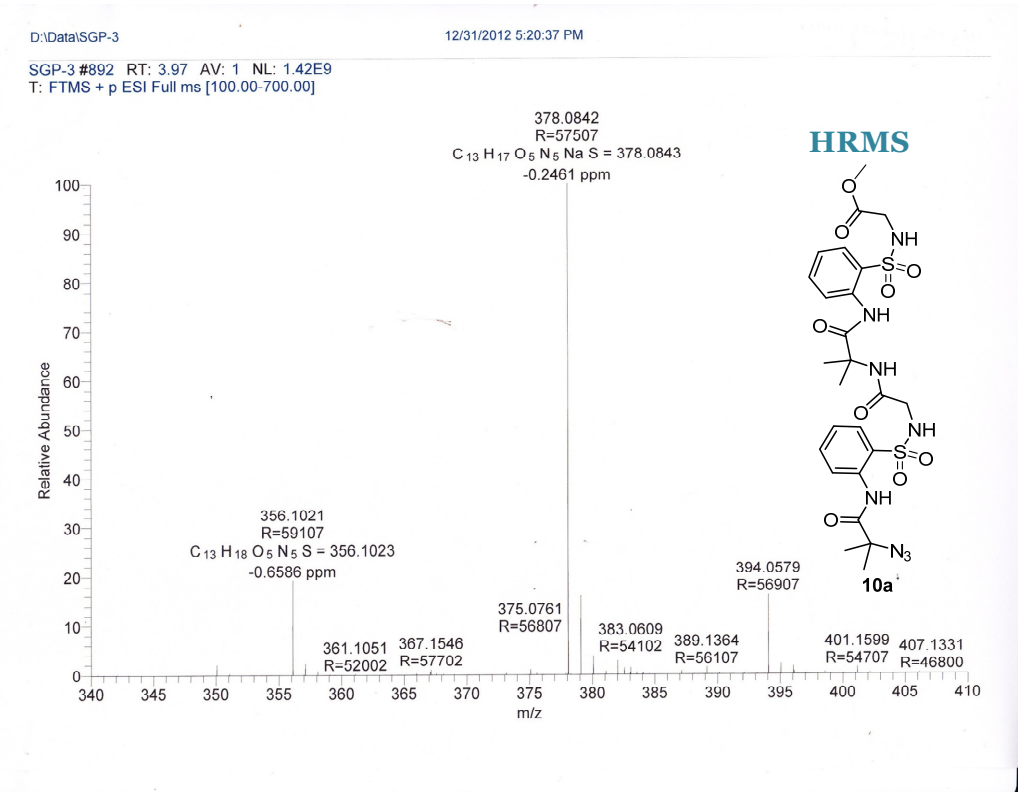
D:\Data\SGP-3
12/31/2012 5:20:37 PM
SGP-3 #892 RT: 3.97 AV: 1 NL: 1.42E9
T: FTMS + p ESI Full ms [100.00-700.00]
378.0842
R=57507
C13 H17 O5 N5 Na S = 378.0843
-0.2461 ppm
HRMS
356.1021
R=59107
C13 H18 O5 N5 S = 356.1023
-0.6586 ppm
361.1051
R=52002
367.1546
R=57702
375.0761
R=56807
383.0609
R=54102
389.1364
R=56107
394.0579
R=56907
401.1599
R=54707
407.1331
R=46800
10a
Relative Abundance
m/z

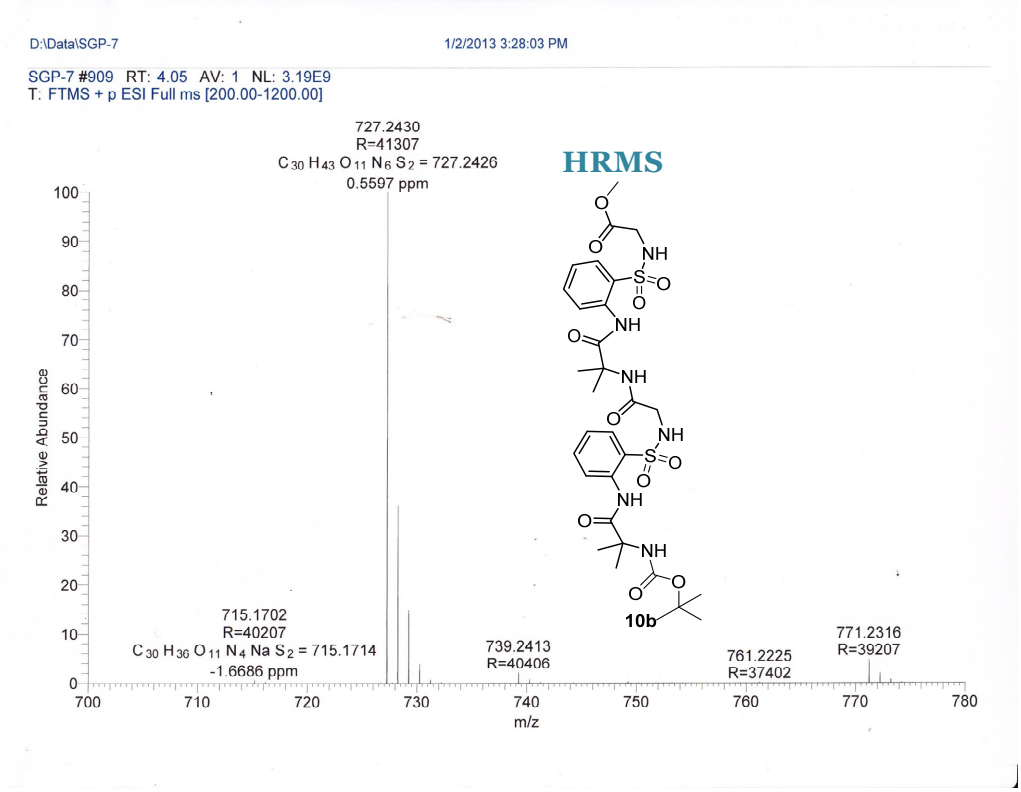
D:\Data\SGP-7
1/2/2013 3:28:03 PM
SGP-7 #909 RT: 4.05 AV: 1 NL: 3.19E9
T: FTMS + p ESI Full ms [200.00-1200.00]
727.2430
R=41307
C30 H43 O11 N6 S2 = 727.2426
0.5597 ppm
HRMS
715.1702
R=40207
C30 H36 O11 N4 Na S2 = 715.1714
-1.6686 ppm
739.2413
R=40406
761.2225
R=37402
771.2316
R=39207
10b
Relative Abundance
m/z

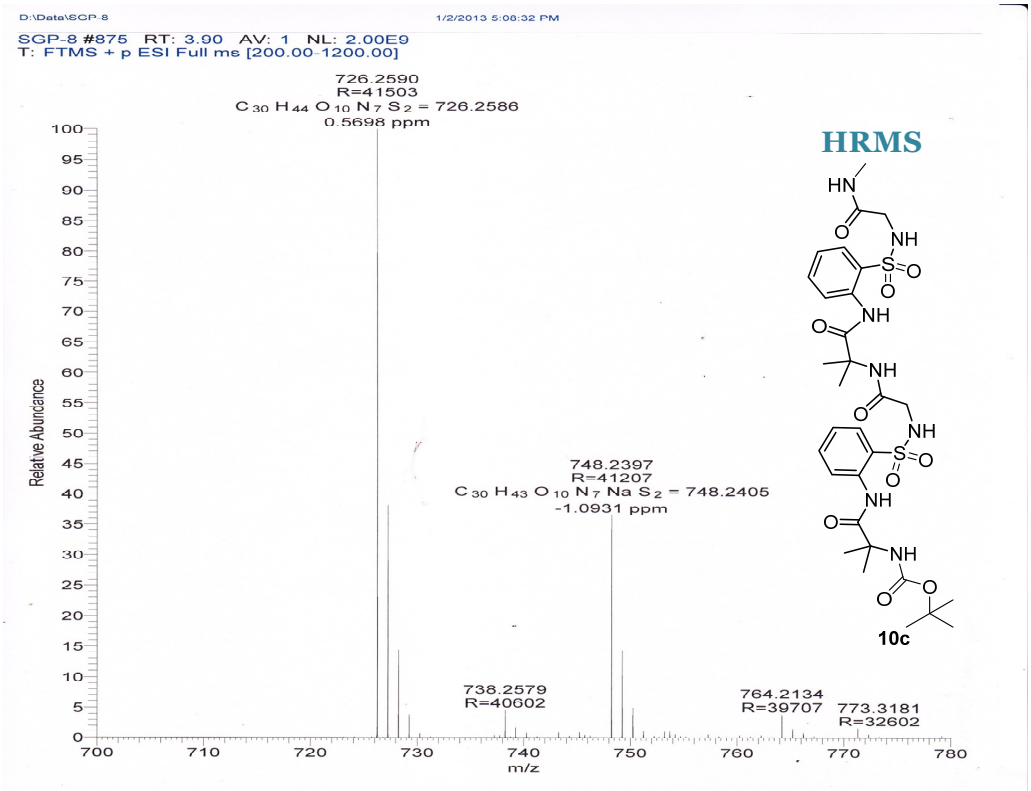
D:\Data\SGP-8
1/2/2013 5:08:32 PM
SGP-8 #875 RT: 3.90 AV: 1 NL: 2.00E9
T: FTMS + p ESI Full ms [200.00-1200.00]
726.2590
R=41503
C30 H44 O10 N7 S2 = 726.2586
0.5698 ppm
748.2397
R=41207
C30 H43 O10 N7 Na S2 = 748.2405
-1.0931 ppm
738.2579
R=40602
764.2134
R=39707
773.3181
R=32602
Relative Abundance
m/z
HRMS
10c

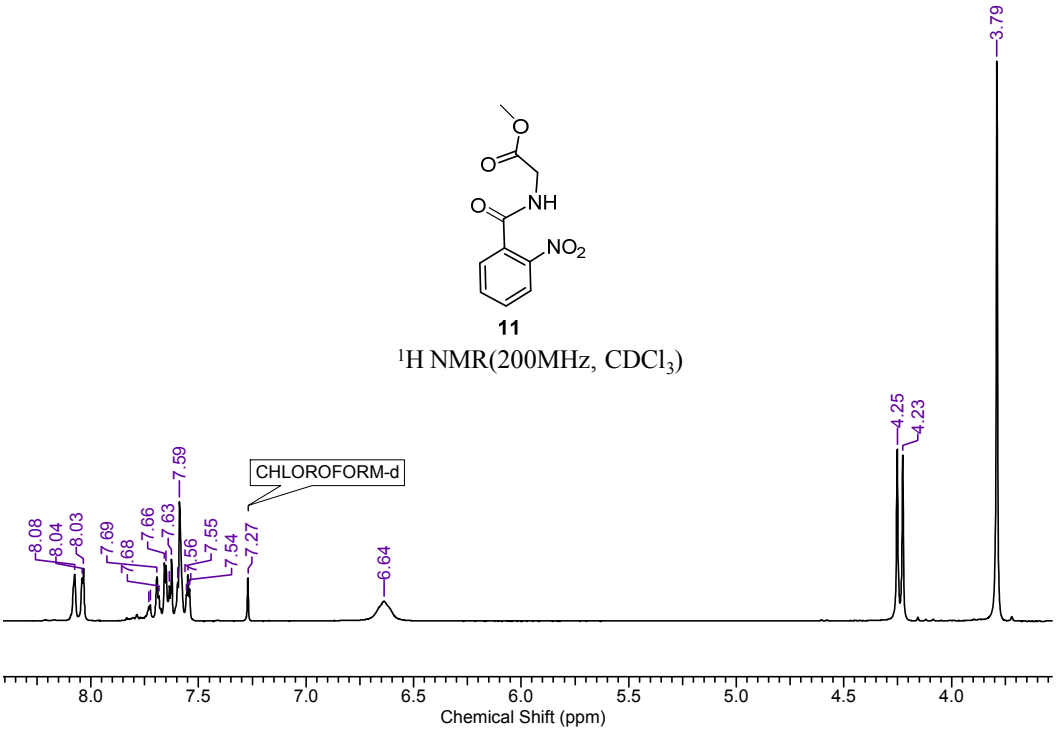
11
1H NMR(200MHz, CDCl3)
CHLOROFORM-d
8.08
8.04
8.03
7.69
7.68
7.66
7.63
7.59
7.56
7.55
7.54
7.27
6.64
4.25
4.23
3.79
Chemical Shift (ppm)

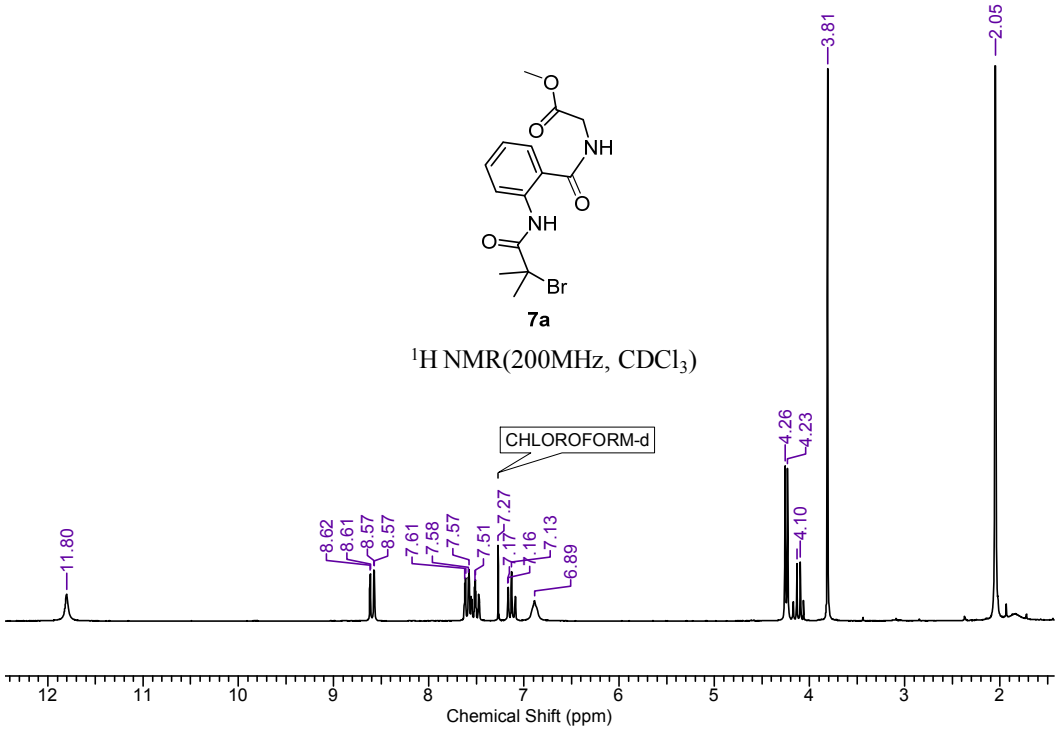

7a

^{1}H NMR(200MHz, $CDCl_3$)

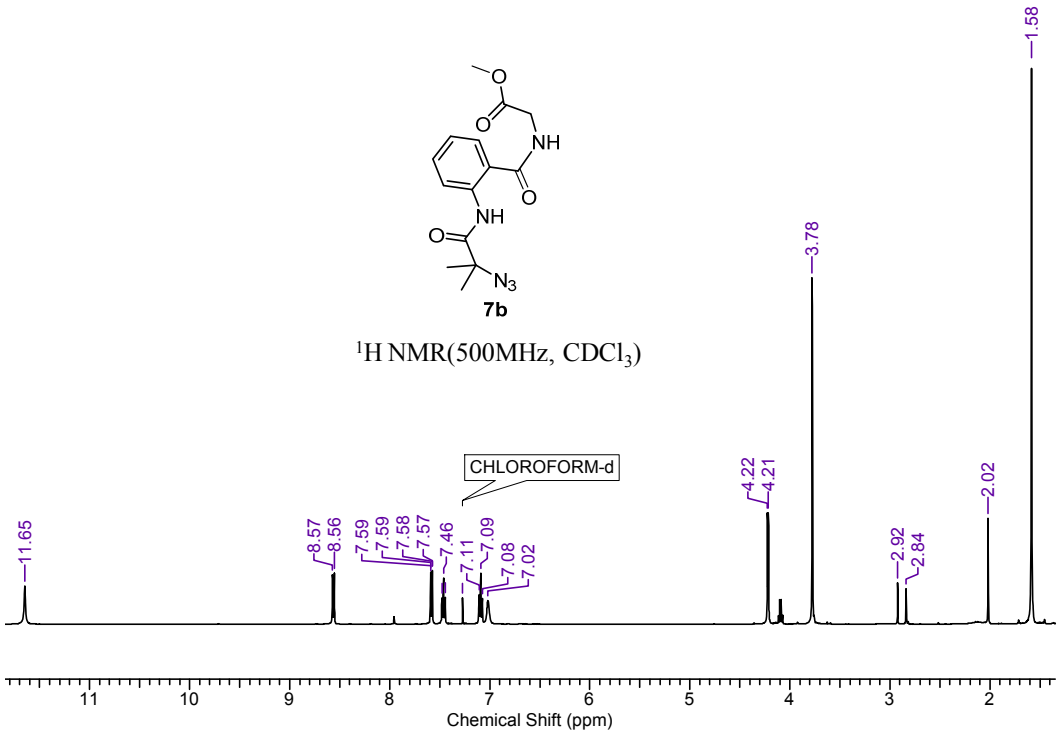

7b

^{1}H NMR(500MHz, $CDCl_3$)

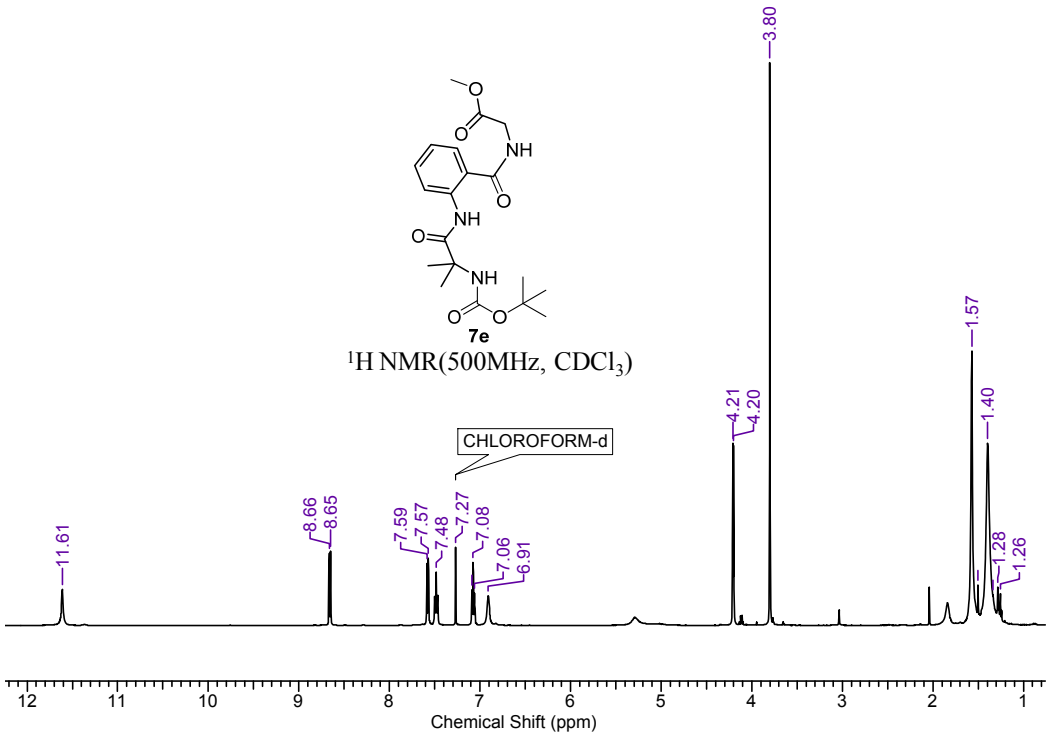

7e

^{1}H NMR(500MHz, $CDCl_3$)

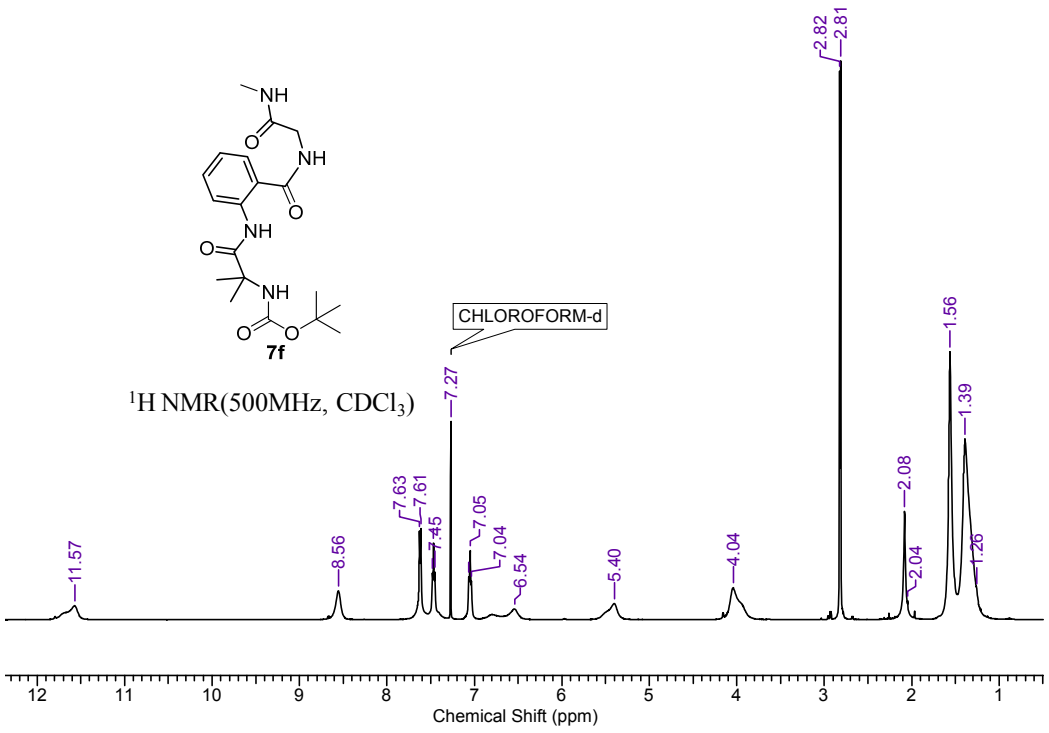

7f

^{1}H NMR(500MHz, $CDCl_3$)

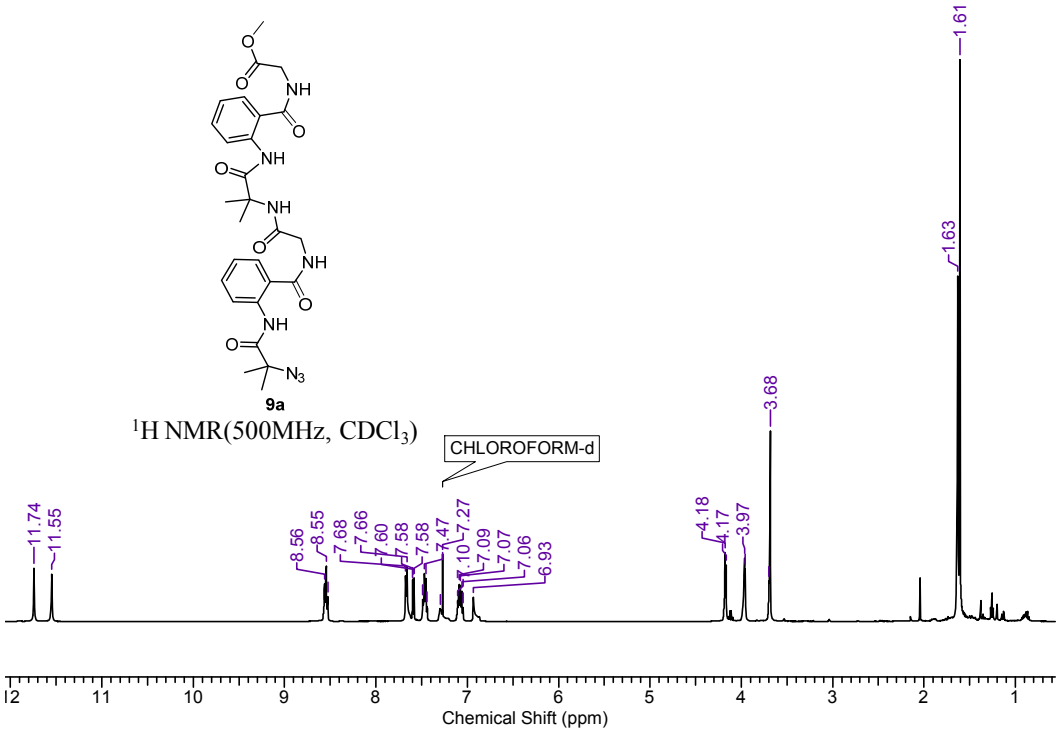
9a
^{1}H NMR(500MHz, $CDCl_3$)
CHLOROFORM-d
11.74
11.55
8.56
8.55
7.68
7.66
7.60
7.58
7.58
7.47
7.27
7.10
7.09
7.07
7.06
6.93
4.18
4.17
3.97
3.68
1.63
1.61
Chemical Shift (ppm)

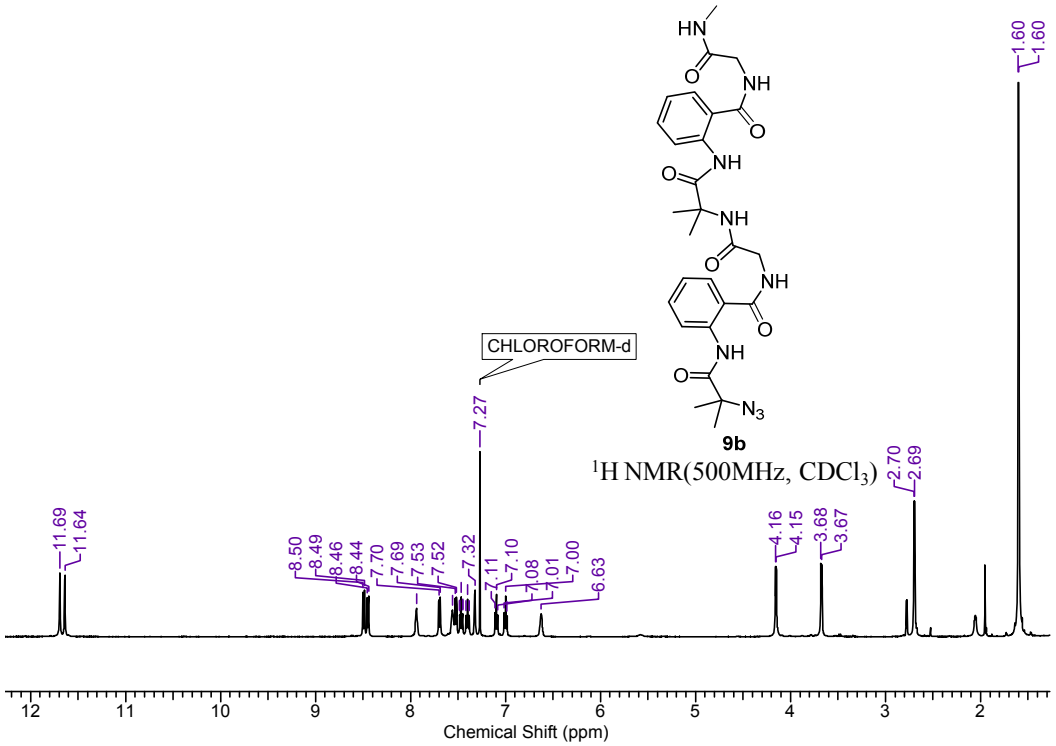
9b
^{1}H NMR(500MHz, $CDCl_3$)
CHLOROFORM-d
11.69
11.64
8.50
8.49
8.46
8.44
7.70
7.69
7.53
7.52
7.32
7.27
7.11
7.10
7.08
7.01
7.00
6.63
4.16
4.15
3.68
3.67
2.70
2.69
1.60
1.60
Chemical Shift (ppm)

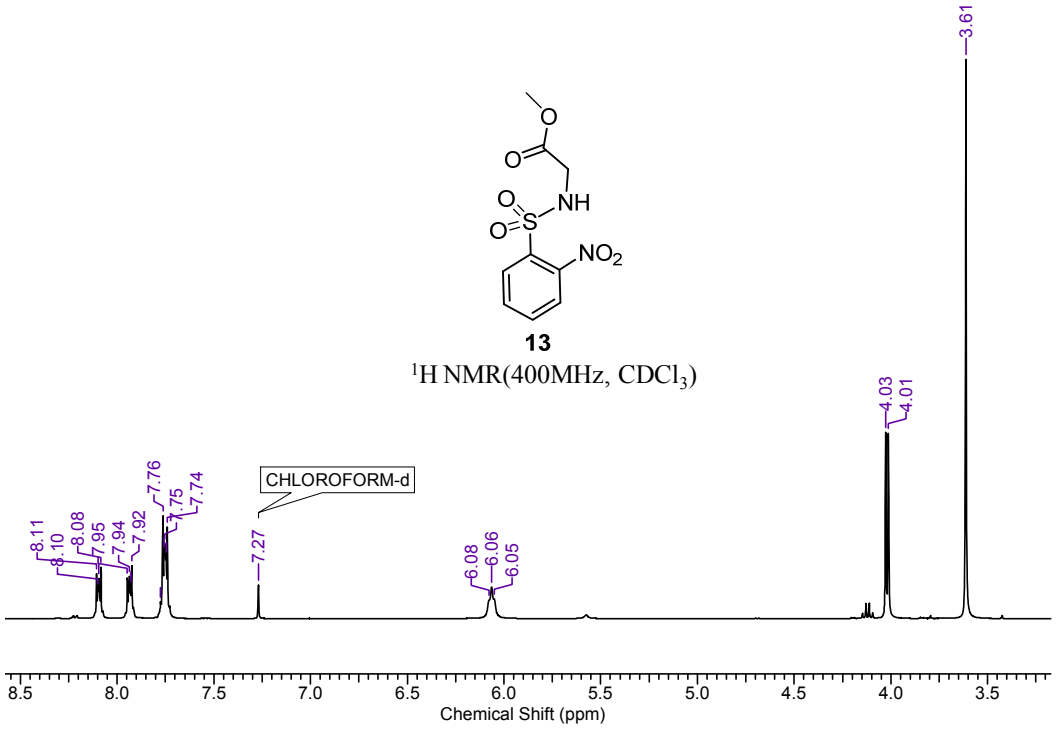
3.61
O
O
NH
O
S
O
NO2
13
1H NMR(400MHz, CDCl3)
4.03
4.01
CHLOROFORM-d
8.11
8.10
8.08
7.95
7.94
7.92
7.76
7.75
7.74
7.27
6.08
6.06
6.05
8.5
8.0
7.5
7.0
6.5
6.0
5.5
5.0
4.5
4.0
3.5
Chemical Shift (ppm)

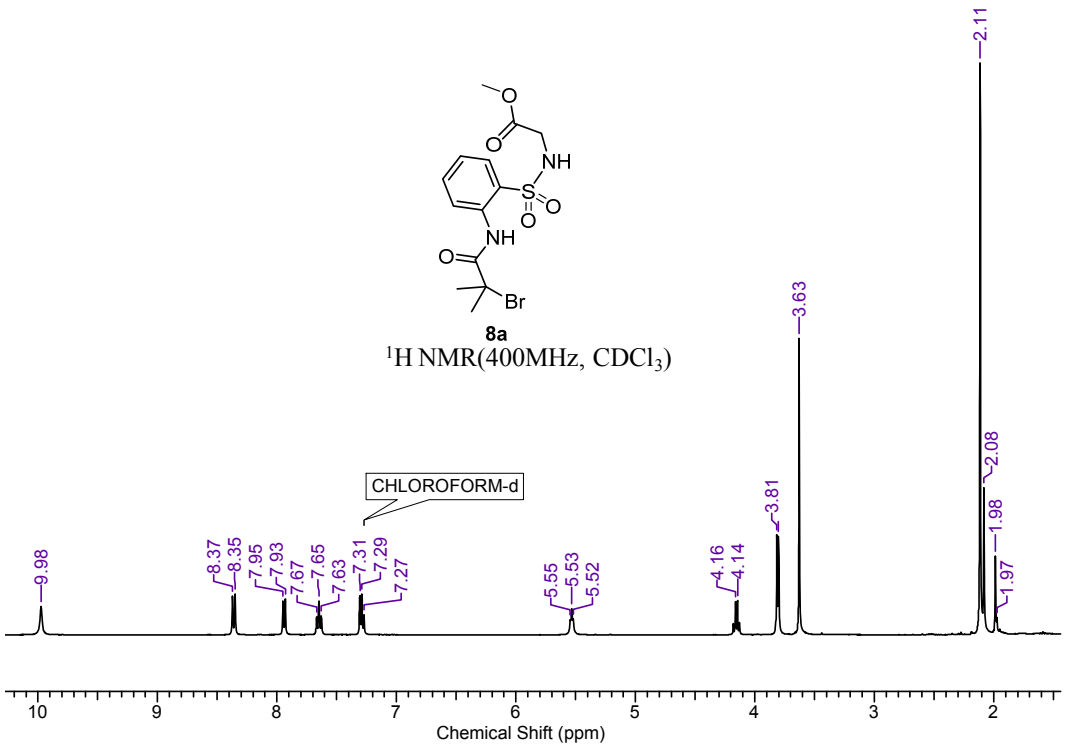
2.11
O
O
NH
S
O
O
NH
O
Br
8a
1H NMR(400MHz, CDCl3)
3.63
2.08
3.81
1.98
1.97
CHLOROFORM-d
9.98
8.37
8.35
7.95
7.93
7.67
7.65
7.63
7.31
7.29
7.27
5.55
5.53
5.52
4.16
4.14
10
9
8
7
6
5
4
3
2
Chemical Shift (ppm)

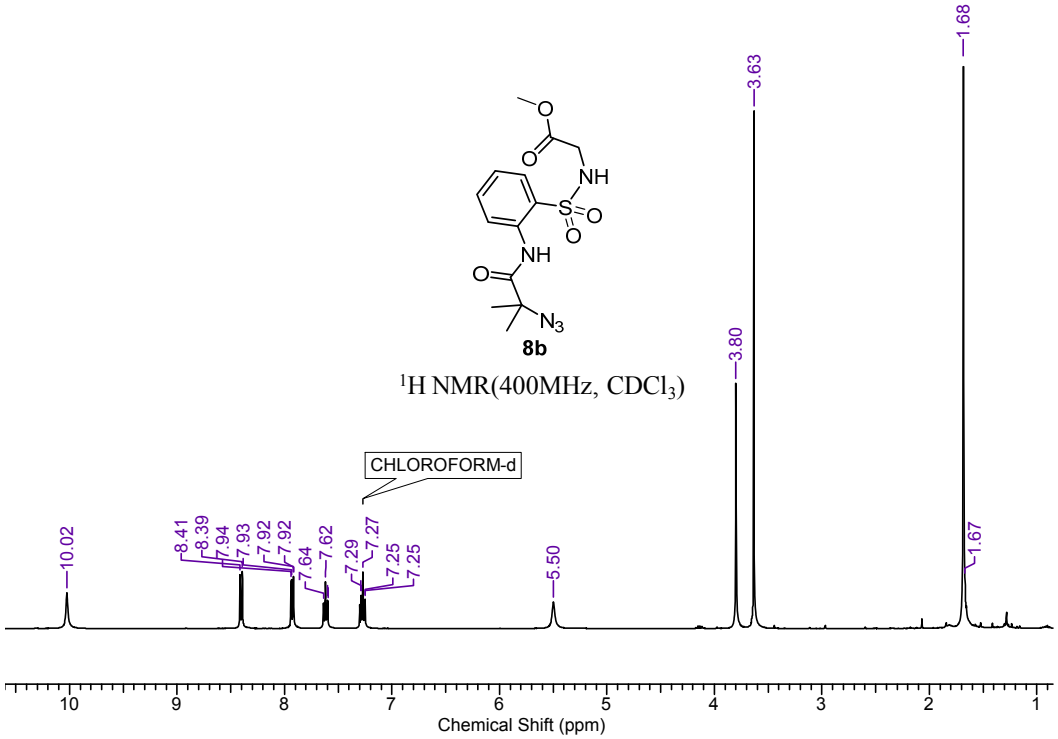
8b
^{1}H NMR(400MHz, $CDCl_3$)
CHLOROFORM-d
10.02
8.41
8.39
7.94
7.93
7.92
7.92
7.64
7.62
7.29
7.27
7.25
7.25
5.50
3.80
3.63
1.68
1.67
Chemical Shift (ppm)

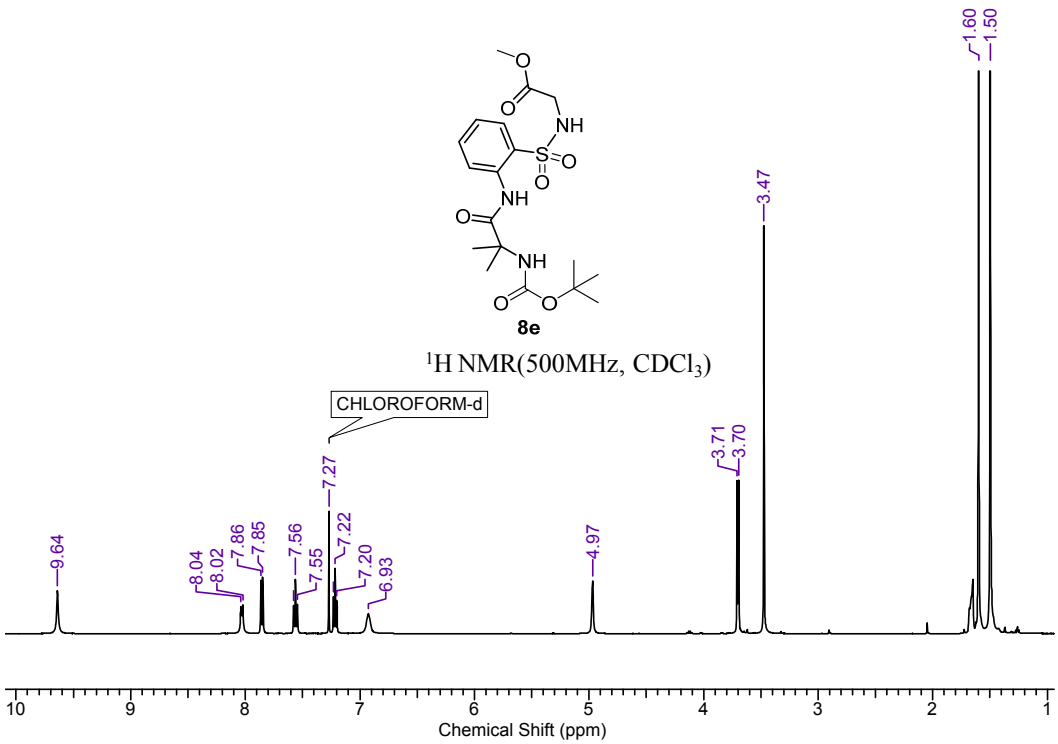
8e
^{1}H NMR(500MHz, $CDCl_3$)
CHLOROFORM-d
9.64
8.04
8.02
7.86
7.85
7.56
7.55
7.27
7.22
7.20
6.93
4.97
3.71
3.70
3.47
1.60
1.50
Chemical Shift (ppm)

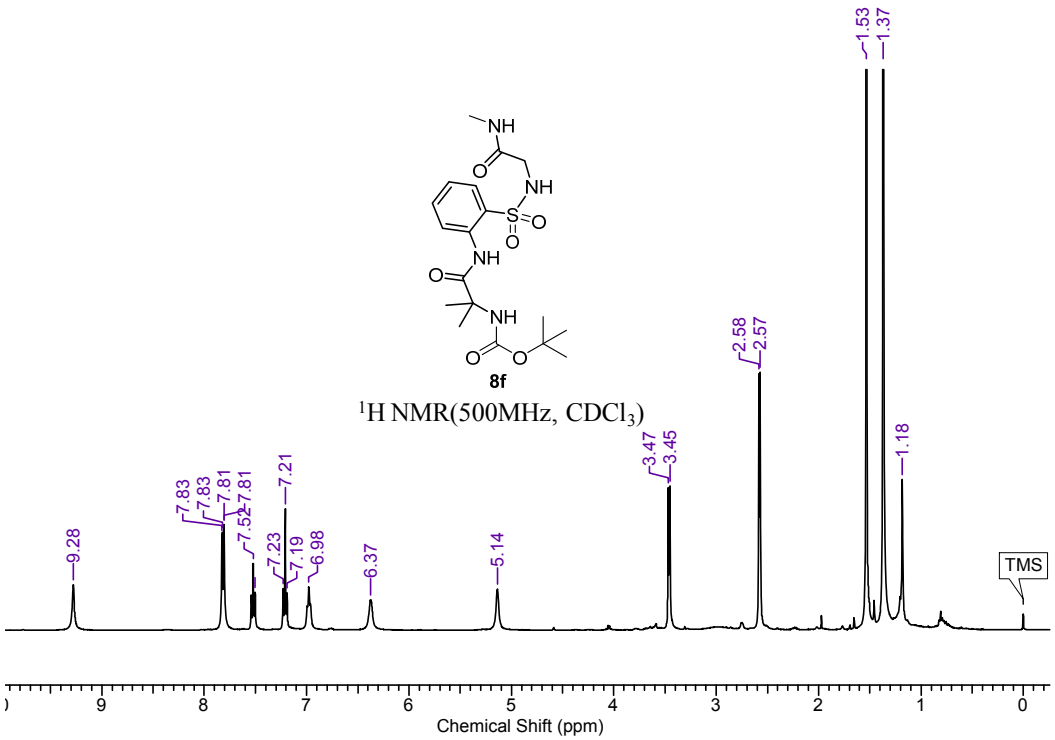
8f
^{1}H NMR(500MHz, CDCl$_3$)
9.28
7.83
7.83
7.81
7.81
7.52
7.23
7.21
7.19
6.98
6.37
5.14
3.47
3.45
2.58
2.57
1.53
1.37
1.18
TMS
Chemical Shift (ppm)

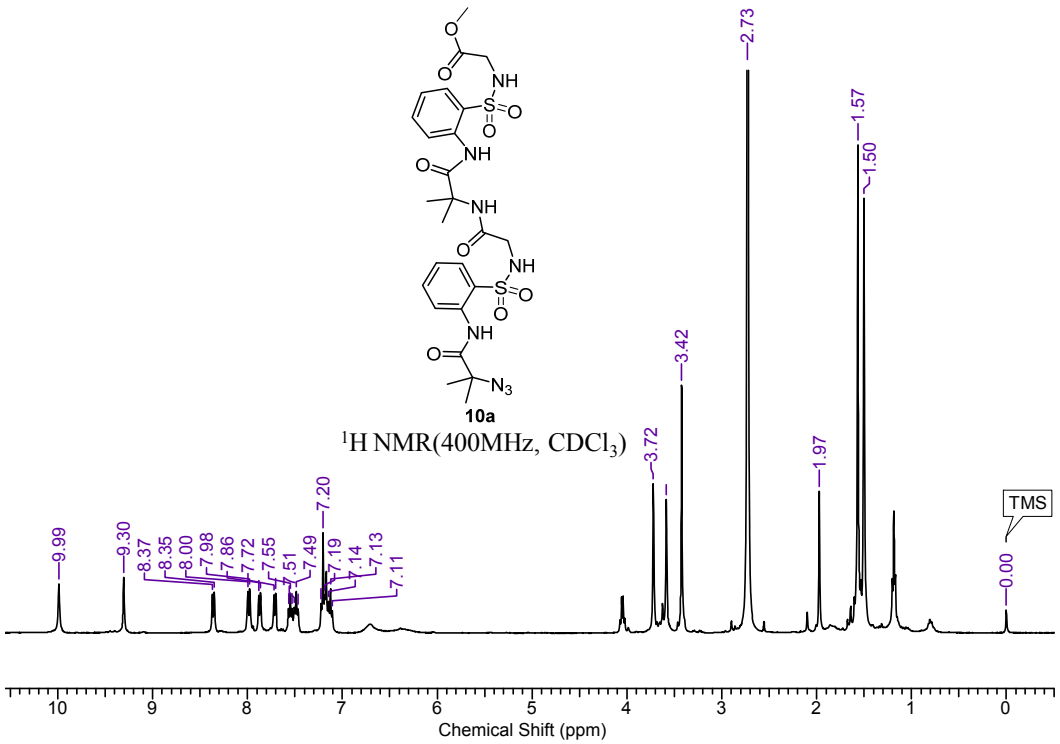
10a
^{1}H NMR(400MHz, CDCl$_3$)
9.99
9.30
8.37
8.35
8.00
7.98
7.86
7.72
7.55
7.51
7.49
7.20
7.19
7.14
7.13
7.11
3.72
3.42
2.73
1.97
1.57
1.50
0.00
TMS
Chemical Shift (ppm)

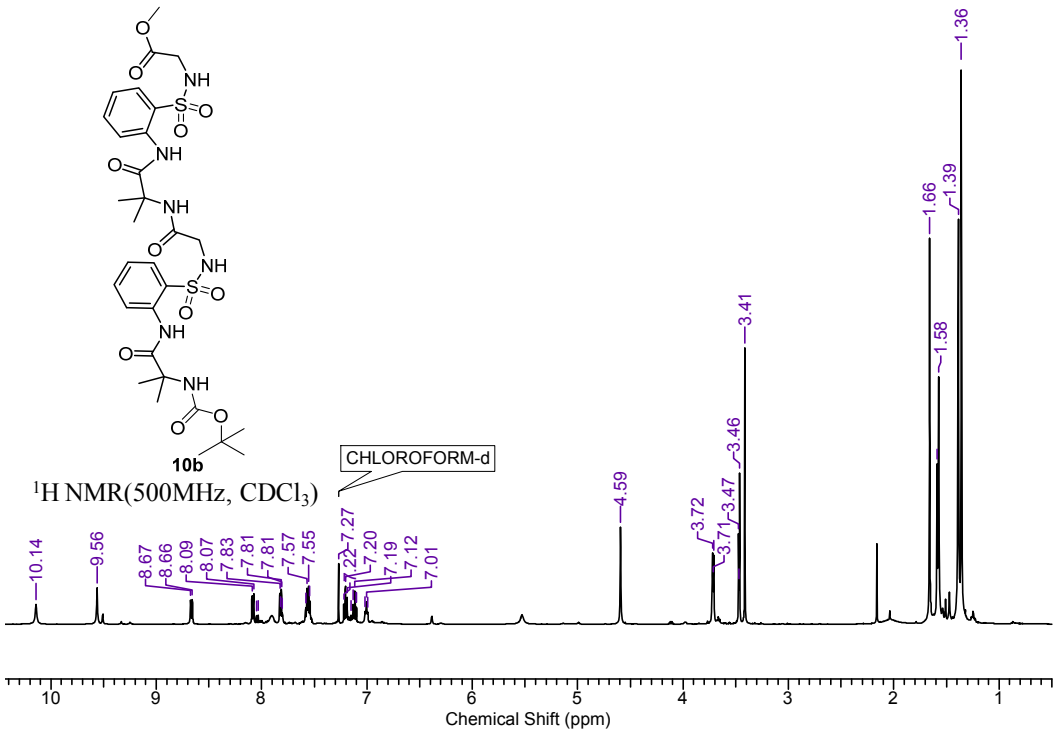
10b
^{1}H NMR(500MHz, $CDCl_3$)
CHLOROFORM-d
10.14
9.56
8.67
8.66
8.09
8.07
7.83
7.81
7.81
7.57
7.55
7.27
7.20
7.19
7.12
7.01
4.59
3.72
3.71
3.47
3.46
3.41
1.66
1.58
1.39
1.36
Chemical Shift (ppm)

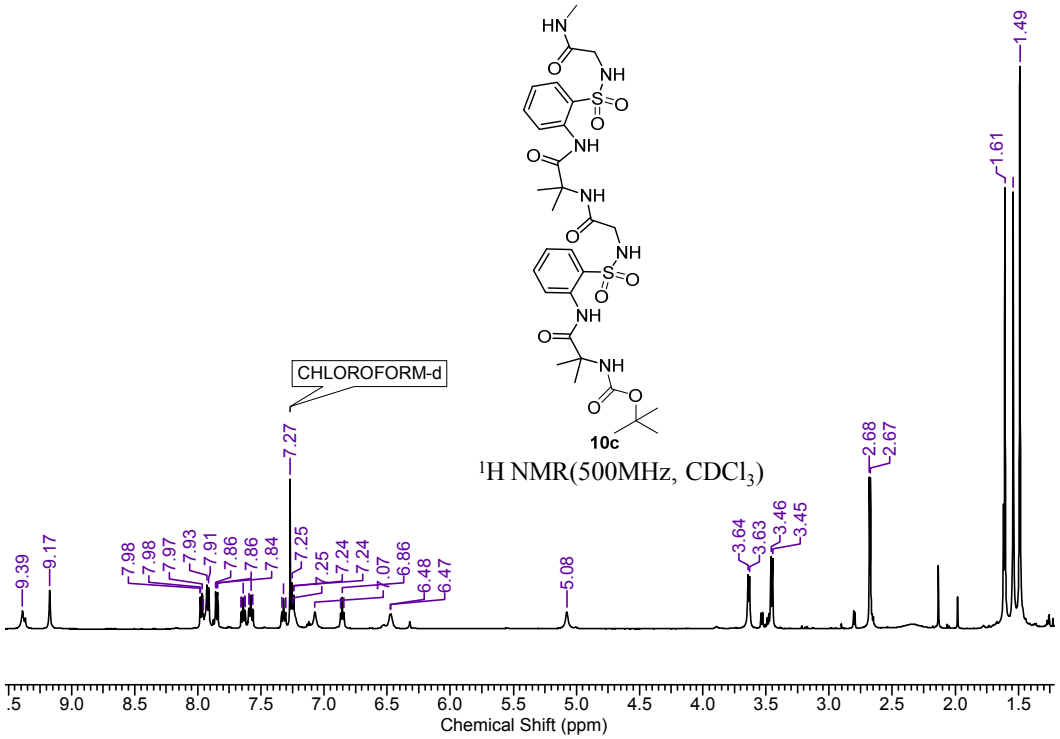
10c
^{1}H NMR(500MHz, $CDCl_3$)
CHLOROFORM-d
9.39
9.17
7.98
7.98
7.97
7.93
7.91
7.86
7.86
7.84
7.27
7.25
7.25
7.24
7.24
7.07
6.86
6.48
6.47
5.08
3.64
3.63
3.46
3.45
2.68
2.67
1.61
1.49
Chemical Shift (ppm)

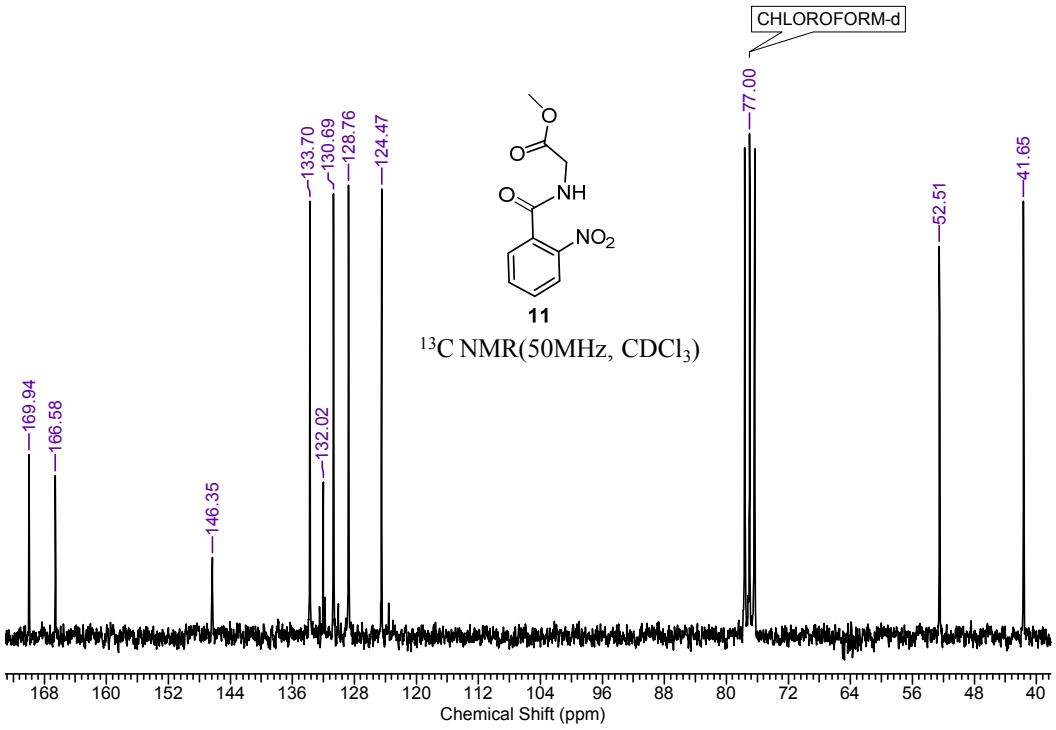
CHLOROFORM-d
77.00
133.70
130.69
128.76
124.47
52.51
41.65
169.94
166.58
146.35
132.02
O
O
NH
O
NO2
11
13C NMR(50MHz, CDCl3)
168 160 152 144 136 128 120 112 104 96 88 80 72 64 56 48 40
Chemical Shift (ppm)

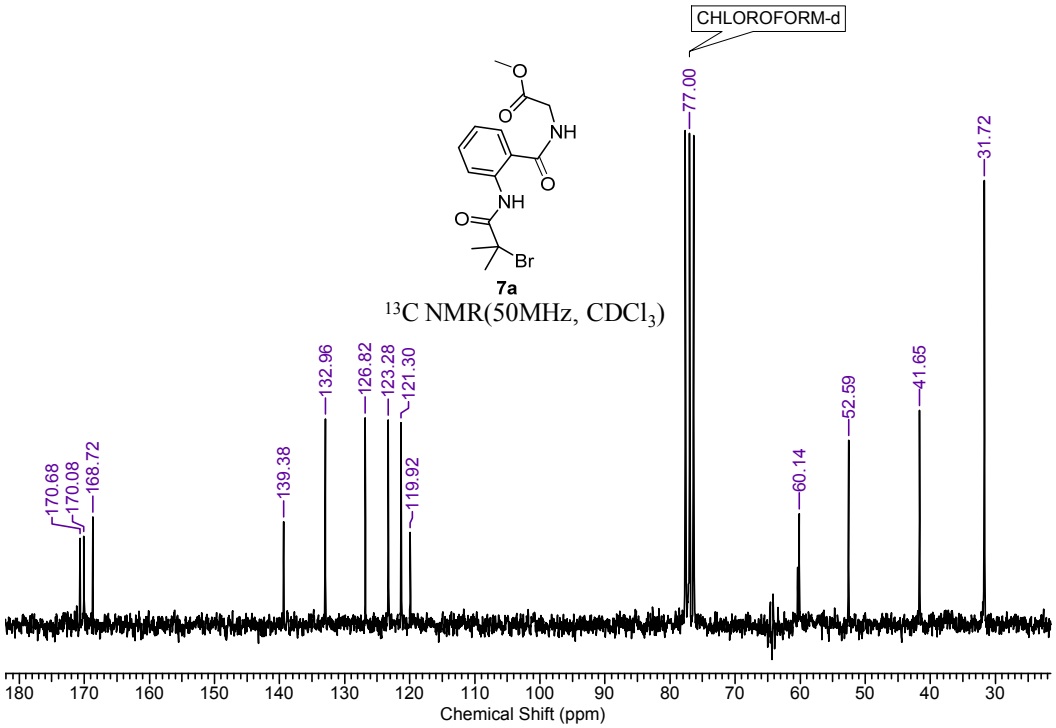
CHLOROFORM-d
77.00
31.72
O
O
NH
O
NH
O
Br
7a
13C NMR(50MHz, CDCl3)
132.96
126.82
123.28
121.30
41.65
52.59
170.68
170.08
168.72
139.38
119.92
60.14
180 170 160 150 140 130 120 110 100 90 80 70 60 50 40 30
Chemical Shift (ppm)

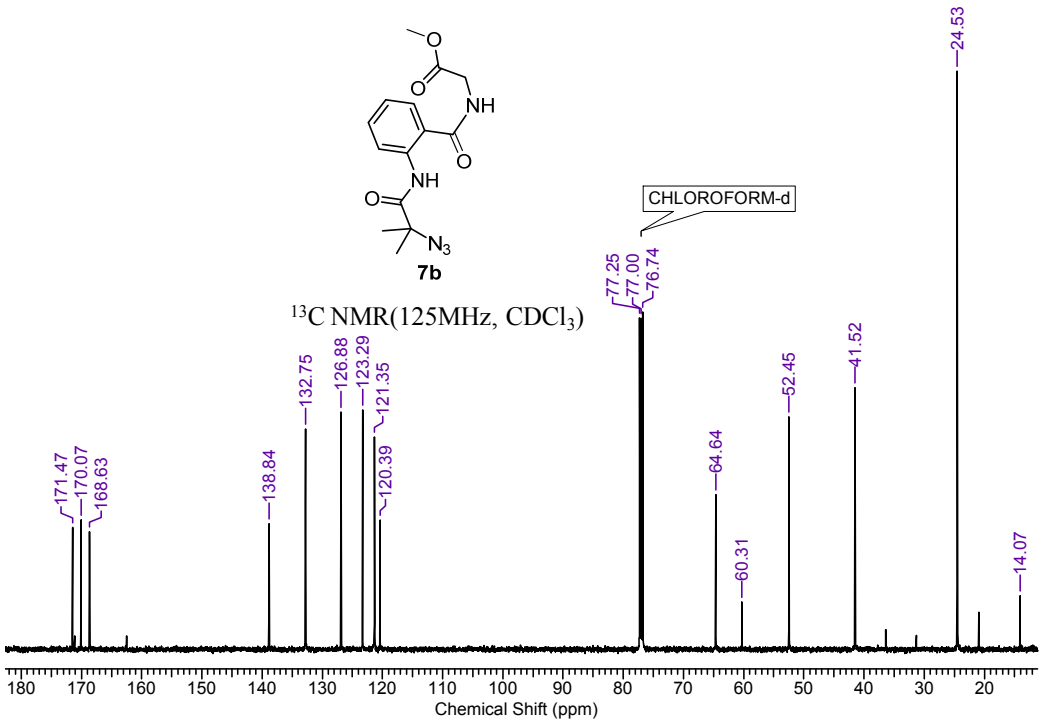
7b
^{13}C NMR(125MHz, CDCl$_3$)
CHLOROFORM-d
77.25
77.00
76.74
171.47
170.07
168.63
138.84
132.75
126.88
123.29
121.35
120.39
64.64
60.31
52.45
41.52
24.53
14.07
Chemical Shift (ppm)

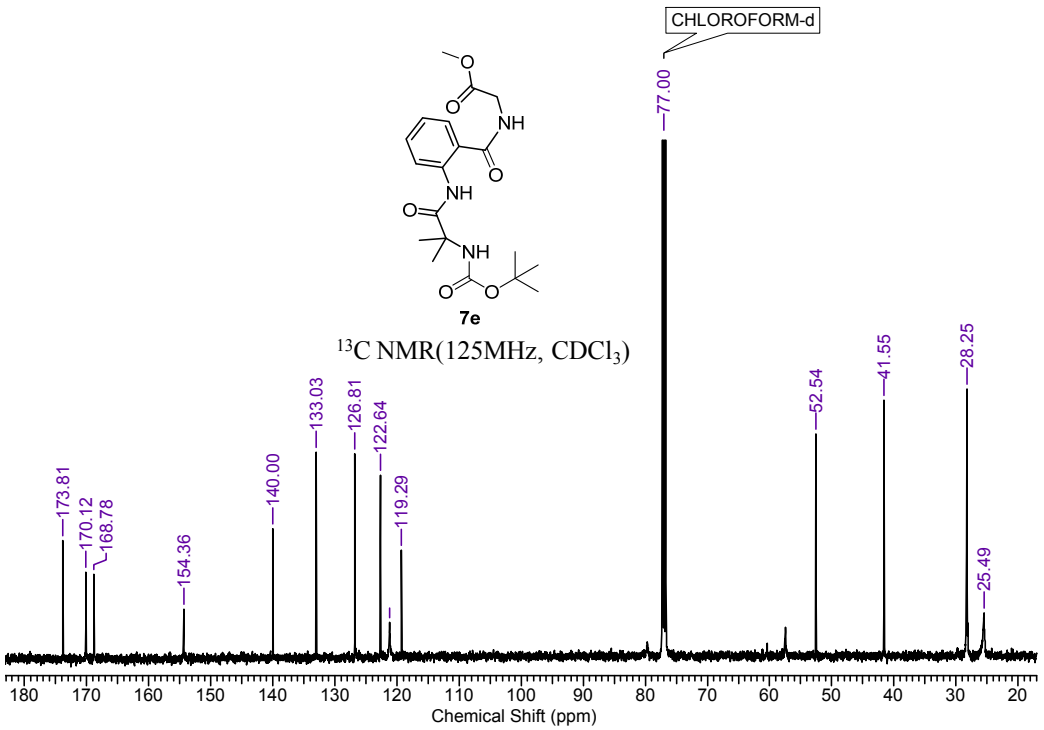
7e
^{13}C NMR(125MHz, CDCl$_3$)
CHLOROFORM-d
77.00
173.81
170.12
168.78
154.36
140.00
133.03
126.81
122.64
119.29
52.54
41.55
28.25
25.49
Chemical Shift (ppm)

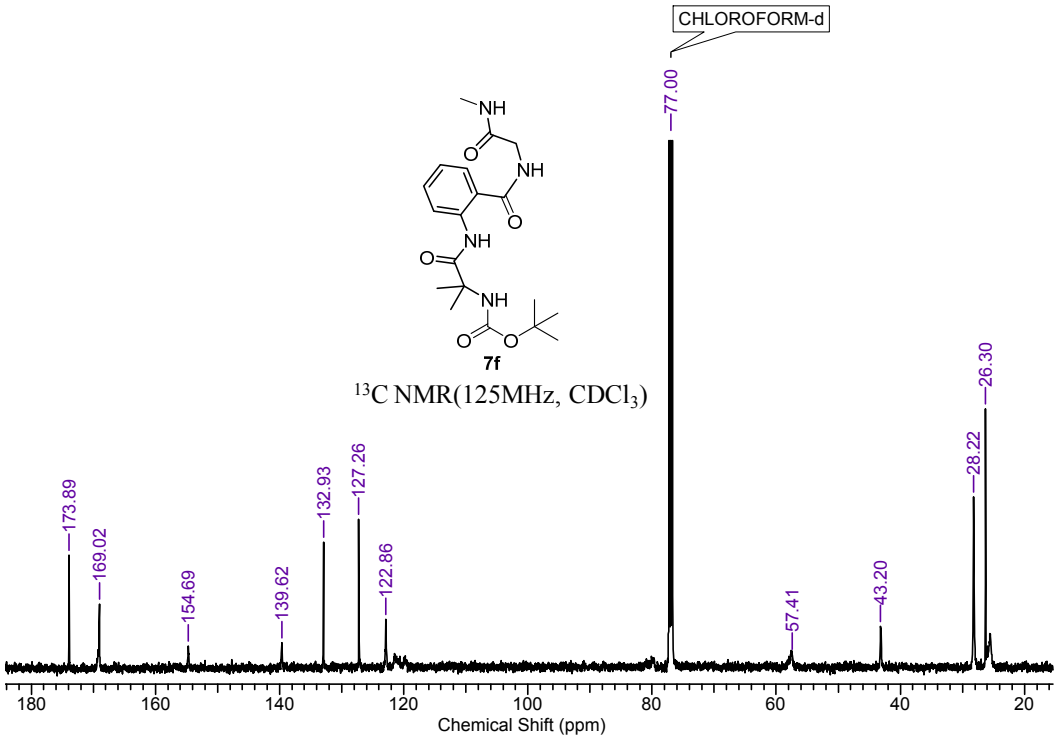
CHLOROFORM-d
77.00
NH
NH
NH
NH
NH
O
O
O
O
O
O
7f
^{13}C NMR(125MHz, CDCl$_3$)
173.89
169.02
154.69
139.62
132.93
127.26
122.86
57.41
43.20
28.22
26.30
180
160
140
120
100
80
60
40
20
Chemical Shift (ppm)

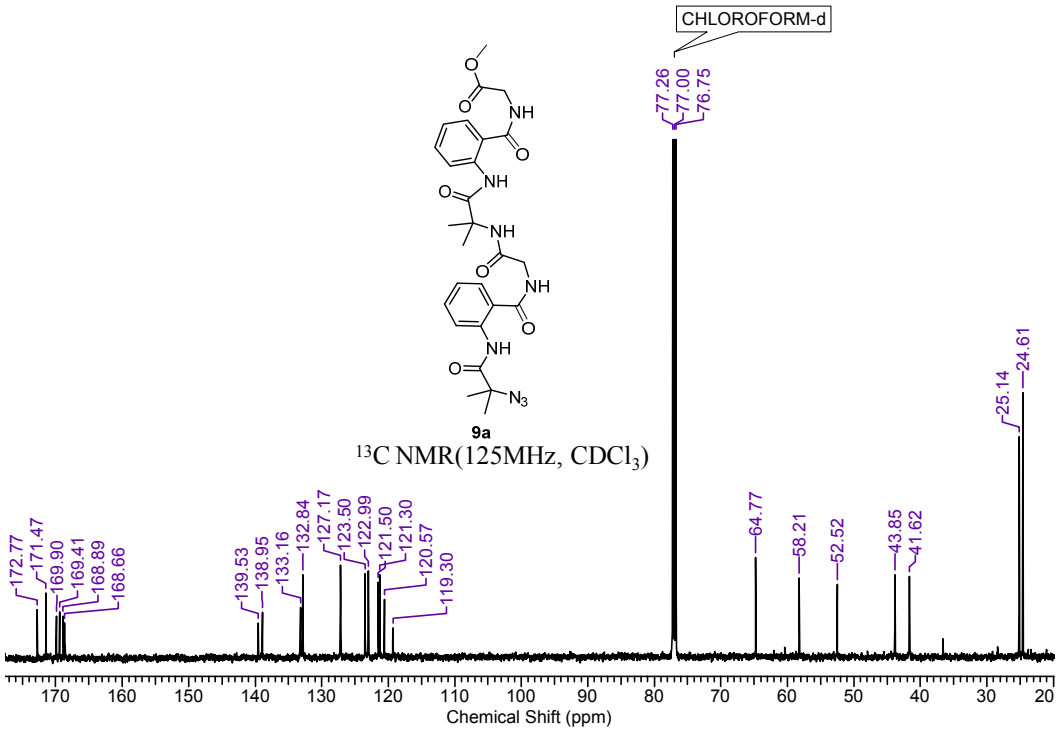
CHLOROFORM-d
77.26
77.00
76.75
NH
NH
NH
NH
NH
O
O
O
O
O
O
N$_3$
9a
^{13}C NMR(125MHz, CDCl$_3$)
172.77
171.47
169.90
169.41
168.89
168.66
139.53
138.95
133.16
132.84
127.17
123.50
122.99
121.50
121.30
120.57
119.30
64.77
58.21
52.52
43.85
41.62
25.14
24.61
170
160
150
140
130
120
110
100
90
80
70
60
50
40
30
20
Chemical Shift (ppm)

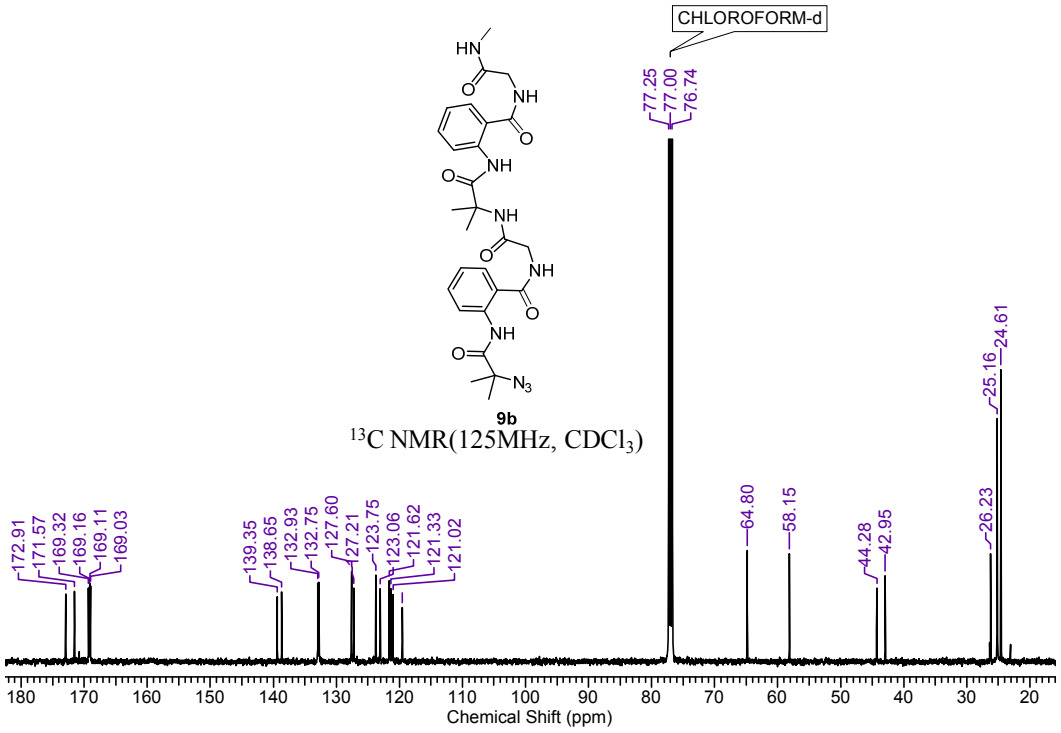

9b

^{13}C NMR(125MHz, $CDCl_3$)

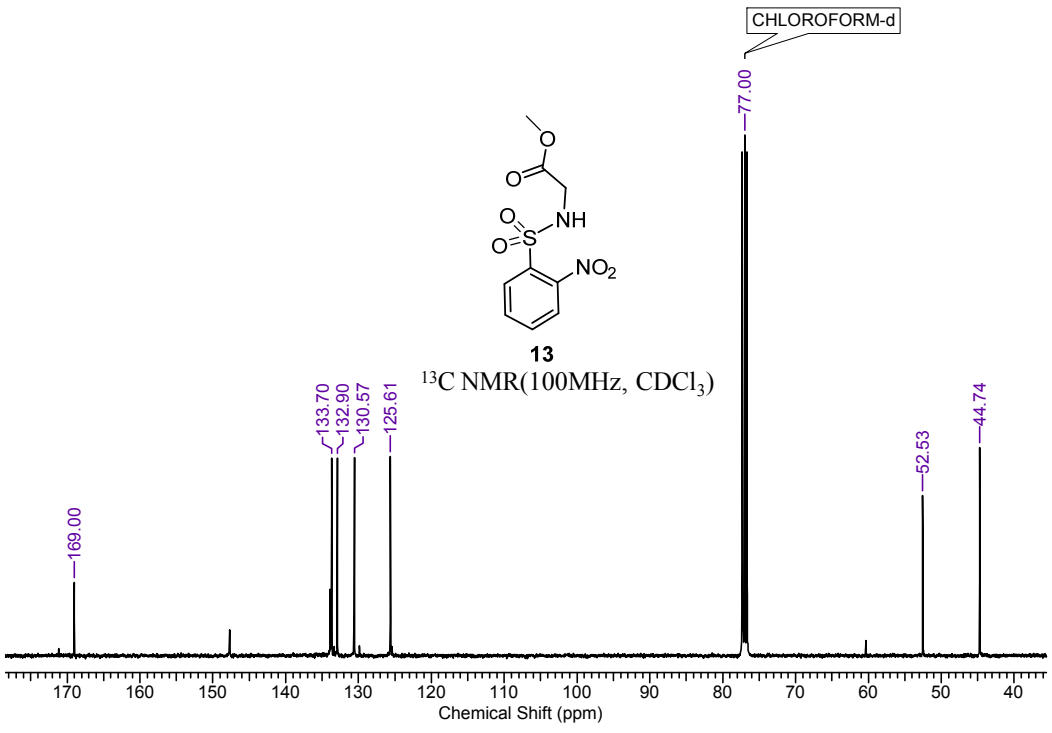

13

^{13}C NMR(100MHz, $CDCl_3$)

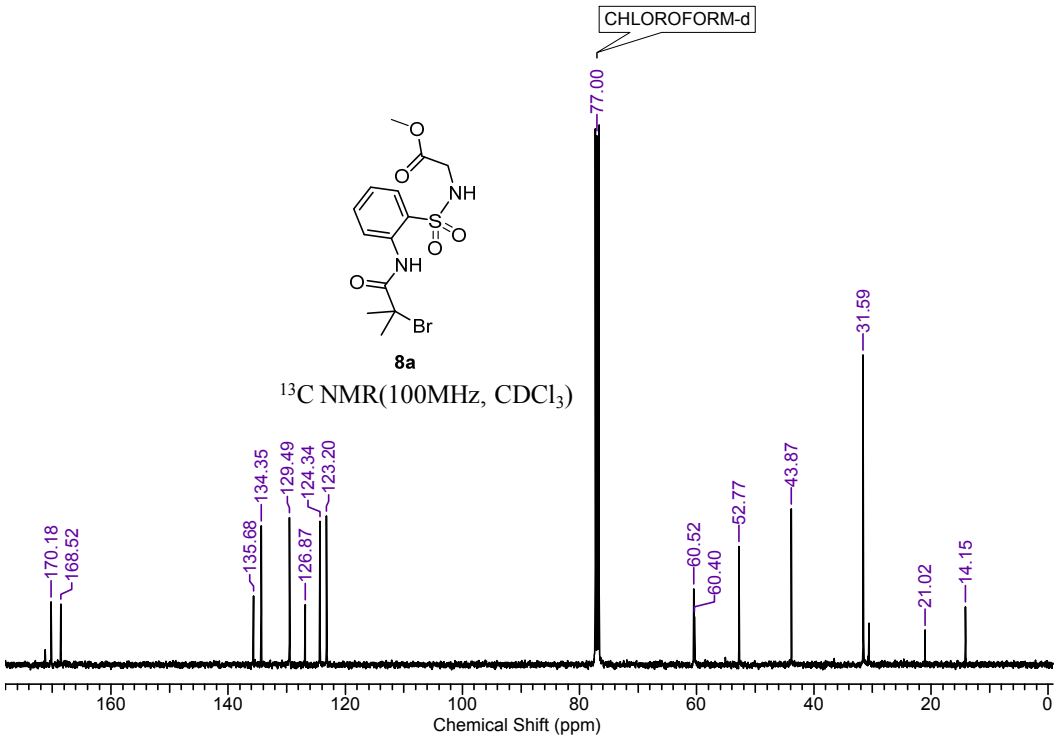

8a

^{13}C NMR(100MHz, $CDCl_3$)

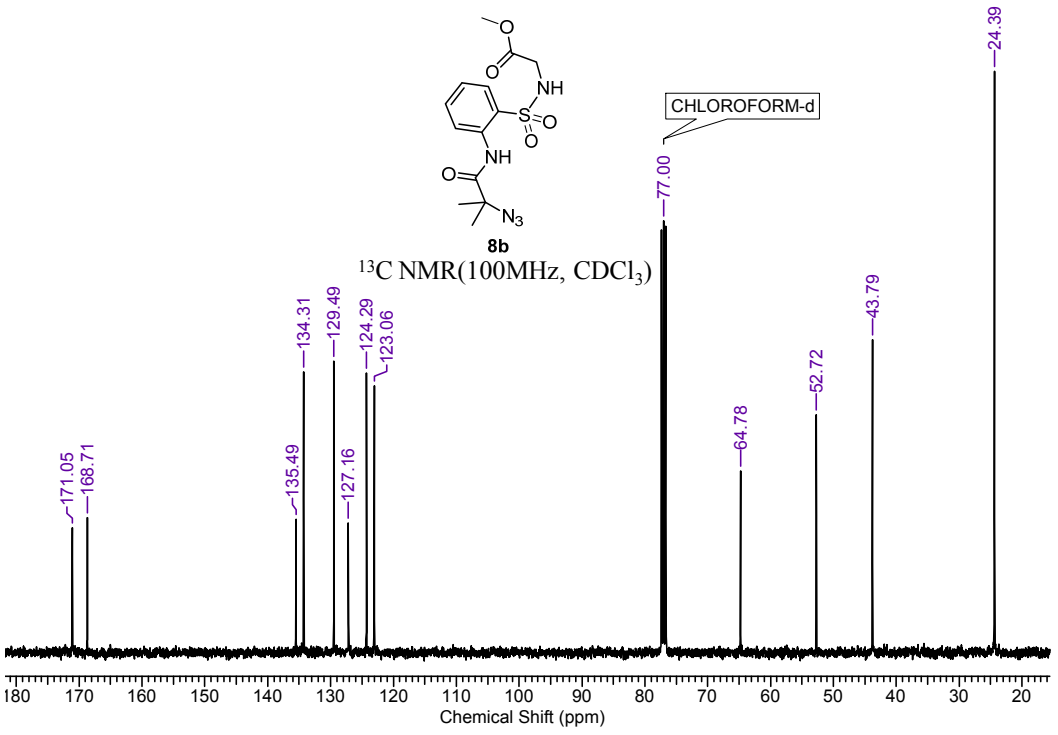

8b

^{13}C NMR(100MHz, $CDCl_3$)

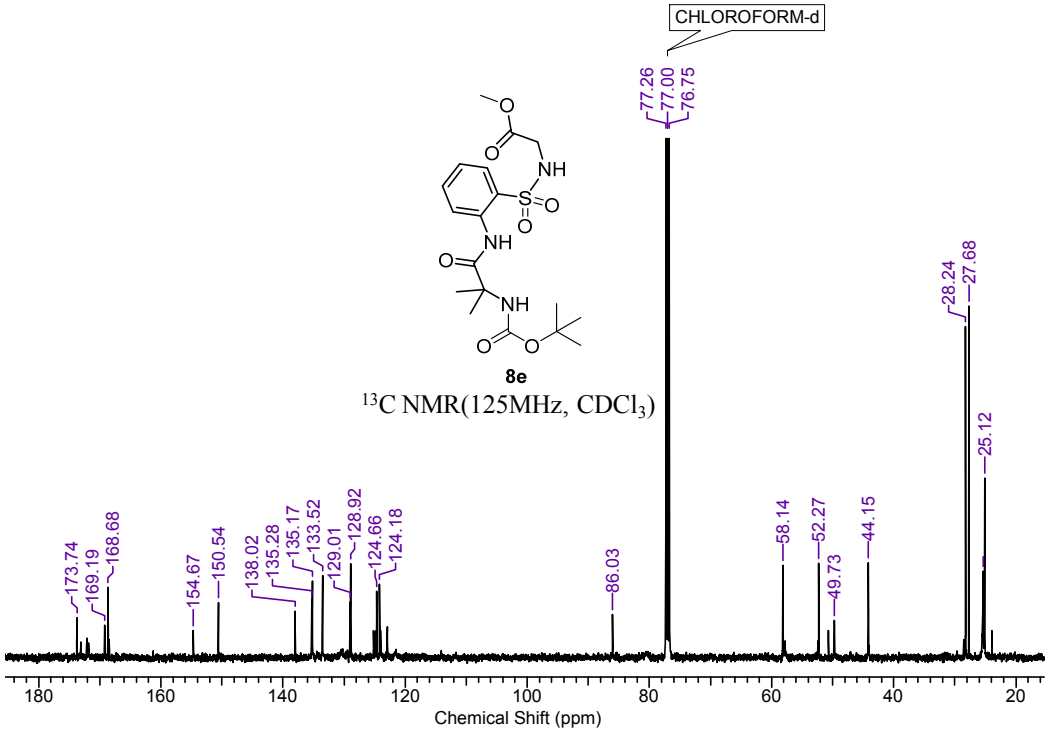

8e

^{13}C NMR(125MHz, $CDCl_3$)

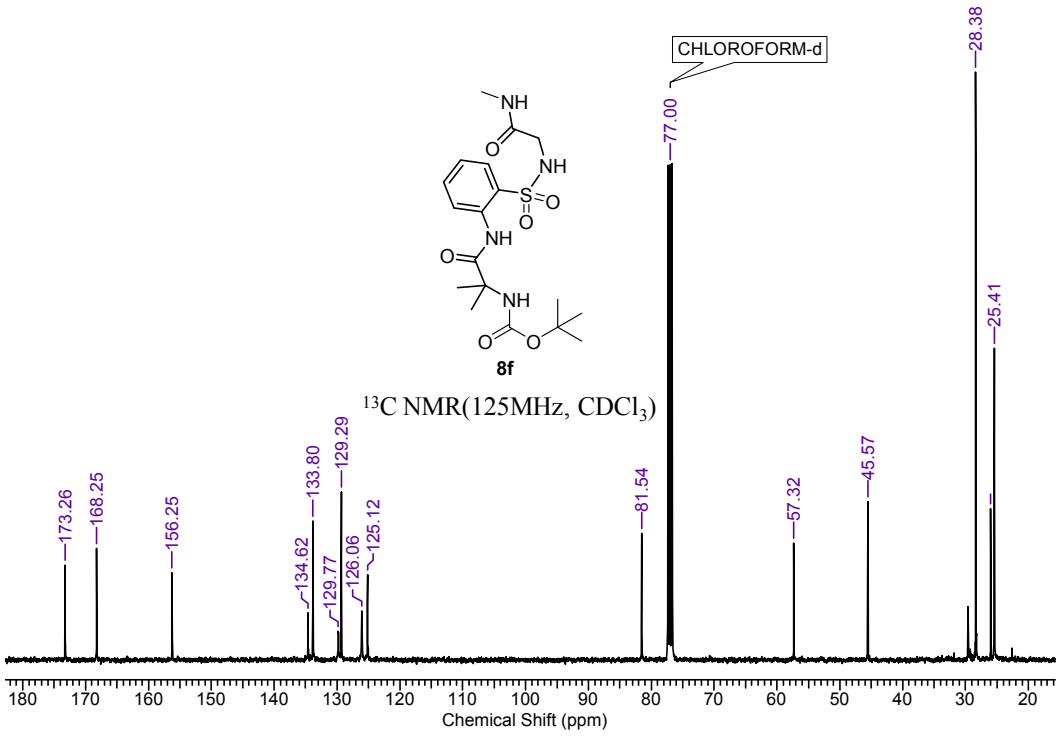

8f

^{13}C NMR(125MHz, $CDCl_3$)

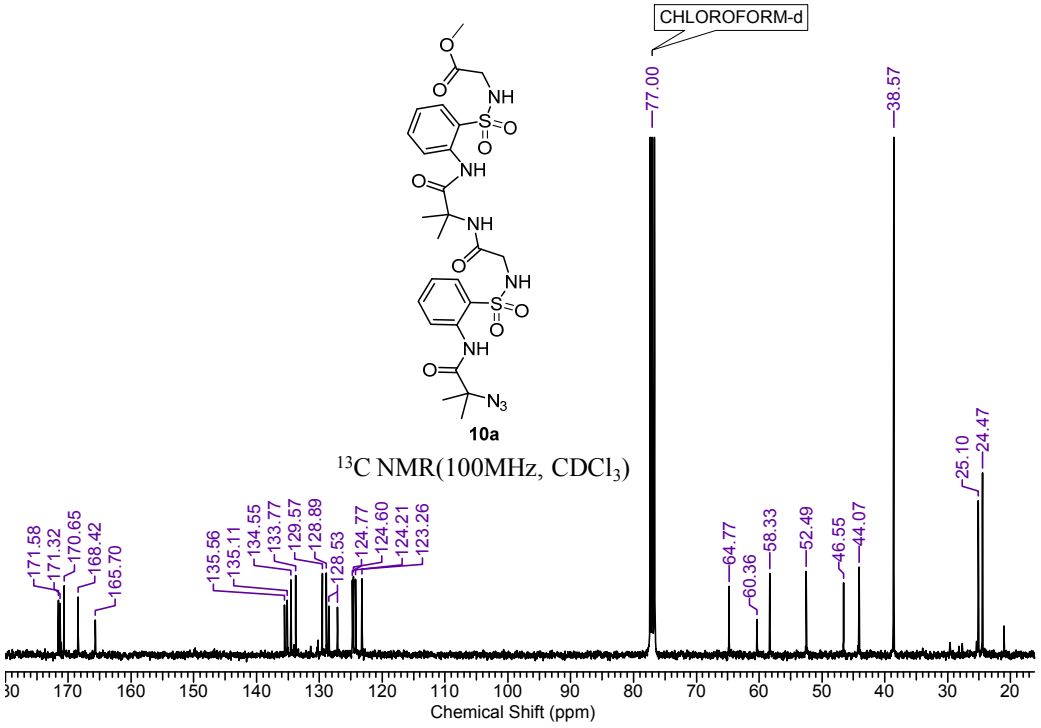

10a

^{13}C NMR(100MHz, $CDCl_3$)

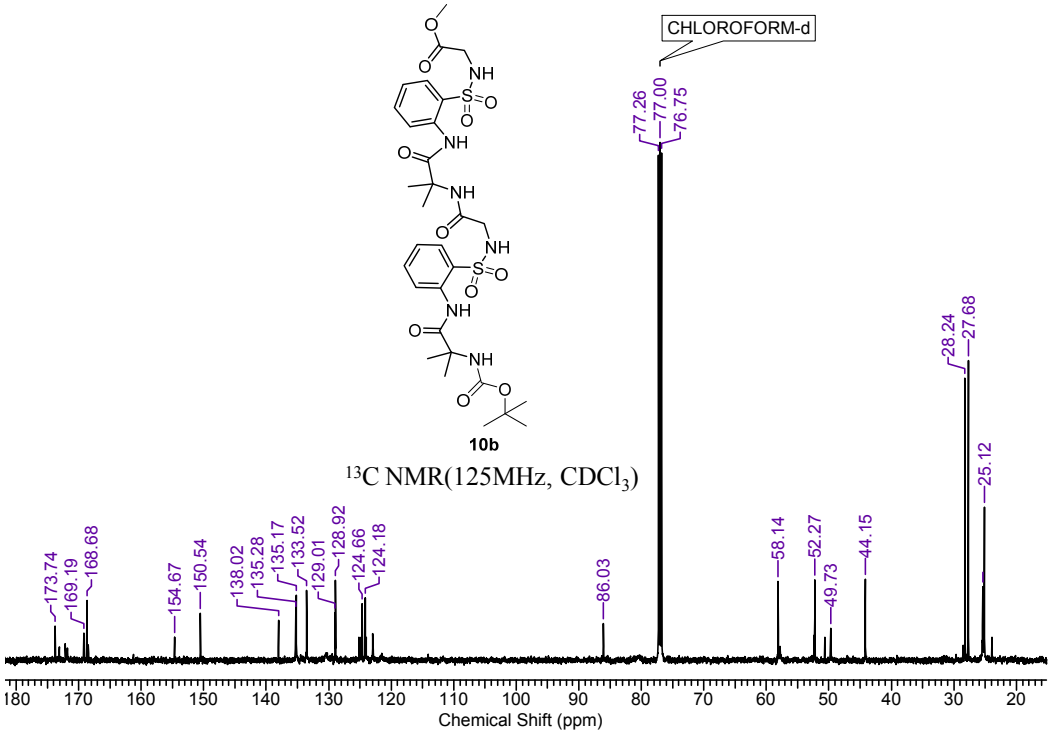

10b

^{13}C NMR(125MHz, $CDCl_3$)

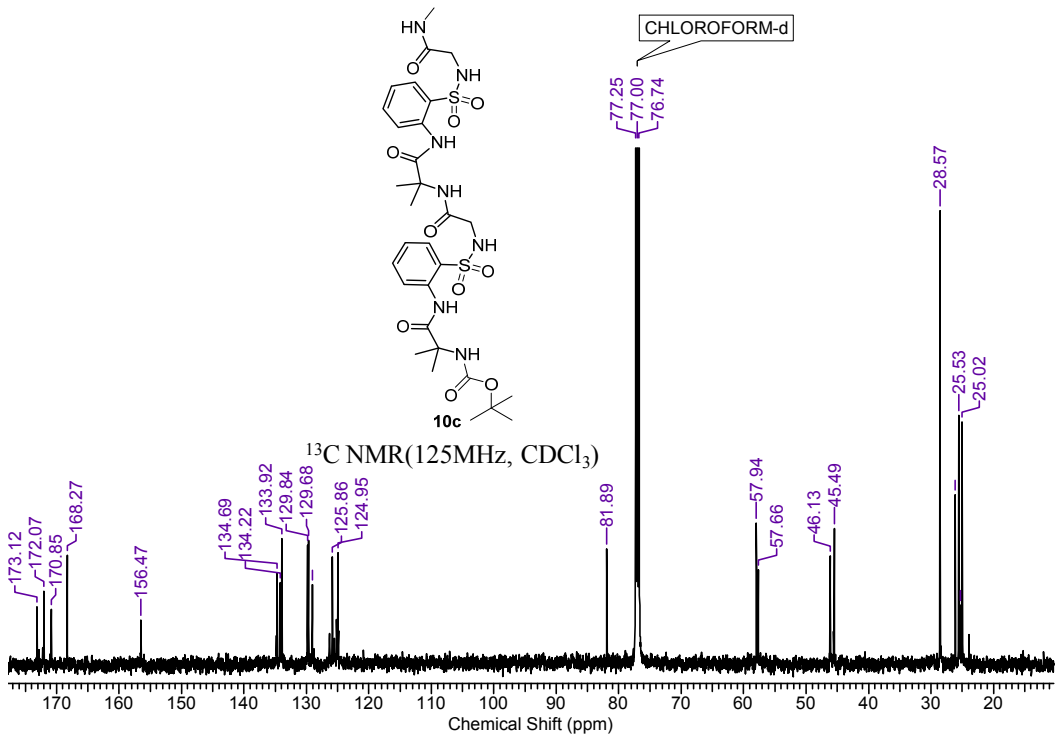
10c
^{13}C NMR(125MHz, CDCl$_3$)
CHLOROFORM-d
77.25
77.00
76.74
28.57
25.53
25.02
173.12
172.07
170.85
168.27
156.47
134.69
134.22
133.92
129.84
129.68
125.86
124.95
81.89
57.94
57.66
46.13
45.49
Chemical Shift (ppm)

Table 2.5. Titration study of 7e in $CDCl_3$ (20 mmol) with DMSO-d_6 (volume of DMSO-d_6 added at each addition = 5 µl)

Volume of DMSO-d_6 added (in µL)	Chemical Shift (in ppm)		
	δNH1	δNH2	δNH3
0	5.27	11.6	6.79
5	5.33	11.6	7.16
10	5.35	11.6	7.42
15	5.4	11.58	7.65
20	5.44	11.57	7.78
25	5.48	11.57	7.84
30	5.48	11.58	7.9
35	5.52	11.55	7.95
40	5.54	11.54	8
45	5.57	11.53	8.04
50	5.59	11.52	8.07

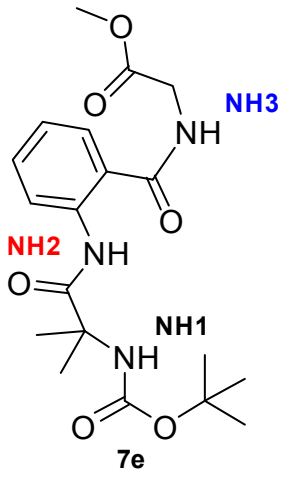

Table 2.6. Titration study of 7f in $CDCl_3$ (20 mmol) with DMSO-d_6 (volume of DMSO-d_6 added at each addition = 5 µl)

Volume of DMSO-d_6 added (in µL)	Chemical Shift (in ppm)			
	δNH1	δNH2	δNH3	δNH4
0	5.31	11.56	7.35	6.3
5	5.33	11.60	7.45	6.55
10	5.37	11.62	7.61	6.69
15	5.41	11.63	7.73	6.8
20	5.44	11.62	7.79	6.87
25	5.48	11.62	7.84	6.92
30	5.51	11.62	7.87	6.94
35	5.54	11.61	7.9	6.98
40	5.58	11.6	7.93	7
45	5.58	11.6	7.94	7
50	5.59	11.59	7.94	7.01

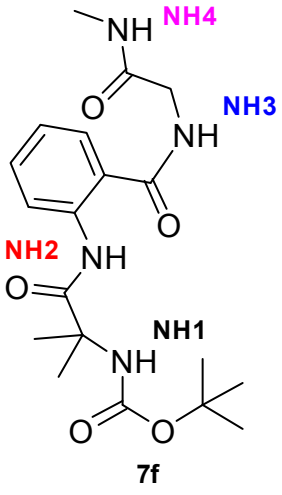

Table 2.7. Titration study of 8e in $CDCl_3$ (20 mmol) with DMSO-d_6 (volume of DMSO-d_6 added at each addition = 5 µl)

Volume of DMSO-d_6 added (in µL)	Chemical Shift (in ppm)		
	δNH1	δNH2	δNH3
0	4.95	9.64	6.93
5	5.1	9.63	6.94
10	5.22	9.61	6.96
15	5.35	9.59	6.98
20	5.52	9.56	7
25	5.61	9.55	7.01
30	5.69	9.53	7.01
35	5.76	9.51	7.02
40	5.81	9.51	7.02
45	5.87	9.49	7.01
50	5.93	9.47	6.98

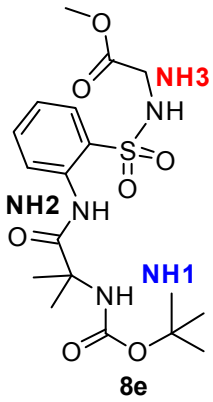

Table 2.8. Titration study of 8f in $CDCl_3$ (20 mmol) with DMSO-d_6 (volume of DMSO-*d6* added at each addition = 5 µl)

Volume of DMSO-d_6 added (in µL)	Chemical Shift (in ppm)			
	δNH1	δNH2	δNH3	δNH4
0	5.06	9.35	7.04	6.41
5	5.21	9.35	7.04	6.41
10	5.41	9.34	7.06	6.42
15	5.52	9.33	7.06	6.43
20	5.64	9.33	7.07	6.44
25	5.7	9.32	7.07	6.44
30	5.77	9.31	7.08	6.44
35	5.83	9.31	7.08	6.45
40	5.92	9.3	7.08	6.46
45	5.96	9.3	7.08	6.46
50	6.02	9.3	7.08	6.47

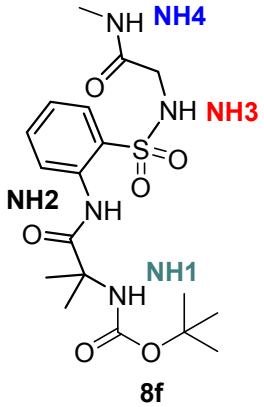

Table 2.9. Titration study of 10c in $CDCl_3$ (20 mmol) with DMSO-d_6 (volume of DMSO-d_6 added at each addition = 5 µl)

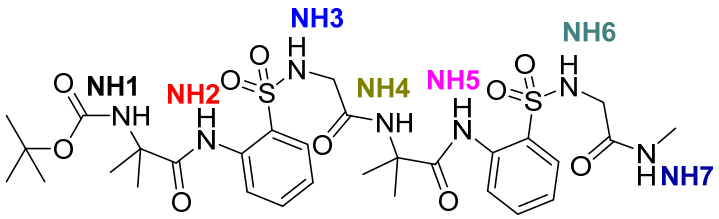

Volume of DMSO- d_6 added in µL	Chemical Shift in ppm						
	δNH1	δNH2	δNH3	δNH4	δNH5	δNH6	δNH7
0	5.04	9.39	7.24	7.06	9.18	6.86	6.45
5	5.18	9.41	7.25	7.13	9.18	6.86	6.48
10	5.65	9.49	7.37	7.17	9.18	6.87	6.65
15	5.77	9.5	7.43	7.19	9.18	6.87	6.69
20	5.81	9.5	7.47	7.19	9.17	6.87	6.72
25	5.96	9.51	7.53	7.2	9.16	6.86	6.75
30	5.98	9.51	7.56	7.18	9.16	6.86	6.77
35	6.05	9.52	7.58	7.17	9.15	6.85	6.78
40	6.07	9.51	7.63	7.17	9.14	6.84	6.8
45	6.11	9.51	7.69	7.15	9.14	6.84	6.84

Table 2.10. Variable temperature study of 7e (20 mmol, 400 MHz, $CDCl_3$).

Temperature (in °K)	Chemical shift in ppm		
	δNH1	δNH2	δNH3
268	5.31	11.67	6.88
273	5.31	11.65	6.86
278	5.3	11.64	6.84
283	5.3	11.63	6.82
288	5.3	11.63	6.81
293	5.28	11.61	6.79
298	5.26	11.6	6.78
303	5.23	11.59	6.77
308	5.2	11.57	6.75
313	5.19	11.56	6.74
318	5.18	11.54	6.73
323	5.18	11.53	6.72

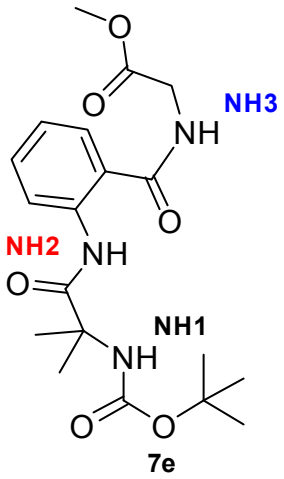

7e

Table 2.11. Variable temperature study of 8e (20 mmol, 400 MHz, $CDCl_3$).

Temperature (in °K)	Chemical shift in ppm		
	δNH1	δNH2	δNH3
268	5.06	9.64	7.01
273	4.99	9.64	7
278	4.97	9.64	6.98
283	4.97	9.64	6.97
288	4.96	9.64	6.96
293	4.95	9.64	6.94
298	4.95	9.64	6.92
303	4.94	9.64	6.9
308	4.94	9.65	6.88
313	4.93	9.65	6.85
318	4.93	9.65	6.82
323	4.92	9.65	6.81

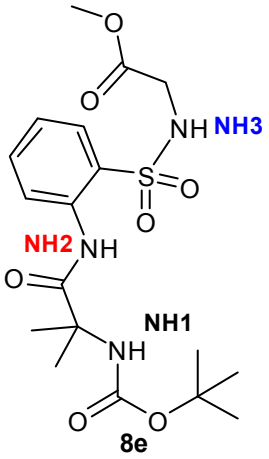

Table 2.12. Variable temperature study of 8f (20 mmol, 400 MHz, $CDCl_3$).

Temperature (in °K)	Chemical Shift (in ppm)			
	δNH1	δNH2	δNH3	δNH4
268	5.1	9.33	7.14	6.48
273	5.09	9.34	7.13	6.48
278	5.09	9.34	7.11	6.47
283	5.08	9.34	7.09	6.45
288	5.07	9.35	7.07	6.43
293	5.06	9.35	7.05	6.42
293	5.06	9.35	7.03	6.4
303	5.05	9.36	7	6.39
308	5.04	9.36	6.99	6.38
313	5.03	9.37	6.96	6.36
318	5.03	9.37	6.95	6.35
323	5.02	9.38	6.92	6.34

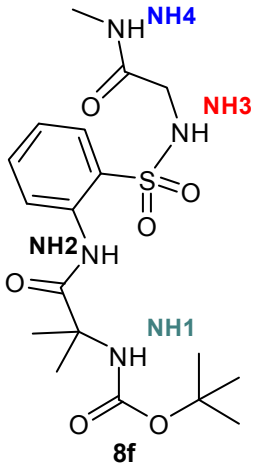

Table 2.13. Variable temperature study of 10c (10 mmol, 400 MHz, $CDCl_3$).

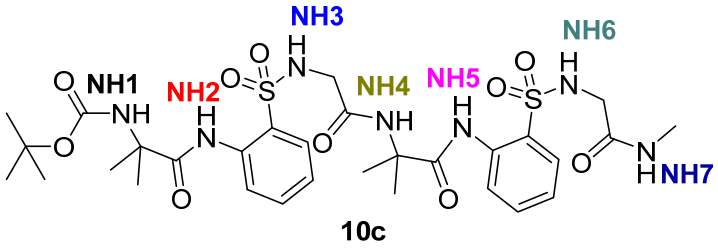

10c

Temperature (in °K)	Chemical Shift in ppm						
	δNH1	δNH2	δNH3	δNH4	δNH5	δNH6	δNH7
268	5.11	9.4	7.27	7.13	9.2	6.92	6.62
273	5.1	9.4	7.27	7.13	9.19	6.91	6.6
278	5.1	9.4	7.26	7.12	9.19	6.9	6.58
283	5.09	9.4	7.26	7.11	9.19	6.89	6.56
288	5.09	9.4	7.26	7.1	9.19	6.88	6.53
293	5.08	9.4	7.26	7.09	9.18	6.86	6.5
298	5.08	9.4	7.25	7.08	9.18	6.85	6.48
303	5.07	9.4	7.21	7.08	9.18	6.83	6.46
308	5.07	9.4	7.19	7.06	9.18	6.82	6.43
313	5.06	9.4	7.17	7.05	9.18	6.8	6.41

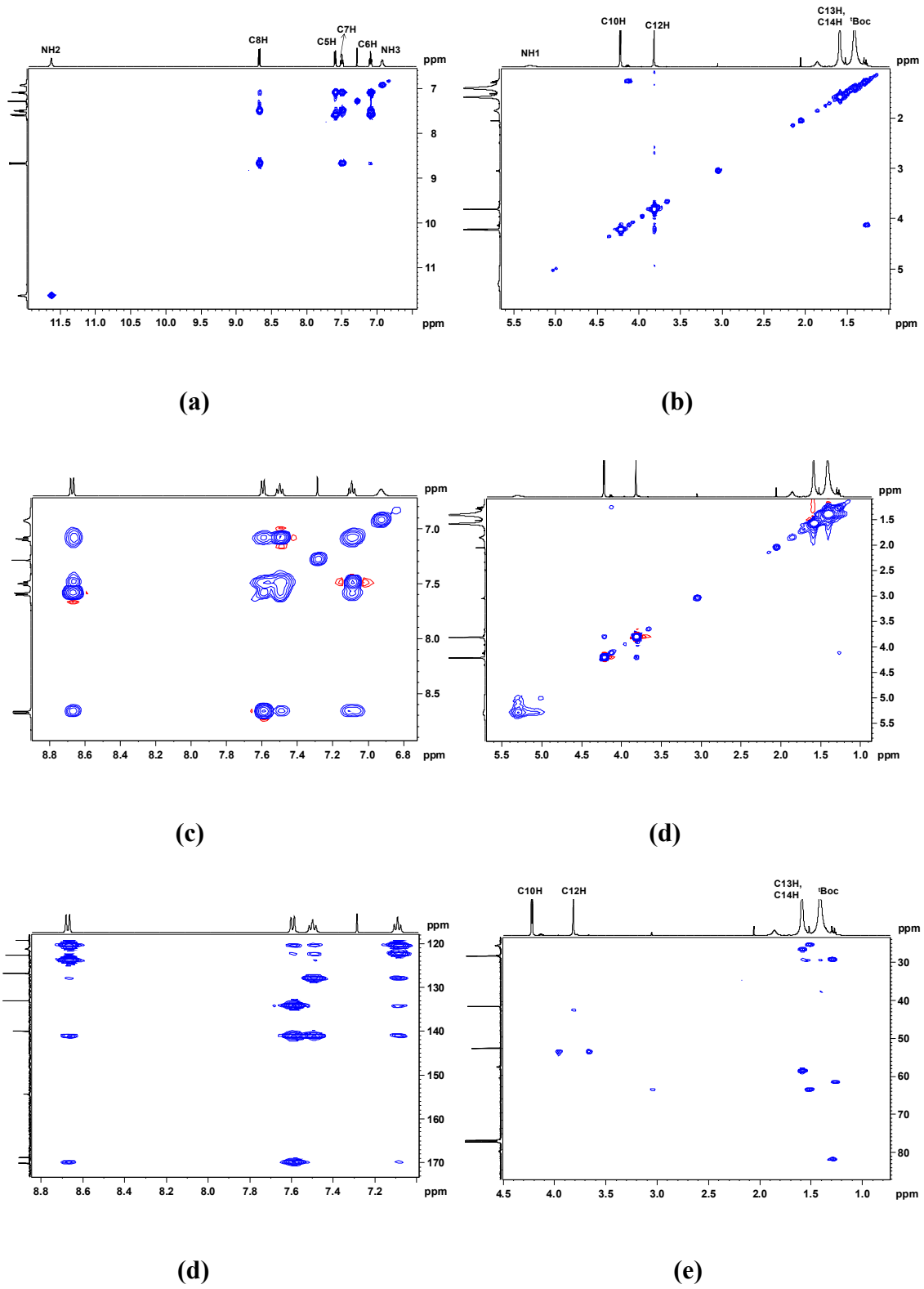

Fig 2.42: Partial COSY (a), (b); TOCSY, (c), (d); and HMBC (e), (f) spectra of **7e** (500 MHz, $CDCl_3$). For better view, aromatic and aliphatic regions are shown separately.

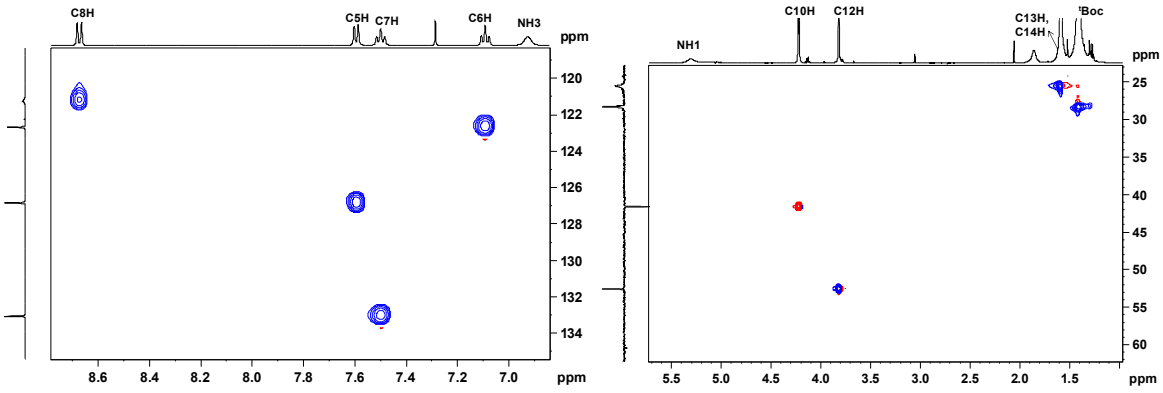

(g) **(h)**

Fig 2.43: Partial HSQC spectra of **7e** (500 MHz, $CDCl_3$). For better view, aromatic and aliphatic regions are shown separately.

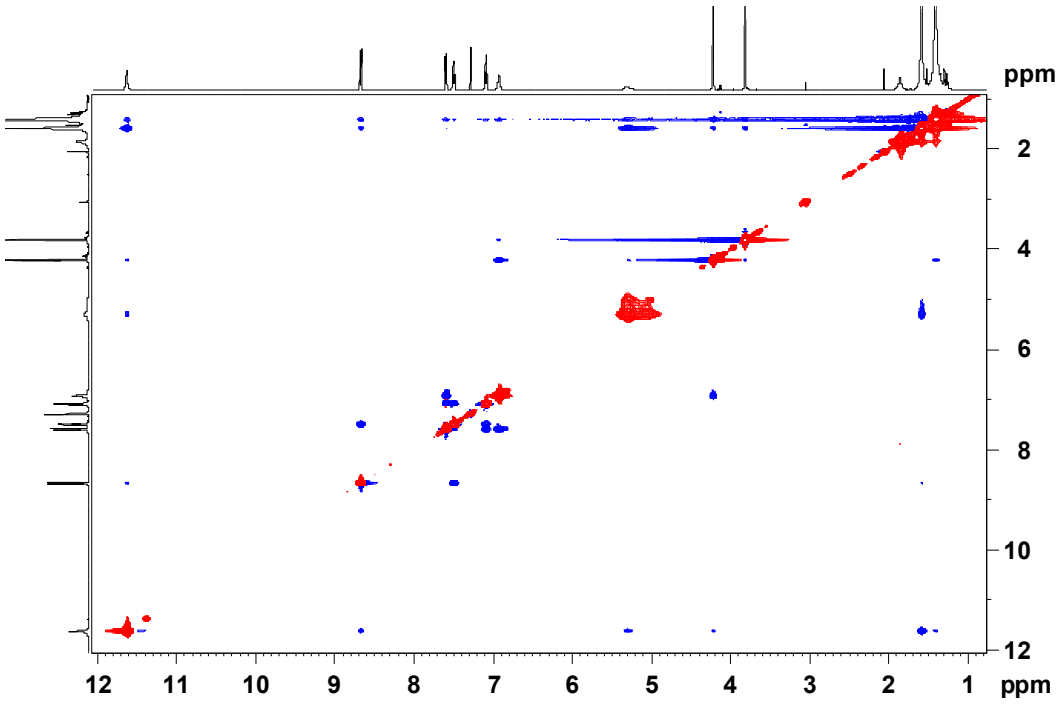

Fig 2.44: Full 2D NOESY spectrum of **7e** (500 MHz, $CDCl_3$).

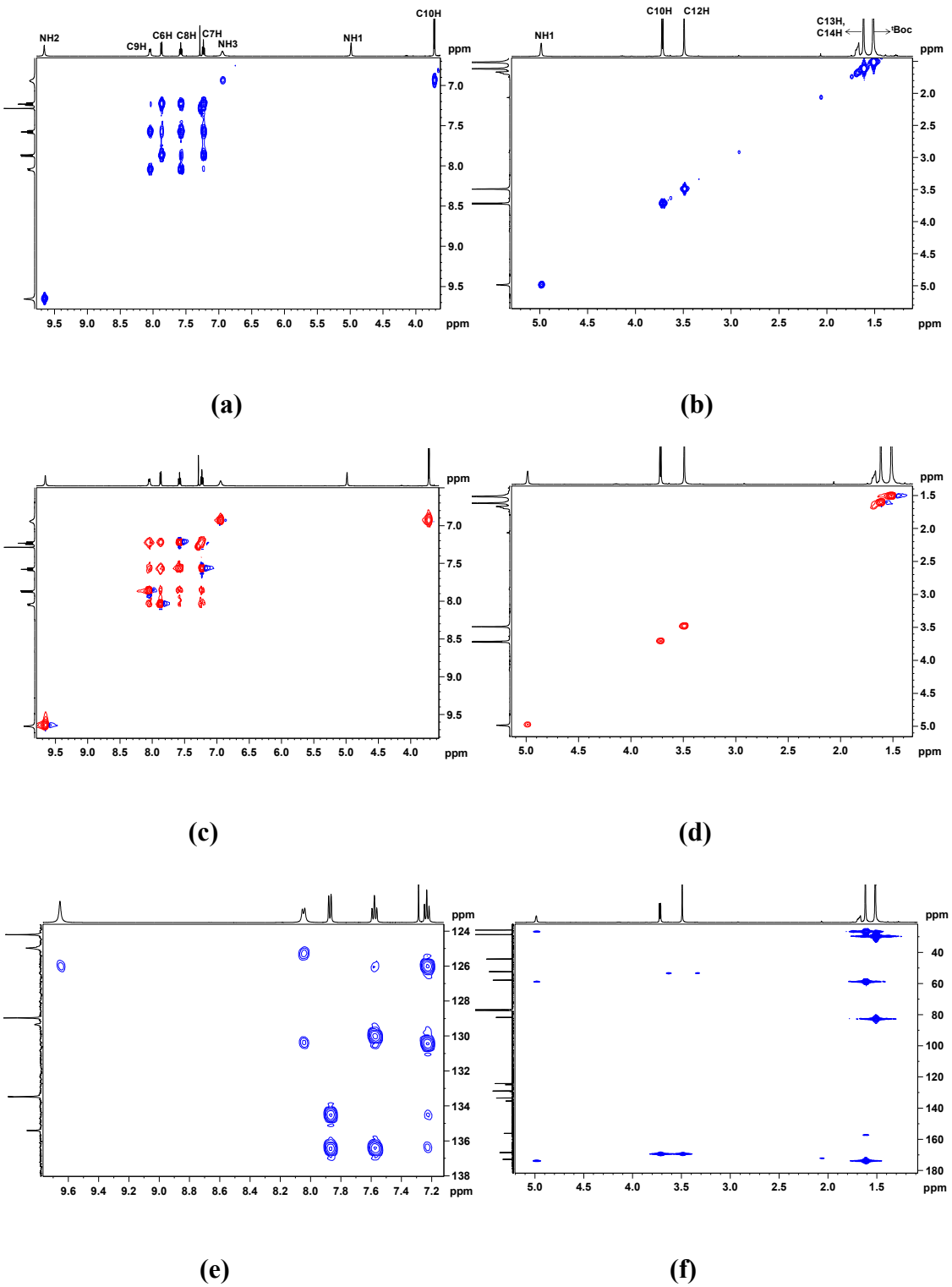

Fig 2.45: Partial COSY (a), (b); TOCSY, (c), (d); and HMBC (e), (f) spectra of **8e** (500 MHz, $CDCl_3$). For better view, aromatic and aliphatic regions are shown separately.

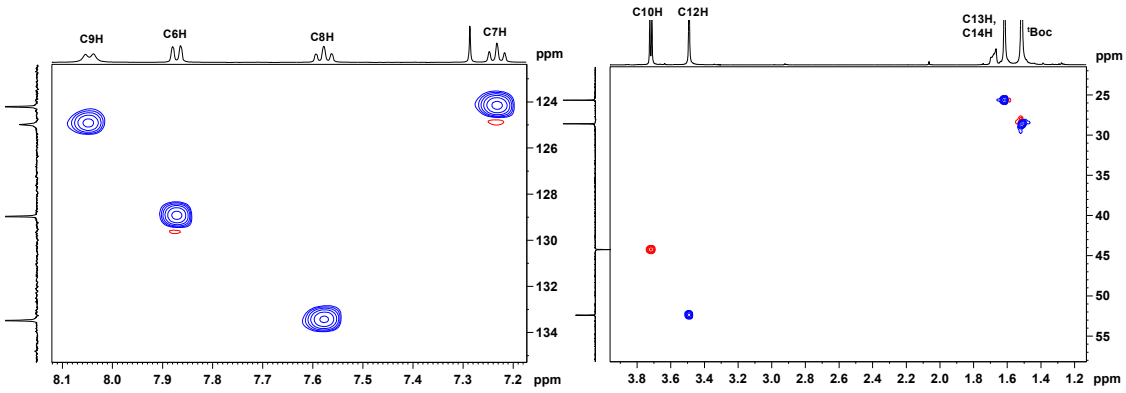

(g) **(h)**

Fig 2.46: Partial HSQC spectra of **8e** (500 MHz, $CDCl_3$). For better view, aromatic and aliphatic regions are shown separately.

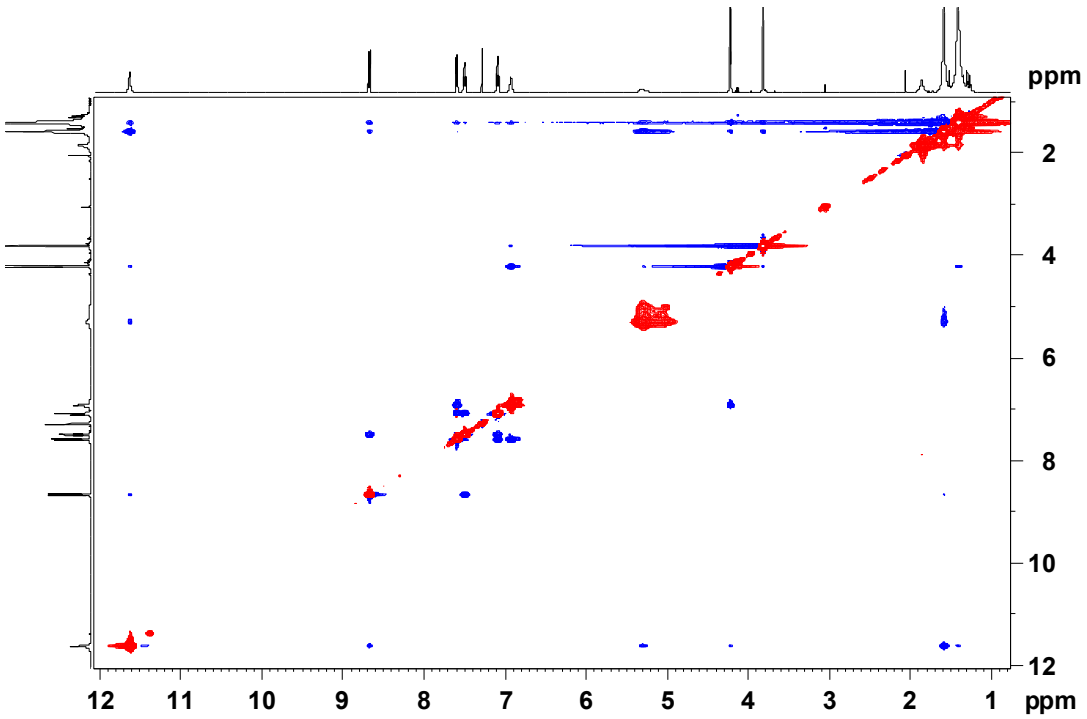

Fig 2.47: Full 2D NOESY spectrum of **8e** (500 MHz, $CDCl_3$).

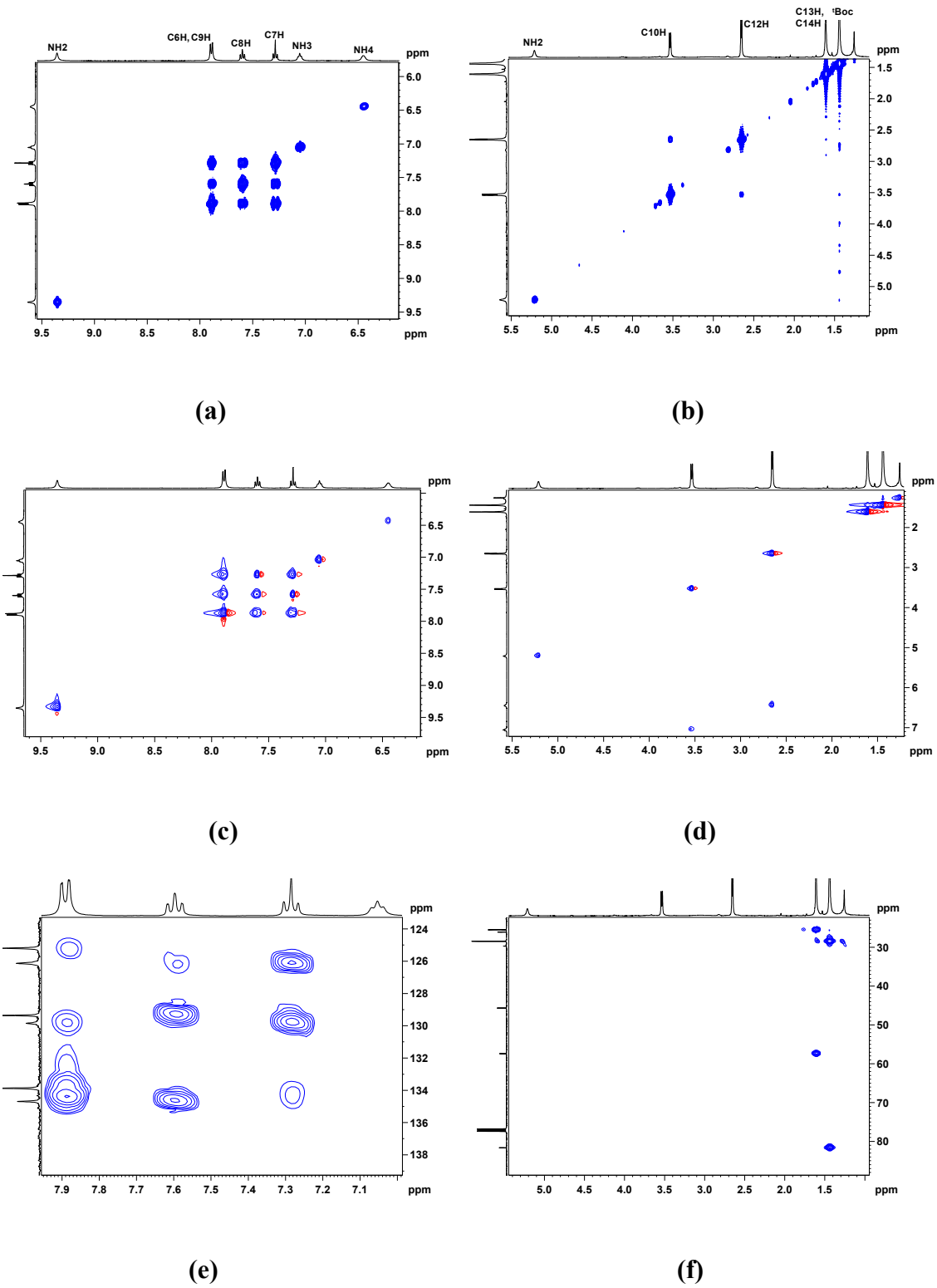

Fig 2.48: Partial COSY (a), (b); TOCSY, (c), (d); and HMBC (e), (f) spectra of **8f** (500 MHz, $CDCl_3$). For better view, aromatic and aliphatic regions are shown separately.

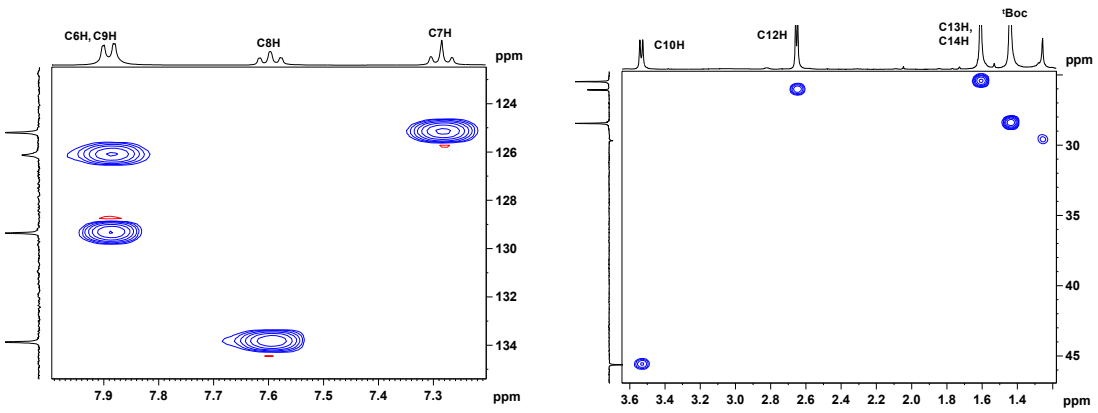

(g) **(h)**

Fig 2.49: Partial HSQC spectra of **8f** (500 MHz, $CDCl_3$). For better view, aromatic and aliphatic regions are shown separately.

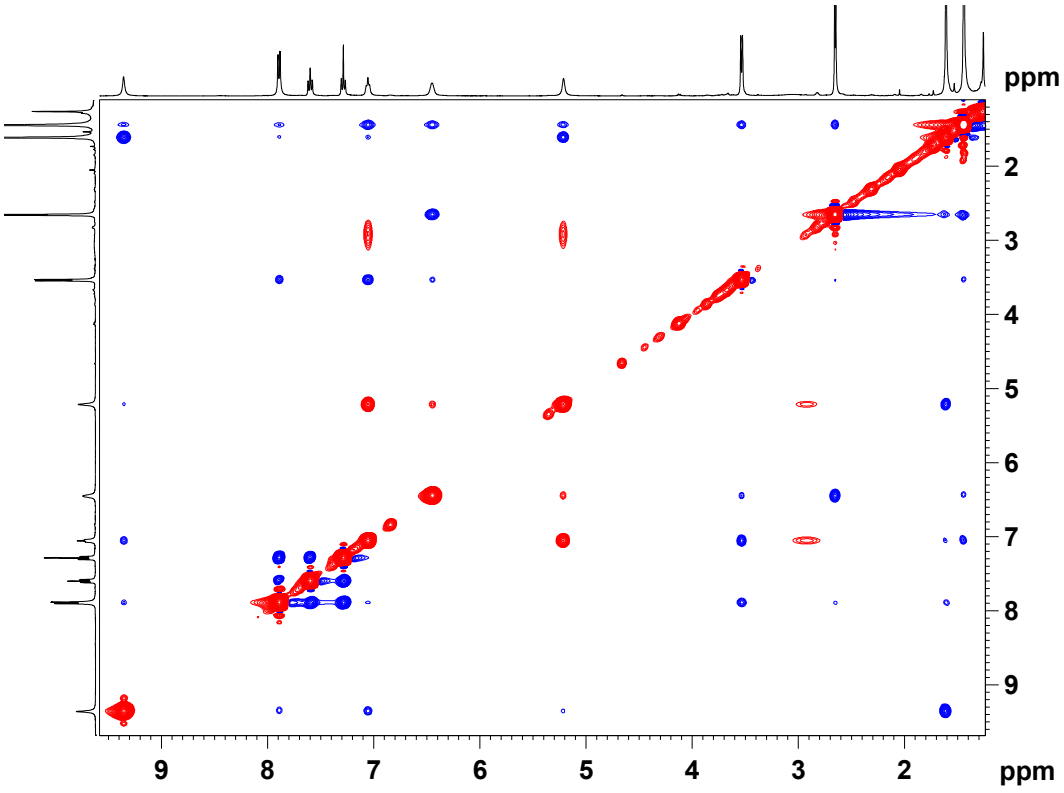

Fig 2.50: Full 2D NOESY spectrum of **8f** (500 MHz, $CDCl_3$).

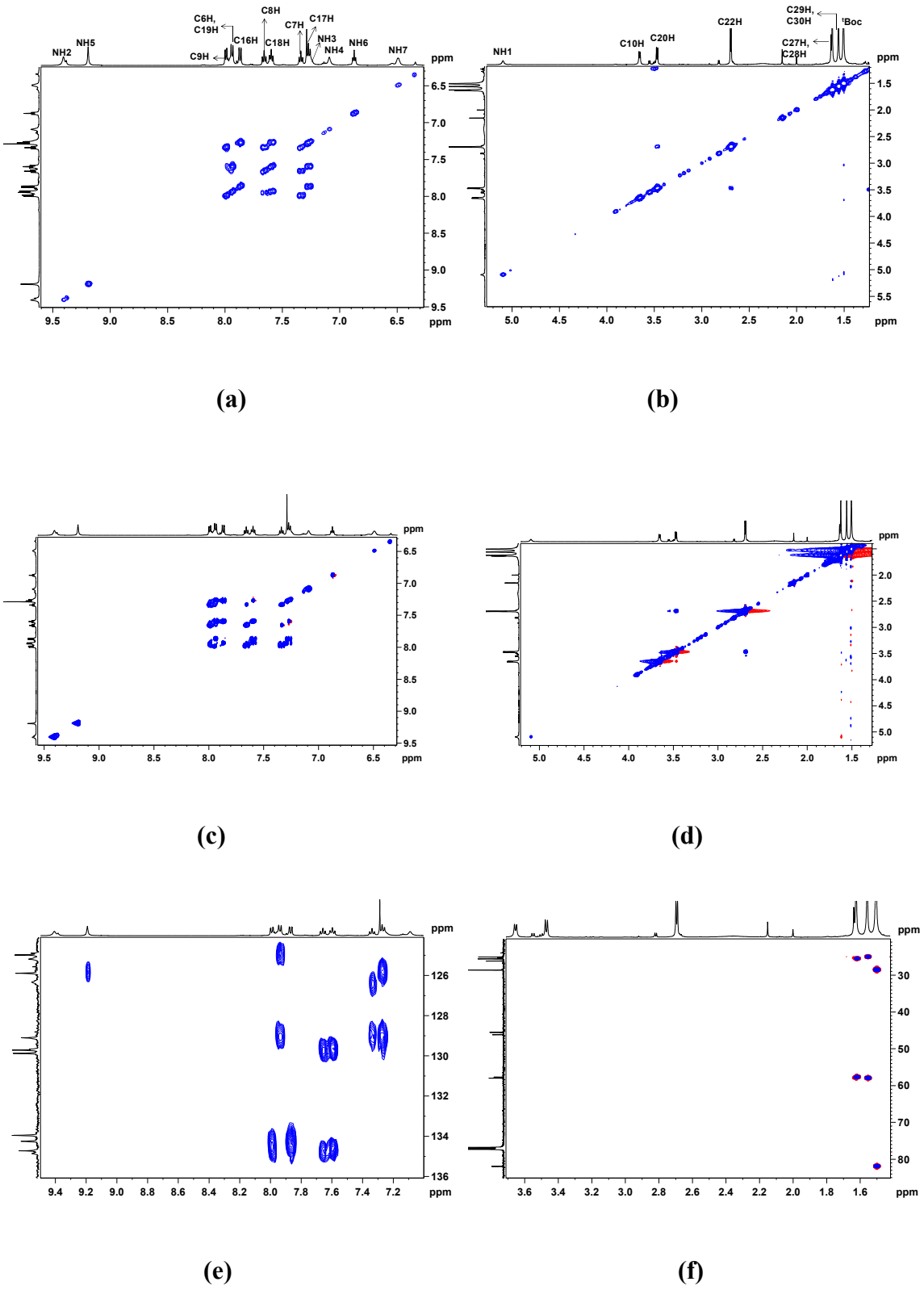

Fig 2.51: Partial COSY (a), (b); TOCSY, (c), (d); and HMBC (e), (f) spectra of **10c** (500 MHz, $CDCl_3$). For better view, aromatic and aliphatic regions are shown separately.

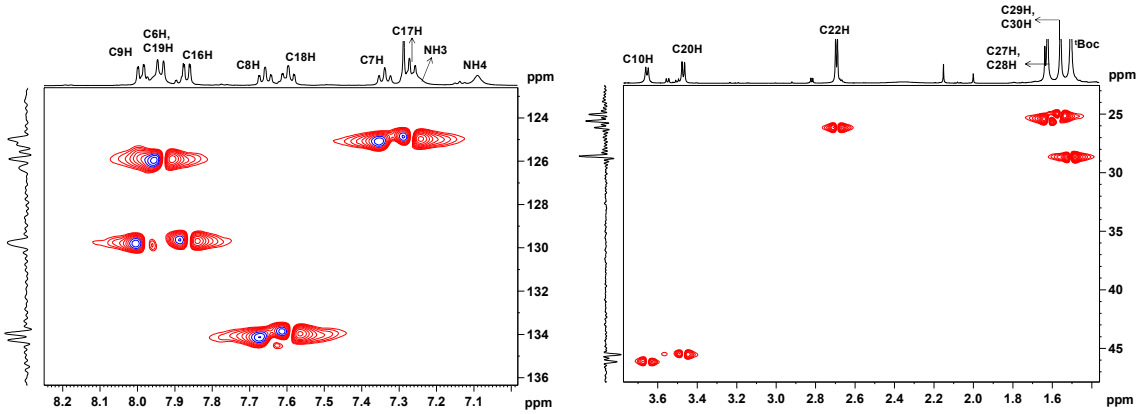

(g) **(h)**

Fig 2.52: Partial HSQC spectra of **10c** (500 MHz, $CDCl_3$). For better view, aromatic and aliphatic regions are shown separately.

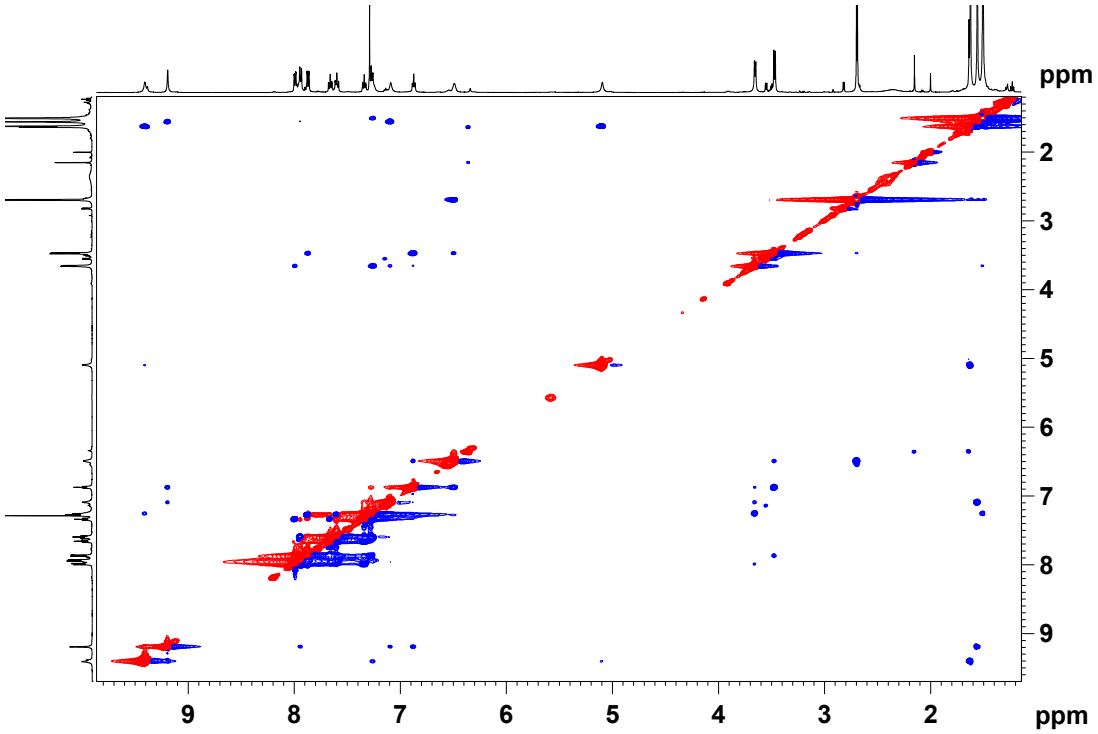

Fig 2.53: Full 2D NOESY spectrum of **10c** (500 MHz, $CDCl_3$).

2.21 Experimental Section (Section C)

Crystal data for 15d:

Single crystals of **15d** were grown by slow evaporation of its solution in DCM and pet. ether. Colorless needle like crystal of approximate size 0.32 x 0.09 x 0.07 mm^3, was used for data collection. Multi-run data acquisition. Total scans = 4, total frames = 1559, exposure / frame = 10.0 sec / frame, θ range = 2.53 to 25.00°, completeness to θ of 25.00 º is 99.9 %. $C_{19}H_{28}N_4O_6S$, *MW* = 440.51, crystals belong to orthorhombic, space group $P2_12_12_1$, *a* = 9.2146(8) Å, *b* = 14.611(1) Å, *c* = 16.096(1) Å, V = 2166.9(3) $Å^3$, *Z* = 4, D_c = 1.35 g/cc, (Mo–K_α) = 0.192 mm^{-1}, 9609 reflections measured, 3803 unique, [I>2σ(I)] R1 = 0.0376, wR2 = 0.0809, largest diff. peak and hole 0.389 and -0.425 e.$Å^{-3}$.

Crystal data for 22:

Single crystals of **22** were grown by slow evaporation of its solution in DCM. Colorless plate like crystal of approximate size 0.46 x 0.28 x 0.13 mm^3, was used for data collection. Multi-run data acquisition. Total scans = 4, total frames = 1559, exposure / frame = 10.0 sec / frame, θ range = 2.63 to 24.99°, completeness to θ of 24.99 º is 99.9 %. $C_{14}H_{18}N_4O_6S.H_2O$, *MW* = 388.4, crystals belong to orthorhombic, space group $P2_1$, *a* = 7.7644(2) Å, *b* = 7.7138(2) Å, *c* = 14.7369(5) Å, V = 879.82(4) $Å^3$, *Z* = 4, D_c = 1.466 g/cc, (Mo–K_α) = 0.23 mm^{-1}, 6578 reflections measured, 2785 unique, [I>2σ(I)] R1 = 0.05, wR2 = 0.1124, largest diff. peak and hole 0.407 and -0.250 e.$Å^{-3}$.

Crystal data for 24:

Single crystals of **24** were grown by slow evaporation of its solution in chloroform. Colorless plate like crystal of approximate size 0.42 x 0.35 x 0.29 mm^3, was used for data collection. Multi-run data acquisition. Total scans = 4, total frames = 1559, exposure / frame = 10.0 sec / frame, θ range = 2.05 to 25.00°, completeness to θ of 25.00 º is 99.9 %. $C_{17}H_{16}N_3O_5Br$, *MW* = 454.3, crystals belong to monoclinic, space group $P2_1$, *a* = 9.6169(1) Å, *b* = 19.8572 (1) Å, *c* = 10.0470 (1) Å, V = 1896.02(4) $Å^3$, *Z* = 4, D_c = 1.592 g/cc, (Mo–K_α) = 2.312 mm^{-1},

28083 reflections measured, 6658 unique, [I>2σ(I)] R1 = 0.0327, wR2 = 0.0670, largest diff. peak and hole 0.27 and -0.258 e.Å^{-3}.

Crystal data for 26a:

Single crystals of **26a** were grown by slow evaporation of the solution in chloroform. Colorless plate like crystal of approximate size 0.42 x 0.31 x 0.08 mm^3, was used for data collection. Multi-run data acquisition. Total scans = 4, total frames = 1559, exposure / frame = 10.0 sec / frame, θ range = 1.90 to 25.00°, completeness to θ of 25.00 º is 99.9 %. $C_{19}H_{19}N_3O_7S$, *MW* = 433.43, crystals belong to monoclinic, space group $P2_1$, *a* = 7.5913(1) Å, *b* = 12.3192 (2) Å, *c* = 11.3409 (2) Å, V = 1004.34(3) Å^3, *Z* = 4, D_c = 1.433 g/cc, (Mo–K$_\alpha$) = 0.209 mm^{-1}, 14526 reflections measured, 3527 unique, [I>2σ(I)] R1 = 0.0344, wR2 = 0.0857, largest diff. peak and hole 0.137 and -0.189 e.Å^{-3}.

Crystal data for 26f:

Single crystals of **26f** were grown by slow evaporation of the solution in acetone. Colorless needle like crystal of approximate size 0.43 x 0.19 x 0.1 mm^3, was used for data collection. Multi-run data acquisition. Total scans = 4, total frames = 1559, exposure / frame = 10.0 sec / frame, θ range = 2.20 to 25.00°, completeness to θ of 25.00 º is 99.9 %. $C_{20}H_{21}N_3O_6S$, *MW* = 431.46, crystals belong to monoclinic, space group $P2_1$, *a* = 10.3772(5) Å, *b* = 10.9443(5) Å, *c* = 17.4395(7) Å, V = 1979.93(15) Å^3, *Z* = 4, D_c = 1.447 g/cc, (Mo–K$_\alpha$) = 0.208 mm^{-1}, 14978 reflections measured, 6559 unique, [I>2σ(I)] R1 = 0.0388, wR2 = 0.1001, largest diff. peak and hole 0.244 and -0.274 e.Å^{-3}.

It was observed that in the crystal lattice of **26f**, there existed two molecules with different conformations. These two structures maintain the C9 H-bonding pattern but vary at the C-terminus proline ring orientation, the overlaid structure of these two conformations of **26f** is shown in Fig 2.44.

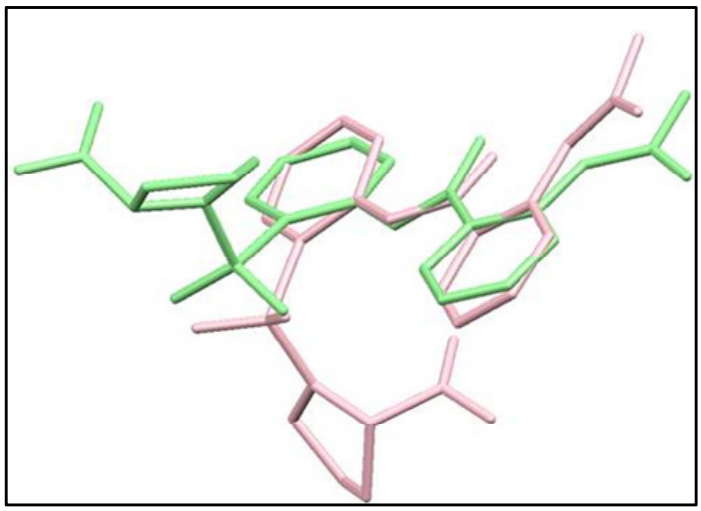

Fig 2.54: Overlaid structure of the two conformers present in crystal lattice of **26f**.

Crystal data for 29a:

Single crystals of **29a** were grown by slow evaporation of the solution in chloroform. Colorless plate like crystal of approximate size 0.41 x 0.40 x 0.11 mm^3, was used for data collection. Multi-run data acquisition. Total scans = 4, total frames = 1559, exposure / frame = 10.0 sec / frame, θ range = 2.03 to 25.00°, completeness to θ of 25.00 º is 99.7 %. $C_{17}H_{21}N_3O_7S$, *MW* = 411.43, crystals belong to monoclinic, space group $P2_1$, *a* = 8.9692(1) Å, *b* = 10.0863(1) Å, *c* = 10.7307(1) Å, V = 909.76(16) $Å^3$, *Z* = 4, D_c = 1.502 g/cc, (Mo–K_α) = 0.226 mm^{-1}, 6993 reflections measured, 2953 unique, [I>2σ(I)] R1 = 0.0221, wR2 = 0.0582, largest diff. peak and hole 0.146 and -0.281 e.$Å^{-3}$.

Crystal data for 29b:

Single crystals of **29b** were grown by slow evaporation of the solution in chloroform. Colorless plate like crystal of approximate size 0.27 x 0.25 x 0.05 mm^3, was used for data collection. Multi-run data acquisition. Total scans = 4, total frames = 1559, exposure / frame = 10.0 sec / frame, θ range = 2.57 to 25.00°, completeness to θ of 25.00 º is 100 %. $C_{17}H_{21}N_3O_7S$, *MW* = 411.43, crystals belong to monoclinic, space group $P2_1$, *a* = 7.8519(2) Å, *b* = 14.9766(4) Å, *c* = 8.2716(2) Å, V = 932.4(4) $Å^3$, *Z* = 4, D_c = 1.465 g/cc, (Mo–K_α) = 0.220 mm^{-1}, 6734 reflections measured, 3124 unique, [I>2σ(I)] R1 = 0.0347, wR2 = 0.0783, largest diff. peak and hole 0.184 and -0.249 e.$Å^{-3}$.

tert-butyl 2-((2-(N-(2-methoxy-2-oxoethyl)sulfamoyl)phenyl)carbamoyl) pyrrolidine-1-carboxylate 15a:

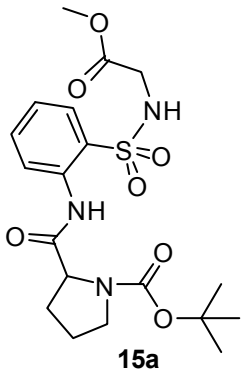

15a

To a two necked round-bottomed flask containing Boc-Pro-OH (0.21 g, 0.98 mmol) in THF, dry Et_3N (0.12 mL, 1.22 and ethyl chloroformate (0.09 mL, 0.98 mmol) were added drop wise at 0 °C followed by the addition of amine **14** (0.2 g, 0.81 mmol). The reaction mixture was stirred at 0 ^oC for 1 h and then refluxed for 48 h. Later, the reaction mixture was cooled to room temperature and filtered. The solvent was evaporated to get the crude product, which was taken into DCM (30 mL) and washed with sat. $NaHCO_3$, brine and sat. $KHSO_4$ solutions. The organic layer was dried over anhydrous Na_2SO_4 and evaporated under reduced pressure to get the crude product which was further purified by column chromatography (eluent: pet ether/ethyl acetate: 30:70, R*f*: 0.5) to furnish **15a** (0.21 g, 60%) as a sticky substance; $[\alpha]^{26}_D$: -110° (*c* 1, $CHCl_3$); IR ($CHCl_3$) ν (cm^{-1}) 3684, 3621, 3344, 3213, 3020, 1742, 1673, 1583, 1519, 1476, 1440, 1392, 1295, 1217, 1157, 1130, 1044, 928, 770, 668, 491; ^1H NMR (500 MHz, $CDCl_3$) δ: 9.47 (s, 1H), 8.11-8.09 (d, *J* = 7.6 Hz, 1H), 7.84-7.82 (dd, *J* = 7.9 Hz, 1.5 Hz, 1H), 7.55-7.52 (t, *J* = 7Hz, 1H), 7.21-7.17 (t, *J* = 7.2 Hz, 1H), 7.08 (bs, 1H), 4.36-4.34 (dd, *J* = 8.5 Hz, 3Hz, 1H), 3.76-3.71 (dd, *J* = 17.7 Hz, 5.8 Hz, 1H), 3.66-3.61 (dd, *J* = 6.4 Hz, 18 Hz, 1H), 3.55-3.51 (m, 1H), 3.42 (s, 3H), 2.3 (bs, 1H), 2.25-2.19 (m, 1H), 1.96-1.91 (m, 2H); ^{13}C NMR (125 MHz, $CDCl_3$) δ: 170.9, 168.4, 156.6, 134.8, 133.4, 129.0, 128.9, 124.4, 124.1, 81.8, 62.0, 52.2, 47.5, 43.8, 30.3, 28.4, 28.2, 24.3; HRMS: $C_{19}H_{28}O_7N_3S$, Calcd: 442.1642 Found: 442.1644; $C_{19}H_{27}O_7N_3SNa$, Calcd: 464.1462 Found: 464.1465.

General procedure for the C-terminus amidation of 15a, 16a, 19c, 20a, 26a, 26d, 27a, and 27d to 15b, 16b, 20b, 26b, 26e, 27b and 27e respectively:

The compounds **15a**, **16a**, **19c, 20a, 26a, 26d, 27a** and **27d** were dissolved in MeOH (2 mL) followed by addition of methanolic methyl amine solution (2 mL) at 0 ^oC. The reaction was monitored by TLC and after completion the solvent was stripped off. The crude product was purified by column chromatography

which yielded the products **15b, 16b, 19f, 20b, 26b, 26e, 27b** and **27e**, respectively.

tert-butyl-2-((2-(N-(2-(methylamino)-2-oxoethyl)sulfamoyl)phenyl) carbamoyl)pyrrolidine-1-carboxylate 15d:

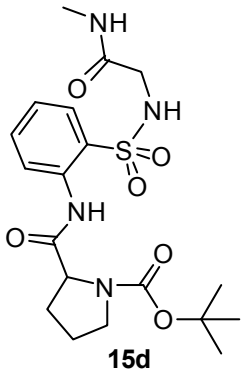
15d

Compound **15d** was isolated as a white solid (eluent: pet. ether/ethyl acetate: 40:60, R*f*: 0.4) in 95% yield; mp: 130-132 ^{o}C; $[\alpha]^{26}_{D}$: -42° (*c* 1, $CHCl_3$); IR ($CHCl_3$) ν (cm^{-1}): 3683, 3618, 3438, 3356, 3192, 3018, 2888, 2400, 1670, 1583, 1523, 1475, 1420, 1394, 1336, 1218, 1158, 927, 847, 771, 590; ^{1}H NMR (500 MHz, $CDCl_3$) δ: 9.26 (s, 1H), 8.03-7.99 (d, *J* = 8.1 Hz, 1H), 7.92-7.87 (dd, *J* = 7.9 Hz, 1.5 Hz, 1H), 7.64-7.56 (m, 1H), 7.33-7.24 (m, 2H), 7.2-7.14 (m, 1H), 6.52-6.49 (m, 1H), 4.3-4.24 (m, 1H), 3.63-3.42 (m, 4H), 2.67-2.64 (d, *J* = 4.8 Hz, 3H), 2.33-2.23 (m, 2H), 2.14-1.89 (m, 2H), 1.47 (s, 9H), ^{13}C NMR (125 MHz, $CDCl_3$) δ: 171.3, 168.1, 156.1, 134.2, 133.8, 129.3, 125.3, 125.0, 81.4, 61.9, 47.5, 45.4, 30.4, 28.4, 25.9, 24.5; HRMS: $C_{19}H_{29}O_6N_4S$, Calcd: 441.1802 Found: 441.1794; $C_{19}H_{28}O_6N_4SNa$, Calcd: 463.1622 Found: 463.1613.

tert-butyl-2-((2-(N-(2-(2-((2-(N-(2-methoxy-2-oxoethyl)sulfamoyl)phenyl)-carbamoyl)pyrrolidin-1-yl)-2-oxoethyl)sulfamoyl)phenyl)carbamoyl) pyrrolidine-1-carboxylate 16a:

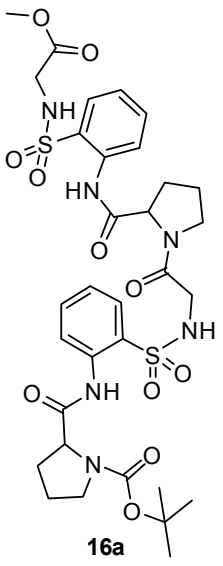
16a

The acid **15c** (0.09 g, 0.22 mmol) was coupled with the amine **15b** (0.07 g, 0.22 mmol) using EDC. HCl (0.05 g, 0.27 mmol), Et_3N (0.09 mL, 0.68 mmol) and HOBt (0.006 g, 0.04 mmol) in dry DCM at 0 °C. The reaction mixture was allowed to attain room temperature and stirred for 12 h. Later, the reaction mixture was washed with sat. $NaHCO_3$, water, sat $KHSO_4$ and brine solutions. The organic layer was dried over anhydrous Na_2SO_4 and evaporated under reduced pressure to get the crude product which on purification by column chromatography (eluent: pet ether/ethyl acetate: 40:60, R*f*: 0.4) yielded **16a** (0.08 g, 50%) as a white solid;

mp: 150-153 °C; $[\alpha]^{26}_D$: -90° (*c* 1, $CHCl_3$); IR ($CHCl_3$) ν (cm^{-1}): 3344, 3017, 1690, 1584, 1525, 1438, 1387, 1332, 1218, 1156, 1126, 847, 770, 480. ^{1}H NMR (400 MHz, $CDCl_3$) δ: 9.75 (s, 1H), 9.36 (s, 1H), 8.27 (d, *J* = 7.7 Hz, 1H), 8.16-8.14 (d, *J* = 8 Hz, 1H), 7.91-7.89 (d, *J* = 7.5 Hz, 1H), 7.82-7.8 (d, *J* = 7.7 Hz, iH), 7.59-7.5 (m, 2H), 7.24-7.16 (m, 2H), 7.01 (bs, 1H), 6.75 (bs, 1H), 4.44-4.4 (m, 2H), 4.15-4.09 (q, ethyl acetate), 3.93-3.82 (m, 1H), 3.77-3.75 (m, 2H), 3.67-3.53 (m, 2H), 3.46 (s, 2H), 3.39-3.36 (m, 1H), 2.3-1.92 (m, 8H), 1.53 (s, 9H); ^{13}C NMR (100 MHz, $CDCl_3$) δ: 171.3, 169.1, 168.5, 156.5, 135.6, 134.8, 133.8, 133.5, 129.1, 129, 128.6, 124.1, 123.7, 81.4, 62.1, 61.9, 60.3, 52.3, 47.6, 46.5, 44.5, 44, 30.4, 28.7, 28.5, 24.8, 24.3; HRMS: $C_{32}H_{43}O_{11}N_6S_2$, Calcd: 751.2426 Found: 751.2418; $C_{32}H_{42}O_{11}N_6S_2Na$, Calcd: 773.2245 Found: 773.2234.

tert-butyl-2-((2-(N-(2-(2-((2-(N-(2-(methylamino)-2-oxoethyl)sulfamoyl) phenyl)carbamoyl)pyrrolidin-1-yl)-2-oxoethyl)sulfamoyl)phenyl)carbamoyl) pyrrolidine-1-carboxylate 16b:

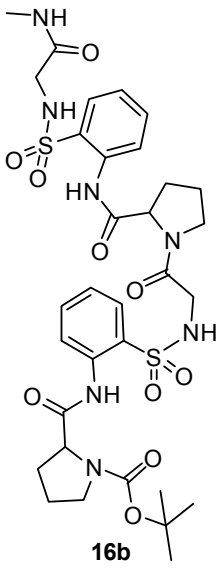

16b

The compound **16b** was isolated as a white solid following the above mentioned procedure in 90% yield; mp: 160-162 °C; $[\alpha]^{26}_D$: -92.3° (*c* 0.26, $CHCl_3$); IR ($CHCl_3$) ν (cm^{-1}): 3684, 3618, 3019, 2400, 1666, 1584, 1523, 1475, 1423, 1334, 1215, 1045, 928, 770, 669, 490; ^{1}H NMR (400 MHz, $CDCl_3$) δ: 9.45 (s, 1H), 9.41 (s, 1H), 8.22-8.2 (d, *J* = 8.2 Hz, 1H), 8.11-8.09 (d, *J* = 7.9 Hz, 1H), 7.94-7.92 (d, *J* = 7.3 Hz, 1H), 7.88-7.86 (d, *J* = 7.3 Hz, 1H), 7.62-7.59 (t, *J* = 7.6 Hz, 1H), 7.58-7.55 (t, *J* = 8.2 Hz, 1H), 7.25-7.21 (m, 2H), 7.01 (bs, 2H), 6.73 (bs, 1H), 4.33-4.32 (dd, *J* = 8.9 Hz, 2.7 Hz, 1H), 4.28-4.27 (d, *J* = 5.2 Hz, 1H), 3.92-3.88 (dd, *J* = 16.9 Hz, 3.2 Hz, 1H), 3.73-3.69 (m, 1H), 3.56-3.42 (m, 5H), 3.31-3.28 (m, 1H), 2.69-2.68 (d, *J* = 4.9 Hz, 3H), 2.3-2.29 (m, 1H), 2.25-2.22 (m, 2H), 2.1-1.93 (m, 5H), 1.53 (s, 9H); ^{13}C NMR (100 MHz, $CDCl_3$) δ: 171.2, 169.3, 168.5, 168.3, 157.1, 135.1, 134.6, 134.2, 130.0, 129.1, 128.7, 126.6, 124.9, 124.4, 124.2, 123.4, 82.1, 62.1, 47.7, 46.6, 45.3, 44.3, 30.5, 29.1, 28.6, 26.6, 24.7, 24.3; HRMS: $C_{32}H_{44}O_{10}N_7S_2$, Calcd: 750.2586 Found: 751.2578; $C_{32}H_{43}O_{10}N_7S_2Na$, Calcd: 772.2405 Found: 772.2386.

Methyl ((2-(2-bromoacetamido)phenyl)sulfonyl)-L-prolinate 19a:

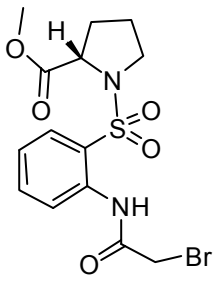

19a

To the solution of amine **18** (1g, 3.5 mmol) in dry DCM at 0 ^{o}C, 2-bromoacetyl bromide (0.36 mL, 4.2 mmol) was added followed by the addition of DIPEA (0.9 mL, 5.2 mmol). The reaction mixture was stirred for 8 h after attaining room temperature. Later, the reaction mixture was diluted with DCM, washed with sat. $NaHCO_3$ and brine solutions. The organic layer was dried over anhydrous Na_2SO_4 and evaporated under reduced pressure to get the crude product which on purification by column chromatography (eluent: pet ether/ethyl acetate: 70:30, R*f*: 0.5) yielded **19a** (0.99 g, 70%); $[\alpha]^{26}_{D}$: -60.6° (*c* 0.3, $CHCl_3$); IR ($CHCl_3$) ν (cm^{-1}): 3305, 3020, 2956, 1742, 1698, 1586, 1531, 1466, 1437, 1337, 1216, 1154, 766, 667, 607, 578; ^{1}H NMR (400 MHz, $CDCl_3$) δ: 10.12 (s, 1H), 8.51-8.47 (dd, *J* = 8.3 Hz, 0.9 Hz, 1H), 7.96-7.91 (dd, *J* = 8 Hz, 1.6 Hz, 1H), 7.66-7.58 (td, *J* = 8.5 Hz, 1.6 Hz, 1H), 7.29-7.21 (td, *J* = 7 Hz, 1.2 Hz, 1H), 4.48-4.42 (dd, *J* = 8.3 Hz, 3.9 Hz, 1H), 4.1-4.09 (m, 2H), 3.7 (s, 3H), 3.4-3.33 (t, *J* = 7Hz, 2H), 2.28-2.18 (m, 1H), 2.13-1.86 (m, 3H); ^{13}C NMR (50 MHz, $CDCl_3$) δ: 172.5, 164.9, 136.1, 134.4, 129.9, 125.7, 124.2, 122.8, 59.5, 52.6, 48.6, 30.9, 29.3, 24.6; HRMS: $C_{14}H_{18}O_5N_2BrS$, Calcd: 407.0094 Found: 407.0089.

Methyl ((2-(2-azidoacetamido)phenyl)sulfonyl)-L-prolinate 19b:

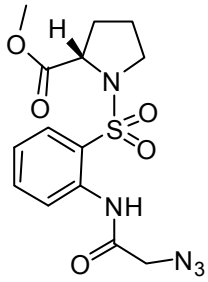

19b

A solution of compound **19a** (0.3g, 0.7 mmol) and NaN_3 (0.14g, 2.2 mmol) in dry DMF was heated at 80 ^{o}C for 5 h exactly. Later, the reaction mixture was taken into ethyl acetate, washed with water and brine solution. The organic layer was then dried over anhydrous Na_2SO_4 and evaporated under reduced pressure to get the crude product which on purification by column chromatography (eluent: petether/ethyl acetate: 70:30, R*f*: 0.5) yielded **19b** (0.24 g, 89%); $[\alpha]^{26}_{D}$: -71.79° (*c* 0.3, $CHCl_3$); IR ($CHCl_3$) ν (cm^{-1}): 3305, 3021, 2116, 1704, 1586, 1531, 1437, 1338, 1284, 1218, 1153, 1021, 771, 668, 608; ^{1}H NMR (400 MHz, $CDCl_3$) δ: 10.12 (s, 1H), 8.55-8.5 (d, *J* = 8.3 Hz, 1H), 7.95-7.9 (dd, *J* = 7.9 Hz, 1.5 Hz, 1H), 7.65-7.56 (td, *J* = 7.7 Hz, 1.5 Hz, 1H), 7.29-7.21 (m, 1H), 6.76-6.7 (m, 1H), 4.46-4.4 (dd, *J* = 8.3 Hz, 3.7 Hz, 1H), 4.18

(s, 2H), 3.67 (s, 3H), 3.41-3.33 (m, 2H), 2.27-1.82 (m, 4H); ^{13}C NMR (100 MHz, $CDCl_3$) δ: 172.3, 165.8, 135.8, 134.4, 129.9, 125.8, 124.8, 122.7, 117.4, 116.6, 59.6, 53.1, 52.6, 48.8, 31, 24.6; HRMS: $C_{14}H_{18}O_5N_5S$, Calcd: 368.1023 Found: 368.1022; $C_{14}H_{17}O_5N_5SNa$, Calcd: 390.0843 Found: 390.0838.

Methyl-((2-(2-((tert-butoxycarbonyl)amino)acetamido)phenyl)sulfonyl)-L-prolinate 19c:

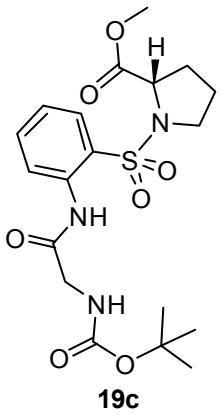

19c

To a solution of **19b** (0.35 g, 1.47 mmol) in methanol (15 mL), 10% Pd/C (0.06 g) was added and subjected to shaking in parr shaker at 60 psi for 12 h to yield amine **19d**. To protect the amine *in situ* as Boc derivative, $(Boc)_2O$ (0.179g, 0.82 mmol) was added to the reaction mixture. Further, the catalyst was filtered through celite and the solvent was evaporated to furnish **19c**, which on purification by column chromatography (eluent: petether/ethyl acetate: 70:30, R*f*: 0.4) yielded the Boc protected compound quantitatively; $[\alpha]^{26}_D$: -46.66° (*c* 0.3, $CHCl_3$); IR ($CHCl_3$) ν (cm^{-1}): 3684, 3615, 3325, 3020, 2980, 2400, 1701, 1586, 1524, 1467, 1438, 1393, 1369, 1340, 1215, 1155, 1072, 1049, 929, 756, 669, 608, 477; ^{1}H NMR (400 MHz, $CDCl_3$) δ: 10.10 (s, 1H), 8.57-8.55 (d, *J* = 7.3 Hz, 1H), 7.9-7.88 (d, *J* = 7.6 Hz, 1H), 7.61-7.57 (t, *J* = 7.3 Hz, 1H), 7.23-7.2 (t, *J* = 7.2 Hz, 1H), 5.46 (s, 1H), 4.37-4.34 (m, 1H), 4.08-4.01 (m, 2H), 3.74 (s, 3H), 3.39-3.36 (m, 1H), 3.33-3.28 (m, 1H), 2.19-2.14 (m, 1H), 2.06-1.92 (m, 3H), 1.88-1.81 (m, 1H), 1.48 (s, 9H); ^{13}C NMR (100 MHz, $CDCl_3$) δ: 172.8, 168.8, 136.5, 134.5, 129.8, 125.8, 123.8, 122.7, 80.3, 59.7, 52.7, 48.7, 45.1, 30.9, 28.2, 24.6; HRMS: $C_{19}H_{28}O_7N_3S$, Calcd: 442.1642 Found: 442.1639; $C_{14}H_{17}O_5N_5SNa$, Calcd: 464.1462 Found: 464.1459.

tert-butyl-(S)-(2-((2-((2-(methylcarbamoyl)pyrrolidin-1-l)sulfonyl)phenyl) amino)-2-oxoethyl)carbamate 19f:

The compound **19f** was synthesized as mentioned in the earlier procedure and was isolated as a pasty mass in quantitative yield. (eluent: ethyl acetate: R*f*: 0.2); $[\alpha]^{26}_D$: +4.65° (*c* 0.4, $CHCl_3$); IR ($CHCl_3$) ν (cm^{-1}): 3678, 3464, 3328, 3018, 2400,

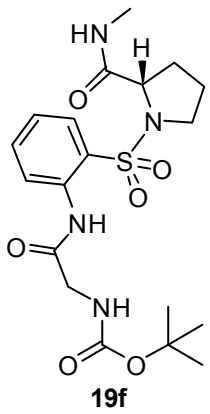
19f

1655, 1535, 1436, 1414, 1369, 1340, 1218, 1155, 1049, 928, 850, 771, 667, 608, 484; ^{1}H NMR (400 MHz, $CDCl_3$) δ: 10.23 (s, 1H), 8.56-8.54 (d, *J* = 8.2 Hz, 1H), 7.84-7.82 (d, *J* = 7.3 Hz, 1H), 7.25-7.22 (t, *J* = 7.6 Hz, 1H), 6.71 (bs, 1H), 5.69 (bs, 1H), 4.16-4.11 (m, *J* = 1H), 4.08-4.06 (dd, *J* = 3.9 Hz, 8.8 Hz, 1H), 3.86-3.81 (m, 1H), 3.58 (bs, 1H), 3.43-3.41 (m, 1H), 3.23-3.18 (m, 1H), 2.03-2.01 (m, 1H), 2.0-1.92 (m, 3H), 1.88-1.83 (m, 2H), 1.76-1.66 (m, 2H), 1.46-1.44 (bs, 9H); ^{13}C NMR (100 MHz, $CDCl_3$) δ: 172.4, 168.9, 136.4, 134.8, 130.3, 129.9, 124.1, 123.8, 122.7, 117.9, 80.4, 62.0, 49.7, 45.3, 31.2, 29.6, 26.3, 24.3; HRMS: $C_{19}H_{29}O_6N_4S$, Calcd: 441.1802 Found: 441.1799.

Methyl-((2-(2-((S)-1-((2-(2-((tert-butoxycarbonyl)amino)acetamido)phenyl) sulfonyl)pyrrolidine-2-carboxamido)acetamido)phenyl)sulfonyl)-prolinate 20a:

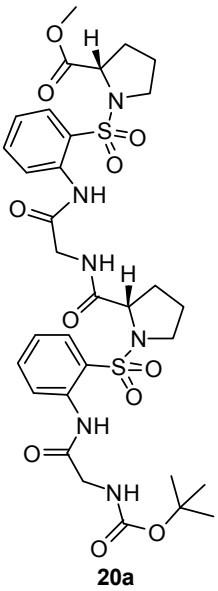
20a

The acid **19c** (0.09 g, 0.22 mmol) was coupled with the amine **19b** (0.07 g, 0.22 mmol) using EDC. HCl (0.05 g, 0.27 mmol), Et_3N (0.09 mL, 0.68 mmol) and HOBt (0.006 g, 0.04 mmol) in dry DCM at 0 °C, the reaction mixture was allowed to attain room temperature and stirred for 12h. Later, the reaction mixture was washed sequentially with sat. $NaHCO_3$, water, sat $KHSO_4$ and brine solutions. The organic layer was dried over anhydrous Na_2SO_4 and evaporated under reduced pressure to get the crude product which on purification by column chromatography (eluent: pet ether/ethyl acetate: 40:60, R*f*: 0.4) yielded 20a (0.08 g, 50%) as a pasty mass; $[\alpha]^{26}_{D}$: -26° (*c* 1, $CHCl_3$); IR ($CHCl_3$) ν (cm^{-1}): 3344, 3017, 1690, 1584, 1525, 1438, 1387, 1332, 1218, 1156, 1126, 847, 770, 480. ^{1}H NMR (400 MHz, $CDCl_3$) δ: 10.28-10.06 (m, 1H), 9.86 (s, 1H), 8.61-8.55 (m, 1H), 8.44-8.43 (d, *J* = 8.2 Hz, 1H), 7.91-7.87 (m, 2H), 7.62-7.58 (m, 2H), 7.26-7.21 (m, 2H), 5.76 (bs, 1H), 4.4-4.36 (m, 2H), 4.22-4.11 (m, 4H), 3.79-3.75 (m, 3H), 3.63-3.63 (m, 1H), 3.36-3.29 (m, 3H), 2.22-2.11 (m, 2H), 2.07-2.04 (m, 2H), 1.98-1.92 (m, 2H),

1.88-1.84 (m, 2H), 1.47-1.46 (m, 9H); ^{13}C NMR (100 MHz, $CDCl_3$) δ: 172.8, 170.3, 169.1, 167.7, 167.6, 136.1, 136, 134.8, 134.6, 134.5, 130, 129.9, 129.8, 124.1, 123.9, 123.5, 122.8, 122.4, 62, 60.3, 59.8, 59.5, 52.9, 49.8, 48.8, 43.9, 43.6, 30.8, 30.7, 28.2, 24.7, 24.4; ESI-MS: $C_{32}H_{42}O_{11}N_6S_2Na$, Calcd: 773.2353 Found: 773.10.

tert-butyl-(2-((2-(((S)-2-((2-((2-(((S)-2-(methylcarbamoyl)pyrrolidin-1-sulfo-nyl)phenyl)amino)-2-oxoethyl)carbamoyl)pyrrolidin-1-yl)sulfonyl)phenyl) amino)-2-oxoethyl)carbamate 20b:

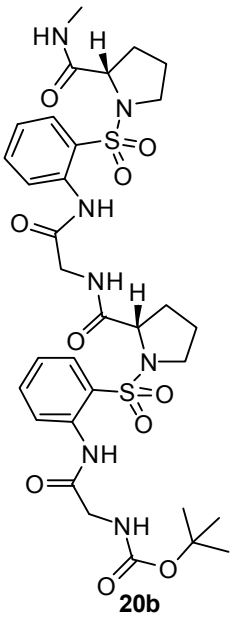

20b

Compound **20b** was isolated as a sticky substance following the above mentioned procedure; $[\alpha]^{26}_D$: -10° (*c* 1, $CHCl_3$); IR ($CHCl_3$) ν (cm^{-1}): 3684, 3618, 3019, 2400, 1666, 1584, 1523, 1475, 1423, 1334, 1215, 1045, 928, 770, 669, 490; ^{1}H NMR (500 MHz, $CDCl_3$) δ: 10.08 (s, 1H), 8.5-8.49 (m, 1H), 7.89-7.88 (d, *J* = 7.9 Hz, 1H), 7.66-7.63 (t, *J* = 7.6 Hz, 1H), 7.36 (bs, 1H), 7.3-7.23 (m, 3H), 7.11-7.05 (m, 1H), 6.81 (bs, 1H), 6.63-6.61 (d, *J* = 8.2 Hz, 2H), 5.85-5.73 (m, 1H), 5.02-4.92 (m, 2H), 4.17-4.04 (m, 2H), 3.97-3.96 (d, *J* = 5.4 Hz, 2H), 3.82-3.81 (d, *J* = 5.8 Hz, 2H), 3.55 (bs, 1H), 3.23-3.21 (m, 1H), 2.84-2.82 (m, 3H), 2.12-1.6 (m, 8H), 1.43 (bs, 9H); ^{13}C NMR (100 MHz, $CDCl_3$) δ: 172.1, 169.2, 168.5, 168.3, 139.2, 130.1, 124, 123, 115.8, 114.8, 82.1, 62.1, 47.7, 43.1, 45.3, 44.3, 33.8, 29.6, 28.2, 22.6.

(S)-N-(2-(methylamino)-2-oxoethyl)-1-((2-nitrophenyl)sulfonyl)pyrrolidine-2-carboxamide 22:

To the amine **21** (0.83 g, 2.8 mmol), 2-nitro benzene sulfonyl chloride (0.62 g, 2.8 mmol) was added followed by the addition of Et_3N (1.18 mL, 8.4 mmol) in DCM at 0 °C. The reaction was allowed to attain room temperature and stirred for 5 h. Then, the reaction mixture was diluted with DCM and washed with $NaHCO_3$ solution, water and brine solution. The organic layer was dried over Na_2SO_4 and evaporated under reduced pressure. The residue obtained was purified through

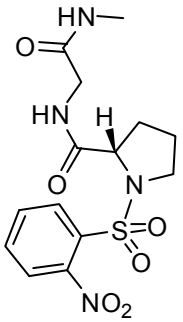

22

column chromatography (eluent: pet ether/ethyl acetate: ethyl acetate R*f*: 0.5) yielded **22** (0.75 g, 72%) as a white solid; mp: 67 °C-69 °C; $[\alpha]^{26}_{D}$: -146° (*c* 1, $CHCl_3$); IR ($CHCl_3$) ν (cm^{-1}): 3685, 3418, 3020, 2401, 1667, 1548, 1416, 1372, 1218, 1165, 1127, 1083, 1008, 928, 852, 667, 572; ^{1}H NMR (400 MHz, $CDCl_3$) δ: 8.07-8.05 (dd, *J* = 7.2 Hz, 1.2 Hz, 1H), 7.8-7.72 (m, 2H), 7.67-7.65 (dd, *J* = 7.5 Hz, 1.7 Hz, 1H), 7.33-7.3 (t, *J* = 6 Hz, 1H), 6.64-6.63 (bs, 1H), 4.43-4.4 (dd, *J* = 8.2 Hz, 4 Hz, 1H), 4.04-3.98 (dd, *J* = 16.8 Hz, 6.5 Hz, 1H), 3.87-3.82 (dd, *J* = 16.8 Hz, 5.5 Hz, 1H), 3.71-3.65 (m, 1H), 3.53-3.47 (m, 1H), 2.77-2.75 (d, *J* = 4.7 Hz, 3H), 2.21-2.12 (m, 1H), 2.08-1.98 (m, 2H), 1.93-1.85 (m, 1H); ^{13}C NMR (100 MHz, $CDCl_3$) δ: 171.6, 169.2, 148.5, 134.4, 131.9, 131.1, 130.1, 124.2, 62.2, 49.8, 43, 31.1, 26.1, 24.6; HRMS: $C_{14}H_{19}O_6N_4S$, Calcd: 371.1020 Found: 371.1017; $C_{14}H_{18}O_6N_4SNa$, Calcd: 393.0839 Found: 393.0833.

N-(4-bromophenyl)-1-((2-nitrophenyl)sulfonyl)pyrrolidine-2-carboxamide 24:

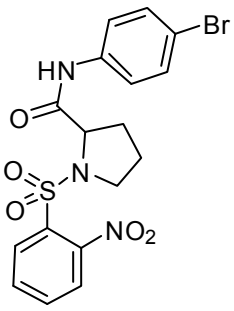

24

To a solution of amine **23b** (0.72 g, 2.7 mmol) in dry DCM (10 mL), Et_3N (1.14 mL, 8.1 mmol) was added and stirred at 0 °C for 15 min. Then, 2-nitrobenzoyl chloride (0.59 g, 2.7 mmol) was added to the reaction mixture. The reaction mixture was allowed to attain room temperature and was further stirred for 12 h. Later, the reaction mixture was washed sequentially with sat. $NaHCO_3$, water, dil. HCl and brine solutions. The organic layer was dried over anhydrous Na_2SO_4 and evaporated under reduced pressure to get the crude product which on purification by column chromatography (eluent: pet ether/ethyl acetate: 75:25, R*f*: 0.5) yielded **24** (0.6 g, 60%); mp: 125-128 °C; $[\alpha]^{26}_{D}$: -224° (*c* 1, $CHCl_3$); IR ($CHCl_3$) ν (cm^{-1}): 3356, 3020, 2400, 1689, 1591, 1545, 1489, 1397, 1370, 1303, 1218, 1164, 1126, 1073, 929, 852, 772, 666, 603, 486; ^{1}H NMR (400 MHz, $CDCl_3$) δ: 8.5 (bs, 1H), 8.1-8.04 (m, 1H), 7.73-7.59 (m, 3H), 7.41-7.3 (m, 4H), 4.57-4.52 (dd, *J* = 2.6 Hz, 8 Hz, 1H), 3.7-3.63 (t, *J* = 6.4 Hz, 2H), 2.47-2.35 (m, 1H), 2.26-2.11 (m, 1H), 2.07-1.92 (m, 2H); ^{13}C NMR (100 MHz, $CDCl_3$) δ: 168.7, 148.1, 136.2, 134.5,

132, 131.8, 131.4, 130.5, 124.2, 121.1, 117.2, 62.6, 49.7, 30.8, 24.5; HRMS: $C_{17}H_{17}O_5N_3BrS$, Calcd: 454.0067 Found: 454.0069.

Methyl ((2-(2-nitrobenzamido)phenyl)sulfonyl)prolinate 26a:

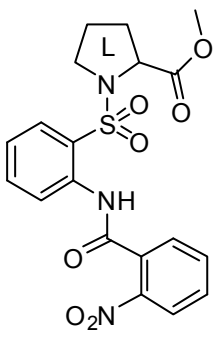

26a

To the solution of amine **18** (0.2 g, 0.7 mmol) in DCM (10 mL), pyridine (0.08 mL, 1.05 mmol) was added followed by the addition of 2-nitro benzoyl chloride (0.19 g, 1.05 mmol) drop wise at 0 °C. The reaction mixture was allowed to attain room temperature and stirred for 5 h. Later, the reaction mixture was diluted with DCM and washed with CuSO4 solution, water, sat. $NaHCO_3$ solutions. The organic layer was dried over Na_2SO_4 and evaporated under reduced pressure. The residue obtained was purified through column chromatography (eluent: pet ether/ethyl acetate: 60:40, R*f*: 0.5) yielded **26a** (0.277 g, 90%); mp: 143-146 ^oC; $[\alpha]^{26}_D$: -164° (*c* 1, $CHCl_3$); IR ($CHCl_3$) ν (cm^{-1}): 3323, 3022, 2400, 1743, 1690, 1586, 1531, 1437, 1348, 1218, 1157, 1077, 1020, 857, 771, 499; ^1H NMR (200 MHz, $CDCl_3$) δ: 10.08 (s, 1H), 8.69-8.65 (d, *J* = 8.2 Hz, 1H), 8.16-8.12 (d, *J* = 7.3 Hz, 1H), 7.99-7.94 (dd, *J* = 7.9 Hz, 1.5 Hz, 1H), 7.78-7.59 (m, 4H), 7.34-7.26 (m, 1H), 4.45-4.38 (dd, *J* = 8.8 Hz, 4.2 Hz, 1H), 3.44 (s, 3H), 3.33-3.21 (m, 2H), 2.29-2.14 (m, 1H), 2.06-1.83 (m, 3H); ^{13}C NMR (50 MHz, $CDCl_3$) δ: 172.4, 164.8, 146.5, 136.3, 134.7, 133.8, 132.9, 130.5, 130, 128.6, 125.7, 124.4, 124.3, 123.4, 59.2, 52.4, 48.7, 30.8, 24.7; HRMS: $C_{19}H_{20}O_7N_3S$, Calcd: 434.1016 Found: 434.1016.

N-methyl-1-((2-(2-nitrobenzamido)phenyl)sulfonyl)pyrrolidine-2-carboxamide 26c:

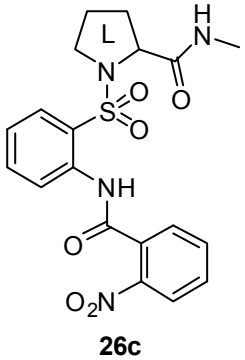

26c

The compound **26c** was isolated as yellow solid in 95% yield. mp: 63-66 ^oC; $[\alpha]^{26}_D$: -136° (*c* 1, $CHCl_3$); IR ($CHCl_3$) ν (cm^{-1}): 3437, 3334, 3019, 1673, 1587, 1533, 1465, 1435, 1349, 1215, 1153, 1153, 1118, 1047, 928, 857, 757, 669, 608; ^1H NMR (500 MHz, $CDCl_3$) δ: 9.99 (s, 1H), 8.64-8.62 (d, *J* = 8.5 Hz, 1H), 8.14-8.12 (d, *J* = 7.3 Hz, 1H), 7.9-7.88 (dd, *J* = 7.9 Hz, 1.5 Hz, 1H), 7.79-7.76 (t, *J* = 6.8 Hz, 1H), 7.72-7.65 (m, 3H), 7.34-7.31 (t, *J* = 7.1 Hz, 1H), 6.53 (bs, 1H), 4.21-

4.18 (dd, *J* = 8.8 Hz, 3 Hz 4.2 Hz, 1H), 3.47-3.44 (m, 1H), 3.37-3.32 (m, 1H), 2.68-2.67 (d, *J* = 4.8 Hz, 3H), 2.19-2.14 (m, 1H), 1.94-1.87 (m, 2H); ^{13}C NMR (125 MHz, $CDCl_3$) δ: 171.1, 164.3, 146.4, 136.4, 135.1, 134.1, 132.4, 131.1, 129.9, 128.3, 124.2, 123.2, 62.3, 49.5, 30.9, 26.2, 24.4; HRMS: $C_{19}H_{21}O_6N_4S$, Calcd: 433.1176 Found: 433.118; $C_{19}H_{21}O_6N_4S$, Calcd: 455.0996 Found: 433.0995.

N-(4-bromophenyl)-1-((2-(2-nitrobenzamido)phenyl)sulfonyl)pyrrolidine-2-carboxamide 26d:

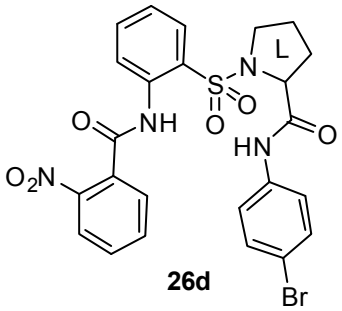

26d

The compound **26d** was synthesized following the similar protocol used for **26a** and it was isolated as a yellow solid; mp: 194-197 ^{o}C; $[\alpha]^{26}_{D}$: -242° (*c* 1, $CHCl_3$); IR ($CHCl_3$) ν (cm^{-1}): 3683, 3622, 3019, 2400, 1692, 1589, 1531, 1434, 1348, 1218, 1046, 928, 771, 668; ^{1}H NMR (500 MHz, $CDCl_3$) δ: 10.02 (s, 1H), 8.68-8.66 (d, *J* = 8.2 Hz, 1H), 8.34 (s, 1H), 8.12-8.1 (d, *J* = 7.9 Hz, 1H), 7.93-7.91 (dd, *J* = 7.9 Hz, 1.2 Hz, 1H), 7.71-7.61 (m, 4H), 7.4-7.38 (m, 2H), 7.35-7.31 (m, 3H), 4.32-4.3 (dd, *J* = 8.5 Hz, 3.3 Hz, 1H), 3.56-3.52 (m, 1H), 3.45-3.38 (m, 1H), 2.32-2.27 (m, 1H), 2.02-1.94 (m, 1H), 1.91-1.83 (m, 2H); ^{13}C NMR (125 MHz, $CDCl_3$) δ: 168.7, 164.4, 146.3, 136.5, 136.1, 135.4, 134.1, 132.4, 131.1, 129.8, 126.2, 124. 2, 124.9, 123.8, 123.3, 121.5, 117.3; HRMS: $C_{19}H_{21}O_6N_4S$, Calcd: 433.1176 Found: 433.118; $C_{24}H_{22}O_6N_4BrS$, Calcd: 575.0417 Found: 575.0414.

General method for N-acetylation of 26a and 27a to yield 26e and 27d:

To the solutions of the nitro compounds **26a** and **27a** in MeOH, 10% Pd/C was added and subjected to shaking on parr shaker at 60 psi for 6 h. Later, the reaction mixture was filtered through celite to remove the catalyst and the residue obtained by evaporating the filtrate under reduced pressure was carried to the next reaction without purification. To these residues in dry DCM, Ac_2O, Et_3N, DMAP were added simultaneously at 0 °C and allowed to stir for 5 h which yielded the acetylated products **26e** and **27d** respectively.

Methyl ((2-(2-acetamidobenzamido)phenyl)sulfonyl)prolinate 26e:

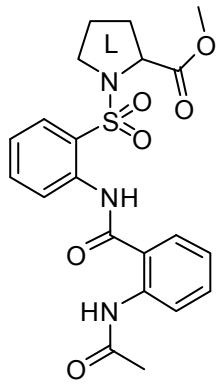

26e

Compound 26e was isolated as white solid. mp: 113-115 ^{o}C; $[\alpha]^{26}_{D}$: -62° (*c* 1, $CHCl_3$); IR ($CHCl_3$) ν (cm^{-1}): 3785, 3682, 3620, 3343, 3018, 2400, 1748, 1686, 1663, 1583, 1522, 1429, 1336, 1294, 1218, 1045, 928, 668; ^{1}H NMR (500 MHz, $CDCl_3$) δ: 11.13 (s, 1H), 8.69-8.67 (d, *J* = 8.2 Hz, 1H), 8.57-8.55 (dd, *J* = 8.5 Hz, 1 Hz, 1H), 7.95-7.94 (dd, *J* = 8.2 Hz, 1.5 Hz, 1H), 7.79-7.78 (dd, *J* = 7.9 Hz, 1.2 Hz, 1H), 7.68-7.64 (t, *J* = 8.6 Hz, 1H), 7.56-7.52 (t, *J* = 8.5 Hz, 1H), 7.31-7.28 (t, *J* = 8.2 Hz, 1H), 7.19-7.15 (t, *J* = 8.2 Hz, 1H), 4.54-4.32 (dd, *J* = 8.5 Hz, 3.3 Hz, 1H), 3.46 (s, 3H), 3.44-3.35 (m, 2H), 2.23 (s, 3H), 2.18-2.08 (m, 1H), 2.04-1.92 (m, 2H), 1.91-1.82 (m, 1H); ^{13}C NMR (125 MHz, $CDCl_3$) δ: 171.8, 168.9, 167.4, 140.5, 136.2, 134.3, 133.4, 129.8, 126.9, 124.3, 123, 121.5, 119.5, 59.9, 52.3, 48.5, 30.9, 25.3, 24.5; HRMS: $C_{21}H_{24}O_6N_3S$, Calcd: 446.138 Found: 446.138; $C_{24}H_{22}O_6N_4BrS$, Calcd: 468.12 Found: 468.1199.

General method for ester hydrolysis:

To the solutions of esters **26b** and **26e** (10 mmol, 1 equiv) in methanol, $LiOH{\cdot}H_2O$ (40 mmol, 4 equiv) dissolved in water (12 mL) was added at 0 °C. After the complete consumption of starting material, the solvent was evaporated under reduced pressure and the residue was treated with sat. $KHSO_4$ solution followed by extraction into DCM (2 X 25 mL). The acid derivatives **26c** and **26f**, respectively obtained after evaporation of the solvent were used for the next reaction without purification.

((2-(2-acetamidobenzamido)phenyl)sulfonyl)proline 26f:

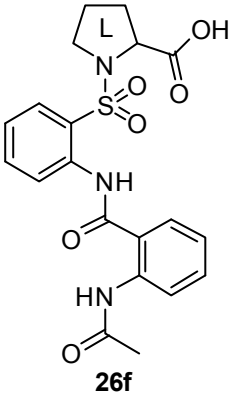

26f

Compound **26f** was isolated as abrown solid. mp: 169-172 ^{o}C; $[\alpha]^{26}_{D}$: -92° (*c* 1, $CHCl_3$); IR ($CHCl_3$) ν (cm^{-1}): 3684, 3619, 3353, 3020, 2400, 1734, 1664, 1583, 1523, 1471, 1430, 1331, 1296, 1217, 1045, 928, 770, 667, 626, 607; ^{1}H NMR (400 MHz, $CDCl_3$) δ: 10.42 (s, 1H), 10.25 (s, 1H), 8.48-8.46 (d, *J* = 8 Hz, 1H), 8.19-8.17 (dd, *J* = 8 Hz, 1H), 7.96-7.94 (d, *J* = 9

Hz, 1H), 7.74-7.72 (d, *J* = 7.7 Hz, 1H), 7.68-7.64 (t, *J* = 7.5 Hz, 1H), 7.55-7.51 (t, *J* = 7.5 Hz, 1H), 7.3-7.23 (m, 4H), 4.47-4.44 (dd, *J* = 3 Hz, J = 8.7 Hz, 1H), 3.46-3.36 (m, 2H), 3.3-3.25 (m, 1H), 2.21 (s, 3H), 2.17-2.04 (m, 2H), 1.94-1.88 (m, 2H); ^{13}C NMR (100 MHz, $CDCl_3$) δ: 173.8, 171.3, 167, 138.1, 136, 134.2, 132.6, 129.8, 127.1, 126.7, 124.6, 124.2, 124, 123, 60, 47.9, 30.9, 24.9, 24.6; HRMS: $C_{20}H_{22}O_6N_3S$, Calcd: 432.1224 Found: 432.1224.

1-((2-(2-acetamidobenzamido)phenyl)sulfonyl)-N-methylpyrrolidine-2-carbox-amide 26g:

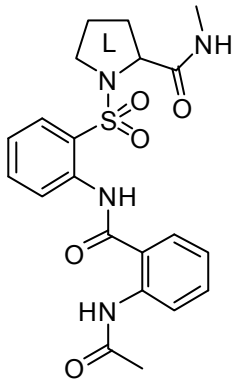

26g

The compound **26e** was amidated to **26g** and isolated as a white solid following the above mentioned procedure; mp: 69-72 °C; $[\alpha]^{26}_D$: -142° (*c* 1, $CHCl_3$); IR ($CHCl_3$) ν (cm^{-1}): 3684, 3621, 3438, 3340, 3020, 2400, 1668, 1582, 1523, 1428, 1338, 1293, 1216, 1046, 928, 771, 669; ^{1}H NMR (500 MHz, $CDCl_3$) δ: 11.08 (s, 1H), 10.52 (s, 1H), 8.67-8.66 (d, *J* = 8.2 Hz, 1H), 8.63-8.61 (dd, *J* = 8.2 Hz, 1 Hz, 1H), 7.9-7.89 (dd, *J* = 7.9 Hz, 1.5 Hz, 1H), 7.77-7.75 (dd, *J* = 7.9 Hz, 1.2 Hz, 1H), 7.72-7.69 (t, *J* = 8.6 Hz, 1H), 7.57-7.54 (t, *J* = 8.5 Hz, 1H), 7.34-7.31 (t, *J* = 8.2 Hz, 1H), 7.19-7.16 (t, *J* = 8.2 Hz, 1H), 6.59 (bs, 1H), 4.18-4.16 (m, 1H), 3.5-3.46 (m, 1H), 3.24-3.19 (m, 1H), 2.76-2.74 (d, *J* = 5.1 Hz, 3H), 2.23 (s, 3H), 2.21-2.17 (m, 1H), 1.81-1.7 (m, 3H); ^{13}C NMR (125 MHz, $CDCl_3$) δ: 170.9, 168.9, 167.3, 140.6, 136.6, 134.9, 133.7, 129.9, 126.6, 124.7, 124.3, 123.2, 123, 121.8, 119.1, 62.5, 49.5, 30.5, 26.3, 25.3, 24.3; HRMS: $C_{21}H_{25}O_5N_4S$, Calcd: 445.154 Found: 445.154; $C_{21}H_{24}O_5N_4SNa$, Calcd: 467.136 Found: 467.136.

General method for N-acetylation of 26d and 27c to yield 26h and 27f:

To the solutions of the nitro compounds **26d** and **27f** in MeOH, $SnCl_2.2H_2O$ was added and refluxed to 80 °C for 12 h. Later, the methanol was evaporated under reduced pressure. The residue was taken into ethyl acetate and washed with sat. $NaHCO_3$ solution. The organic layer was dried over Na_2SO_4 and evaporated under vacum to give the respective amines as residues. To these residues in dry DCM, Ac_2O, Et_3N, DMAP were added simultaneously at 0 °C and

allowed to stir for 5 h which yielded the acetylated products **26h** and **27f** respectively.

1-((2-(2-acetamidobenzamido)phenyl)sulfonyl)-N-(4-bromophenyl) pyrrolidine-2-carboxamide 26h:

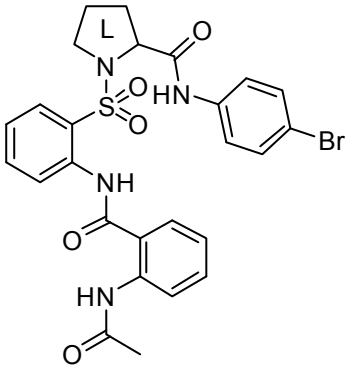

26h

Compound **26h** was isolated as a fluffy mass following the above mentioned protocol; $[\alpha]^{26}_{D}$: -110° (*c* 1, $CHCl_3$); IR ($CHCl_3$) ν (cm^{-1}): 3684, 3619, 3348, 3019, 2400, 1689, 1582, 1521, 1427, 1337, 1292, 1218, 1046, 928, 771, 667; ^{1}H NMR (500 MHz, $CDCl_3$) δ: 11.02 (s, 1H), 10.51 (s, 1H), 8.65-8.63 (d, *J* = 8.2 Hz, 1H), 8.62-8.61 (dd, *J* = 8.5 Hz, 1 Hz, 1H), 8.5 (s, 1H), 7.93-7.91 (dd, *J* = 7.9 Hz, 1.2 Hz, 1H), 7.73-7.69 (m, 2H), 7.52-7.49 (t, *J* = 8.5 Hz, 1H), 7.42-7.36 (m, 4H), 7.34-7.31 (t, *J* = 8 Hz, 1H), 7.08-7.04 (t, *J* = 8.2 Hz, 1H), 4.25-4.23 (dd, *J* = 7.9 Hz, 2.4 Hz, 1H), 3.6-3.56 (m, 1H), 3.31-3.26 (m, 1H), 2.3-2.28 (m, 1H), 2.22 (s, 3H), 1.87-1.84 (m, 2H), 1.83-1.76 (m, 1H); ^{13}C NMR (125 MHz, $CDCl_3$) δ: 169, 168.4, 167.3, 140.4, 136.7, 136.1, 133.7, 131.8, 129.8, 126.5, 124.8, 124, 123.2, 121.8, 121.4, 119.1, 117.3, 82.7, 49.9, 30.4, 25.3, 24.4; HRMS: $C_{21}H_{25}O_5N_4S$, Calcd: 445.154 Found: 445.154; $C_{26}H_{26}O_4N_4BrS$, Calcd: 587.0781 Found: 587.0778.

N-methyl-1-(((2-(2-nitrobenzamido)phenyl)sulfonyl)prolyl)pyrrolidine-2-carbox-amide 27b:

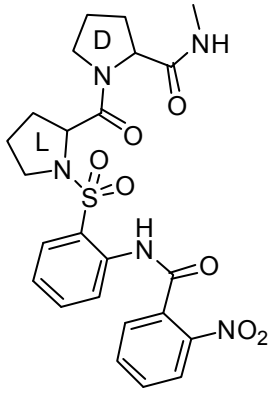

27b

The acid **26b** was coupled to hydro chloride salt of D-Pro-OMe to obtain the ester compound **27a**. The ester was converted to its methyl amide derivative **27b** following the mentioned procedure as a sticky substance; $[\alpha]^{26}_{D}$: +100° (*c* 0.1, $CHCl_3$); IR ($CHCl_3$) ν (cm^{-1}): 3683, 3620, 3421, 3020, 2400, 1658, 1581, 1529, 1436, 1349, 1296, 1217, 1046, 928, 770, 668, 627, 607; ^{1}H NMR (500 MHz, $CDCl_3$) δ: 10.28 (s, 1H), 8.84-8.83 (d, *J* = 8.2 Hz, 1H), 8.1-

8.08 (dd, *J* = 8.2 Hz, 1 Hz, 1H), 8.05-8.03 (dd, J = 8.2 Hz, 1.5 Hz, 1H), 7.74-7.7 (m, 2H), 7.61-7.57 (t, *J* = 8.5 Hz, 1H), 7.48-7.46 (dd, J = 7.6 Hz, 1.5 Hz, 1H), 7.29-7.26 (t, *J* = 8.2 Hz, 1H), 6.5 (bs, 1H), 4.46-4.43 (t, *J* = 7.9 Hz, 1H), 3.97-3.95 (d, *J* = 6.4 Hz, 1H), 3.76-3.72 (t, *J* = 9.7 Hz, 1H), 3.33-3.28 (m, 1H), 3.24-3.2 (m, 1H), 3.03-2.99 (m, 1H), 2.69-2.68 (d, *J* = 4.8 Hz, 3H), 2.3-2.26 (m, 1H), 2.22-2.16 (sex, *J* = 12.2 Hz, 6.7 Hz, 1H), 2.04-1.97 (m, 2H), 1.94-1.86 (m, 4H), 1.85-1.77 (m, 2H); ^{13}C NMR (125 MHz, $CDCl_3$) δ: 170.8, 170.5, 166.4, 146.5, 137.4, 135.4, 134.1, 133.3, 130.6, 128.8, 123.9, 123.7, 123.2, 60.5, 57.7, 48.4, 46.7, 29.6, 28.7, 26.2, 25.2, 23.9; HRMS: $C_{24}H_{28}O_7N_5S$, Calcd: 530.1704 Found: 530.1706; $C_{26}H_{26}O_4N_4NaS$, Calcd: 552.1523 Found: 552.1522.

N-(4-bromophenyl)-1-(((2-(2-nitrobenzamido)phenyl)sulfonyl)prolyl) pyrrolidine-2-carboxamide 27c:

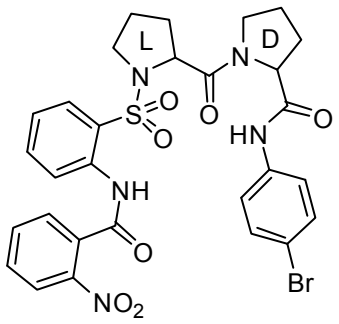

27c

To the acid **26b** (0.22 g, 0.54 mmol), the amine **23d** (0.14 g, 0.54 mmol), EDC.HCl (0.12 g, 0.65 mmol), HOBt (0.01 g, 0.01 mmol), Et_3N (0.09 mL, 0.65 mmol) in DCM were added at 0 °C and the reaction mixture was allowed to stirring for 12 h. Then, the reaction mixture was diluted with DCM followed by washing with sat. NaHCO3, brine and sat KHSO4 solutions sequentially. The organic layer was dried over Na2SO4 and evaporated under reduced pressure. The residue was purified through column chromatography that yielded the product **27c** (0.178 g, 50%); $[\alpha]^{26}_D$: +46° (*c* 1, $CHCl_3$); IR ($CHCl_3$) ν (cm^{-1}): 3684, 3620, 3421, 3020, 2400, 1689, 1582, 1521, 1427, 1337, 1292, 1218, 1046, 928, 771, 667; ^{1}H NMR (500 MHz, $CDCl_3$) δ: 10.25 (s, 1H), 8.85-8.83 (d, *J* = 8.2 Hz, 1H), 8.07-8.05 (d, *J* = 8 Hz, 3H), 7.74-7.7 (t, *J* = 7.2 Hz, 1H), 7.55-7.51 (m, 3H), 7.46-7.42 (t, *J* = 6.7 Hz, 1H), 7.38-7.35 (d, *J* = 8.7 Hz, 2H), 7.3-7.27 (t, *J* = 7.2 Hz, 2H), 7.06-7.04 (t, *J* = 7.5 Hz, 1H), 4.53-4.49 (t, *J* = 7.7 Hz, 1H), 4.07-4.08 (d, *J* = 6.2 Hz, 1H), 3.82-3.78 (t, *J* = 9.2 Hz, 1H), 3.37-3.35 (m, 1H), 3.25-3.2 (m, 1H), 3.07-3.02 (m, 1H), 2.42-2.4 (m, 1H), 2.27-2.21 (m, 1H), 2.05-1.81 (m, 4H), 1.61-1.51 (m, 2H); ^{13}C NMR (125 MHz, $CDCl_3$) δ: 171.7, 168.4, 166.2, 146.4, 137.3, 136.9, 135.8, 134.1, 133, 131.8, 130.7, 128.8,

123.8, 123.3, 121.3, 116.9, 61.1, 57.7, 48.4, 47, 36.5, 29.7, 28.7, 25.2, 24.1; HRMS: $C_{29}H_{29}O_7N_5BrS$, Calcd: 672.0945 Found: 672.0945.

1-(((2-(2-acetamidobenzamido)phenyl)sulfonyl)prolyl)-N-methylpyrrolidine-2-carboxamide 27e:

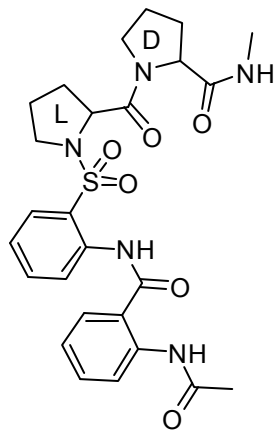

27e

The acetylated compound **27e** was synthesized from the corresponding ester **27d** following the mentioned protocol. $[\alpha]^{26}_D$: +125° (*c* 1.3, $CHCl_3$); IR ($CHCl_3$) ν (cm^{-1}): 3684, 3618, 3418, 2400, 1661, 1583, 1523, 1429, 1295, 1216, 1045, 928, 771, 668, 627; ^1H NMR (500 MHz, $CDCl_3$) δ: 11.02 (s, 1H), 10.25 (s, 1H), 8.65-8.62 (d, *J* = 8.2 Hz, 1H), 8.49-8.47 (d, *J* = 8.2 Hz, 1H), 8.0-7.97 (dd, J = 8 Hz, 1.5 Hz, 1H), 7.81-7.79 (dd, *J* = 8 Hz, 1.2 Hz, 1H), 7.62-7.64 (t, *J* = 8.7 Hz, 1H), 7.56-7.52 (t, *J* = 8.5 Hz, 1H), 7.33-7.29 (t, *J* = 8.2 Hz, 2H), 7.18-7.14 (t, *J* = 8 Hz, 1H), 6.74-6.73 (bs, 1H), 4.55-4.53 (d, *J* = 6.2 Hz, 1H), 4.5-4.47 (dd, *J* = 7.5 Hz, 5.2 Hz, 1H), 3.63 (m, 1H), 3.58-3.54 (m, 1H), 3.47-3.41 (m, 1H), 3.34-3.27 (m, 2H), 2.66-2.65 (d, *J* = 4.7 Hz, 3H), 2.36-2.29 (m, 1H), 2.17-2.1 (m, 3H), 2.01-1.85 (m, 4H); ^{13}C NMR (125 MHz, $CDCl_3$) δ: 171, 170.9, 168.9, 167.4, 140.2, 136.1, 134.3, 133.5, 129.5, 126.9, 126.8, 124.7, 123.4, 123.1, 121.7, 119.4, 60.5, 59.6, 48.1, 46.9, 30, 26.2, 26.1, 25, 24.3; HRMS: $C_{26}H_{32}O_6N_5S$, Calcd: 542.2068 Found: 542.2068; $C_{26}H_{32}O_6N_5NaS$, Calcd: 564.1887 Found: 564.1884.

1-(((2-(2-acetamidobenzamido)phenyl)sulfonyl)prolyl)-N-(4-bromophenyl) pyrrolidine-2-carboxamide 27f:

Compound **27f** was synthesized following the procedure mentioned above. $[\alpha]^{26}_D$: +78° (*c* 1, $CHCl_3$); IR ($CHCl_3$) ν (cm^{-1}): 3683, 3620, 3420, 3020, 2400, 1689, 1582, 1524, 1427, 1337, 1292, 1221, 1046, 928, 771, 669; ^1H NMR (500 MHz, $CDCl_3$) δ: 11.0 (s, 1H), 10.37 (s, 1H), 8.73 (s, 1H), 8.63-8.62 (d, *J* = 8.2 Hz, 1H), 8.39-8.38 (d, *J* = 8.2 Hz, 1H), 7.98-7.96 (dd, *J* = 7.9 Hz, 1.5 Hz, 1H), 7.78-7.76 (dd, *J* = 7.9 Hz, 1.2 Hz, 1H), 7.61-7.58 (t, *J* = 8.6 Hz, 1H), 7.53-7.5 (t, *J* = 7.9 Hz, 1H), 7.44-7.42 (d, *J* = 8.8 Hz, 2H), 7.33-7.31 (d, *J* = 8.8 Hz, 2H), 7.24-7.21 (t,

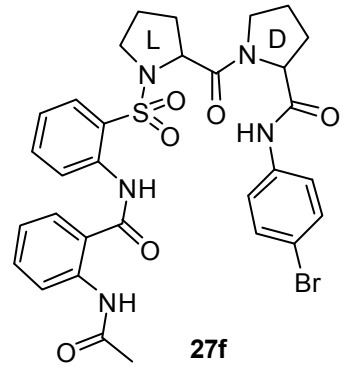

27f

J = 8.2 Hz, 1H), 7.08-7.05 (t, *J* = 8 Hz, 1H), 4.68-4.67 (d, *J* = 6.1 Hz, 1H), 4.51-4.49 (t, *J* = 6.3 Hz, 1H), 4.13-4.09 (q, ethyl acetate), 3.52-3.49 (m, 2H), 3.24-3.28 (m, 2H), 2.46-2.44 (m, 1H), 2.2 (s, 3H), 2.18-2.12 (m, 2H), 1.98-1.86 (m, 6H); ^{13}C NMR (125 MHz, $CDCl_3$) δ: 171.8, 168.9, 168.5, 167.4, 140.3, 137, 136, 134.3, 133.6, 131.5, 129.5, 127, 126.9, 124.7, 123.6, 123, 121.5, 61.2, 59.7, 48.1, 47, 30, 27.7, 25.3, 25; HRMS: $C_{31}H_{33}O_6N_5BrS$, Calcd: 684.1309 Found: 684.1312.

Methyl ((2-nitrophenyl)sulfonyl)-L-prolyl-D-prolinate 29a:

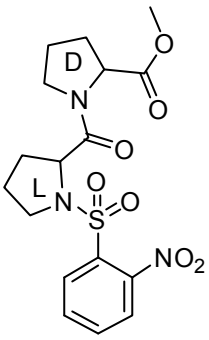

29a

The procedure followed to synthesize **29a** was exactly similar to that of **24**. The compound 29a was isolated a white solid; mp: 154-156 °C; $[\alpha]^{26}_D$: +40° (*c* 0.3, $CHCl_3$); IR ($CHCl_3$) ν (cm^{-1}): 3684, 3618, 34410, 3019, 2400, 1741, 1654, 1545, 1436, 1371, 1215, 1046, 928, 877, 770, 669; ^{1}H NMR (200 MHz, $CDCl_3$) δ: 8.16-8.02 (m, 1H), 7.74-7.58 (m, 3H), 4.92-4.81 (m, 1H), 4.59-4.32 (m, 1H), 4-3.9 (m, 1H), 3.77 (s, 1H), 3.66-3.58 (m, 3H), 3.57-3.38 (m, 2H), 2.38-1.80 (m, 8H); ^{13}C NMR (125 MHz, $CDCl_3$) δ: 172.7, 172.1, 170.8, 169.9, 148.1, 133.2, 132.9, 131.6, 130.5, 128.9, 123.6, 60.1, 59.2, 52.5, 51.9, 48.9, 46.7, 31.1, 30.9, 30.5, 28.8, 25.1, 24.8, 24.6, 22.4; HRMS: $C_{17}H_{22}O_7N_3S$, Calcd: 412.1173 Found: 412.1175; $C_{17}H_{22}O_7N_3NaS$,Calcd: 434.0992 Found: 434.0991.

Methyl ((2-nitrophenyl)sulfonyl)-L-prolyl-L-prolinate 29b:

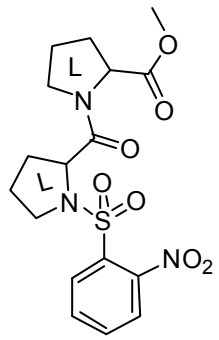

29b

Compound **29b** was synthesized following the similar protocol as **24** was synthesized. It was isolated as a white solid; mp: 128-130 °C; $[\alpha]^{26}_D$: -102° (*c* 1, $CHCl_3$); IR ($CHCl_3$) ν (cm^{-1}): 3684, 3618, 34410, 3019, 2400, 1741, 1654, 1545, 1436, 1371, 1215, 1046, 928, 877, 770, 669; ^{1}H NMR (200 MHz, $CDCl_3$) δ: 8.24-8.15 (m, 1H), 7.72-7.57 (m, 3H), 4.87-4.82 (dd, *J* = 7.9 Hz, 3.2 Hz, 1H), 4.51-4.45 (dd, *J* = 8.4 Hz, 4Hz, 1H), 3.85-3.73 (m, 1H), 3.69 (s, 3H), 3.66-3.47 (m, 3H), 2.33-1.89 (m, 8H);

^{13}C NMR (125 MHz, $CDCl_3$) δ: 172.7, 172.1, 170.8, 169.9, 148.1, 133.2, 132.9, 131.6, 130.5, 128.9, 123.6, 60.1, 59.2, 52.5, 51.9, 48.9, 46.7, 31.1, 30.9, 30.5, 28.8, 25.1, 24.8, 24.6, 22.4; HRMS: $C_{17}H_{22}O_7N_3S$, Calcd: 412.1173 Found: 412.1175; $C_{17}H_{22}O_7N_3NaS$,Calcd: 434.0992 Found: 434.0991.

N-methyl-1-(((2-nitrophenyl)sulfonyl)prolyl)pyrrolidine-2-carboxamide 29c:

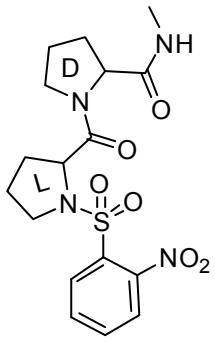

29c

Compound 29c was prepared by amidating 29[a] following the same procedure mentioned above. $[\alpha]^{26}_D$: +12° (*c* 1, $CHCl_3$); IR ($CHCl_3$) ν (cm^{-1}): 3684, 3618, 34410, 3019, 2400, 1741, 1654, 1545, 1436, 1371, 1215, 1046, 928, 877, 770, 669; ^{1}H NMR (500 MHz, $CDCl_3$) δ: 8.22-8.19 (m, 1H), 7.74-7.71 (m, 2H), 7.67-7.65 (m, 1H), 6.73 (bs, 1H), 4.80-4.77 (dd, *J* = 7.6 Hz, 4.8 Hz, 1H), 4.6-4.59 (d, *J* = 6.1 Hz, 1H), 3.95-3.91 (quin, *J* = 9.7 Hz, 5.1 Hz, 1H), 3.65-3.6 (m, 1H), 3.54-3.4 (m, 3H), 2.64-2.63 (d, *J* = 4.8 Hz, 3H), 2.36-2.33 (m, 1H), 2.3-2.21 (m, 2H), 2.09-1.9 (m, 5H); ^{13}C NMR (125 MHz, $CDCl_3$) δ: 172.7, 172.1, 170.8, 169.9, 148.1, 133.2, 132.9, 131.6, 130.5, 128.9, 123.6, 60.1, 59.2, 52.5, 51.9, 48.9, 46.7, 31.1, 30.9, 30.5, 28.8, 25.1, 24.8, 24.6, 22.4; HRMS: $C_{17}H_{23}O_6N_4S$, Calcd: 411.1333 Found: 411.1333; $C_{17}H_{22}O_7N_3NaS$,Calcd: 433.1152 Found: 433.1150.

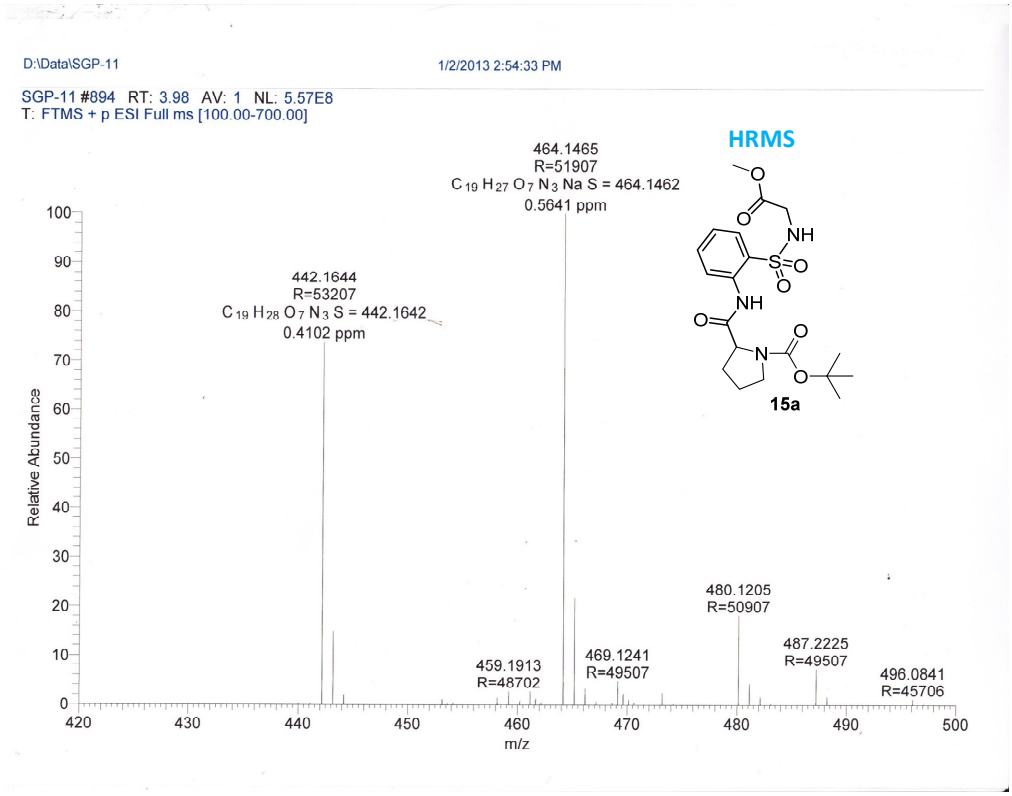
D:\Data\SGP-11
1/2/2013 2:54:33 PM
SGP-11 #894 RT: 3.98 AV: 1 NL: 5.57E8
T: FTMS + p ESI Full ms [100.00-700.00]
HRMS
464.1465
R=51907
C 19 H 27 O 7 N 3 Na S = 464.1462
0.5641 ppm
442.1644
R=53207
C 19 H 28 O 7 N 3 S = 442.1642
0.4102 ppm
480.1205
R=50907
487.2225
R=49507
459.1913
R=48702
469.1241
R=49507
496.0841
R=45706
15a
Relative Abundance
m/z

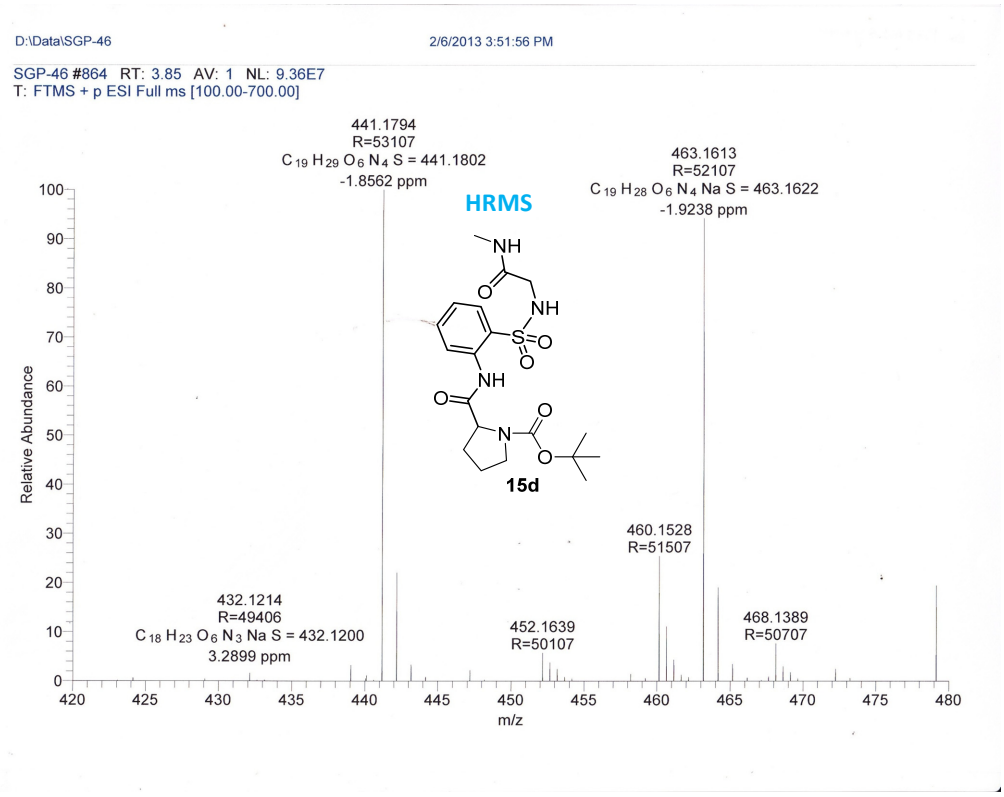
D:\Data\SGP-46
2/6/2013 3:51:56 PM
SGP-46 #864 RT: 3.85 AV: 1 NL: 9.36E7
T: FTMS + p ESI Full ms [100.00-700.00]
441.1794
R=53107
C 19 H 29 O 6 N 4 S = 441.1802
-1.8562 ppm
HRMS
463.1613
R=52107
C 19 H 28 O 6 N 4 Na S = 463.1622
-1.9238 ppm
460.1528
R=51507
432.1214
R=49406
C 18 H 23 O 6 N 3 Na S = 432.1200
3.2899 ppm
452.1639
R=50107
468.1389
R=50707
15d
Relative Abundance
m/z

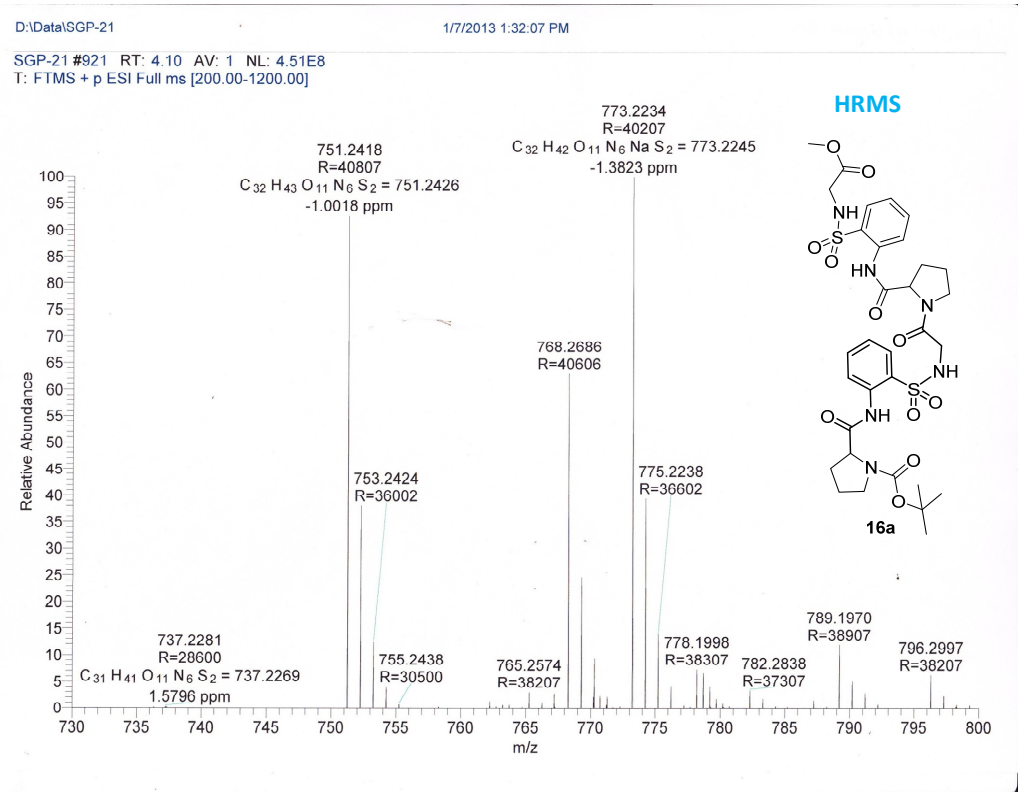
D:\Data\SGP-21
1/7/2013 1:32:07 PM
SGP-21 #921 RT: 4.10 AV: 1 NL: 4.51E8
T: FTMS + p ESI Full ms [200.00-1200.00]
HRMS
773.2234
R=40207
C32 H42 O11 N6 Na S2 = 773.2245
-1.3823 ppm
751.2418
R=40807
C32 H43 O11 N6 S2 = 751.2426
-1.0018 ppm
768.2686
R=40606
753.2424
R=36002
775.2238
R=36602
737.2281
R=28600
C31 H41 O11 N6 S2 = 737.2269
1.5796 ppm
755.2438
R=30500
765.2574
R=38207
778.1998
R=38307
782.2838
R=37307
789.1970
R=38907
796.2997
R=38207
16a
Relative Abundance
m/z

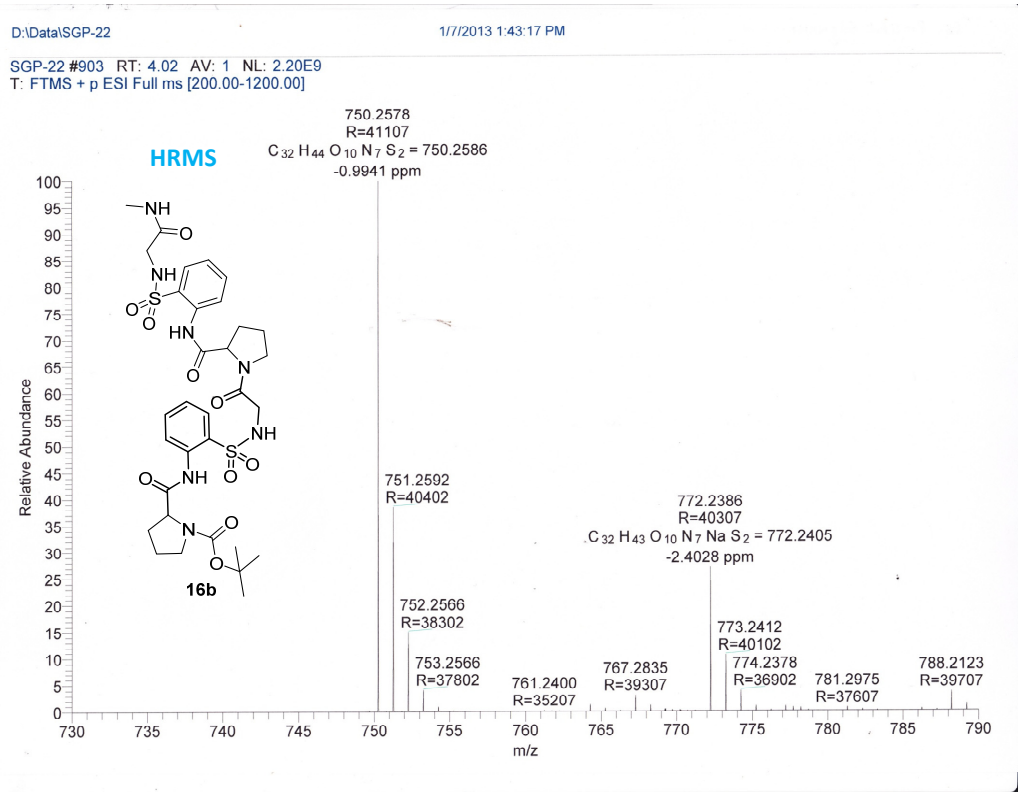
D:\Data\SGP-22
1/7/2013 1:43:17 PM
SGP-22 #903 RT: 4.02 AV: 1 NL: 2.20E9
T: FTMS + p ESI Full ms [200.00-1200.00]
HRMS
750.2578
R=41107
C32 H44 O10 N7 S2 = 750.2586
-0.9941 ppm
751.2592
R=40402
772.2386
R=40307
C32 H43 O10 N7 Na S2 = 772.2405
-2.4028 ppm
752.2566
R=38302
773.2412
R=40102
753.2566
R=37802
761.2400
R=35207
767.2835
R=39307
774.2378
R=36902
781.2975
R=37607
788.2123
R=39707
16b
Relative Abundance
m/z

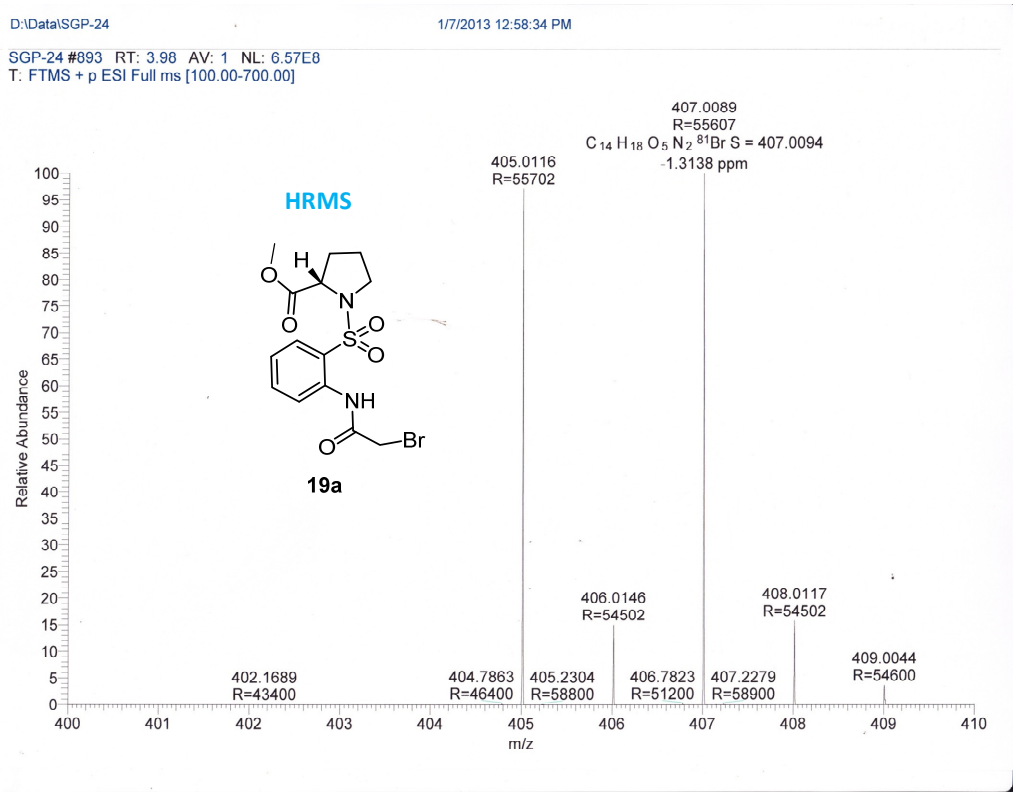
D:\Data\SGP-24
1/7/2013 12:58:34 PM
SGP-24 #893 RT: 3.98 AV: 1 NL: 6.57E8
T: FTMS + p ESI Full ms [100.00-700.00]
HRMS
19a
407.0089
R=55607
C 14 H 18 O 5 N 2 81Br S = 407.0094
-1.3138 ppm
405.0116
R=55702
406.0146
R=54502
408.0117
R=54502
409.0044
R=54600
402.1689
R=43400
404.7863
R=46400
405.2304
R=58800
406.7823
R=51200
407.2279
R=58900
Relative Abundance
m/z

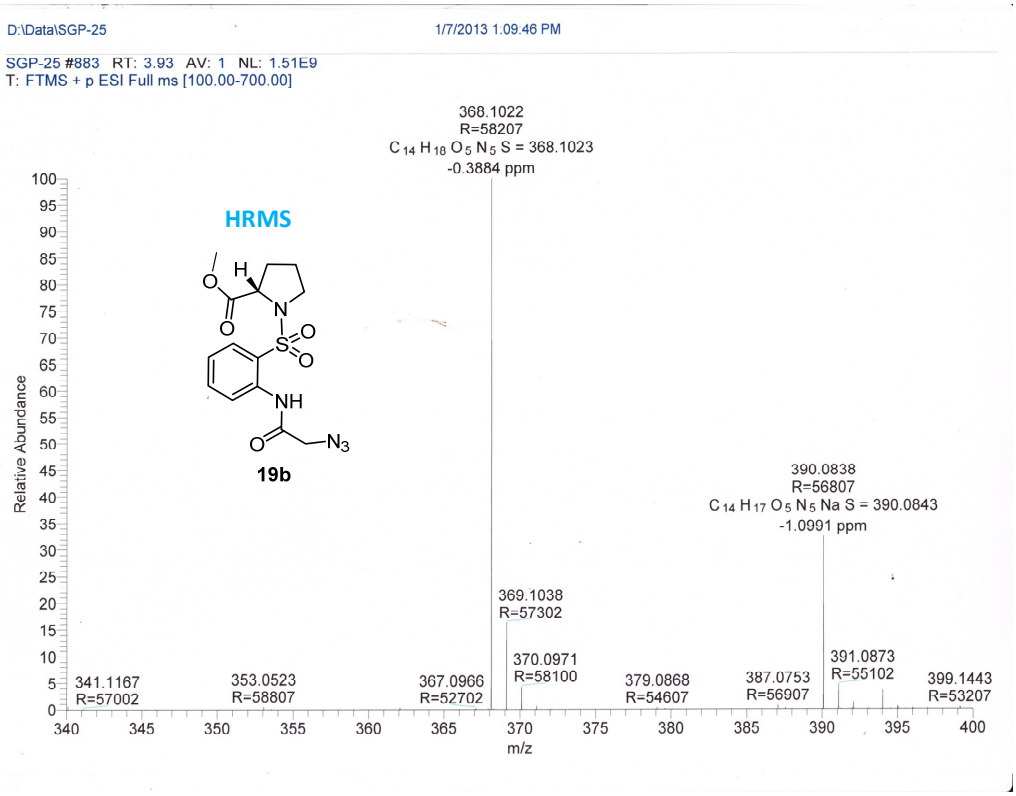
D:\Data\SGP-25
1/7/2013 1.09:46 PM
SGP-25 #883 RT: 3.93 AV: 1 NL: 1.51E9
T: FTMS + p ESI Full ms [100.00-700.00]
HRMS
19b
368.1022
R=58207
C 14 H 18 O 5 N 5 S = 368.1023
-0.3884 ppm
390.0838
R=56807
C 14 H 17 O 5 N 5 Na S = 390.0843
-1.0991 ppm
369.1038
R=57302
370.0971
R=58100
391.0873
R=55102
341.1167
R=57002
353.0523
R=58807
367.0966
R=52702
379.0868
R=54607
387.0753
R=56907
399.1443
R=53207
Relative Abundance
m/z

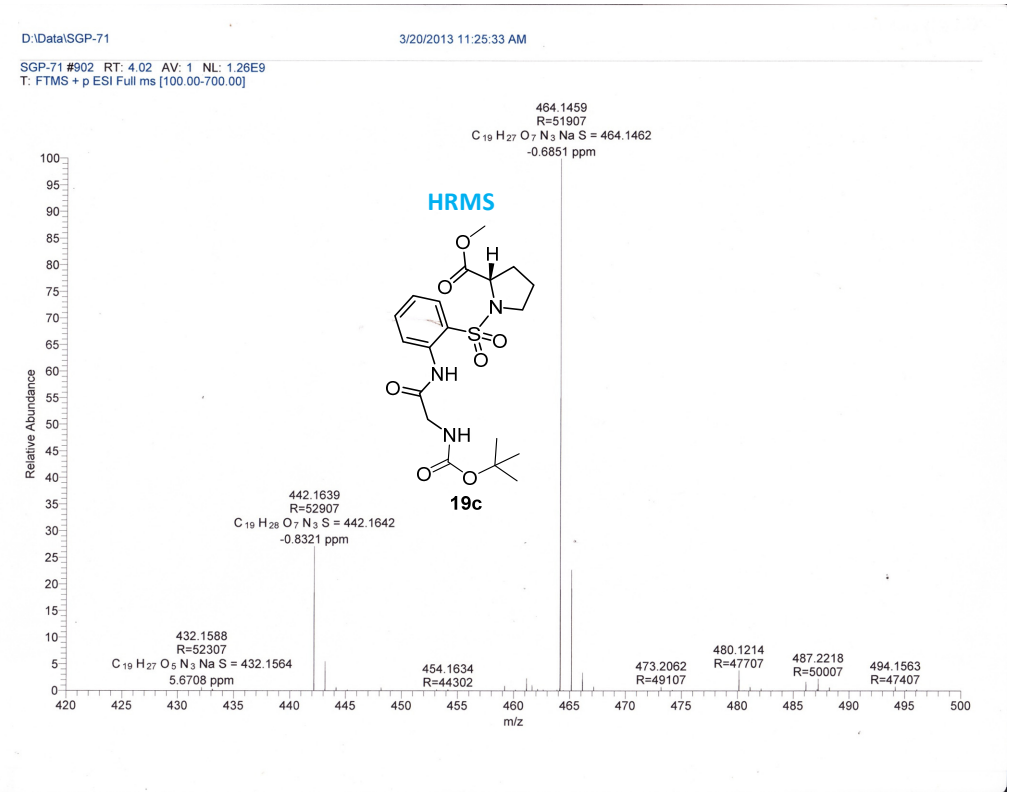
D:\Data\SGP-71
3/20/2013 11:25:33 AM
SGP-71 #902 RT: 4.02 AV: 1 NL: 1.26E9
T: FTMS + p ESI Full ms [100.00-700.00]
464.1459
R=51907
C19 H27 O7 N3 Na S = 464.1462
-0.6851 ppm
HRMS
19c
442.1639
R=52907
C19 H28 O7 N3 S = 442.1642
-0.8321 ppm
432.1588
R=52307
C19 H27 O5 N3 Na S = 432.1564
5.6708 ppm
454.1634
R=44302
473.2062
R=49107
480.1214
R=47707
487.2218
R=50007
494.1563
R=47407
Relative Abundance
m/z

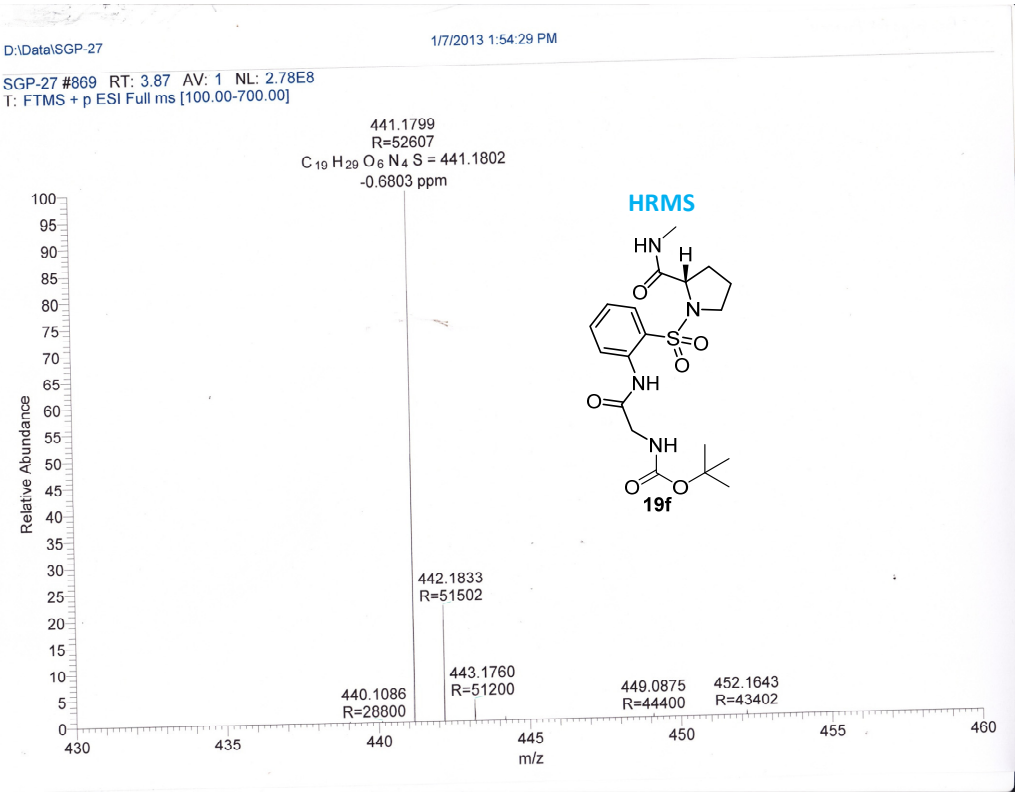
D:\Data\SGP-27
1/7/2013 1:54:29 PM
SGP-27 #869 RT: 3.87 AV: 1 NL: 2.78E8
T: FTMS + p ESI Full ms [100.00-700.00]
441.1799
R=52607
C19 H29 O6 N4 S = 441.1802
-0.6803 ppm
HRMS
19f
442.1833
R=51502
443.1760
R=51200
440.1086
R=28800
449.0875
R=44400
452.1643
R=43402
Relative Abundance
m/z

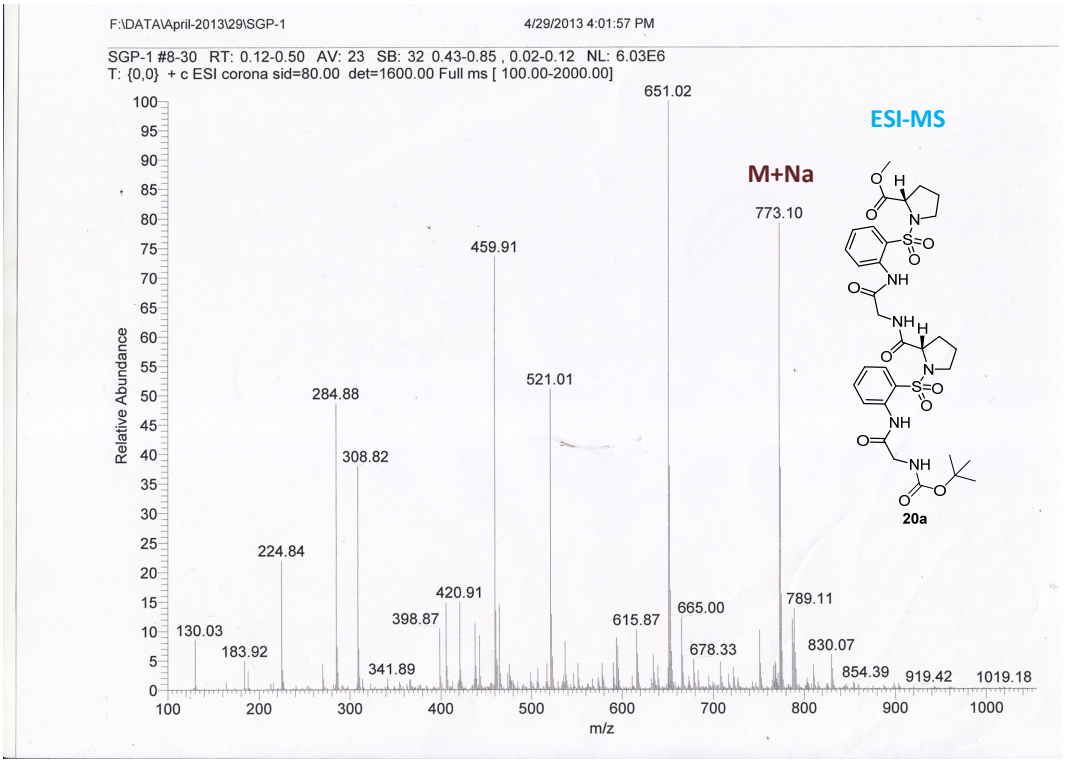
F:\DATA\April-2013\29\SGP-1 4/29/2013 4:01:57 PM
SGP-1 #8-30 RT: 0.12-0.50 AV: 23 SB: 32 0.43-0.85 , 0.02-0.12 NL: 6.03E6
T: {0,0} + c ESI corona sid=80.00 det=1600.00 Full ms [100.00-2000.00]
ESI-MS
M+Na
651.02
773.10
459.91
521.01
284.88
308.82
224.84
420.91
398.87
615.87
665.00
789.11
678.33
830.07
130.03
183.92
341.89
854.39
919.42
1019.18
Relative Abundance
m/z
20a

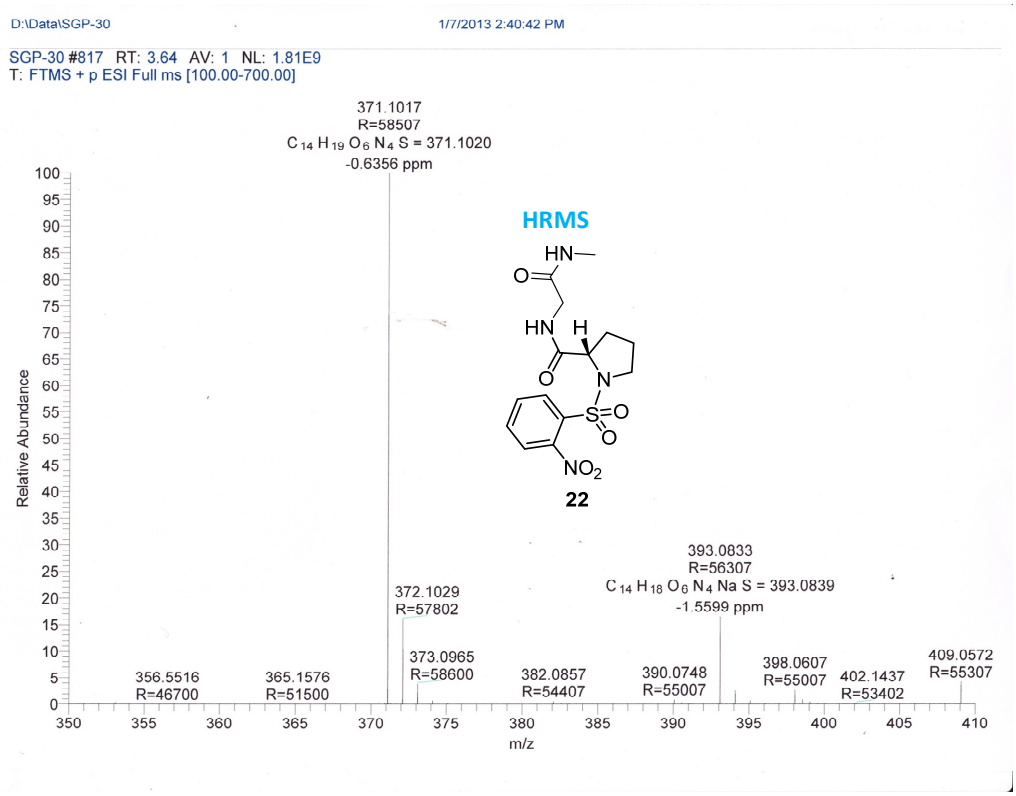
D:\Data\SGP-30 1/7/2013 2:40:42 PM
SGP-30 #817 RT: 3.64 AV: 1 NL: 1.81E9
T: FTMS + p ESI Full ms [100.00-700.00]
371.1017
R=58507
C 14 H 19 O 6 N 4 S = 371.1020
-0.6356 ppm
HRMS
22
393.0833
R=56307
C 14 H 18 O 6 N 4 Na S = 393.0839
-1.5599 ppm
372.1029
R=57802
373.0965
R=58600
356.5516
R=46700
365.1576
R=51500
382.0857
R=54407
390.0748
R=55007
398.0607
R=55007
402.1437
R=53402
409.0572
R=55307
Relative Abundance
m/z

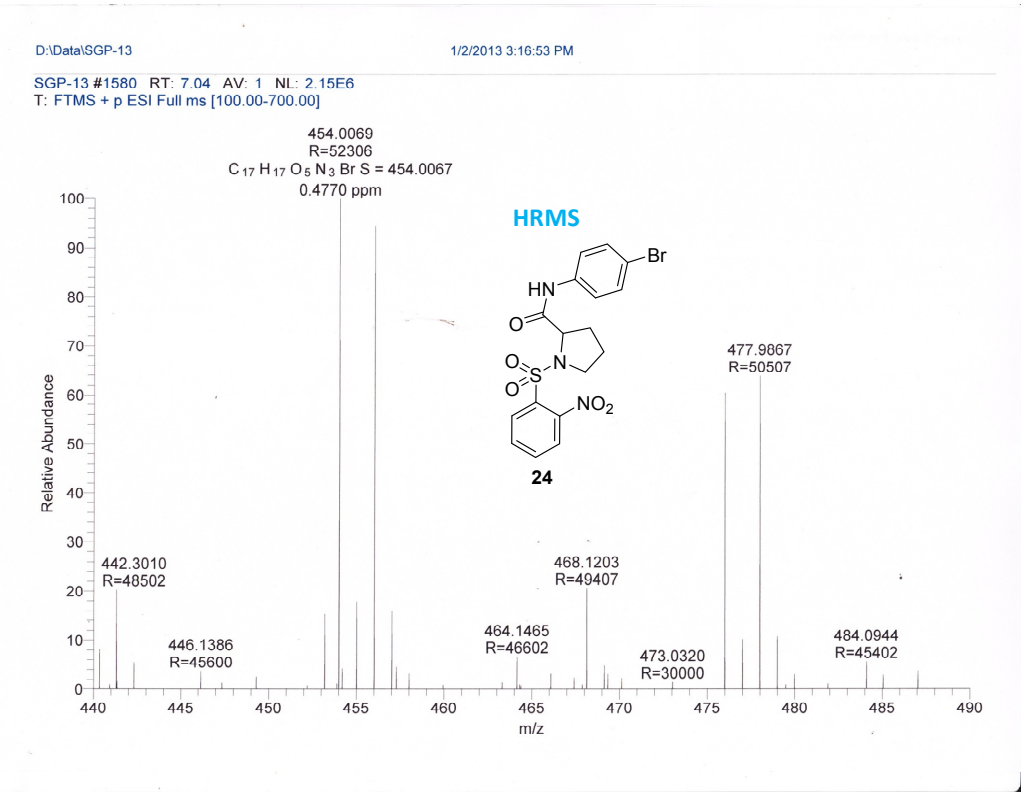
D:\Data\SGP-13
1/2/2013 3:16:53 PM
SGP-13 #1580 RT: 7.04 AV: 1 NL: 2.15E6
T: FTMS + p ESI Full ms [100.00-700.00]
454.0069
R=52306
C 17 H 17 O 5 N 3 Br S = 454.0067
0.4770 ppm
HRMS
Br
HN
O
O
S
O
N
NO2
24
477.9867
R=50507
442.3010
R=48502
446.1386
R=45600
464.1465
R=46602
468.1203
R=49407
473.0320
R=30000
484.0944
R=45402
Relative Abundance
m/z

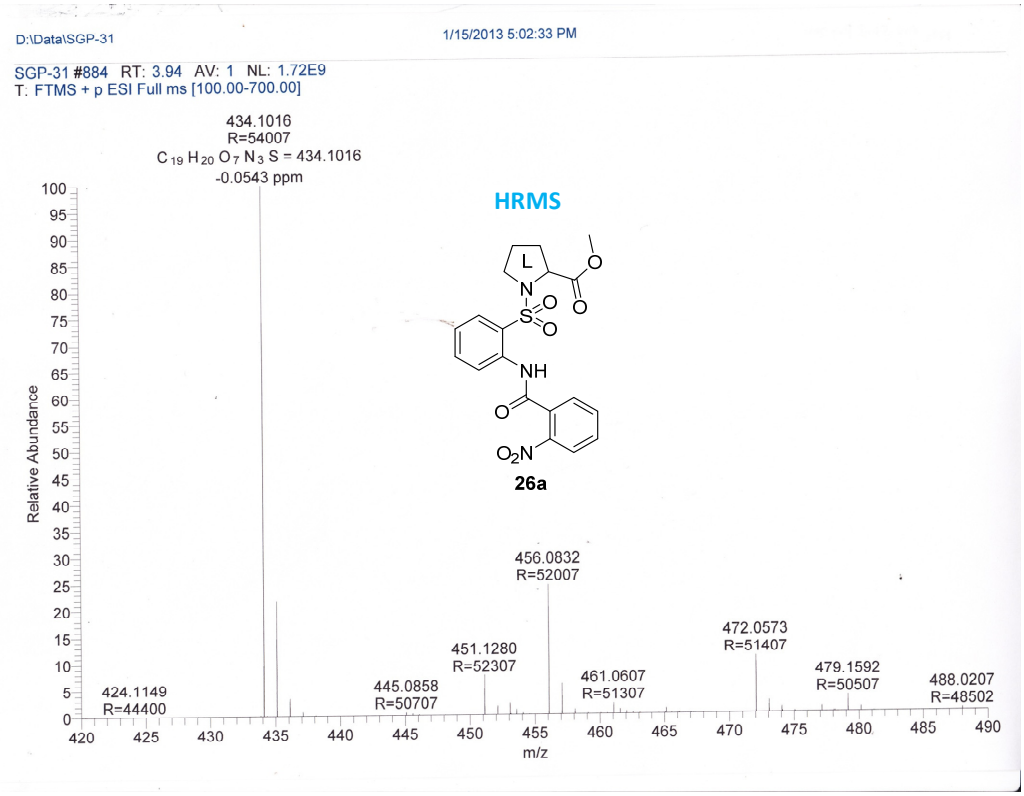
D:\Data\SGP-31
1/15/2013 5:02:33 PM
SGP-31 #884 RT: 3.94 AV: 1 NL: 1.72E9
T. FTMS + p ESI Full ms [100.00-700.00]
434.1016
R=54007
C 19 H 20 O 7 N 3 S = 434.1016
-0.0543 ppm
HRMS
L
N
O
O
S
O
O
NH
O
O2N
26a
456.0832
R=52007
424.1149
R=44400
445.0858
R=50707
451.1280
R=52307
461.0607
R=51307
472.0573
R=51407
479.1592
R=50507
488.0207
R=48502
Relative Abundance
m/z

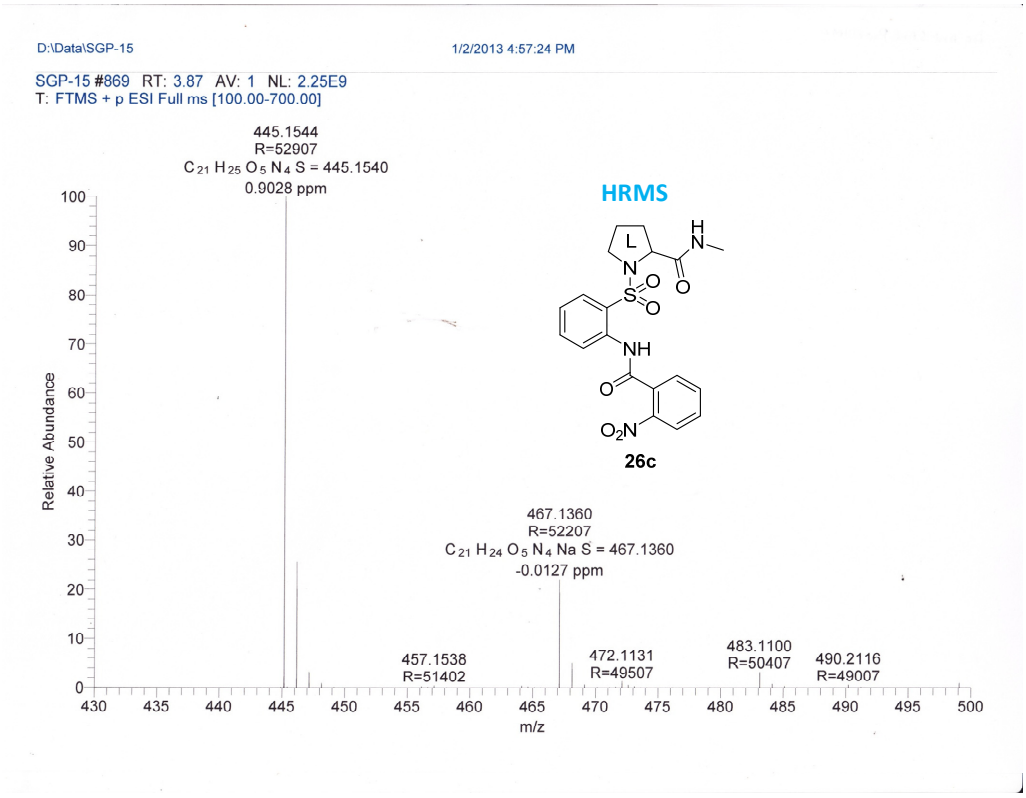
D:\Data\SGP-15
1/2/2013 4:57:24 PM
SGP-15 #869 RT: 3.87 AV: 1 NL: 2.25E9
T: FTMS + p ESI Full ms [100.00-700.00]
445.1544
R=52907
C21 H25 O5 N4 S = 445.1540
0.9028 ppm
HRMS
26c
467.1360
R=52207
C21 H24 O5 N4 Na S = 467.1360
-0.0127 ppm
457.1538
R=51402
472.1131
R=49507
483.1100
R=50407
490.2116
R=49007
Relative Abundance
m/z

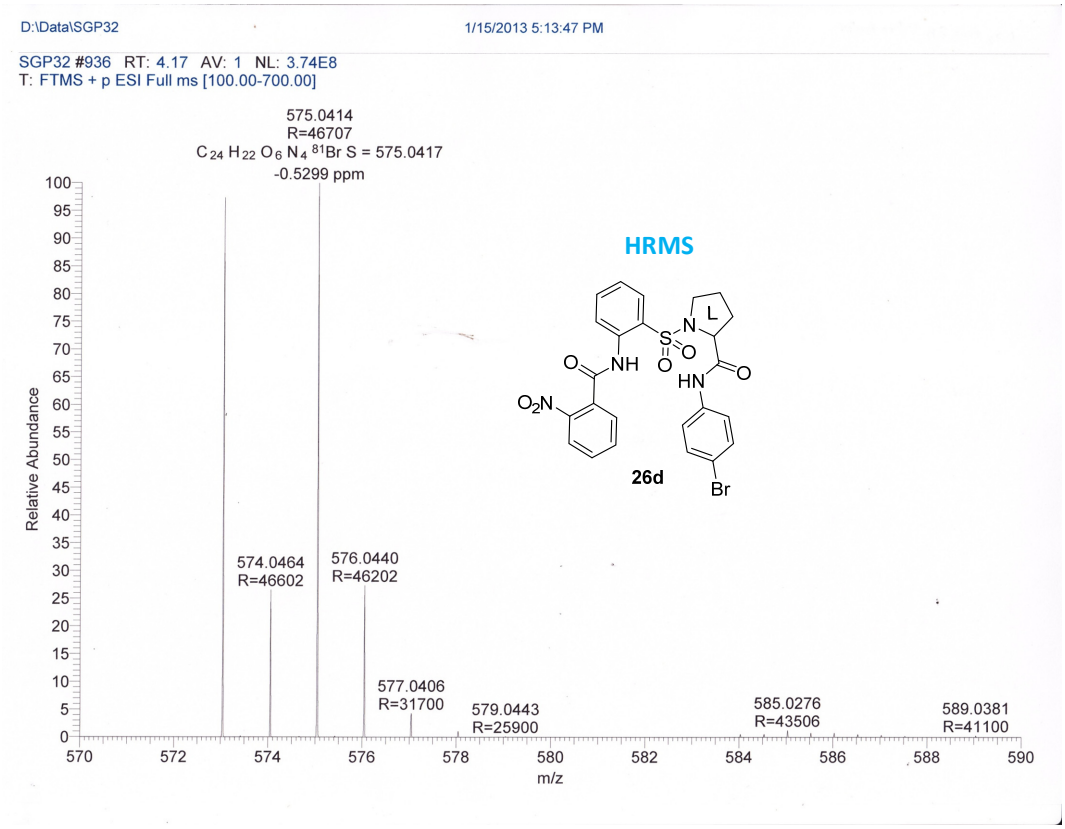
D:\Data\SGP32
1/15/2013 5:13:47 PM
SGP32 #936 RT: 4.17 AV: 1 NL: 3.74E8
T: FTMS + p ESI Full ms [100.00-700.00]
575.0414
R=46707
C24 H22 O6 N4 81Br S = 575.0417
-0.5299 ppm
HRMS
26d
574.0464
R=46602
576.0440
R=46202
577.0406
R=31700
579.0443
R=25900
585.0276
R=43506
589.0381
R=41100
Relative Abundance
m/z

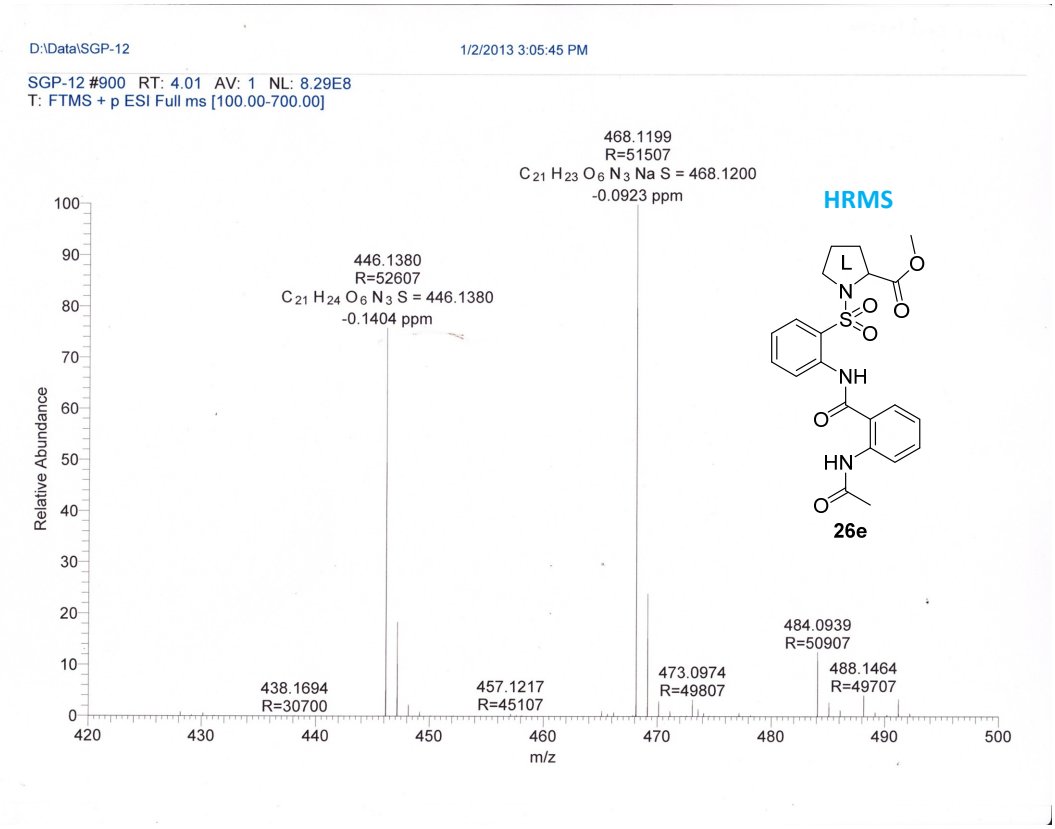
D:\Data\SGP-12
1/2/2013 3:05:45 PM
SGP-12 #900 RT: 4.01 AV: 1 NL: 8.29E8
T: FTMS + p ESI Full ms [100.00-700.00]
468.1199
R=51507
C21 H23 O6 N3 Na S = 468.1200
-0.0923 ppm
HRMS
446.1380
R=52607
C21 H24 O6 N3 S = 446.1380
-0.1404 ppm
26e
484.0939
R=50907
438.1694
R=30700
457.1217
R=45107
473.0974
R=49807
488.1464
R=49707
Relative Abundance
m/z

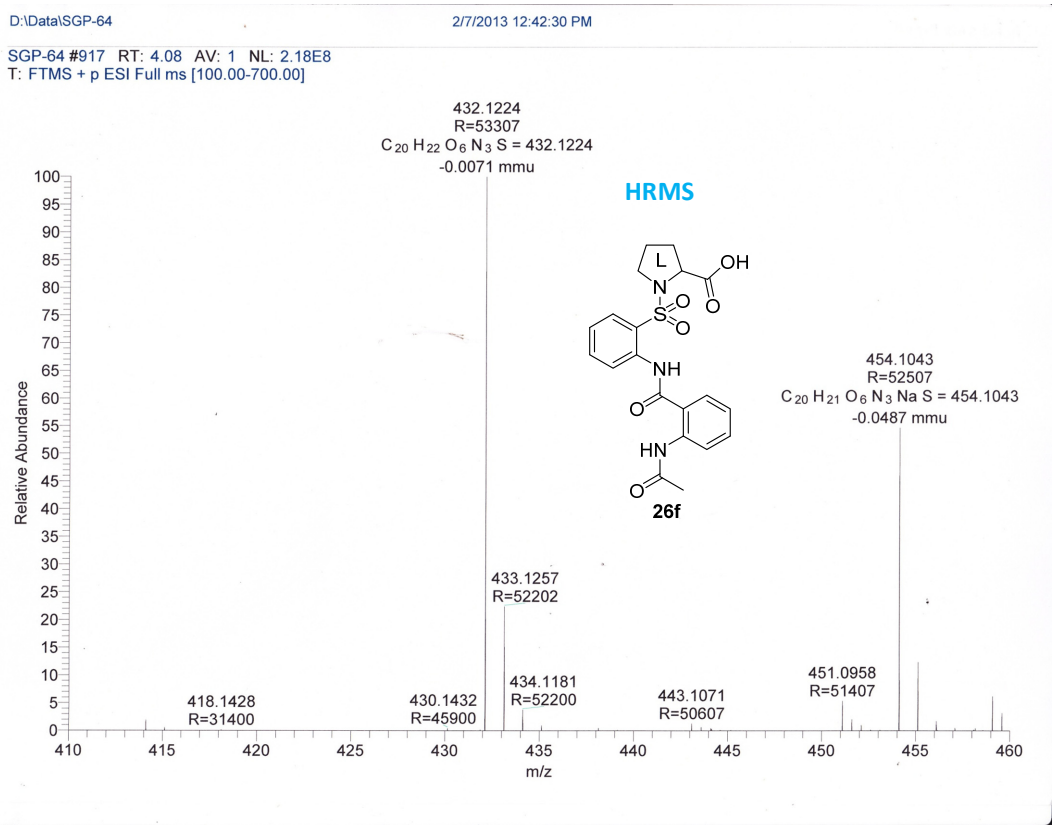
D:\Data\SGP-64
2/7/2013 12:42:30 PM
SGP-64 #917 RT: 4.08 AV: 1 NL: 2.18E8
T: FTMS + p ESI Full ms [100.00-700.00]
432.1224
R=53307
C20 H22 O6 N3 S = 432.1224
-0.0071 mmu
HRMS
26f
454.1043
R=52507
C20 H21 O6 N3 Na S = 454.1043
-0.0487 mmu
433.1257
R=52202
418.1428
R=31400
430.1432
R=45900
434.1181
R=52200
443.1071
R=50607
451.0958
R=51407
Relative Abundance
m/z

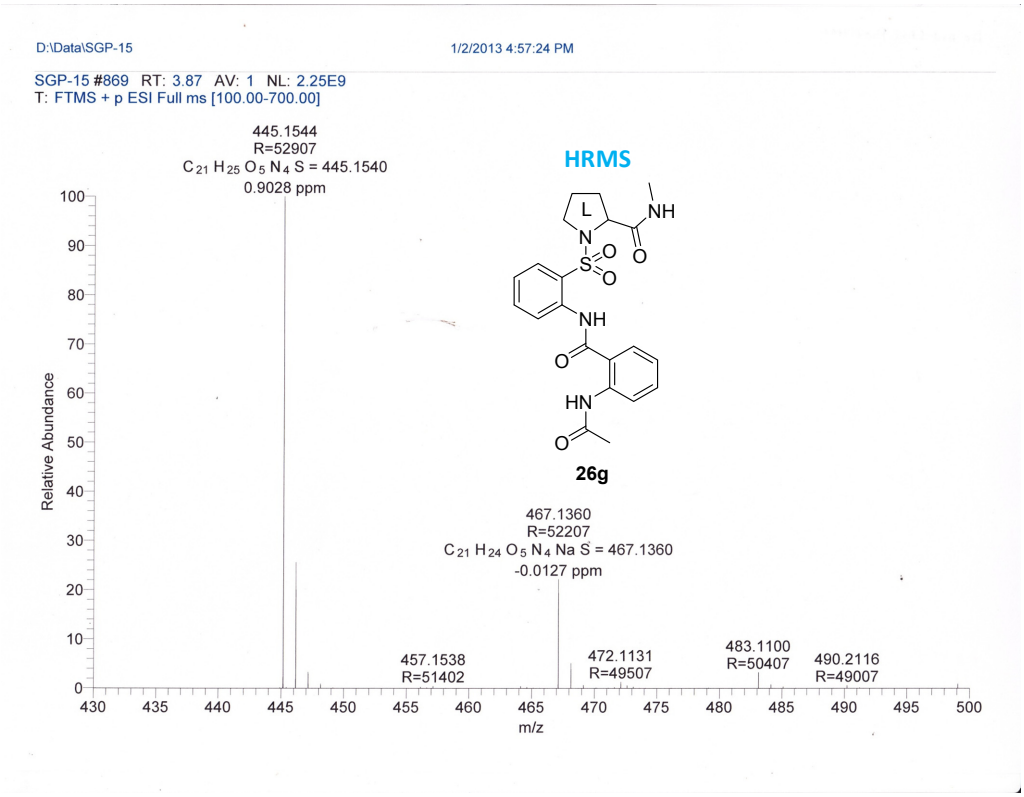
D:\Data\SGP-15
1/2/2013 4:57:24 PM
SGP-15 #869 RT: 3.87 AV: 1 NL: 2.25E9
T: FTMS + p ESI Full ms [100.00-700.00]
445.1544
R=52907
C21 H25 O5 N4 S = 445.1540
0.9028 ppm
HRMS
26g
467.1360
R=52207
C21 H24 O5 N4 Na S = 467.1360
-0.0127 ppm
457.1538
R=51402
472.1131
R=49507
483.1100
R=50407
490.2116
R=49007
Relative Abundance
m/z

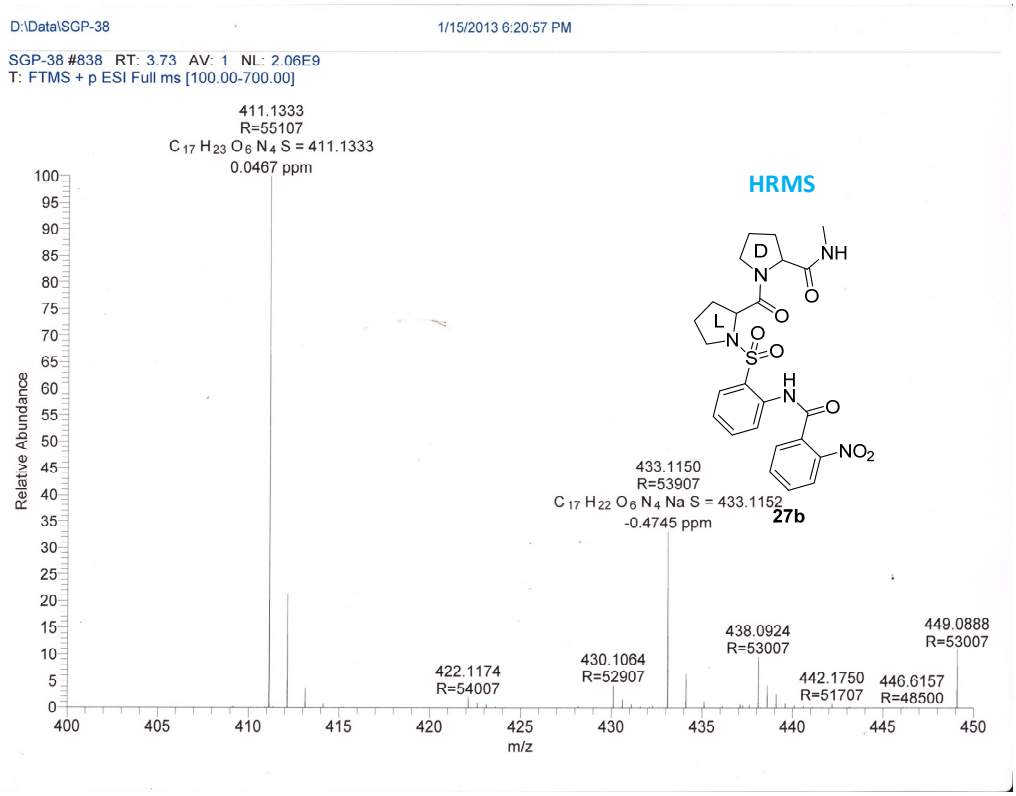
D:\Data\SGP-38
1/15/2013 6:20:57 PM
SGP-38 #838 RT: 3.73 AV: 1 NL: 2.06E9
T: FTMS + p ESI Full ms [100.00-700.00]
411.1333
R=55107
C17 H23 O6 N4 S = 411.1333
0.0467 ppm
HRMS
27b
433.1150
R=53907
C17 H22 O6 N4 Na S = 433.1152
-0.4745 ppm
422.1174
R=54007
430.1064
R=52907
438.0924
R=53007
442.1750
R=51707
446.6157
R=48500
449.0888
R=53007
Relative Abundance
m/z

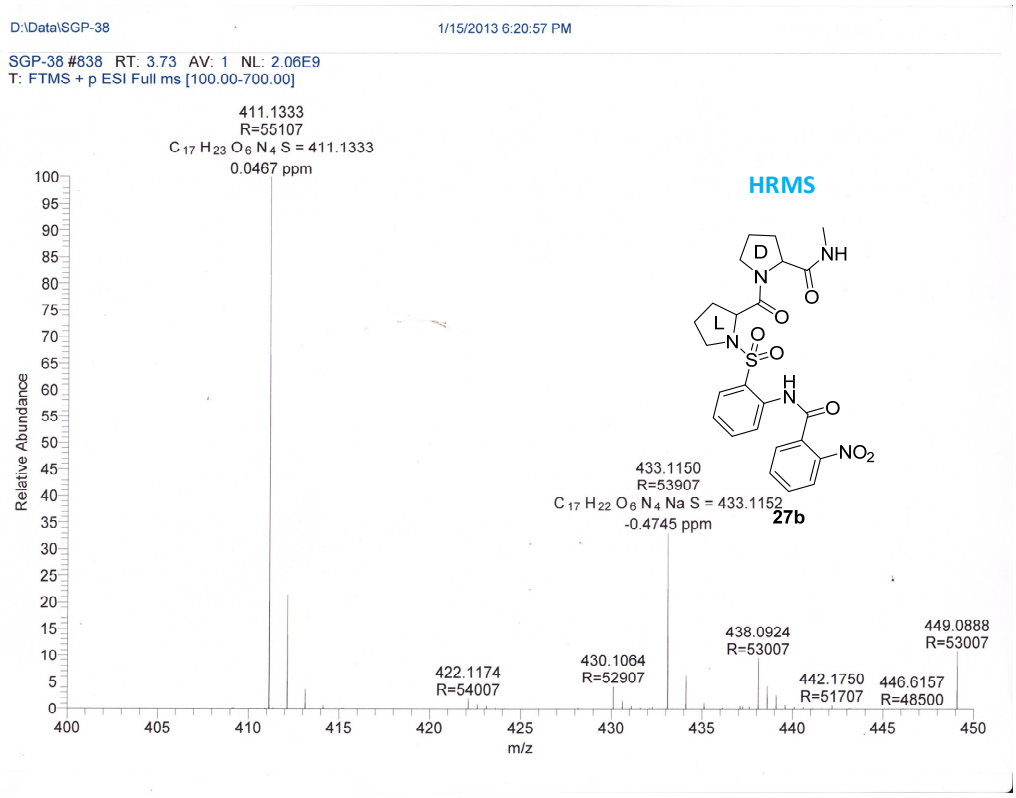
D:\Data\SGP-38
1/15/2013 6:20:57 PM
SGP-38 #838 RT: 3.73 AV: 1 NL: 2.06E9
T: FTMS + p ESI Full ms [100.00-700.00]
411.1333
R=55107
C 17 H 23 O 6 N 4 S = 411.1333
0.0467 ppm
HRMS
433.1150
R=53907
C 17 H 22 O 6 N 4 Na S = 433.1152
-0.4745 ppm
27b
422.1174
R=54007
430.1064
R=52907
438.0924
R=53007
442.1750
R=51707
446.6157
R=48500
449.0888
R=53007
Relative Abundance
m/z

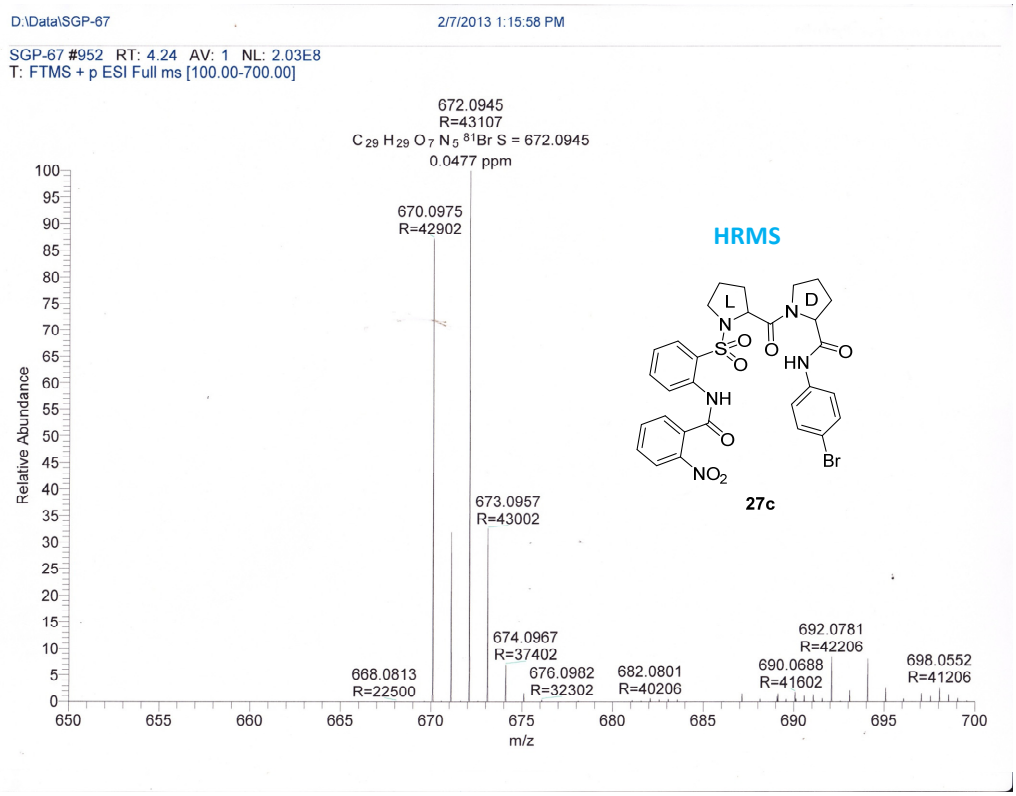
D:\Data\SGP-67
2/7/2013 1:15:58 PM
SGP-67 #952 RT: 4.24 AV: 1 NL: 2.03E8
T: FTMS + p ESI Full ms [100.00-700.00]
672.0945
R=43107
C 29 H 29 O 7 N 5 81Br S = 672.0945
0.0477 ppm
HRMS
670.0975
R=42902
673.0957
R=43002
674.0967
R=37402
668.0813
R=22500
676.0982
R=32302
682.0801
R=40206
690.0688
R=41602
692.0781
R=42206
698.0552
R=41206
27c
Relative Abundance
m/z

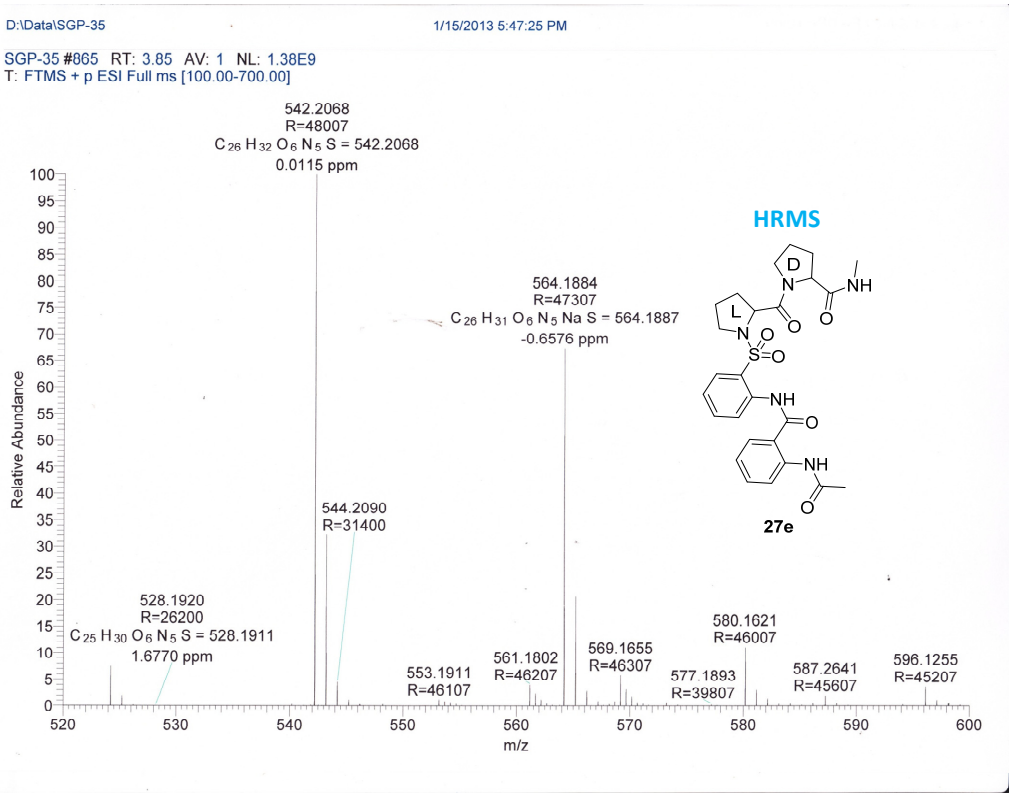
D:\Data\SGP-35
1/15/2013 5:47:25 PM
SGP-35 #865 RT: 3.85 AV: 1 NL: 1.38E9
T: FTMS + p ESI Full ms [100.00-700.00]
542.2068
R=48007
C26 H32 O6 N5 S = 542.2068
0.0115 ppm
564.1884
R=47307
C26 H31 O6 N5 Na S = 564.1887
-0.6576 ppm
544.2090
R=31400
528.1920
R=26200
C25 H30 O6 N5 S = 528.1911
1.6770 ppm
553.1911
R=46107
561.1802
R=46207
569.1655
R=46307
577.1893
R=39807
580.1621
R=46007
587.2641
R=45607
596.1255
R=45207
HRMS
27e
Relative Abundance
m/z

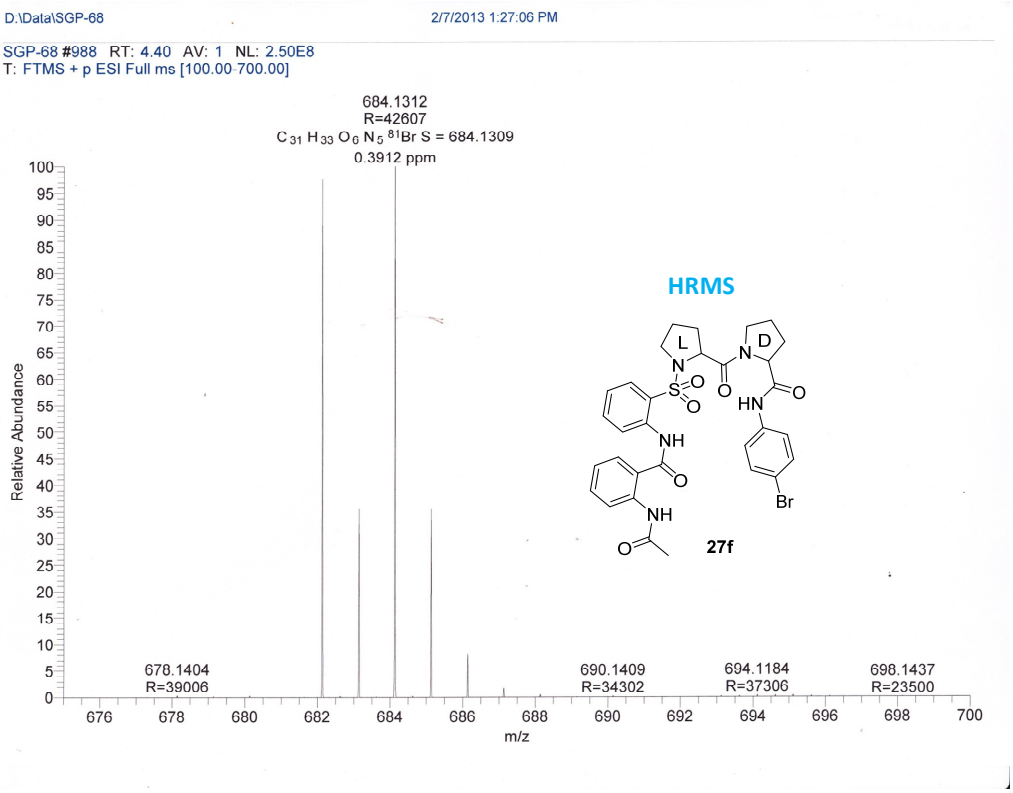
D:\Data\SGP-68
2/7/2013 1:27:06 PM
SGP-68 #988 RT: 4.40 AV: 1 NL: 2.50E8
T: FTMS + p ESI Full ms [100.00-700.00]
684.1312
R=42607
C31 H33 O6 N5 81Br S = 684.1309
0.3912 ppm
678.1404
R=39006
690.1409
R=34302
694.1184
R=37306
698.1437
R=23500
HRMS
27f
Relative Abundance
m/z

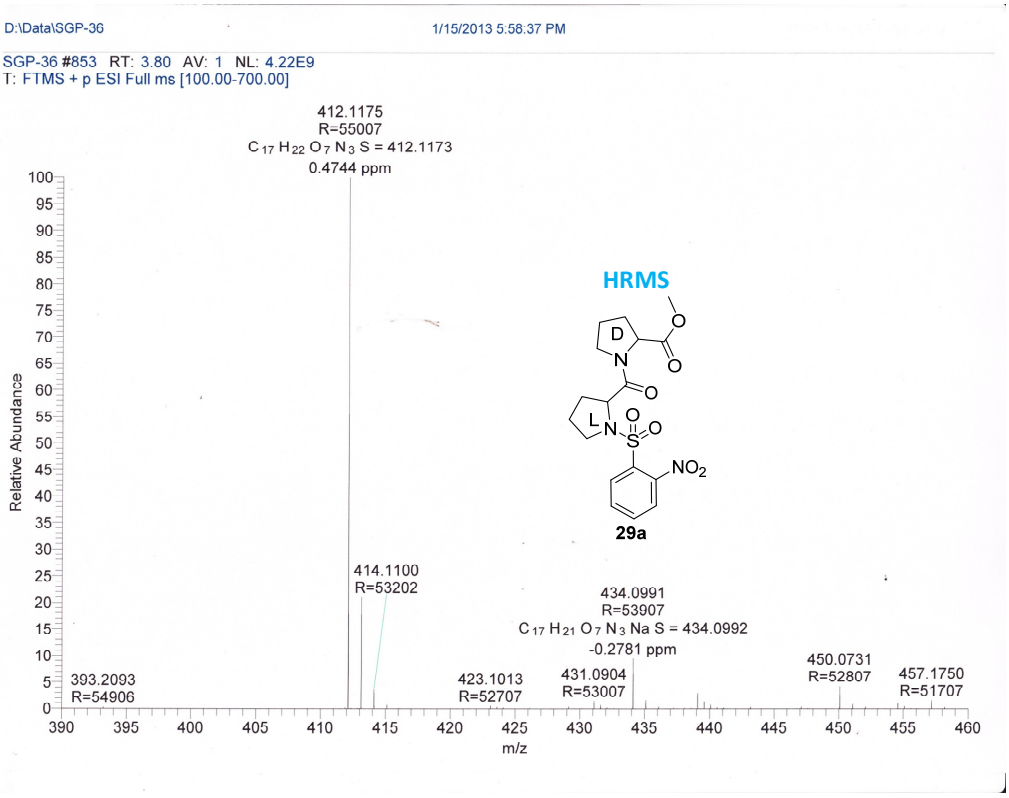
D:\Data\SGP-36
1/15/2013 5:58:37 PM
SGP-36 #853 RT: 3.80 AV: 1 NL: 4.22E9
T: FTMS + p ESI Full ms [100.00-700.00]
412.1175
R=55007
C 17 H 22 O 7 N 3 S = 412.1173
0.4744 ppm
HRMS
29a
414.1100
R=53202
434.0991
R=53907
C 17 H 21 O 7 N 3 Na S = 434.0992
-0.2781 ppm
393.2093
R=54906
423.1013
R=52707
431.0904
R=53007
450.0731
R=52807
457.1750
R=51707
Relative Abundance
m/z

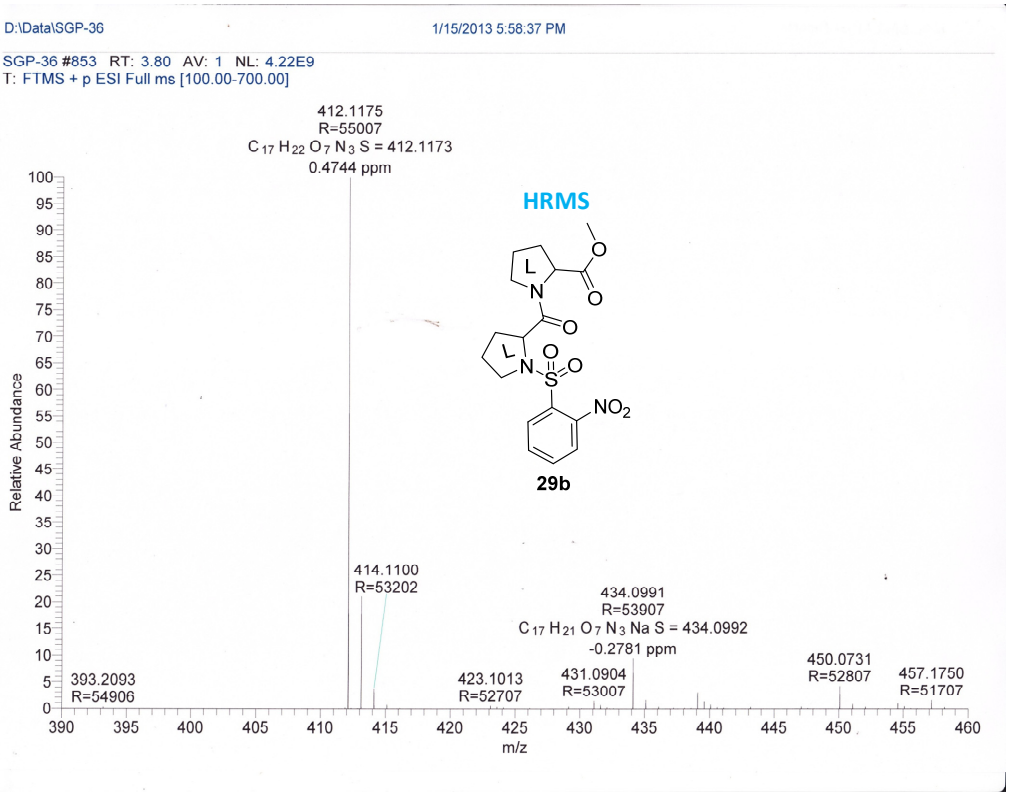
D:\Data\SGP-36
1/15/2013 5:58:37 PM
SGP-36 #853 RT: 3.80 AV: 1 NL: 4.22E9
T: FTMS + p ESI Full ms [100.00-700.00]
412.1175
R=55007
C 17 H 22 O 7 N 3 S = 412.1173
0.4744 ppm
HRMS
29b
414.1100
R=53202
434.0991
R=53907
C 17 H 21 O 7 N 3 Na S = 434.0992
-0.2781 ppm
393.2093
R=54906
423.1013
R=52707
431.0904
R=53007
450.0731
R=52807
457.1750
R=51707
Relative Abundance
m/z

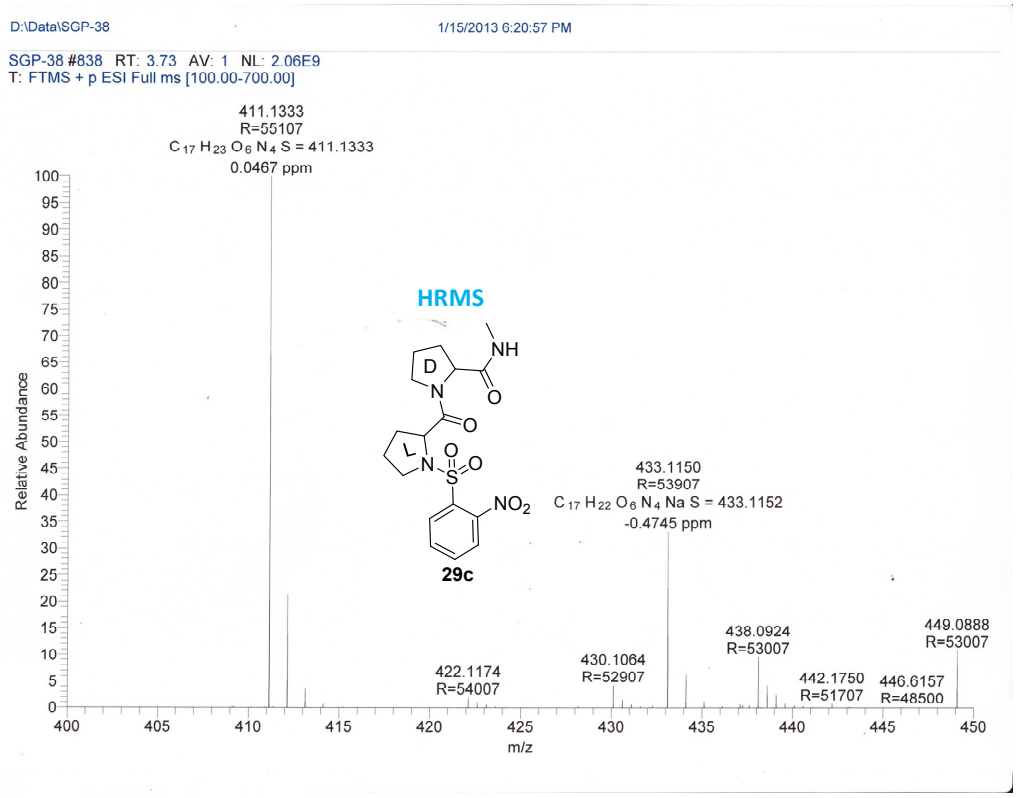
D:\Data\SGP-38
1/15/2013 6:20:57 PM
SGP-38 #838 RT: 3.73 AV: 1 NL: 2.06E9
T: FTMS + p ESI Full ms [100.00-700.00]
411.1333
R=55107
C17 H23 O6 N4 S = 411.1333
0.0467 ppm
HRMS
29c
433.1150
R=53907
C17 H22 O6 N4 Na S = 433.1152
-0.4745 ppm
438.0924
R=53007
449.0888
R=53007
422.1174
R=54007
430.1064
R=52907
442.1750
R=51707
446.0157
R=48500
Relative Abundance
m/z

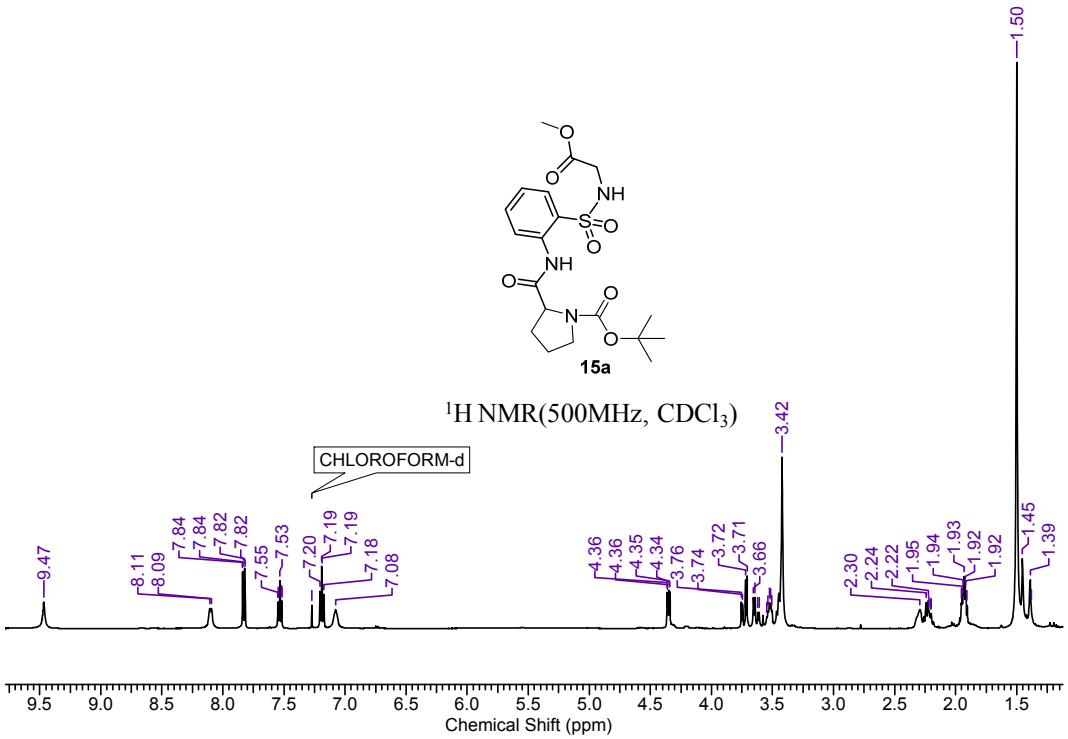
15a
1H NMR(500MHz, CDCl3)
CHLOROFORM-d
Chemical Shift (ppm)

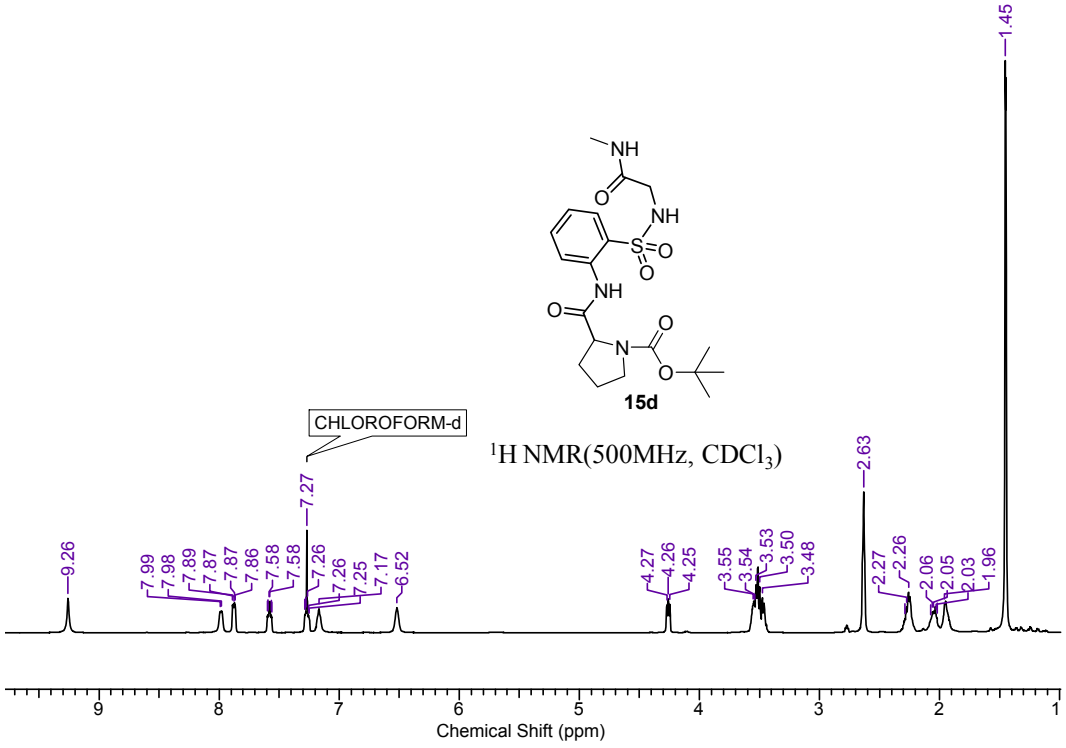
15d
CHLOROFORM-d
^{1}H NMR(500MHz, $CDCl_3$)
Chemical Shift (ppm)

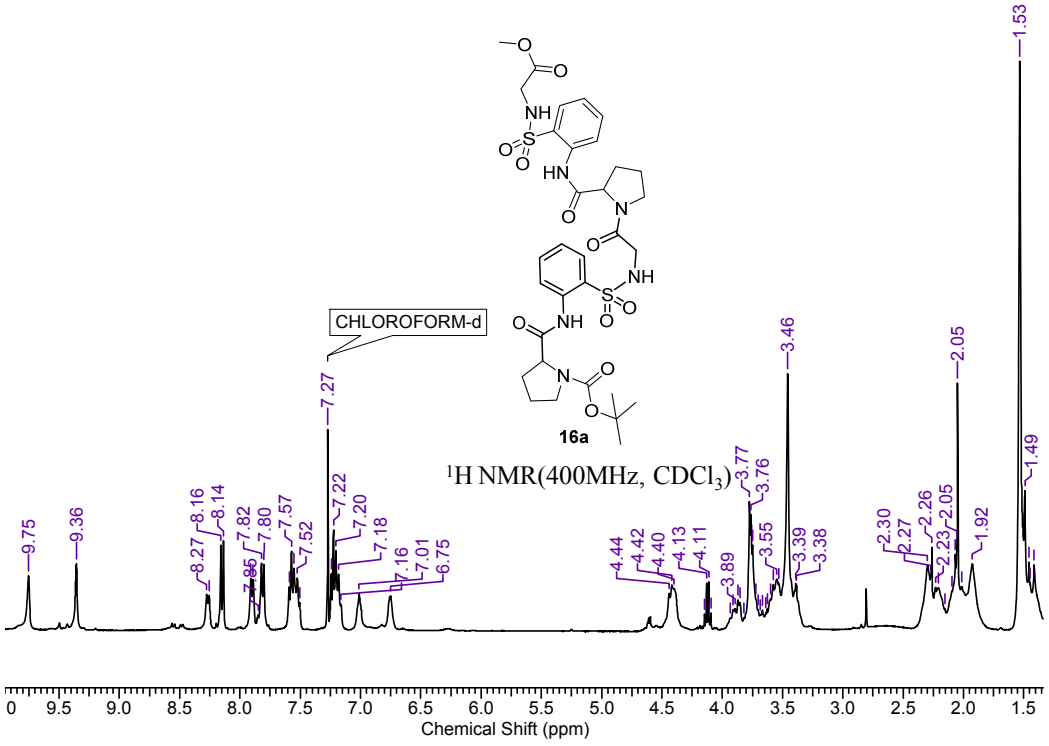
16a
CHLOROFORM-d
^{1}H NMR(400MHz, $CDCl_3$)
Chemical Shift (ppm)

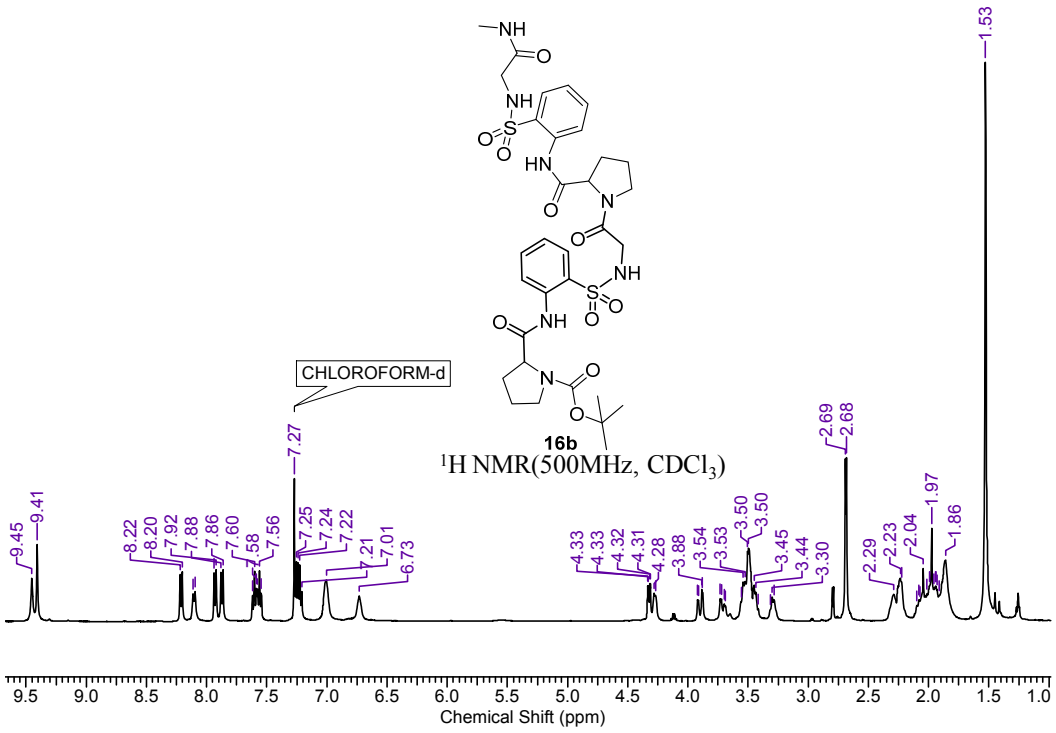

16b

^{1}H NMR(500MHz, $CDCl_3$)

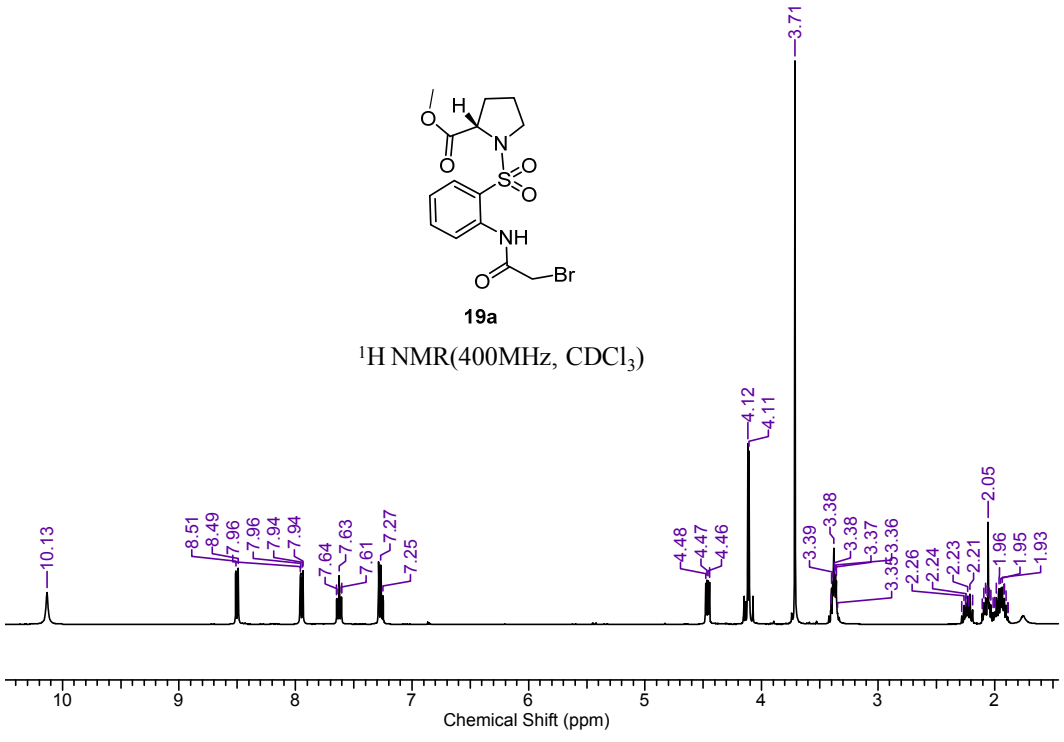

19a

^{1}H NMR(400MHz, $CDCl_3$)

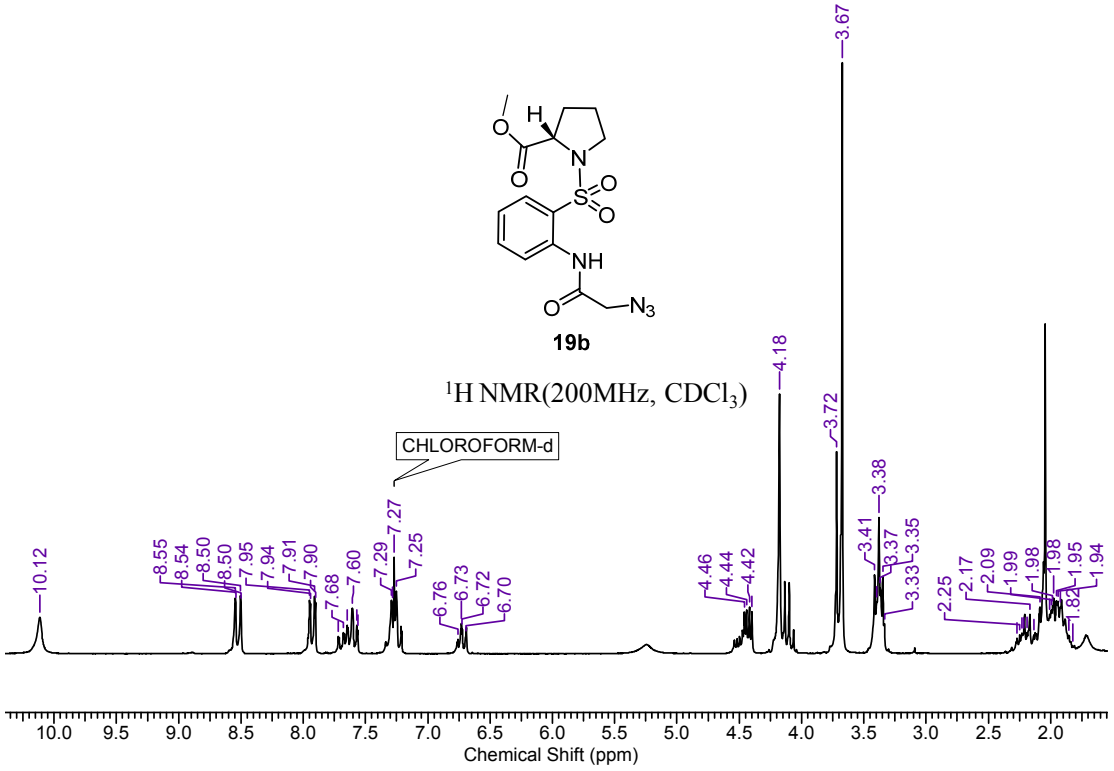
19b
^{1}H NMR(200MHz, CDCl$_3$)
CHLOROFORM-d
Chemical Shift (ppm)

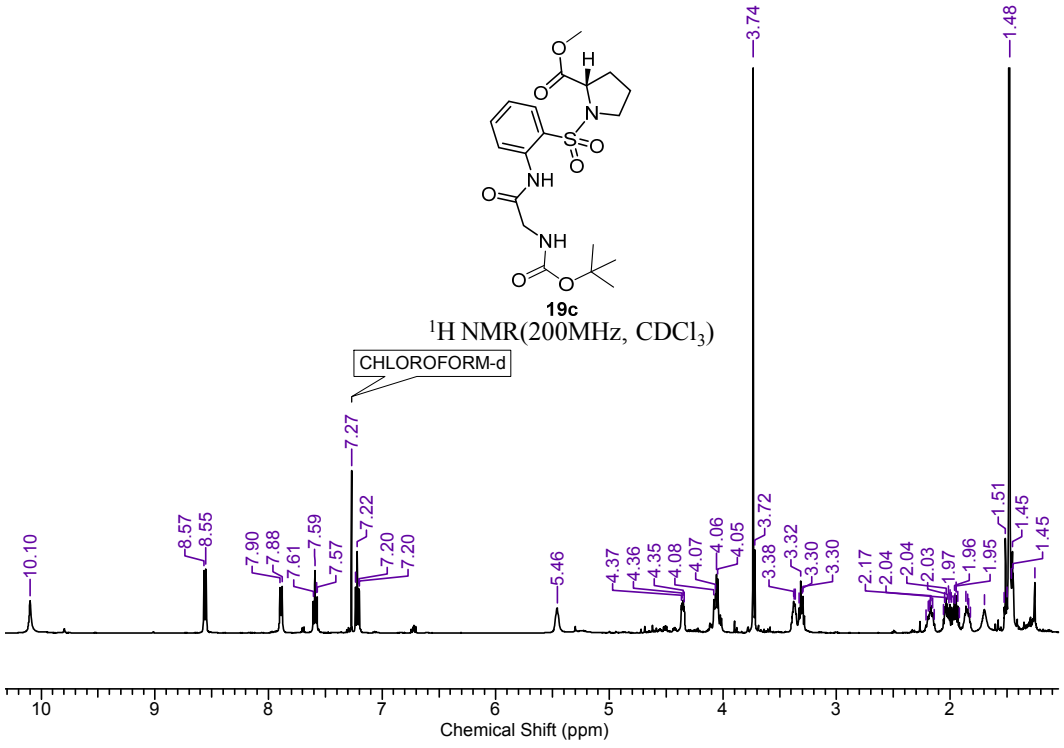
19c
^{1}H NMR(200MHz, CDCl$_3$)
CHLOROFORM-d
Chemical Shift (ppm)

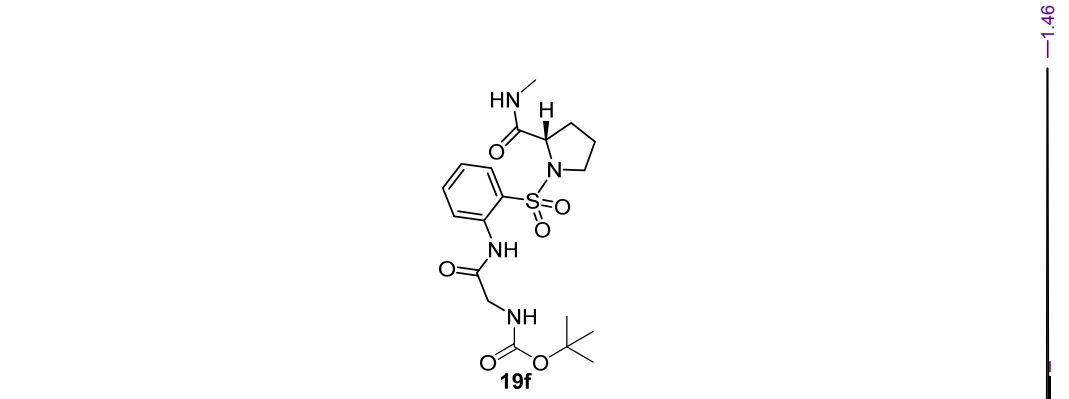

19f

^{1}H NMR(500MHz, $CDCl_3$)

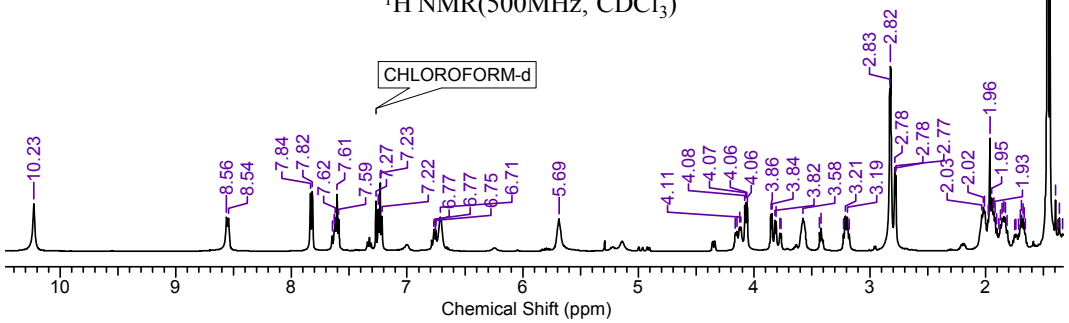

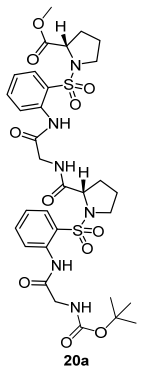

20a

^{1}H NMR(500MHz, $CDCl_3$)

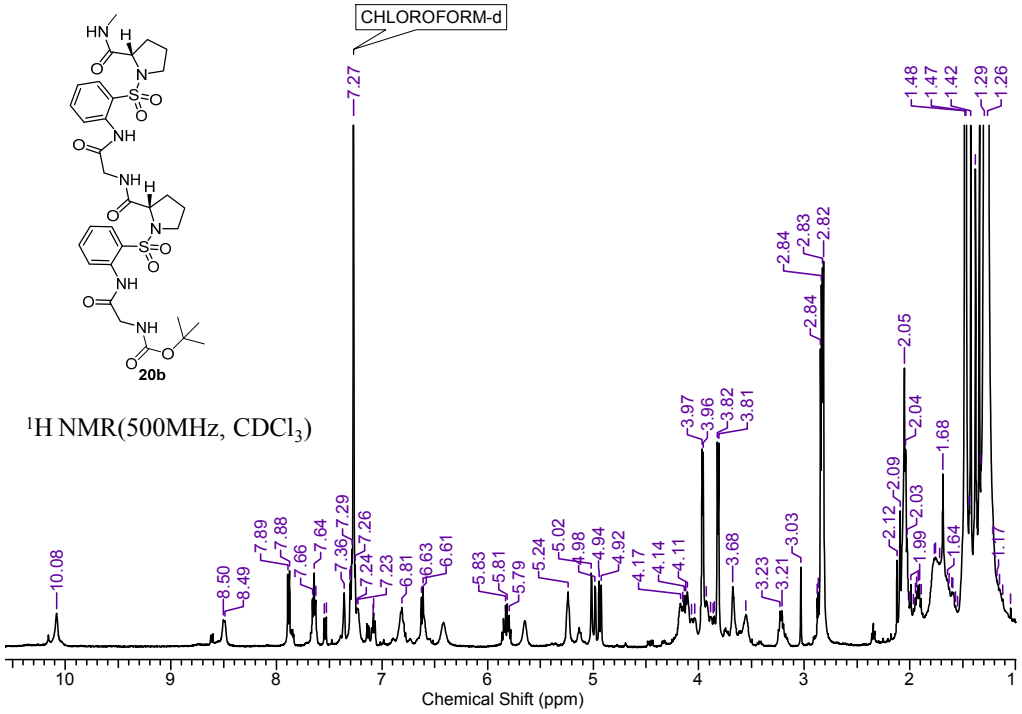
CHLOROFORM-d
20b
^{1}H NMR(500MHz, $CDCl_3$)
Chemical Shift (ppm)

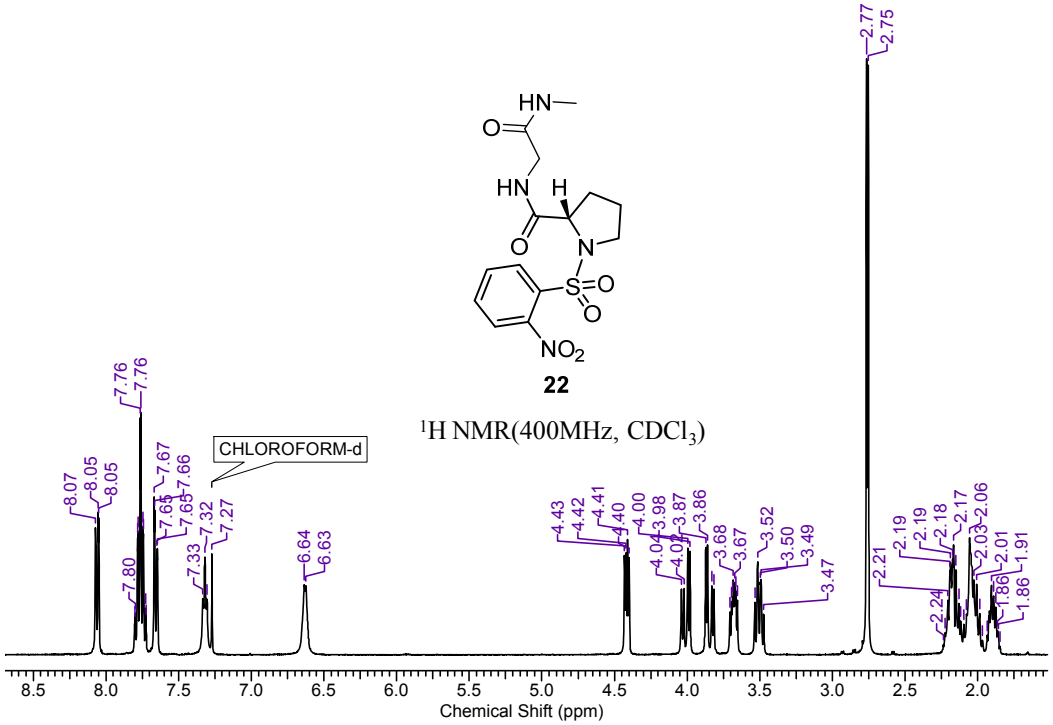
22
^{1}H NMR(400MHz, $CDCl_3$)
CHLOROFORM-d
Chemical Shift (ppm)

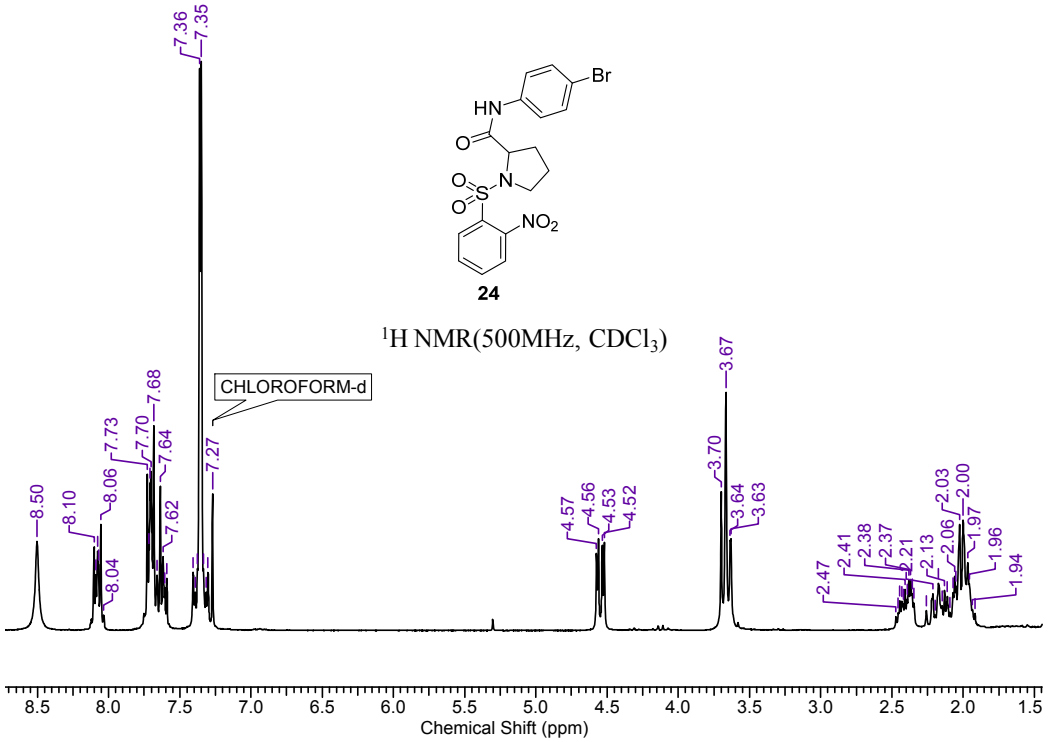
Br
HN
O
O
S
O
N
NO2
24
1H NMR(500MHz, CDCl3)
CHLOROFORM-d
7.36
7.35
7.73
7.70
7.68
7.64
7.62
8.50
8.10
8.06
8.04
7.27
4.57
4.56
4.53
4.52
3.67
3.70
3.64
3.63
2.47
2.41
2.38
2.37
2.21
2.13
2.06
2.03
2.00
1.97
1.96
1.94
8.5
8.0
7.5
7.0
6.5
6.0
5.5
5.0
4.5
4.0
3.5
3.0
2.5
2.0
1.5
Chemical Shift (ppm)

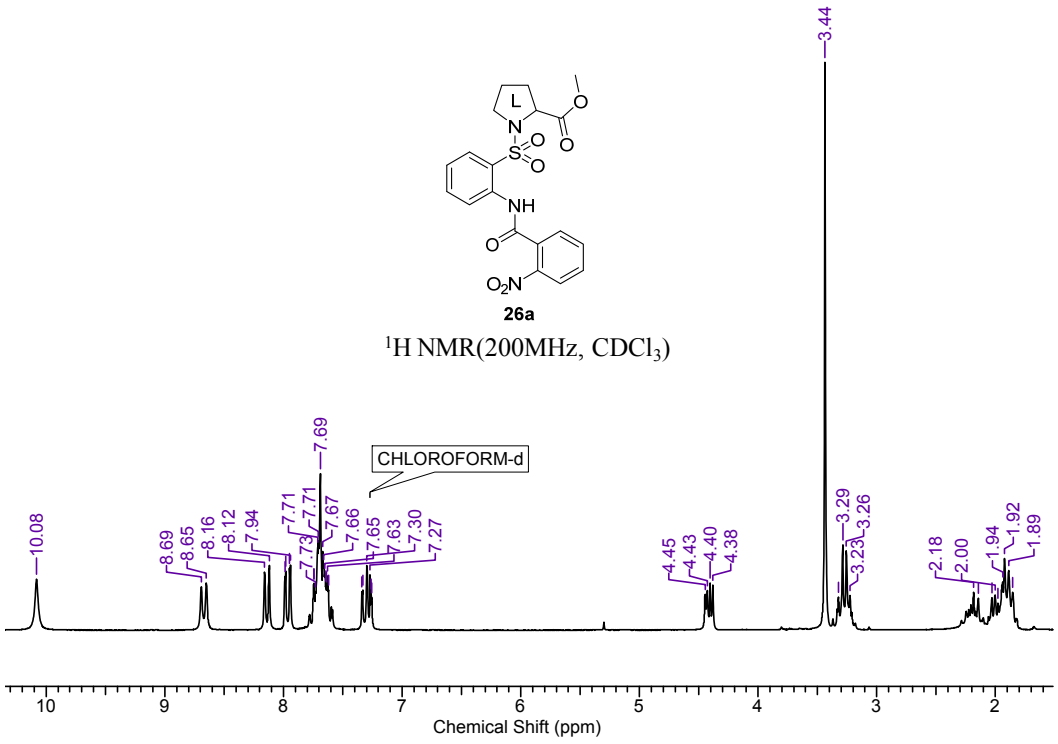
L
N
O
O
S
O
O
NH
O
O2N
26a
1H NMR(200MHz, CDCl3)
CHLOROFORM-d
10.08
8.69
8.65
8.16
8.12
7.94
7.73
7.71
7.71
7.69
7.67
7.66
7.65
7.63
7.30
7.27
4.45
4.43
4.40
4.38
3.44
3.29
3.26
3.23
2.18
2.00
1.94
1.92
1.89
10
9
8
7
6
5
4
3
2
Chemical Shift (ppm)

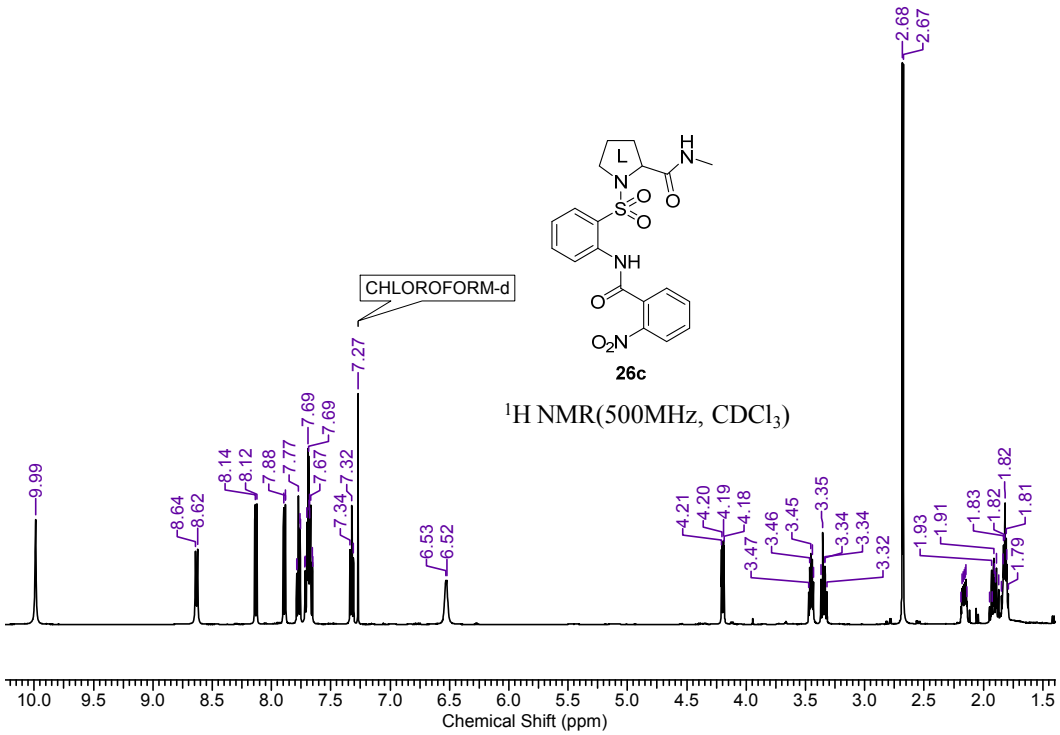
CHLOROFORM-d
26c
^{1}H NMR(500MHz, CDCl$_3$)
Chemical Shift (ppm)

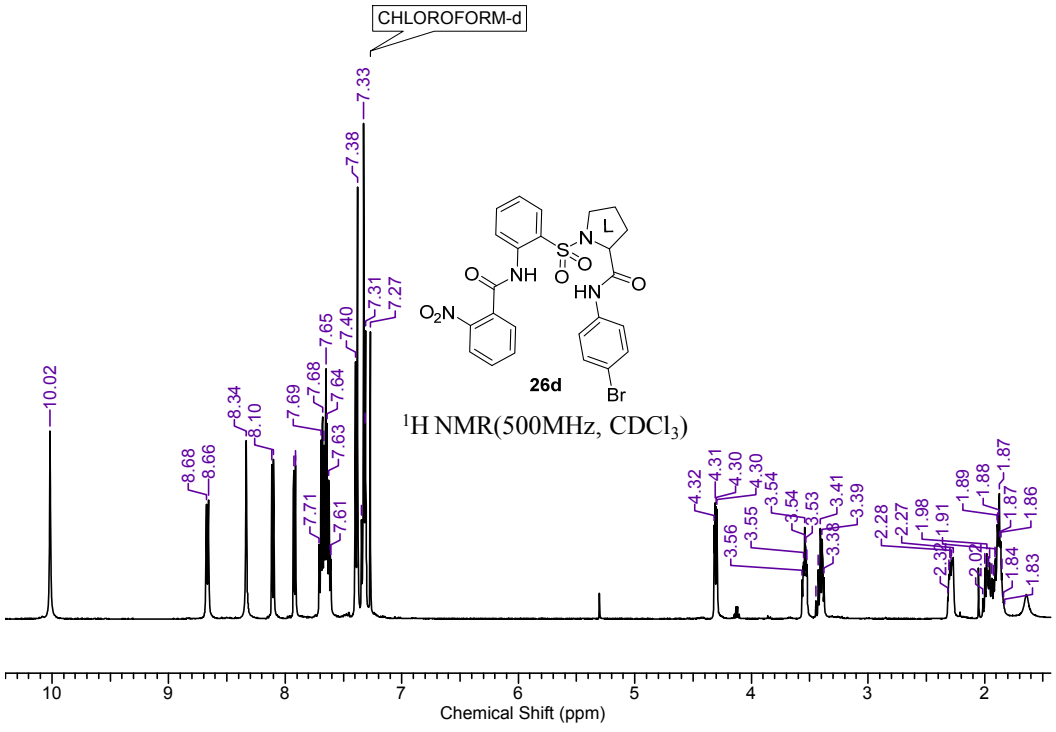
CHLOROFORM-d
26d
^{1}H NMR(500MHz, CDCl$_3$)
Chemical Shift (ppm)

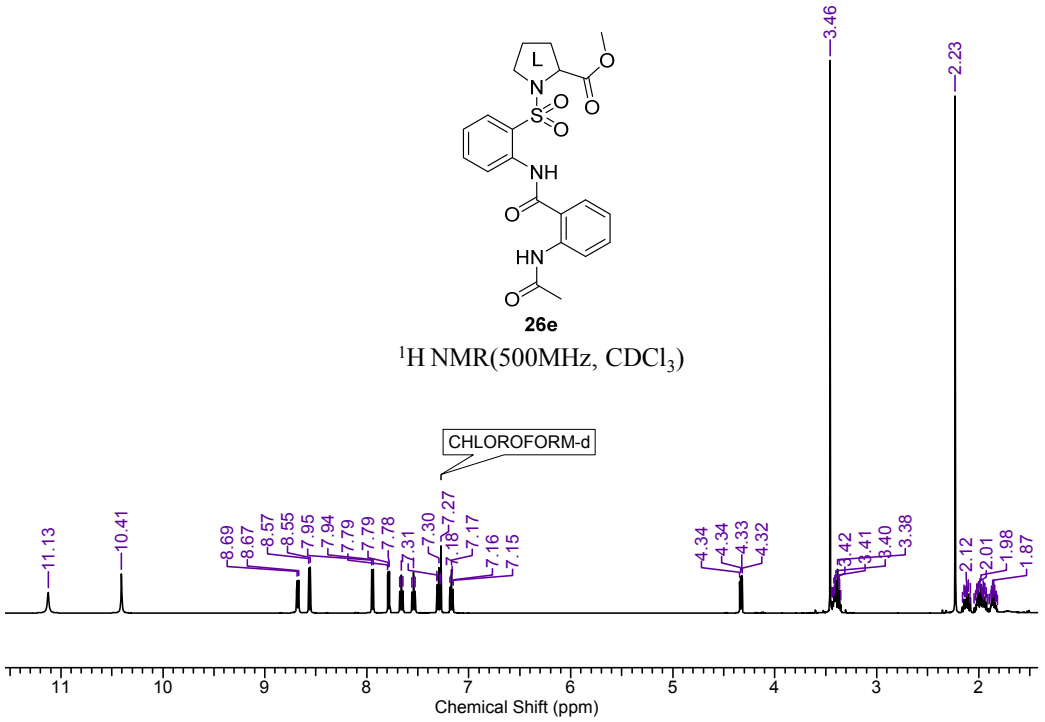
26e
^{1}H NMR(500MHz, $CDCl_3$)
CHLOROFORM-d
Chemical Shift (ppm)

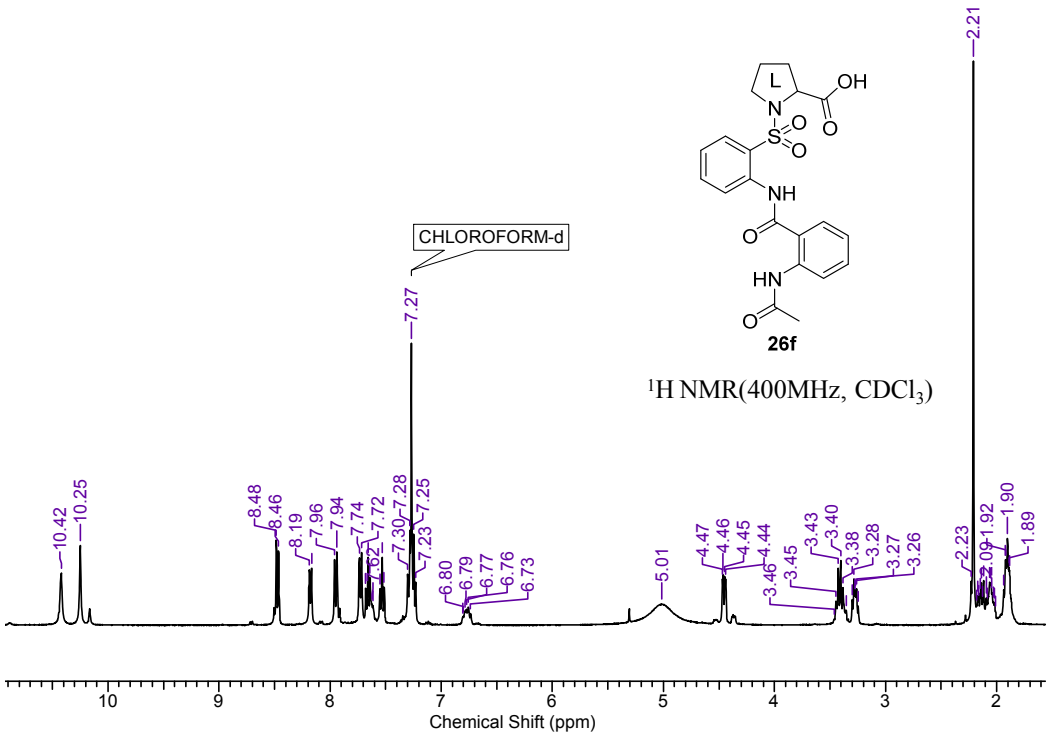
26f
^{1}H NMR(400MHz, $CDCl_3$)
CHLOROFORM-d
Chemical Shift (ppm)

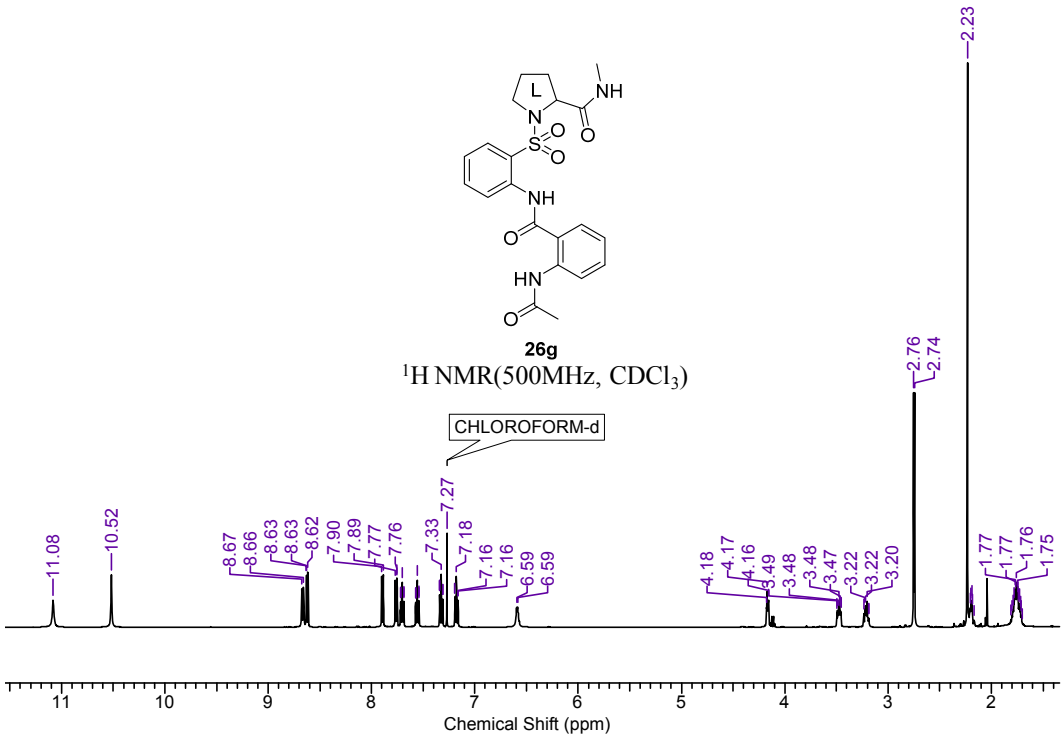
26g
^{1}H NMR(500MHz, CDCl$_3$)
CHLOROFORM-d
Chemical Shift (ppm)

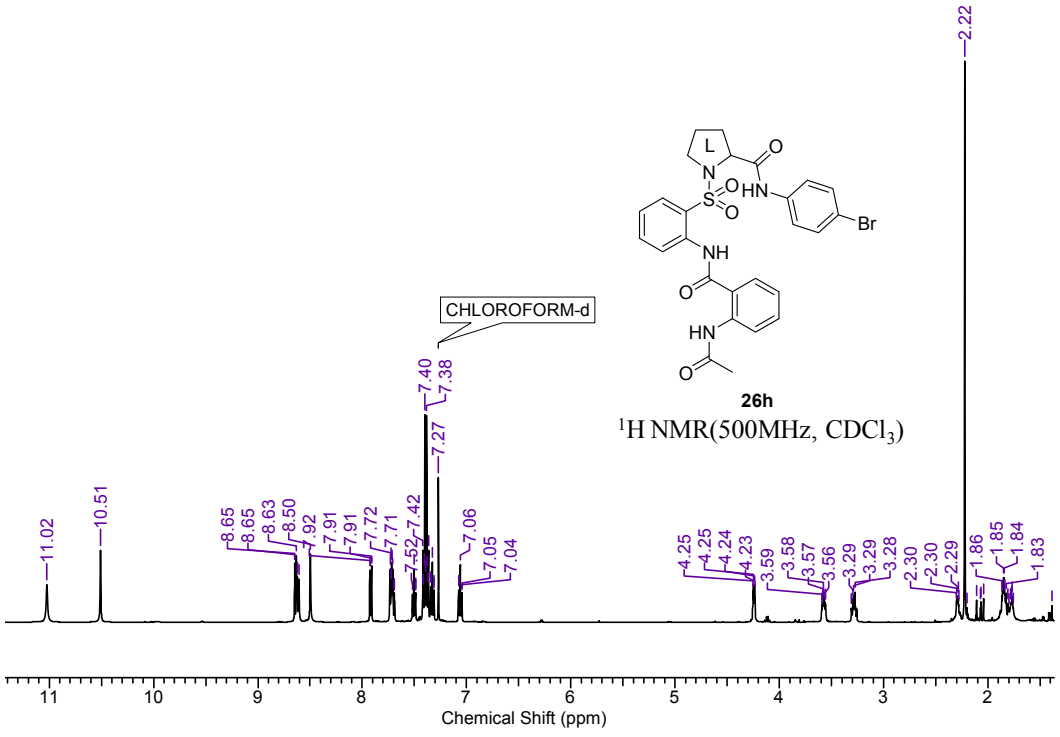
26h
^{1}H NMR(500MHz, CDCl$_3$)
CHLOROFORM-d
Chemical Shift (ppm)

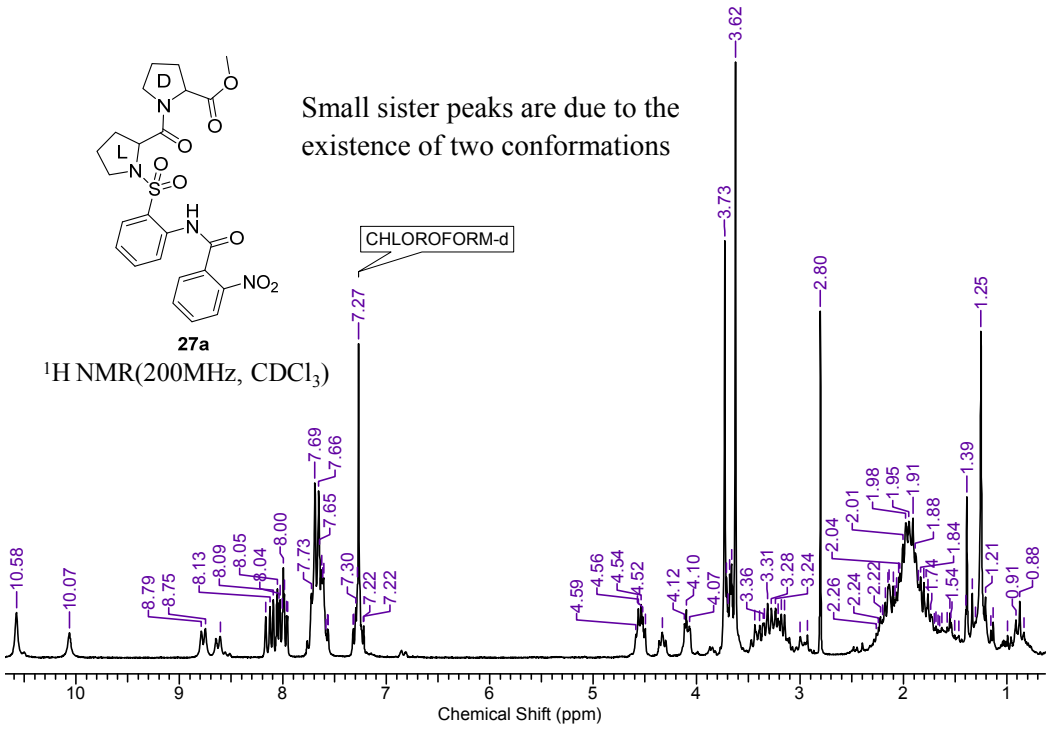

27a

^{1}H NMR(200MHz, $CDCl_3$)

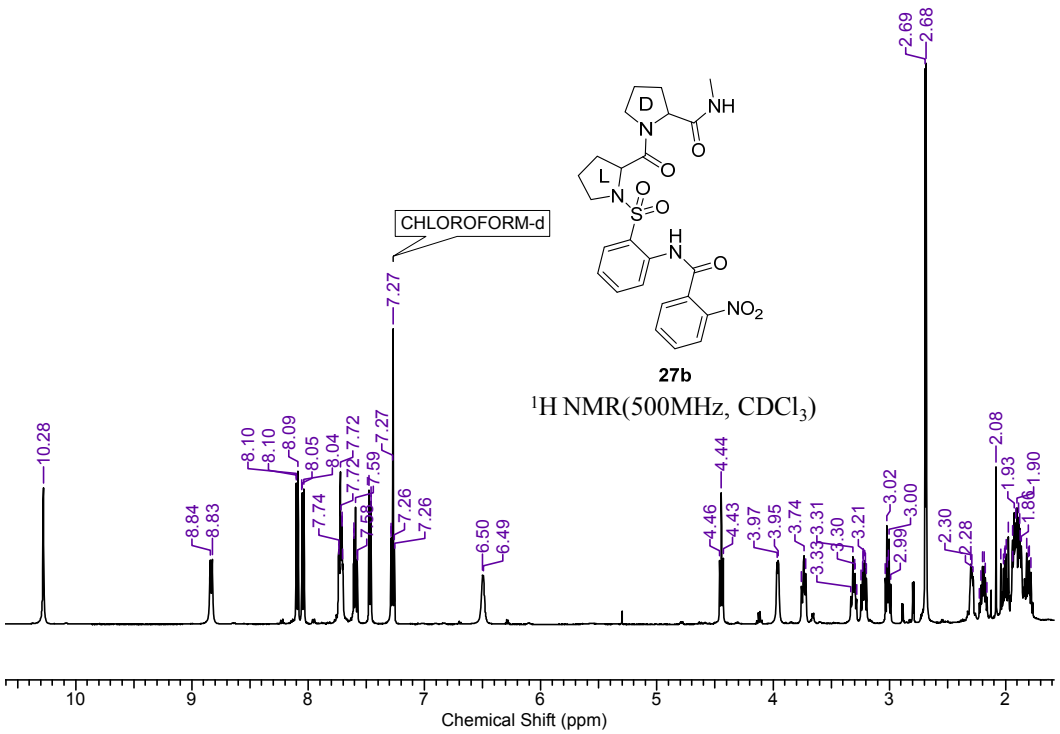

27b

^{1}H NMR(500MHz, $CDCl_3$)

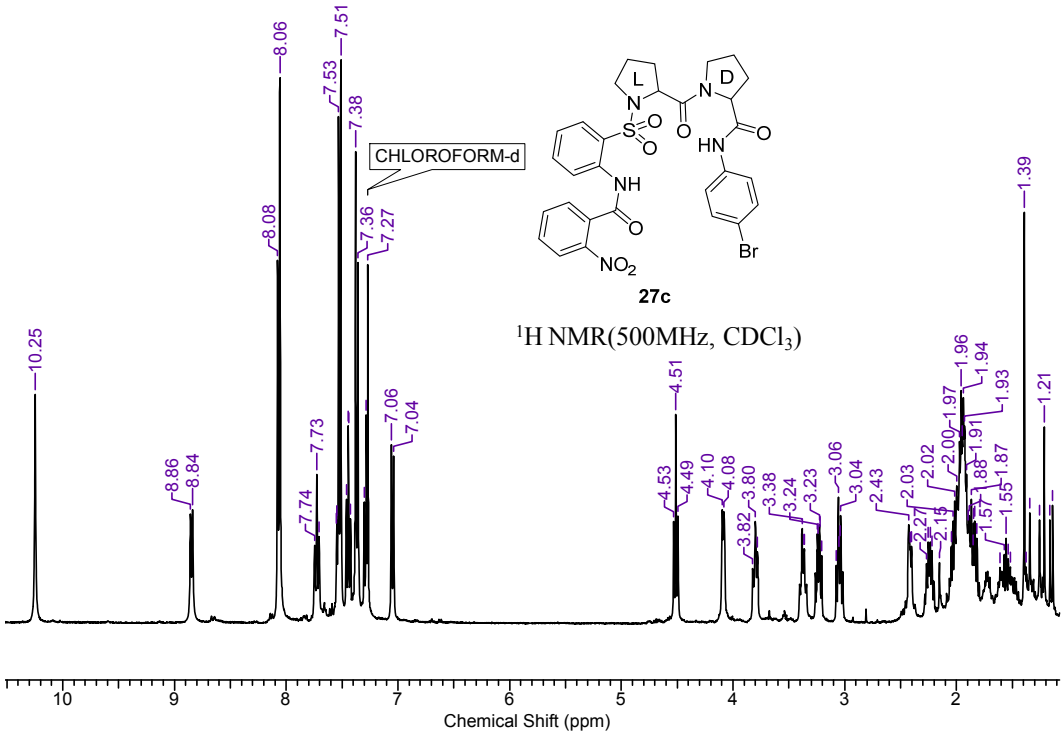
CHLOROFORM-d
27c
^{1}H NMR(500MHz, CDCl$_3$)
Chemical Shift (ppm)

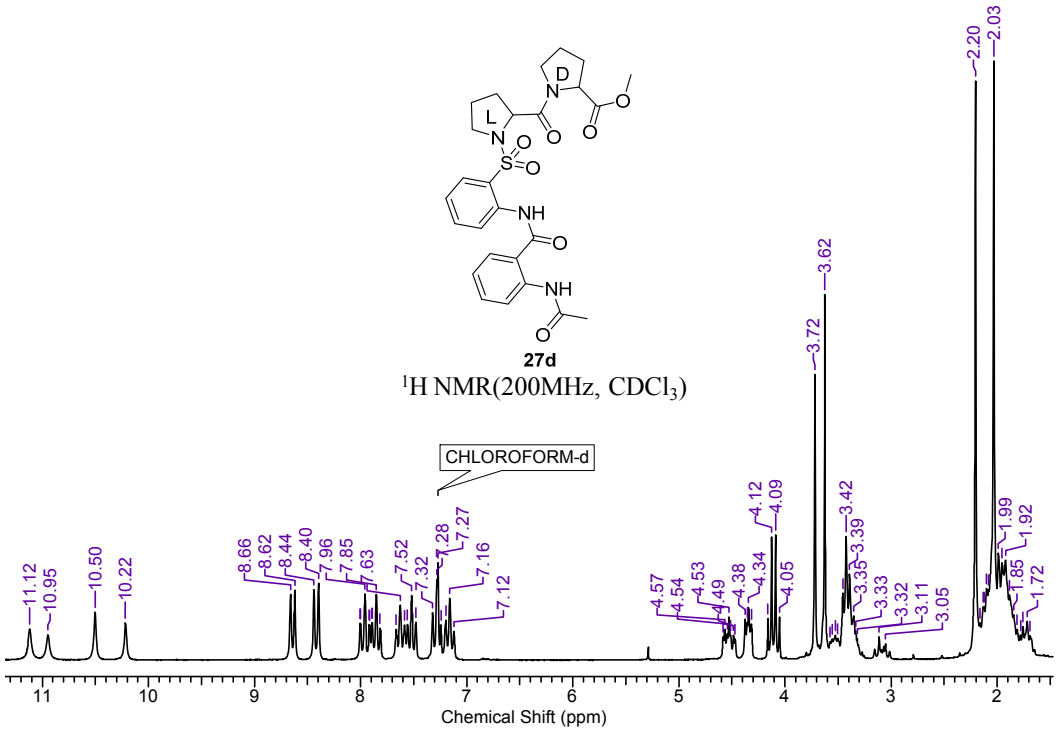
CHLOROFORM-d
27d
^{1}H NMR(200MHz, CDCl$_3$)
Chemical Shift (ppm)

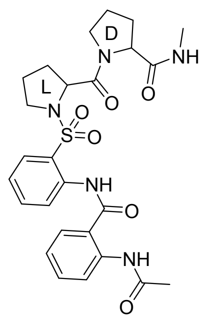

27e

^{1}H NMR(400MHz, $CDCl_3$)

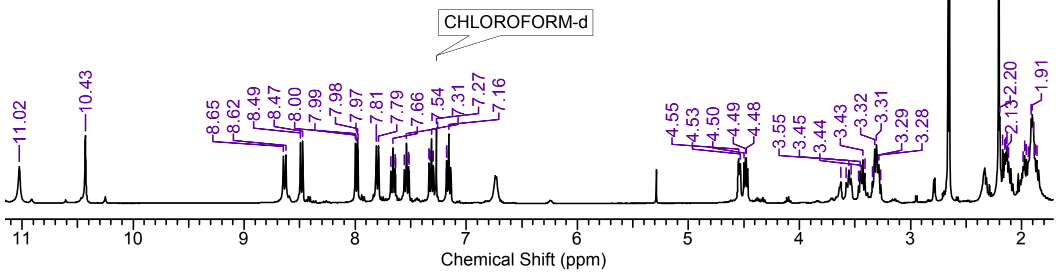

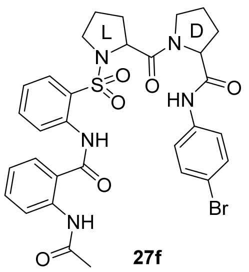

27f

^{1}H NMR(500MHz, $CDCl_3$)

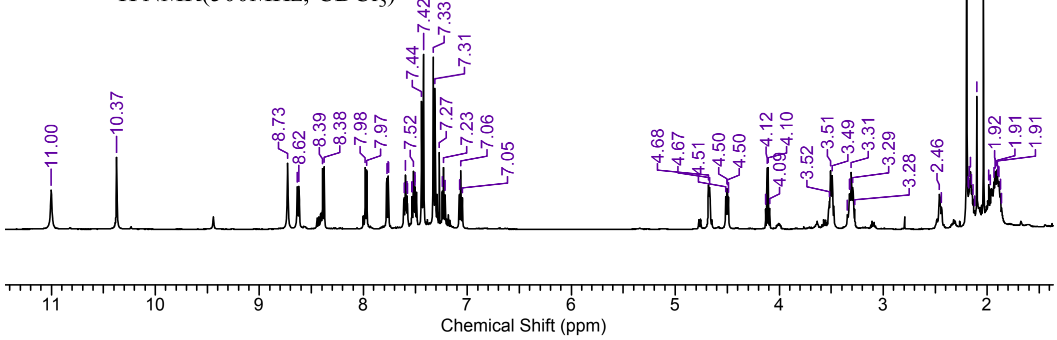

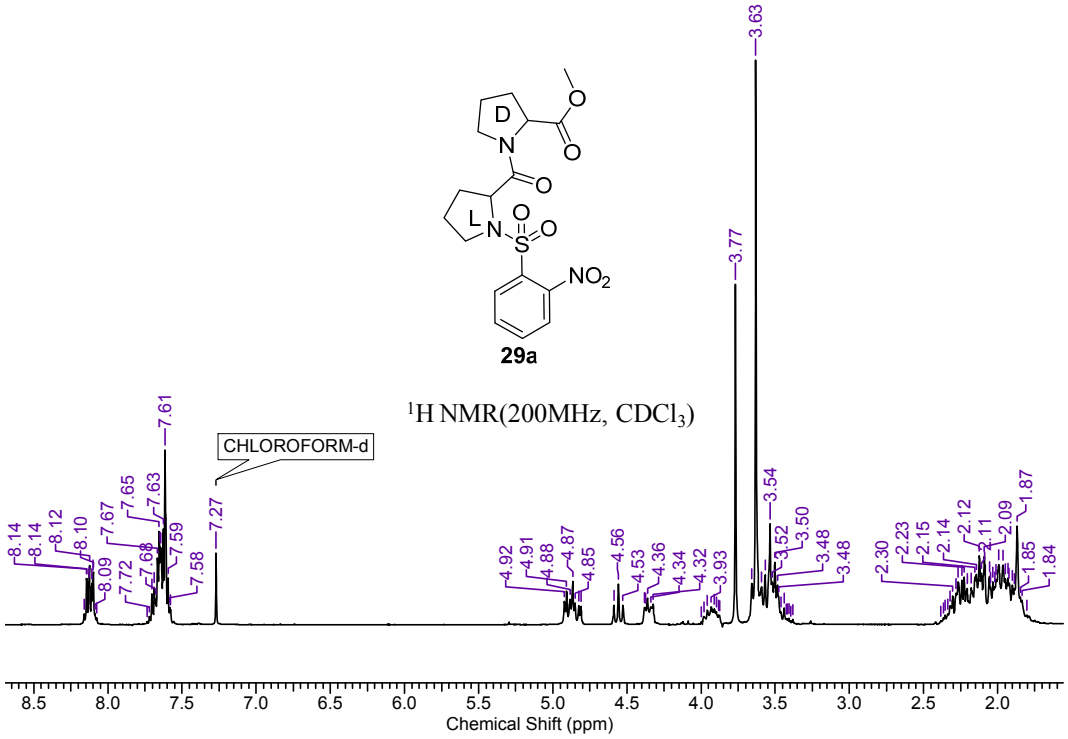
D
L
NO2
29a
1H NMR(200MHz, CDCl3)
CHLOROFORM-d
Chemical Shift (ppm)

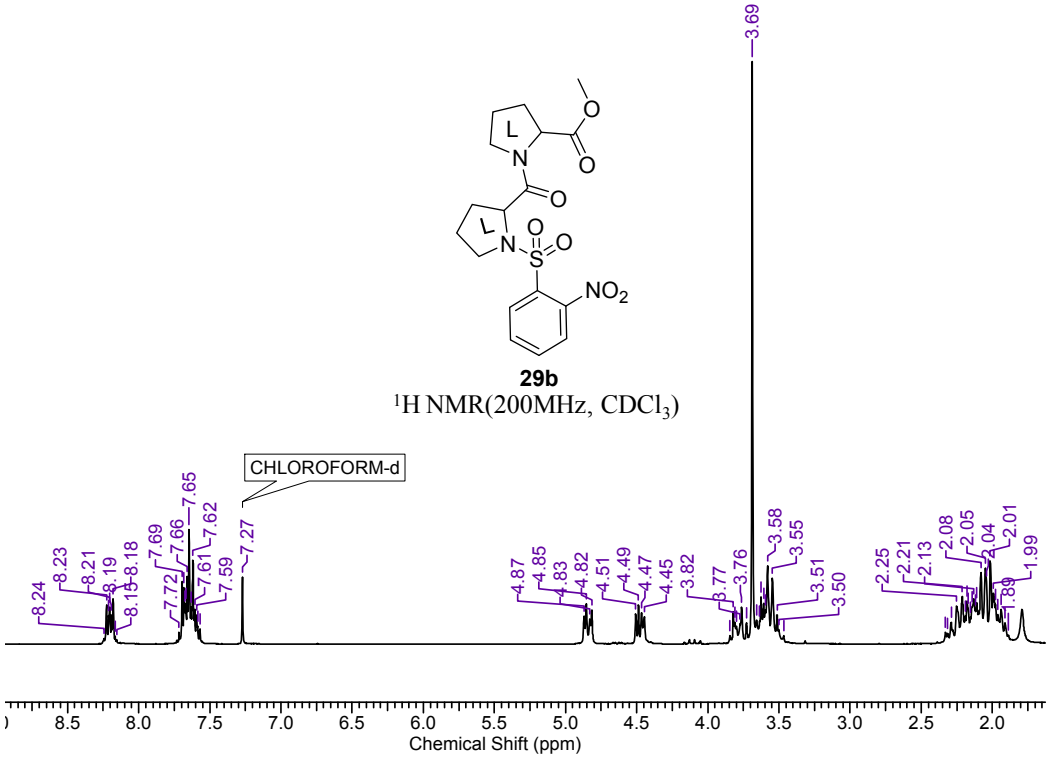
L
L
NO2
29b
1H NMR(200MHz, CDCl3)
CHLOROFORM-d
Chemical Shift (ppm)

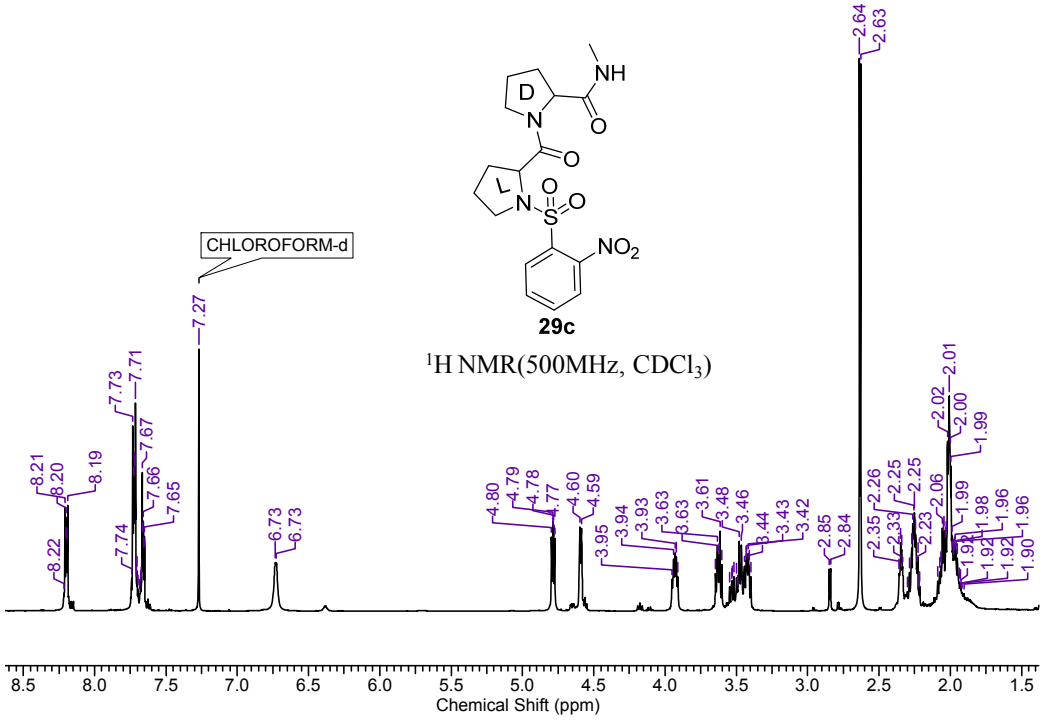
CHLOROFORM-d
29c
^{1}H NMR(500MHz, $CDCl_3$)
Chemical Shift (ppm)

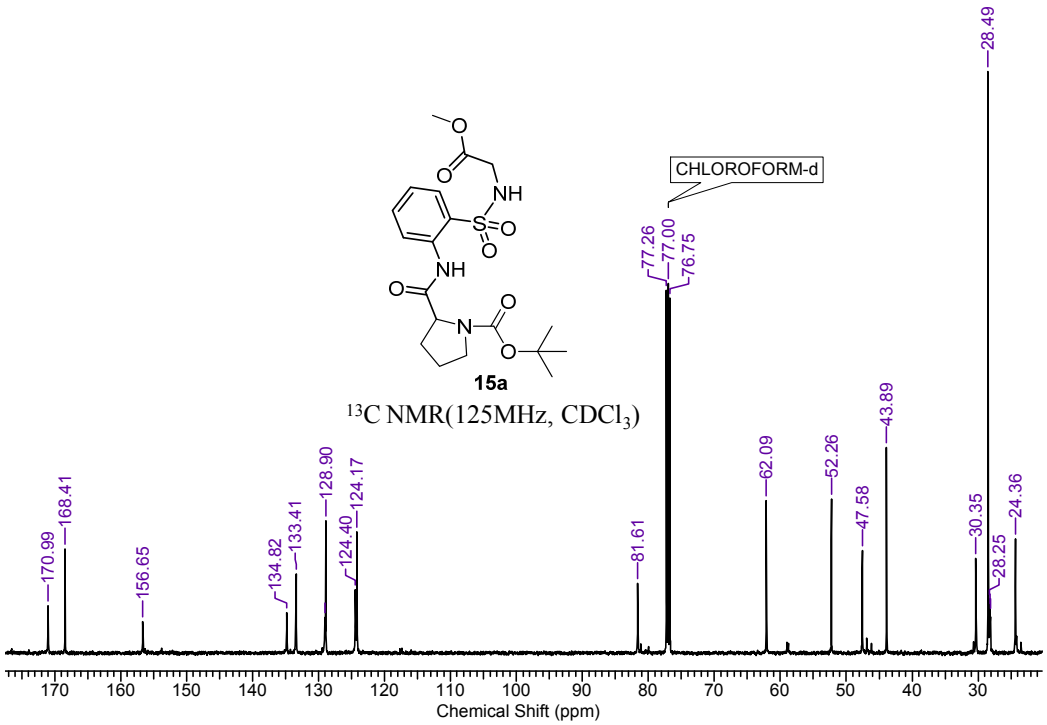
CHLOROFORM-d
15a
^{13}C NMR(125MHz, $CDCl_3$)
Chemical Shift (ppm)

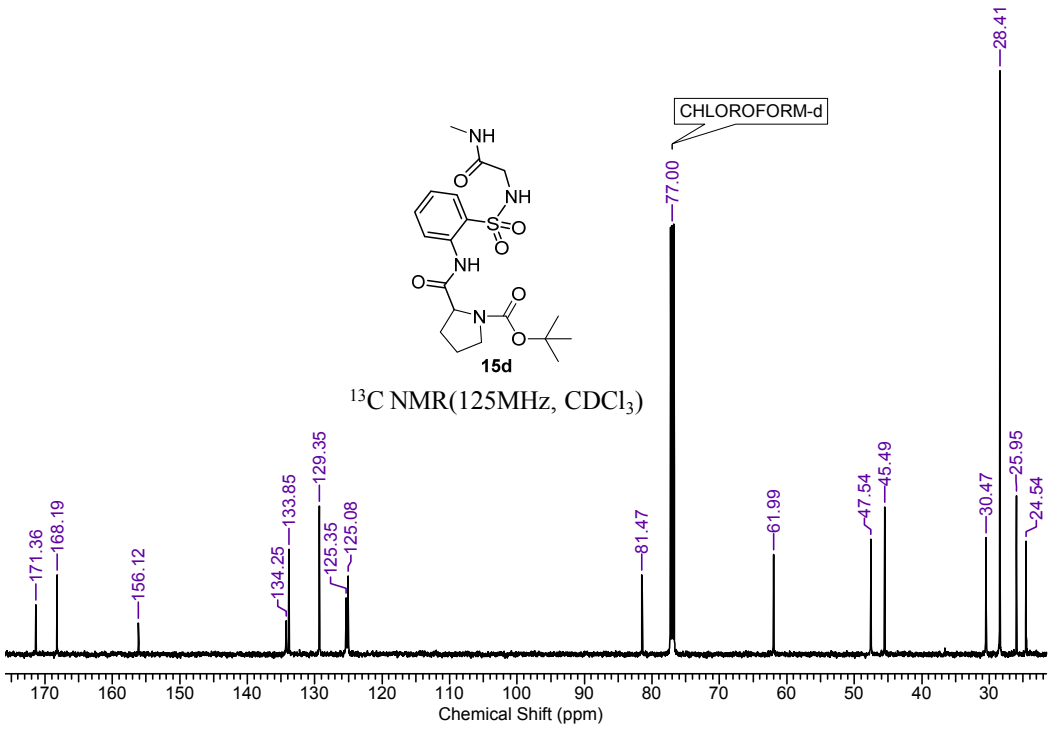

15d

^{13}C NMR(125MHz, $CDCl_3$)

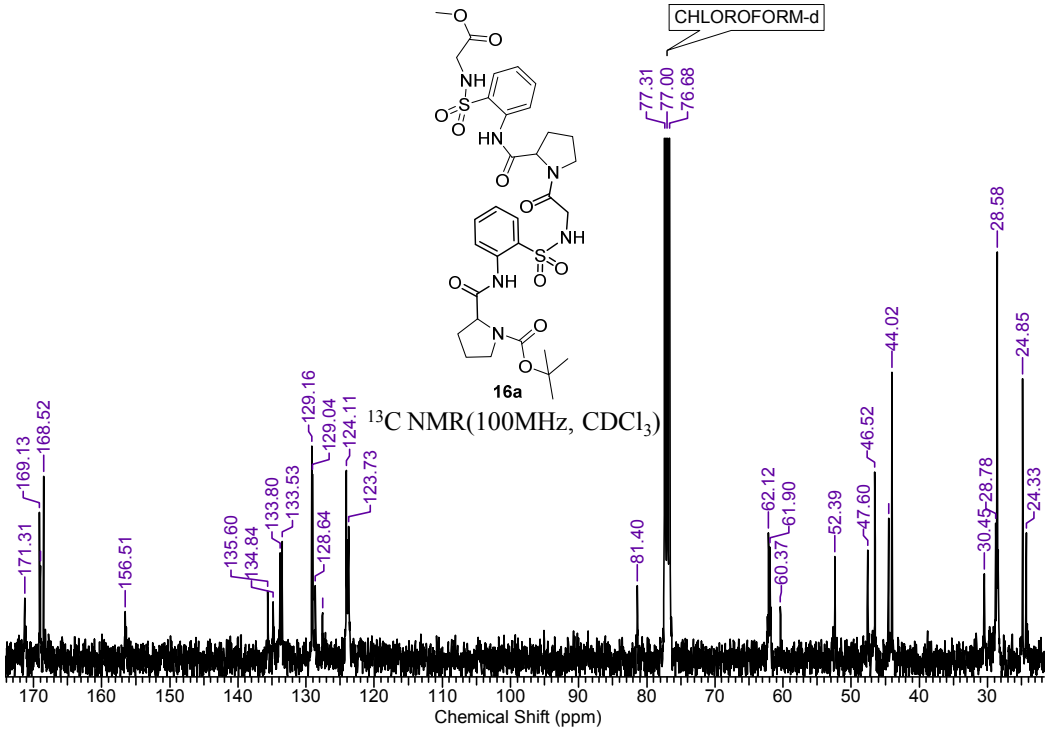

16a

^{13}C NMR(100MHz, $CDCl_3$)

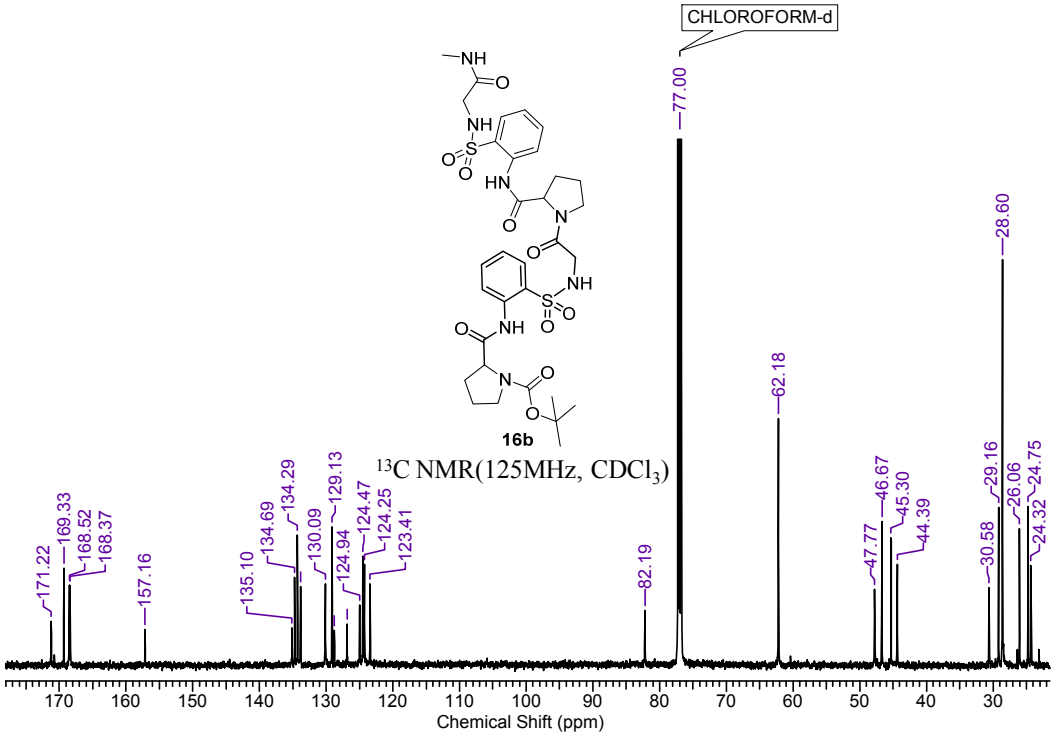

16b

^{13}C NMR(125MHz, $CDCl_3$)

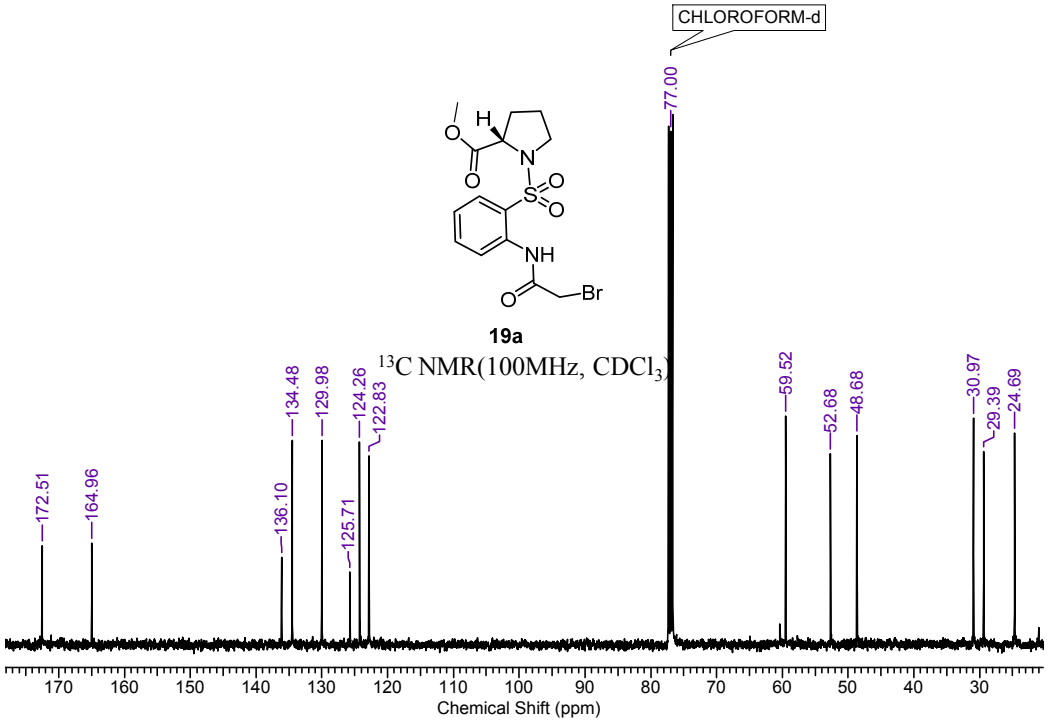

19a

^{13}C NMR(100MHz, $CDCl_3$)

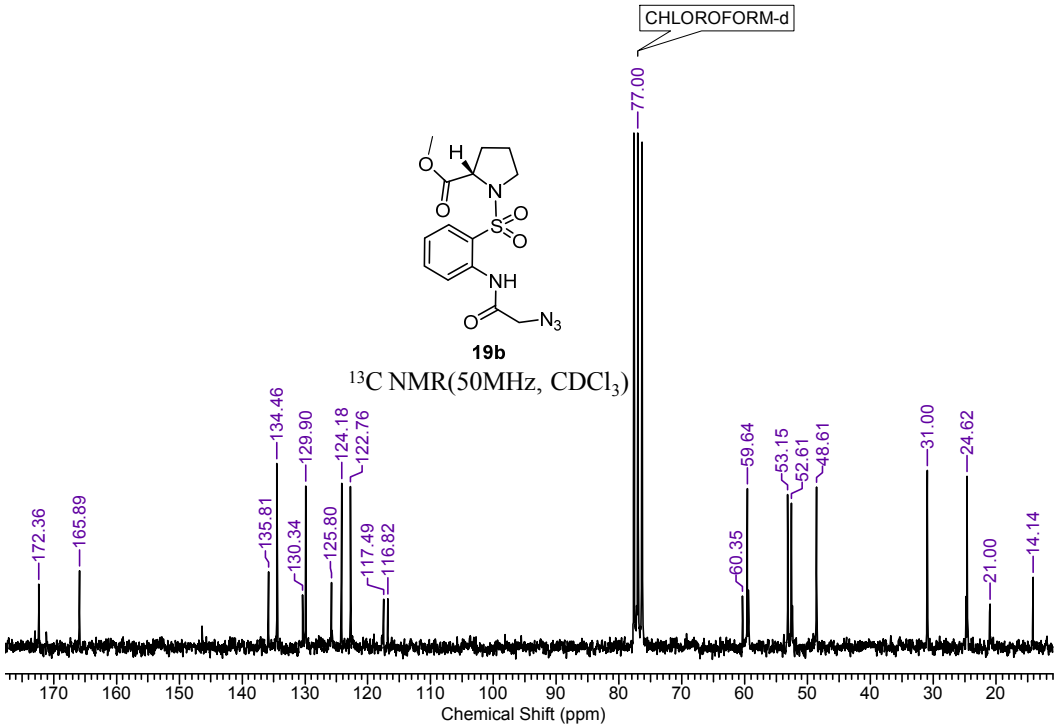
CHLOROFORM-d
77.00
19b
^{13}C NMR(50MHz, $CDCl_3$)
172.36
165.89
135.81
134.46
130.34
129.90
125.80
124.18
122.76
117.49
116.82
60.35
59.64
53.15
52.61
48.61
31.00
24.62
21.00
14.14
Chemical Shift (ppm)

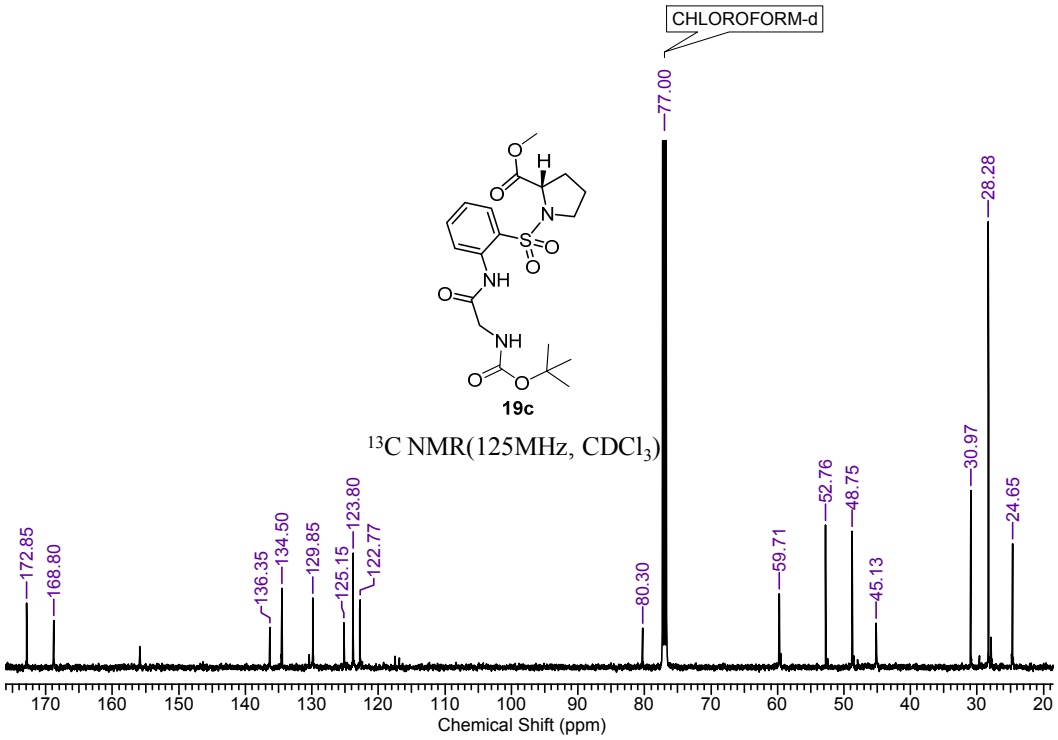
CHLOROFORM-d
77.00
19c
^{13}C NMR(125MHz, $CDCl_3$)
172.85
168.80
136.35
134.50
129.85
125.15
123.80
122.77
80.30
59.71
52.76
48.75
45.13
30.97
28.28
24.65
Chemical Shift (ppm)

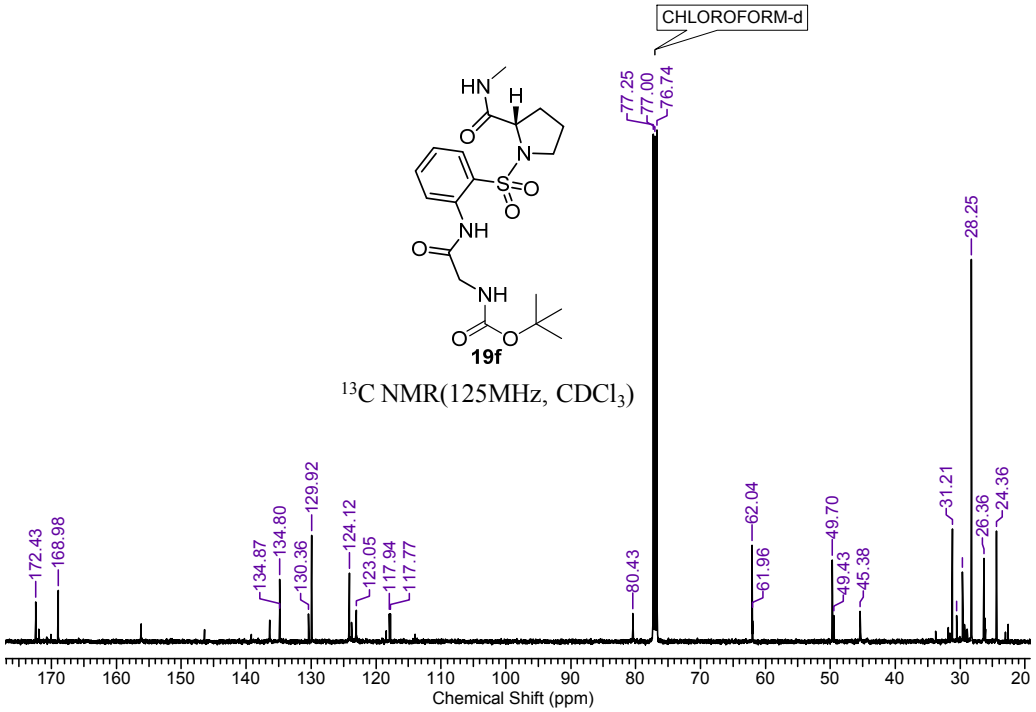

19f

^{13}C NMR(125MHz, $CDCl_3$)

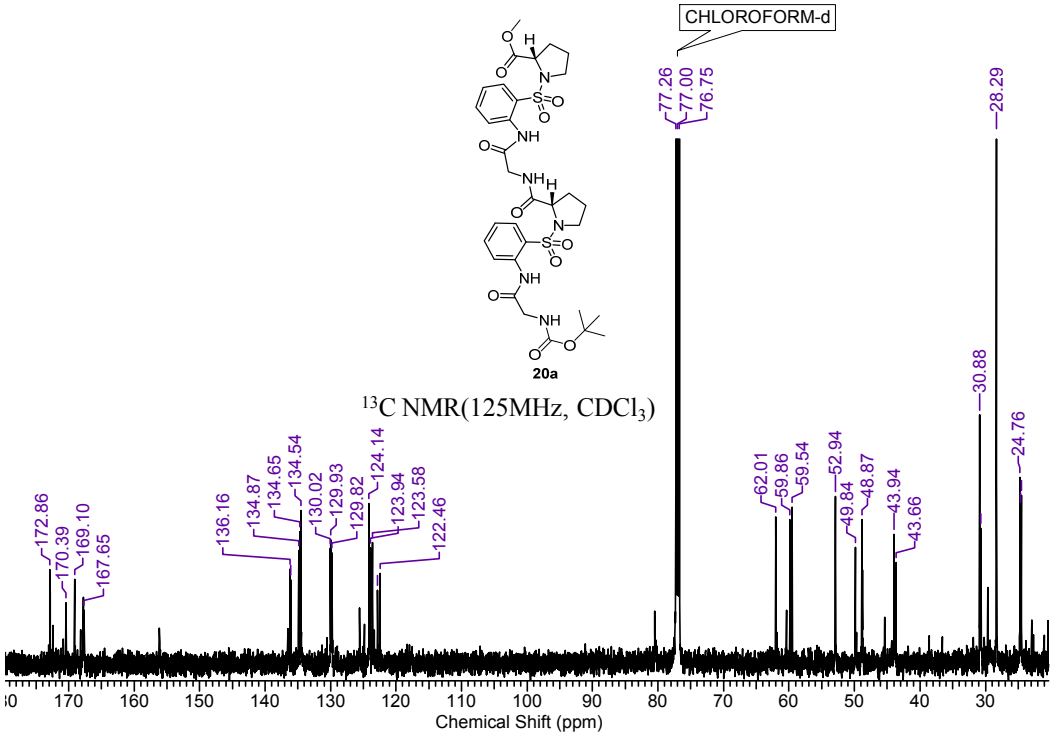

20a

^{13}C NMR(125MHz, $CDCl_3$)

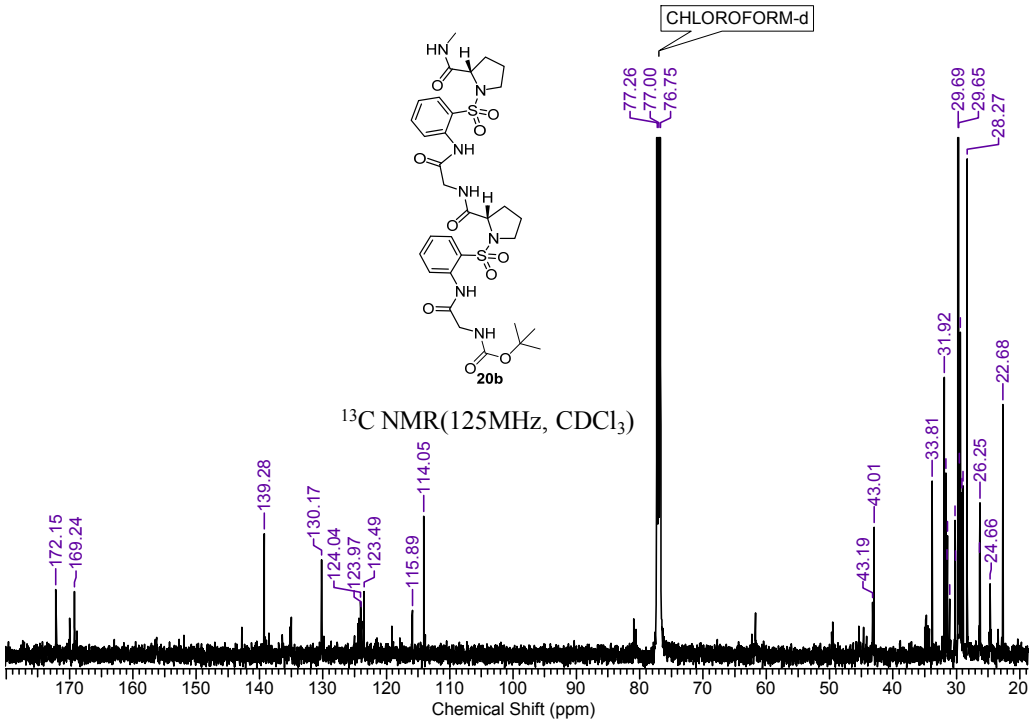

20b

^{13}C NMR(125MHz, $CDCl_3$)

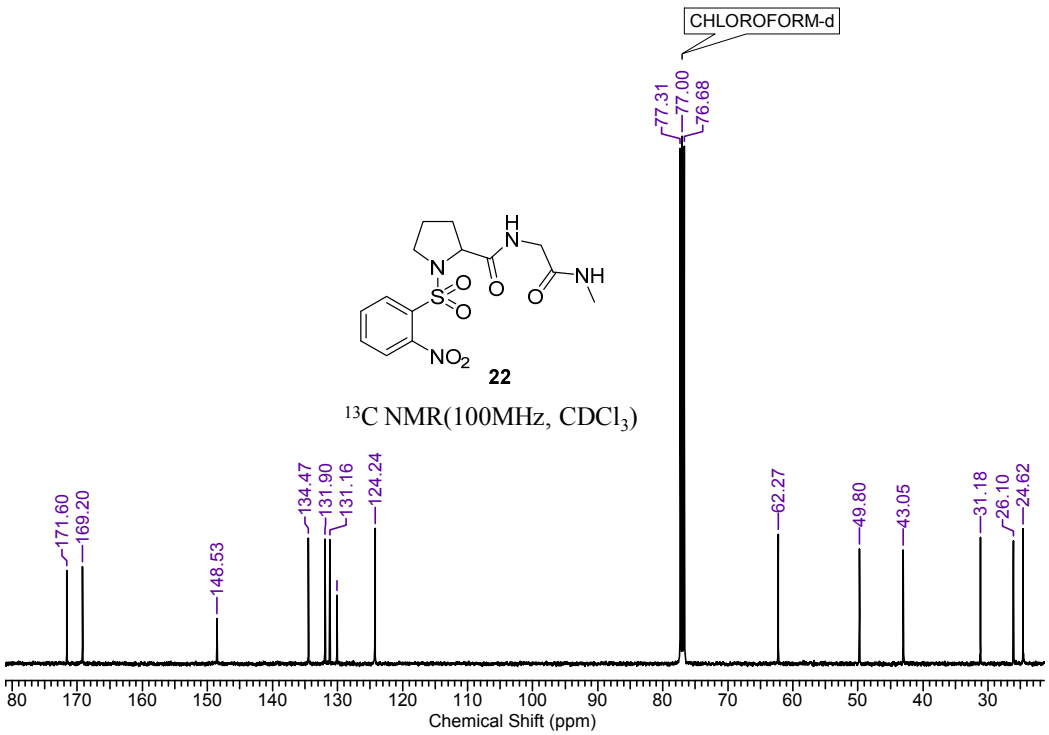

22

^{13}C NMR(100MHz, $CDCl_3$)

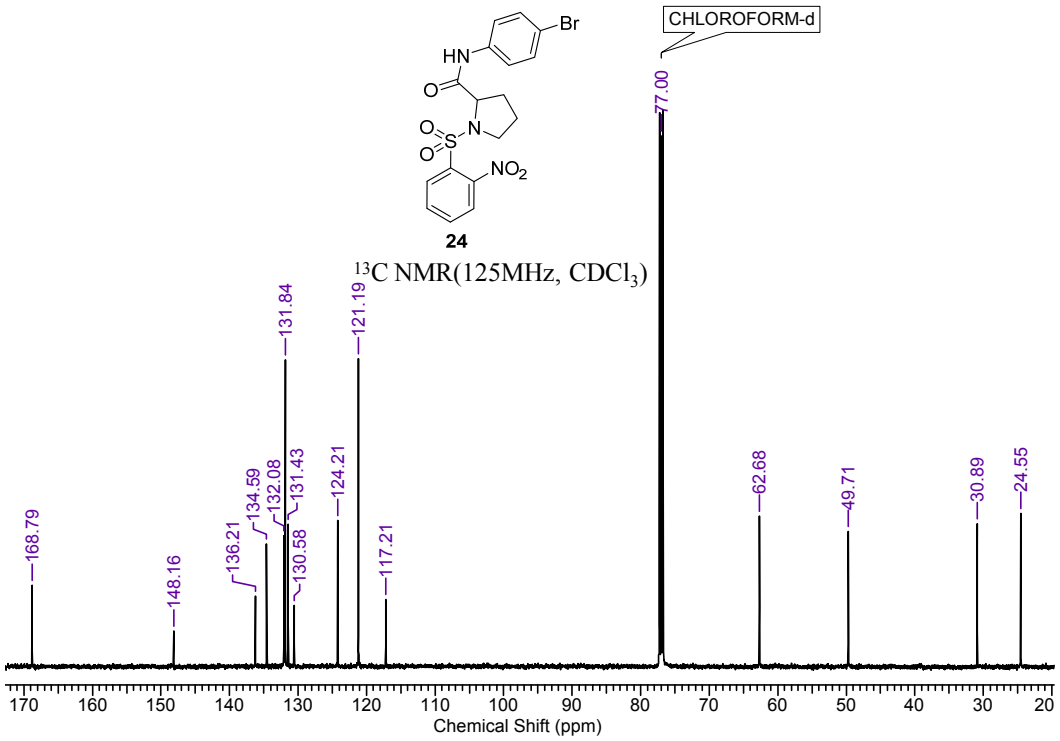
CHLOROFORM-d
77.00
Br
HN
O
O
S
O
N
NO2
24
13C NMR(125MHz, CDCl3)
131.84
121.19
168.79
148.16
136.21
134.59
132.08
131.43
130.58
124.21
117.21
62.68
49.71
30.89
24.55
Chemical Shift (ppm)

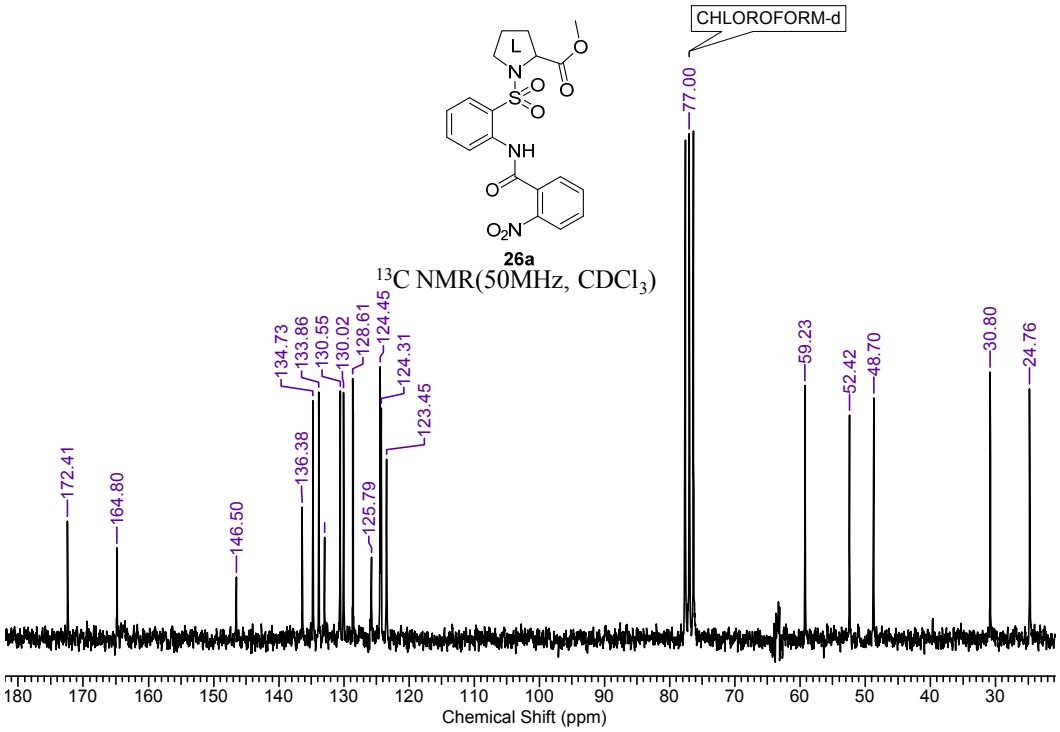
CHLOROFORM-d
77.00
L
N
O
O
S
O
O
NH
O
O2N
26a
13C NMR(50MHz, CDCl3)
134.73
133.86
130.55
130.02
128.61
124.45
124.31
123.45
136.38
125.79
172.41
164.80
146.50
59.23
52.42
48.70
30.80
24.76
Chemical Shift (ppm)

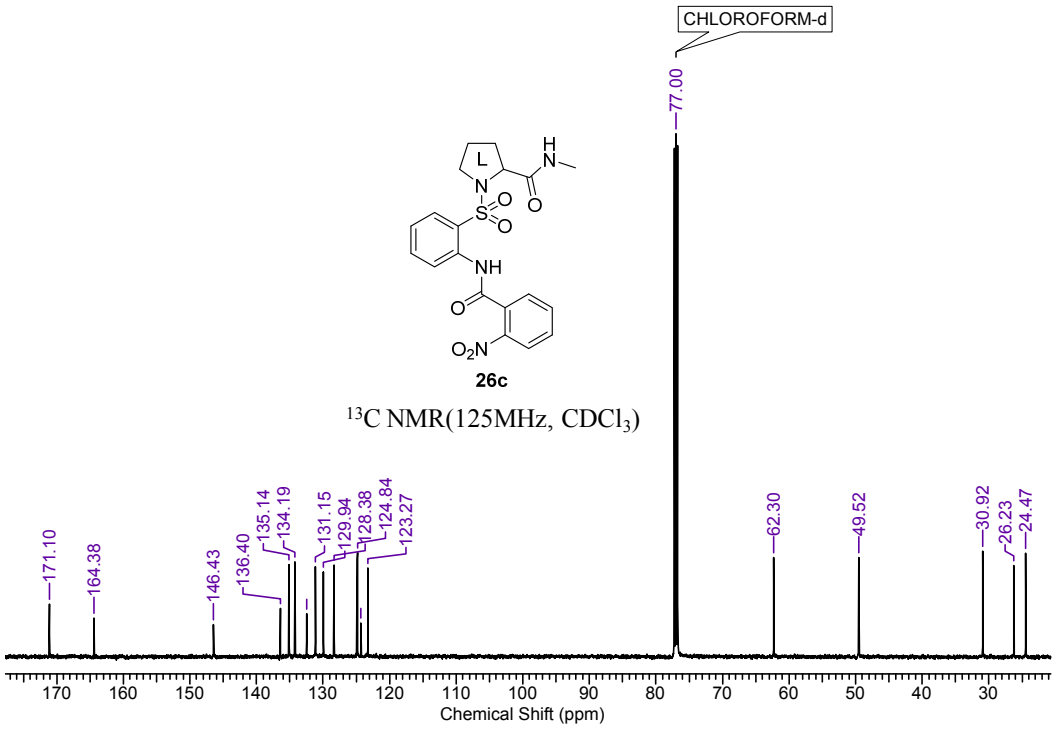

26c

^{13}C NMR(125MHz, $CDCl_3$)

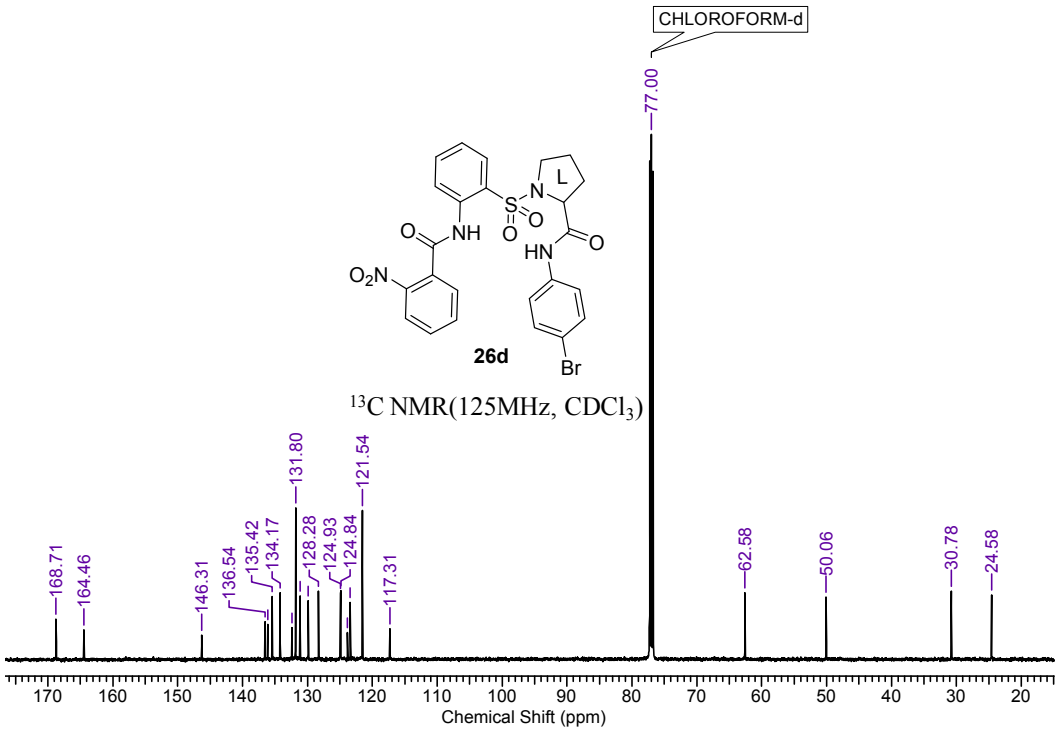

26d

^{13}C NMR(125MHz, $CDCl_3$)

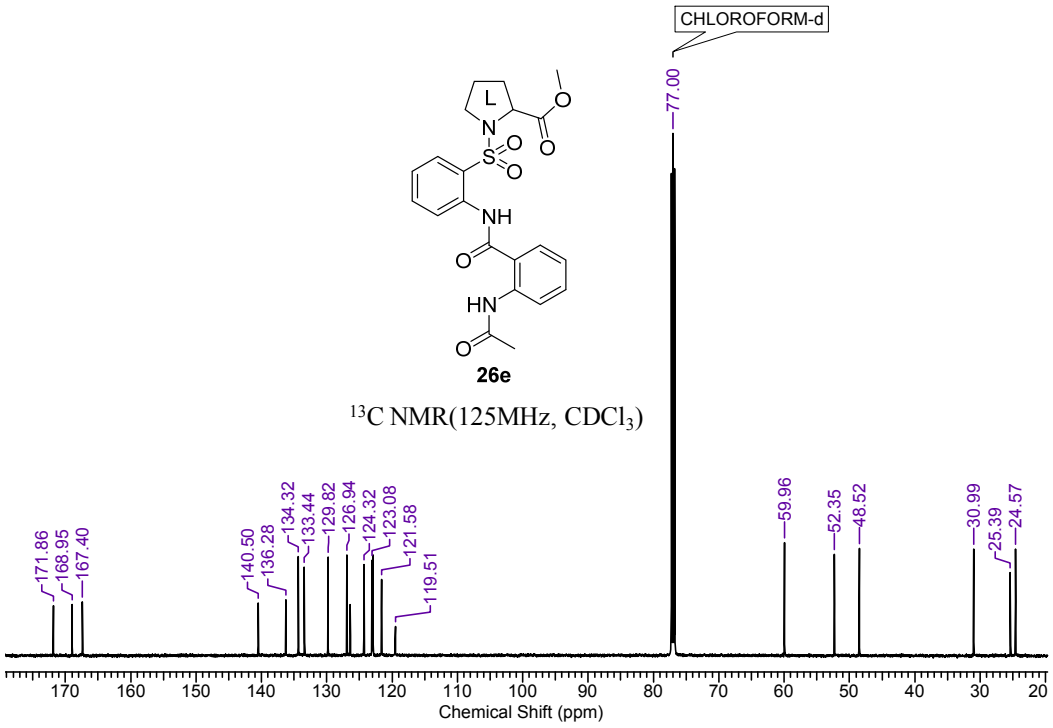

26e

^{13}C NMR(125MHz, $CDCl_3$)

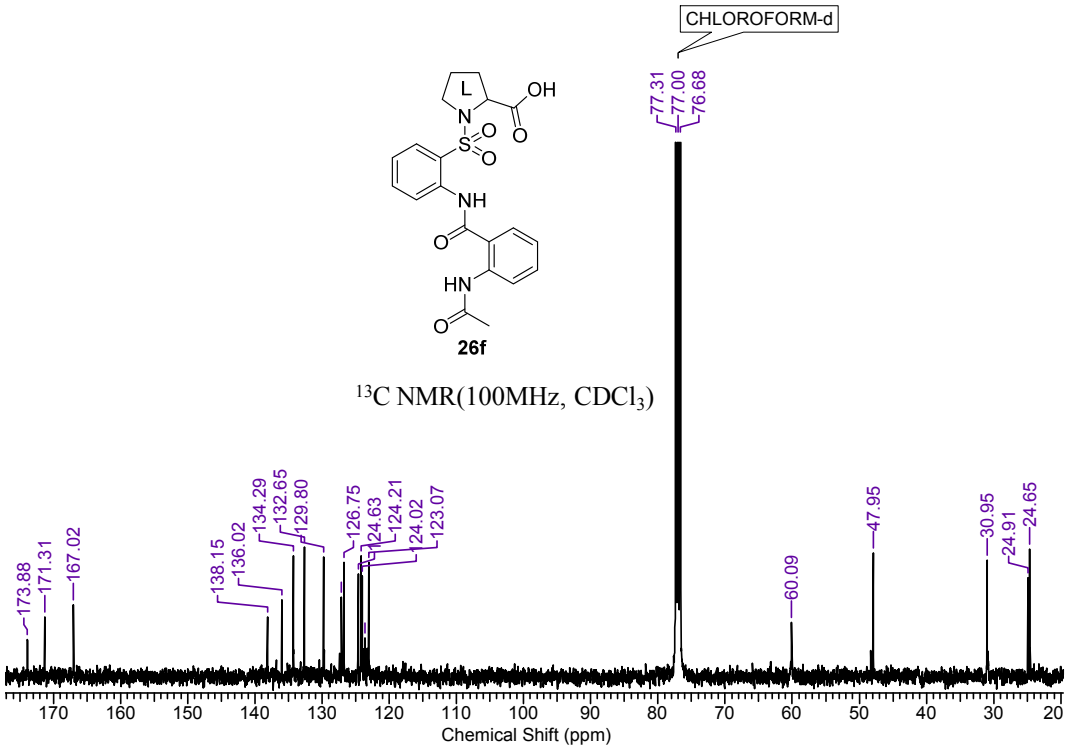

26f

^{13}C NMR(100MHz, $CDCl_3$)

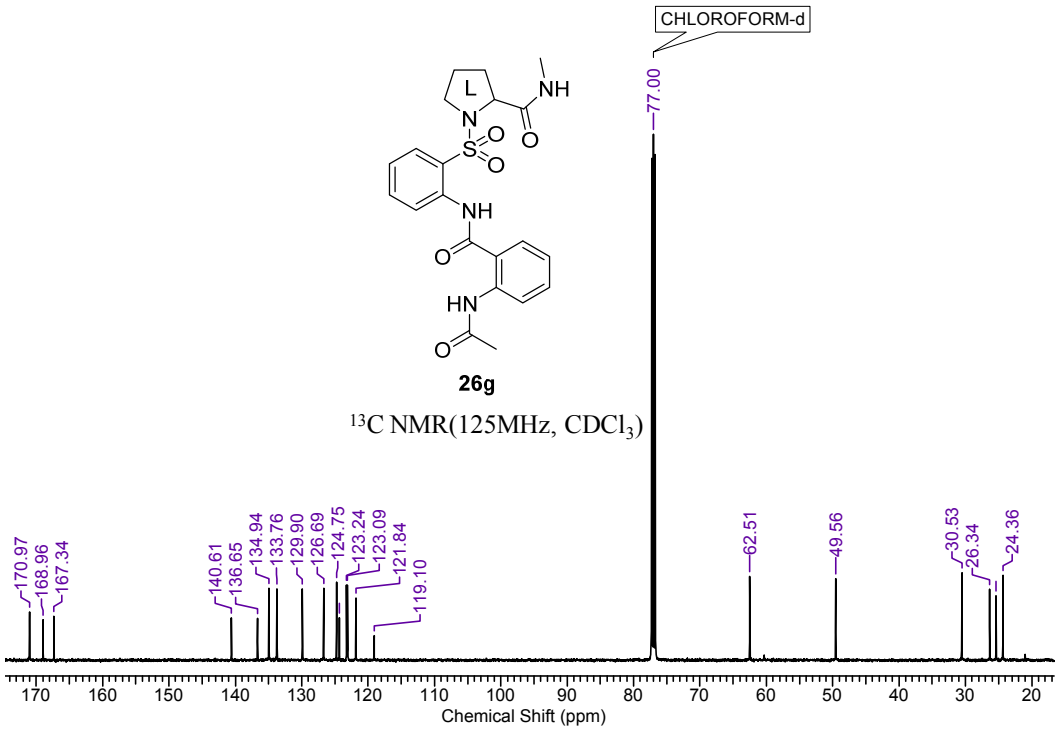

26g

^{13}C NMR(125MHz, $CDCl_3$)

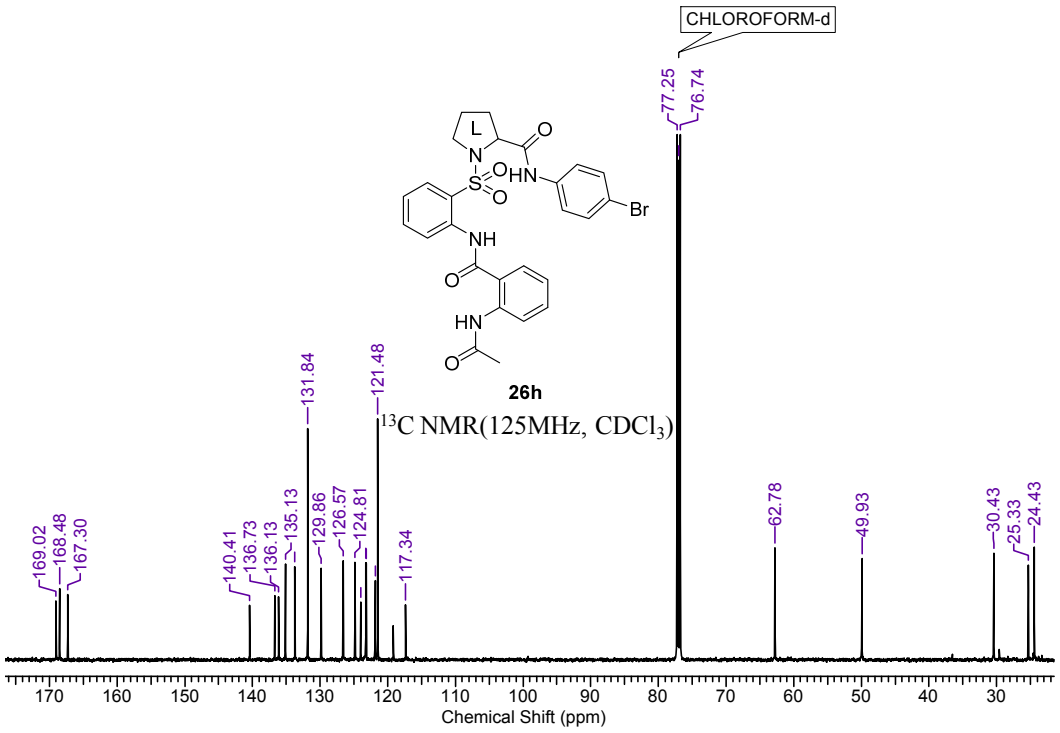

26h

^{13}C NMR(125MHz, $CDCl_3$)

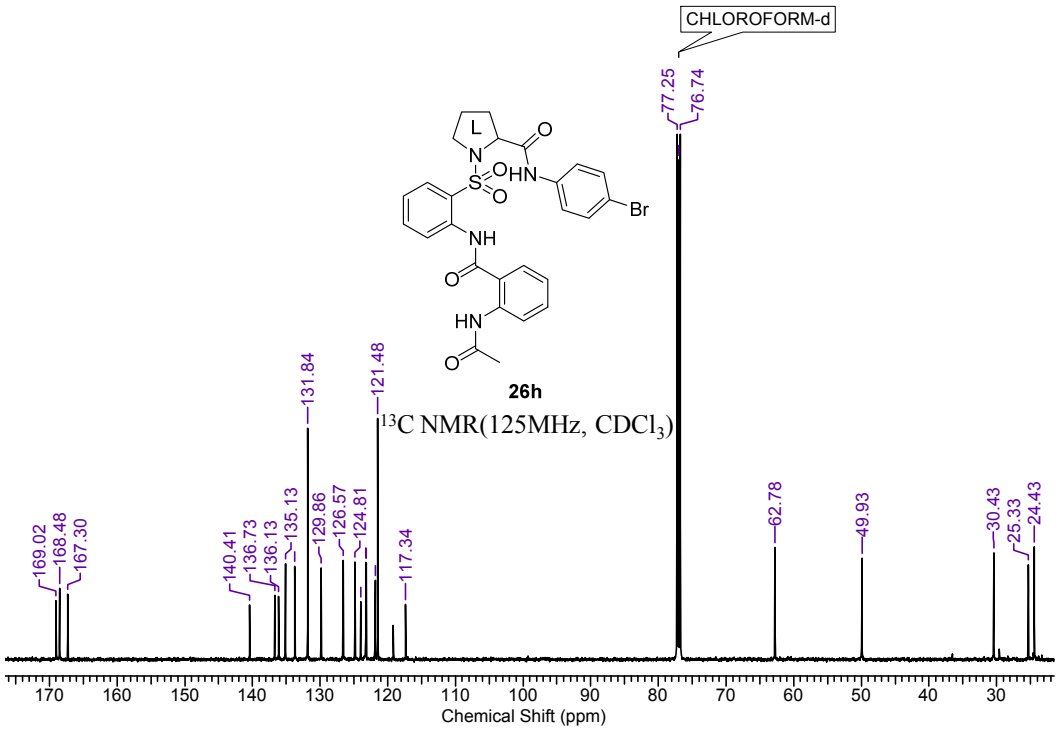

26h

^{13}C NMR(125MHz, $CDCl_3$)

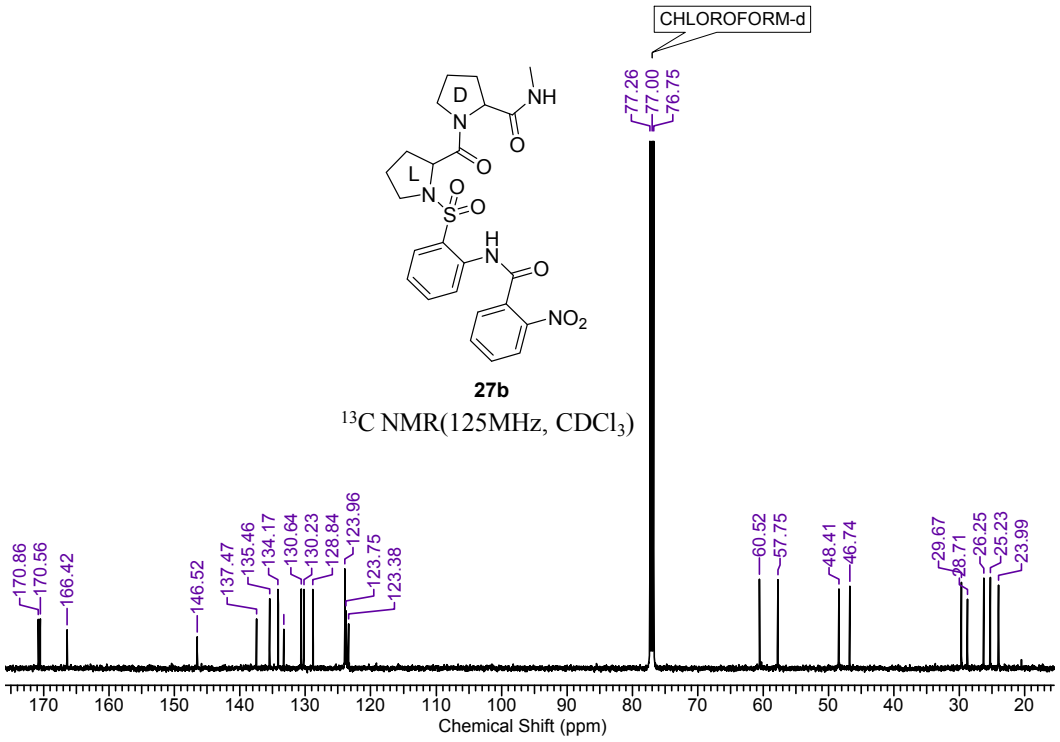

27b

^{13}C NMR(125MHz, $CDCl_3$)

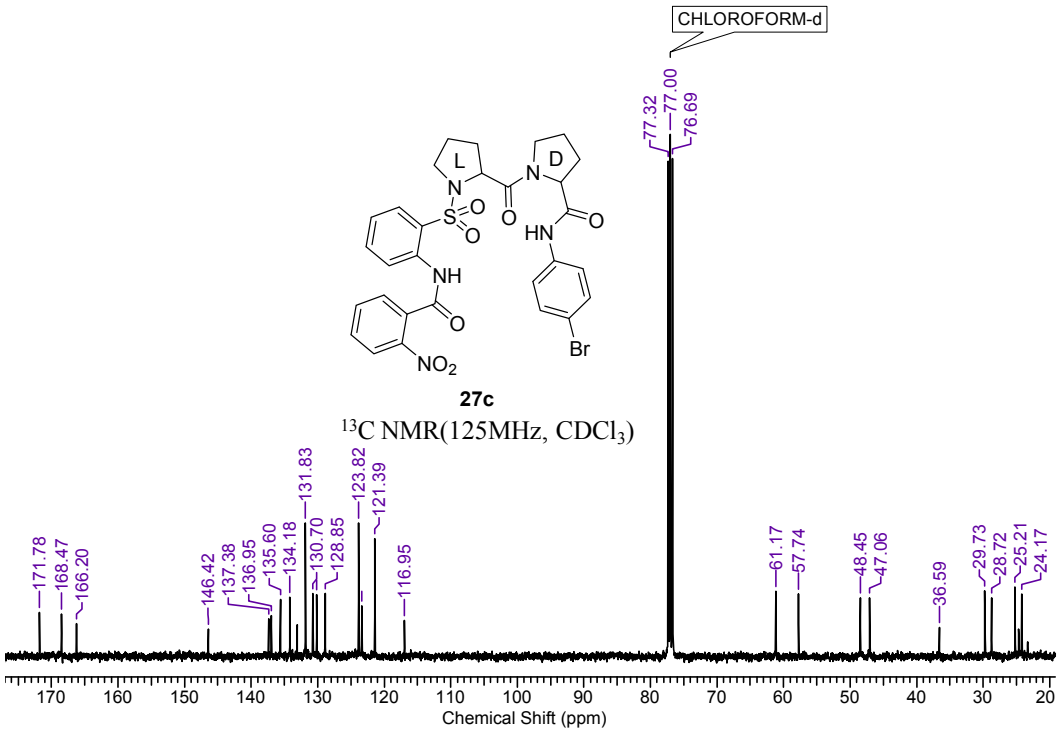

27c

^{13}C NMR(125MHz, $CDCl_3$)

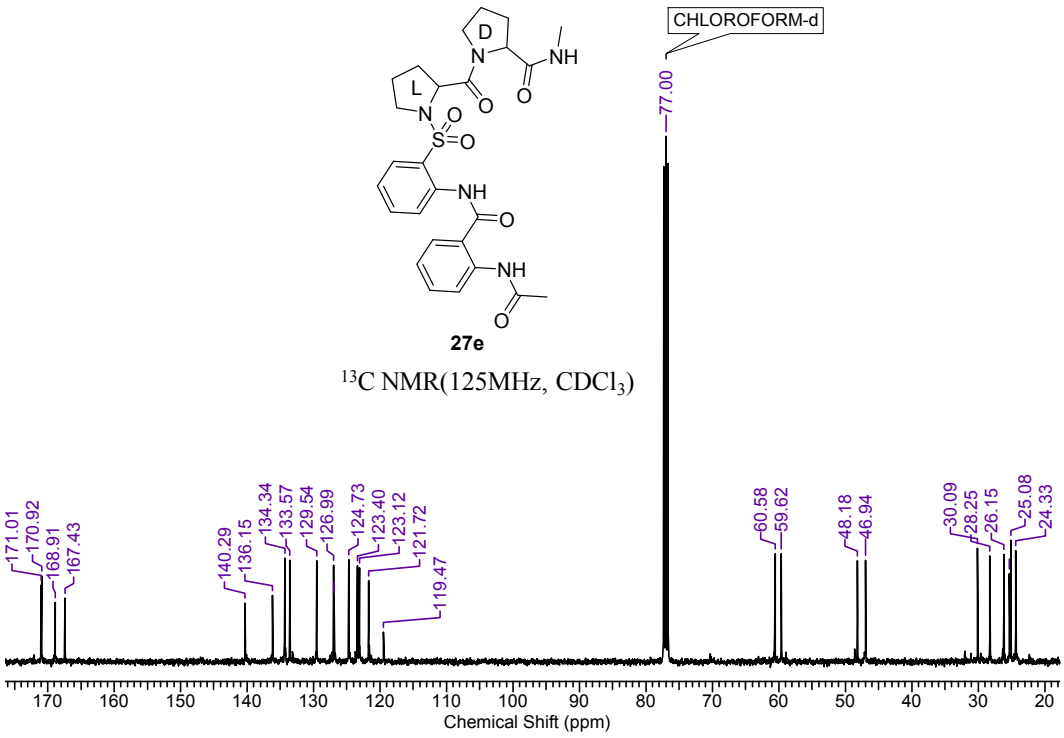

27e

^{13}C NMR(125MHz, $CDCl_3$)

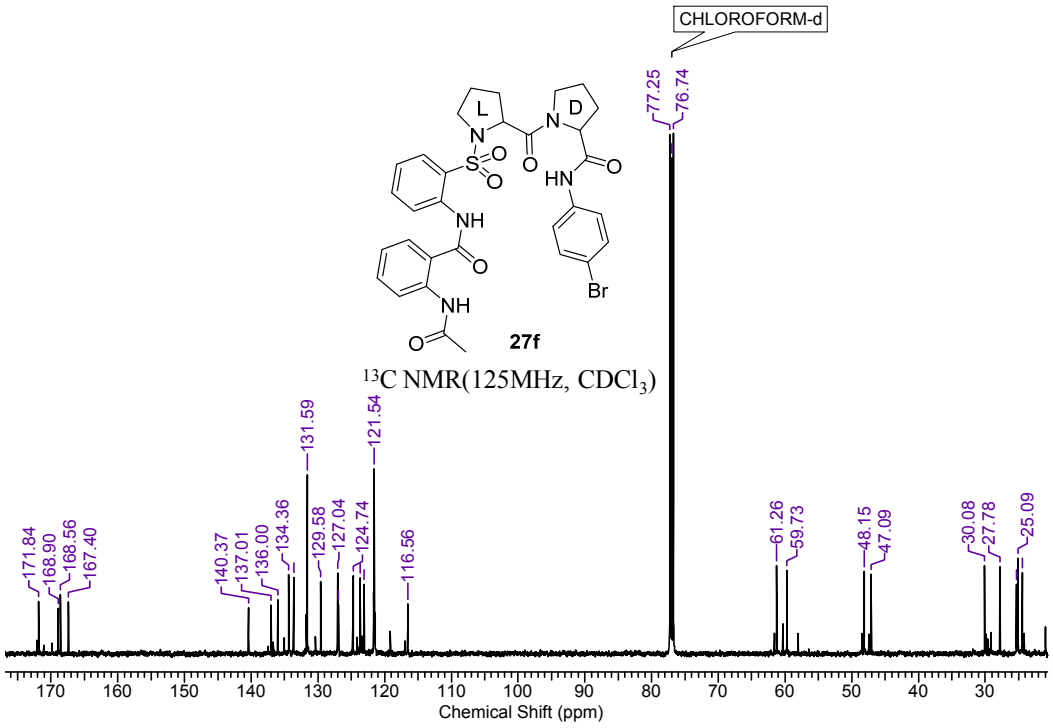
CHLOROFORM-d
77.25
76.74
L
D
N
S
O
HN
NH
Br
27f
^{13}C NMR(125MHz, CDCl$_3$)
171.84
168.90
168.56
167.40
140.37
137.01
136.00
134.36
131.59
129.58
127.04
124.74
121.54
116.56
61.26
59.73
48.15
47.09
30.08
27.78
25.09
Chemical Shift (ppm)

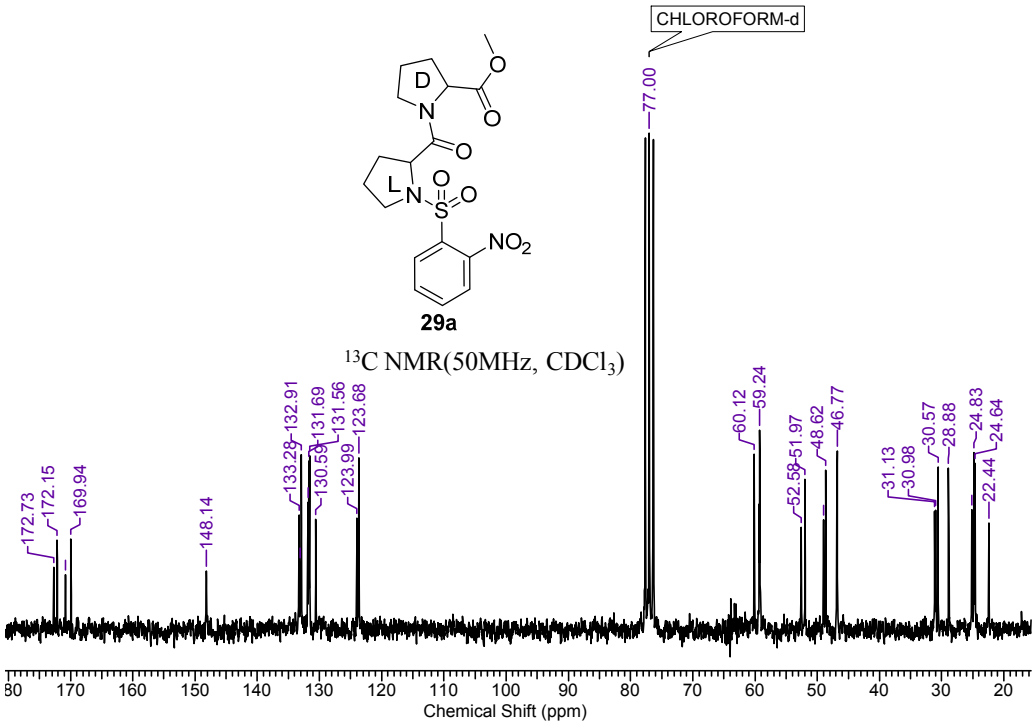
CHLOROFORM-d
77.00
D
L
N
S
O
NO$_2$
29a
^{13}C NMR(50MHz, CDCl$_3$)
172.73
172.15
169.94
148.14
133.28
132.91
131.69
131.56
130.59
123.99
123.68
60.12
59.24
52.59
51.97
48.62
46.77
31.13
30.98
30.57
28.88
24.83
24.64
22.44
Chemical Shift (ppm)

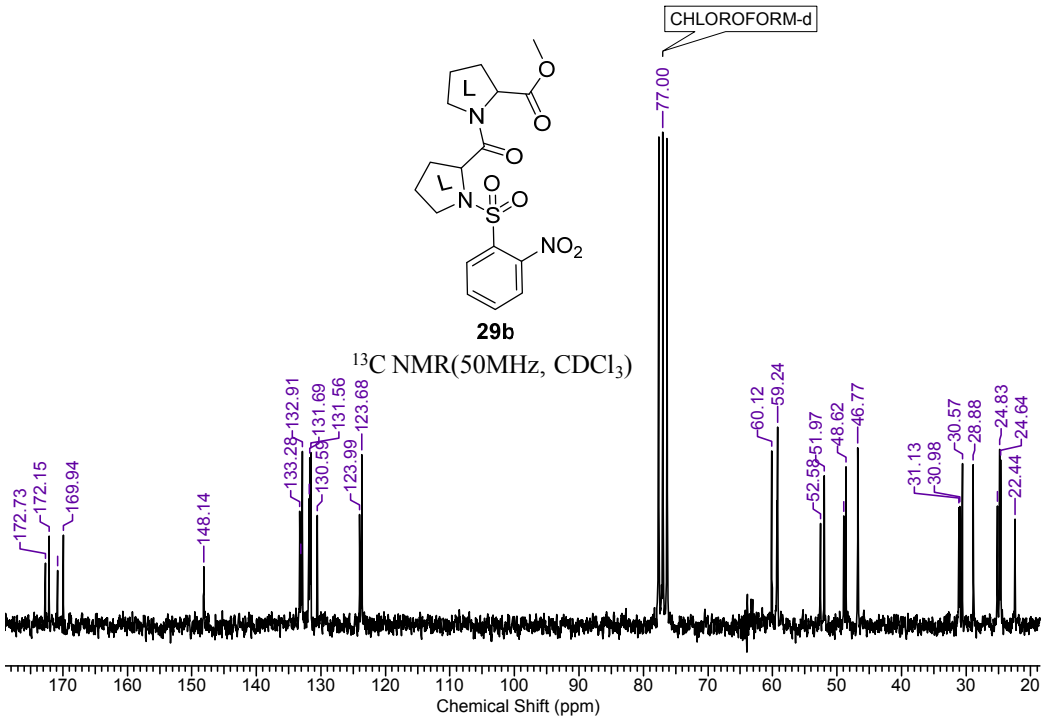

29b

^{13}C NMR(50MHz, $CDCl_3$)

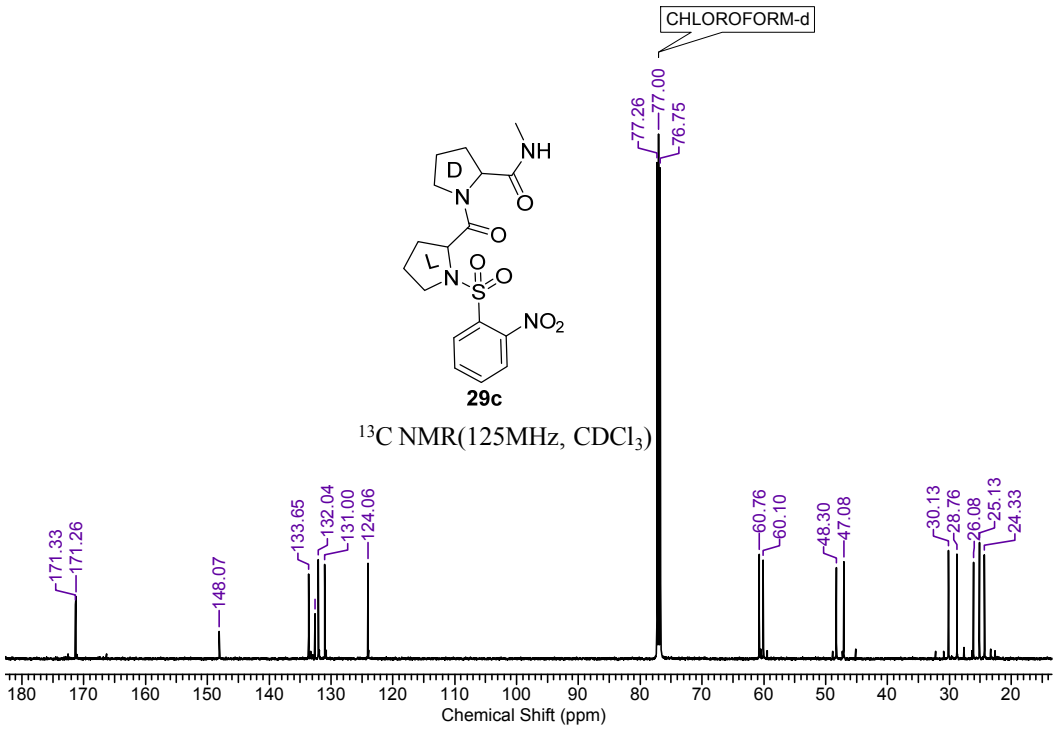

29c

^{13}C NMR(125MHz, $CDCl_3$)

Table 2.14. Titration study of 15d in $CDCl_3$ (20 mmol) with DMSO-d_6 (volume of DMSO-d_6 added at each addition = 5 µl)

Volume of DMSO-d_6 added (in µL)	Chemical Shift (in ppm)		
	δNH1	δNH2	δNH3
5	9.26	7.17	6.5
10	9.26	7.17	6.51
15	9.26	7.17	6.51
20	9.27	7.17	6.51
25	9.27	7.18	6.52
30	9.27	7.18	6.53
35	9.28	7.18	6.54
40	9.28	7.18	6.54
45	9.28	7.18	6.55
50	9.29	7.19	6.56

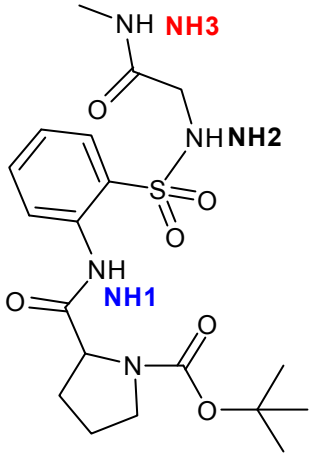

15d

Table 2.15. Titration study of 22 in $CDCl_3$ (20 mmol) with DMSO-d_6 (volume of DMSO-d_6 added at each addition = 5 µl)

Volume of DMSO-d_6 added (in µL)	Chemical Shift (in ppm)	
	δNH1	δNH2
0	7.01	6.41
5	7.04	6.48
10	7.35	6.61
15	7.4	6.65
20	7.54	6.69
25	7.55	6.69
30	7.61	6.72
35	7.69	6.77
40	7.72	6.78
45	7.74	6.78

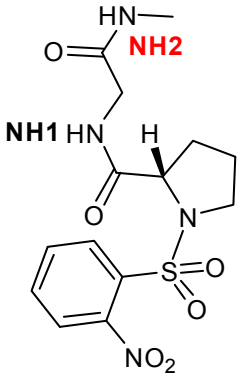

22

Table 2.16. Titration study of 16b in $CDCl_3$ (20 mmol) with DMSO-d_6 (volume of DMSO-d_6 added at each addition = 5 µl)

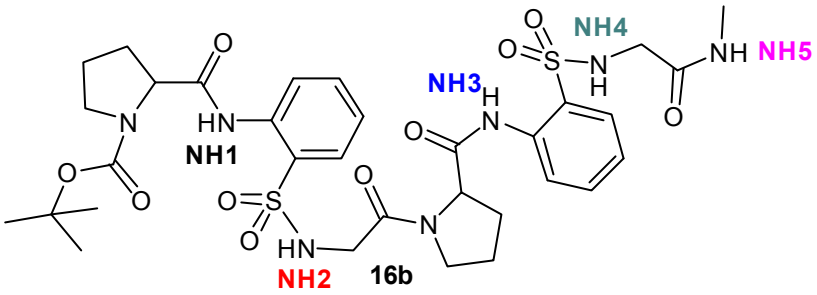

Volume of DMSO-d_6 added (in µL)	Chemical Shift (in ppm)				
	δNH1	δNH2	δNH3	δNH4	δNH5
5	9.45	7.01	9.41	6.72	7.01
10	9.46	7.01	9.41	6.74	7.01
15	9.46	7.01	9.4	6.75	7.01
20	9.46	6.99	9.39	6.75	6.99
25	9.46	6.98	9.38	6.77	6.98
30	9.46	6.98	9.37	6.77	6.98
35	9.46	6.97	9.36	6.79	6.97
40	9.46	6.97	9.36	6.78	6.97
45	9.46	6.96	9.35	6.79	6.96
50	9.46	6.96	9.34	6.8	6.96

Table 2.17. Titration study of 26g in $CDCl_3$ (20 mmol) with DMSO-d_6 (volume of DMSO-d_6 added at each addition = 5 µl)

Volume of DMSO-d_6 added (in µL)	Chemical Shift (in ppm)		
	δNH1	δNH2	δNH3
0	11.1	10.53	6.57
5	11.09	10.52	6.59
10	11.06	10.51	6.63
15	11.02	10.48	6.68
20	11	10.48	6.7
25	10.99	10.48	6.72
30	10.96	10.45	6.77
35	10.93	10.41	6.79
40	10.92	10.41	6.8
45	10.9	10.39	6.82
50	10.89	10.38	6.83

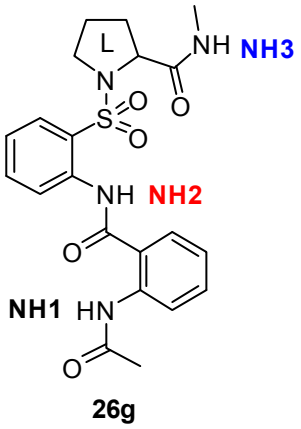

Table 2.18. Titration study of 27e in $CDCl_3$ (20 mmol) with DMSO-d_6 (volume of DMSO-d_6 added at each addition = 5 µl)

Volume of DMSO-d_6 added (in µL)	Chemical Shift (in ppm)		
	δNH1	δNH2	δNH3
0	11.04	10.45	6.75
5	11.02	10.44	6.73
10	11.01	10.42	6.72
15	10.99	10.4	6.71
20	10.98	10.39	6.69
25	10.96	10.38	6.68
30	10.95	10.36	6.67
35	10.94	10.35	6.66
40	10.92	10.33	6.65
45	10.91	10.32	6.64
50	10.89	10.31	6.62

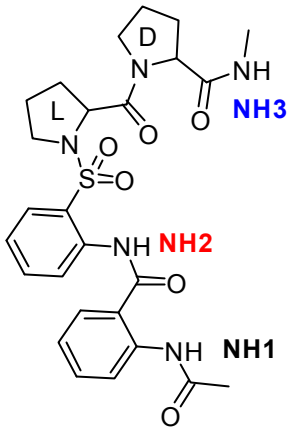

27e

Table 2.19. Variable temperature of 15d in $CDCl_3$ (20 mmol) with DMSO-d_6 (volume of DMSO-d_6 added at each addition = 5 µl)

Temperature (in °K)	Chemical shift in ppm		
	δNH1	δNH2	δNH3
268	9.26	7.26	6.57
273	9.26	7.24	6.56
278	9.26	7.23	6.55
283	9.26	7.21	6.53
288	9.26	7.21	6.52
293	9.26	7.17	6.5
298	9.26	7.16	6.49
303	9.26	7.13	6.47
308	9.27	7.11	6.46
313	9.27	7.09	6.45
318	9.27	7.06	6.43
323	9.27	7.04	6.42

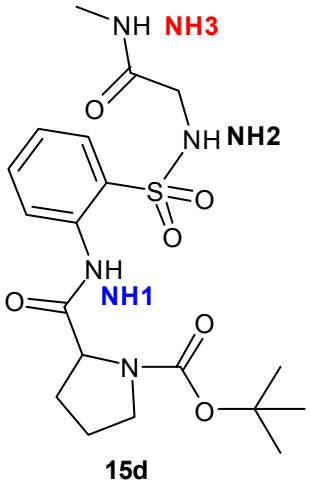

15d

Table 2.20. Variable temperature study of 22 (20 mmol, 400 MHz, $CDCl_3$).

Temperature in °K	Chemical Shift (in ppm)	
	δNH1	δNH2
273	7.14	6.6
278	7.12	6.56
283	7.1	6.53
288	7.08	6.49
293	7.06	6.46
298	7.04	6.43
303	7.03	6.4
308	7.01	6.37
313	7	6.34
318	6.99	6.32

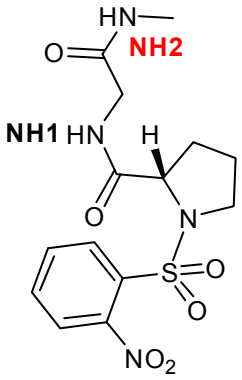

22

Table 2.21. Variable temperature study of 26g (20 mmol, 400 MHz, $CDCl_3$).

Temperature (in °K)	Chemical shift in ppm		
	δNH1	δNH2	δNH3
273	11.07	10.48	6.78
278	11.07	10.47	6.77
283	11.06	10.47	6.76
288	11.05	10.46	6.75
293	11.05	10.45	6.75
298	11.04	10.45	6.75
303	11.02	10.44	6.73
308	11.02	10.43	6.73
313	11.01	10.43	6.72
318	11	10.42	6.7
323	10.99	10.42	6.7
273	11.07	10.48	6.78

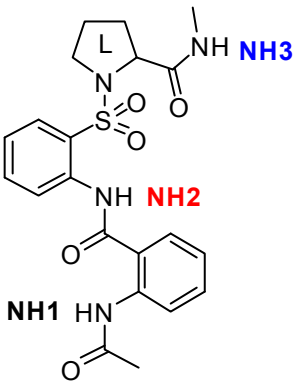

26g

Table 2.22. Variable temperature study of 27e (20 mmol, 400 MHz, $CDCl_3$).

Temperature (in °K)	Chemical shift in ppm		
	δNH1	δNH2	δNH3
273	11.13	10.57	6.66
278	11.13	10.56	6.65
283	11.12	10.56	6.65
288	11.12	10.55	6.61
293	11.11	10.54	6.58
298	11.1	10.53	6.56
303	11.09	10.52	6.55
308	11.08	10.51	6.53
313	11.07	10.51	6.51
318	11.05	10.5	6.49
323	11.04	10.49	6.47

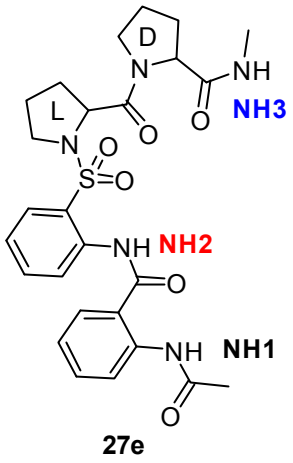

27e

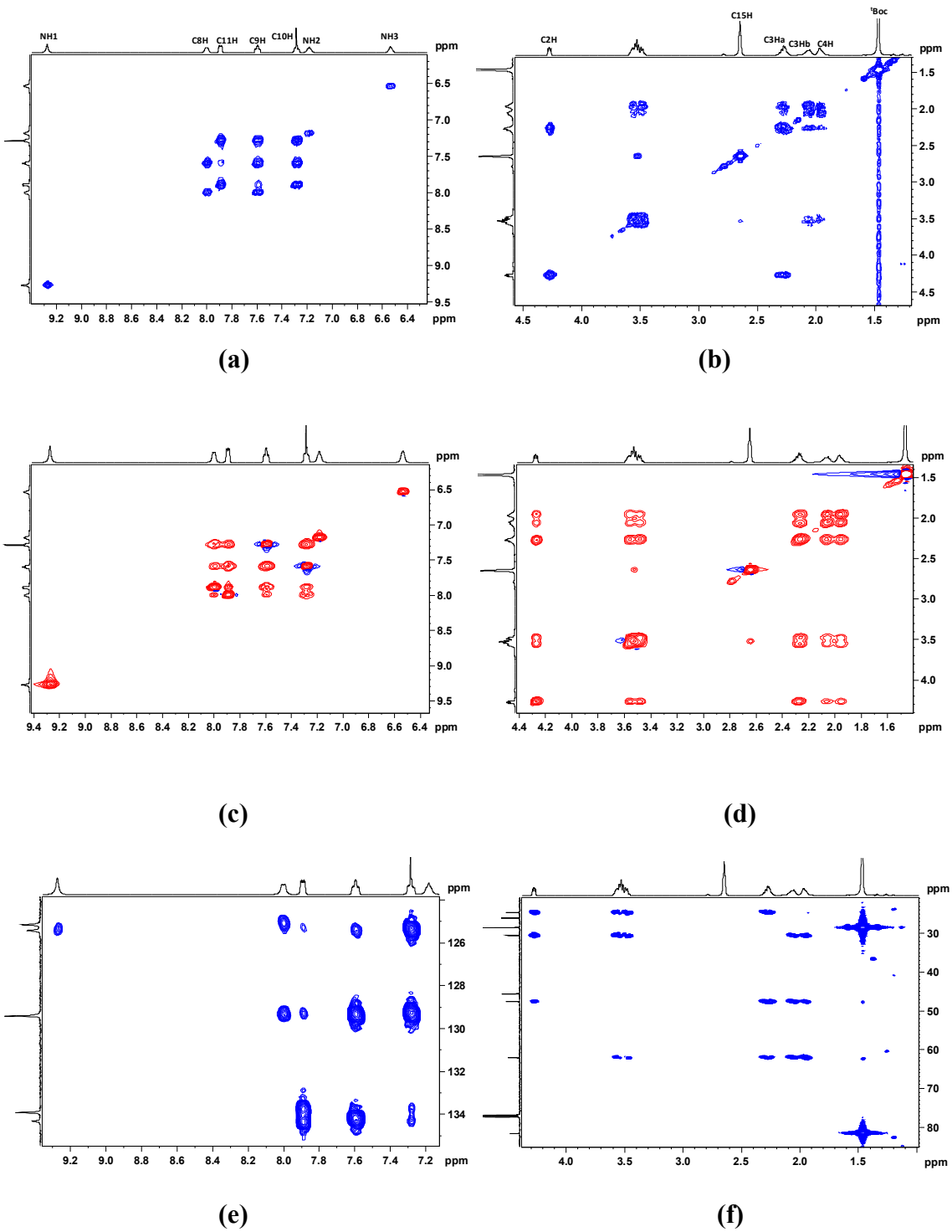

Fig 2.55: Partial COSY (a), (b); TOCSY, (c), (d); and HMBC (e), (f) spectra of **15d** (400 MHz, $CDCl_3$). For better view, aromatic and aliphatic regions are shown separately.

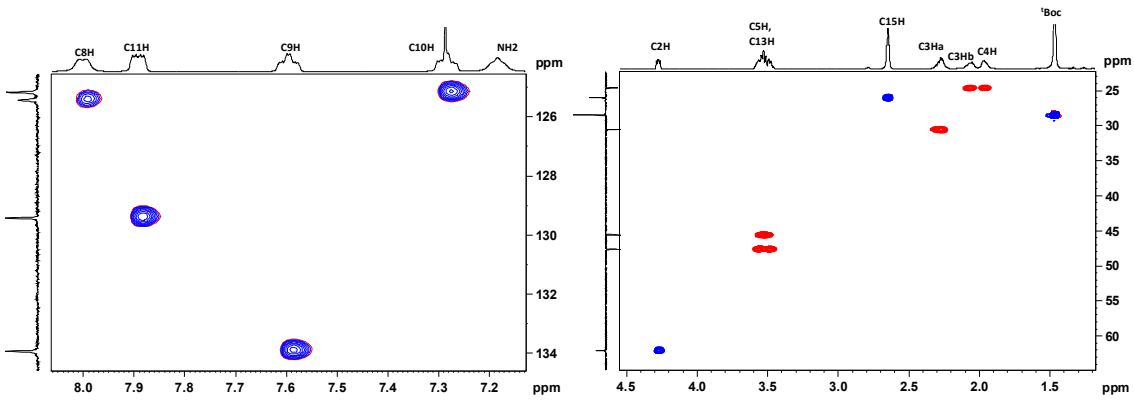

(g) **(h)**

Fig 2.56: Partial HSQC (g), (h) spectra of **15d** (400 MHz, $CDCl_3$). For better view, aromatic and aliphatic regions are shown separately.

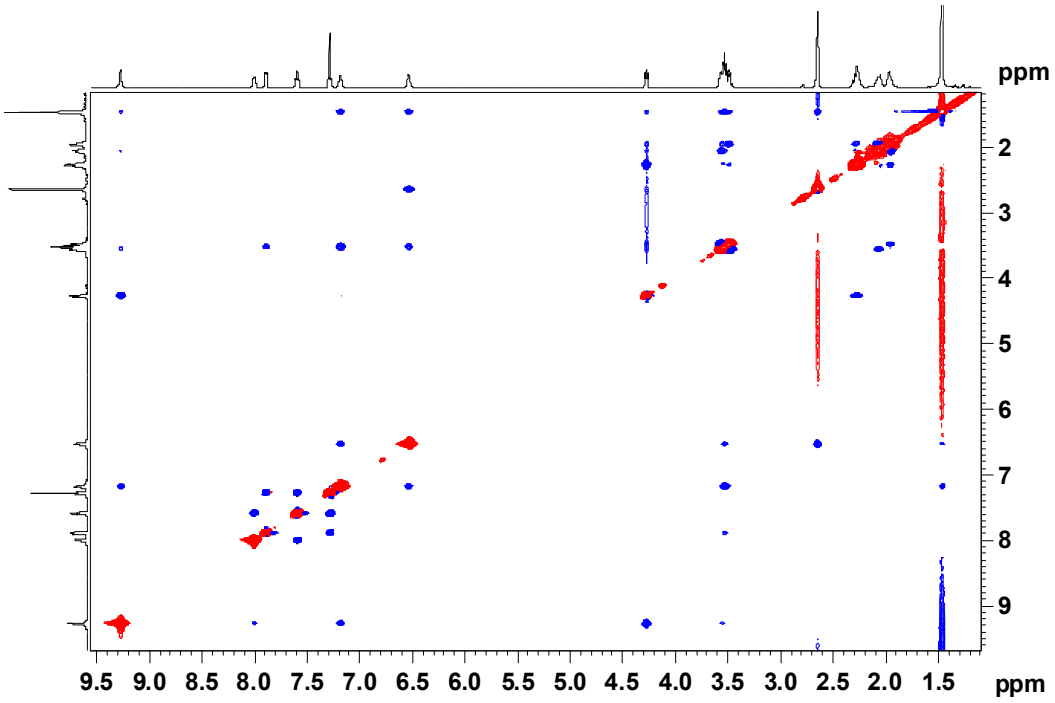

Fig 2.57: Full 2D NOESY spectrum of **15d** (400 MHz, $CDCl_3$).

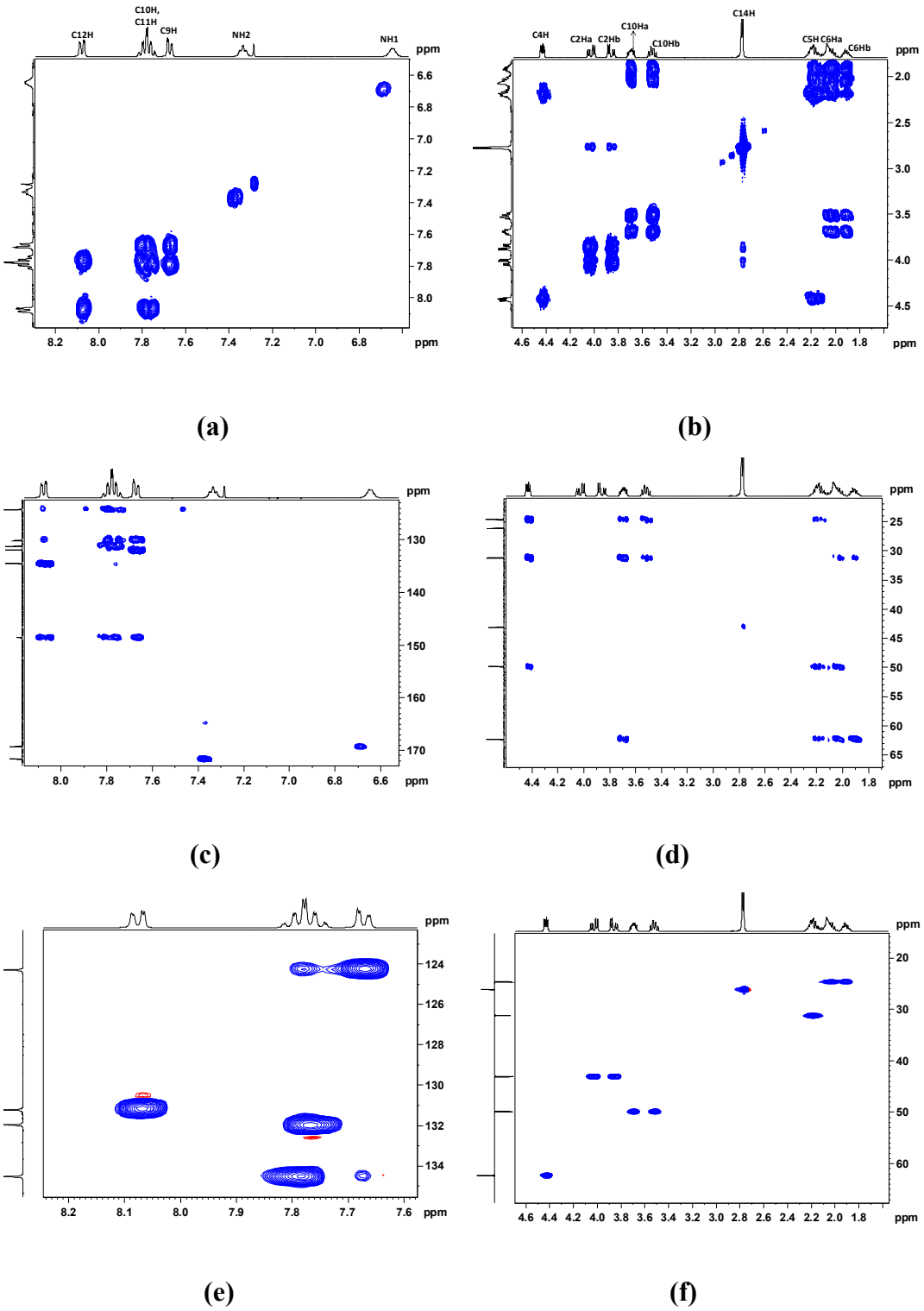

Fig 2.58: Partial COSY (a), (b); HMBC (c), (d); and HSQC (e), (f) spectra of **22** (400 MHz, $CDCl_3$). For better view, aromatic and aliphatic regions are shown separately.

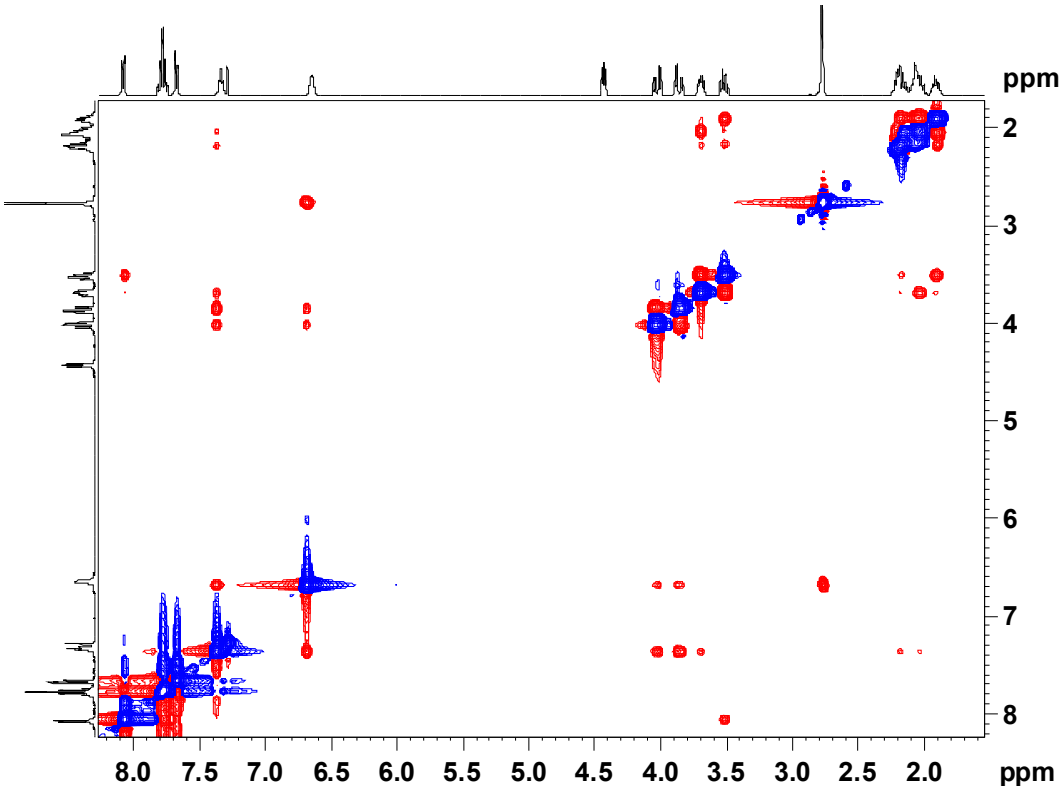

Fig 2.59: Full 2D NOESY spectrum of **22** (400 MHz, $CDCl_3$).

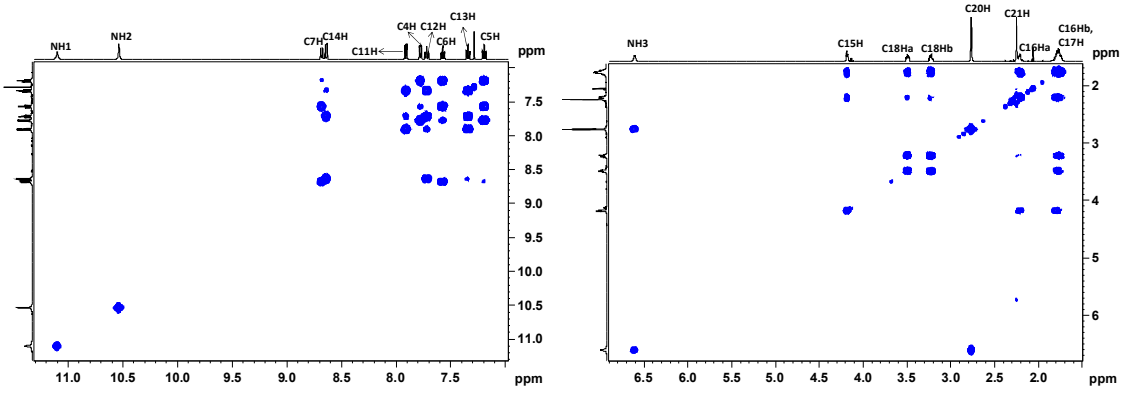

(a) **(b)**

Fig 2.60: Partial COSY (a), (b) spectra of **26g** (400 MHz, $CDCl_3$). For better view, aromatic and aliphatic regions are shown separately.

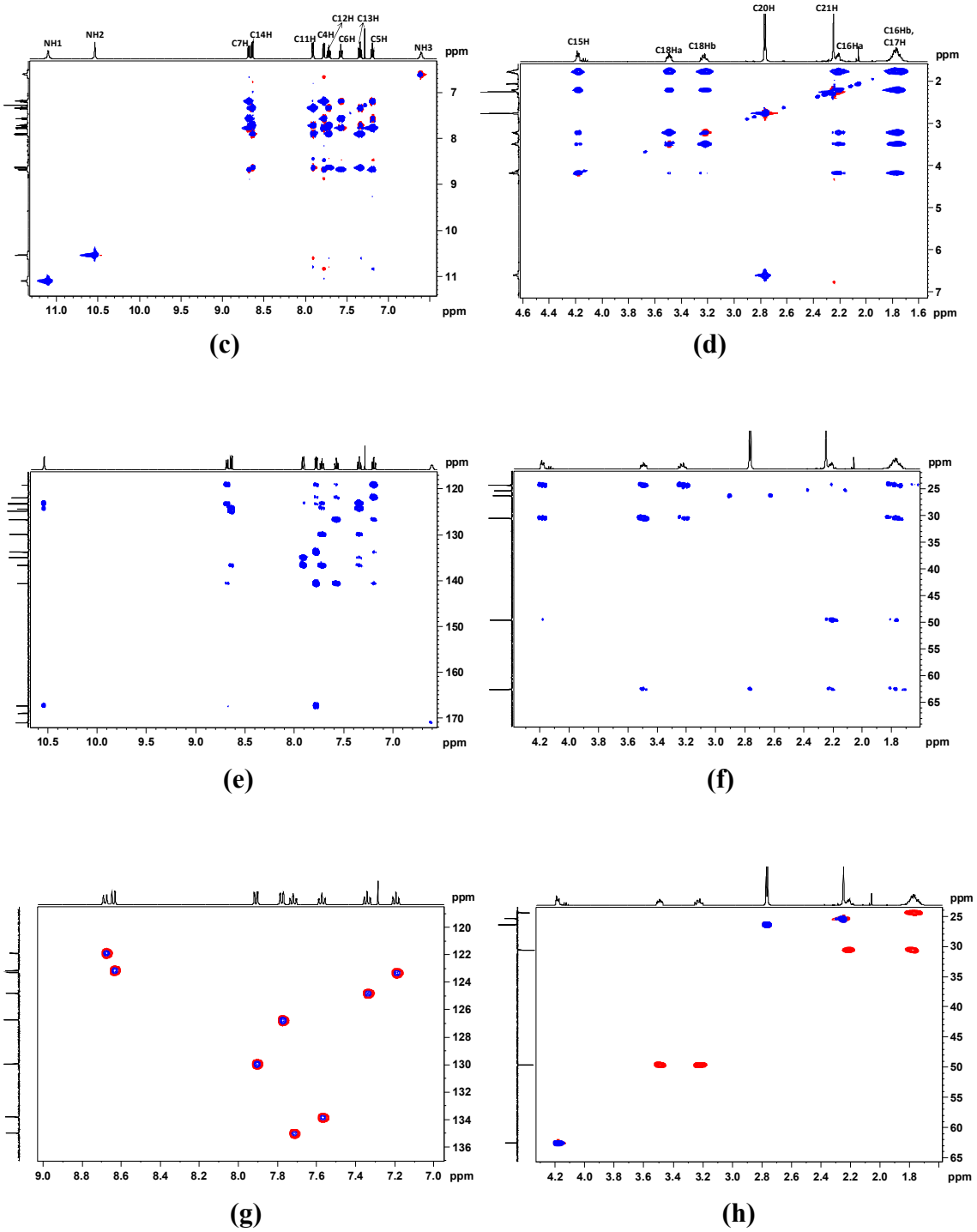

Fig 2.61: Partial TOCSY (c), (d); HMBC (e), (f) and HSQC (g), (h) spectra of **26g** (400 MHz, $CDCl_3$). For better view, aromatic and aliphatic regions are shown separately.

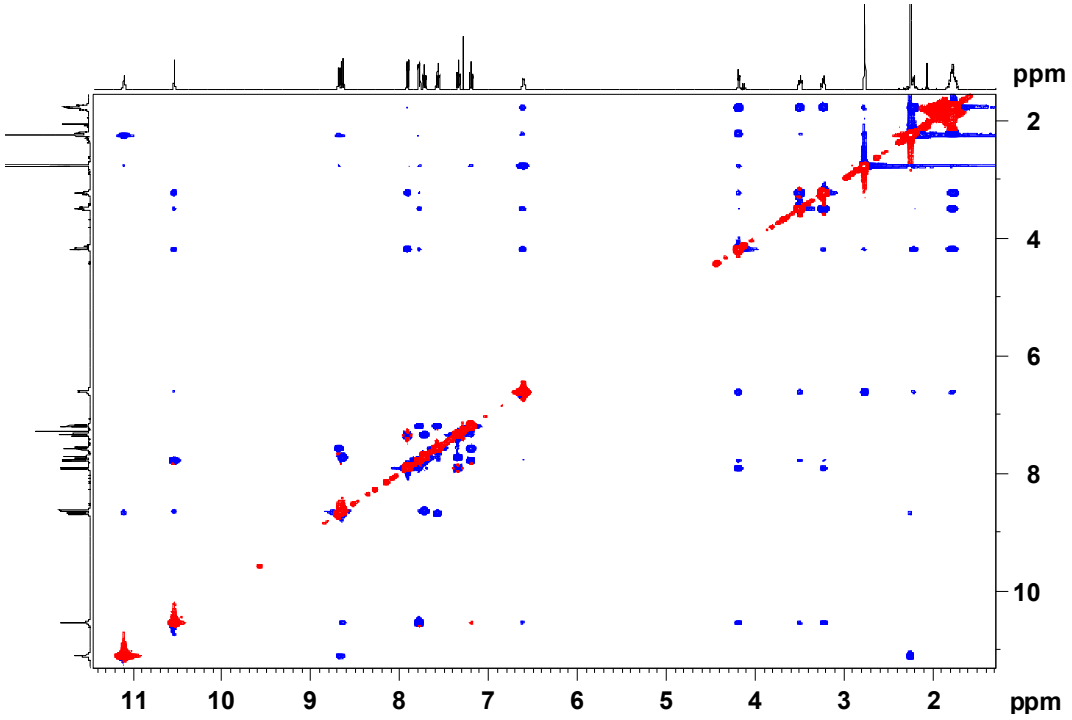

Fig 2.62: Full 2D NOESY spectrum of **26g** (400 MHz, $CDCl_3$).

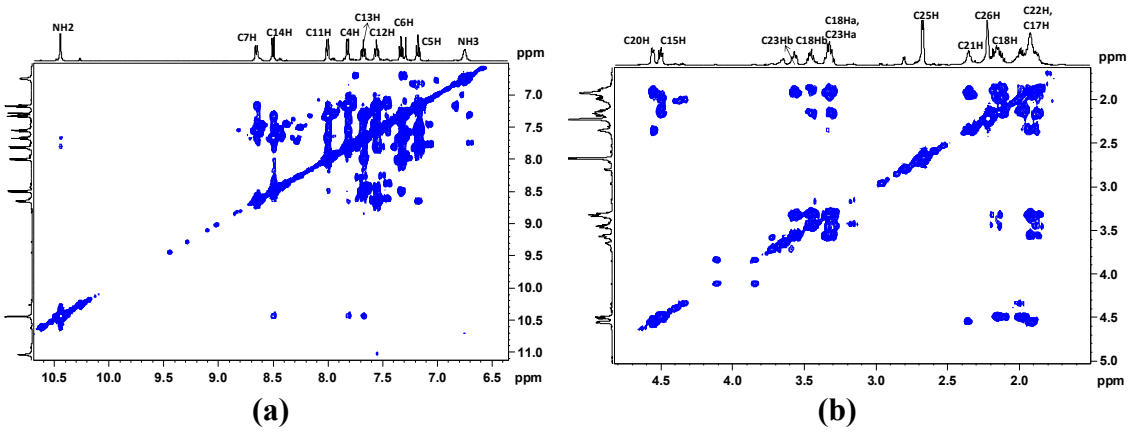

Fig 2.63: Partial COSY (a), (b) spectra of **27e** (400 MHz, $CDCl_3$). For better view, aromatic and aliphatic regions are shown separately.

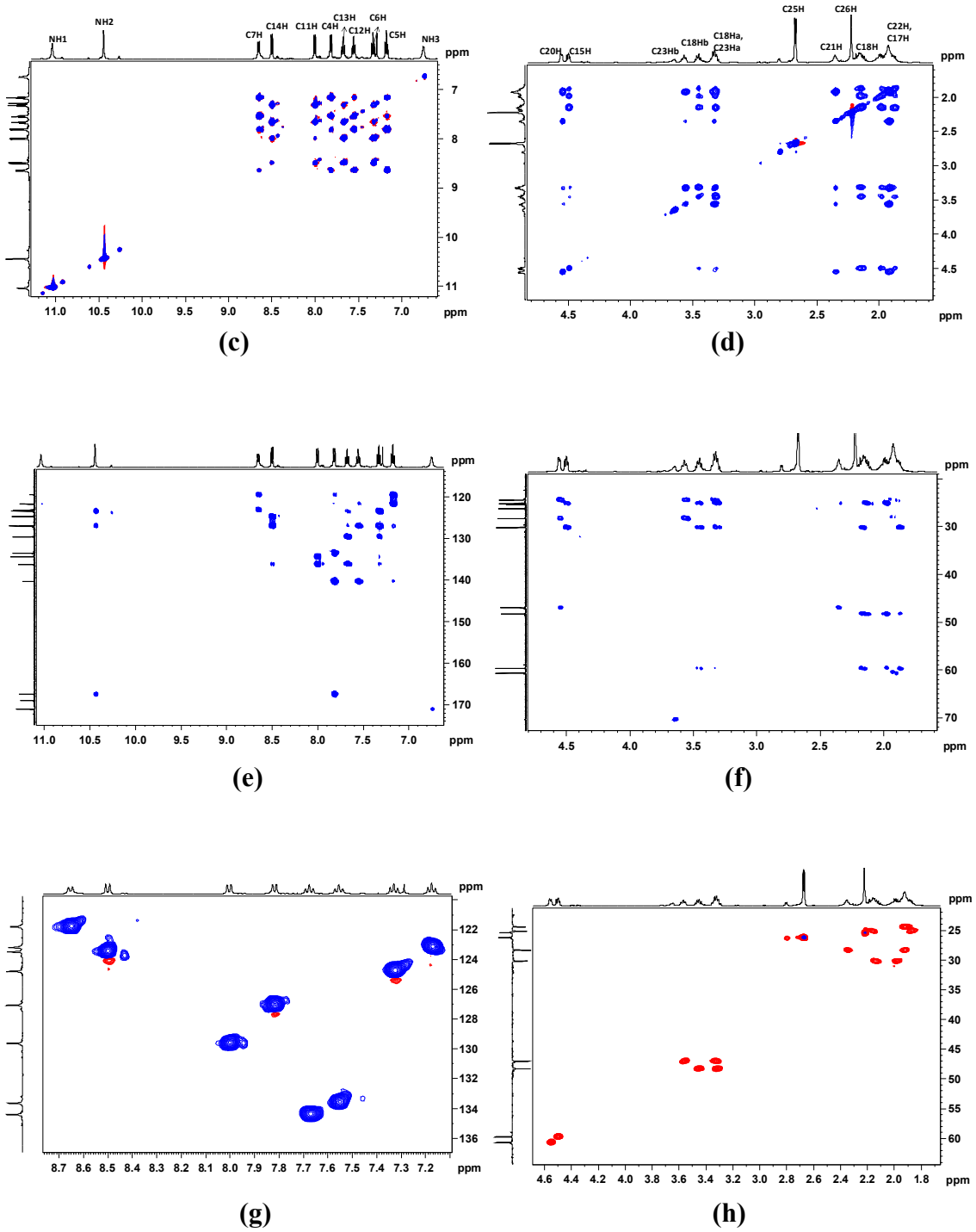

Fig 2.64: Partial TOCSY (c), (d); HMBC (e), (f) and HSQC (g), (h) spectra of **27e** (400 MHz, $CDCl_3$). For better view, aromatic and aliphatic regions are shown separately.

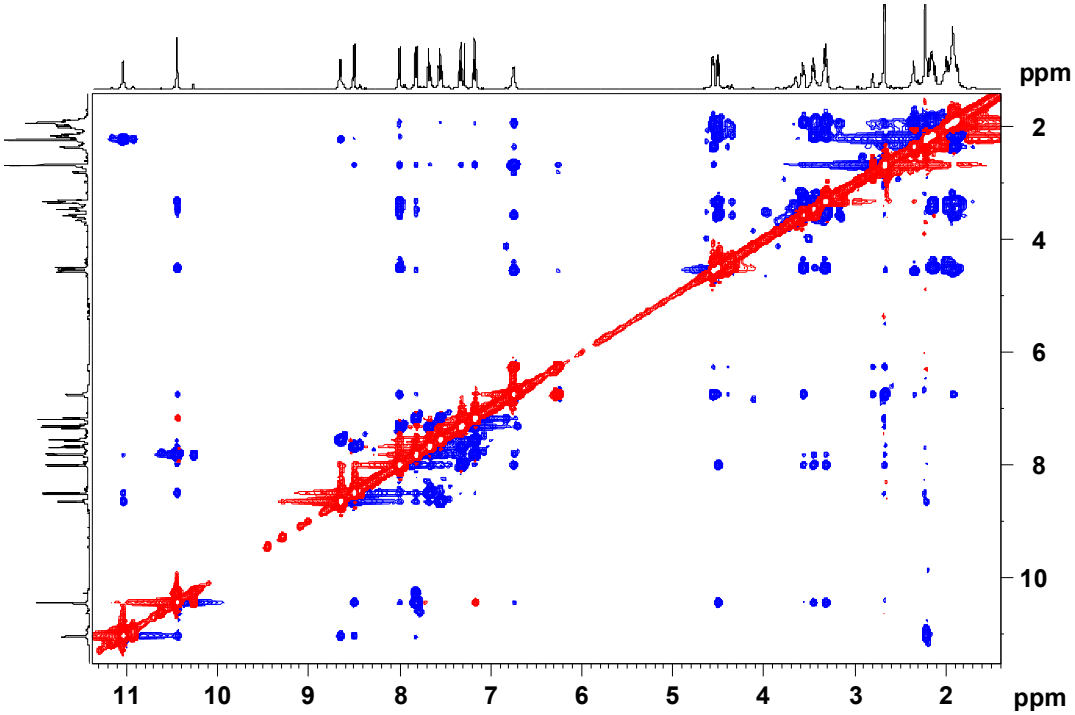

Fig 2.65: Full 2D NOESY spectrum of **27e** (400 MHz, $CDCl_3$).

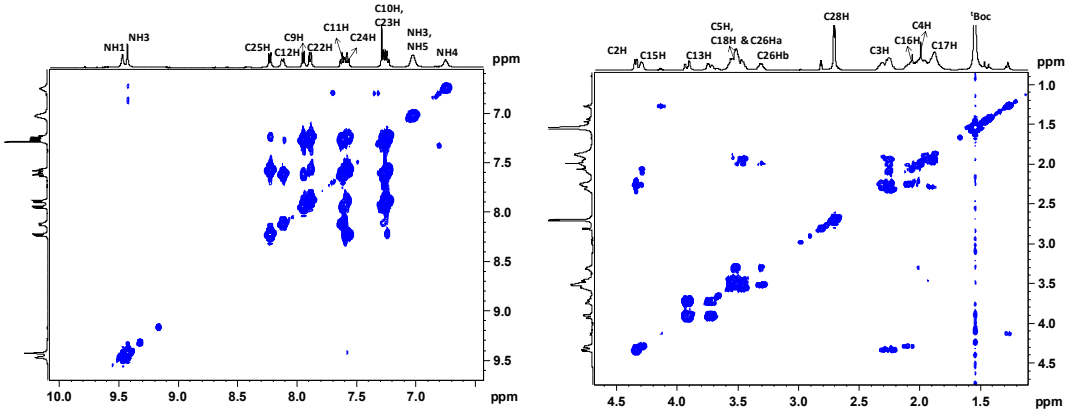

(a) **(b)**

Fig 2.66: Partial COSY (a), (b) spectra of **16b** (400 MHz, $CDCl_3$). For better view, aromatic and aliphatic regions are shown separately.

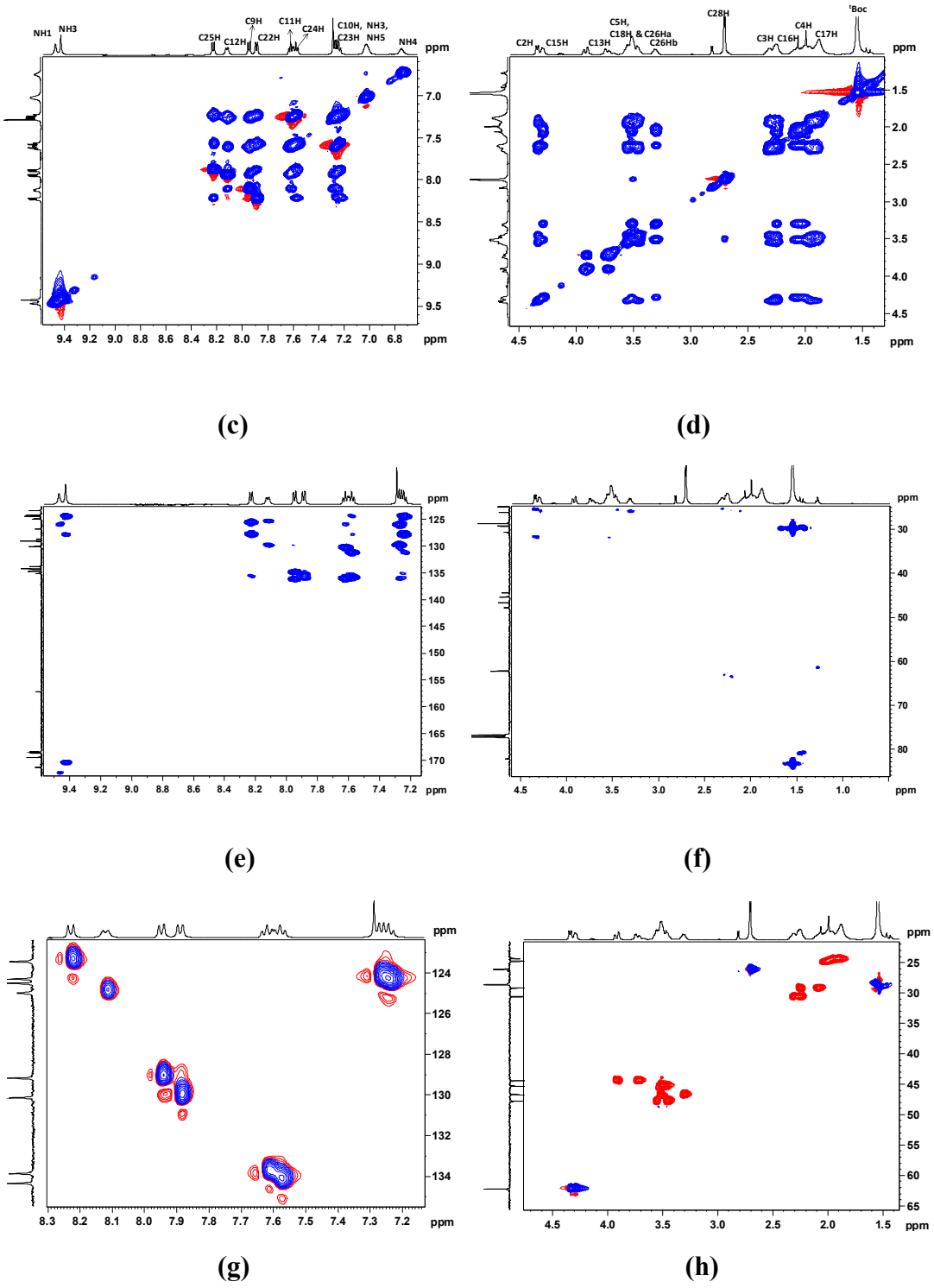

Fig 2.67: Partial TOCSY (c), (d); HMBC (e), (f) and HSQC (g), (h) spectra of **16b** (400 MHz, $CDCl_3$). For better view, aromatic and aliphatic regions are shown separately.

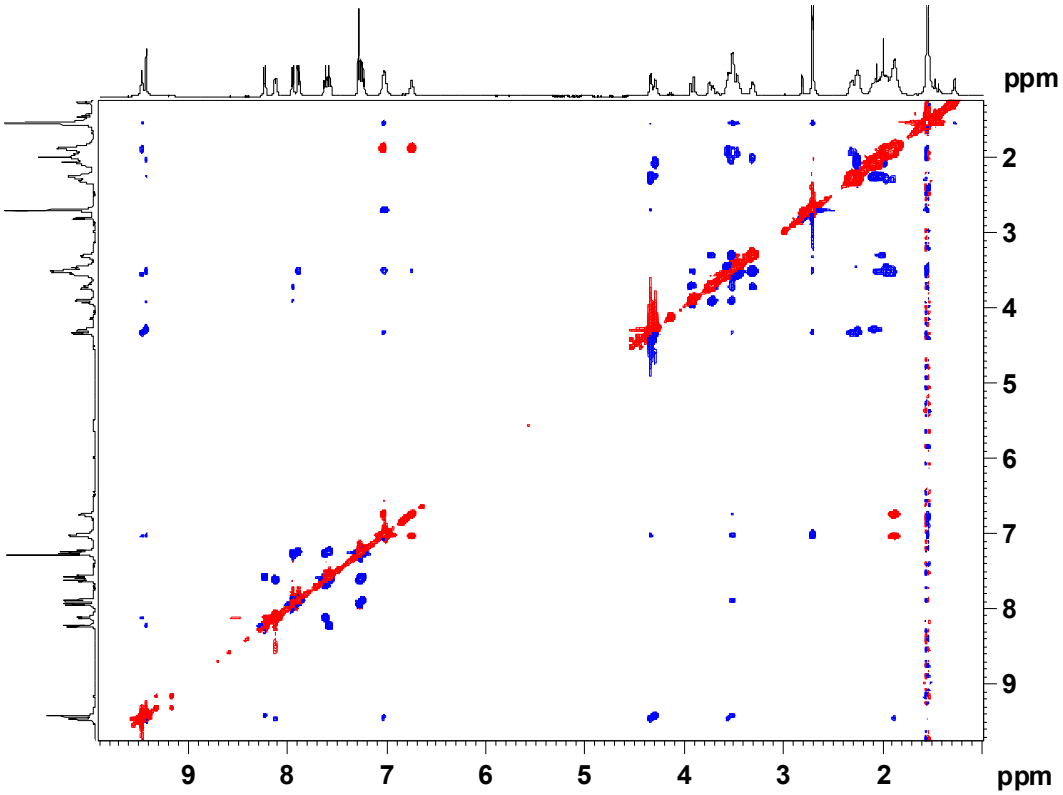

Fig 2.68: Full 2D NOESY spectrum of **16b** (400 MHz, $CDCl_3$).

2.22 References and Notes

(1) Vander, A. J.; Sherman, J. H.; Luciano, D. S. *Human. Physiology. ed*. Prancan, K.M.; Bradley, J. W. McGraw-Hill, New York, **1994**.

(2) (a) Ramachandran, G. N.; Sasisekharan, V. *Adv. Prot. Chem*. **1968**, *23*, 283. (b) Anfinsen, C. B. *Science*, **1973**, *181*, 223. (c) Mackay, D. H. J.; Cross, A. J.; Hagler, A. T. *Prediction of Protein Structure and the Principles of Protein conformation* (Ed.:G. D. Fasman), Plenum, New York, **1989**.

(3) (a) Wilmot, C. M.; Thornton, J. M. *J. Mol. Biol.* **1988**, *203*, 221. (b) K. C. Chou, *Anal. Biochem.* **2000**, *286*, 1.

(4) (a) Craik, D. J.; Fairlie, D. P.; Liras, S.; Price, D. *Chem. Biol. Drug. Des.* **2013**, *81*, 136. (b) Giannis, A.; Rubsam, F. *Adv. Drug. Res.* **1997**, *29*, 1. (c) Gante, J. *Angew. Chem. Int. Ed.* **1994**, *33*, 1699. (d) Giannis, A.; Kolter, T. *Angew. Chem. Int. Ed.* **1993**, *32*, 1244. (e) Goodman, M.; Ro, S. *Burger's Medicinal Chemistry and Drug Discovery*. Ed. M. E. Wolff. New York, John Wiley & Sons, Inc. **1995**, 803. (f) Liskamp, R. M. J. *Recl. Trav. Chim. Pays. Bas.* **1994**, *113*, 1. (g) Ripka, A. S.; Rich, D. H. *Curr. Opin. Chem. Bio*. **1998**, *2*, 441. (h) Fauchere, J. L.; Thurieau, C. *Adv. Drug. Res.* **1992**, *23*, 127. (i) Marshall, G. R. *Tetrahedron.* **1993**, *49*, 3547. (j) Hirshmann, R. *Angew. Chem. Int. Ed. Eng.* **1991**, *30*, 1278.

(5) (a) Hirschmann, R. F; Nicolaou, K. C.; Angeles, A. R.; Chen, J. S.; Smith, A. B. *Acc. Chem. Res*. **2009**, *42*, 1511. (b) Vasudev, P. G.; Chatterjee, S.; Shamala, N.; Balaram, P. *Acc. Chem. Res.* **2009**, *42*, 1628. (c) Ross, N. T.; Katt, W. P.; Hamilton, A. D. *Philos. Trans. R. Soc. London Ser. A* **2010**, *368*, 989. (d) Holub, J. M.; Kirshenbaum, K. *Chem. Soc. Rev.* **2010**, *39*, 1325. (e) Liskamp, R. M. J.; Rijkers, D. T. S.; Kruijtzer, J. A. W.; Kemmink, J. *Chem. Bio. Chem.* **2011**, *12*, 1626. (f) Martinek, T. A.; Fulop, F. *Chem. Soc. Rev*. **2012**, *41*, 687.

(6) (a) Haase, H. S.; Peterson-Kaufman, K. J.; Lan Levengood, S. K.; Checco, J. W.; Murphy, W. L.; Gellman, S. H. *J. Am. Chem. Soc.* **2012,** *134*, 7652. (b) Johnson, L. M.; Mortenson, D. E.; Yun, H. G.; Horne, W. S.; Ketas, T. J.;

Lu, M.; Moore, J. P.; Gellman, S. H. *J. Am. Chem. Soc.* **2012,** *134*, 7317. (c) Cheng, R. P.; Gellman, S. H.; DeGrado, W. F. *Chem. Rev*. **2001**, *101*, 3219. (d) T. A. Martinek and F. Fulop, *Chem. Soc. Rev*. **2012**, *41*, 687. (e) Seebach, D.; Matthews, J. L. *Chem. Commun*. **1997**, 2015. (d) Pilsl, L. K. A.; Reiser, O. *Amino Acids.* **2011**, *41*, 709. (e) Rai, R.; Raghothama, S.; Sridharan, R.; Balaram, P. *Pept. Sci.* **2007,** *88*, 350. (e) Bomar, M. G.; Song, B.; Kibler, P.; Kodukula, K.; Galande, A. K. *Org. Lett.* **2011,** *13*, 5878.

(7) (a) Adessi, C.; Soto, C. *Curr. Med. Chem.* **2002***, 9*, 963. (b) Moore, G. J. *Trends. Pharmacol. Sci.* **1994,** *15*, 124. (b) Chorev, M. *Biopolymers.* **2005,** *80*, 67. (c) Tanaka, M. *Chem. Pharm. Bull*. **2007**, *55*, 349. (d) Moore, S. B.; Grant, M.; Rew, Y.; Bosa, E.; Fabbri, M.; Kumar, U.; Goodman, M. *J. Pep. Res.* **2005,** *66*, 404. (e) Erchegyi, J.; Penke, B.; Simon, L.; Michaelson, S.; Wenger, S.; Waser, B.; Cescato, R.; Schaer, J.-C.; Reubi, J. C.; Rivier, J. *J. Med. Chem.* **2003,** *46*, 5587. (f) Tóth, G.; Ioja, E.; Tömböly, C.; Ballet, S.; Tourwé, D.; Péter, A.; Martinek, T.; Chung, N. N.; Schiller, P. W.; Benyhe, S.; Borsodi, A. *J. Med. Chem.* **2006,** *50*, 328.

(8) (a) Vasudev, P. G.; Chatterjee, S.; Shamala, N.; Balaram, P. *Chem. Rev*. **2011**, *111*, 657. (b) Guichard, G.; Huc, I. *Chem. Commun*. **2011**, *47*, 5933. (c) Tomasini, C.; Angelici G.; Castellucci, N. *Eur. J. Org. Chem*. **2011**, 3648. (d) Risseeuw, M. D. P.; Overhand, M.; Fleet, G. W. J.; Simon, M. I. *Tetrahedron: Asymmetry.* **2007**, *18*, 2001. (e) Martinek, T. A.; Toth, G. K.; Vass, E.; Hollosi M. Fulop, F. *Angew. Chem. Int. Ed.* **2002**, *41*, 1718. (f) Seebach, D.; Abele, S.; Gademann, K. Jaun, B. *Angew. Chem. Int. Ed*. **1999**, *38*, 1595.

(9) De Pol, S.; Zorn, C.; Klein, C. D.; Zerbe O.; Reiser, O. *Angew. Chem. Int. Ed*. **2004**, *43*, 511.

(10) Gellman, S. H. *Acc. Chem. Res*. **1998**, *31*, 173.

(11) (a) Seth Horne W.; Gellman, S. H. *Acc. Chem. Res*. **2008**, *41*, 1399. (b) Mandity, I. M.; Fulop, L.; Vass, E.; Toth, G. K.; Martinek, T. A.; Fulop, F. *Org. Lett*. **2010**, *12*, 5584.

(12) (a) Prabhakaran, P.; Kale, S. S.; Puranik, V. G.; Rajamohanan, P. R.; Chetina, O.; Howard, J. A. K.; Hofmann, H. J.; Sanjayan, G. J. *J. Am. Chem. Soc.* **2008**, *130*, 17743. (b) Ramesh, V. V .E.; Priya, G.; Kotmale, A. S.; Gonnade, R. G.; Rajamohanan, P. R.; Sanjayan, G. J. *Chem. Commun.* **2012**, *48*, 11205. (c) Kale, S. S.; Kotmale, A. S.; Dutta, A. K.; Pal, S.; Rajamohanan, P. R.; Sanjayan, G. J. *Org. Biomol. Chem.* **2012,** *10*, 8426.

(13) André, C.; Legrand, B.; Deng, C.; Didierjean, C.; Pickaert, G.; Martinez, J.; Averlant-Petit, M. C.; Amblard, M.; Calmes, M. *Org. Lett.* **2012**, *14*, 960.

(14) (a) Gennari, C.; Salom, B.; Potenza, D.; Williams, A. *Angew. Chem. Int. Ed.* **1994**, *33*, 2067. (b) Moree, W. J.; van der Marel, G. A.; Liskamp, R. J. *J. Org. Chem.* **1995,** *60*, 5157. (c) Gude, M.; Piarulli, U.; Potenza, D.; Salom, B.; Gennari, C. *Tetrahedron Lett.* **1996,** *37*, 8589. (d) Monnee, M. C. F.; Marijne, M. F.; Brouwer, A. J.; Liskamp, R. M. J. *Tetrahedron Lett.* **2000,** *41*, 7991. (e) Gennari, C.; Salom, B.; Potenza, D.; Longari, C.; Fioravanzo, E.; Carugo, O.; Sardone, N. *Chem. Eur. J.* **1996**, *2*, 644. (f) Vijayadas, K. N.; Davis, H. C.; Kotmale, A. S.; Gawade, R. L.; Puranik, V. G.; Rajamohanan, P. R.; Sanjayan, G. J. *Chem. Commun.* **2012**, *48*, 9747. (g) Bindal, R. D.; Golab, J. T.; Katzenellenbogen, J. A. *J. Am. Chem.Soc.* **1990**, *112*, 7861. (h) Radkiewicz, J. L.; McAllister, M. A.; Goldstein, E.; Houk, K. N. *J. Org. Chem.* **1998**, *63*, 1419. (i) Gennari, C.; Gude, M.; Potenza, D.; Piarulli, U. *Chem. Eur. J.* **1998**, *4*, 1924. (j) Turcotte, S.; Gervais, S. H. B.; Lubell, W. D. *Org. Lett*. **2012**, *14*, 1318. (k) Baldauf, C.; Gunther, R.; Hofmann, H.-J. *THEOCHEM*, **2004**, *675*, 19.

(15) Bolm, C.; Moll, G.; Kahmann, J. D. *Chem. Eur. J.* **2001**, *7*, 1118.

(16) Langenhan, J. M.; Fisk, J. D.; Gellman, S. H. *Org. Lett.* **2001**, *3*, 2559.

(17) Hu, Z.-Q.; Chen, C.-F. *Chem. Commun*. **2005**, *19*, 2445.

(18) Ramesh, V. V. E.; Kale, S. S.; Kotmale, A. S.; Gawade, R. L.; Puranik, V. G.; Rajamohanan, P. R.; Sanjayan, G. J. *Org. Lett.* **2013**, *15*, 1504.

(19) Liskamp, R. M. J.; Kruijtzer, J. A. W. *Mol. Diversity*, **2004**, *8*, 79.

(20) Supuran, C. T.; Casini, A. Scozzafava, A. *Med. Res. Rev*. **2003**, *23*, 535.

(21) Schueler-Furman, O.; Wang, C.; Bradley, P.; Misura, K.; Baker, D. *Science.* **2005**, *310*, 638.

(22) (a) Powers, E. T.; Deechongkit, S.; Kelly, J. W. *Adv. Protein. Chem.* 2005, *72*, 39. (b) Lu, W.; Qasim, M. A.; Laskowski, M.; Kent, S. B. H. *Biochemistry.* **1997**, *36*, 673. (c) Koh, J. T.; Cornish, V. W.; Schultz, P. G. *Biochemistry.* **1997**, *36*, 11314. (d) Karle, I. L.; Das, C.; Balaram, P. *Biopolymers.* **2001**, *59*, 276. (e) Beligere, G. S.; Dawson, P. E. *J. Am. Chem. Soc.* **2000**, *122*, 12079. (f) Gordon, D. J.; Meredith, S. C. *Biochemistry.* **2003**, *42*, 475. (g) Silinski, P.; Fitzgerald, M. C. *Biochemistry.* **2003**, *42*, 6620. (h) Deechongkit, S.; Nguyen, H.; Powers, E. T.; Dawson, P. E.; Gruebele, M.; Kelly, J. W. *Nature.* **2004**, *430*, 101. (i) Gao, J.; Bosco, D. A.; Powers, E. T.; Kelly, J. W. *Nat. Struct. Mol. Biol.* **2009**, *16*, 684.

(23) (a) Giuliano, M. W.; Horne, W. S.; Gellman, S. H. *J. Am. Chem. Soc*. **2009**, *131*, 9860. (b) Price, J. L.; Horne, W. S.; Gellman, S. H. *J. Am. Chem. Soc*. **2010**, *132*, 12378.

(24) Sanford, A. R.; Yamato, K.; Yang, X.; Yuan, L.; Han, Y.; Gong, B. *Eur. J. Biochem*. **2004**, *271*, 1416.

(25) Roy, R. S.; Karle, I. L.; Raghothama, S. Balaram, P. *Proc. Natl. Acad. Sci. U. S. A*. **2004**, *101*, 16478.

(26) Schmitt, M. A.; Choi, S. H.; Guzei, I. A.; Gellman, S. H. *J. Am. Chem. Soc*. **2006**, *128*, 4538.

(27) (a) Brahmachari, S. K.; Ananthanarayanan, V. S. *Proc. Nat. Acad. Sci.* **1979**, *76*, 5119. (b) Stimson, E. R.; Zimmerman, S. S.; Scheraga, H. A. *Macromolecules.* **1977**, *10*, 1049. (c) Zimmerman, S. S.; Scheraga, H. A. *Biopolymers*. **1977**, *16*, 811.

(28) Némethy, G.; Scheraga, H. A. *Biopolymers.* **1982**, *21*, 1535.

(29) Chatterjee, B.; Saha, I.; Raghothama, S.; Aravinda, S.; Rai, R.; Shamala, N.; Balaram, P. *Chem. Eur. J.* **2008**, *14*, 6192.

Chapter 3

Synthesis and Biological Evaluation of Structural Analogs of peptide-based antimitotic agents

Section A: Pro-Atc dipeptide-based peptidomimetic analogues as antimitotic agents

Section B: Synthesis of analogs of Ixorapeptides-their biological evaluation

Pro-Atc dipeptide-based peptidomimetic analogues as antimitotic agents

3.1 Introduction

The latest advances in various fields of science like molecular biology, biochemistry, structural chemistry, molecular pharmacology, neuro chemistry, molecular endocrinology and immunology make it clear that proteins and peptides constitute the major segment of bioactive ligands, pointing them as specific targets for drug design. The design and synthesis of peptidomimetics are the crucial stepladders to develop novel drug molecules since the peptides and protein-protein interactions dwell a dominant pose in molecular recognition and cell signaling, particularly in the living systems.[1] Now-a-days there exists, enormously elevated demand for synthesis and screening of natural-like biopolymers and their derivatives, the so called peptide mimics (***peptidomimetics***) that feature improved stability profiles and pharmacokinetic properties.

3.2 Peptidomimetics

Peptidomimetics are regular organic molecules that mimic the structure of endogenous peptide. These molecules are considered to possess advantages over the natural peptide drugs since the natural peptides are in general biologically unstable, poorly absorbed and rapidly metabolized in the biological systems. The synthetic peptidomimetic molecules possess the abilities to overcome such draw backs by offering specificity in binding, ready oral availability and improved pharmacokinetic profiles.[2]

3.3 Therapeutic applications

The peptidomimetic molecules possess wide range of applications and are used as therapeutics. These molecules are well recognized to show anti-microbial activity,[4] anti-cancer activity,[5] anti-viral activity,[6] immune detection and suppressant activity,[7] anti-malarial activity,[8] amino-peptidase N-inhibition activity,[9] motilin antagonist activity[10] and analgesic activity.[11] The peptidomimetic molecules have a lot of advantages over conventional drug molecules since they do not cause any detrimental effect on the normal cells with their remarkable stability and pharmacokinetic profiles in the biological systems. Although peptide

drugs and their mimetics (Fig 3.1) exhibit extensive applications, in this part of study the significance of these moieties as anti-cancer agents is discussed in brief.

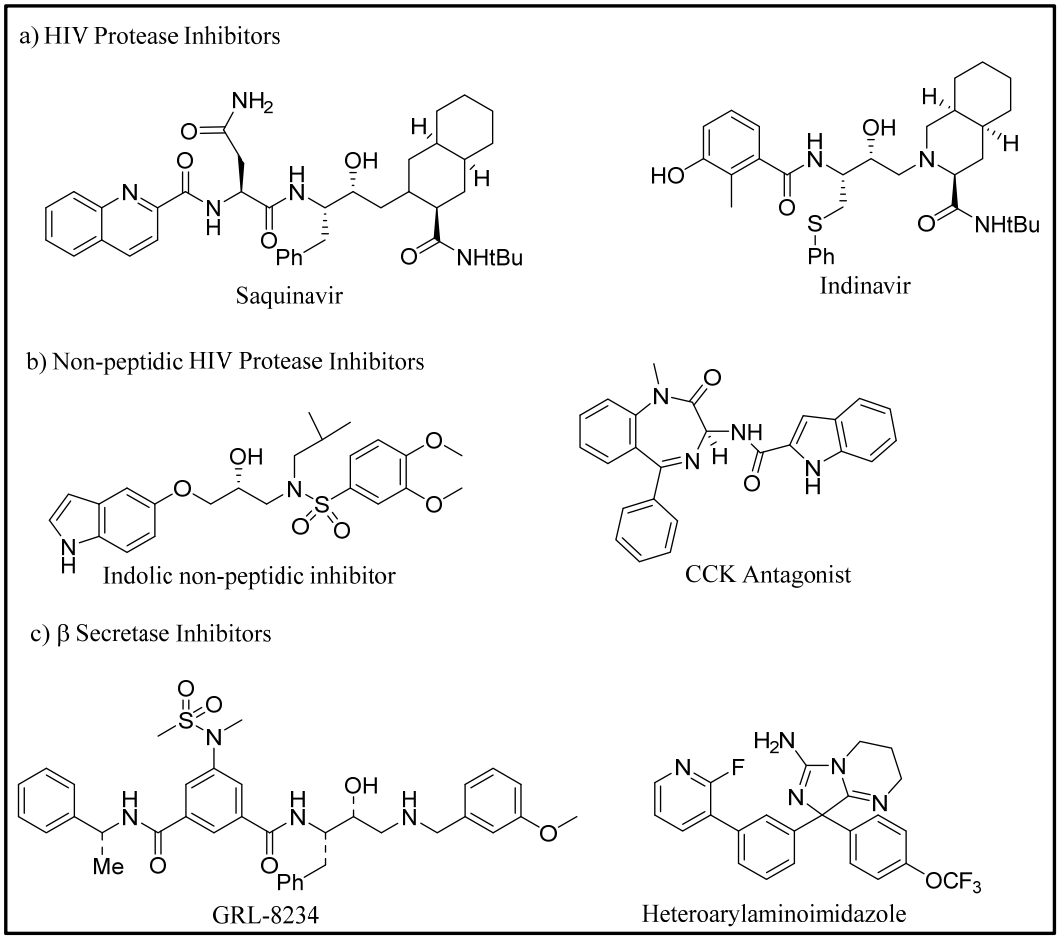

Fig 3.1: Selected examples of peptidomimetic molecules that possess bio-medical applications.[12, 13]

3.4 Cancer therapy using peptides

3.4.1 Cancer

Cancer is defined as the uncontrolled division of cells (mitosis), the ability of these cells to assault other tissues leading to formation of tumour mass, vascularization (abnormal or pathological formation of blood vessels that develops proliferative capillaries) and metastasis (spreading to other parts of the body).[14] About 7 million people die from cancer related cases per year and it is estimated that there will be more than 16 million new cases by 2020.[15] Chemotherapy although associated with certain disadvantages like altered bio-

distribution, bio-transformation and drug clearance, it has been used as a powerful tool to treat cancer.[16]

3.4.2 Role of microtubules in cancer

The process of cell division-mitosis, plays a pivotal role in causing cancer which involves the microtubule polymerization and depolymerization processes. Hence, these microtubules become important cellular targets in treating cancer.[17] Microtubules are made of α or β tubulin heterodimers which undergo polymerization leading to the formation of protofilaments. These protofilaments form a bundle and form hollow cylinders which are capable to grow or shrink. Since the microtubules are hetero-dimers, they are polarized, possessing α-tubulin at the minus end (slow growing end) and β-tubulin at the plus end (fast growing end). Both the α- subunits and β-subunits bind to GTP, the β-subunit hydrolyses the GTP once it gets incorporated into the microtubule.

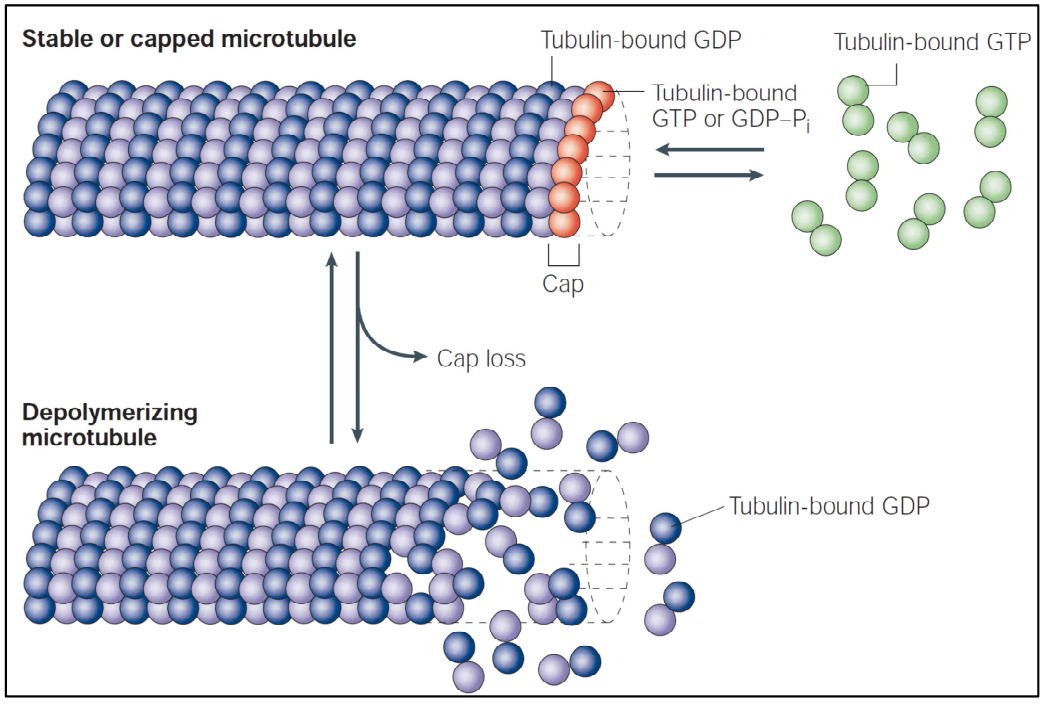

Fig 3.2: Polymerization and depolymerization dynamics of Tubulin.[17]

GTP hydrolysis lags behind the subunit addition process which leads to the formation of a 'GTP cap' at the plus end. This process stabilizes the plus end and further enhances the polymerization of tubulin. When the rate of subunit addition decreases, the hydrolysis of GTP catches up, the GTP cap is lost leading to

depolymerization (Fig 3.2). The switch from growth to shrink is called 'catastrophe' and the switch from shrink to growth is called 'rescue'. This phenomemon of switching rapidly between the two states is called 'dynamic instability'. This dynamic instability plays a significant role during mitosis, since it leads to the formation of mitotic spindles.[18]

3.4.3 Function of anti-mitotic drugs

The agents which are capable to interfere with the dynamics of tubulin by preventing the normal spindle assembly and disrupting the mitotic cell division process are termed as '***anti-mitotic agents***'.[19] Several chemically diverse substances originating from natural sources are reported to bind to the tubulin or microtubules, altering the microtubule polymerization and depolymerization dynamics in different ways. When the cells are exposed to anti-mitotic agent such as taxol, they arrest the mitosis due to chronic activation of the spindle assembly which may result in cell death or unequally divide to produce aneuploid (abnormal number of chromosomes) daughter cells. Alternatively, the cells would exit the mitotic cell division process. Such cells may eventually die in interphase or might get arrested in interphase or they might proceed with the further cellular processes (Fig 3.3).

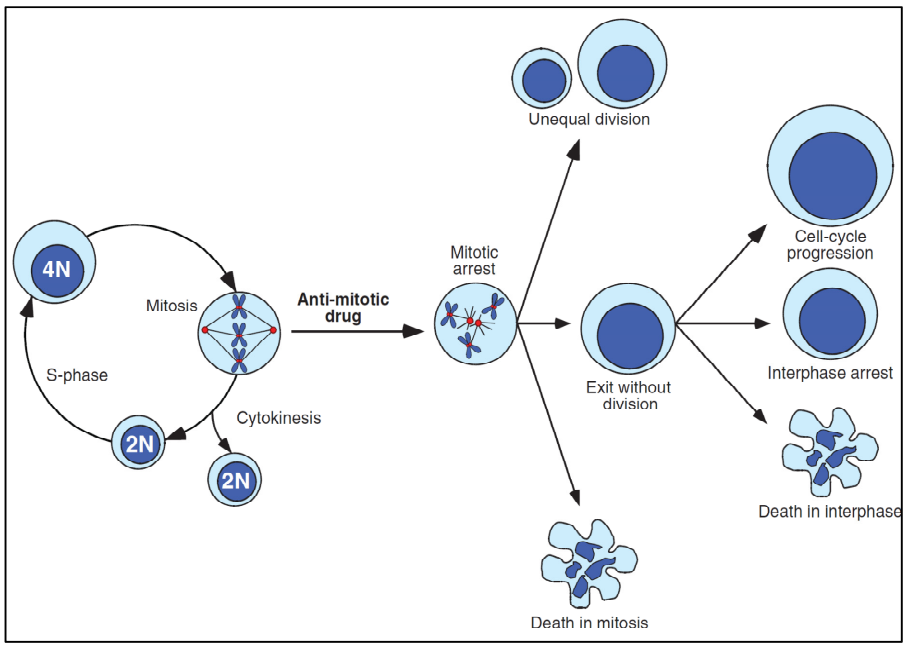

Fig 3.3: The fate of cancer cell when administered with anti-mitotic drug.[18]

There are many such anti-mitotic drugs known, that inhibit cell proliferation by binding to tubulin at different sites and suppress the tubulin dynamics during the vulnerable mitotic stage of the cell cycle. According to the various binding sites on tubulin, these anti-mitotic drugs have been classified into vinca-domain binders (vinflunine, cevipabulin, eribulin etc.), colchicine-domain binders (combretastatins, ombrabulin, indibulin, 2-methoxyoestradiol etc.), taxol-domain binders (discodermalide, ixabepilone, cyclostreptin, eleutherobin etc.) and many other peptide drugs (cryptomycin, dolastatins, hemiasterlin, milnamide, HTI-286, tubulysin etc.).[21]

3.5. Peptides as anti-cancer agents

Over the years, peptides molecules are proven to be successful in treating cancer. [21] Being the most bio-compatible substances, they can be used in a variety of mechanistic pathways to treat cancer.[22] Peptides can be utilized as anticancer drugs as they possess the ability to be cytotoxic drug carriers, vaccines, hormones, radio-nuclide carriers, receptors and anti-mitotic agents.

3.5.1Peptide Horomones

Peptide hormones are reported to be one of the best classical examples in cancer treatment where LHRH (luteinizing hormone-releasing hormone) acts as an agonist as reported by Schally *et. al*. Various formulations of LHRH agonists such as buserelin, leuprolide, goseralin, triptorelin were developed to treat prostate cancer. Cetrorelix was the first LHRH agonist that was clinically approved and marketed drug.[23]

3.5.2 Radionuclide Peptides

Peptide receptor radionuclide therapy (PRRT) utilizes the combination of a peptide with radionuclide (a radioactive substance) to form highly specialized molecules called radio-peptide analogues.[24] For instance, radiolabelled somastatin analogues comprise of a cyclic octapeptide-Tyr3-octerotide, a chelator-DOTA (tetra azacyclododecane tetraacetic acid) and a radioactive element-111In or 90Y or 177Lu which emit radiations and kill the cancer cell.[25]

3.5.3 Peptide vaccines

Peptide based vaccines are also finding applications in treating cancer since they are less expensive, easy to synthesize and have a defined structure since they are synthetically designed. Many peptide vaccines underwent I/II/III stage clinical phase trials and show promising immunological as well as clinical response. Few examples of the known peptide vaccines[26] are HER-2/neu immunodominant peptide (lung, breast and ovarian cancers), Mucin-1 peptide (breast and colon cancer), carcinoembryonic antigen (colorectal, gastric, breast, pancreatic and non small cell lung cancers). Many other peptide vaccines are well explored to be anti-cancer agents.

3.5.4 Peptide drug carriers

Peptides can be conjugated with a cytotoxic drug to deliver it to a cancer cell expressing the corresponding peptide receptor. Such peptides are known as cell targeting peptides since they can specifically target a cell expressing its receptor. The potential drug candidate AEZS-108 couples a peptide LHRH with the chemotherapeutic agent doxorubicin to directly target those LHRH receptors, especially in case of prostate cancer cells.[27]

3.5.5 Anti mitotic Peptides

Apart from the above mentioned drugs, there are some peptide molecules isolated from marine sources[28] that include dolastatins[29] (dolastatin 10, dolastatin 15, dolastatin 18 etc.), hemiasterlin,[30] milnamide,[31] didemin, HTI-286[32] etc, which are in clinical phase or pre-clinical phase trials and are proved to be potent anti-cancer drugs. Few synthetic analogues of these natural compounds, designed and synthesized in the laboratory subsequently using the peptidomimetic chemistry are known to be active against various cancer cell lines and more potent compared to the parent natural peptides.

The peptidomimetic drugs are advantageous since they are small in size, have ability to penetrate the tumor and possess bio-compatibility. However, they possess few disadvantages, as the protein/peptide drugs are notorious to undergo proteolytic degradation. Incorporation of D-amino acids, cyclization and

constructing a conformationally rigid peptide can solve the issues of proteolysis to a maximum extent, making the drug more potent. It is noteworthy that the SAR profiles of these potential anti-mitotic peptides clearly suggest that the conformation of these peptides is accountable for their bio-active profiles.

3.6 Objective of the present work

Peptide drugs that disrupt microtubule polymerization are of particular interest in treating cancer. This class of drugs comprises of small peptide molecules that include a group of tri, tetra, penta peptides and depsipeptides (peptides in which one or more amide bonds are replaced by ester bonds). When these compounds bind to tubulin, they induce formation of short curved oligomers of tubulin by distorting tubulin-tubulin contacts and thereby causing microtubule depolymerization. Few synthetic analogues of the naturally occurring peptides are known to be highly potent showing cell growth inhibition in sub-nanomolar range and most of these are in clinical phase trials. The SAR profiles of the potent anti-mitotic agents reveal that a folded conformation is accountable for their activity. A closer look at the solid state conformation of dolastatin reveals a 'S shaped conformation'[33a] while the other natural peptides such as hemiasterlin, milnamide and many other drugs possess a 'U shaped/bent conformations'.[33b] This conformational feature of the peptides intrigues the synthetic chemists to design and synthesize folded synthetic peptides featuring side chains that are capable of establishing interactions with tubulin polymer and has become the major area of interest.

Looking at the future, computational and synthetic developments may be reliable prospects to design and identify peptides of desired conformation and biological profiles. The discovery process would rely on the structure and not the function so that hypothetical inhibitors can be produced with the knowledge of the functions or interactions established by the inhibitor moieties as such, on the target receptors. If this approach can be streamlined, it would be helpful in producing molecules that interfere tubulin dynamics and also could be a route to downstream the functions involved in such dynamic interactions.

3.7 Design Strategy

As mentioned in Chapter I, we successfully developed folded peptides devoid of inter-residual hydrogen bonding, featuring a reverse turn conformation. We extended our research to probe the biological applications of such folded peptides since it is a well established fact that majority of the folded peptides are biologically active exhibiting anti-mitotic activity. Using the principles of peptide mimicry, we introduced D-amino acids (in the analogue **C**) on the backbone of the designed peptides in order to account the proteolytic cleavage of the peptide. We designed few peptides with a variety of side chains[34] like O-TBDMS and O-benzyl (as in the analogues **F-I**) that are capable to establish interactions with the bio-receptors. The strategy followed in the design of such synthetic peptides was to retain the turn inducing segment (Pro-Atc, turn segment was retained in all the analogues **A-I**) of the peptide which was surrounded by diverse classes of hydrophobic as well as rigid amino acids possessing variety of side chains. Our design strategy also included the incorporation of hydrophobic groups at the termini of the peptide analogues (**B** and **E**). The synthetic Pro-Atc dipeptide-based peptidomimetic analogues designed are shown below in Fig 3.6.

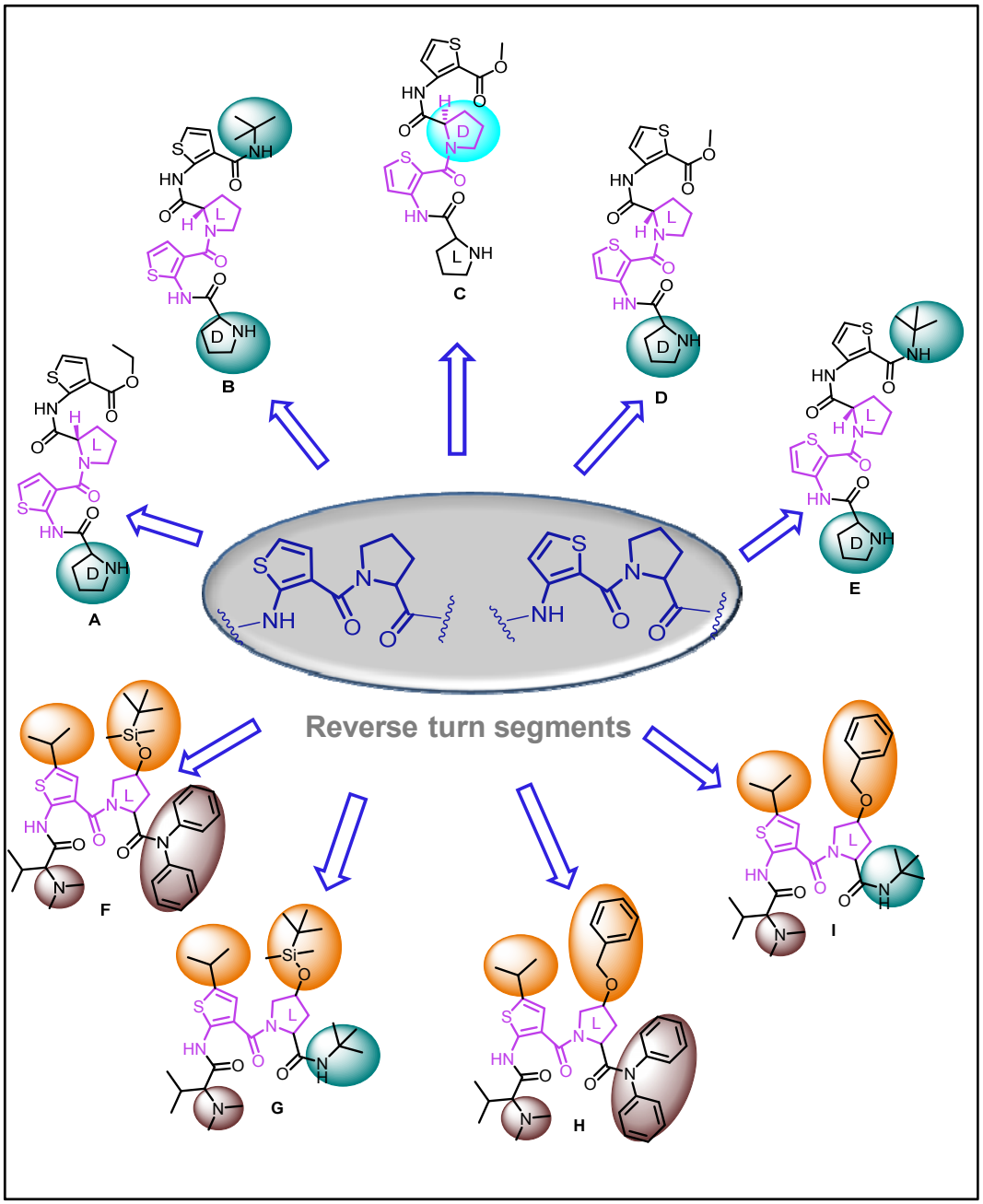

Fig 3.6: Design of folded Pro-Atc dipeptide based analogues featuring modifications on backbone (highlighted in green), turn segment (highlighted in cyan), termini (highlighted in brown), side chain (highlighted in orange) around the turn inducing segments (highlighted in purple).

3.8 Synthesis

3.8.1 Synthesis of the analogues A and B

The compounds **1a**, **1d** and **3g** were subjected to Boc deprotection that yielded the respective amines **1c, 1e, A** in quantitative yields. Further, **3g** was subjected to ester hydrolysis which gave **3h**. To synthesize **3i**, **3h** was coupled with $^{t}BuNH_2$ using DCC as a coupling agent. The C-terminus amidated analogue **3i** was subjected to Boc deprotection to yield **B** directly (Scheme 3.1).

Scheme 3.1

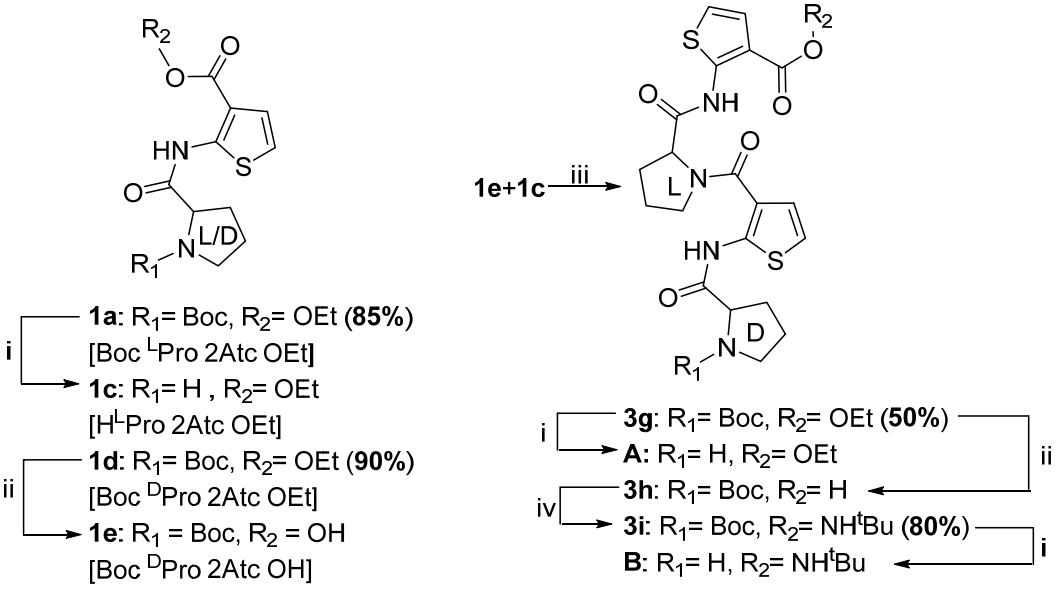

Scheme 3.1: Reagents and conditions: (i) TFA:DCM (1:1), rt, 2 h; (ii) aq. LiOH, MeOH, rt, 4 h; (iii) DCC, HOBt, Et_3N, DCM, rt, 12 h; (iv) $^{t}BuNH_2$, HBTU, HOBt, Et_3N, CH_3CN, rt, 12 h

[*Note*: The numbering of the compounds except for the final analogues is either similar or continued according to the numbering done in Chapter 1. The synthetic protocols used to synthesize **1d** and **3g** were similar to those used in Chapter 1].

3.8.2 Synthesis of the analogues C, D and E

In order to obtain **C**, **D** and **E**, the similar deprotection protocol was followed with the compounds **4g**, **4h** and **4i,** respectively. Thus, the analogues **A-E** were successfully synthesized that feature a folded conformation with necessary hydrophobic functionalities ($^{t}BuNH$- group at the C-terminus) as well as polar

sites, (exposed -NH of proline) that are required to establish essential interactions with the bio-receptors (Scheme 3.2).

Scheme 3.2

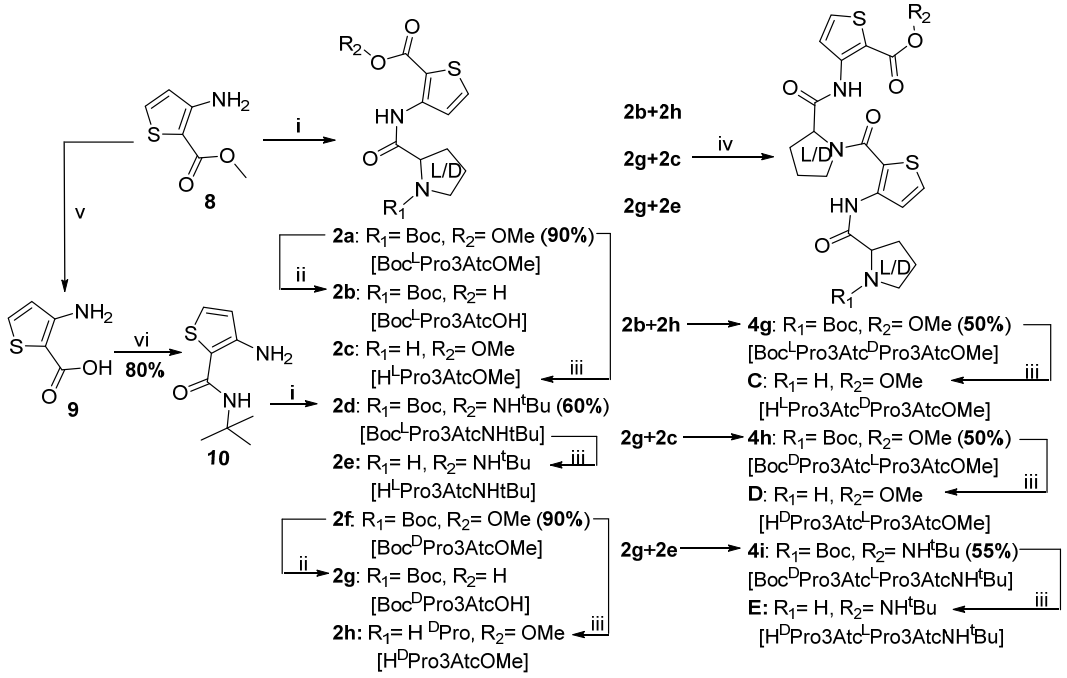

Scheme 3.2: Reagents and conditions: (i) Boc ^{L}Pro-OH, ethyl chloroformate, Et_3N, DCM, 80 ^{0}C, 48 h; (ii) aq. LiOH, MeOH, rt, 4 h; (iii) TFA:DCM (1:1), rt, 2 h; (iv) DCC, HOBt, Et_3N, DCM, rt, 12 h; (v) 2N NaOH, 60 ^{0}C, 5 h; (vi) $^{t}BuNH_2$, EDC.HCl, Et_3N, CH_3CN, rt, 12 h.

[*Note*: The numbering of the compounds except for the final analogues is either similar or continued according to the numbering done in Chapter 1. Also the synthetic protocols followed to synthesize **2a**, **2d**, **2f**, **4g**, **4h**, and **4i** were similar to those used in Chapter 1].

3.8.3 Synthesis of the analogues F and G

Compound **5** was synthesized according to the reported procedure.[35] This amine **5,** was coupled with Cbz-valine using EDC.HCl to get the dipeptide **6**. The Cbz group of the dipeptide **6** was removed using HBr.AcOH, the free amine obtained was N, N dimethylated *in situ* using formaldehyde in the presence of $NaBH_3CN$ to give **7**. Later, compound **7** was subjected to hydrolysis to yield **7a**-one of the counterparts of the target molecules. In order to synthesize the C-terminus counterpart, we started with O-TBDMS protected hydroxy proline **11**, which was subjected to hydrolysis to yield **11a**. Compound **11a** was coupled with benzhydryl amine and tertiary butyl amine simultaneously using EDC.HCl as the

coupling agent to obtain the compounds **12a** and **12b** respectively. Then, **12a** and **12b** were subjected to boc deprotection to yield the respective amines **12c** and **12d**. Further, these amines, **12c** and **12d** were coupled with **7a** using EDC.HCl as a coupling agent to give **F** and **G**, respectively as shown in Scheme 3.3.

Scheme 3.3

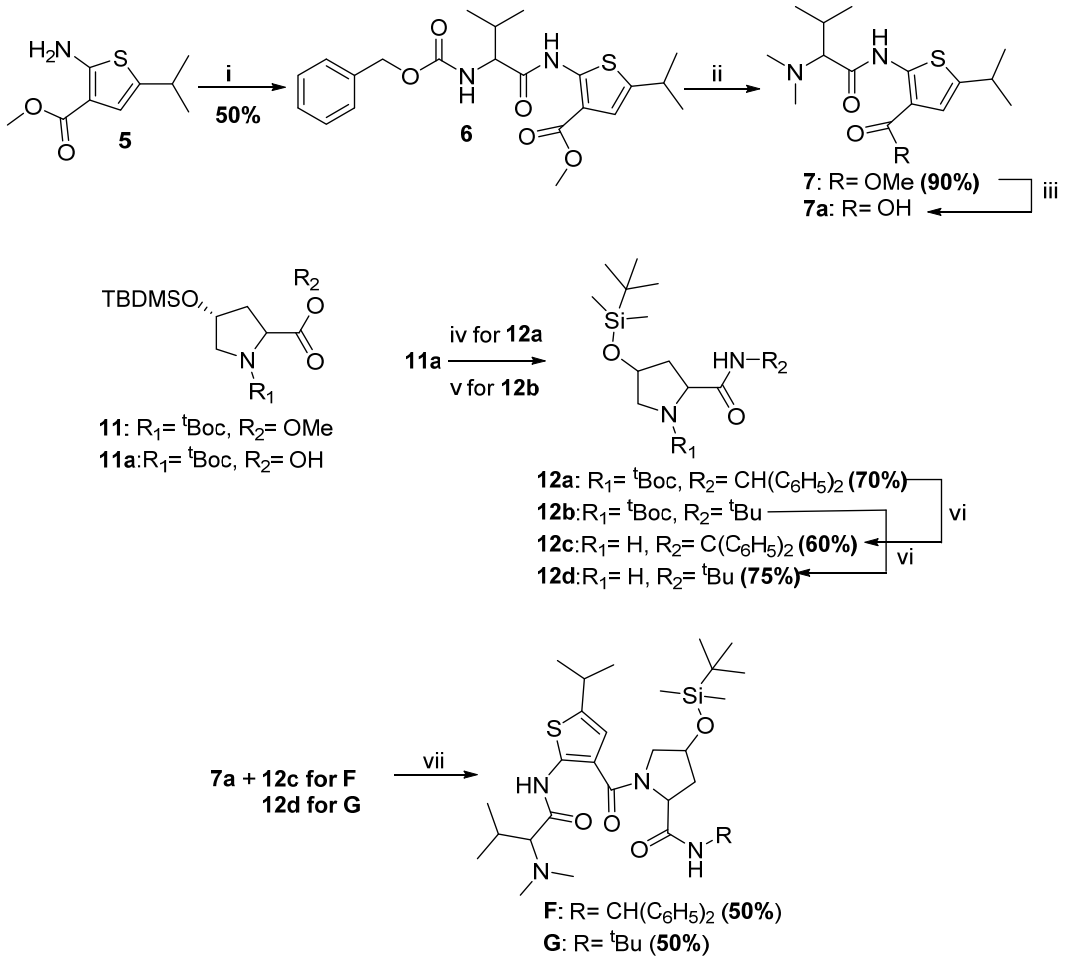

Scheme 3.3: Reagents and conditions: (i) EDC.HCl, DCM, rt, 12 h; (ii) a) HBr.AcOH b) $NaBH_3CN$, HCHO, MeOH; (iii) aq. LiOH, MeOH, rt, 4 h; (iv) $CH(C_6H_5)_2NH_2$, EDC.HCl, HOBt, Et_3N, DCM; (v) $^tBuNH_2$, EDC.HCl, HOBt, Et_3N, DCM; (vi) TFA:DCM (1:1), rt, 2 h; (vii) EDC.HCl, HOBt, Et_3N, DCM.

3.8.4 Synthesis of the analogues H and I

To synthesize the target molecules **H** and **I**, we started with O-benzyl protected hydroxy proline **13**, which was subjected to hydrolysis to give **13a**. The acid **13a** was coupled with benzhydryl amine and tertiary butyl amine respectively using EDC.HCl as the coupling agent to give the compounds **14a** and **14b**. Then, **14a** and **14b** which were further subjected to boc deprotection to yield the

respective amines **14c** and **14d**. Later, these amines, **14c** and **14d** were coupled with **7a** using EDC.HCl to give **H** and **I**, respectively as mentioned in Scheme 3.4. Thus, all the designed peptides **A-I** were synthesized successfully.

Scheme 3.4

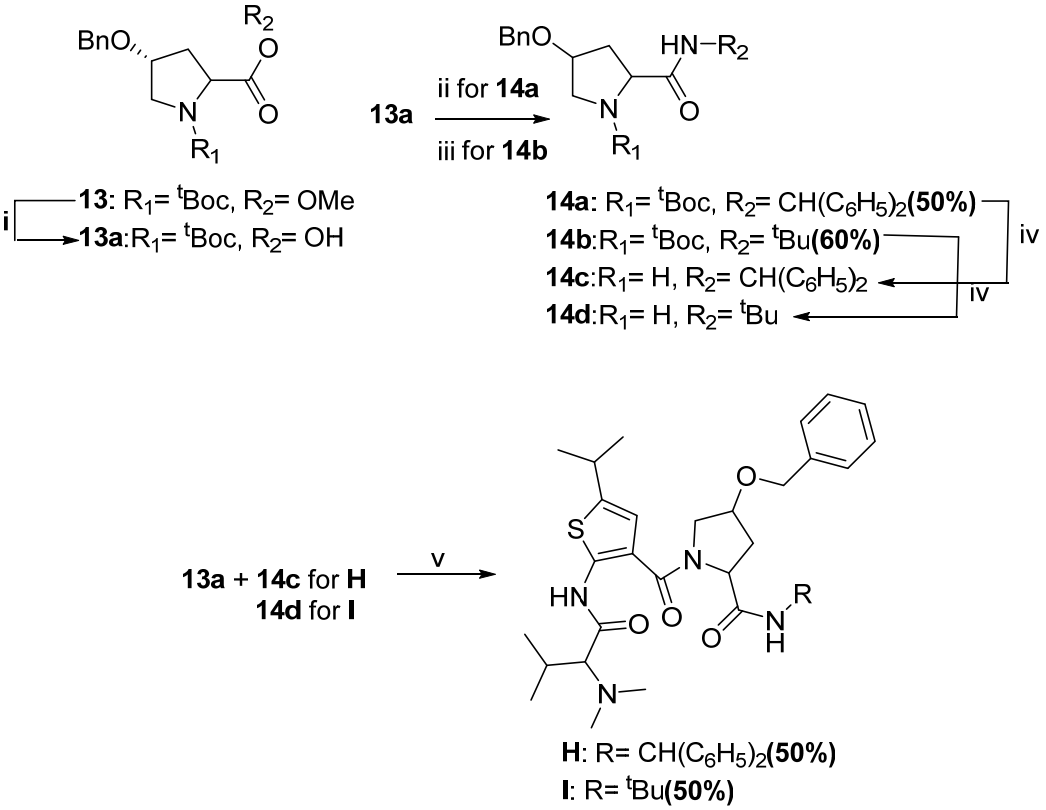

Scheme 3.4: Reagents and conditions: (i) aq. LiOH, MeOH; (ii) $CH(C_6H_5)_2NH_2$, EDC.HCl, HOBt, Et_3N, DCM, 12 h; (iii) $^tBuNH_2$, EDC.HCl, HOBt, Et_3N, DCM, 12 h; (iv) TFA:DCM (1:1), rt, 2 h; (v) EDC.HCl, HOBt, Et_3N, DCM, 12 h.

3.9 Conclusion

In summary, we could synthesize Pro-Atc dipeptide based peptidomimetic analogues **A-I**, featuring modifications on backbone, chirality of the residues of the turn segment, termini and side chains, around the Pro-2Atc and Pro-3Atc reverse turn segments which may result in potential anti-mitotic drugs, as they possess a pre-defined rigid conformational feature. The study of these peptidomimetic molecules might open avenues for the development of a 'new class' of peptide anti-mitotic agents.

Synthesis of analogues of Ixorapeptide I-their biological evaluation.

3.10 Introduction

Ixorapeptide I, a flavonoid was isolated from the MeOH extracts of *Ixora coccinea*. It exhibits selective potency against Hep 3B liver cancer cell line with IC_{50} value 3.36 µg/mL. *Ixora*, belonging to Rubiaceae is a class of shrubs found in tropical asia and africa. *Ixora coccinea Linn*, a plant with red flowers, widely spread in Taiwan is the source of Ixorapeptide I. In addition to anti-tumour activity, the extracts from *Ixora coccinea* exhibit anti-bacterial, antifungal, anti-oxidative and analgesic activities.[36] The flowers, roots and stem are used to treat various ailments and is also used in several folk medicines.

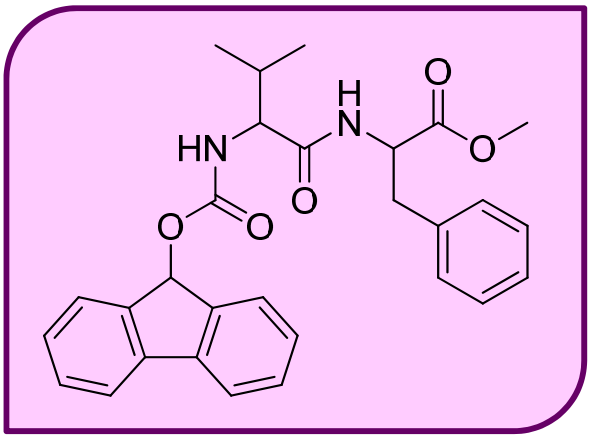

Fig 3.7: Chemical structure of Ixora peptide I.

3.11 Objective of the present work

Our basic effort was to synthesize peptidomimetic analogues of Ixora peptide I and find their applications in biological systems if they can serve as anti-mitotic drugs. It is a known fact that many natural as well as synthetic peptides bind and disrupt the tubulin dynamics, leading to apoptosis. Our thought was to explore the utility of the designed peptidomimetic analogues of Ixora peptide I as a tubulin binding agents. The possible modifications that can be done on the dipeptide, to improve the hydrophobic nature, essential for binding to tubulin and to increase its potency are shown in the figure (Fig 3.8).

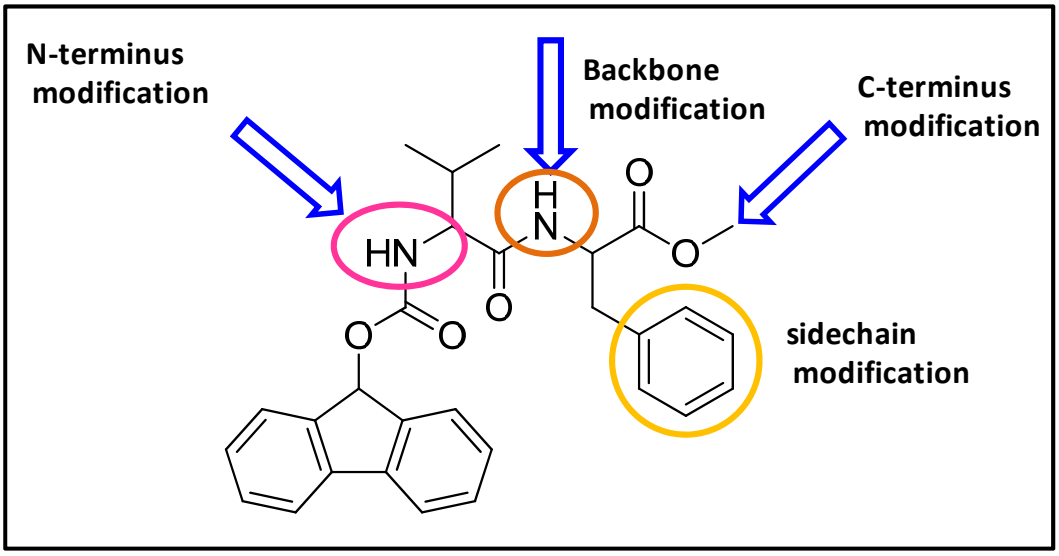

Fig 3.8: Possible structural modifications on the dipeptide, Ixora peptide I.

3.12 Design Strategy

Keeping in view, the advantages of peptidomimetics, we designed few analogues featuring N-methylated amino acids, hydrophobic side chains, amide bond surrogates, building block modifications and termini modifications (Fig 3.9).

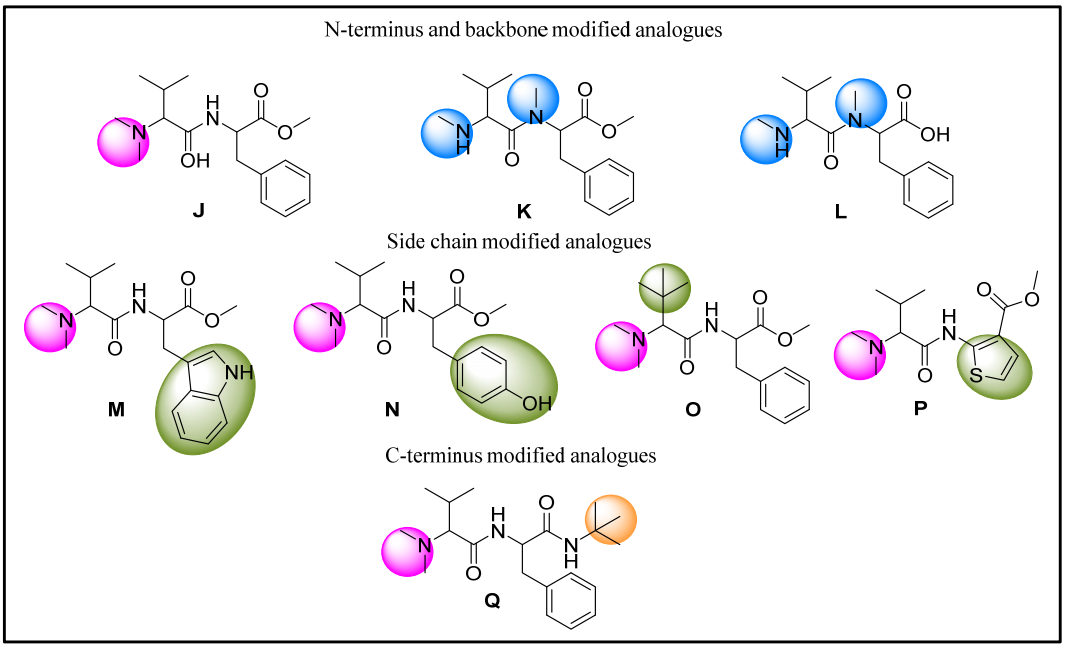

Fig 3.9: Structures of the designed synthetic analogues of Ixorapeptide I with N-terminus modifications (highlighted in pink), backbone modifications (highlighted in blue), side chain modifications (highlighted in green) and C-terminus modification (highlighted in orange).

3.12.1 N-methylation

N-methylation/N, N dimethylation was attempted as a key modification in the designed synthetic analogues. The N-terminus Fmoc group was substituted by N, N, dimethyl group in the analogues **J-Q** (Fig 3.9) and the amide group was substituted by N-methylated amide functionality in **K** and **L** (Fig 3.9). N, N dimethylated/N-methylated peptides are very well known to be biologically active.[37] N-methylation of amide bonds in peptides is not a post-translational modification strategy. However, there are several cyclic or linear N-methylated peptides known till date (Fig 3.10). The N-methylated peptides in nature are synthesized enzymatically to induce certain physical & biological properties and to modulate few protein-protein interactions. Such N-methylated peptides are known to target cell membranes,[38a] microtubules,[38b-e] DNA,[39] ribosomes[40] and protein phosphatases.[41] N, N dimethylation strategy of amino acids had resulted in analogues with improved pharmacokinetic properties such as enzymatic stability, receptor selectivity, enhanced potency and bioavailability. Therefore, mono and multiple N-methylation scan of peptides would continue to be a powerful approach in finding better lead structures which can modulate the biological properties of several peptides.

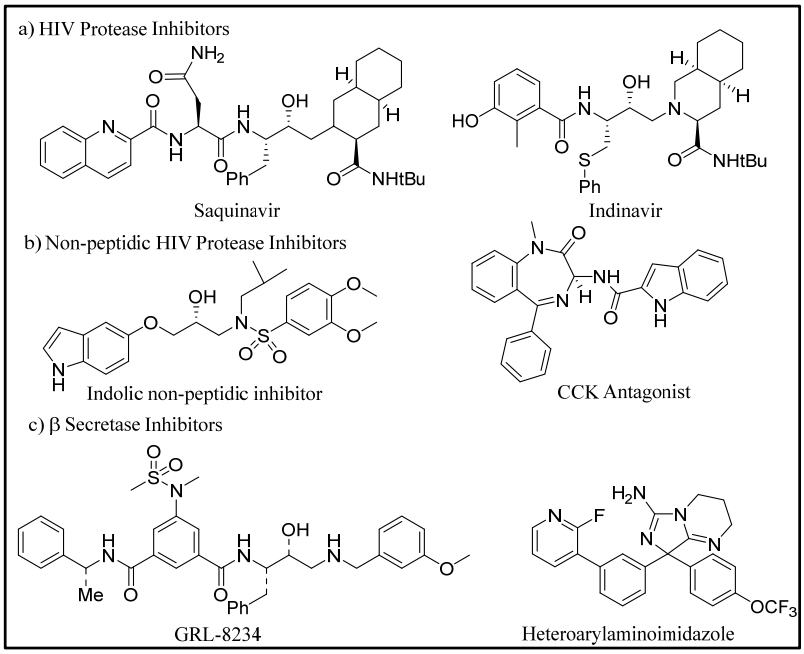

Fig 3.10: N-methylated peptides currently in clinical trials used as various types of cancer.[37]

3.12.2 Side chain modification

Ixorapeptide I is a dipeptide with valine as the first residue and phenyl alanine as the second residue. In general, the side chains of the amino acids play crucial role in establishing interactions with the target peptides. Hence, we designed analogues wherein the following side chain modifications were done. The phenyl side chain of the second residue in Ixorapeptide I was substituted by indole moiety, substituted phenyl side chains and a heterocyclic ring in **M-P** (Fig. 3.9) respectively. The analogue with tryptophan (Fig 3.9, **M**) as the second residue features an exposed –NH group which might enhance the binding ability to tubulin protein. The analogue with tyrosine amino acid (Fig 3.9, **N**) as the second residue possesses unmasked -OH group on the phenyl ring which can enhance the hydrogen bonding probability of the peptide. The analogue with a heterocyclic ring contains a sulfur atom as a hetero atom (Fig 3.9, **P**). This was chosen as its incorporation was observed to enhance the anti-mitotic activity of many peptide analogues.[42] In one of the analogues, the first residue valine was substituted by L-tert leucine (Fig 3.9, **O**) which contains an hydrophobic tert butyl side chain. The side chains such as tert butyl group, indole group and phenylic groups were specifically chosen since they are extensively found in many natural peptides like Hemiasterlin, HTI-286, E7974 etc (Fig 3.11).

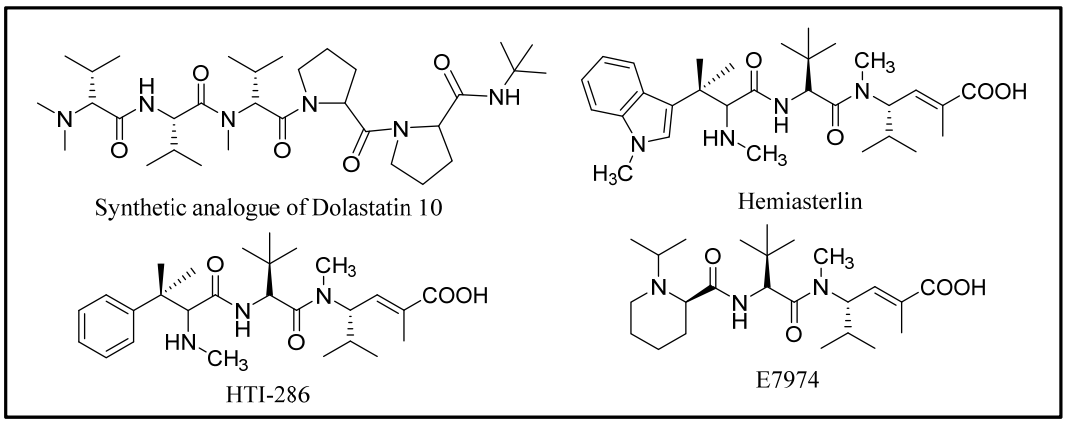

Fig 3.11: Peptides featuring specific side chains and C-terminus groups necessary for bio-activity.

3.12.3 C-Terminus modification

C-terminus modification was also attempted in one of the designed peptides. The C-terminus ester of Ixora peptide I was translated to an amide

featuring tert-butyl group to increase its hydrophobicity (Fig 3.9 **Q**). Similar modification in one of the synthetic analogues of dolastatin resulted in improved biological profile of the peptide and is in clinical phase trials now (Fig 3.11).

3.13 Synthesis

All the analogues **J-Q**, were synthesized as shown below:

3.13.1 Synthesis of the analogues J, Q, M, N, O

Scheme 3. 5

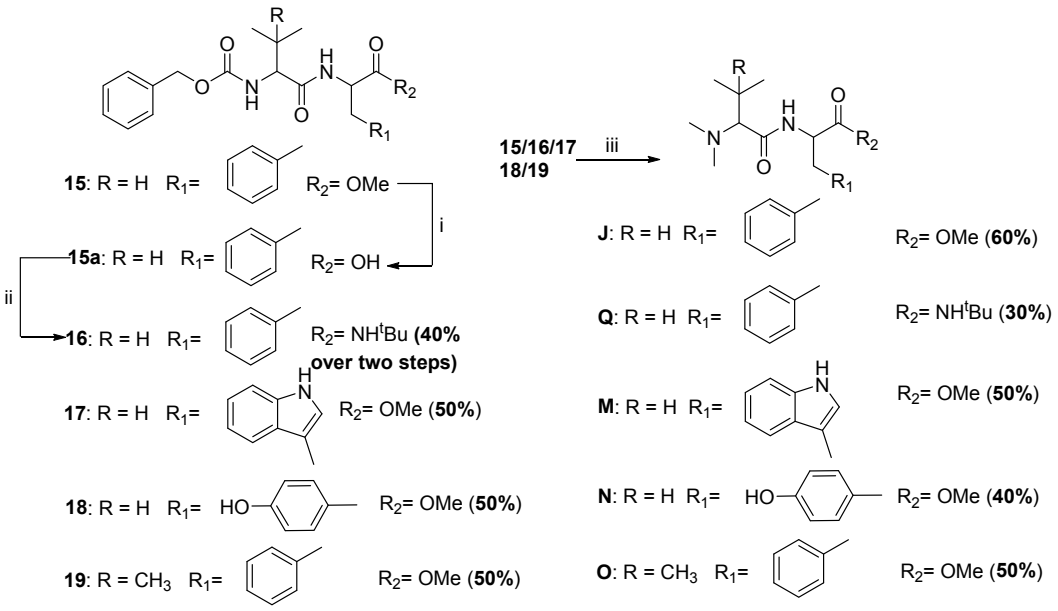

Scheme 3.5: Reagents and conditions: (i) aq. LiOH, MeOH, rt, 12 h; (ii) $^{t}BuNH_2$, HBTU, HOBt, CH_3CN, rt, 12 h; (iii) Pd/C, HCHO, MeOH, H_2, 60 psi, 3 days.

The dipeptide **15** was synthesized following the reported procedure.[43] Later, the dipeptide **15** was subjected to hydrolysis to get the acid **5a**. This acid **5a** was then coupled with tertiary butyl amine to obtain the C-terminus amidated analogue **16**. The dipeptides **17** and **18** were synthesized by coupling Cbz-valine with the respective hydrochloride salts of tryptophan methyl ester and tyrosine methyl ester using EDC.HCl as coupling agent. All the dipeptide analogues **15**, **16**, **17**, **18** and **19** were treated with formaldehyde in the presence of 10% Pd/C catalyst under H_2 pressure at 60 psi in methanol for 3 days to yield the respective N, N dimethylated analogues **J**, **Q**, **M**, **N**, **O**, respectively. The details of the synthetic procedures used to synthesize the compounds are given in Scheme 3.5.

3.13.2 Synthesis of the analogues K and L

The dipeptide **15** was subjected to methylation using silver oxide and methyl iodide in DMF, which gave a mixture of products **20**. This mixture was subjected to Cbz-deprotection using 10% Pd/C as a catalyst under H_2 pressure at 60 psi in methanol. The products obtained were **K** and **L** (Scheme 3.6), confirmed by the NMR and HRMS analysis.

Scheme 3.6

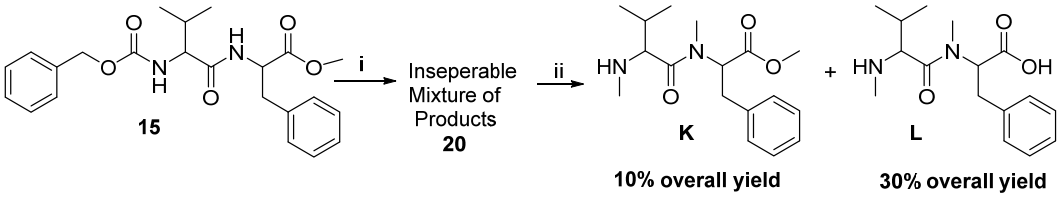

Scheme 3.6: Reagents and conditions: (i) Ag_2O, CH_3I, DMF, 12 h; (ii) Pd/C, MeOH, H_2, 60 psi, 8 h.

3.13.3 Synthesis of the analogue P

The analogue **P** was synthesized by coupling Cbz-valine to methyl 2-amino thiophene 3-carboxylate using EDC.HCl as coupling agent followed by N, N- dimethylation of the resultant dipeptide **22**. The dipeptide **22** was subjected to Cbz-deprotection using HBr.AcOH. The amine obtained was N, N alkylated using $NaBH_3CN$ and formaldehyde in methanol which yielded the analogue **P** (Scheme 3.7).

Scheme 3.7

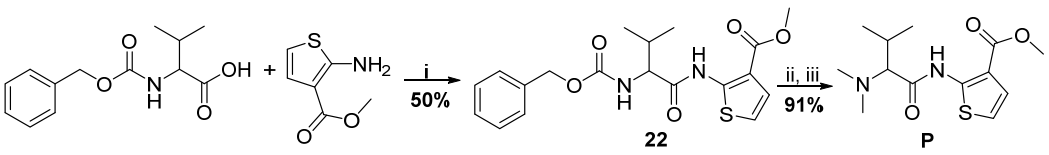

Scheme 3.7: Reagents and conditions: (i) EDC.HCl, HOBt, Et_3N, CH_3CN, rt, 12 h; (ii) HBr. AcOH, rt, 20 min; (iii) $NaBH_3CN$, HCHO, MeOH, 6 h.

3.14 Biological evaluation-Tubulin polymerization assay

Preliminary studies

For invitro tubulin polymerization assay,[44] tubulin, BRB-80 buffer and GTP were used. BRB-80, GTP and **J** were taken into a 96 well plate that was maintained at 0 °C. To this mixture, the compound **J** was added followed by the addition of tubulin and then it was introduced into the spectrophotometer which was pre-incubated at 37 °C for 20 min. The tubulin polymerization was studied based on the increased levels of turbidity at 340 nm in the reaction mixture, comparing the activity with a known control, nocodazole.[45] The results clearly suggest that **J** acts as anti-tubulin polymerization agent (Fig 3.12).

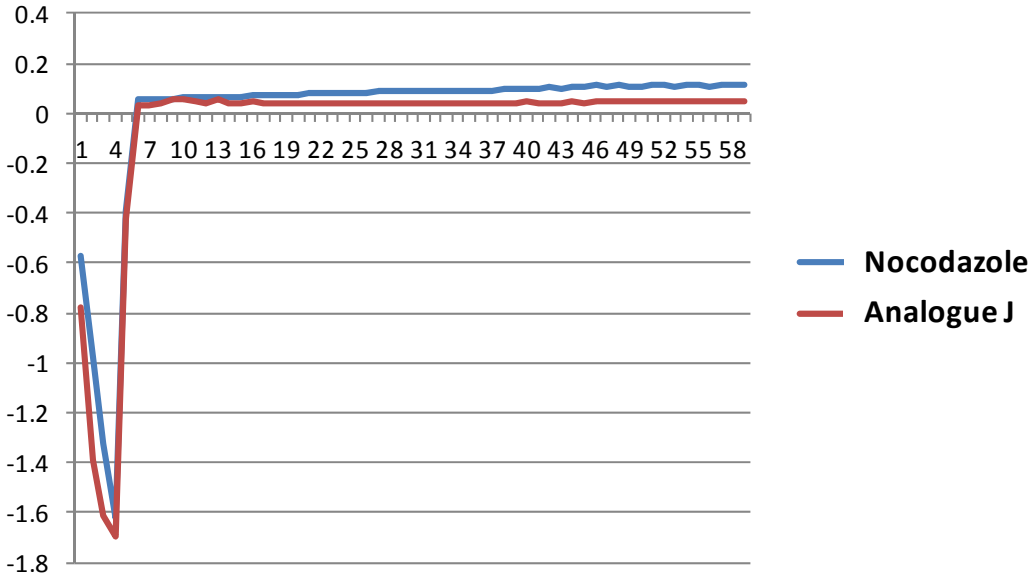

Fig 3.12: Turbidity progress curve when tubulin undergoes polymerization.

3.15 Conclusion

In summary, we could successfully synthesize the synthetic analogues of Ixorapeptide I and evaluate the bio-activity profile of one of the analogues **J**, which showed a promising tubulin binding activity. Hence, the analogues could be valuable tubulin polymerization inhibiting agents. Further, structural modifications on these analogues might furnish a potent anti-mitotic drug.

3.16 Experimental Section (Section A)

General methods for synthesis of dipeptides 1d, 2f and tetrapeptides 3g, 4g, 4h:

The dipeptides **1d**, **2f** and tetrapeptides **3g**, **4g**, **4h** were synthesized following the procedures mentioned in Chapter I. D-Proline has been used instead of L-Proline wherever mentioned according to the design strategy.

tert-butyl-2-((3-(ethoxycarbonyl)thiophen-2-yl)carbamoyl)pyrrolidine-1-carboxylate 1d:

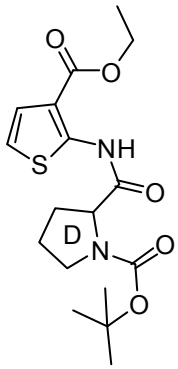

1d

Compound **1d** was isolated as a yellow solid (0.3 g, 85%); m.p: 63-66 °C; $[\alpha]^{26}_{D}$: -132° (*c* = 1, $CHCl_3$); IR ($CHCl_3$) ν (cm^{-1}): 3684, 3276, 3018, 2980, 2889, 2400, 1685, 1550, 1498, 1384, 1291, 1217, 1089, 1034, 928, 770, 668, 626, 484. ^{1}H NMR (400 MHz, $CDCl_3$) δ: $11.51_{rotamer}$(0.45H), $11.36_{rotamer}$(0.55H), 7.17-7.14 (d, *J* = 5.5 Hz, 1H), 6.71-6.68 (d, *J* = 5.3 Hz, 1H), 4.34-4.23 (q, *J* = 6.9 Hz, 14 Hz, 2H), 3.57 (bs, 2H), 2.21-2.13 (bs, 2H), 1.93-1.86 (m, 2H), 1.45 (s, 3H), $1.34_{rotamer}$ (5H), $1.27_{rotamer}$ (4H); ^{13}C NMR (100 MHz, $CDCl_3$) δ: 170.4, 169.8, 164.8, 147.8, 123.6, 115.7, 113.2, 80.3, 61, 60.4, 46.7, 28, 24.1, 23.7, 14.4; HRMS: $C_{11}H_{18}O_3N_3S$, Calcd: 369.1479 Found: 369.1479.

tert-butyl-(R)-2-((3-((S)-2-((3-(ethoxycarbonyl)thiophen-2-yl)carbamoyl) pyrrolidine-1-carbonyl)thiophen-2-yl)carbamoyl)pyrrolidine-1-carboxylate 3g:

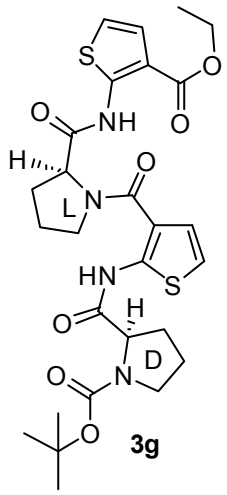

3g

The compound **3g** was isolated as a white solid; mp: 136-138 °C; $[\alpha]^{26}_{D}$: -82° (*c* = 1, $CHCl_3$); IR ($CHCl_3$) ν (cm^{-1}): 3272, 3019, 1681, 1551, 1399, 1215, 702, 668; ^{1}H NMR (400 MHz, $CDCl_3$) δ: 11.73 (bs, 1H), 11.60 (bs, 1H), 7.27-7.25 (bs, 1H), 7.21-7.18 (d, *J* = 5.8 Hz, 1H), 6.82-6.80 (m, 1H), 6.75-6.73 (d, *J* = 5.7 Hz, 1H), 4.97-4.91 (m, 1H), 4.51-4.48 (m, 1H), 4.34-4.24 (q, *J* = 6.9 Hz, 2H), 4.04-3.87 (m, 2H), 3.53-3.33 (m, 2H), 2.37-1.85 (m, 8H), $1.49_{rotamer}$ (4H), 1.40-1.33 (m, 3H),

$1.29_{rotamer}$ (5H); ^{13}C NMR (100 MHz, $CDCl_3$) δ: 170.5, 169.9, 168.9, 166.6, 165.1, 155.0, 153.7, 148.0, 147.2, 123.7, 123.2, 115.9, 115.2, 113.4, 96.0, 80.2, 80.1, 79.4, 61.1, 60.5, 57.4, 50.0, 46.9, 46.5, 36.5, 31.2, 29.8, 28.3, 25.7, 25.1, 24.2, 23.7, 14.2; ESI-MS: 613.4067 $(M+Na)^+$; Elemental analysis calculated for $C_{27}H_{34}N_4O_7S_2$: C, 54.90; H, 5.80; N, 9.48; S, 10.86; Found: C, 52.54; H, 5.42; N, 10.01; S, 10.66.

tert-butyl-(R)-2-((3-((S)-2-((3-(tert-butylcarbamoyl)thiophen-2-yl)carbamoyl) pyrrolidine-1-carbonyl)thiophen-2-yl)carbamoyl)pyrrolidine-1-carboxylate 3i:

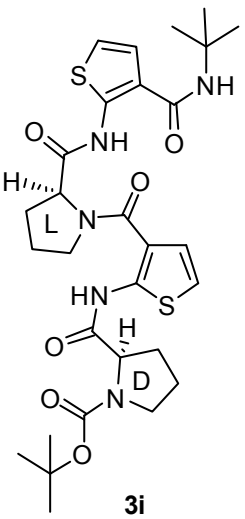

3i

The acid **3h** (0.18 g, 0.33 mmol, 1equiv) was coupled with $^tBuNH_2$ (0.1 mL, 1.01 mmol, using HBTU (0.19 g, 0.5 mmol, 1.5 equiv) and DIPEA (0.11 mL, 0.6 mmol, 2 equiv). Work up, as that described for **1a** followed by column chromatographic purification yielded compound **3i** (0.1 g, 50%) as yellow solid; mp: 85-88 °C; $[\alpha]^{26}_D$: -60° (*c* = 1, $CHCl_3$); IR ($CHCl_3$) ν (cm^{-1}): 3683, 2978, 2400, 1684, 1628, 1545, 1485, 1396, 1217, 1047, 927, 769, 666, 482; ^{1}H NMR (200 MHz, $CDCl_3$) δ: 12.64 (s, 1H), $11.7_{rotamer}$ (0.4H), 11.64 (s, 1H), 7.39 (bs, 1H), 6.87-6.85 (m,1H), 6.78-6.72 (m, 2H), 5.75-5.73 (m, 1H), 4.91 (bs, 1H), $4.42_{rotamer}$ (0.5H), $4.27_{rotamer}$ (0.5H), 4.03-3.99 (m, 1H), 3.9-3.88 (m, 1H), 3.57 (bs, 1H), 3.49-3.36 (m, 1H), 2.39 (bs, 1H), 2.17-1.86 (m, 7H), $1.47_{rotamer}$ (4H), 1.34 (s, 9H), $1.28_{rotamer}$ (5H); ^{13}C NMR (100 MHz, $CDCl_3$) δ: 169.4, 166.5, 164.7, 146.4, 145.7, 123.7, 120.7, 115.9, 115.3, 80.1, 60.9, 51.5, 50.6, 49.9, 46.7, 38.4, 28.6, 28.0, 24.3; MALDI-TOF: 639.7768 $(M+Na-1)^+$, 640.7768 $(M+Na)^+$, 641.7773 $(M+Na+1)^+$, 655.7349 $(M+K-1)^+$, 656.7327 $(M+K)^+$, 657.7293 $(M+Na+1)^+$; Elemental analysis calculated for $C_{29}H_{39}N_5O_6S_2$: C, 54.96; H, 5.21; N, 11.15; S, 12.76; Found: C, 55.5; H, 5.8; N, 10.9; S, 12.8.

tert-butyl-(R)-2-((2-(methoxycarbonyl)thiophen-3-yl)carbamoyl)pyrrolidine-1-carboxylate 2f:

The didpeptide **2f** was isolated as a pasty mass. $[\alpha]^{26}_D$: -172° (*c* = 1, $CHCl_3$); IR ($CHCl_3$) ν (cm^{-1}): 3308, 3015, 1684, 1570, 1388, 1282, 1216, 1160, 1095, 755; ^{1}H NMR (400 MHz, $CDCl_3$) δ: $10.75_{rotamer}$ (0.45H), $10.62_{rotamer}$ (0.55H), 8.15-8.12 (d,

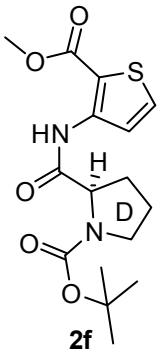

2f

J = 5.6 Hz, 1H), 7.47 (bs, 1H), 4.44$_{rotamer}$ (0.45H), 4.30$_{rotamer}$ (0.55H), 4.16-4.06 (q, ethyl acetate), 3.87 (s, 3H), 3.64-3.58 (m, 2H), 2.20-2.17 (m, 2H), 2.04 (s, ethyl acetate), 1.93 (m,2H), 1.49$_{rotamer}$ (4H), 1.33$_{rotamer}$ (5H); ^{13}C NMR (100 MHz, $CDCl_3$) δ: 171.0, 170.4, 164.1,154.1, 143.8, 131.6, 122.0, 110.7, 80.4, 61.9, 61.3, 51.9, 46.8, 31.3, 30.0, 28.1 23.1, 14.0; HRMS: $C_{16}H_{23}O_5N_2S$, Calcd: 369.1479 Found: 369.1479. $C_{16}H_{23}O_5N_2NaS$, Calcd: 377.1442 Found: 377.1444.

tert-butyl-(S)-2-((2-((R)-2-((2-(methoxycarbonyl)thiophen-3-yl)carbamoyl) pyrrolidine-1-carbonyl)thiophen-3-yl)carbamoyl)pyrrolidine-1-carboxylate 4g:

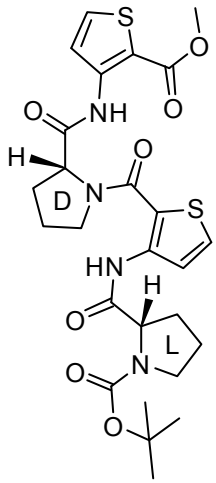

4g

The compound **4g** was isolated as a white solid; mp: 91-93 °C; $[\alpha]^{26}_D$: +80° (*c* = 0.1, $CHCl_3$); IR ($CHCl_3$) ν (cm^{-1}): 3684, 3619, 3441, 3019, 2400, 1679, 1522, 1476, 1423, 1215, 1046, 928, 766, 669, 626; ^{1}H NMR (400 MHz, $CDCl_3$) δ: 11.75$_{rotamer}$ (0.5H), 11.59$_{rotamer}$ (0.5H), 10.68 (s, 1H), 8.27-8.22 (t, *J* = 5 Hz, 1H), 8.12-8.09 (d, *J* = 5.4 Hz, 1H), 7.47-7.44 (d, *J* = 4.8 Hz, 2H), 4.92-4.87 (t, *J* = 5.1 Hz, 1H), 4.41$_{rotamer}$ (0.5H), 4.25$_{rotamer}$ (1.5H), 4.07-3.97 (m, 1H), 3.8 (bs, 3H), 3.69-3.58 (m, 1H), 3.52-3.53 (m, 1H), 2.25-2.09 (m, 6H), 1.93-1.84 (m, 2H), 1.31$_{rotamer}$ (4H), 1.26$_{rotamer}$ (5H); ^{13}C NMR (100 MHz, $CDCl_3$) δ: 170.5, 169.9, 168.9, 166.6, 165.1, 155.0, 153.7, 148.0, 147.2, 123.7, 123.2, 115.9, 115.2, 113.4, 96.0, 80.2, 80.1, 79.4, 61.1, 60.5, 57.4, 50.0, 46.9, 46.5, 36.5, 31.2, 29.8, 28.3, 25.7, 25.1, 24.2, 23.7, 14.2; ESI-MS: 599.7709 $(M+Na)^+$; Elemental analysis calculated for $C_{26}H_{32}N_4O_7S_2$: C, 54.15; H, 5.59; N, 9.72; S, 11.42; Found: C, 56.1; H, 4.8; N, 9.67; S, 10.5.

tert-butyl-(R)-2-((2-((S)-2-((2-(methoxycarbonyl)thiophen-3-yl)carbamoyl) pyrrolidine-1-carbonyl)thiophen-3-yl)carbamoyl)pyrrolidine-1-carboxylate 4h:

The compound **4h** was isolated as a white solid; mp: 91-93 °C; $[\alpha]^{26}_D$: -30° (*c* = 1, $CHCl_3$); IR ($CHCl_3$) ν (cm^{-1}): 3684, 3620, 3307, 3019, 2978, 2887, 2400, 1679, 1554, 1476, 1422, 1403, 1283, 1216, 1123, 1088, 1046, 928, 877, 849, 770, 668,

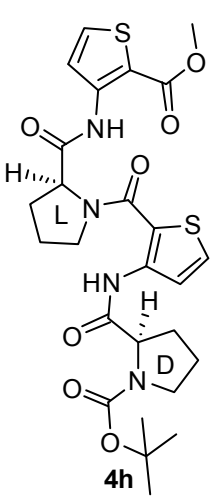

626; ^{1}H NMR (400 MHz, $CDCl_3$) δ: 11.74$_{rotamer}$ (0.5H), 11.59$_{rotamer}$ (0.5H), 10.67 (s, 1H), 8.26-8.23 (q, *J* = 10.9 Hz, 5.4 Hz, 1H), 8.12-8.11 (d, *J* = 4.5 Hz, 1H), 7.47-7.44 (m, 2H), 4.9 (bs, 1H), 4.39$_{rotamer}$ (0.5H), 4.22$_{rotamer}$ (1.5H), 4.17rotamer (0.5H), 4.02$_{rotamer}$ (0.5H), 3.82-3.8 (d, *J* = 8.8 Hz, 3H), 3.65-3.61 (m, 1H), 3.53$_{rotamer}$ (0.5H), 3.43$_{rotamer}$(0.5H), 2.26-2.13 (m, 6H), 1.95-1.83 (m, 2H), 1.31$_{rotamer}$ (4H), 1.26$_{rotamer}$ (5H); ^{13}C NMR (100 MHz, $CDCl_3$) δ: 169.3, 164.4, 145, 143.9, 131.4, 129, 111.9, 79.9, 62.9, 51.8, 48.9, 46.9, 28.1; ESI-MS: 599.7709 $(M+Na)^+$; Elemental analysis calculated for $C_{26}H_{32}N_4O_7S_2$: C, 54.15; H, 5.59; N, 9.72; S, 11.42; Found: C, 55.4; H, 5.3; N, 9.01; S, 10.8.

tert-butyl (R)-2-((2-((S)-2-((2-(tert-butylcarbamoyl)thiophen-3-yl)carbamoyl) pyrrolidine-1-carbonyl)thiophen-3-yl)carbamoyl)pyrrolidine-1-carboxylate 4i:

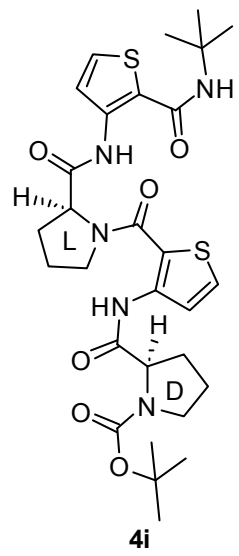

The compound **4i** was isolated as brown solid; mp: 110-113 °C; $[\alpha]^{26}_{D}$: -60° (*c* = 1, $CHCl_3$); IR ($CHCl_3$) ν (cm^{-1}): 3684, 3618, 3422, 3019, 2400, 1685, 1555, 1423, 1403, 1367, 1289, 1215, 1121, 1046, 929, 877, 849, 770, 669, 626; ^{1}H NMR (400 MHz, $CDCl_3$) δ: 11.81$_{rotamer}$ (0.4H), 11.64$_{rotamer}$ (0.5H), 8.24-8.21 (t, *J* = 7Hz, 1H), 8.11-8.1 (d, *J* = 3.7 Hz, 1H),7.46-7.42 (dd, *J* = 11.5 Hz, 4.5 Hz, 1H), 7.25-7.22 (t, *J* = 5.7 Hz, 1H), 5.41-5.38 (d, *J* = 9.2 Hz, 1H), 4.9 (bs, 1H), 4.39$_{rotamer}$ (0.5H), 4.24$_{rotamer}$ (1.5H), 4.02-4 (m, 1H), 3.64-3.61 (m, 1H), 3.53$_{rotamer}$ (0.5H), 3.45$_{rotamer}$ (0.5H), 2.28-2.04 (m, 6H), 1.98-1.8 (m, 2H), 1.33 (s, 9H), 1.28 (s, 9H); ^{13}C NMR (100 MHz, $CDCl_3$) δ: 169.4, 166.5, 164.7, 146.4, 145.7, 123.7, 120.7, 115.9, 115.3, 80.1, 60.9, 51.5, 50.6, 49.9, 46.7, 38.4, 28.6, 28.0, 24.3; MALDI-TOF: 639.7768 $(M+Na-1)^+$, 640.7768 $(M+Na)^+$, 641.7773 $(M+Na+1)^+$, 655.7349 $(M+K-1)^+$, 656.7327 $(M+K)^+$, 657.7293 $(M+Na+1)^+$; Elemental analysis calculated for $C_{29}H_{39}N_5O_6S_2$: C, 54.96; H, 5.21; N, 11.15; S, 12.76; Found: C, 55.5; H, 5.8; N, 10.9; S, 12.8.

General method for the synthesis of A-E:

The analogues **A-E** have been synthesized by removing the N-terminus Boc group. The solutions of Boc-peptides **3g**, **3i**, **4g**, **4h** and **4i** (3 mmol) were subjected to deprotection using DCM/TFA (1:1, 5 mL) at 0 °C. After completion of the reaction (~2 h), the solvent was stripped off, the residue was taken into DCM (30 mL), washed with sat.$NaHCO_3$ solution (3x10 mL) and the product was repeatedly extracted. The organic layer was dried over anhydrous Na_2SO_4. The residues **A**, **B**, **C**, **D** and **E**, respectively, obtained after evaporation of the solvent were the required final analogues.

Ethyl-2-((S)-1-(2-((R)-pyrrolidine-2-carboxamido)thiophene-3-carbonyl) pyrrolidine-2-carboxamido)thiophene-3-carboxylate A:

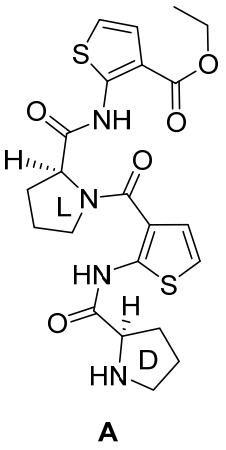

A

The analogue **A** was isolated as a yellow solid. mp: 71-74 °C; $[\alpha]^{26}_D$: -160° (*c* = 0.5, $CHCl_3$); IR ($CHCl_3$) ν (cm^{-1}): 3683, 3617, 3259, 3018, 2980, 2400, 1671, 1603, 1551, 1493, 1399, 1355, 1291, 1215, 1181, 1095, 1035, 927, 770, 668, 481; ^{1}H NMR (400 MHz, $CDCl_3$) δ: 11.59 (s, 1H), 7.26 (bs, 1H), 7.19-7.17 (d, *J* = 5.5 Hz, 1H), 6.82-6.8 (d, *J* = 5.7 Hz, 1H), 6.74-6.72 (d, *J* = 5.7 Hz, 1H), 5.29 (s, 1H), 4.95 (m, 1H), 4.31-4.26 (q, *J* = 14 Hz, 7 Hz, 2H), 3.97-3.88 (m, 2H), 3.29-3.18 (m, 2H), 2.4-2.28 (m, 2H), 2.22-1.95 (m, 4H), 1.9-1.87 (m, 2H), 1.34-1.33 (t, *J* = 7Hz, 3H); ^{13}C NMR (100 MHz, $CDCl_3$) δ: 169.6, 169.1, 166.6, 165.2, 148, 146, 123.8, 123.3, 116.3, 116, 113.5, 60.6, 60.1, 46.6, 30.1, 25.2, 14.2; ESI-MS: 491.22 $(M+H)^+$, 513.18 $(M+Na)^+$; Elemental analysis calculated for $C_{22}H_{26}N_4O_5S_2$: C, 53.86; H, 5.34; N, 11.42; S, 13.07; Found: C, 54.4; H, 5.7; N, 11.01; S, 13.8.

(S)-N-(3-(tert-butylcarbamoyl)thiophen-2-yl)-1-(2-((R)-pyrrolidine-2-carboxamido)thiophene-3-carbonyl)pyrrolidine-2-carboxamide B:

The analogue **B** was isolated as a brown solid. mp: 104-107 °C; $[\alpha]^{26}_D$: -124° (*c* = 1, $CHCl_3$); IR ($CHCl_3$) ν (cm^{-1}): 3684, 3619, 3451, 3019, 2977, 2400, 1672, 1632, 1538, 1486, 1422, 1357, 1308, 1216, 1046, 928, 771, 668, 481; ^{1}H NMR (400 MHz, $CDCl_3$) δ: 12.67 (s, 1H), 12.13 (bs, 1H), 7.42 (bs, 1H), 6.85-6.84 (d, *J* = 5.7 Hz, 1H), 6.77-6.76 (d, *J* = 5.7 Hz, 1H), 6.71-6.69 (d, *J* = 5.7 Hz, 1H), 5.75 (s, 1H),

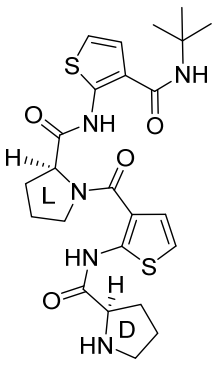

B

4.99 (bs, 1H), 4.02-3.98 (m, 1H), 3.92-3.88 (m, 2H), 3.08-2.96 (m, 2H), 2.18-2.08 (m, 4H), 2.04-1.94 (m, 2H), 1.78-1.67 (m, 2H), 1.36 (s, 9H); ^{13}C NMR (100 MHz, $CDCl_3$) δ: 173.2, 169.2, 166.7, 164.8, 146.2, 145.9, 120.5, 116.2, 116.1, 115.8, 60.4, 51.6, 47.2, 38.5, 30.7, 28.8, 28.1; ESI-MS: 518.23 $(M+H)^+$, 540.24 $(M+Na)^+$; Elemental analysis calculated for $C_{24}H_{31}N_5O_4S_2$: C, 55.69; H, 6.04; N, 13.53; S, 12.39; Found: C, 56.2; H, 6.5; N, 13.5; S, 12.5.

Methyl-3-((S)-1-(3-((S)-pyrrolidine-2-carboxamido)thiophene-2-carbonyl) pyrrolidine-2-carboxamido)thiophene-2-carboxylate C:

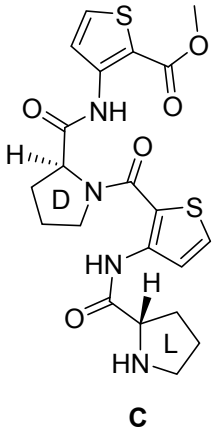

C

The analogue **C** was isolated as a white solid. mp: 93-95 °C; $[\alpha]^{26}_D$: +124° (*c* = 1, $CHCl_3$); IR ($CHCl_3$) ν (cm^{-1}): 3684, 3620, 3455, 3019, 2977, 2985, 2400, 1677, 1572, 1547, 1475, 1423, 1403, 1357, 1283, 1216, 1046, 929, 877, 849, 771, 669, 626, 477; ^{1}H NMR (400 MHz, $CDCl_3$) δ: 11.99 (s, 1H), 10.71 (s, 1H), 8.22-8.21 (d, J = 5.5 Hz, 1H), 8.12-8.1 (d, *J* = 5.2 Hz, 1H), 7.46-7.43 (t, *J* = 5.5 Hz, 2H), 4.98-4.95 (t, *J* = 5.5 Hz, 1H), 4.17-4.1 (m, 1H), 4.03-3.98 (m, 1H), 3.95-3.91 (m, 1H), 3.8 (s, 3H), 3.11-3.08 (m, 2H), 2.28-2.23 (m, 3H), 2.21-2.06 (m, 3H), 2.04-1.96 (m, 1H), 1.83-1.71 (m, 2H); ^{13}C NMR (100 MHz, $CDCl_3$) δ: 172.3, 169.3, 164.5, 163.5, 143.8, 142.5, 128.4, 125.7, 123, 122, 113.7, 113.1, 62.6, 61.1, 52.1, 49.1, 47, 30.7, 28.7, 25.8; ESI-MS: 477.14 $(M+H)^+$, 499 $(M+Na)^+$; Elemental analysis calculated for $C_{21}H_{24}N_4O_5S_2$: C, 52.93; H, 5.08; N, 11.76; S, 13.45; Found: C, 53.21; H, 5.18; N, 11.82; S, 13.6.

Methyl-3-((S)-1-(3-((R)-pyrrolidine-2-carboxamido)thiophene-2-carbonyl) pyrrolidine-2-carboxamido)thiophene-2-carboxylate D:

The analogue **D** was isolated as a white solid. mp: 80-83 °C; $[\alpha]^{26}_D$: -90° (*c* = 0.2, $CHCl_3$); IR ($CHCl_3$) ν (cm^{-1}): 3684, 3618, 3310, 3019, 2977, 2400, 1677, 1572, 1548, 1423, 1403, 1356, 1283, 1216, 1085, 1046, 928, 877, 848, 770, 669, 474; ^{1}H NMR (400 MHz, $CDCl_3$) δ: 11.98 (s, 1H), 10.71 (s, 1H), 8.2-8.19 (d, *J* = 5.5 Hz, 1H), 8.11-8.1 (d, *J* = 5.2 Hz, 1H), 7.46-7.43 (t, *J* = 5.5 Hz, 2H), 5.29 (s, 1H), 4.96-4.93 (t, *J* = 5.5 Hz, 1H), 4.15-4.11 (m, 2H), 4.03-3.97 (m, 2H), 3.81 (s, 3H), 3.14-

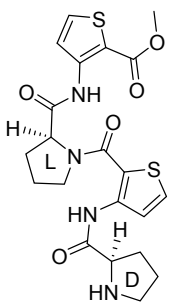

D

3.1 (m, 2H), 2.28-2.22 (m, 4H), 2.13-2.1 (m, 1H), 2.04-2 (m, 1H), 1.81-1.77 (m, 2H); ^{13}C NMR (100 MHz, $CDCl_3$) δ: 172.2, 169.3, 164.3, 144, 143.9, 131.4, 128.6, 122.2, 122.1, 112.7, 62.6, 61.1, 51.8, 49.1, 47, 30.7, 25.7, 25.8; ESI-MS: 477.17 $(M+H)^+$, 499.19 $(M+Na)^+$; Elemental analysis calculated for $C_{21}H_{24}N_4O_5S_2$: C, 52.93; H, 5.08; N, 11.76; S, 13.45; Found: C, 53.1; H, 5.92; N, 11.9; S, 13.4.

(S)-N-(2-(tert-butylcarbamoyl)thiophen-3-yl)-1-(3-((R)-pyrrolidine-2-carbox-amido)thiophene-2-carbonyl)pyrrolidine-2-carboxamide E:

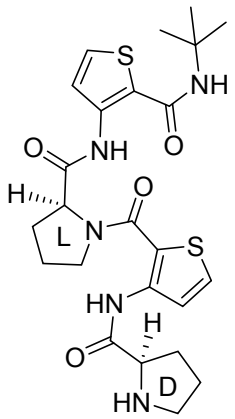

E

The analogue **E** was isolated as a white solid. mp: 102-105 °C; $[\alpha]^{26}_D$: -60° (*c* = 1, $CHCl_3$); IR ($CHCl_3$) ν (cm^{-1}): 3684, 3619, 3422, 3236, 3019, 2977, 2400, 1682, 1634, 1549, 1424, 1403, 1365, 1290, 1217, 1046, 929, 877, 849, 771, 667, 491; ^{1}H NMR (400 MHz, $CDCl_3$) δ: 12.02 (s, 1H), 11.65 (s, 1H), 8.2-8.19 (d, *J* = 5.5 Hz, 1H), 8.1-8.08 (d, *J* = 5.2 Hz, 1H), 7.43-7.42 (d, *J* = 5.2 Hz, 1H), 7.23-7.22 (d, *J* = 5.5 Hz, 1H), 5.42 (s, 1H), 4.96-4.93 (dd, *J* = 7.7 Hz, 4 Hz, 1H), 4.22-4.18 (m, 1H), 4.03-3.94 (m, 2H), 3.11-3.1 (m, 2H), 2.34-2.12 (m, 5H), 2.1-2.06 (m, 1H), 2.03-1.95 (m, 1H), 1.8-1.73 (m, 2H), 1.33 (s, 9H); ^{13}C NMR (100 MHz, $CDCl_3$) δ: 172.3, 169.3, 164.5, 163.5, 143.8, 142.5, 128.4, 125.7, 123, 122, 113.7, 113.1, 62.6, 61.1, 52.1, 49.1, 47, 30.7, 28.7, 25.8; ESI-MS: 518.22 $(M+H)^+$, 540.2 $(M+Na)^+$; Elemental analysis calculated for $C_{24}H_{31}N_5O_4S_2$: C, 55.69; H, 6.04; N, 13.53; S, 12.39; Found: C, 55.32; H, 6.7; N, 12.09; S, 13.1.

Methyl-2-(2-(((benzyloxy)carbonyl)amino)-3-methylbutanamido)-5-isopropyl thiophene-3-carboxylate 6:

Compound **5** was prepared following the reported procedure. To the solution of Cbz-valine (0.3 g, 1.4 mmol) in dry DCM, the amine **5** (0.35 g, 1.4 mmol) was added at 0 °C followed by the addition of EDC.HCl (0.32 g, 1.6 mmol) . The reation mixture was allowed to stirring for 12 h after it reached room temperature. Then, the reaction mixture was diluted with DCM and washed with sat. solutions of $NaHCO_3$, sat. brine, water and sat. $KHSO_4$ sequentially. The organic layer was

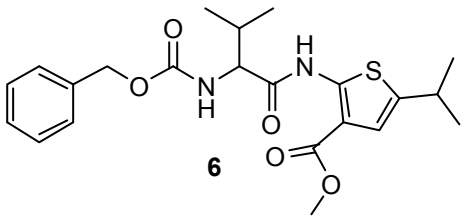

dried over Na_2SO_4 and was evaporated under reduced pressure, The residue obtained was purified through column chromatography (eluent: pet ether/ethyl acetate: 70:30, R*f*: 0.5) which yielded the dipeptide **6** (0.3 g, 50%). mp: 73-75 °C; $[\alpha]^{26}_D$: -22° (*c* = 1, $CHCl_3$); IR ($CHCl_3$) ν (cm^{-1}): 3685, 3617, 3434, 3285, 3020, 2969, 2401, 1716, 1673, 1563, 1532, 1455, 1392, 1309, 1219, 1093, 1045, 929, 877, 848, 771, 667, 626, 505; ^{1}H NMR (200 MHz, $CDCl_3$) δ: 11.3 (s, 1H), 7.36 (bs, 5H), 6.87 (s, 1H), 5.66-5.63 (m, 1H), 5.15 (s, 2H), 4.4-4.33 (m, 1H), 3.84 (s, 3H), 3.14-2.94 (sep, 1H), 2.41-2.25 (sex, 1H), 1.32-1.28 (d, *J* = 6.9 Hz, 6H), 1.04-1.01 (d, *J* = 6.8 Hz, 3H), 0.97-0.94 (d, *J* = 6.8 Hz, 3H); ^{13}C NMR (50 MHz, $CDCl_3$) δ: 168.4, 165.6, 156.3, 145.6, 142.9, 136, 128.3, 127.9, 117.6, 112.3, 67.1, 60.4, 51.5, 30.7, 29.3, 24.2, 19, 17.4; HRMS: $C_{22}H_{29}O_5N_2S$, Calcd: 433.1792 Found: 433.1791; $C_{22}H_{29}O_5N_2NaS$, Calcd: 455.1611 Found: 455.1606.

Methyl 2-(2-(dimethylamino)-3-methylbutanamido)-5-isopropylthiophene-3-carboxylate 7:

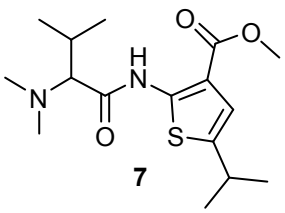

Compound **6** (0.18 g, 0.49 mmol) was taken in HBr. AcOH (2 mL) and stirred at room temperature for 30 min. Later, dry ether was added to the reaction mixture, that yielded a white precipitate. This precipitate was kept over KOH in dessicator overnight. To the precipitate taken in MeOH, Et_3N (0.34 mL, 0.24 mmol) was added followed by the addition of HCHO (3 mL) and $NaBH_3CN$ (0.15 g, 0.24 mmol). The reaction mixture was allowed to stir for 6 h. The MeOH was eveporated, the residue obtained was taken into DCM and washed with water and the organic layer was dried over Na_2SO_4 and evaporated under reduced pressure. The residue obtained was purified through column chromatography (eluent: pet ether/ethyl acetate: 80:20, R*f*: 0.5) giving compound **7** (0.14 g, 90%) as a sticky substance. $[\alpha]^{26}_D$: -42.42° (*c* = 1, $CHCl_3$); IR ($CHCl_3$) ν (cm^{-1}): 3683, 3619, 3283, 3020, 2967, 2875, 2400, 1673, 1557, 1529, 1450, 1386, 1350, 1308, 1217, 1160, 1114, 1035, 929, 880, 847, 756, 667, 626, 589, 469; ^{1}H NMR (400 MHz, $CDCl_3$) δ: 11.33 (s, 1H), 6.87 (s, 1H), 3.85 (s, 3H), 3.08-3 (sep, 1H), 2.73-

2.72 (d, *J* = 6.2 Hz, 1H), 2.35 (s, 6H), 2.23-2.14 (sex, 1H), 1.3-1.28 (d, *J* = 6.7 Hz, 3H), 1.04-1.02 (d, *J* = 6.7 Hz, 3H), 0.94-0.92 (d, *J* = 6.5 Hz, 3H); ^{13}C NMR (50 MHz, $CDCl_3$) δ: 168.8, 165.5, 145.7, 142.5, 117.6, 111.8, 75.9, 51.4, 42.7, 29.4, 27.7, 24.2, 20, 17.6; HRMS: $C_{16}H_{27}O_3N_2S$, Calcd: 327.1737 Found: 327.1737; $C_{22}H_{29}O_5N_2NaS$, Calcd: 349.1556 Found: 349.1550.

tert-butyl-(2S, 4R)-2-(benzhydrylcarbamoyl)-4-((tert-butyldimethylsilyl)oxy) pyrrolidine-1-carboxylate 12a:

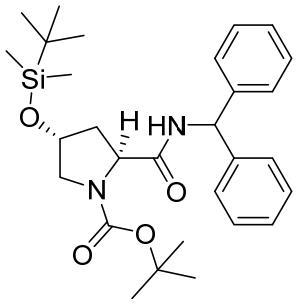

12a

To the solution of **11a** (0.3 g, 0.86 mmol) in dry DCM, benzhydryl amine (0.15 mL, 0.86 mmol) was added followed by the addition of Et_3N (0.24 mL, 1.7 mmol), EDC.HCl (0.19 g, 1.04 mmol) and HOBt (0.02 g, 0.17 mmol) at 0 °C. The reaction mixture was allowed for stirring for 12 h. Later, the reaction mixture was diluted with DCM and washed with sat. $NaHCO_3$, brine, water and sat. $KHSO_4$ solutions sequentially. The organic layer was dried over Na_2SO_4 and was evaporated under reduced pressure, The residue obtained was purified through column chromatography (eluent: pet ether/ethyl acetate: 80:20, R*f*: 0.4) which yielded the compound **12a** (0.31 g, 70%) as pasty mass; $[\alpha]^{26}_D$: +4° (*c* = 1, $CHCl_3$); IR ($CHCl_3$) ν (cm^{-1}): 3683, 3615, 3545, 3319, 2974, 2400, 1523, 1422, 1318, 1215, 1045, 928, 877, 849, 756, 669, 626, 469; ^{1}H NMR (200 MHz, $CDCl_3$) δ: 7.98 (bs, 1H), 7.27 (m, 10H), 6.21 (bs, 1H), 4.47 (bs, 2H), 3.45-3.37 (dd, *J* = 10.9 Hz, 4.9 Hz, 1H), 3.35-3.25 (bs, 1H), 1.64 (s, 2H), $1.47_{rotamer}$(6H), $1.34_{rotamer}$ (3H), 0.87 (s, 9H), 0.07 (s, 6H); HRMS: $C_{29}H_{43}O_4N_2Si$, Calcd: 511.2987, Found: 511.2987.

tert-butyl-(2S,4R)-2-(tert-butylcarbamoyl)-4-((tert-butyldimethylsilyl)oxy) pyrrolidine-1-carboxylate 12b:

To the solution of **11a** (0.2 g, 0.57 mmol) in dry DCM, tert. butyl amine (0.18 mL, 1.7 mmol) was added, followed by the addition of Et_3N (0.08 mL, 0.86 mmol) and EDC.HCl (0.13 g, 0.69 mmol) 0 °C. The reaction mixture was allowed for stirring for 12 h. Later, the reaction mixture was diluted with DCM and washed with sat. $NaHCO_3$, brine, water and sat. $KHSO_4$ solutions sequentially. The organic layer was dried over Na_2SO_4 and was evaporated under reduced pressure, The residue

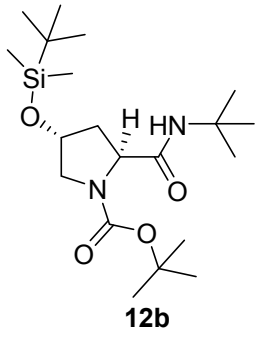

12b

obtained was purified through column chromatography (eluent: pet ether/ethyl acetate: 90:10, R*f*: 0.5) which yielded the compound **12b** (0.17 g, 75%) as pasty mass; $[\alpha]^{26}_{D}$: -70° (*c* = 1, $CHCl_3$); IR ($CHCl_3$) ν (cm^{-1}): 3684, 3625, 3413, 3019, 2931, 2858, 2400, 1679, 1518, 1473, 1393, 1367, 1215, 1162, 1117, 1094, 1025, 928, 837, 770, 669, 626, 487; ^{1}H NMR (400 MHz, $CDCl_3$) δ: $6.9_{rotamer}$ (0.5H), $5.83_{rotamer}$ (0.5H), 4.4-4.21 (m, 2H), $3.58_{rotamer}$ (0.5H), 3.42-3.38 (dd, J = 4.5 Hz, 11.2 Hz, 1H), $3.31_{rotamer}$ (0.5H), $2.2_{rotamer}$ (0.5H), 2.12 (bs, 1H), $1.99_{rotamer}$ (0.5H), $1.88_{rotamer}$ (0.5H), 1.46 (s, 9H), 1.33 (bs, 9H), 0.85 (s, 9H), 0.06-0.05 (bs, 6H); ^{13}C NMR (100 MHz, $CDCl_3$) δ: 80.4, 70.4, 69.8, 60.7, 59.2, 55.2, 54.8, 50.8, 40.2, 36.4, 28.6, 28.2, 25.6, 17.8,-4.9; HRMS: $C_{20}H_{41}O_4N_2Si$, Calcd: 401.283, Found: 401.283.

tert-butyl-(2S, 4R)-2-(benzhydrylcarbamoyl)-4-(benzyloxy)pyrrolidine-1-carboxylate 14a:

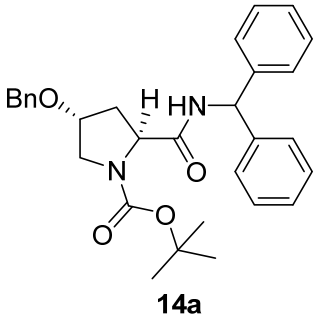

14a

To the solution of **13a** (0.24 g, 0.76 mmol) in dry DCM, benzhydryl amine (0.13 mL, 0.76 mmol) was added followed by the addition of Et_3N (0.24 mL, 1.7 mmol), EDC.HCl (0.21 g, 1.04 mmol) and HOBt (0.02 g, 0.15 mmol) at 0 °C. The reaction mixture was allowed for stirring for 12 h. Later, the reaction mixture was diluted with DCM and washed with sat. $NaHCO_3$, brine, water and sat. $KHSO_4$ solutions sequentially. The organic layer was dried over Na_2SO_4 and was evaporated under reduced pressure, The residue obtained was purified through column chromatography (eluent: pet ether/ethyl acetate: 70:30, R*f*: 0.4) which yielded the compound **14a** (0.22 g, 60%) as pasty substance; $[\alpha]^{26}_{D}$: -120° (*c* = 1, $CHCl_3$); IR ($CHCl_3$) ν (cm^{-1}): 3683, 3615, 3545, 3319, 2974, 2400, 1523, 1422, 1318, 1215, 1045, 928, 877, 849, 756, 669, 626, 469; ^{1}H NMR (400 MHz, $CDCl_3$) δ: 7.93 (bs, 1H), 7.35-7.24 (m, 15H), 6.18 (s, 1H), 4.5-4.49 (m, 3H), $4.25_{rotamer}$ (0.5H), $4.14_{rotamer}$ (0.5H), 3.46-3.45 (m, 2H), 2.62-2.43 (m, 1H), $2.22_{rotamer}$ (0.6H), $2.03_{rotamer}$ (0.4H), $1.45_{rotamer}$ (6H), $1.31_{rotamer}$ (3H); ^{13}C NMR (50 MHz, $CDCl_3$) δ: 171.2, 170.2, 156, 155.1, 141.7, 141.5, 141.3, 137.8, 128.5, 128.4, 127.7, 127.5,

127.3, 127, 80.7, 71.3, 60.1, 58.5, 56.9, 51.6, 36.9, 33.1, 28.2; HRMS: $C_{30}H_{35}O_4N_2$, Calcd: 487.2591, Found: 487.2589.

tert-butyl-(2S, 4R)-4-(benzyloxy)-2-(tert-butylcarbamoyl)pyrrolidine-1-carboxylate 14b:

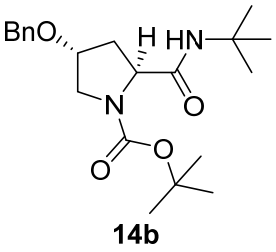

14b

To the solution of **13a** (0.26 g, 0.81 mmol) in dry DCM, tert.butyl amine (0.42 mL, 4 mmol) was added followed by the addition of Et_3N (0.24 mL, 1.7 mmol), EDC.HCl (0.18 g, 0.97 mmol) and HOBt (0.02 g, 0.16 mmol) at 0 °C. The reaction mixture was allowed for stirring for 12 h. Later, the reaction mixture was diluted with DCM and washed with sat. $NaHCO_3$, brine, water and sat. $KHSO_4$ solutions sequentially. The organic layer was dried over Na_2SO_4 and was evaporated under reduced pressure, The residue obtained was purified through column chromatography (eluent: pet ether/ethyl acetate: 70:30, R*f*: 0.5) which yielded the compound **14b** (0.18 g, 60%) as pasty mass; $[\alpha]^{26}_D$: -300° (*c* = 1, $CHCl_3$); IR ($CHCl_3$) ν (cm^{-1}): 3682, 3621, 3415, 3334, 3018, 2978, 2401, 1681, 1516, 1477, 1455, 1367, 1217, 1163, 1117, 929, 852, 770, 698, 667, 626, 495; ^{1}H NMR (500 MHz, $CDCl_3$) δ: 7.36-7.29 (m, 5H), $6.83_{rotamer}$ (0.5H), $5.75_{rotamer}$ (0.5H), 4.51 (s, 2H), 4.32-4.14 (m, 2H), $3.85_{rotamer}$ (0.5H), 3.49-$3.46_{rotamer}$ (1.5H), 2.58 (0.5H), $2.41_{rotamer}$ (0.5H), $2.12_{rotamer}$ (0.5H), $2.03_{rotamer}$ (0.5H), $1.61_{rotamer}$ (1H), 1.48 (s, 9H), $1.34_{rotamer}$ (8H); ^{13}C NMR (125 MHz, $CDCl_3$) δ: 128.4, 127.6, 80.5, 71.3, 71, 60.4, 58.2, 51.7, 50.9, 37, 33.3, 28.3; HRMS: $C_{21}H_{33}O_4N_2$, Calcd: 377.2435, Found: 377.2429.

General method for the synthesis of the analogues F-I:

The analogues **F-I** have been synthesized using the routine coupling protocol. To the solution of acid **7a**, the amines **12c**, **12d**, **14c** and **14d** were added respectively in four different RB flasks seperately, at 0 °C followed by the addition of EDC.HCl, Et_3N and HOBt. The reaction mixtures were allowed for stirring for 12 h. Later, the reaction mixtures were diluted with DCM and washed with water and then the organic layer was dried over Na_2SO_4. The residues obtained after evaporation of the organics were purified through column chromatography which yielded the respective products **F**, **G**, **H** and **I** (50% yield in each case respectively).

(2R,4S)-N-benzhydryl-4-((tert-butyldimethylsilyl)oxy)-1-(2-(2-(dimethyl-amino)-3-methylbutanamido)-5-isopropylthiophene-3-carbonyl)pyrrolidine-2-carbox-amide F:

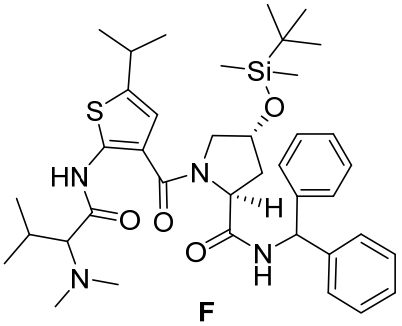

F

The analogue **F** was isolated as a sticky substance; $[\alpha]^{26}_{D}$: -68° (*c* = 1, $CHCl_3$); IR ($CHCl_3$) ν (cm^{-1}): 3684, 3622, 3424, 3020, 2976, 2400, 1602, 1521, 1475, 1423, 1218, 1046, 928, 877, 771, 668, 626; ^{1}H NMR (400 MHz, $CDCl_3$) δ: 11.55 (s, 1H), 7.77 (s, 1H), 7.32-7.21 (m, 10H), 6.67 (s, 1H), 6.18 (s, 1H), 5.05-5.01 (s, 1H), 4.48 (s, 1H), 3.77-3.75 (dd, *J* = 10.5 Hz, 3.5 Hz, 2H), 3.74-3.66 (d, *J* = 10.7 Hz, 2H), 3.13-3.07 (m, 1H), 3-2.95 (m, 1H), 2.8 (bs, 1H), 2.51-2.47 (m, 2H), 2.41 (s, 6H), 2.23-2.18 (m, 2H), 2.10-2.02 (m, 2H), 1.34-1.32 (d, *J* = 6.5 Hz, 6H), 1.09-1.07 (d, *J* = 6.7 Hz, 3H), 0.95-0.93 (d, *J* = 6.5 Hz, 3H), 0.87 (s, 6H), 0.79 (s, 9H), -0.04 (bs, 6H); ^{13}C NMR (100 MHz, $CDCl_3$) δ: 169.9, 168.1, 141.6, 141.4, 128.6, 128.5, 127.4, 126.9, 117.4, 74.1, 70.9, 58.9, 57.4, 42.2, 36, 29.6, 27.7, 25.7, 25.5, 24.3, 19.9, 18.4, 17.7, -4.8, -5; HRMS: $C_{21}H_{33}O_4N_2SSi$, Calcd: 705.3864, Found: 705.3864; $C_{21}H_{33}O_4N_2SSiNa$, Calcd: 727.3684, Found: 705.3662.

(2S,4R)-N-(tert-butyl)-4-((tert-butyldimethylsilyl)oxy)-1-(2-(2-(dimethyl amino)-3-methylbutanamido)-5-isopropylthiophene-3-carbonyl)pyrrolidine-2-carbox-amide G:

The analogue **G** was isolated as a pasty mass; $[\alpha]^{26}_{D}$: -66.66° (*c* = 1, $CHCl_3$); IR

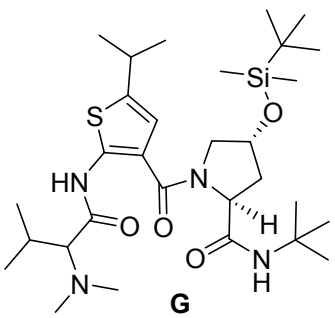

G

($CHCl_3$) ν (cm^{-1}): 3684, 3618, 3426, 3312, 3019, 2967, 2932, 2787, 2400, 1669, 1555, 1519, 1463, 1403, 1366, 1256, 1215, 1096, 1031, 928, 878, 837, 767, 668, 626; ^{1}H NMR (400 MHz, $CDCl_3$) δ: 11.47 (s, 1H), 6.77 (s, 1H), 6.68 (s, 1H), 4.77-4.74 (t, *J* = 7 Hz, 1H), 4.47 (bs, 1H), 3.79-3.76 (d, *J* = 13 Hz, 1H), 3.65-3.63 (d, *J* = 10.2 Hz, 1H), 3.1-3.03 (quin, *J* = 13.5 Hz, 6.5 Hz, 1H), 2.71-2.69 (d, *J* = 7.7 Hz, 1H), 2.33 (s, 6H), 2.2-2.13 (m, 2H), 2-1.97 (m, 1H), 1.32-1.29 (m, 15H), 1.03-1.01 (d, *J* = 6.7 Hz, 3H), 0.93-0.91 (d, *J* = 6.7 Hz, 3H), 0.78 (s, 9H), -0.04 (s, 6H); ^{13}C NMR (100 MHz, $CDCl_3$) δ: 170.1, 168.6, 167.6,

143.7, 142.2, 128.9, 125.2, 120.2, 117.4, 114.7, 109.2, 75.9, 70.8, 60.3, 59.3, 58.7, 51.1, 42.3, 36.6, 36.4, 29.5, 28.5, 27.6, 25.5, 24.3, 19.8, 18.3, -4.8, -5; HRMS: $C_{30}H_{55}O_4N_4SSi$, Calcd: 595.3708, Found: 595.3708.

(2S,4R)-N-benzhydryl-4-(benzyloxy)-1-(2-(2-(dimethylamino)-3-methyl butanamido)-5-isopropylthiophene-3-carbonyl)pyrrolidine-2-carboxamide H:

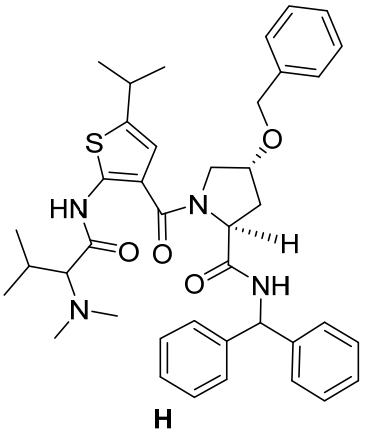

H

The analogue **H** was isolated as a sticky substance; $[\alpha]^{26}_D$: -75° (*c* = 1, $CHCl_3$); IR ($CHCl_3$) ν (cm^{-1}): 3684, 3625, 3428, 3019, 2975, 2400, 1673, 1519, 1423, 1216, 1046, 928, 877, 771, 669, 626; ^{1}H NMR (500 MHz, $CDCl_3$) δ: 11.51 (s, 1H), 7.68 (s, 1H), 7.26-7.15 (m, 11H), 7.11 (s, 4H), 6.55 (s, 1H), 6.09-6.07 (d, *J* = 7.9 Hz, 1H), 4.97-4.94 (t, *J* = 7.6 Hz, 1H), 4.47-4.45 (d, *J* = 11.9 Hz, 1H), 4.33-4.31 (d, *J* = 11.9 Hz, 1H), 4.19 (bs, 1H), 3.81-3.79 (d, *J* = 10.9 Hz, 1H), 3.69-3.66 (dd, *J* = 3.6 Hz, 10.9 Hz, 1H), 3.01-2.96 (m, 1H), 2.62-2.6 (d, J = 7.6 Hz, 1H), 2.53-2.49 (m, 1H), 2.24 (s, 6H), 2.21-2.17 (m, 1H), 2.14-2.07 (m, 1H), 1.24-1.23 (d, *J* = 6.7 Hz, 6H), 0.97-0.95 (d, *J* = 6.7 Hz, 3H), 0.87-0.86 (d, *J* = 6.7 Hz, 3H); ^{13}C NMR (125 MHz, $CDCl_3$) δ: 169.9, 168.1, 141.6, 141.4, 128.6, 128.5, 127.4, 126.9, 117.4, 74.1, 70.9, 58.9, 57.4, 42.2, 36, 29.6, 27.7, 25.7, 25.5, 24.3, 19.9, 18.4, 17.7, -4.8, -5; HRMS: $C_{40}H_{49}O_4N_2S$, Calcd: 681.3469, Found: 681.346.

(2S,4R)-4-(benzyloxy)-N-(tert-butyl)-1-(2-(2-(dimethylamino)-3-methyl butanamido)-5-isopropylthiophene-3-carbonyl)pyrrolidine-2-carboxamide I:

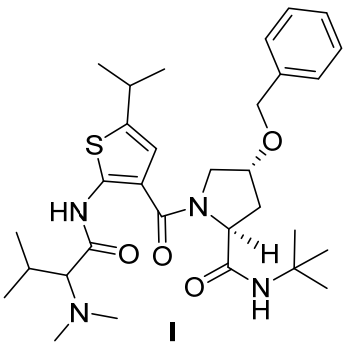

I

The analogue **I** was isolated as a pasty substance; $[\alpha]^{26}_D$: -73.33° (*c* = 1, $CHCl_3$); IR($CHCl_3$) ν (cm^{-1}): 3684, 3622, 3425, 3028, 2976, 2400, 1669, 1519, 1476, 1423, 1219, 1046, 928, 877, 850, 771, 667, 627, 511; ^{1}H NMR (500 MHz, $CDCl_3$) δ: 11.5 (s, 1H), 7.21-7.17 (m, 5H), 6.67 (bs, 1H), 6.59 (s, 1H), 4.7 (bs, 1H), 4.47-4.45 (d, *J* = 11.9 Hz, 1H), 4.35-4.32 (d, *J* = 11.9 Hz, 1H), 4.22 (bs, 1H), 3.75-3.72 (m, 2H), 3-2.95 (quin, *J* = 13.4 Hz, 6.7 Hz, 1H), 2.65 (d, *J* = 7.6 Hz, 1H), 2.39 (bs,

1H), 2.26 (s, 6H), 2.14-2.07 (m, 2H), 1.25-1.22 (m, 15H), 0.96-0.95 (d, *J* = 6.7 Hz, 3H), 0.67-0.66 (d, J = 6.7 Hz, 3H); ^{13}C NMR (125 MHz, $CDCl_3$) δ: 169.9, 168.5, 167.2, 144.4, 142.1, 137.6, 128.3, 127.7, 127.4, 117.2, 114.4, 77.6, 75.9, 71.1, 59.6, 55.3, 51.1, 42.3, 32.8, 29.5, 28.5, 27.5, 24.4, 24.3, 19.7, 18.3; HRMS: $C_{30}H_{55}O_4N_4SSi$, Calcd: 571.3313, Found: 571.3312.

.

3.17 Experimental Section (Section B)

Benzyl-(1-((1-(tert-butylamino)-1-oxo-3-phenylpropan-2-yl)amino)-3-methyl-1-oxobutan-2-yl)carbamate 16:

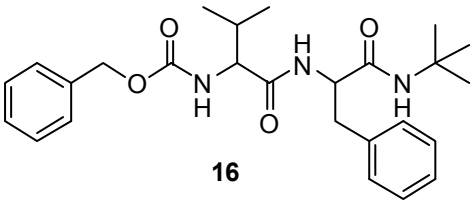

16

The dipeptide **15** was synthesized according to the reported procedure which was subjected to hydrolysis to give the corresponding acid **15a**. To the acid **15a** (0.09 g, 0.24 mmol) in CH_3CN, tert. butyl amine (0.12 mL, 1.21 mmol) was added at 0 °C followed by the addition of Et_3N (0.06 mL, 0.48 mmol), and EDC.HCl (0.05 g, 0.29mmol). The reaction mixture was stirred for 12 h at room temperature. Then, the solvent was removed under reduced pressure and extracted with DCM which was washed with sat. $NaHCO_3$, brine and sat. $KHSO_4$ solutions in a sequence. The residue obtained was purified by column chromatography (eluent: pet ether/ethyl acetate: 70:30, R*f*: 0.3) which yielded the compound **16** (0.04 g, 40% over two steps) as white solid; mp: 153-156 °C; $[\alpha]^{26}_D$: -20° (*c* = 1, $CHCl_3$); IR ($CHCl_3$) ν (cm^{-1}): 3420, 3019, 2400, 1661, 1517, 1422, 1216, 1045, 928, 771, 668, 468; ^{1}H NMR (400 MHz, $CDCl_3$) δ: 7.36 (bs, 5H), 7.31-7.28 (m, 2H), 7.25-7.21 (m, 3H), 6.67-6.65 (d, *J* = 7.7 Hz, 1H), 5.37 (bs, 1H), 5.31-5.29 (d, *J* = 7.7 Hz, 1H), 5.13-5.06 (m, 2H), 4.5-4.45 (q, *J* = 13.8 Hz, 7.5 Hz, 1H), 4.05-4.01 (t, *J* = 7 Hz, 1H), 3.12-3.07 (dd, *J* = 13 Hz, 5.7 Hz, 1H), 2.96-2.91 (dd, *J* = 12.8 Hz, 8.5 Hz, 1H), 2.17-2.09 (sex, *J* = 12.5 Hz, 6Hz, 1H), 1.19 (s, 9H), 0.94-0.92 (d, *J* = 6.7 Hz, 3H), 0.85-0.83 (d, *J* = 6.7 Hz, 3H); ^{13}C NMR (100 MHz, $CDCl_3$) δ: 170.8, 169.1, 156.3, 136.6, 136.1, 129.3, 128.8, 128.5, 128.2, 127, 67.1, 60.4, 54.9. 51.3, 38.6, 30.9, 28.4, 19.1, 17.4; HRMS: $C_{26}H_{36}O_4N_3$, Calcd: 454.27, Found: 455.27; $C_{26}H_{35}O_4N_3Na$, Calcd: 476.252, Found: 476.2515.

General method for the preparation of dipeptides 17 and 18:

To a solution of Cbz-valine in dry DCM, the hydrochloride salts of tryptophan methyl ester and tyrosine methyl ester were added respectively followed by the addition of Et_3N, EDC.HCl and HOBt. The reaction mixtures were stirred at room temperature for 12 h. Later, the reaction mixtures were diluted with DCM and washed with sat. $NaHCO_3$, brine and sat. $KHSO_4$ solutions

simultaneously in all the cases and the organic layers were dried over Na_2SO_4. The solvent was removed under reduced pressure. The residues obtained were purified by column chromatography which yielded the corresponding compounds **17** and **18** (50% in each case).

Methyl ((benzyloxy)carbonyl)valyltryptophanate 17:

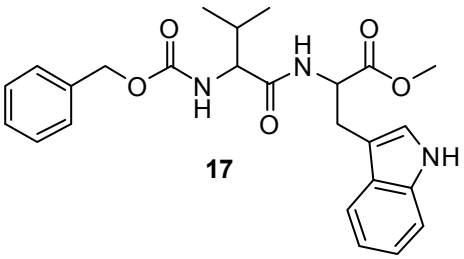

17

The dipeptide **17** was isolated as yellow crystalline solid; mp: 104-106 °C; $[\alpha]^{26}_D$: +54° (*c* = 1, $CHCl_3$); IR ($CHCl_3$) ν (cm^{-1}): 3685, 3617, 3478, 3426, 3019, 2974, 2400, 1715, 1673, 1514, 1440, 1371, 1217, 1093, 1045, 929, 771, 668, 626; ^1H NMR (400 MHz, $CDCl_3$) δ: 8.12 (bs, 1H), 7.52-7.5 (d, *J* = 8 Hz, 1H), 7.34-7.31 (m, 6H), 7.19-7.15 (m, 1H), 7.11-7.08 (m, 1H), 6.94-6.92 (m, 1H), 8.56 (bs, 1H), 5.41 (bs, 1H), 5.15-5.02 (m, 1H), 4.99-4.91 (m, 1H), 4.11 (bs, 1H), 3.68-3.67 (m, 3H), 3.31-3.28 (m, 2H), 2.09-2.03 (sextet, 1H), 1.68 (bs, 1H), 0.94-0.92 (d, *J* = 6.5 Hz, 3H), 0.88-0.86 (d, *J* = 6.5 Hz, 3H); ^{13}C NMR (100 MHz, $CDCl_3$) δ: 171.9, 171, 156.3, 136, 128.5, 128, 123.1, 122.1, 119.6, 118.3, 111.2, 109.4, 66.9, 60, 52.6, 52.3, 31.3, 27.5, 19, 17.5; HRMS: $C_{25}H_{30}O_5N_3$, Calcd: 452.218, Found: 452.218.

Methyl ((benzyloxy)carbonyl)valyltyrosinate 18:

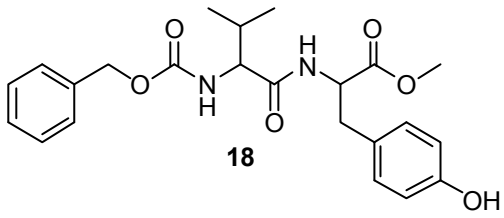

18

The dipeptide **18** was isolated as white solid; mp: 143-145 °C; $[\alpha]^{26}_D$: +38° (*c* = 1, $CHCl_3$); IR ($CHCl_3$) ν (cm^{-1}): 3684, 3618, 3424, 3019, 2400, 1717, 1672, 1614, 1516, 1423, 1217, 1045, 928, 771, 669, 626, 492; ^1H NMR (200 MHz, $CDCl_3$) δ: 7.34 (bs, 5H), 7.12 (bs, 1H), 6.93-6.88 (m, 2H), 6.77-6.67 (m, 3H), 5.56-5.52 (d, *J* = 9 Hz, 1H), 5.15-4.97 (q, 2H), 4.92-4.82 (m, 1H), 4.19-4.05 (m, 1H), 3.71 (s, 3H), 3.03-3 (m, 2H), 2.13-1.96 (m, 1H), 0.94-0.86 (t, *J* = 7.2 Hz, 6H); ^{13}C NMR (50 MHz, $CDCl_3$) δ: 171.7, 171.3, 156.5, 155.4, 136, 130, 128.5, 128.1, 127.9, 126.7, 115.5, 67.1, 60.1, 53.3, 52.3, 37, 31.1, 19, 17.7; HRMS: $C_{23}H_{29}O_6N_2$, Calcd: 429.2020, Found: 429.2019.

Methyl-((S)-2-(((benzyloxy)carbonyl)amino)-3,3-dimethylbutanoyl)phenyl alaninate 19:

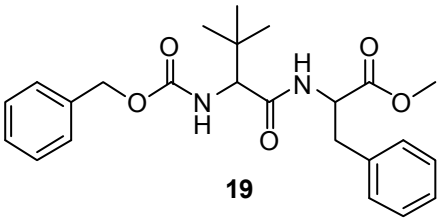

19

Cbz-tert.Leucine (0.2 g, 0.75 mmol) was prepared following the reported protocol. To the solution of Cbz-tert. Leucine in dry DCM, hydrochloride salt of phenyl alanine methyl ester (0.16 g, .075 mmol) was added followed by the addition of Et3N (0.31 mL, 0.15 mmol), EDC.HCl (0.17 g, 0.9 mmol) and HOBt (0.02 g, 0.01 mmol) at 0 °C and it was allowed to stir for 12 h. The reaction mixture was diluted with DCM and washed sequentially with sat. $NaHCO_3$, brine and sat. $KHSO_4$ solutions. Then, the organic layer was dried over Na_2SO_4 and evaporated under vacuum. The residue thus obtained is subjected to column chromatographic purification which yielded **19** (0.16 g, 50%) as a pasty substance; $[\alpha]^{26}_D$: -52.3° (*c* = 1, $CHCl_3$); IR ($CHCl_3$) ν (cm^{-1}): 3682, 3620, 3430, 3019, 2971, 2400, 1718, 1676, 1508, 1439, 1369, 1218, 1111, 1051, 928, 772, 668, 626, 505, 491; ^{1}H NMR (500 MHz, $CDCl_3$) δ: 7.37-7.36 (d, *J* = 4.5 Hz, 5H), 7.35-7.29 (m, 2H), 7.26-7.19 (m, 3H), 7.1-7.09 (d, *J* = 7 Hz, 2H), 6.54-6.52 (d, *J* = 7.6 Hz, 1H), 5.61-5.59 (d, *J* = 9.4 Hz, 1H), 5.13-5.11 (d, *J* = 12 Hz, 1H), 5.05-5.03 (d, *J* = 12.2 Hz, 1H), 3.7 (s, 3H), 3.1-3.08 (t, *J* = 6.4 Hz, 2H), 0.98 (s, 6H); ^{13}C NMR (125 MHz, $CDCl_3$) δ: 171.6, 170.2, 156.2, 136.2, 135.4, 129.1, 128.5, 128, 127.9, 127.1, 126.6, 66.8, 62.5, 53, 52.1, 37.8, 34.6; HRMS: $C_{24}H_{31}O_5N_2$, Calcd: 427.2227, Found: 427.2227.

General method for N, N dimethylation of 15, 16, 17, 18, 19 and 22:

To the dipeptide compounds **15**, **16**, **17**, **18**, **19** and **22** in MeOH (5 mmol), 10% Pd/C and HCHO (3 mL) were added and were subjected to shaking under H_2 pressure at 60 psi for 3days. Later, the catalyst was removed by filtration through celite. The solvent was evaporated under vacuum. The residues obtained were taken into ethyl acetate and washed with water. The organic layers were dried over Na_2SO_4 and then evaporated, the residues obtained were purified by column chromagraphy which yielded the required analogues **J**, **Q**, **M**, **N**, **O** (30% overall yield) respectively.

Methyl dimethylvalylphenylalaninate J:

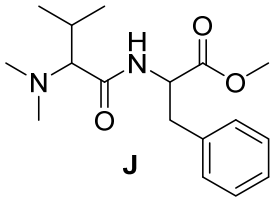

J

The analogue **J** was isolated as a white solid; mp: 104-106 °C; $[\alpha]^{26}_{D}$: +1.33° (*c* = 1, $CHCl_3$); IR ($CHCl_3$) ν (cm^{-1}): 3684, 3423, 3430, 3020, 2975, 2400, 1742, 1669, 1505, 1438, 1218, 1046, 929, 771, 668, 513; ^{1}H NMR (200 MHz, $CDCl_3$) δ: 7.31-7.13 (m, 5H), 6.73-6.69 (m, 1H), 4.98-4.87 (m, 1H), 3.69 (s, 3H), 3.23-3.13 (dd, *J* = 14 Hz, 5.4 Hz, 1H), 3.04-2.92 (dd, *J* = 14 Hz, 8.3 Hz, 1H), 2.4-2.37 (d, *J* = 6.8 Hz, 3H), 2.18 (s, 6H), 2.05-1.84 (m, 1H), 0.87-0.84 (d, *J* = 6.8 Hz, 3H), 0.65-0.62 (d, *J* = 6.6 Hz, 3H); ^{13}C NMR (50 MHz, $CDCl_3$) δ: 172.2, 171.3, 136, 128.9, 128.4, 126.9, 75.8, 52.4, 52, 42.7, 38, 27.3, 19.8, 17; HRMS: $C_{17}H_{27}O_3N_2$, Calcd: 307.2016, Found: 307.2016; $C_{17}H_{26}O_3N_2Na$, Calcd: 329.1836, Found: 329.1829.

N-(1-(tert-butylamino)-1-oxo-3-phenylpropan-2-yl)-2-(dimethylamino)-3-methylbutanamide Q:

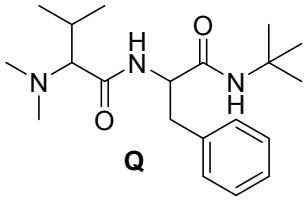

Q

The analogue **Q** was isolated as a white solid; mp: 155-157 °C; $[\alpha]^{26}_{D}$: -85.71° (*c* = 1, $CHCl_3$); IR ($CHCl_3$) ν (cm^{-1}): 3684, 3620, 3019, 2976, 2400, 1658, 1602, 1521, 1477, 1423, 1215, 1046, 928, 877, 849, 764, 669, 626, 472; ^{1}H NMR (500 MHz, $CDCl_3$) δ: 7.31-7.21 (m, 5H), 5.7 (bs, 1H), 4.57-4.52 (q, *J* = 7.9 Hz, 1H), 3.06-3.05 (d, *J* = 7.6 Hz, 2H), 2.2 (s, 6H), 2.07-2 (sext, *J* = 13.1 Hz, 6.4 Hz, 1H), 1.23 (s, 9H), 0.94-0.93 (d, *J* = 6.7 Hz, 3H), 0.72-0.71 (d, *J* = 6.4 Hz, 3H); ^{13}C NMR (125 MHz, $CDCl_3$) δ: 169.6, 137.1, 129.3, 128.6, 126.8, 54.8, 51.2, 42.5, 38.1, 28.4, 27.4, 19.9, 17.4; HRMS: $C_{20}H_{34}O_2N_3$, Calcd: 348.2646, Found: 348.2648.

Methyl dimethylvalyltryptophanate M:

The analogue **M** was isolated as a pasty mass; $[\alpha]^{26}_{D}$: +8° (*c* = 1, $CHCl_3$); IR ($CHCl_3$) ν (cm^{-1}): 3477, 3354, 3018, 2970, 2876, 2832, 2788, 2400, 1740, 1667, 1505, 1439, 1370, 1215, 1095, 1047, 928, 909, 769, 668, 504; ^{1}H NMR (500 MHz, $CDCl_3$) δ: 8.57 (bs, 1H), 7.59-7.58 (d, *J* = 7.9 Hz, 1H), 7.36-7.34 (d, *J* = 8.2 Hz, 1H), 7.2-7.17 (t, *J* = 7 Hz, 1H), 7.13-7.1 (t, *J* = 7 Hz, 1H), 7.04-7.03 (bs, 1H),

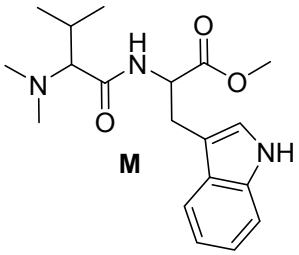

M

6.86-6.85 (d, *J* = 7.9 Hz, 1H), 5-4.96 (dd, *J* = 7.3 Hz, 13.7 Hz, 1H), 3.68 (s, 3H), 3.3-3.28 (dd, *J* = 5.4 Hz, 3.3 Hz, 2H) 2.47-2.46 (d, *J* = 6.4 Hz, 1H), 2.21 (s, 6H), 2.01-1.97 (m, 1H), 0.91-0.9 (d, *J* = 6.7 Hz, 3H), 0.71-0.7 (d, *J* = 6.7 Hz, 3H); ^{13}C NMR (125 MHz, $CDCl_3$) δ: 172.6, 171.3, 136.1, 127.3, 122.7, 122, 119.4, 111.2, 110, 75.6, 52.1, 42.5, 27.9, 27.5, 19.9, 17.3; HRMS: $C_{19}H_{28}O_3N_3$, Calcd: 346.2125, Found: 346.2126.

Methyl dimethylvalyltyrosinate N:

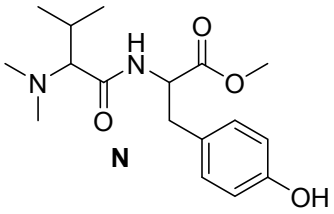

N

The analogue **N** was isolated as a pasty mass; $[\alpha]^{26}_D$: -142° (*c* = 1, $CHCl_3$); IR ($CHCl_3$) ν (cm^{-1}): 3681, 3609, 3358, 3019, 2973, 2789, 2400, 1886, 1738, 1662, 1516, 1438, 1372, 1216, 1113, 1046, 928, 758, 668, 627; ^{1}H NMR (400 MHz, $CDCl_3$) δ: 7.03-7.01 (d, *J* = 8.5 Hz, 1H), 6.89-6.87 (d, *J* = 8.5 Hz, 1H), 6.78-6.76 (d, *J* = 8.2 Hz, 2H), 4.98-4.92 (m, 1H), 3.73 (s, 3H), 3.18-3.13 (dd, *J* = 5 Hz, 14.3 Hz, 1H) 2.92-2.86 (dd, *J* = 9 Hz, 14.3 Hz, 1H), 2.52-2.51 (d, 6.2 Hz, 1H), 2.22 (s, 6H), 2.04-1.96 (m, 1H), 0.85-0.83 (d, *J* = 6.7 Hz, 3H), 0.72-0.7 (d, *J* = 6.5 Hz, 3H); ^{13}C NMR (100 MHz, $CDCl_3$) δ: 172.3, 171.5, 155.6, 130, 127.1, 115.5, 75.7, 52.7, 52.3, 42.6, 37.4, 27.5, 19.8, 17.1; HRMS: $C_{17}H_{27}O_4N_2$, Calcd: 323.1965, Found: 323.1965.

Methyl (2-(dimethylamino)-3,3-dimethylbutanoyl)phenylalaninate O:

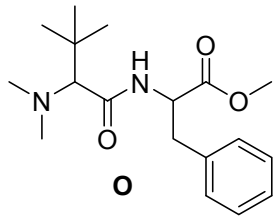

O

The analogue **O** was isolated as a white solid; mp: 63-66 °C; $[\alpha]^{26}_D$: +21.27° (*c* = 1, $CHCl_3$); IR ($CHCl_3$) ν (cm^{-1}): 3684, 3431, 3019, 2956, 2400, 1740, 1673, 1497, 1436, 1364, 1215, 1021, 929, 770, 669, 626; ^{1}H NMR (200 MHz, $CDCl_3$) δ: 7.31-7.28 (t, *J* = 7 Hz, 2H), 7.25-7.22 (t, *J* = 7.3 Hz, 1H), 7.18-7.17 (d, *J* = 7 Hz, 2H), 6.26-6.24 (d, *J* = 7.6 Hz, 1H), 4.96-4.93 (m, 1H), 4.92-4.89 (m, 1H), 3.74 (s, 1H), 3.22-3.18 (dd, *J* = 5.4 Hz, 5.4 Hz, 1H), 3.05-3.01 (dd, *J* = 13.7 Hz, 7.6 Hz, 1H), 2.29 (s, 6H), 0.97 (s, 9H); ^{13}C NMR (50 MHz, $CDCl_3$) δ: 172.3, 170.9, 136, 129.1, 128.6, 127, 77.6, 52.5, 52.2, 44.7, 38.2, 34.8, 27.8; HRMS: $C_{18}H_{28}O_3N_2Na$, Calcd: 343.1992, Found: 343.1986.

Synthesis of the analogues K and L:

To dipeptide **15** in DMF, silver oxide and methyl iodide were added at 0 °C and stirred for 12 h. Later, the reaction mixture was extracted into ethyl acetate, then washed with water and brine solution to remove excess DMF. The organic layer was dried over Na_2SO_4 and evaporated under vacuum. The residue obtained was purified through column chromatography which yielded the compound **20**. Compound **20** was found to be a mixture of products. The mixture was subjected to Z-deprotection using 10% Pd/C in MeOH under H_2 pressure at 60 psi in parr shaker. The catalyst was filtered out by passing the reaction mixture through celite. The organics were evaporated and the residue was purified through column chromatography which yielded the products **K** and **L**.

Methyl N-(dimethylvalyl)-N-methylphenylalaninate K:

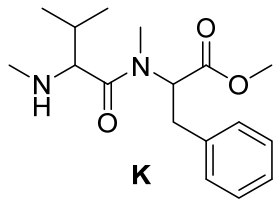

K

The analogue **K** was isolated as a yellow solid; mp: 77-80 °C; $[\alpha]^{26}_{D}$: -112° (*c* = 1, $CHCl_3$); IR ($CHCl_3$) ν (cm^{-1}): 3406, 3019, 2974, 2400, 1740, 1651, 1471, 1215, 1045, 928, 768, 668; ^{1}H NMR (200 MHz, $CDCl_3$) δ: 7.31-7.18 (m, 5H), 5.75-5.66 (dd, *J* = 11.7 Hz, 4.9 Hz, 1H), 3.74 (s, 3H), 3.52-3.43 (dd, *J* = 14.9 Hz, 4.9 Hz, 1H), 3.1-2.95 (m, 2H), 2.91 (s, 3H), 2.13-2.04 (m, 1H), 1.9 (s, 3H), 0.97-0.94 (d, *J* = 6.5 Hz, 3H), 0.9-0.87 (d, *J* = 6.5 Hz, 3H); ^{13}C NMR (50 MHz, $CDCl_3$) δ: 170.6, 136.4, 129.4, 128.8, 127.1, 68.8, 66.7, 65, 57.1, 52.4, 40.2, 34.3, 32.4, 29, 19.9, 18.9, HRMS: $C_{17}H_{27}O_3N_2$, Calcd: 307.2016, Found: 307.2015.

N-methyl-N-(methylvalyl)phenylalanine L:

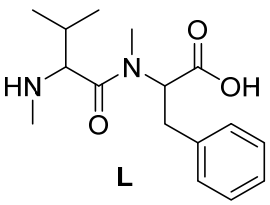

L

The analogue **L** was isolated as a white solid; mp: 77-80 °C; $[\alpha]^{26}_{D}$: -84° (*c* = 1, $CHCl_3$); IR ($CHCl_3$) ν (cm^{-1}): 3684, 3619, 3422, 3019, 2400, 1654, 1522, 1476, 1423, 1216, 1045, 928, 771, 669, 488; ^{1}H NMR (200 MHz, CDCl3) δ: 7.35-7.19 (m, 5H), 4.15-4.09 (dd, *J* = 7.5 Hz, 4.2 Hz, 1H), 3.55-3.52 (d, *J* = 7.2 Hz, 1H), 3.41-3.32 (dd, *J* = 14 Hz, 4.4 Hz, 1H), 3.13-3.02 (dd, *J* = 14 Hz, 7Hz, 1H), 3.00 (s, 3H), 2.65 (s, 3H), 1.73-1.56 (sextet, *J* = 13.7 Hz, 6.9 Hz, 1H), 1.02-0.98 (d, *J* = 6.9 Hz, 3H), 0.94-0.91 (d, *J* = 6.8 Hz, 3H); ^{13}C NMR (50 MHz,

$CDCl_3$) δ: 166.3, 165.6, 136.9, 129.3, 128.8, 127.1, 68.7, 64.9, 40, 35.7, 33.7, 33.4, 20.4, 19.4; ESI-MS: 296.1787 $(M+H)^+$; Elemental analysis calculated for $C_{16}H_{24}N_2O_2$: C, 65.73; H, 8.27; N, 9.58 Found: C, 65.54; H, 7.85; N, 9.01.

Methyl-2-(2-(((benzyloxy)carbonyl)amino)-3-methylbutanamido)thiophene-3-carboxylate 22:

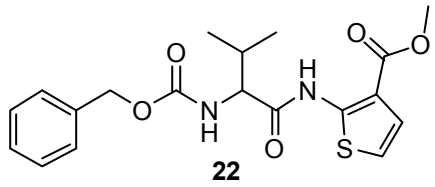

22

To a solution of Cbz-valine (1.74 g, 6.96 mmol) in dry DCM, the amine **21** (1 g, 6.32 mmol) was added followed by the addition of EDC.HCl (1.45 g, 7.59 mmol). The reaction mixture was stirred at room temperature for 12 h. Later, the reaction mixture was diluted with DCM and washed with sat. $NaHCO_3$, brine and sat. $KHSO_4$ solution in a sequence. Then, the organic layer was dried over Na_2SO_4 and was evaporated under reduced pressure. The residue obtained was purified by column chromatography which yielded the corresponding dipeptide **22** (1.35 g, 50%) as a white solid; mp: 116-118 °C; $[\alpha]^{26}_D$: -18.05° (*c* = 1, $CHCl_3$); IR ($CHCl_3$) ν (cm^{-1}): 3683, 3616, 3283, 3019, 2969, 2400, 1722, 1679, 1553, 1498, 1445, 1393, 1292, 1215, 1166, 1089, 1026, 928, 889, 849, 758, 701, 668, 626; ^{1}H NMR (200 MHz, $CDCl_3$) δ: 11.4 (s, 1H), 7.4-7.33 (m, 5H), 7.22-7.21 (d, *J* = 5.8 Hz, 1H), 6.77-6.76 (d, *J* = 5.8 Hz, 1H), 5.43-5.41 (d, *J* = 7 Hz, 1H), 5.2-5.13 (q, *J* = 11.9 Hz, 2H), 4.39 (bs, 1H), 3.69 (s, 3H), 2.37-2.33 (m, 1H), 1.67-1.66 (bs, 1H), 1.05-1.04 (d, *J* = 6.7 Hz, 3H), 0.98-0.96 (d, *J* = 6.7 Hz, 3H); ^{13}C NMR (50 MHz, $CDCl_3$) δ: 168.7, 165.7, 156.3, 147.9, 136.1, 128.1, 123.8, 116.3, 113.3, 67.3, 60.5, 51.7, 30.9, 19.2, 17.4; HRMS: $C_{19}H_{22}O_5N_2S$, Calcd: 391.1322, Found: 391.1322. $C_{19}H_{21}O_5N_2NaS$, Calcd: 413.1142, Found: 413.1137.

Methyl-2-(2-(dimethylamino)-3-methylbutanamido)thiophene-3-carboxylate P:

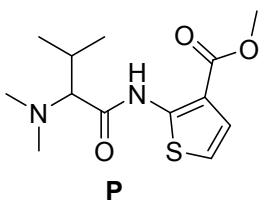

P

N,N dimethylation of **22** was carried out using the above mentioned procedure. The analogue **P** was isolated as a brown solid; mp: 40-42 °C; $[\alpha]^{26}_D$: +38° (*c* = 1, $CHCl_3$); IR ($CHCl_3$) ν (cm^{-1}): 3683, 3621, 3280, 3020, 2877, 2833, 2788, 2400, 1674, 1543, 1495, 1444, 1382, 1292, 1215, 1165, 1089, 1026, 929,

881, 769, 701, 668, 627; ^{1}H NMR (200 MHz, CDCl3) δ: 11.46 (s, 1H), 7.22-7.19 (d, *J* = 5.8 Hz, 1H), 6.74-6.71 (d, *J* = 5.6 Hz, 1H), 3.89 (s, 3H), 2.75-2.72 (d, *J* = 6.3 Hz, 1H), 2.35 (s, 6H), 2.26-2.12 (sextet, *J* = 6.6 Hz, 1H), 1.06-1.02 (d, *J* = 6.8 Hz, 3H), 0.96-0.93 (d, *J* = 6.6 Hz, 3H); ^{13}C NMR (50 MHz, $CDCl_3$) δ: 169.4, 165.5, 147.9, 123.8, 115.8, 112.6, 51.6, 42.9, 27.8, 20, 17.5; ESI-MS: 306.89 $(M+Na)^+$; Elemental analysis calculated for $C_{13}H_{20}N_2O_3S$: C, 54.90; H, 7.09; N, 9.85; S, 11.27; Found: C, 52.54; H, 7.42; N, 11.01; S, 10.86.

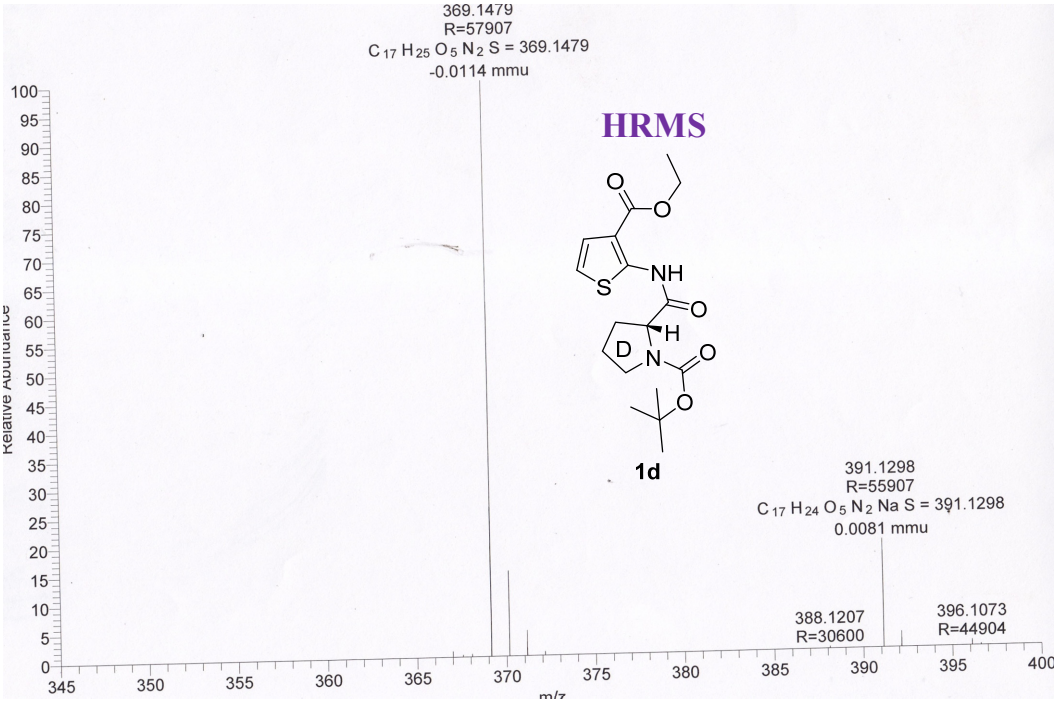
369.1479
R=57907
C 17 H 25 O 5 N 2 S = 369.1479
-0.0114 mmu
HRMS
1d
391.1298
R=55907
C 17 H 24 O 5 N 2 Na S = 391.1298
0.0081 mmu
388.1207
R=30600
396.1073
R=44904
Relative Abundance
m/z

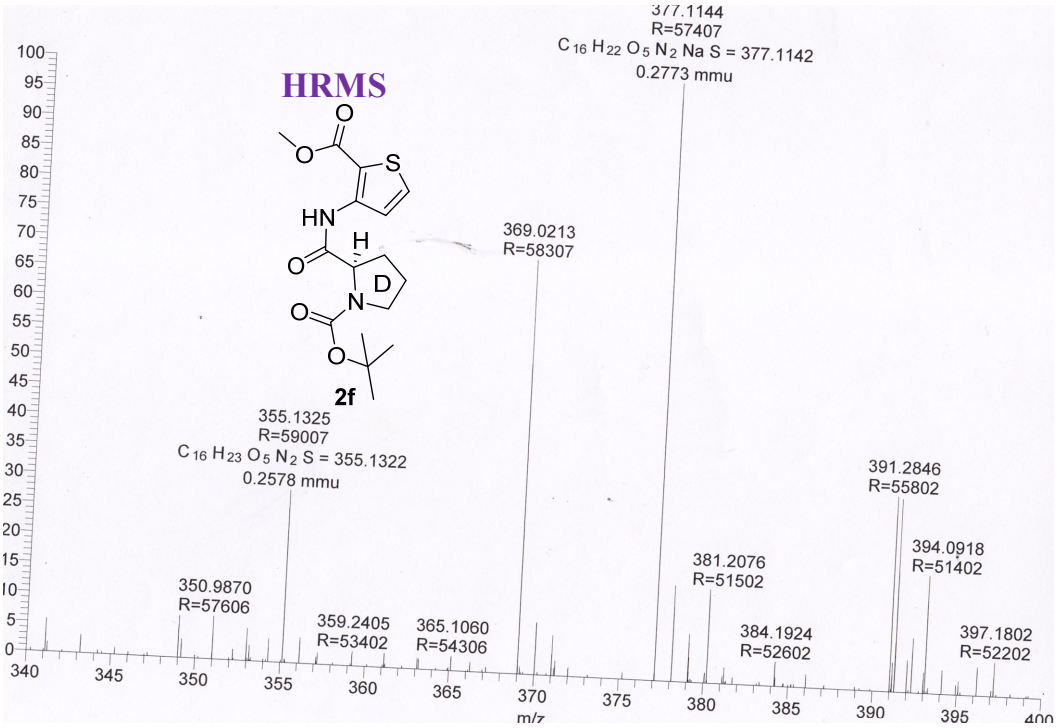
377.1144
R=57407
C 16 H 22 O 5 N 2 Na S = 377.1142
0.2773 mmu
HRMS
2f
369.0213
R=58307
355.1325
R=59007
C 16 H 23 O 5 N 2 S = 355.1322
0.2578 mmu
391.2846
R=55802
394.0918
R=51402
381.2076
R=51502
350.9870
R=57606
359.2405
R=53402
365.1060
R=54306
384.1924
R=52602
397.1802
R=52202
m/z

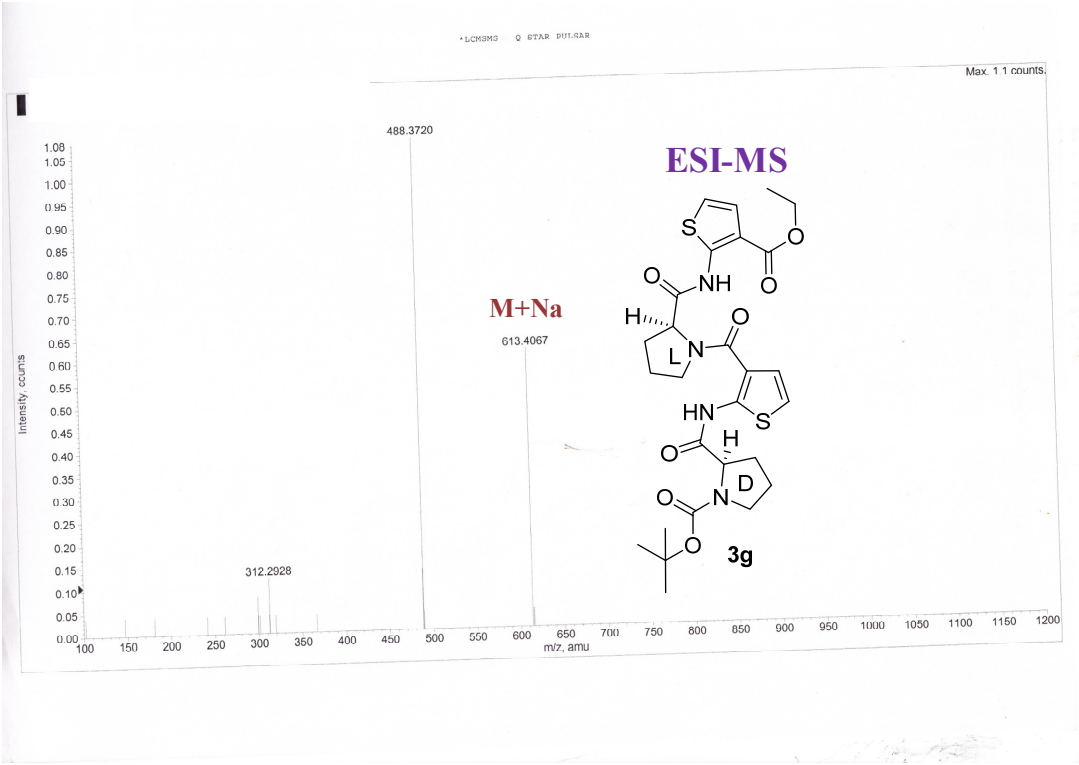
ESI-MS
Max. 1.1 counts.
488.3720
M+Na
613.4067
312.2928
Intensity, counts
m/z, amu
3g

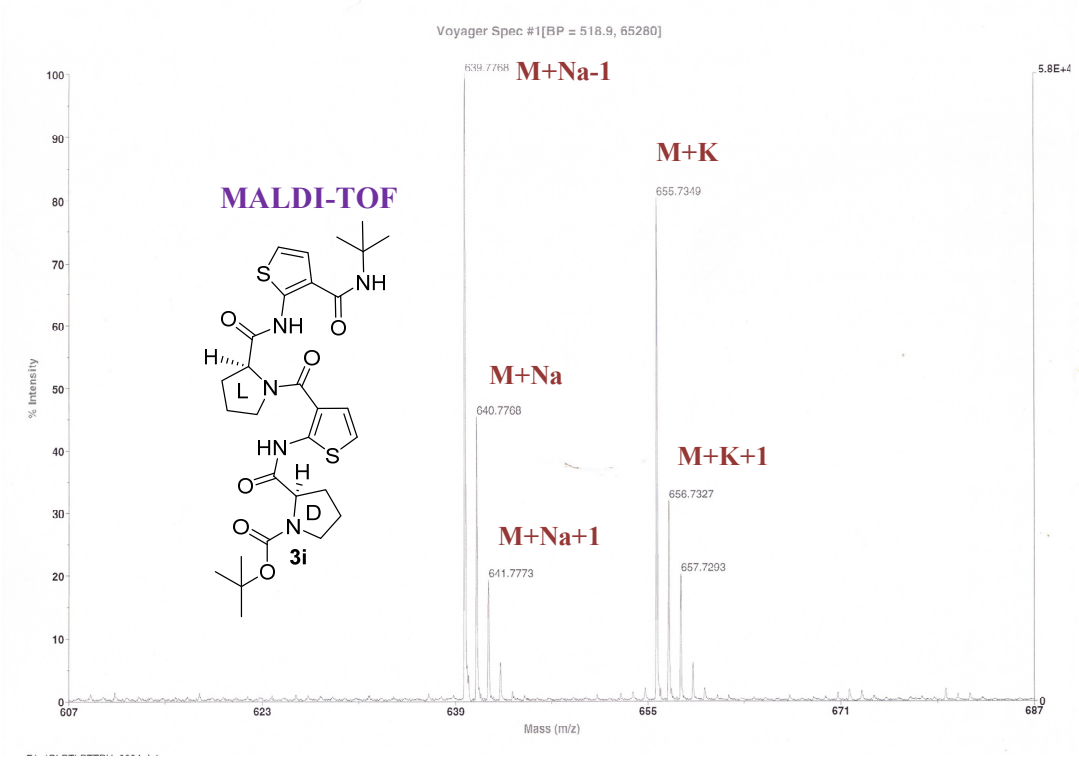
Voyager Spec #1[BP = 518.9, 65280]
MALDI-TOF
M+Na-1
639.7768
M+K
655.7349
M+Na
640.7768
M+K+1
656.7327
M+Na+1
641.7773
657.7203
% Intensity
Mass (m/z)
3i

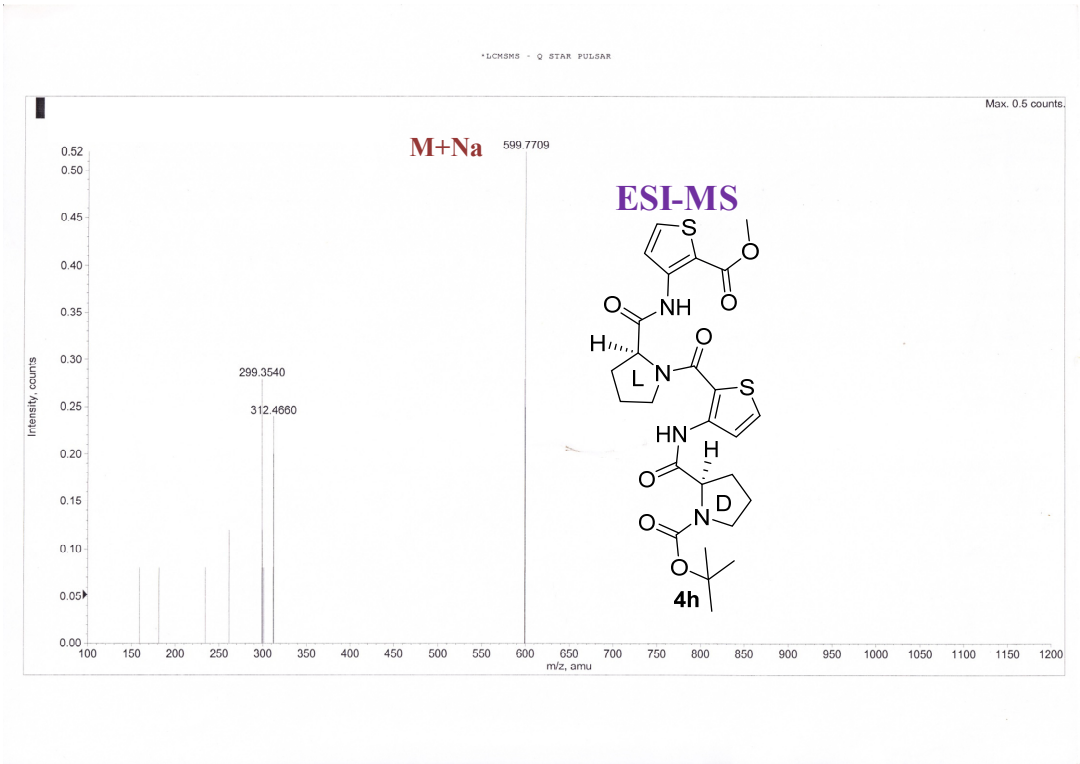
*LCMSMS - Q STAR PULSAR
Max. 0.5 counts.
M+Na
599.7709
ESI-MS
299.3540
312.4660
Intensity, counts
m/z, amu
4h

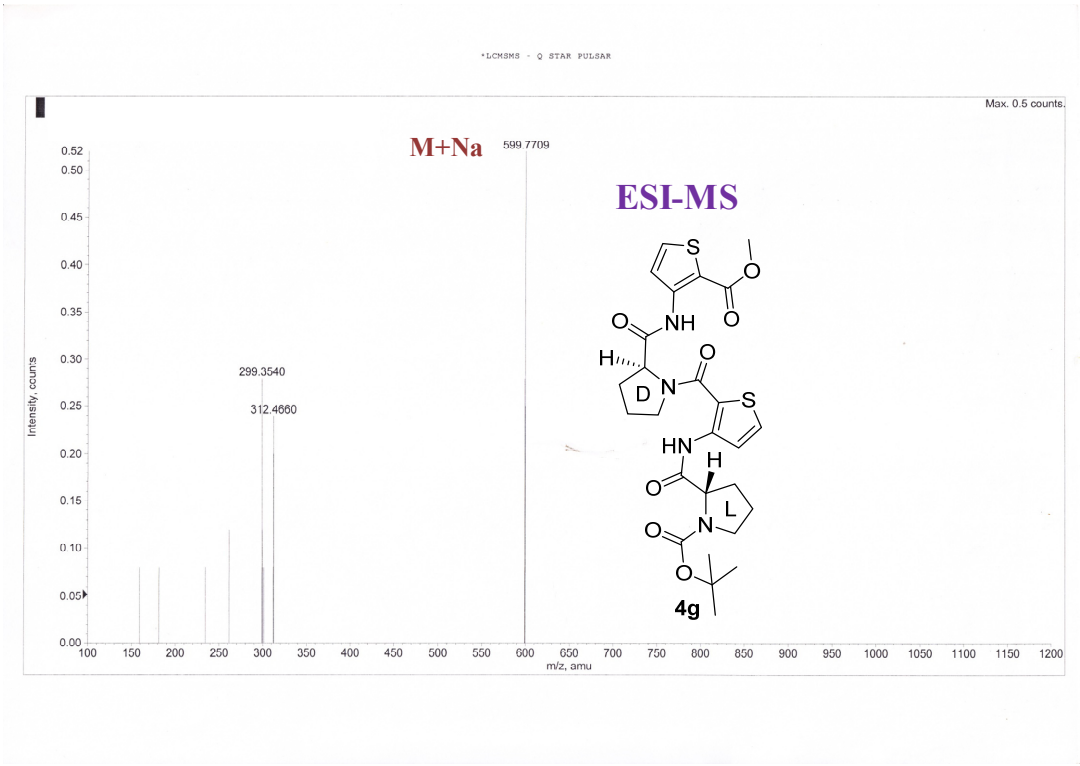
*LCMSMS - Q STAR PULSAR
Max. 0.5 counts.
M+Na
599.7709
ESI-MS
299.3540
312.4660
Intensity, counts
m/z, amu
4g

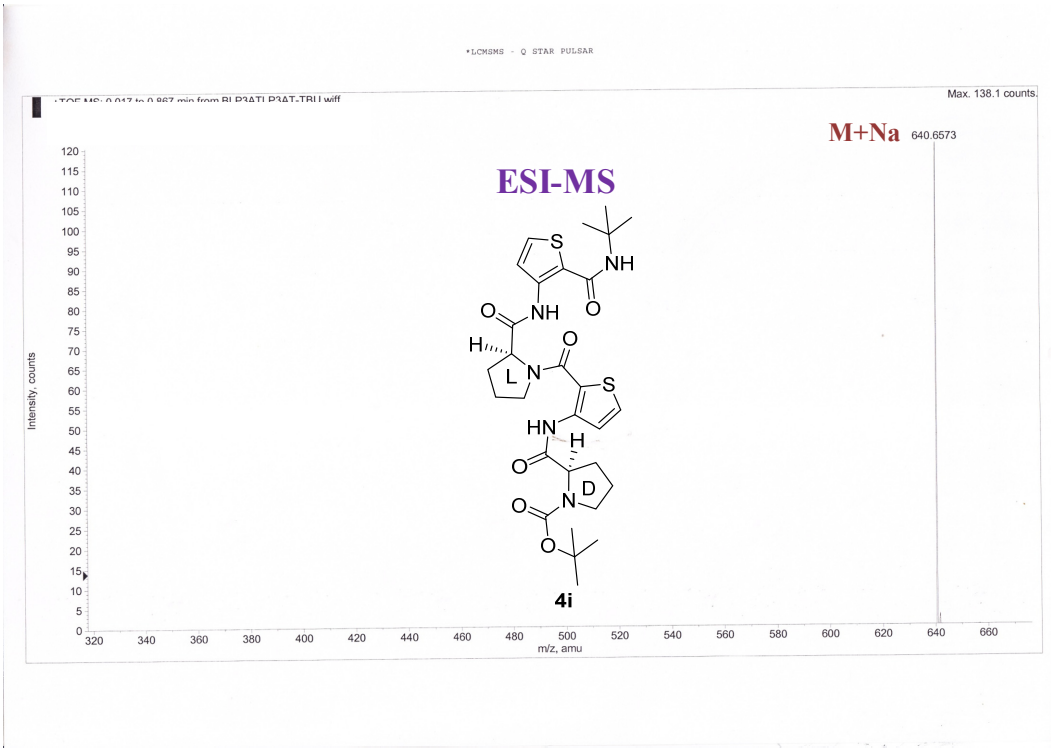
*LCMSMS - Q STAR PULSAR
Max. 138.1 counts.
M+Na 640.6573
ESI-MS
Intensity, counts
m/z, amu
4i

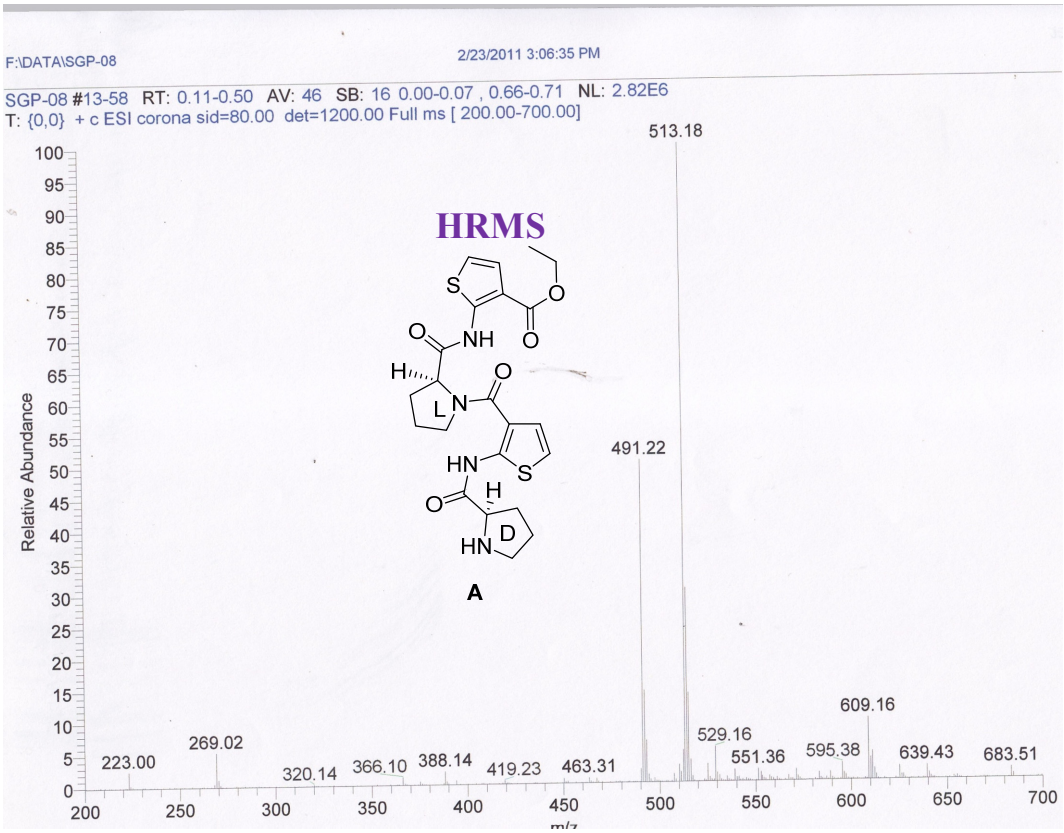
F:\DATA\SGP-08
2/23/2011 3:06:35 PM
SGP-08 #13-58 RT: 0.11-0.50 AV: 46 SB: 16 0.00-0.07 , 0.66-0.71 NL: 2.82E6
T: {0,0} + c ESI corona sid=80.00 det=1200.00 Full ms [200.00-700.00]
HRMS
513.18
491.22
609.16
529.16
269.02
223.00
320.14
366.10
388.14
419.23
463.31
551.36
595.38
639.43
683.51
Relative Abundance
m/z
A

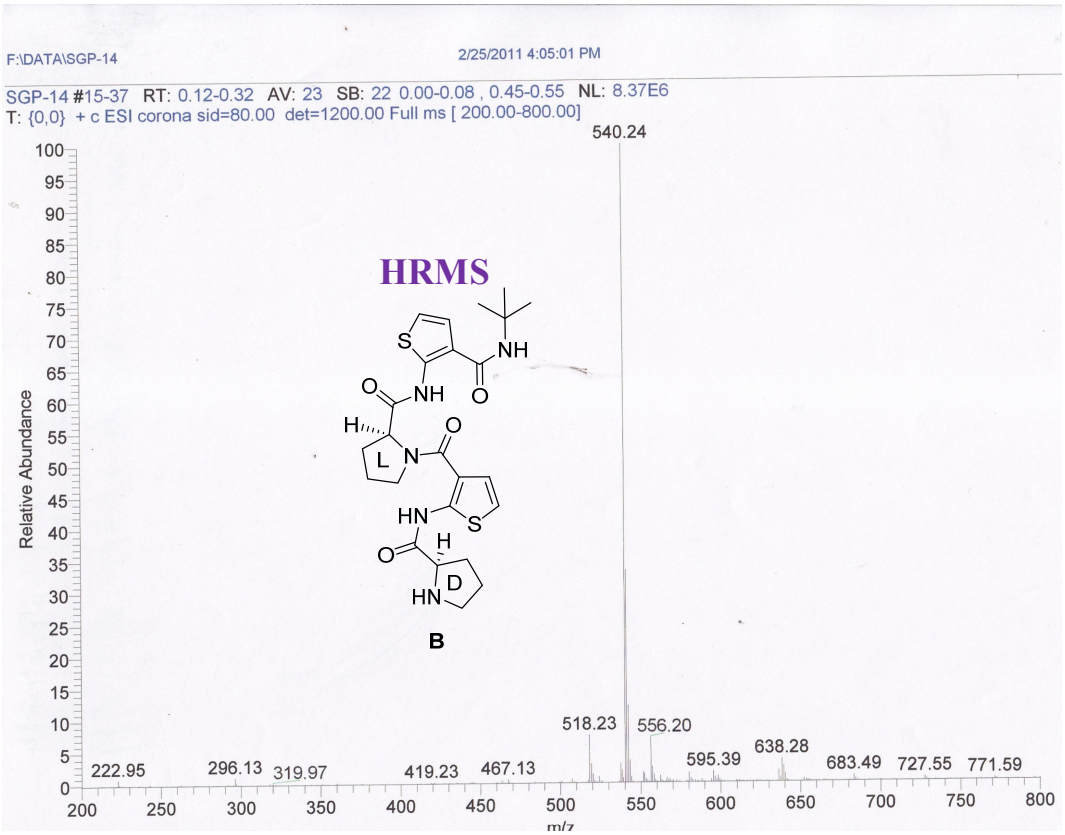
F:\DATA\SGP-14
2/25/2011 4:05:01 PM
SGP-14 #15-37 RT: 0.12-0.32 AV: 23 SB: 22 0.00-0.08 , 0.45-0.55 NL: 8.37E6
T: {0,0} + c ESI corona sid=80.00 det=1200.00 Full ms [200.00-800.00]
540.24
HRMS
B
Relative Abundance
m/z
518.23
556.20
595.39
638.28
683.49
727.55
771.59
222.95
296.13
319.97
419.23
467.13

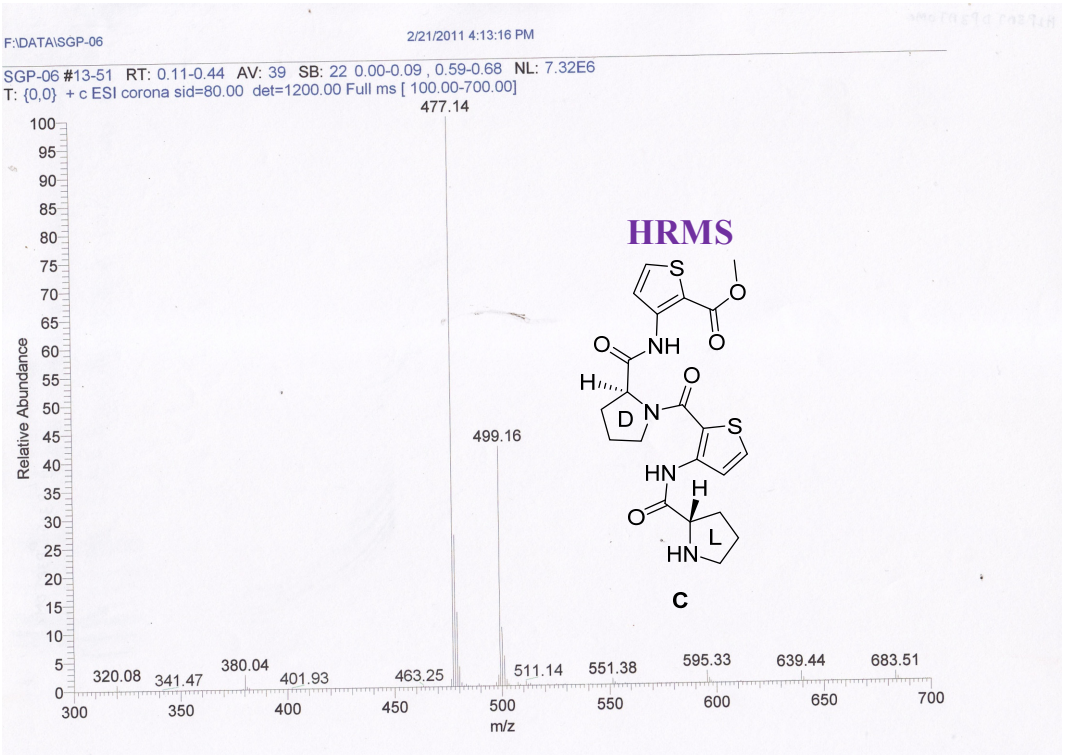
F:\DATA\SGP-06
2/21/2011 4:13:16 PM
SGP-06 #13-51 RT: 0.11-0.44 AV: 39 SB: 22 0.00-0.09 , 0.59-0.68 NL: 7.32E6
T: {0,0} + c ESI corona sid=80.00 det=1200.00 Full ms [100.00-700.00]
477.14
HRMS
C
Relative Abundance
m/z
499.16
511.14
551.38
595.33
639.44
683.51
320.08
341.47
380.04
401.93
463.25

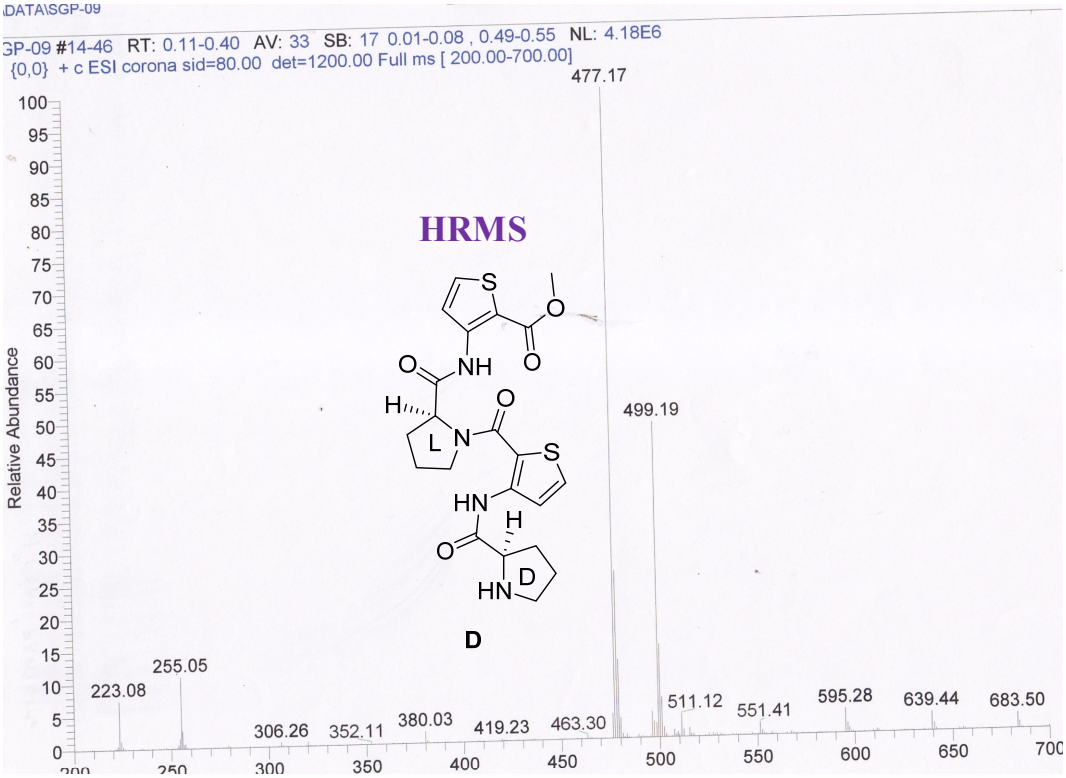
DATA\SGP-09
GP-09 #14-46 RT: 0.11-0.40 AV: 33 SB: 17 0.01-0.08 , 0.49-0.55 NL: 4.18E6
{0,0} + c ESI corona sid=80.00 det=1200.00 Full ms [200.00-700.00]
HRMS
Relative Abundance
477.17
499.19
255.05
223.08
306.26
352.11
380.03
419.23
463.30
511.12
551.41
595.28
639.44
683.50
D

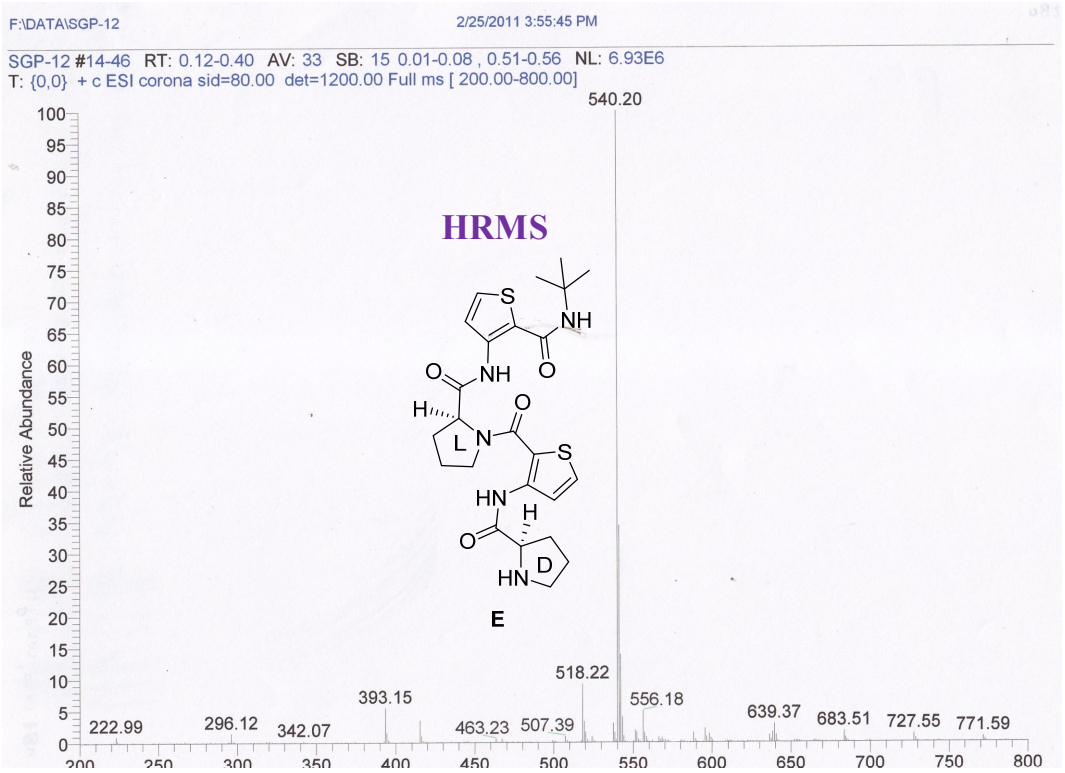
F:\DATA\SGP-12
2/25/2011 3:55:45 PM
SGP-12 #14-46 RT: 0.12-0.40 AV: 33 SB: 15 0.01-0.08 , 0.51-0.56 NL: 6.93E6
T: {0,0} + c ESI corona sid=80.00 det=1200.00 Full ms [200.00-800.00]
HRMS
Relative Abundance
540.20
518.22
393.15
222.99
296.12
342.07
463.23
507.39
556.18
639.37
683.51
727.55
771.59
E

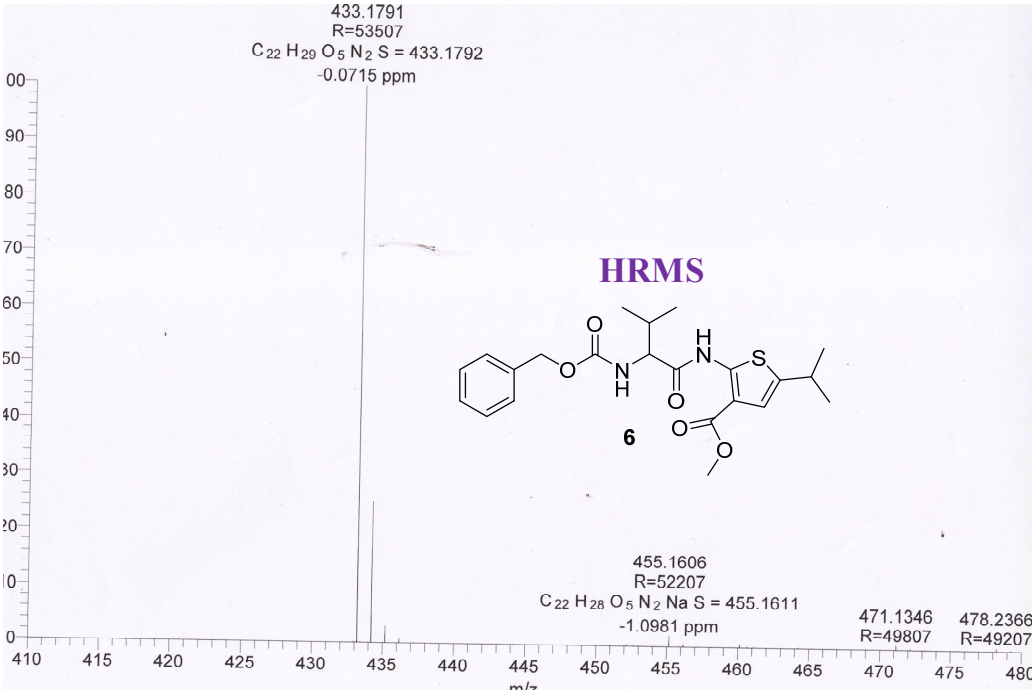
433.1791
R=53507
C22 H29 O5 N2 S = 433.1792
-0.0715 ppm
HRMS
6
455.1606
R=52207
C22 H28 O5 N2 Na S = 455.1611
-1.0981 ppm
471.1346
R=49807
478.2366
R=49207

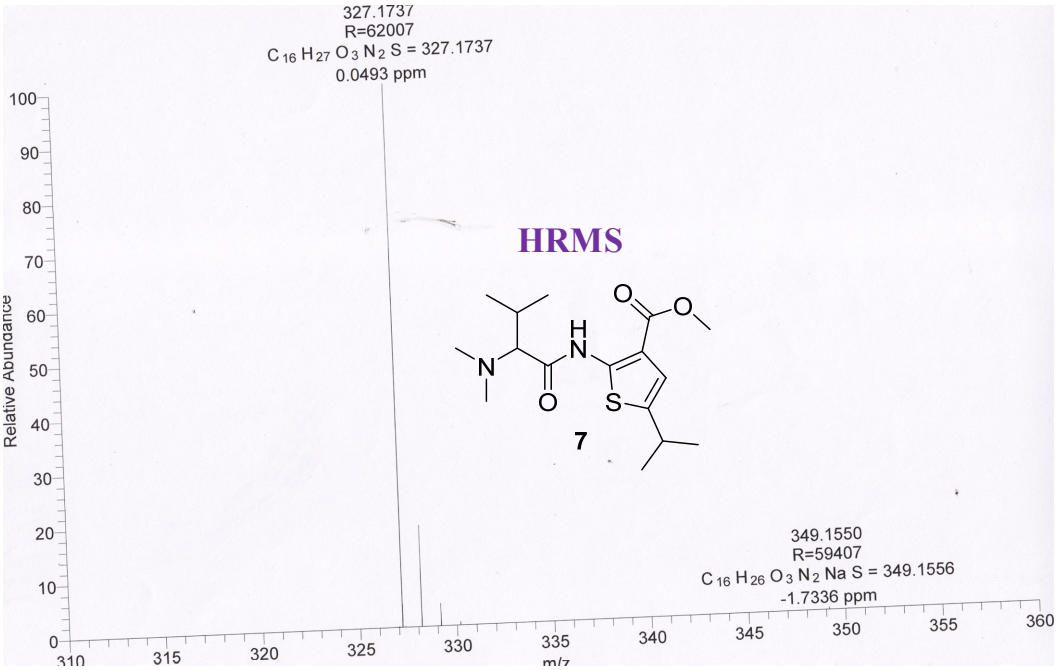
327.1737
R=62007
C16 H27 O3 N2 S = 327.1737
0.0493 ppm
HRMS
7
Relative Abundance
349.1550
R=59407
C16 H26 O3 N2 Na S = 349.1556
-1.7336 ppm

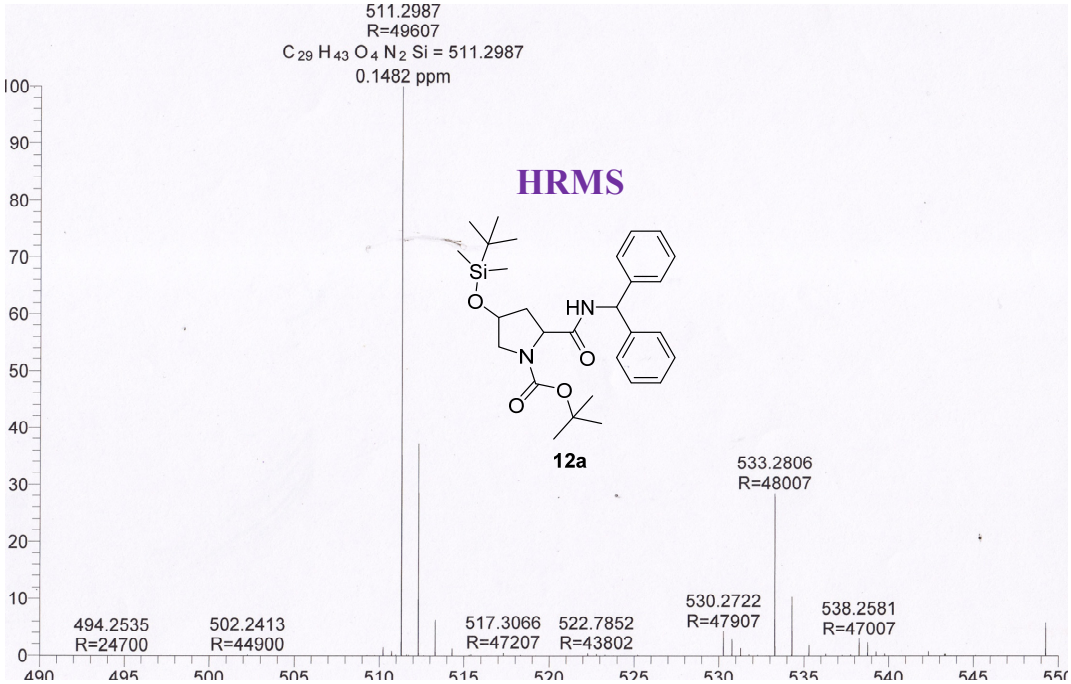
511.2987
R=49607
C 29 H 43 O 4 N 2 Si = 511.2987
0.1482 ppm
HRMS
12a
533.2806
R=48007
494.2535
R=24700
502.2413
R=44900
517.3066
R=47207
522.7852
R=43802
530.2722
R=47907
538.2581
R=47007

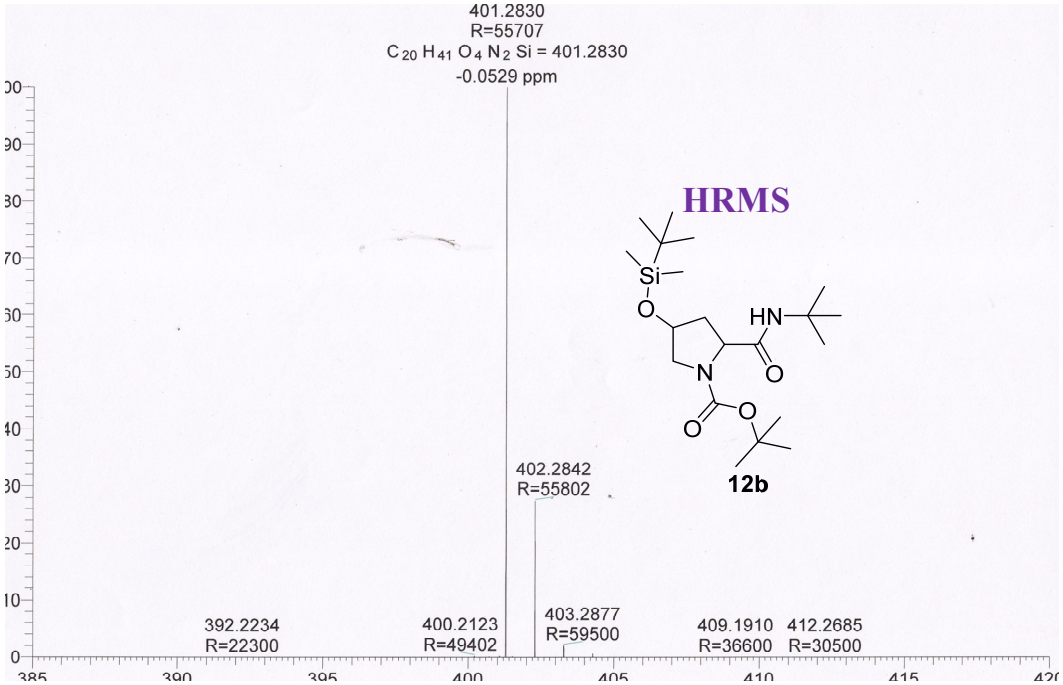
401.2830
R=55707
C 20 H 41 O 4 N 2 Si = 401.2830
-0.0529 ppm
HRMS
12b
402.2842
R=55802
392.2234
R=22300
400.2123
R=49402
403.2877
R=59500
409.1910
R=36600
412.2685
R=30500

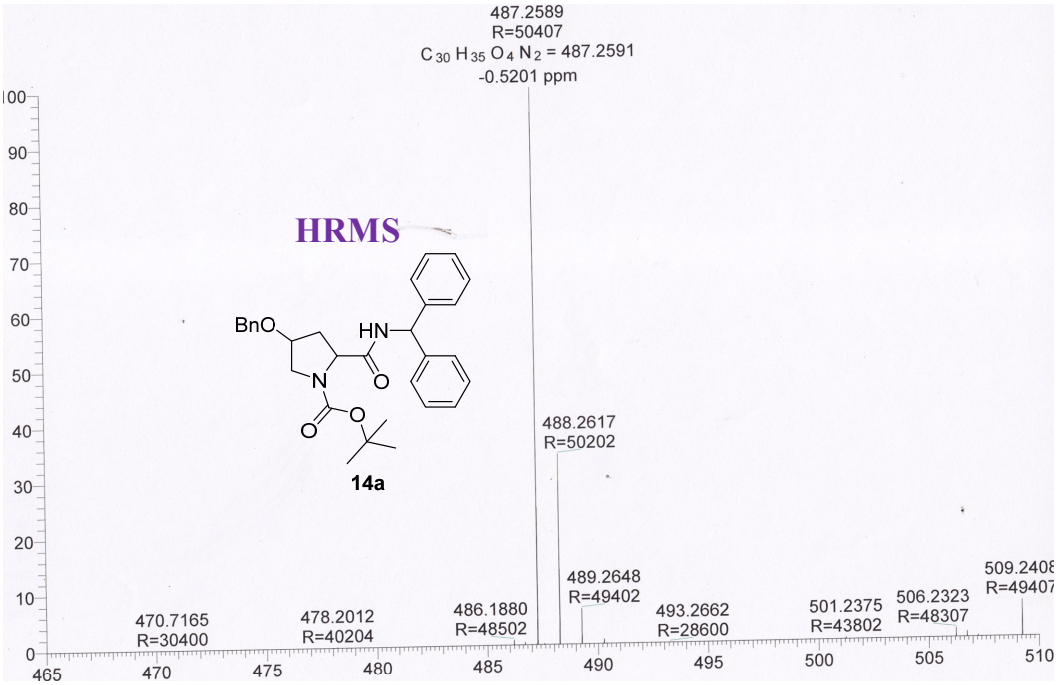
487.2589
R=50407
C 30 H 35 O 4 N 2 = 487.2591
-0.5201 ppm
HRMS
BnO
HN
N
O
O
O
14a
488.2617
R=50202
489.2648
R=49402
470.7165
R=30400
478.2012
R=40204
486.1880
R=48502
493.2662
R=28600
501.2375
R=43802
506.2323
R=48307
509.2408
R=49407

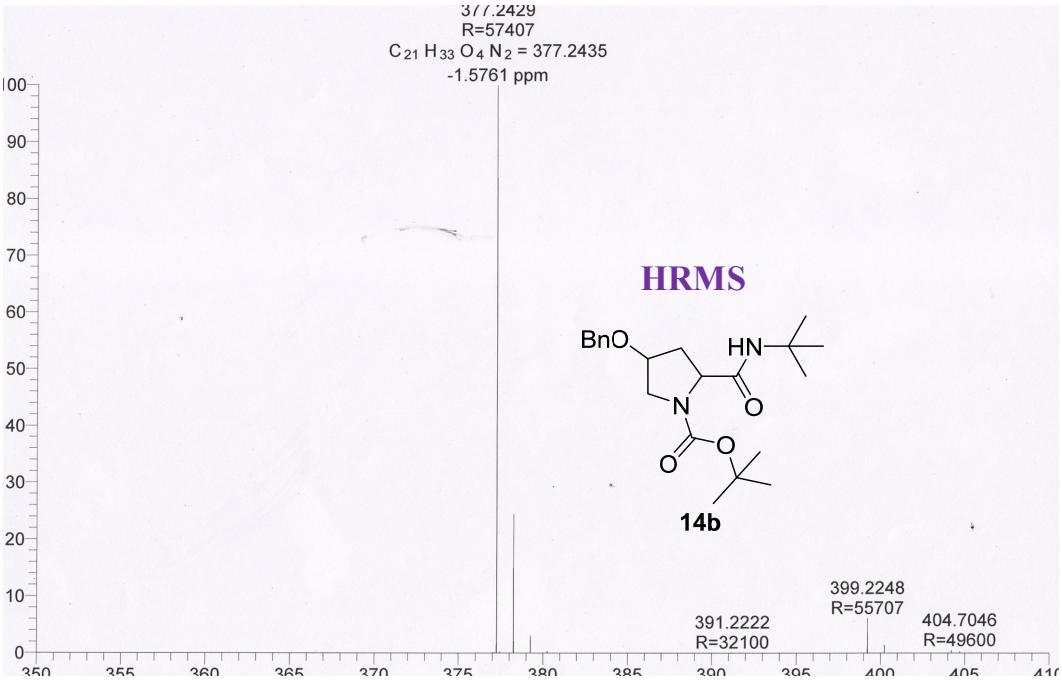
377.2429
R=57407
C 21 H 33 O 4 N 2 = 377.2435
-1.5761 ppm
HRMS
BnO
HN
N
O
O
O
14b
399.2248
R=55707
391.2222
R=32100
404.7046
R=49600

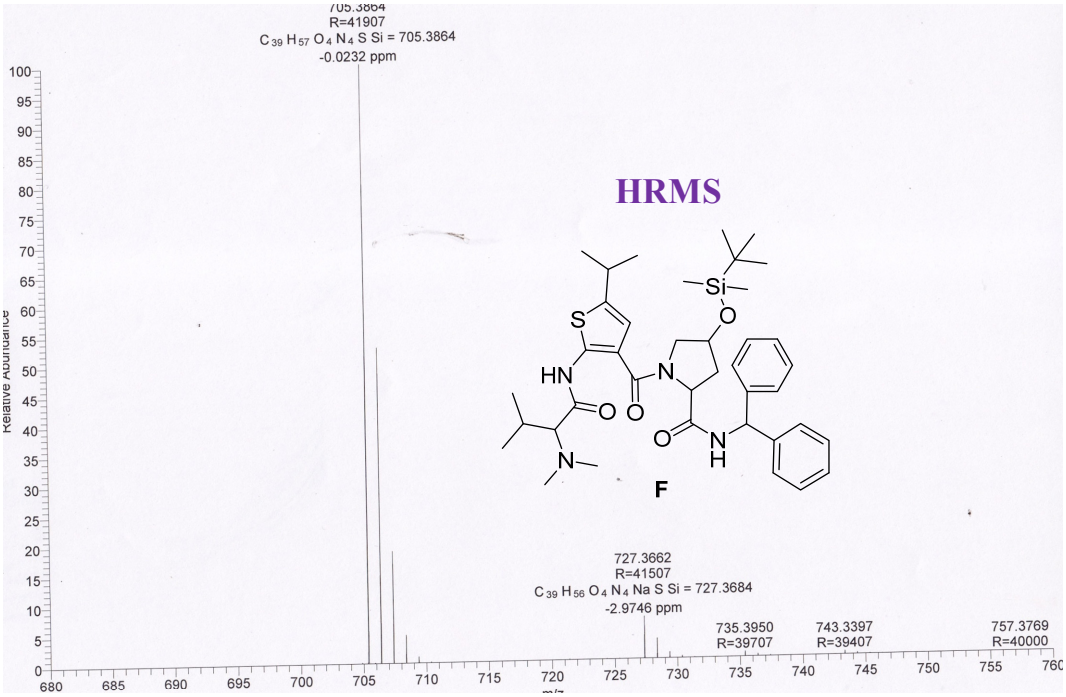
705.3864
R=41907
C 39 H 57 O 4 N 4 S Si = 705.3864
-0.0232 ppm
HRMS
F
727.3662
R=41507
C 39 H 56 O 4 N 4 Na S Si = 727.3684
-2.9746 ppm
735.3950
R=39707
743.3397
R=39407
757.3769
R=40000

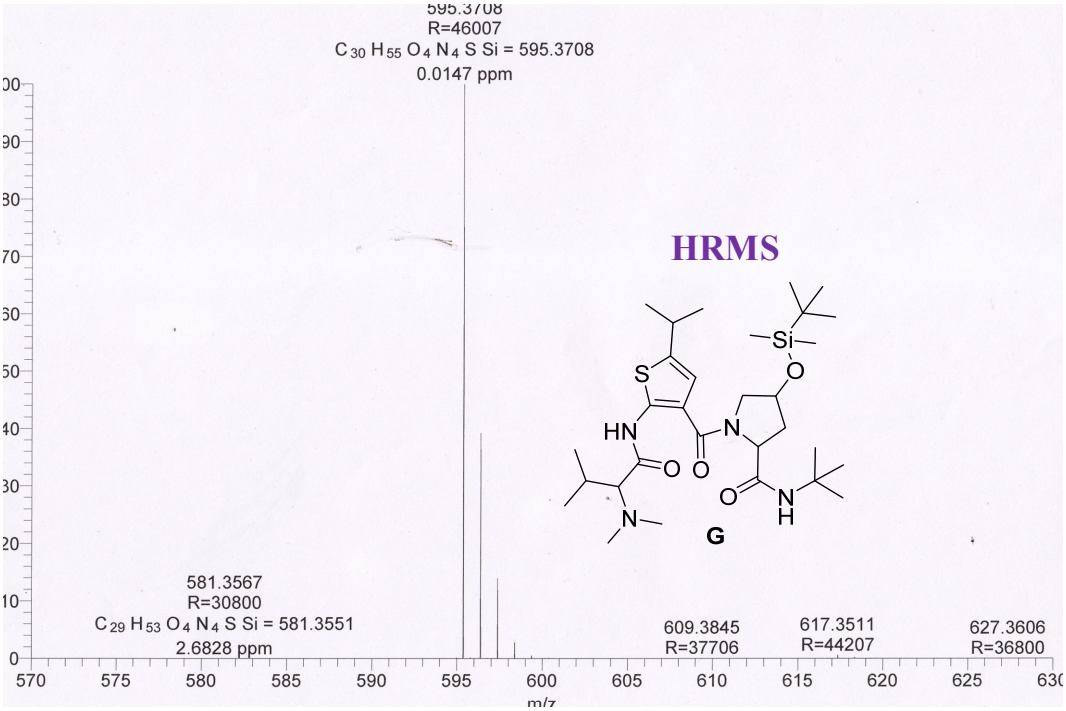
595.3708
R=46007
C 30 H 55 O 4 N 4 S Si = 595.3708
0.0147 ppm
HRMS
G
581.3567
R=30800
C 29 H 53 O 4 N 4 S Si = 581.3551
2.6828 ppm
609.3845
R=37706
617.3511
R=44207
627.3606
R=36800

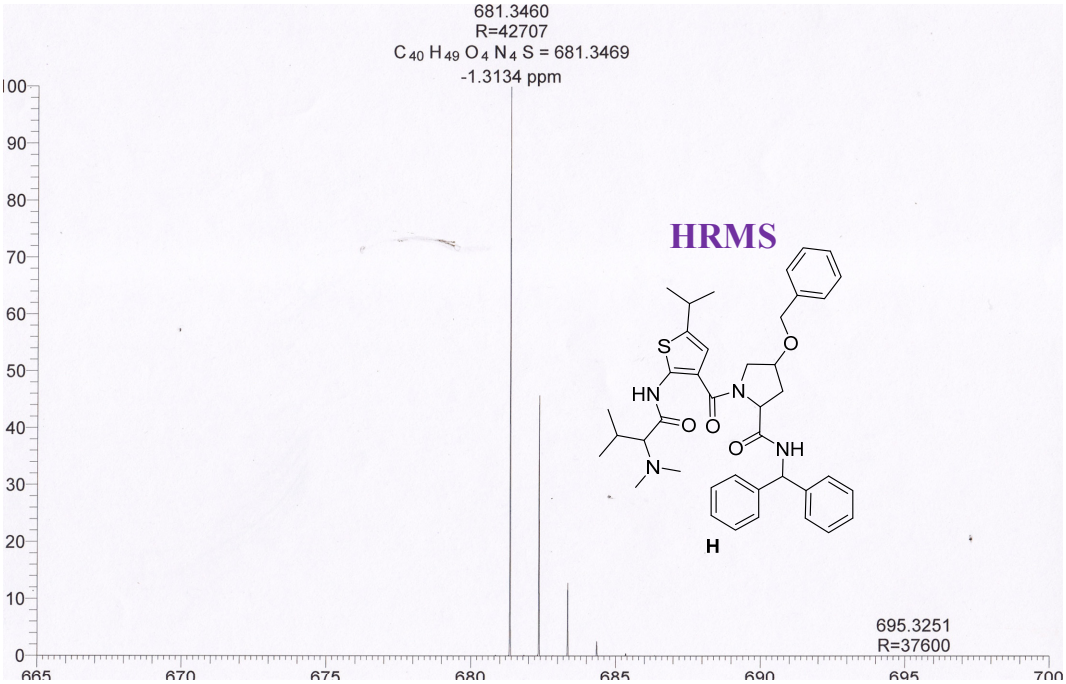
681.3460
R=42707
C40 H49 O4 N4 S = 681.3469
-1.3134 ppm
HRMS
695.3251
R=37600
H

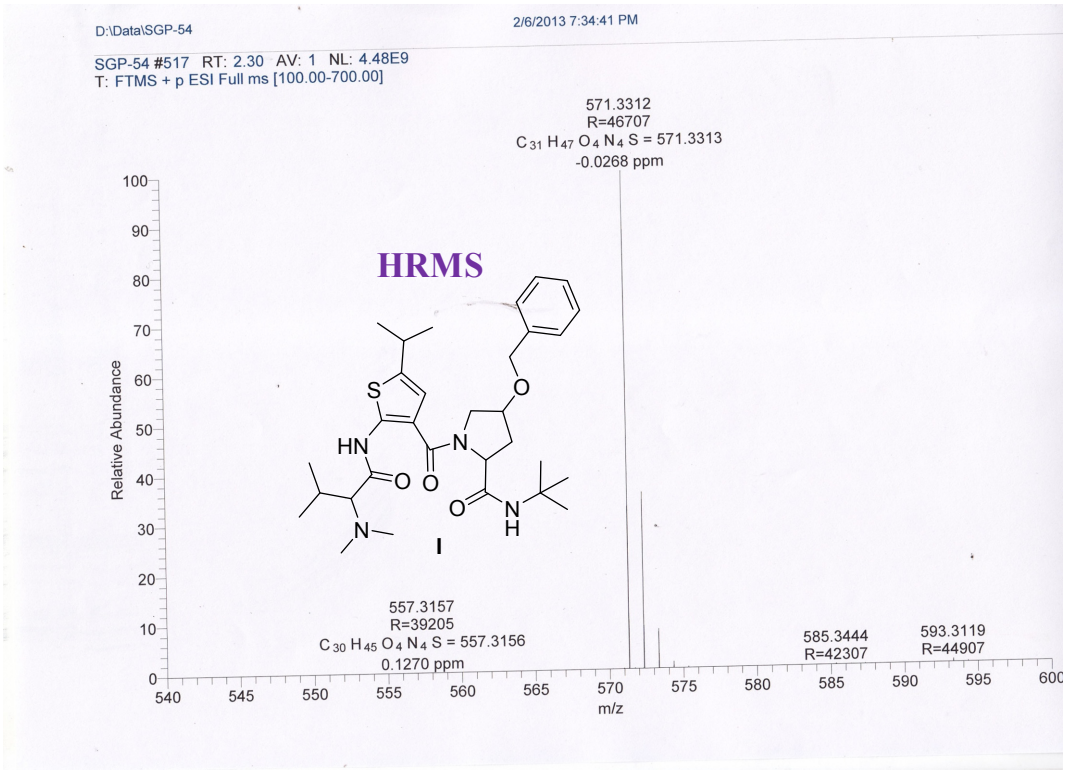
D:\Data\SGP-54
2/6/2013 7:34:41 PM
SGP-54 #517 RT: 2.30 AV: 1 NL: 4.48E9
T: FTMS + p ESI Full ms [100.00-700.00]
571.3312
R=46707
C31 H47 O4 N4 S = 571.3313
-0.0268 ppm
HRMS
Relative Abundance
m/z
I
557.3157
R=39205
C30 H45 O4 N4 S = 557.3156
0.1270 ppm
585.3444
R=42307
593.3119
R=44907

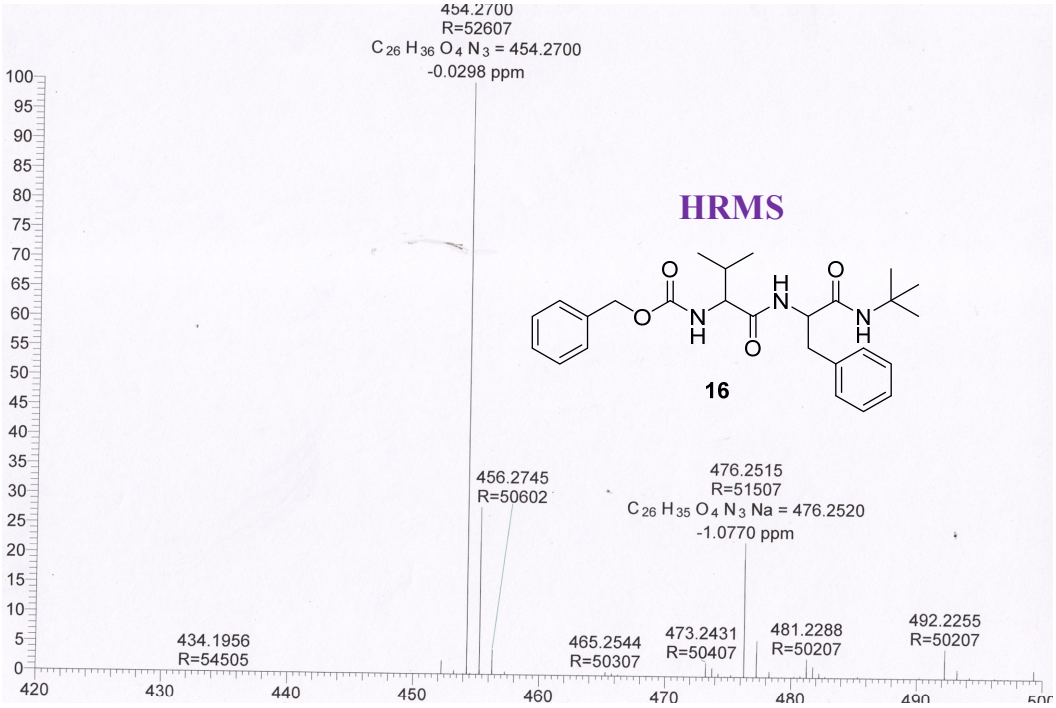
454.2700
R=52607
C26 H36 O4 N3 = 454.2700
-0.0298 ppm
HRMS
16
456.2745
R=50602
476.2515
R=51507
C26 H35 O4 N3 Na = 476.2520
-1.0770 ppm
434.1956
R=54505
465.2544
R=50307
473.2431
R=50407
481.2288
R=50207
492.2255
R=50207

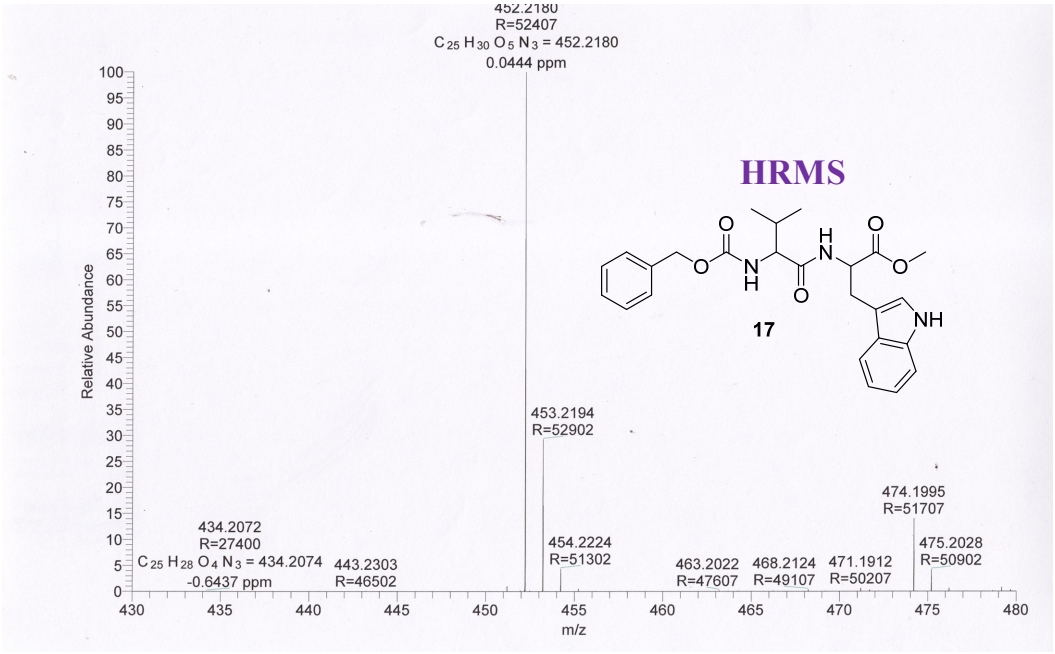
452.2180
R=52407
C25 H30 O5 N3 = 452.2180
0.0444 ppm
HRMS
17
Relative Abundance
m/z
453.2194
R=52902
434.2072
R=27400
C25 H28 O4 N3 = 434.2074
-0.6437 ppm
443.2303
R=46502
454.2224
R=51302
463.2022
R=47607
468.2124
R=49107
471.1912
R=50207
474.1995
R=51707
475.2028
R=50902

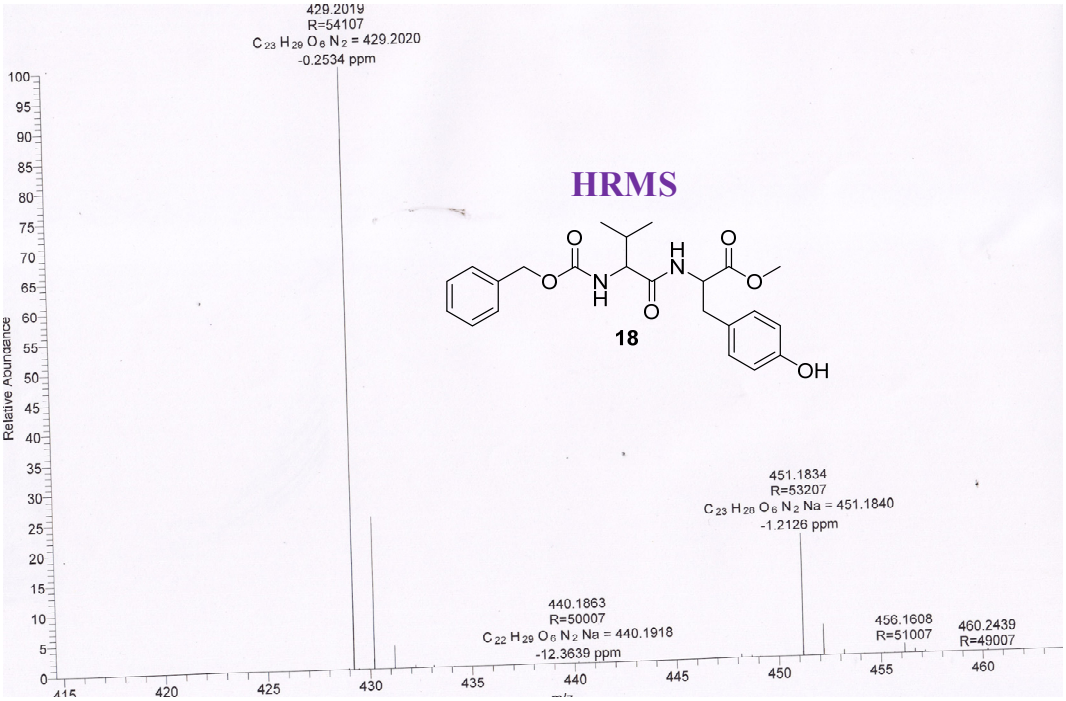
429.2019
R=54107
C23 H29 O6 N2 = 429.2020
-0.2534 ppm
HRMS
18
OH
Relative Abundance
451.1834
R=53207
C23 H28 O6 N2 Na = 451.1840
-1.2126 ppm
440.1863
R=50007
C22 H29 O6 N2 Na = 440.1918
-12.3639 ppm
456.1608
R=51007
460.2439
R=49007

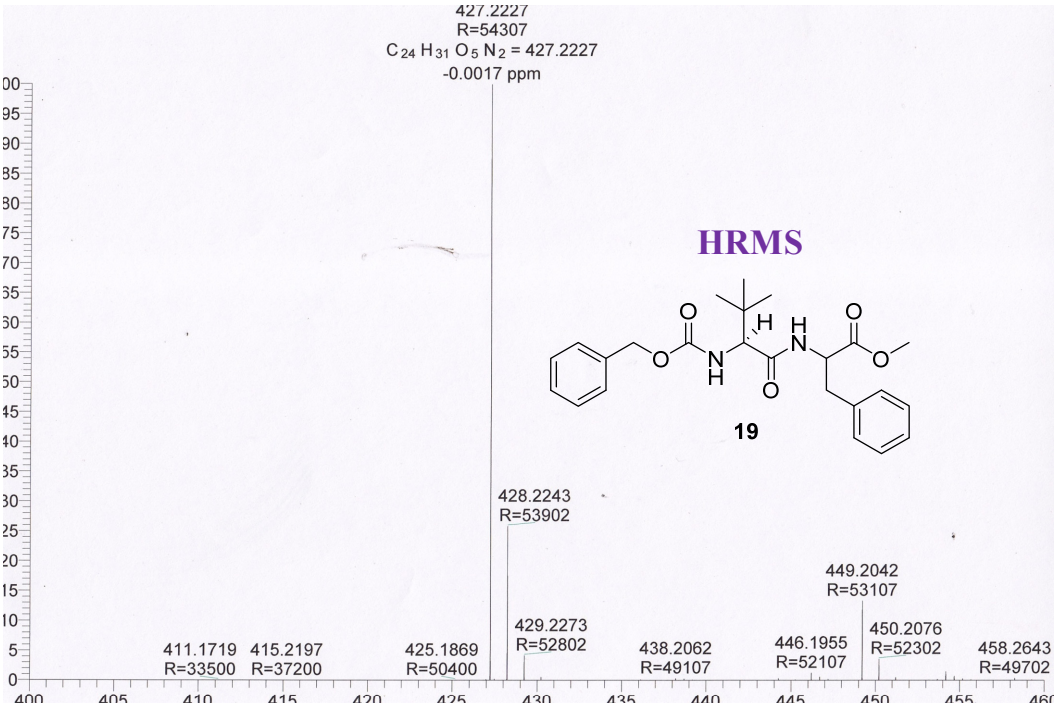
427.2227
R=54307
C24 H31 O5 N2 = 427.2227
-0.0017 ppm
HRMS
19
428.2243
R=53902
449.2042
R=53107
429.2273
R=52802
450.2076
R=52302
411.1719
R=33500
415.2197
R=37200
425.1869
R=50400
438.2062
R=49107
446.1955
R=52107
458.2643
R=49702

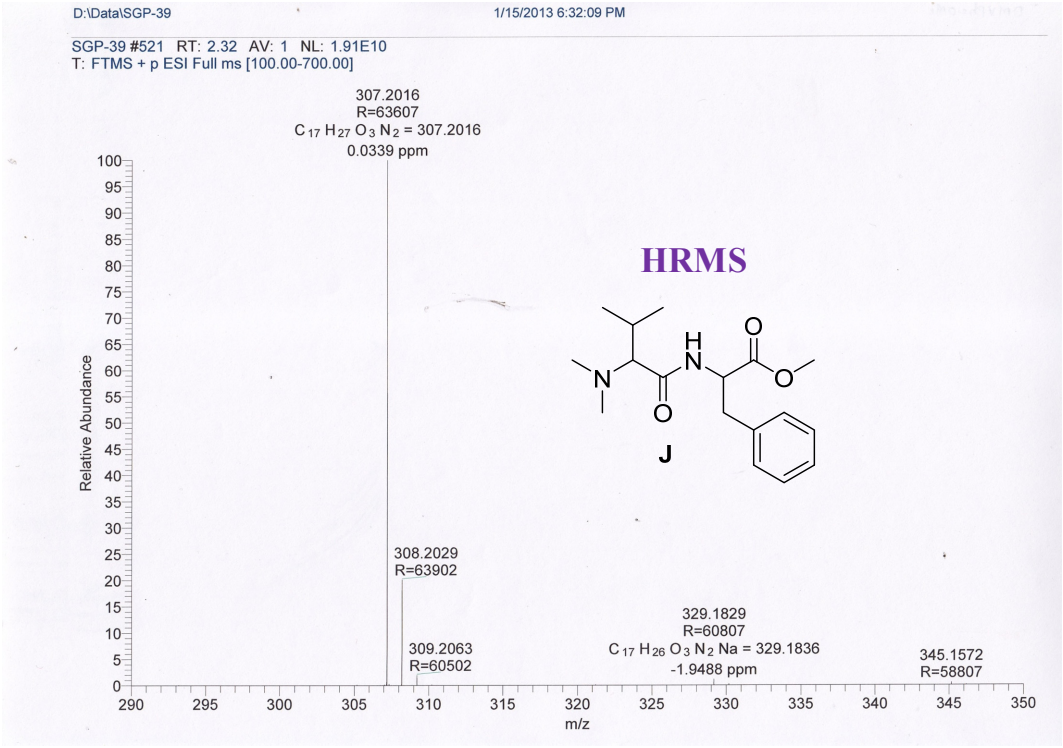
D:\Data\SGP-39
1/15/2013 6:32:09 PM
SGP-39 #521 RT: 2.32 AV: 1 NL: 1.91E10
T: FTMS + p ESI Full ms [100.00-700.00]
307.2016
R=63607
C 17 H 27 O 3 N 2 = 307.2016
0.0339 ppm
HRMS
J
308.2029
R=63902
309.2063
R=60502
329.1829
R=60807
C 17 H 26 O 3 N 2 Na = 329.1836
-1.9488 ppm
345.1572
R=58807
Relative Abundance
m/z

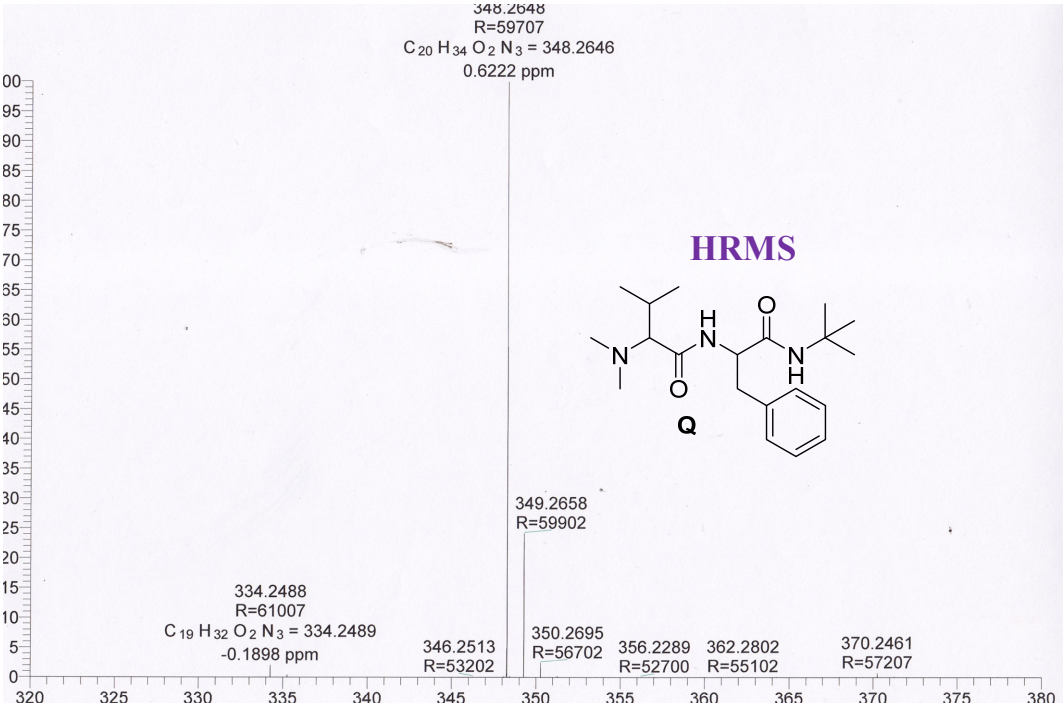
348.2648
R=59707
C 20 H 34 O 2 N 3 = 348.2646
0.6222 ppm
HRMS
Q
349.2658
R=59902
334.2488
R=61007
C 19 H 32 O 2 N 3 = 334.2489
-0.1898 ppm
346.2513
R=53202
350.2695
R=56702
356.2289
R=52700
362.2802
R=55102
370.2461
R=57207

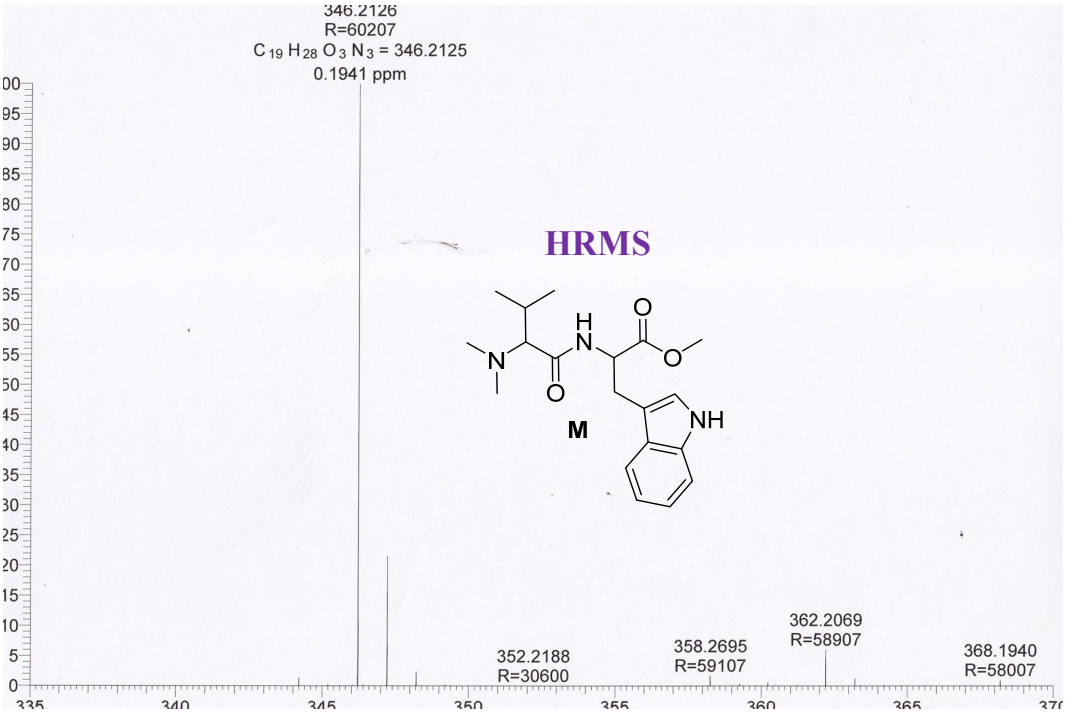
346.2126
R=60207
C 19 H 28 O 3 N 3 = 346.2125
0.1941 ppm
HRMS
M
352.2188
R=30600
358.2695
R=59107
362.2069
R=58907
368.1940
R=58007

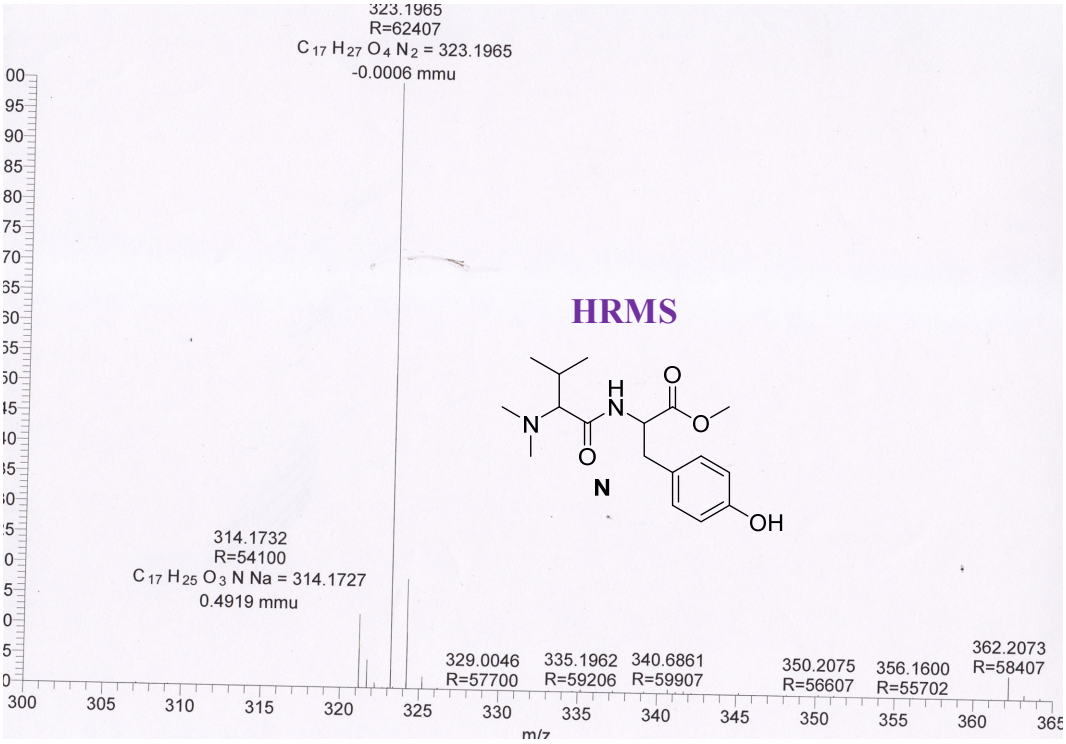
323.1965
R=62407
C 17 H 27 O 4 N 2 = 323.1965
-0.0006 mmu
HRMS
N
314.1732
R=54100
C 17 H 25 O 3 N Na = 314.1727
0.4919 mmu
329.0046
R=57700
335.1962
R=59206
340.6861
R=59907
350.2075
R=56607
356.1600
R=55702
362.2073
R=58407
m/z

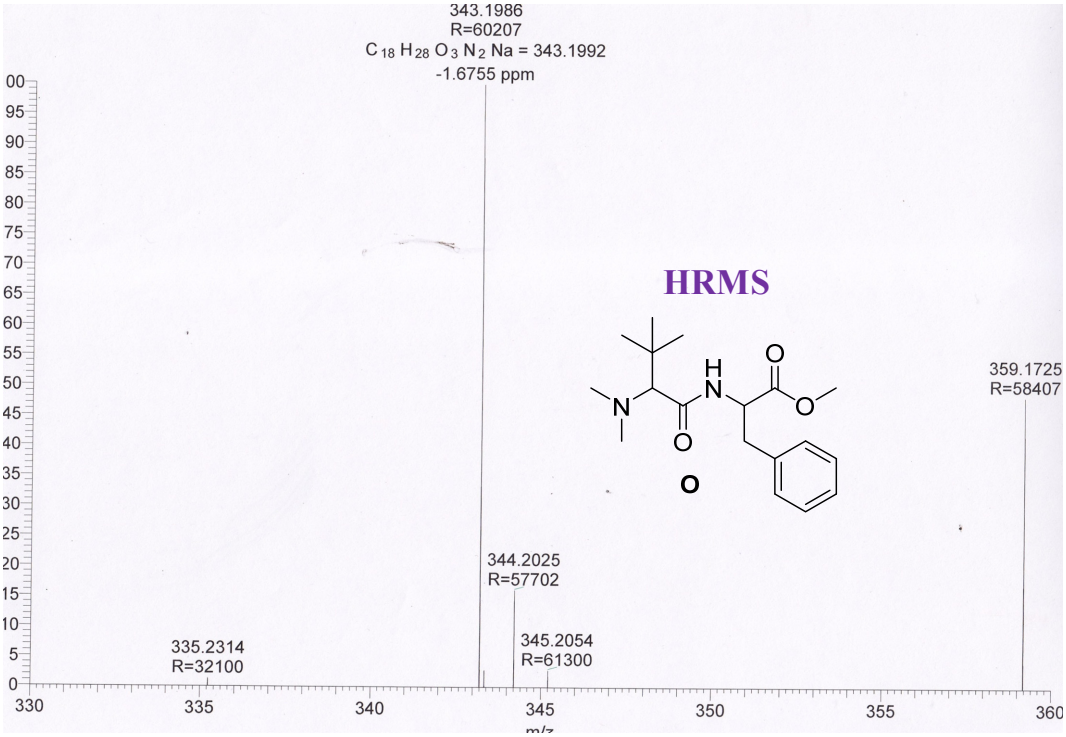
343.1986
R=60207
C 18 H 28 O 3 N 2 Na = 343.1992
-1.6755 ppm
HRMS
359.1725
R=58407
344.2025
R=57702
345.2054
R=61300
335.2314
R=32100
O
m/z

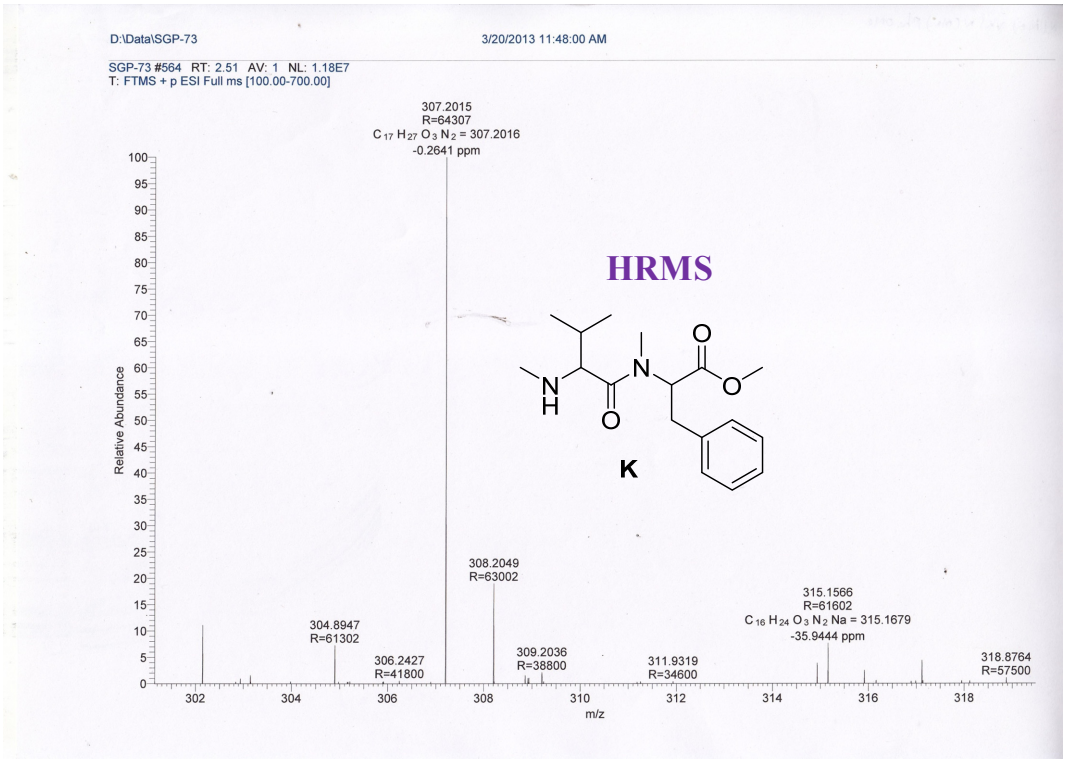
D:\Data\SGP-73
3/20/2013 11:48:00 AM
SGP-73 #564 RT: 2.51 AV: 1 NL: 1.18E7
T: FTMS + p ESI Full ms [100.00-700.00]
307.2015
R=64307
C 17 H 27 O 3 N 2 = 307.2016
-0.2641 ppm
HRMS
K
Relative Abundance
308.2049
R=63002
315.1566
R=61602
C 16 H 24 O 3 N 2 Na = 315.1679
-35.9444 ppm
304.8947
R=61302
306.2427
R=41800
309.2036
R=38800
311.9319
R=34600
318.8764
R=57500
m/z

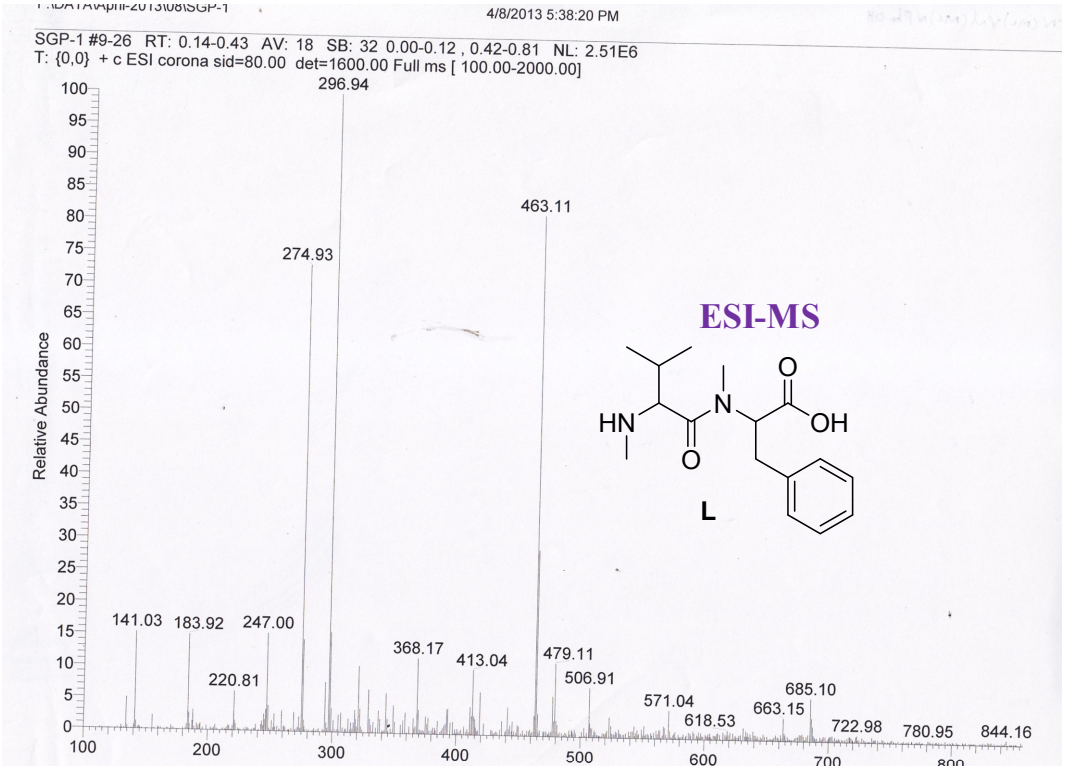
4/8/2013 5:38:20 PM
SGP-1 #9-26 RT: 0.14-0.43 AV: 18 SB: 32 0.00-0.12 , 0.42-0.81 NL: 2.51E6
T: {0,0} + c ESI corona sid=80.00 det=1600.00 Full ms [100.00-2000.00]
Relative Abundance
296.94
463.11
274.93
141.03
183.92
247.00
220.81
368.17
413.04
479.11
506.91
571.04
618.53
663.15
685.10
722.98
780.95
844.16
ESI-MS
HN
N
O
OH
O
L

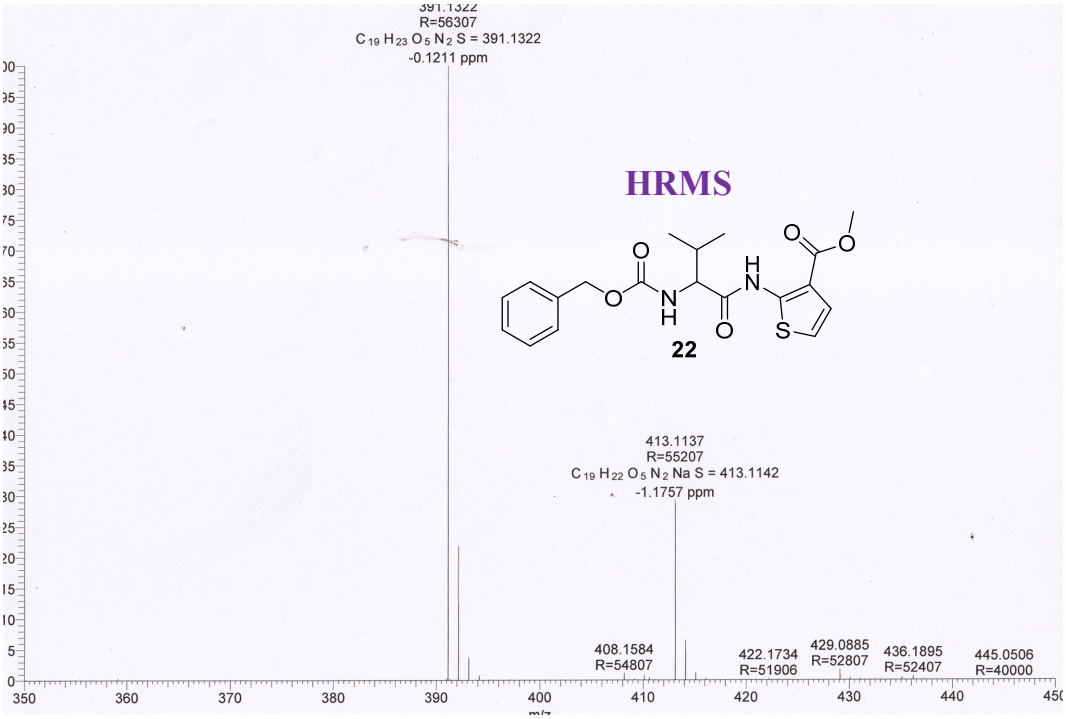
391.1322
R=56307
C 19 H 23 O 5 N 2 S = 391.1322
-0.1211 ppm
HRMS
O
O
N
H
H
N
O
O
O
S
22
413.1137
R=55207
C 19 H 22 O 5 N 2 Na S = 413.1142
-1.1757 ppm
408.1584
R=54807
422.1734
R=51906
429.0885
R=52807
436.1895
R=52407
445.0506
R=40000

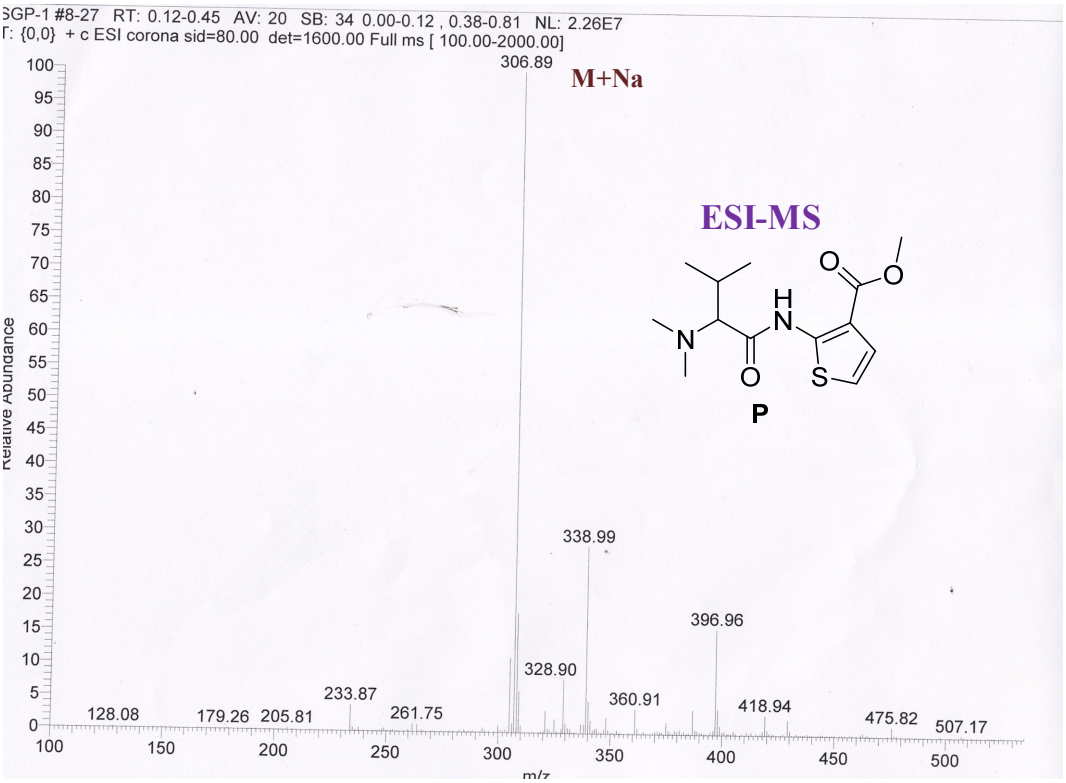
SGP-1 #8-27 RT: 0.12-0.45 AV: 20 SB: 34 0.00-0.12 , 0.38-0.81 NL: 2.26E7
T: {0,0} + c ESI corona sid=80.00 det=1600.00 Full ms [100.00-2000.00]
306.89
M+Na
ESI-MS
338.99
396.96
328.90
360.91
233.87
418.94
128.08
179.26
205.81
261.75
475.82
507.17
Relative Abundance
m/z
P

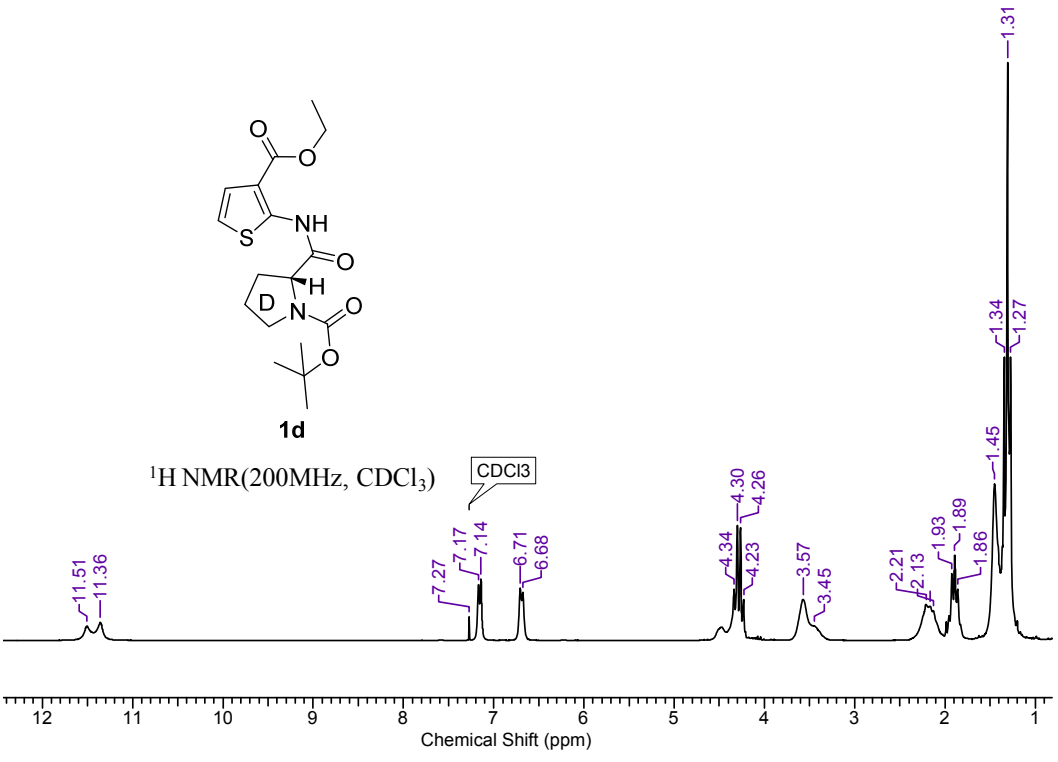
1d
1H NMR(200MHz, CDCl3)
CDCl3
11.51
11.36
7.27
7.17
7.14
6.71
6.68
4.34
4.30
4.26
4.23
3.57
3.45
2.21
2.13
1.93
1.89
1.86
1.45
1.34
1.31
1.27
Chemical Shift (ppm)

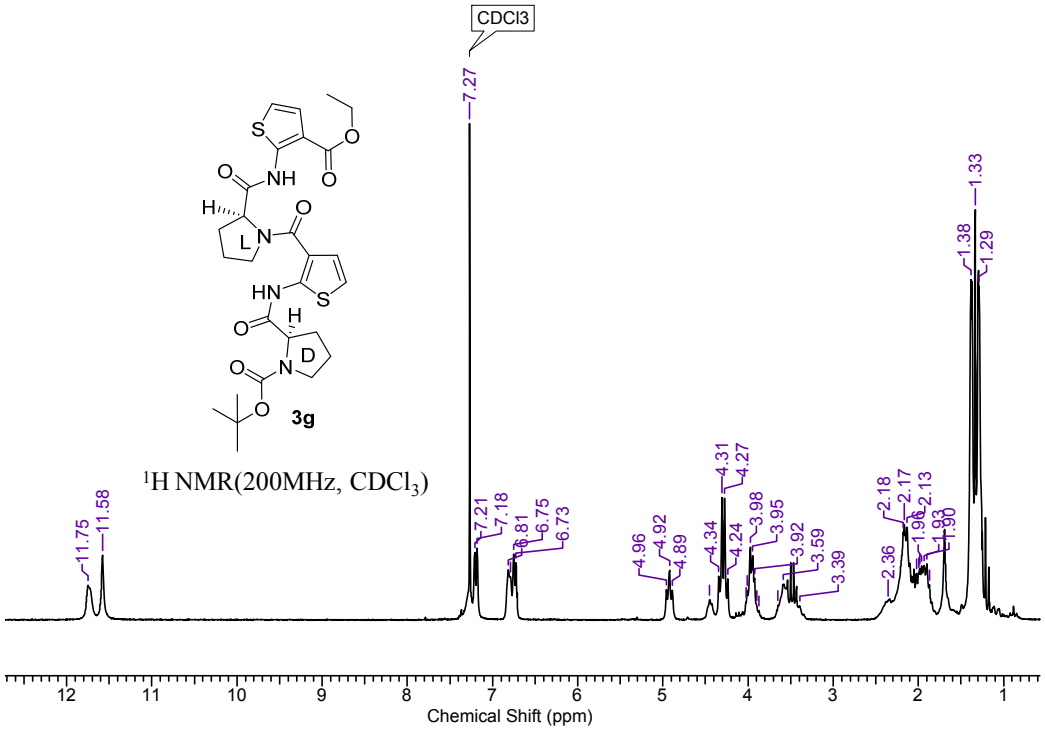
CDCl3
7.27
1.33
1.38
1.29
11.75
11.58
7.21
7.18
6.81
6.75
6.73
4.96
4.92
4.89
4.34
4.31
4.27
4.24
3.98
3.95
3.92
3.59
3.39
2.36
2.18
2.17
2.13
1.96
1.93
1.90
3g
1H NMR(200MHz, CDCl3)
Chemical Shift (ppm)

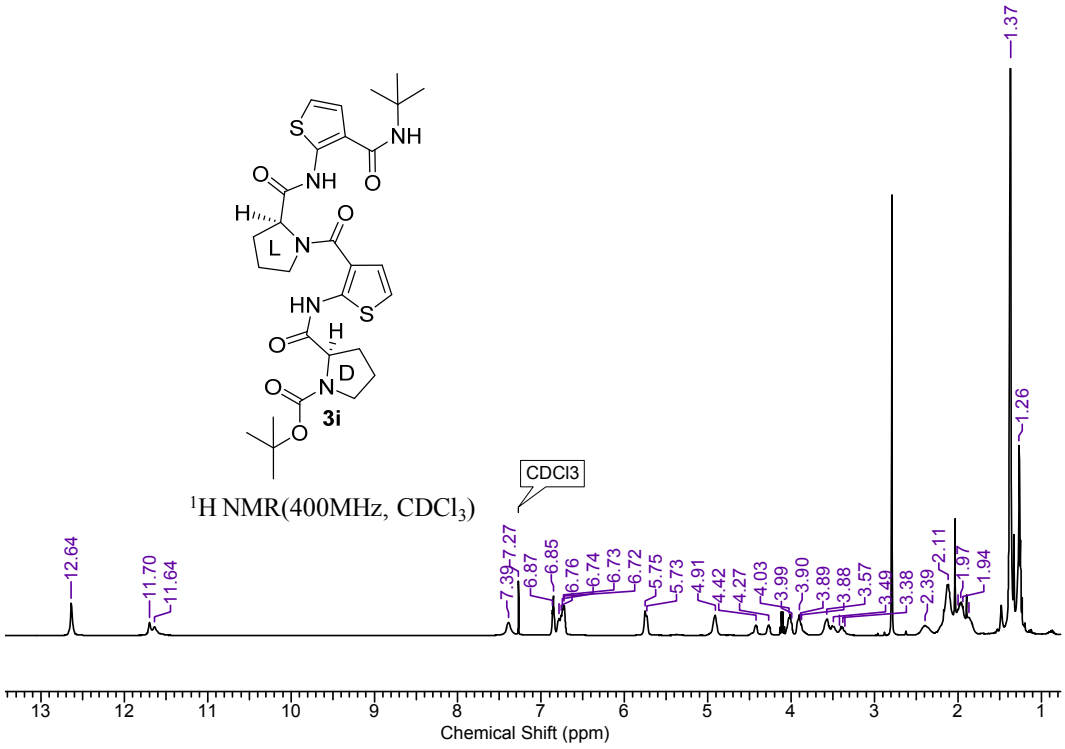
1.37
1.26
CDCl3
12.64
11.70
11.64
7.39
7.27
6.87
6.85
6.76
6.74
6.73
6.72
5.75
5.73
4.91
4.42
4.27
4.03
3.99
3.90
3.89
3.88
3.57
3.49
3.38
2.39
2.11
1.97
1.94
3i
1H NMR(400MHz, CDCl3)
Chemical Shift (ppm)

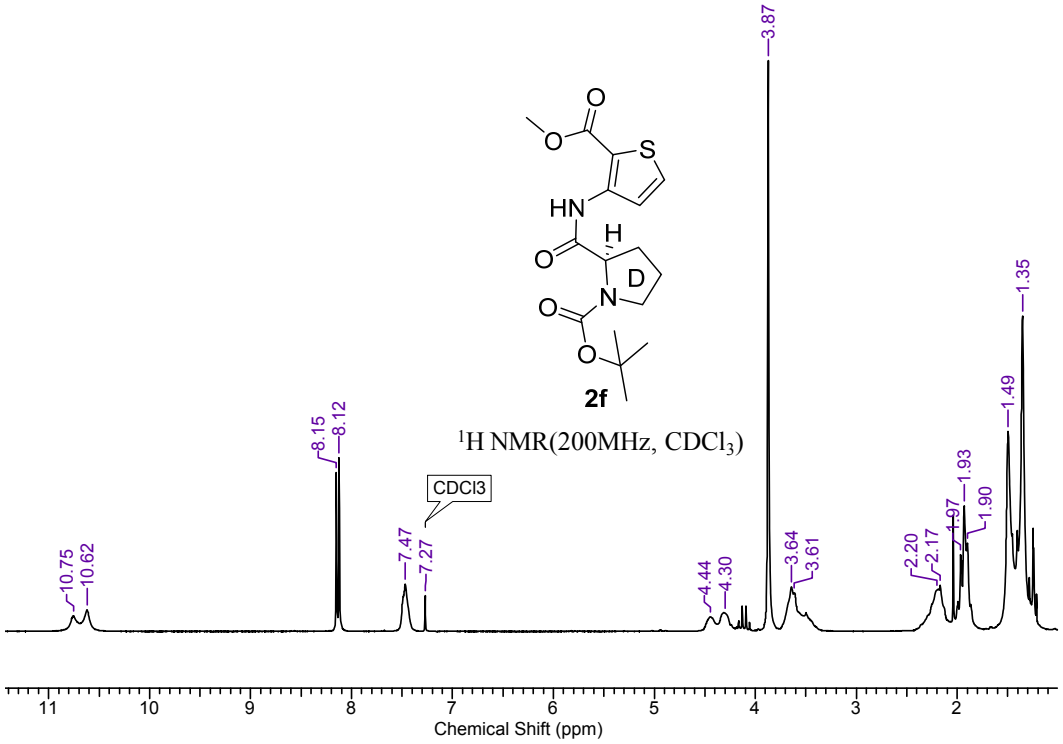
2f
^{1}H NMR(200MHz, $CDCl_3$)
CDCl3
Chemical Shift (ppm)

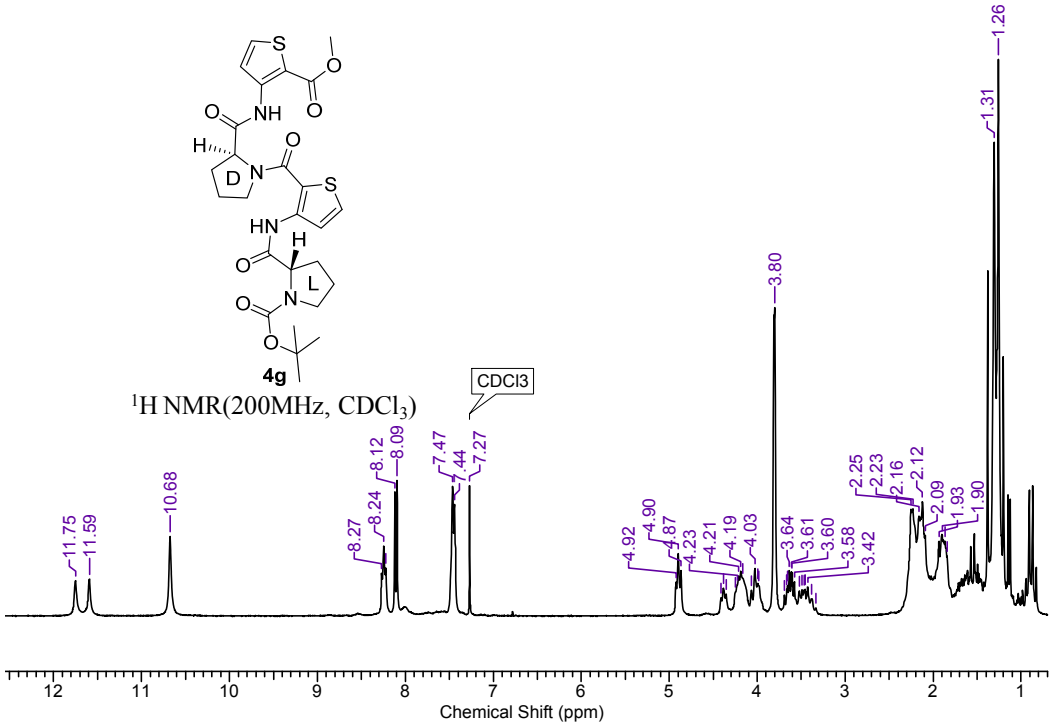
4g
^{1}H NMR(200MHz, $CDCl_3$)
CDCl3
Chemical Shift (ppm)

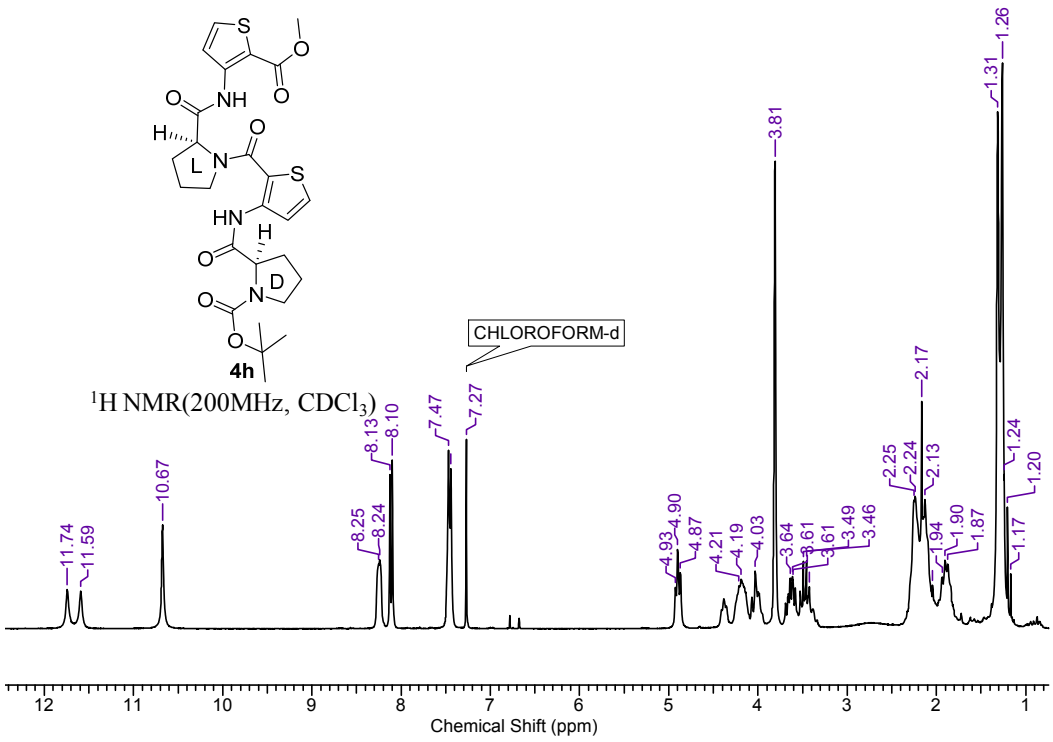
4h
^{1}H NMR(200MHz, $CDCl_3$)
CHLOROFORM-d
11.74
11.59
10.67
8.25
8.24
8.13
8.10
7.47
7.27
4.93
4.90
4.87
4.21
4.19
4.03
3.81
3.64
3.61
3.61
3.49
3.46
2.25
2.24
2.17
2.13
1.94
1.90
1.87
1.31
1.26
1.24
1.20
1.17
Chemical Shift (ppm)

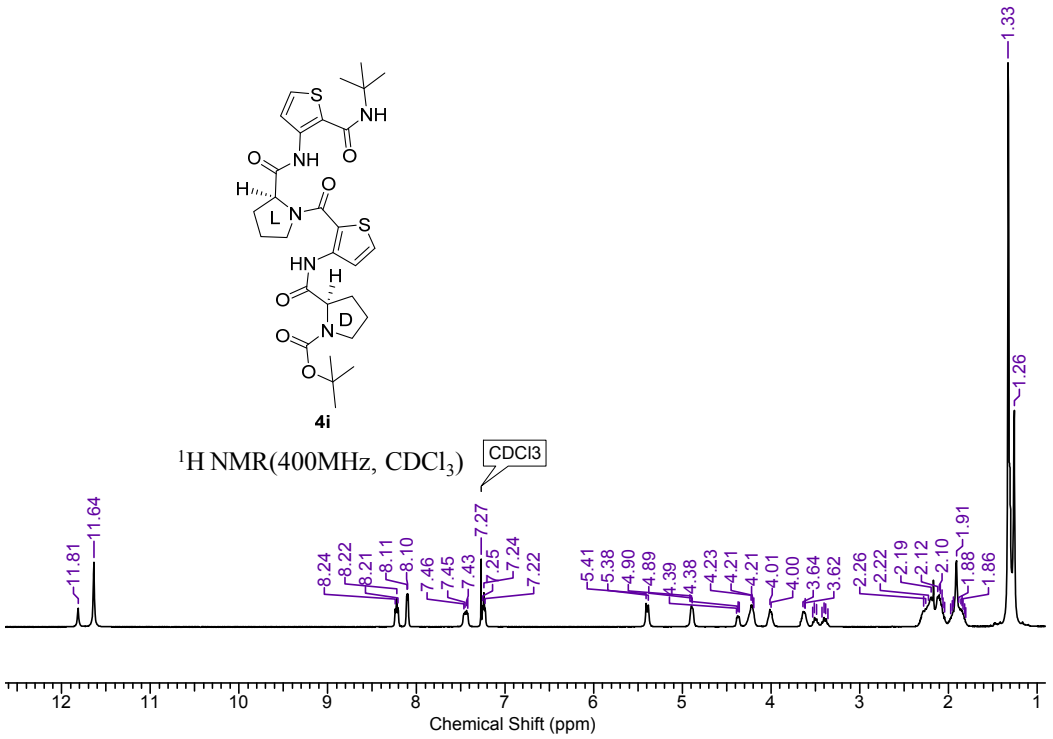
4i
^{1}H NMR(400MHz, $CDCl_3$)
CDCl3
11.81
11.64
8.24
8.22
8.21
8.11
8.10
7.46
7.45
7.43
7.27
7.25
7.24
7.22
5.41
5.38
4.90
4.89
4.39
4.38
4.23
4.21
4.21
4.01
4.00
3.64
3.62
2.26
2.22
2.19
2.12
2.10
1.91
1.88
1.86
1.33
1.26
Chemical Shift (ppm)

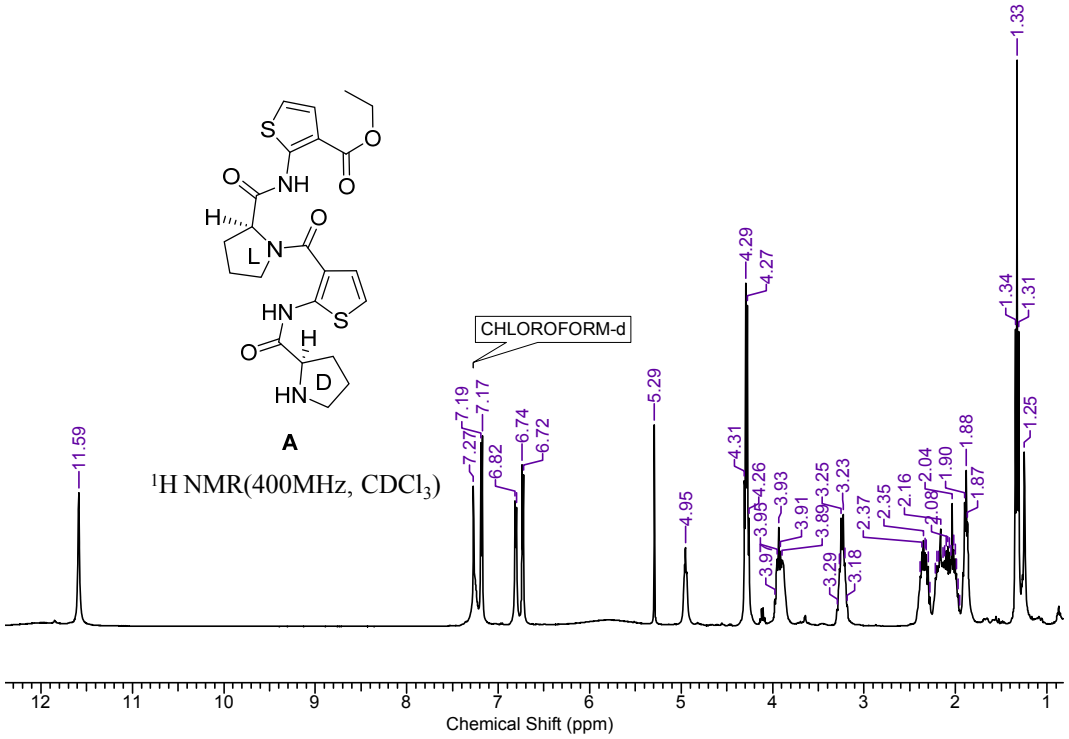
A
^{1}H NMR(400MHz, $CDCl_3$)
CHLOROFORM-d
Chemical Shift (ppm)

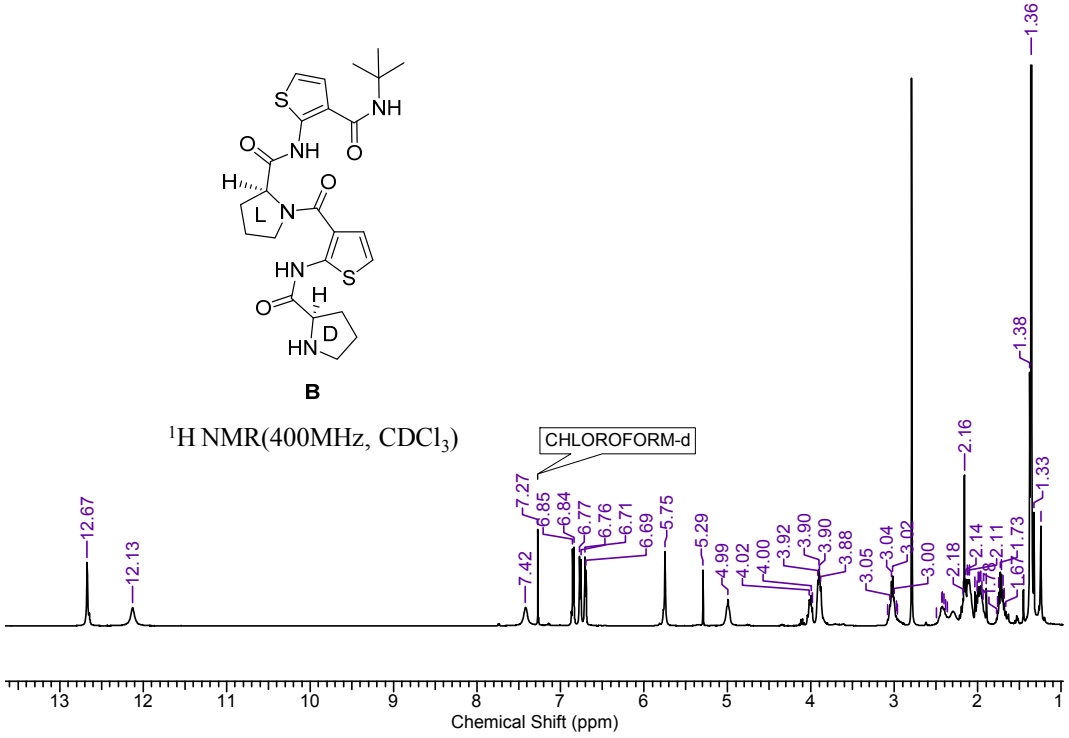
B
^{1}H NMR(400MHz, $CDCl_3$)
CHLOROFORM-d
Chemical Shift (ppm)

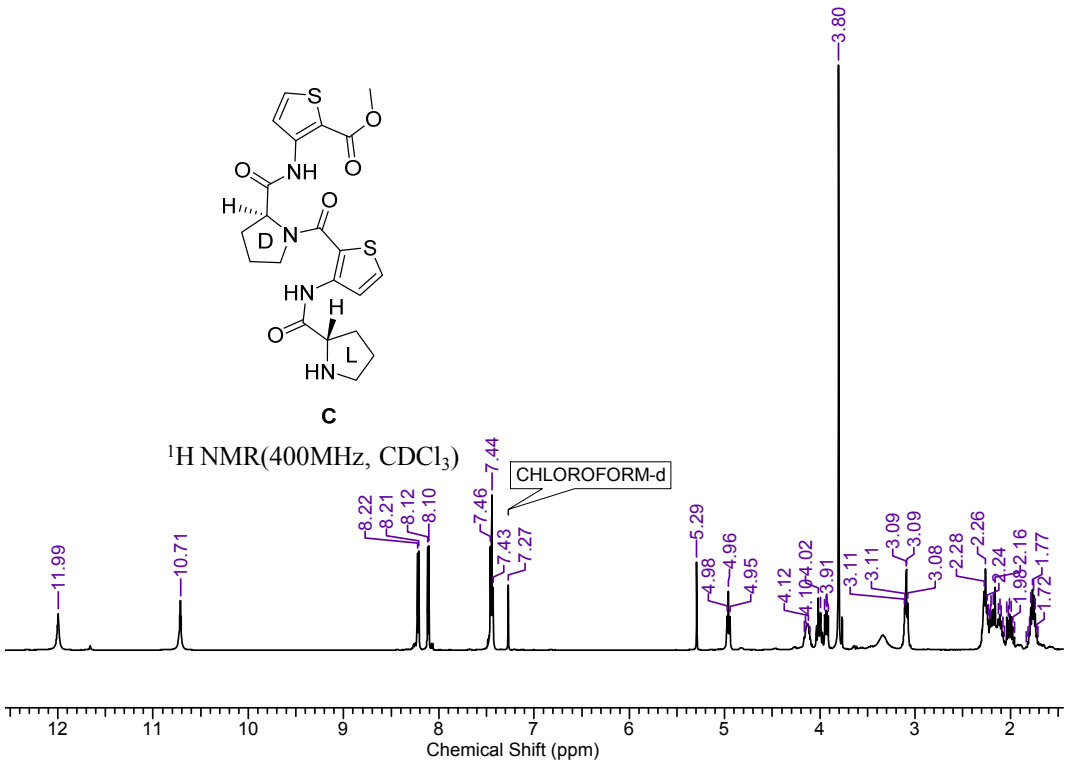
C
^{1}H NMR(400MHz, CDCl$_3$)
CHLOROFORM-d
Chemical Shift (ppm)

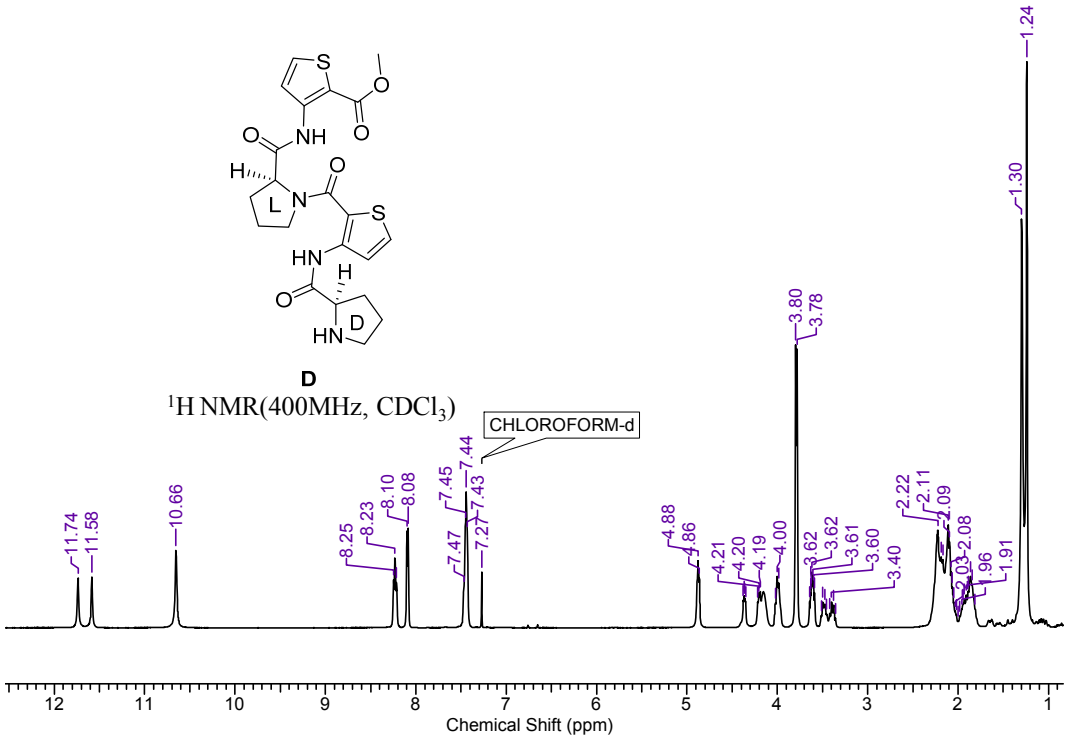
D
^{1}H NMR(400MHz, CDCl$_3$)
CHLOROFORM-d
Chemical Shift (ppm)

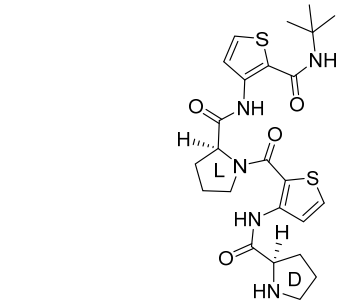

E

^{1}H NMR(400MHz, $CDCl_3$)

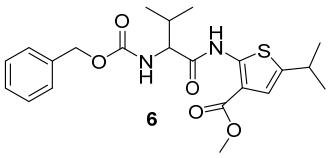

6

^{1}H NMR(200MHz, $CDCl_3$)

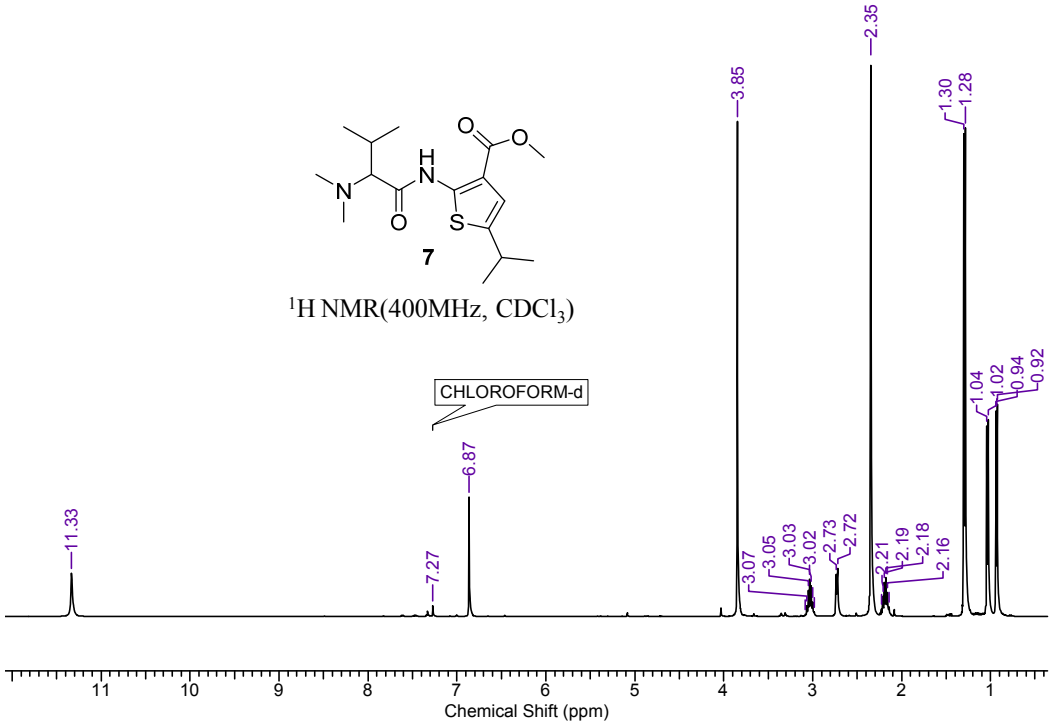
7
^{1}H NMR(400MHz, $CDCl_3$)
CHLOROFORM-d
11.33
7.27
6.87
3.85
2.35
1.30
1.28
1.04
1.02
0.94
0.92
3.07
3.05
3.03
3.02
2.73
2.72
2.21
2.19
2.18
2.16
Chemical Shift (ppm)

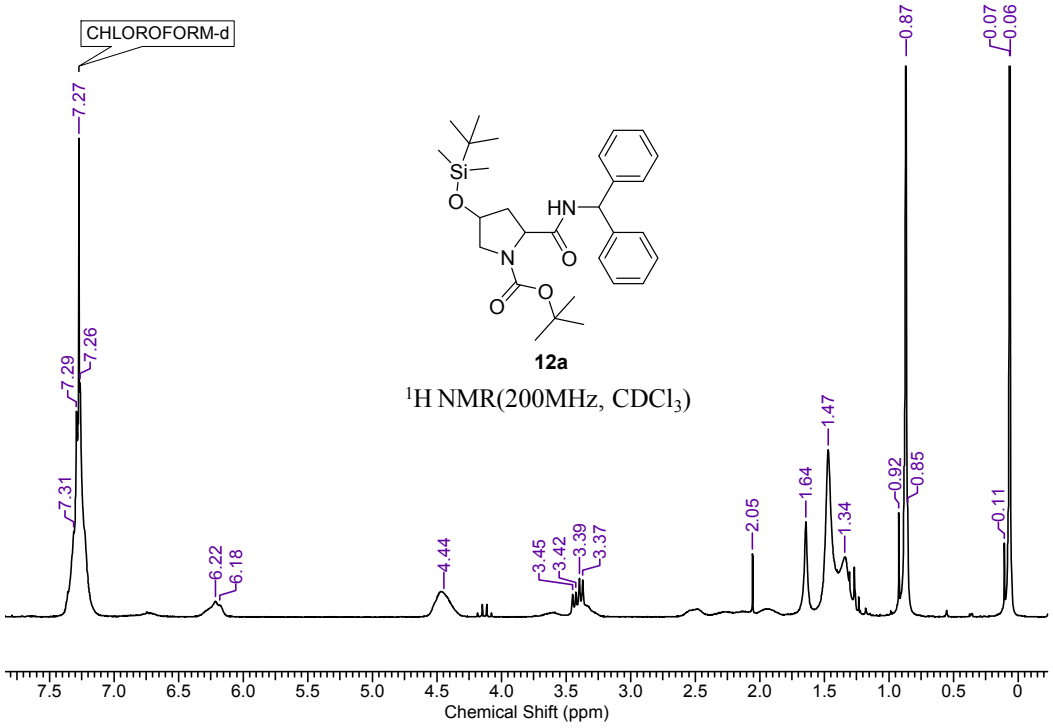
12a
^{1}H NMR(200MHz, $CDCl_3$)
CHLOROFORM-d
7.27
7.29
7.26
7.31
6.22
6.18
4.44
3.45
3.42
3.39
3.37
2.05
1.64
1.47
1.34
0.92
0.87
0.85
0.11
0.07
0.06
Chemical Shift (ppm)

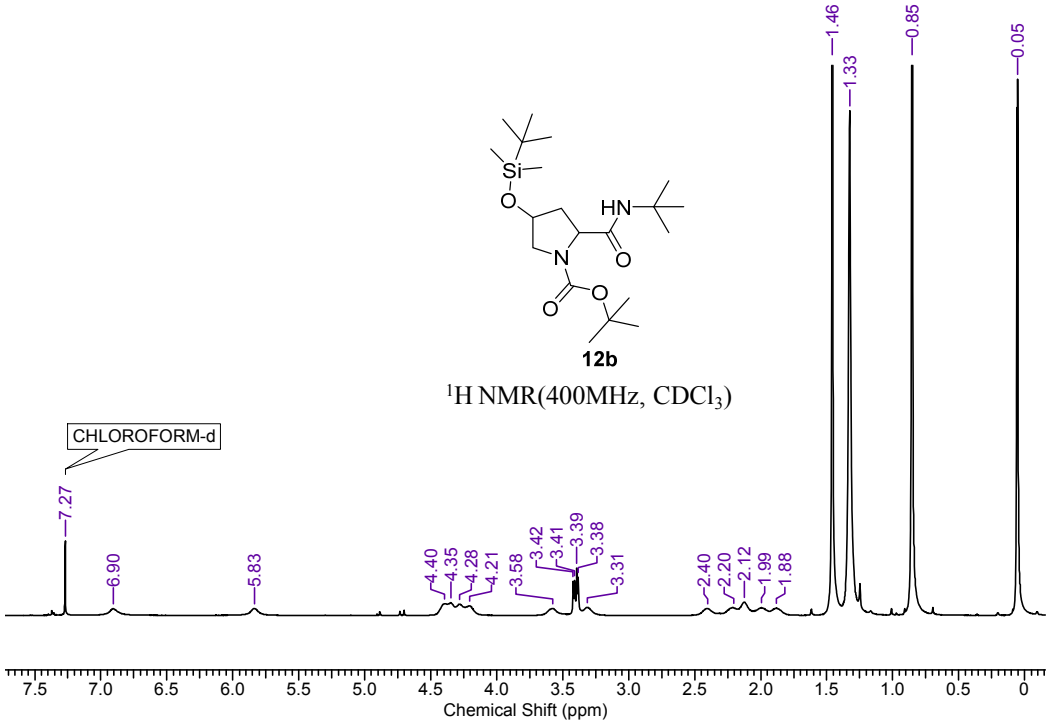

12b

^{1}H NMR(400MHz, $CDCl_3$)

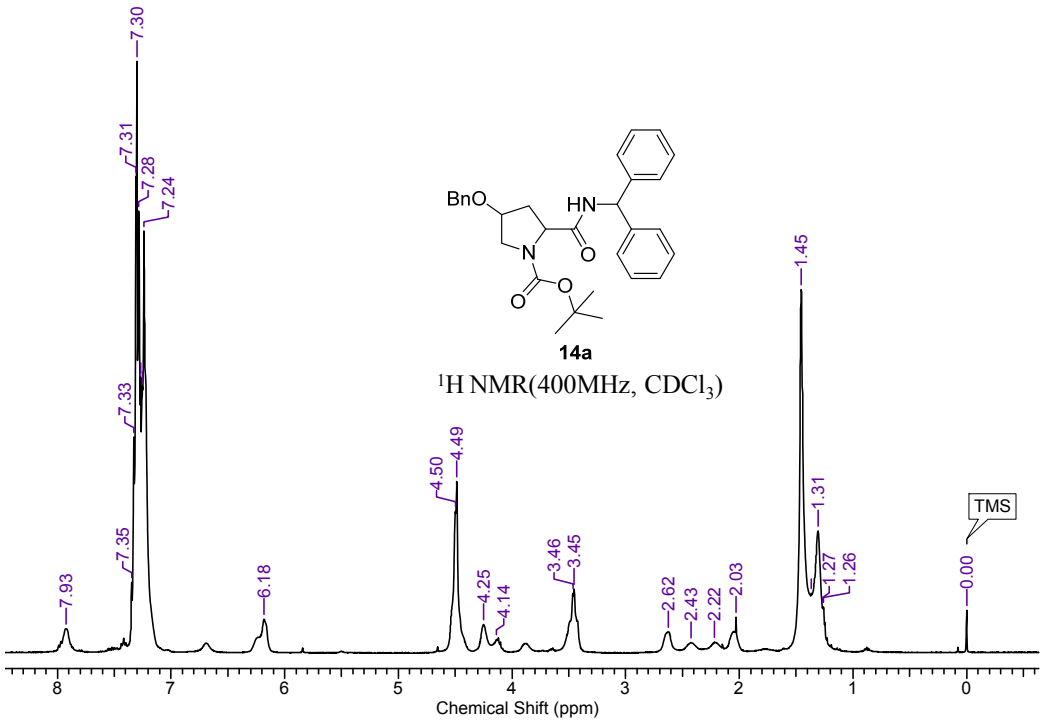

14a

^{1}H NMR(400MHz, $CDCl_3$)

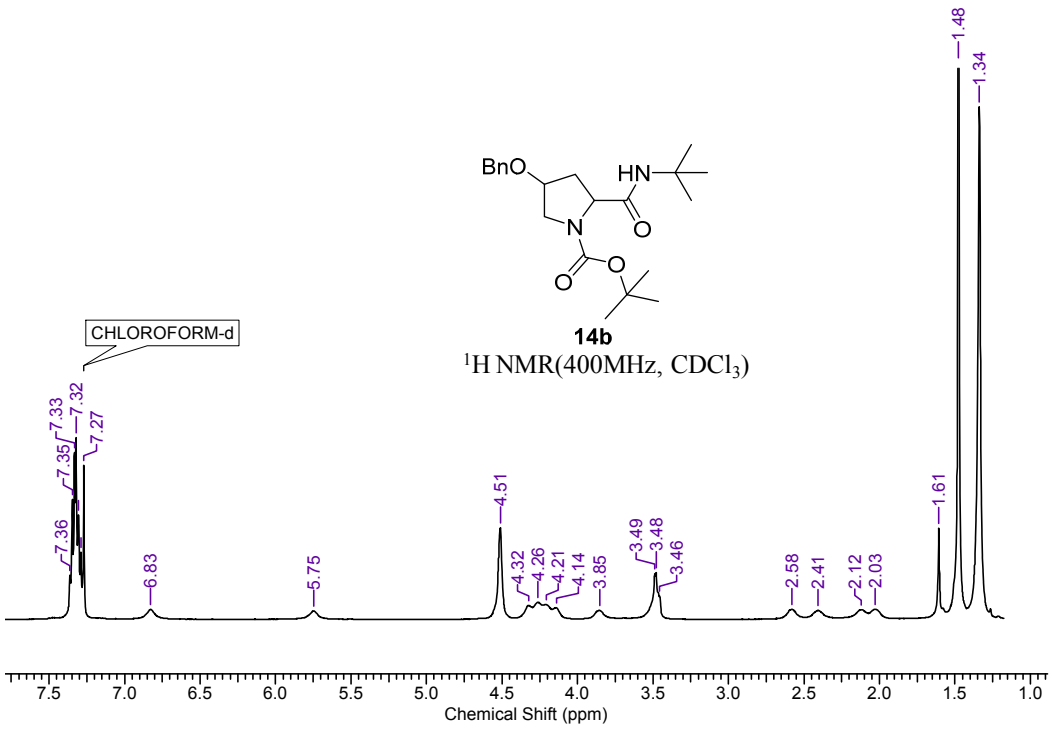
BnO
HN
N
O
O
O
14b
^{1}H NMR(400MHz, $CDCl_3$)
CHLOROFORM-d
7.33
7.32
7.35
7.27
7.36
6.83
5.75
4.51
4.32
4.26
4.21
4.14
3.85
3.49
3.48
3.46
2.58
2.41
2.12
2.03
1.61
1.48
1.34
Chemical Shift (ppm)

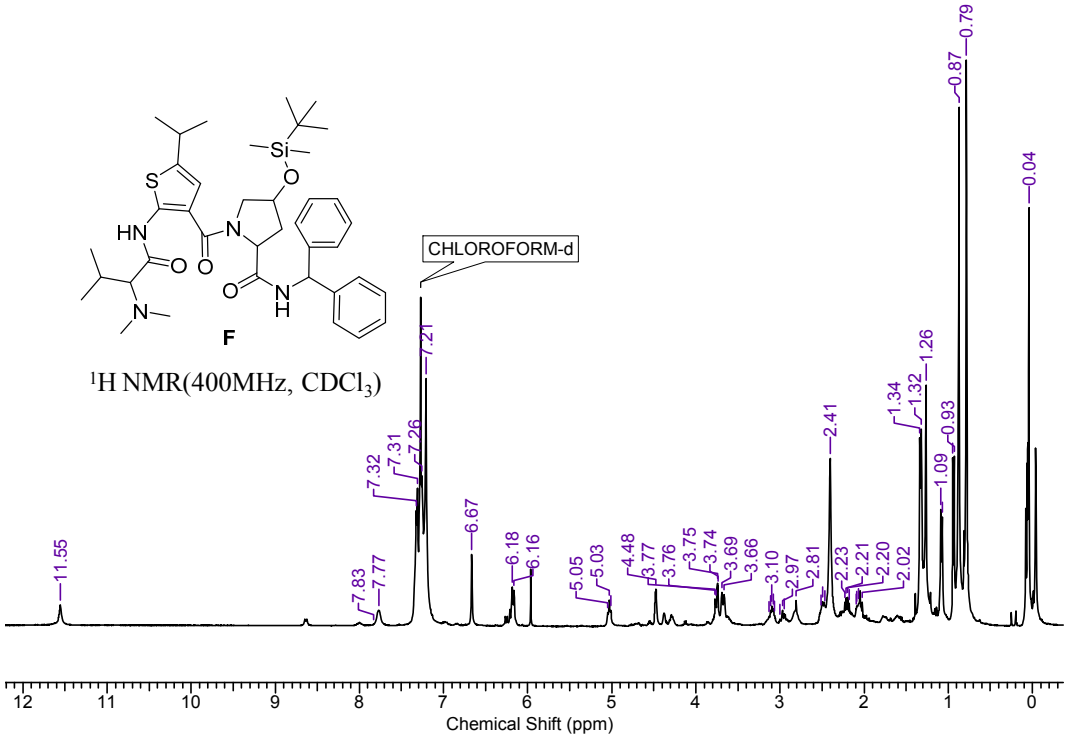
Si
O
S
HN
O
O
N
O
N
H
N
F
^{1}H NMR(400MHz, $CDCl_3$)
CHLOROFORM-d
11.55
7.83
7.77
7.32
7.31
7.26
7.21
6.67
6.18
6.16
5.05
5.03
4.48
3.77
3.76
3.75
3.74
3.69
3.66
3.10
2.97
2.81
2.41
2.23
2.21
2.20
2.02
1.34
1.32
1.26
1.09
0.93
0.87
0.79
0.04
Chemical Shift (ppm)

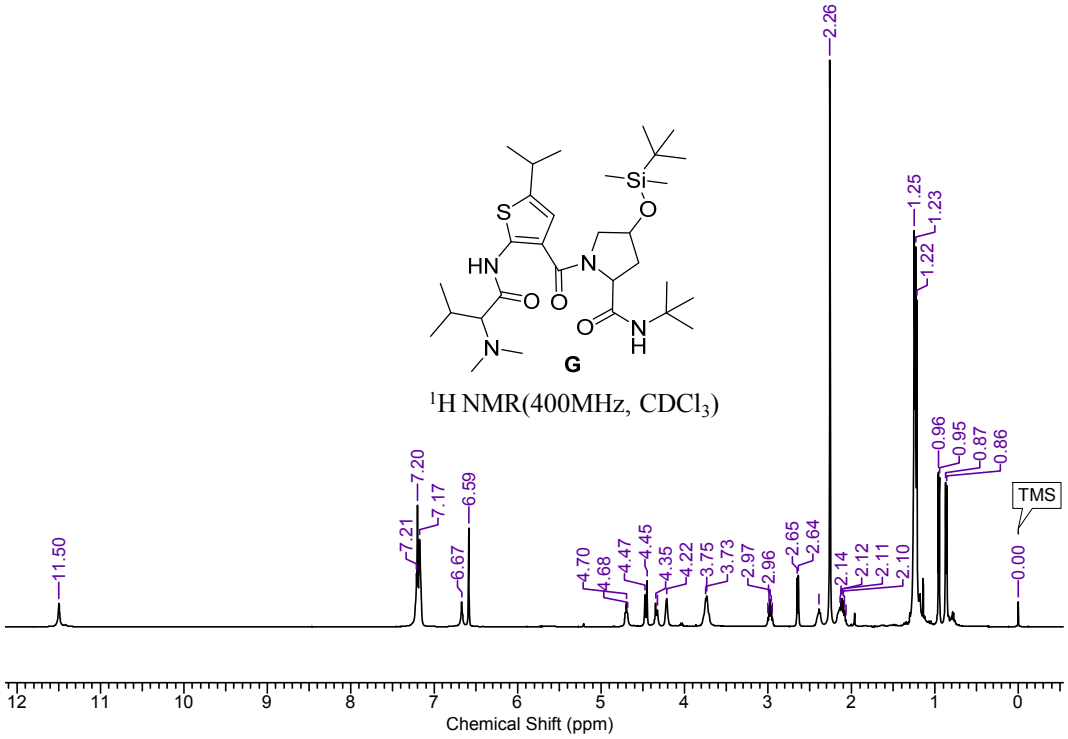
G
^{1}H NMR(400MHz, CDCl$_3$)
Chemical Shift (ppm)
TMS

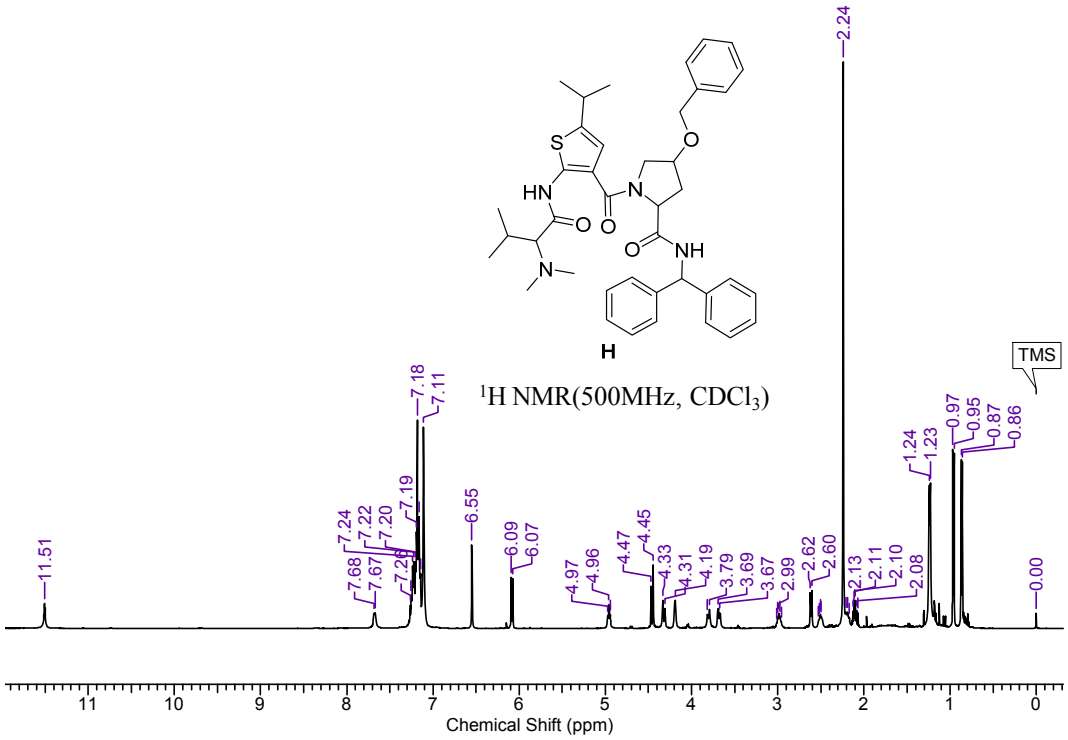
H
^{1}H NMR(500MHz, CDCl$_3$)
Chemical Shift (ppm)
TMS

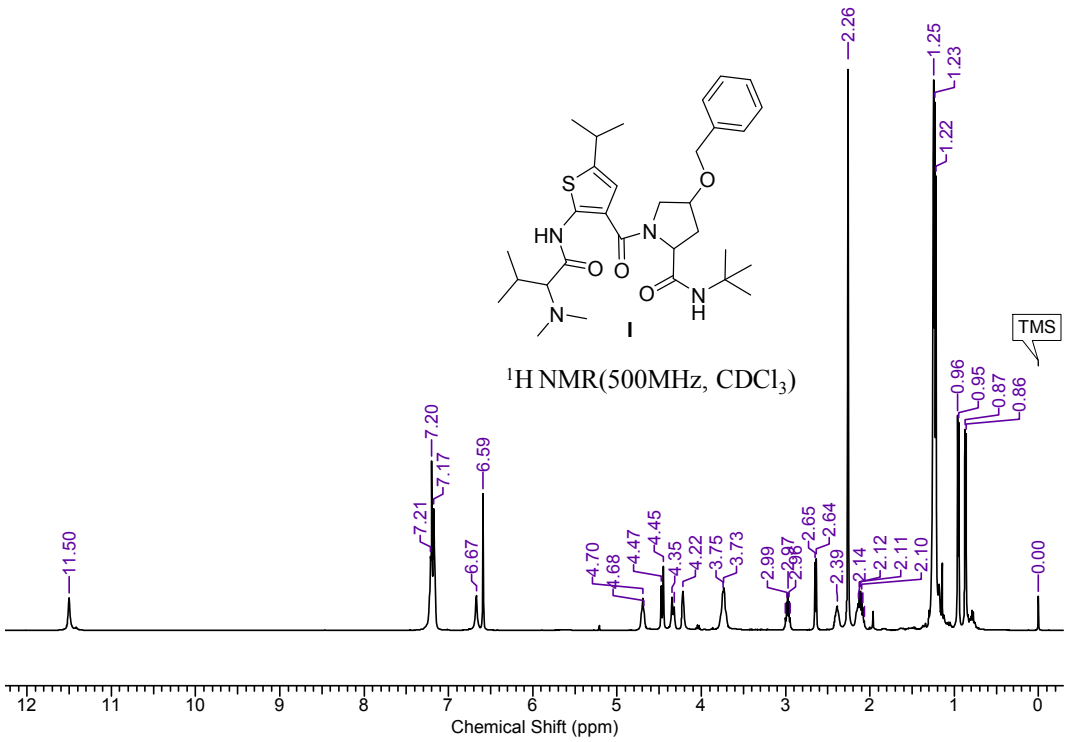
I
^{1}H NMR(500MHz, CDCl$_3$)
TMS
Chemical Shift (ppm)

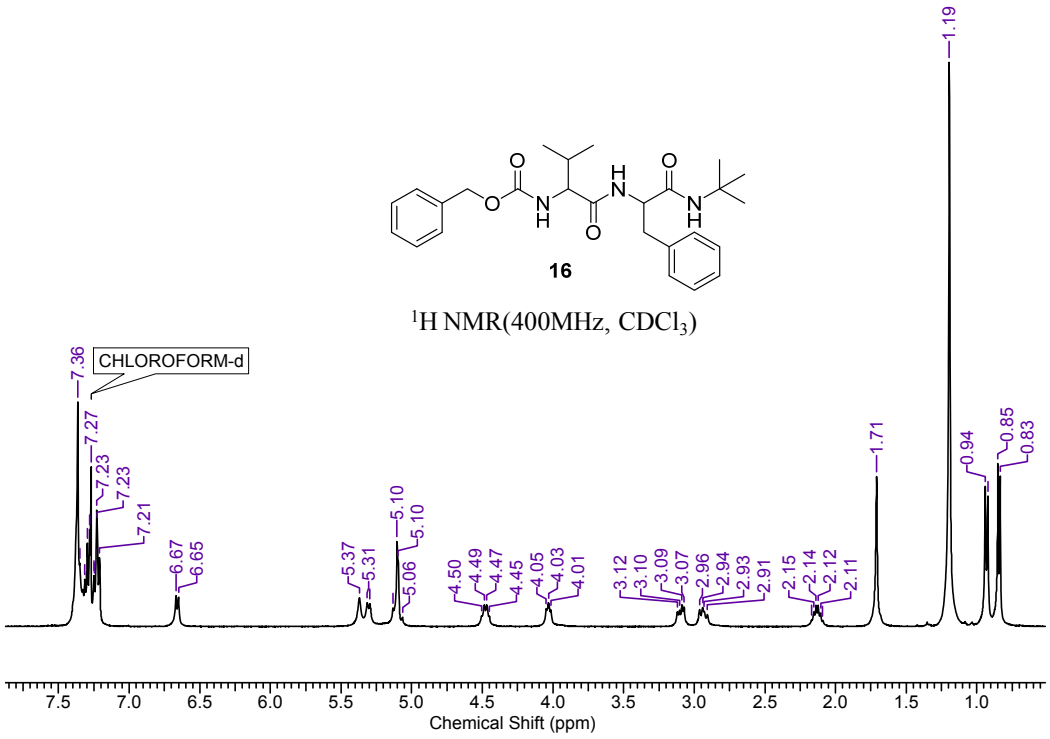
16
^{1}H NMR(400MHz, CDCl$_3$)
CHLOROFORM-d
Chemical Shift (ppm)

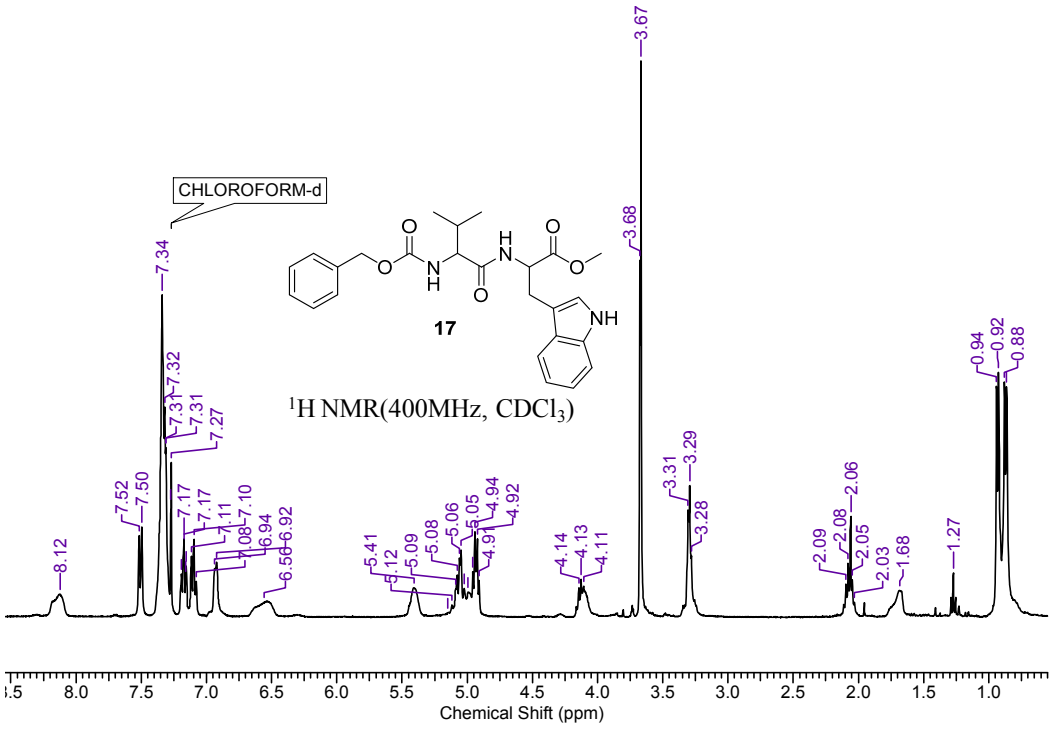
CHLOROFORM-d
17
^{1}H NMR(400MHz, $CDCl_3$)
Chemical Shift (ppm)

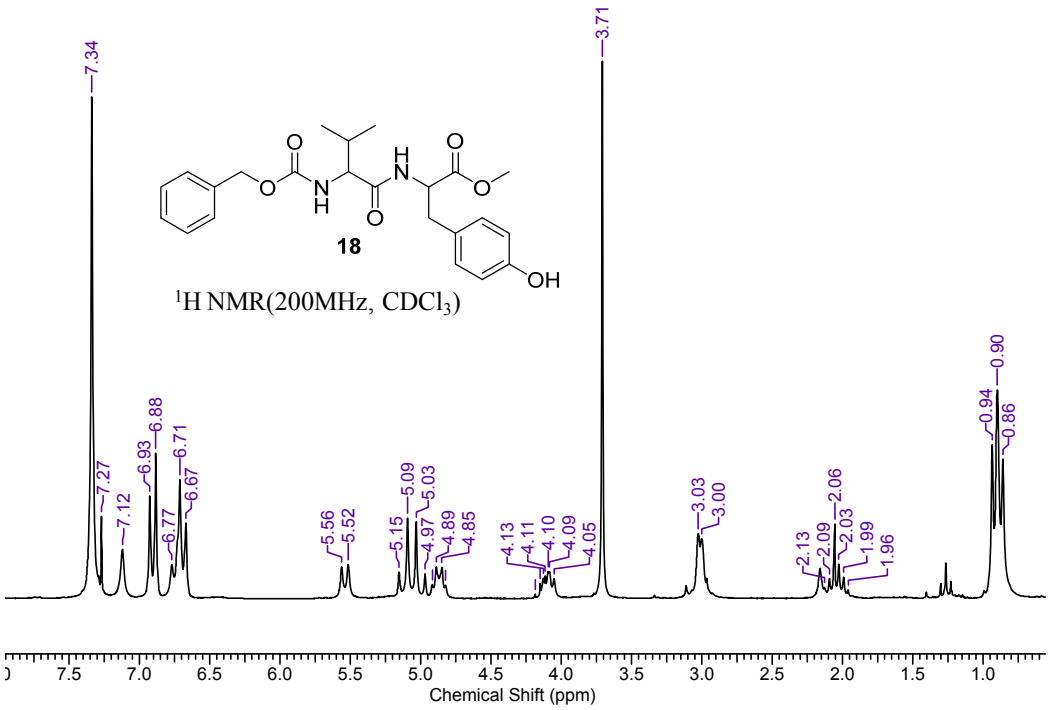
18
^{1}H NMR(200MHz, $CDCl_3$)
Chemical Shift (ppm)

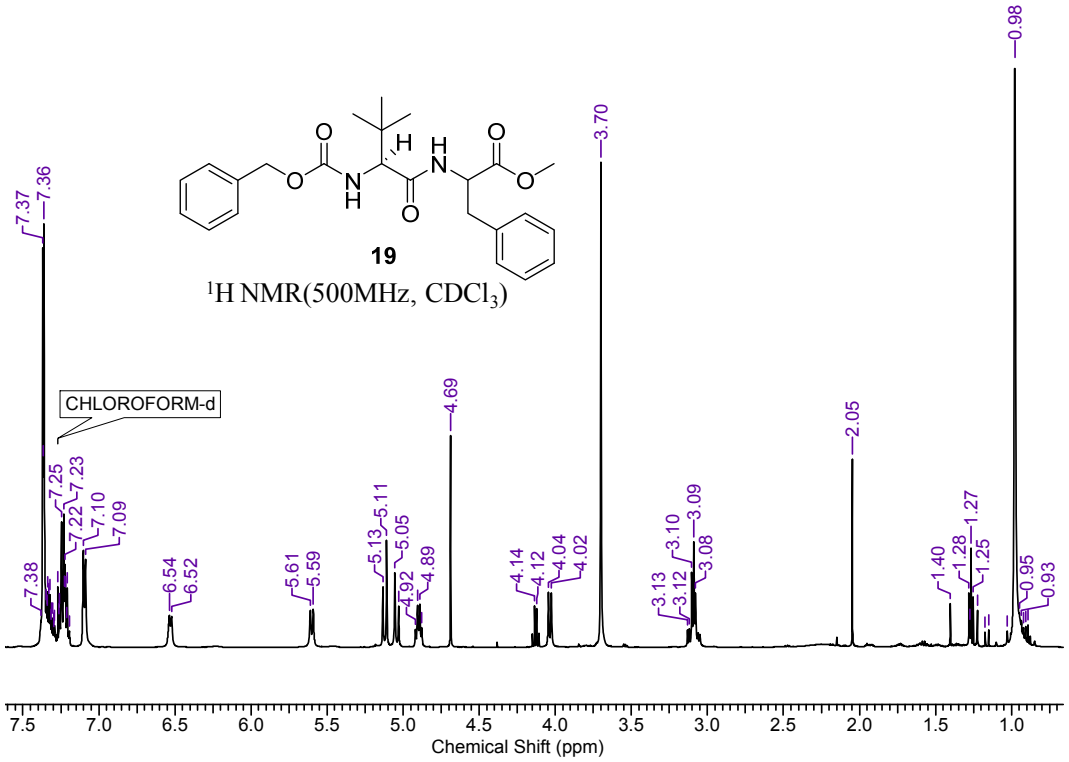
19
^{1}H NMR(500MHz, $CDCl_3$)
CHLOROFORM-d
Chemical Shift (ppm)

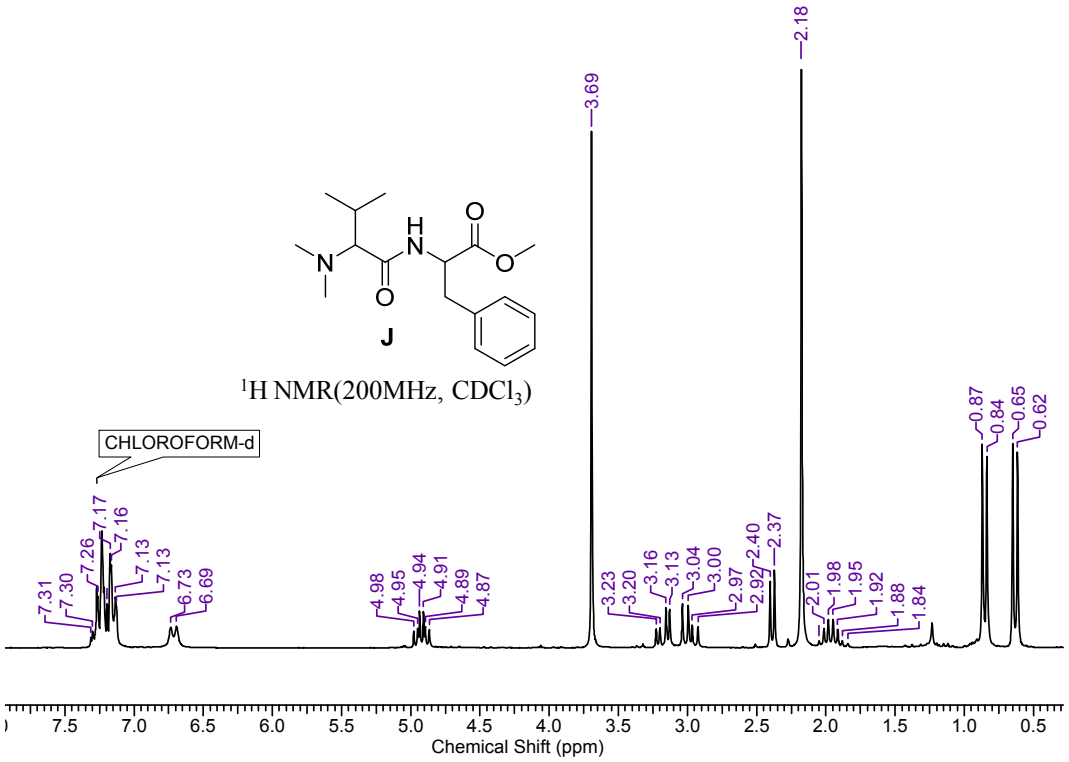
J
^{1}H NMR(200MHz, $CDCl_3$)
CHLOROFORM-d
Chemical Shift (ppm)

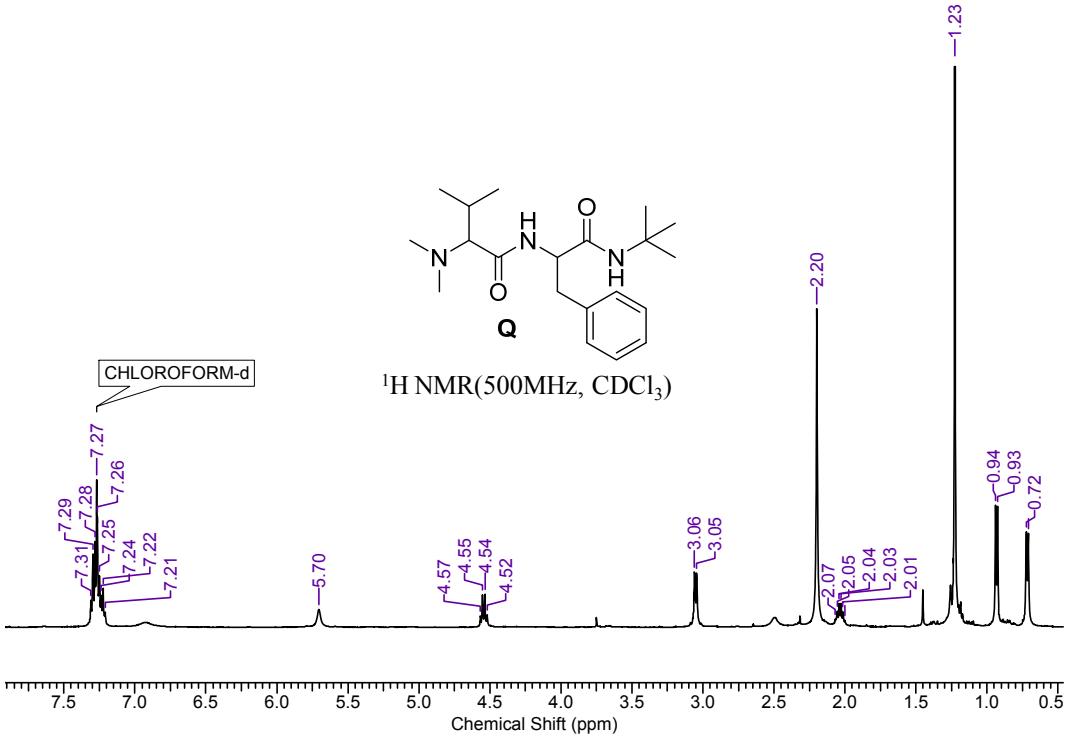
Q
^{1}H NMR(500MHz, $CDCl_3$)
CHLOROFORM-d
Chemical Shift (ppm)

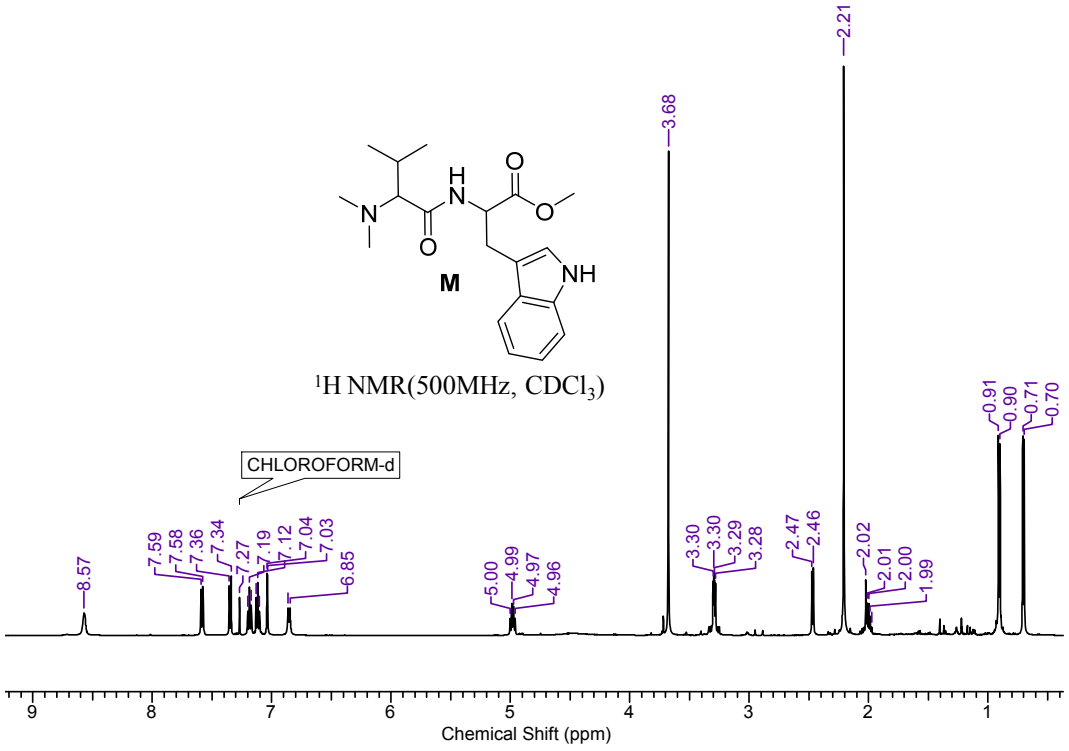
M
^{1}H NMR(500MHz, $CDCl_3$)
CHLOROFORM-d
Chemical Shift (ppm)

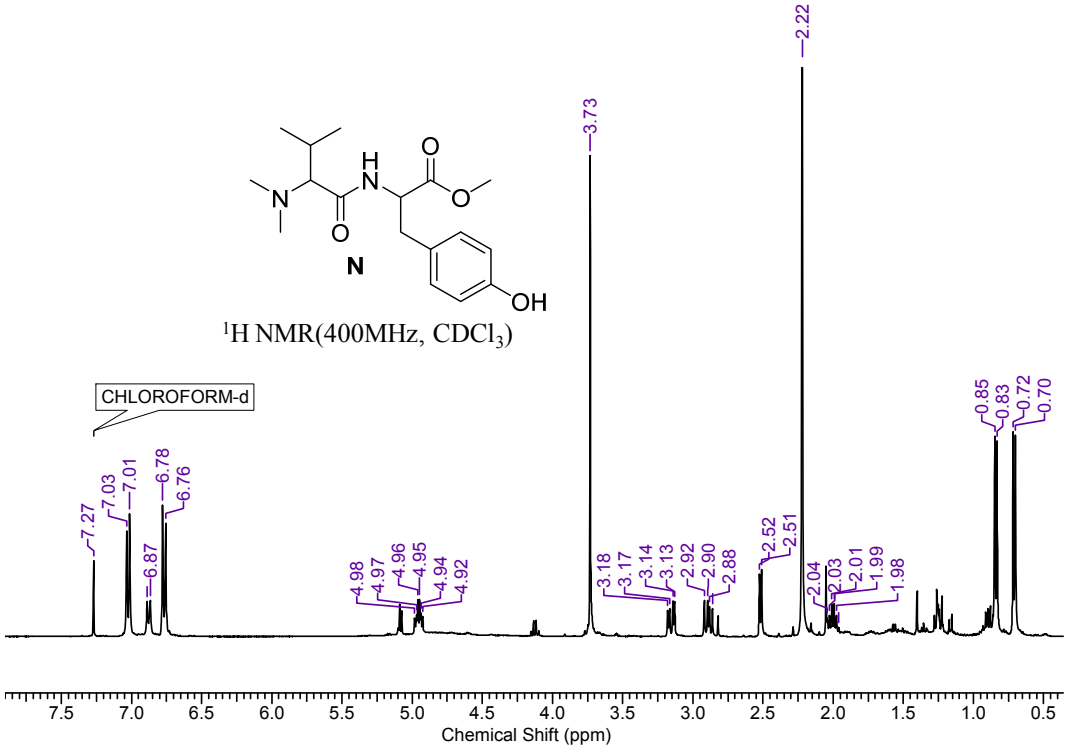
N
OH
^{1}H NMR(400MHz, $CDCl_3$)
CHLOROFORM-d
2.22
3.73
0.85
0.83
0.72
0.70
7.27
7.03
7.01
6.78
6.76
6.87
4.98
4.97
4.96
4.95
4.94
4.92
3.18
3.17
3.14
3.13
2.92
2.90
2.88
2.52
2.51
2.04
2.03
2.01
1.99
1.98
7.5 7.0 6.5 6.0 5.5 5.0 4.5 4.0 3.5 3.0 2.5 2.0 1.5 1.0 0.5
Chemical Shift (ppm)

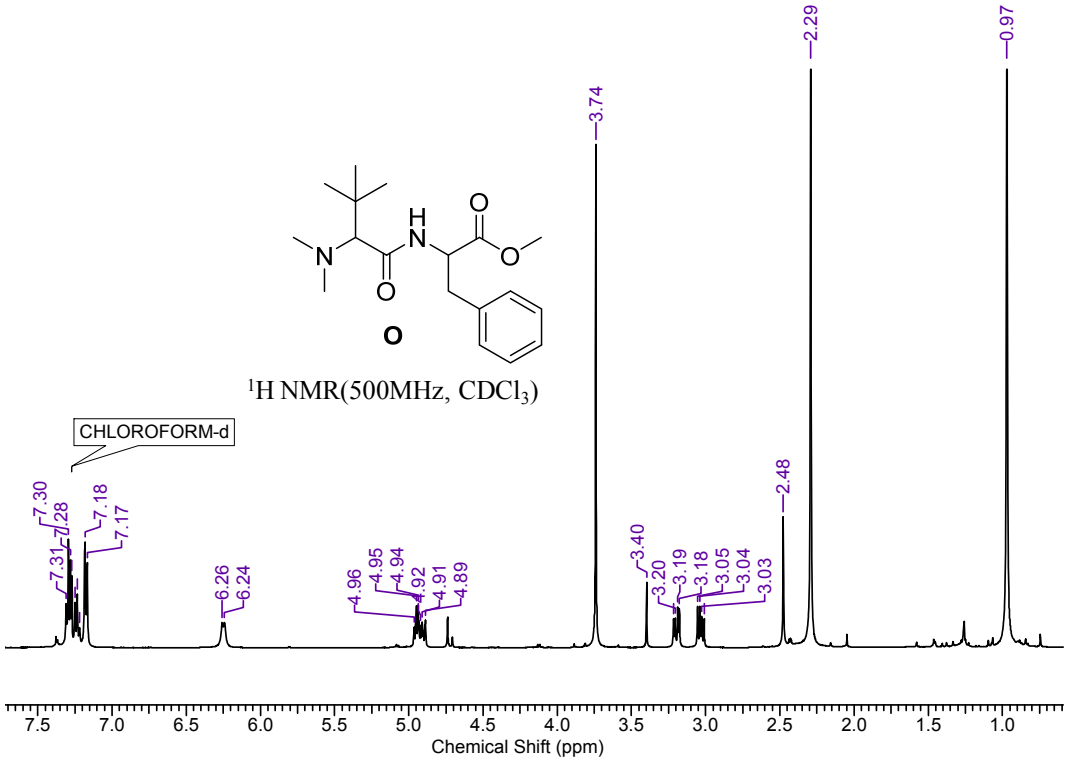
O
^{1}H NMR(500MHz, $CDCl_3$)
CHLOROFORM-d
2.29
0.97
3.74
7.30
7.28
7.18
7.17
7.31
6.26
6.24
4.96
4.95
4.94
4.92
4.91
4.89
3.40
3.20
3.19
3.18
3.05
3.04
3.03
2.48
7.5 7.0 6.5 6.0 5.5 5.0 4.5 4.0 3.5 3.0 2.5 2.0 1.5 1.0
Chemical Shift (ppm)

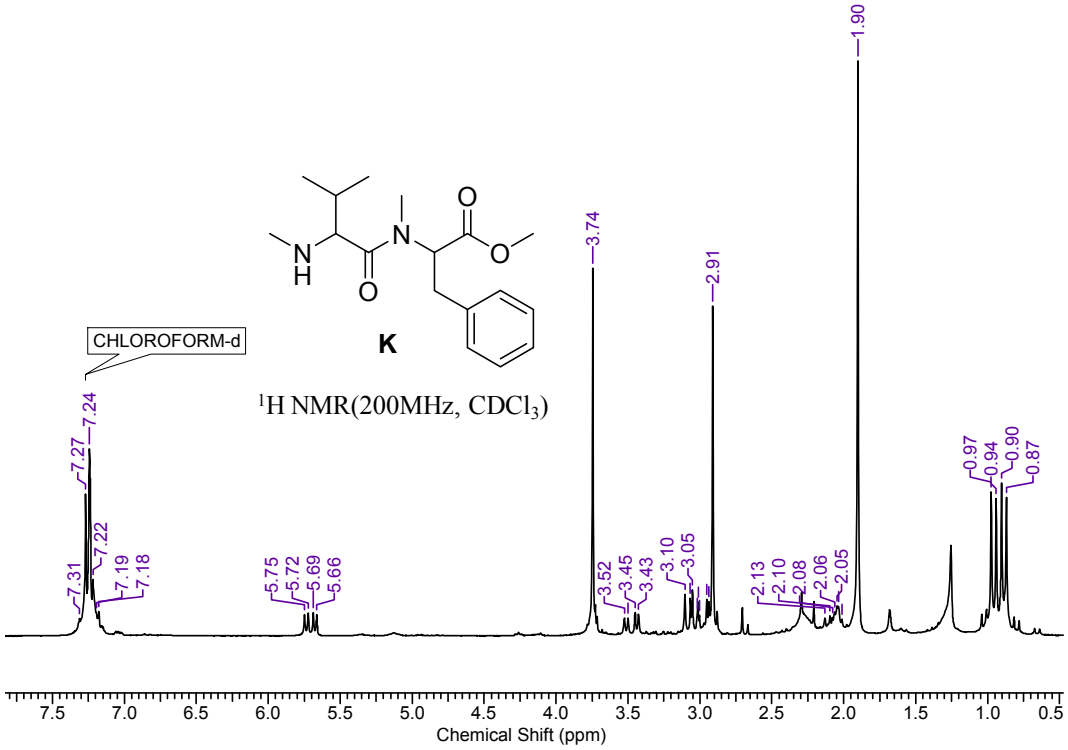
K
^{1}H NMR(200MHz, CDCl$_3$)
CHLOROFORM-d
Chemical Shift (ppm)

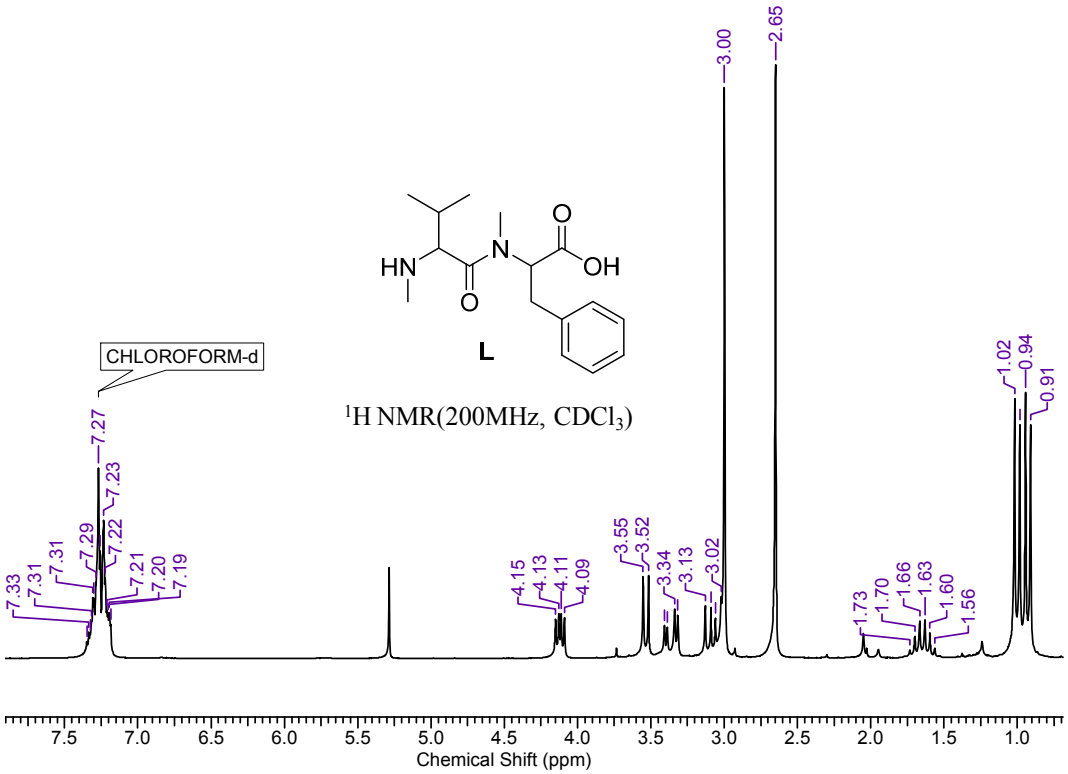
L
^{1}H NMR(200MHz, CDCl$_3$)
CHLOROFORM-d
Chemical Shift (ppm)

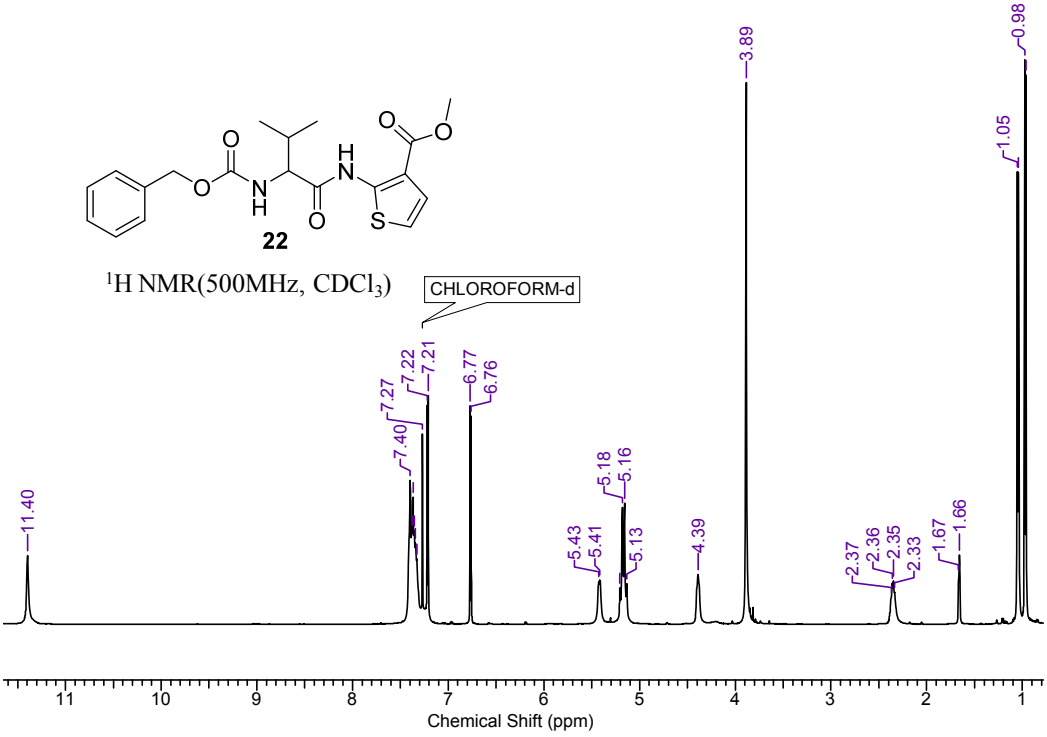
22
^{1}H NMR(500MHz, CDCl$_3$)
CHLOROFORM-d
11.40
7.40
7.27
7.22
7.21
6.77
6.76
5.43
5.41
5.18
5.16
5.13
4.39
3.89
2.37
2.36
2.35
2.33
1.67
1.66
1.05
0.98
Chemical Shift (ppm)

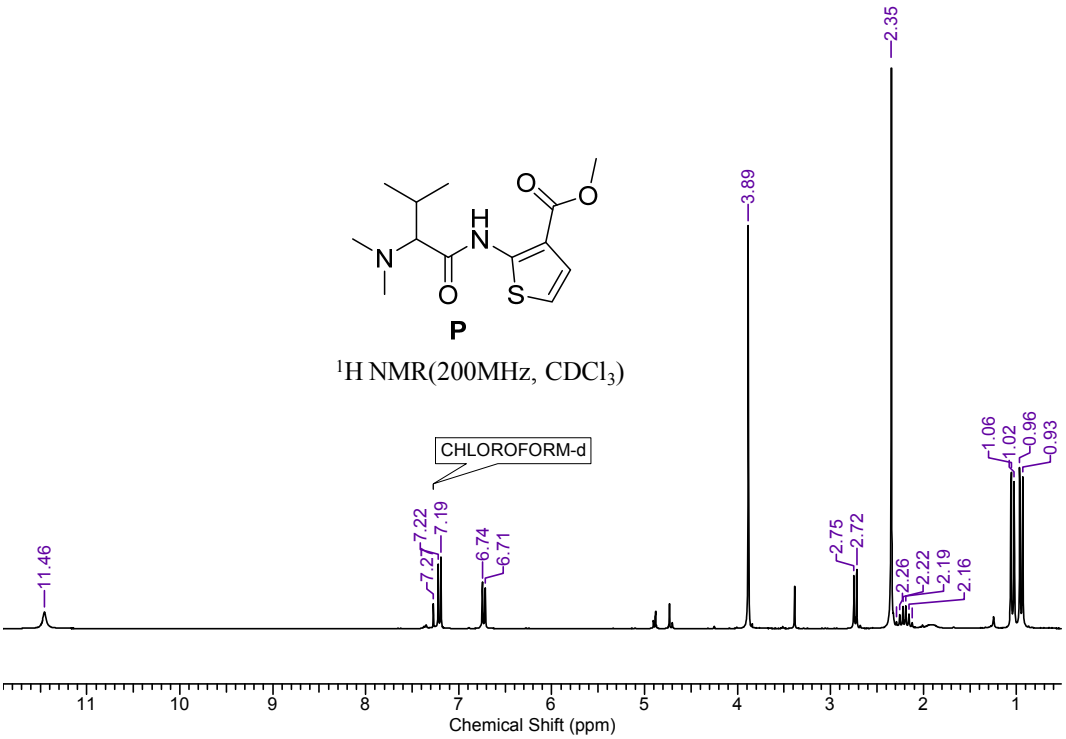
P
^{1}H NMR(200MHz, CDCl$_3$)
CHLOROFORM-d
11.46
7.27
7.22
7.19
6.74
6.71
3.89
2.75
2.72
2.35
2.26
2.22
2.19
2.16
1.06
1.02
0.96
0.93
Chemical Shift (ppm)

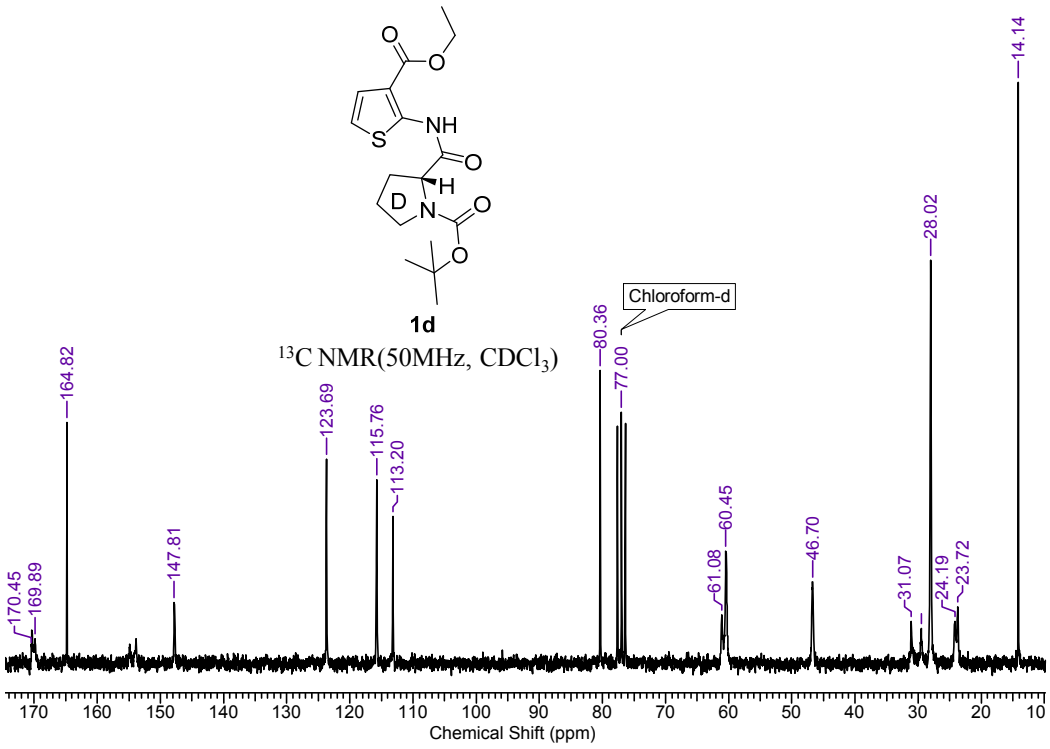
1d
^{13}C NMR(50MHz, $CDCl_3$)
Chloroform-d
164.82
147.81
123.69
115.76
113.20
80.36
77.00
61.08
60.45
46.70
31.07
28.02
24.19
23.72
14.14
170.45
169.89
Chemical Shift (ppm)

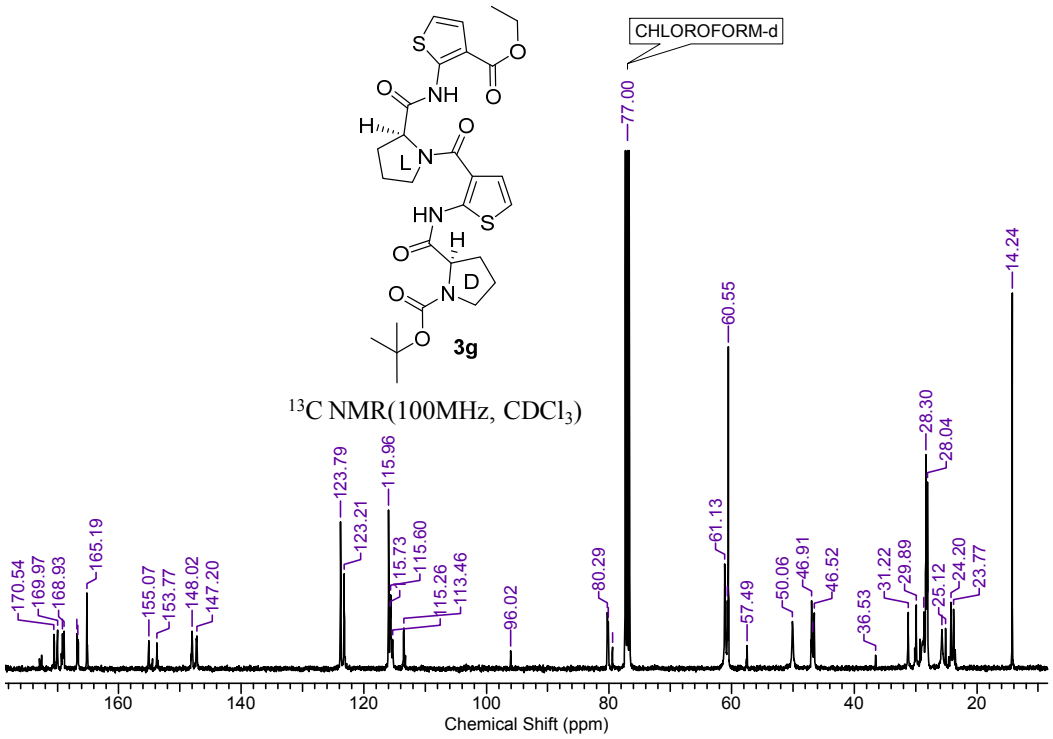
3g
^{13}C NMR(100MHz, $CDCl_3$)
CHLOROFORM-d
77.00
60.55
14.24
123.79
123.21
115.96
115.73
115.60
115.26
113.46
165.19
80.29
61.13
57.49
50.06
46.91
46.52
36.53
31.22
29.89
28.30
28.04
25.12
24.20
23.77
96.02
155.07
153.77
148.02
147.20
170.54
169.97
168.93
Chemical Shift (ppm)

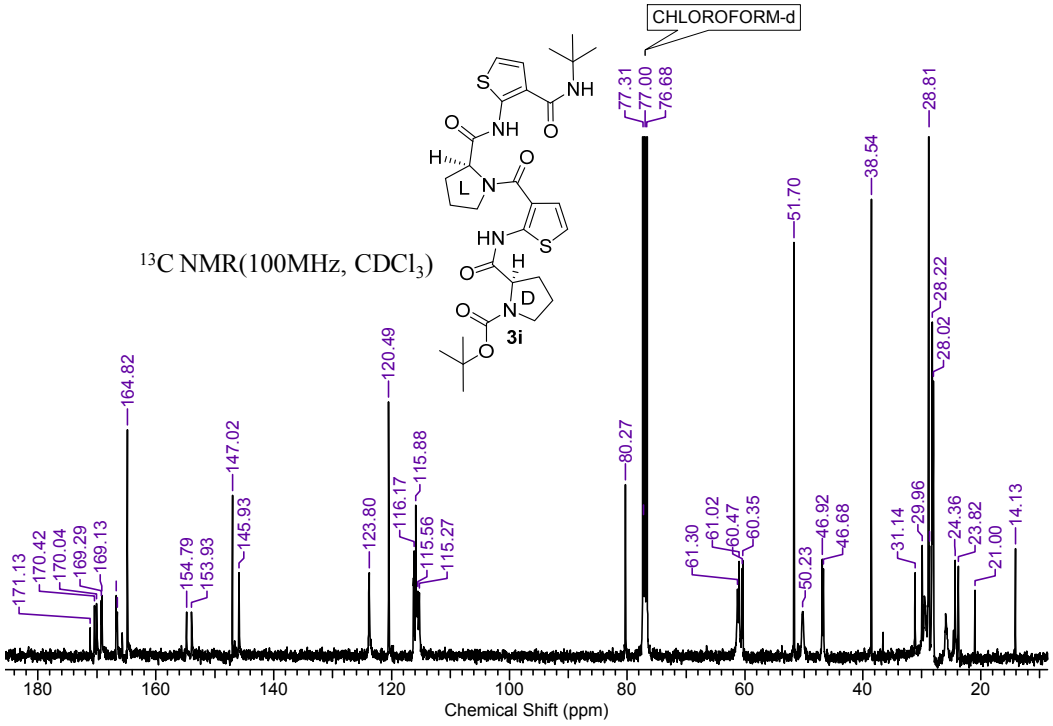
CHLOROFORM-d
^{13}C NMR(100MHz, $CDCl_3$)
3i
Chemical Shift (ppm)

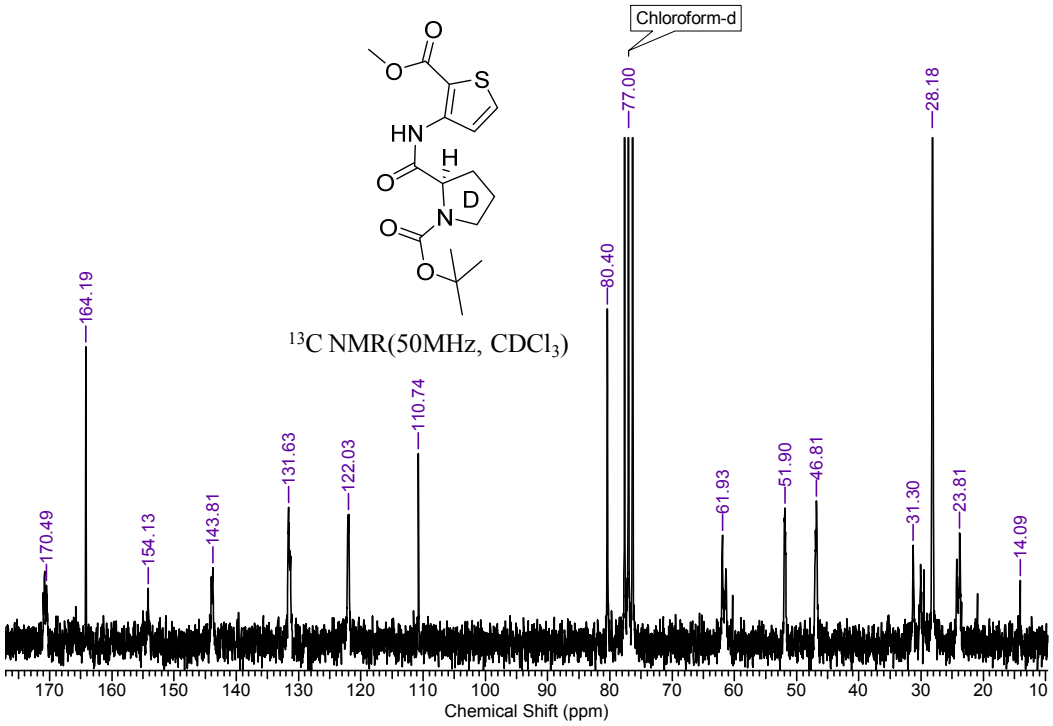
Chloroform-d
^{13}C NMR(50MHz, $CDCl_3$)
Chemical Shift (ppm)

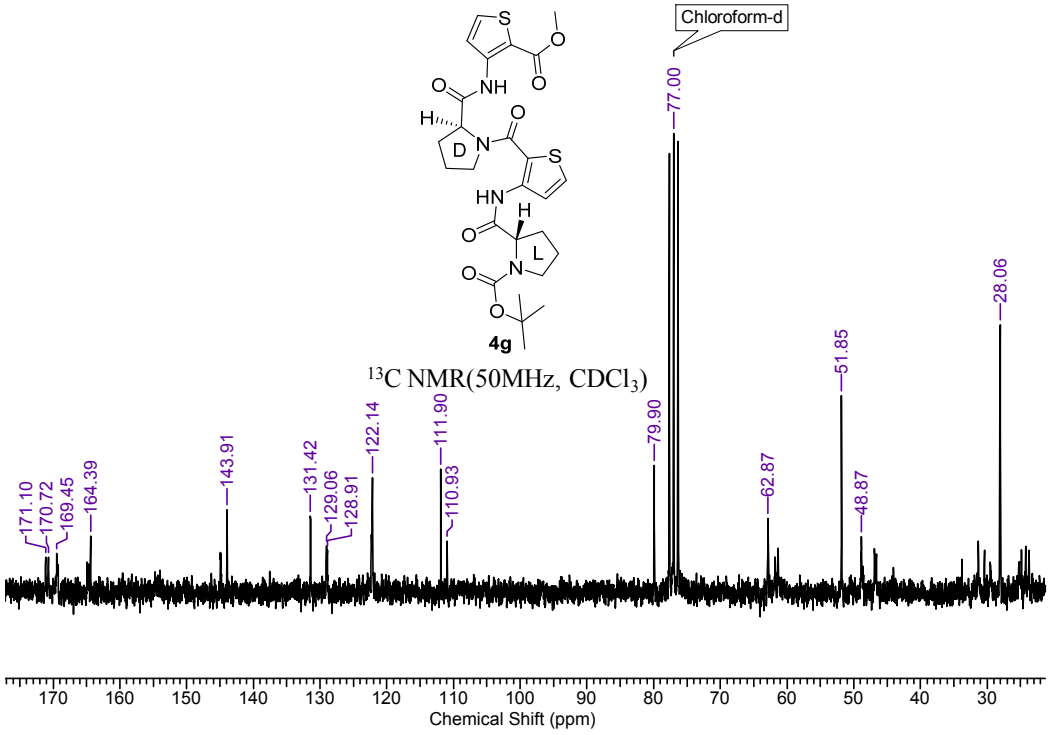
Chloroform-d
77.00
28.06
51.85
79.90
62.87
48.87
122.14
111.90
143.91
131.42
129.06
128.91
110.93
171.10
170.72
169.45
164.39
4g
13C NMR(50MHz, CDCl3)
Chemical Shift (ppm)

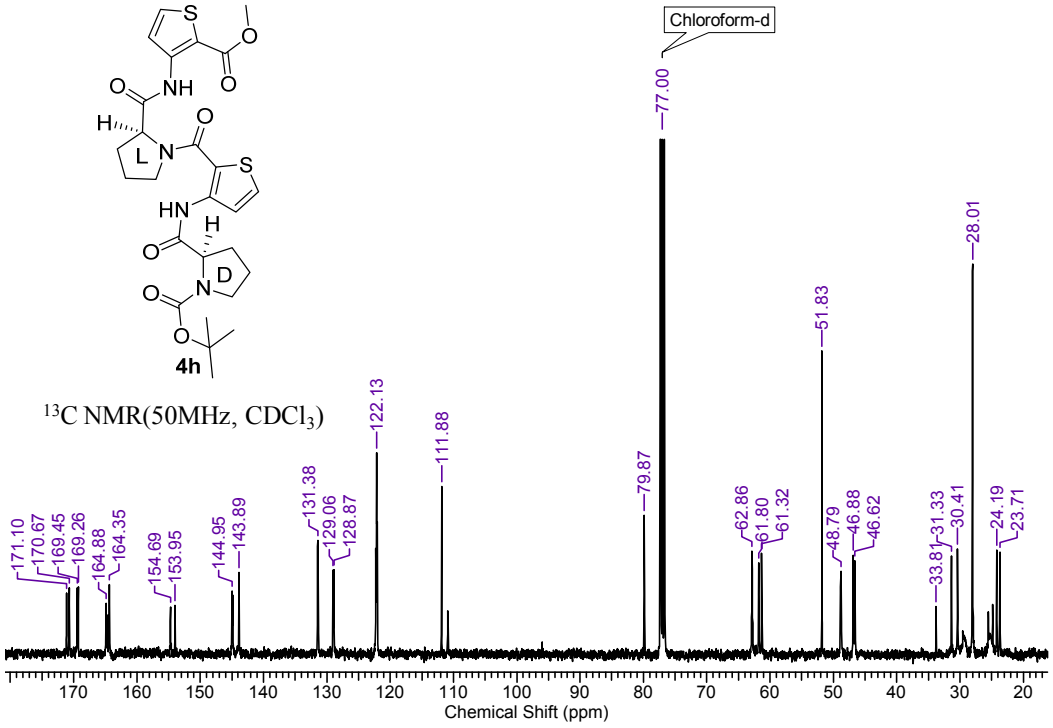
Chloroform-d
77.00
28.01
51.83
122.13
111.88
79.87
131.38
129.06
128.87
62.86
61.80
61.32
48.79
46.88
46.62
33.81
31.33
30.41
24.19
23.71
171.10
170.67
169.45
169.26
164.88
164.35
154.69
153.95
144.95
143.89
4h
13C NMR(50MHz, CDCl3)
Chemical Shift (ppm)

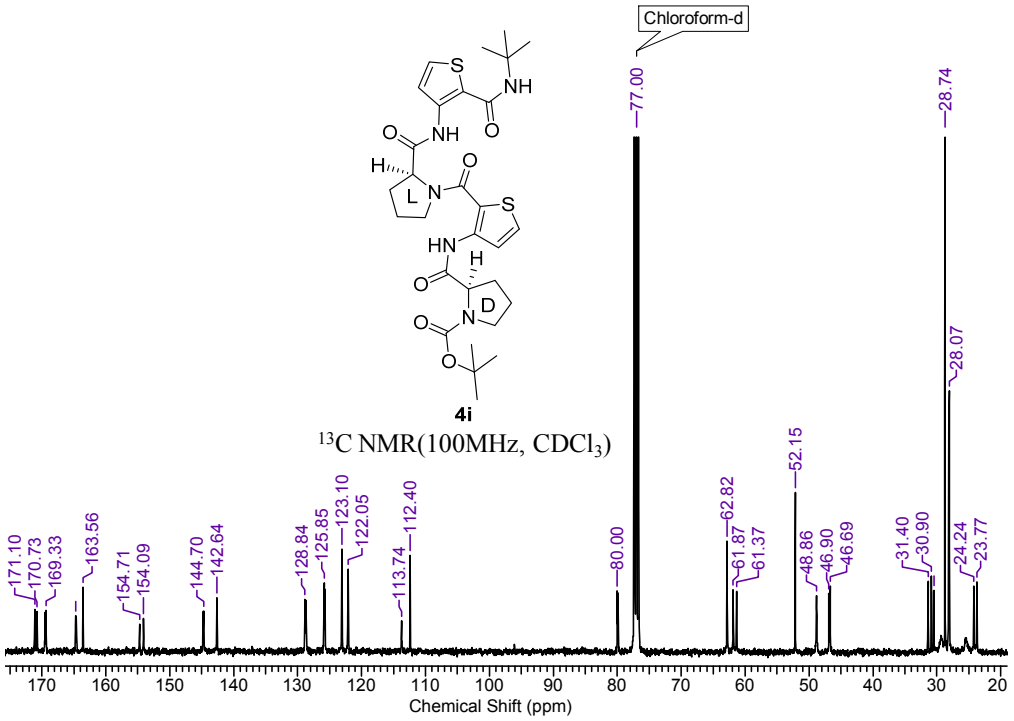

4i

^{13}C NMR(100MHz, $CDCl_3$)

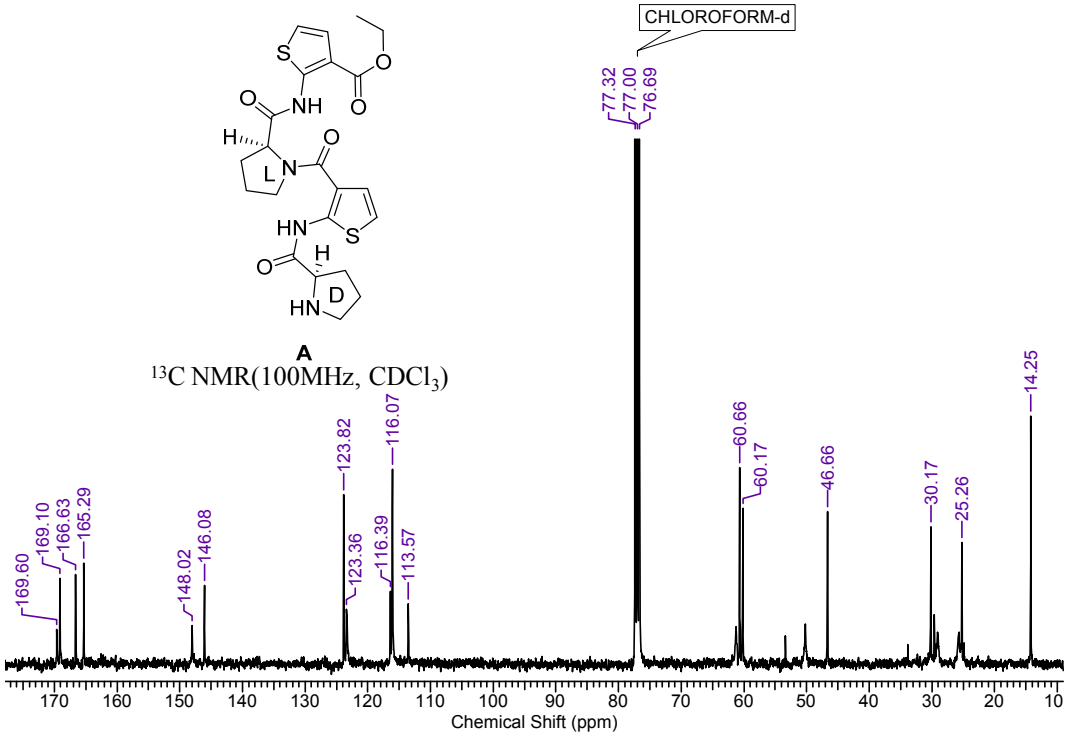

A

^{13}C NMR(100MHz, $CDCl_3$)

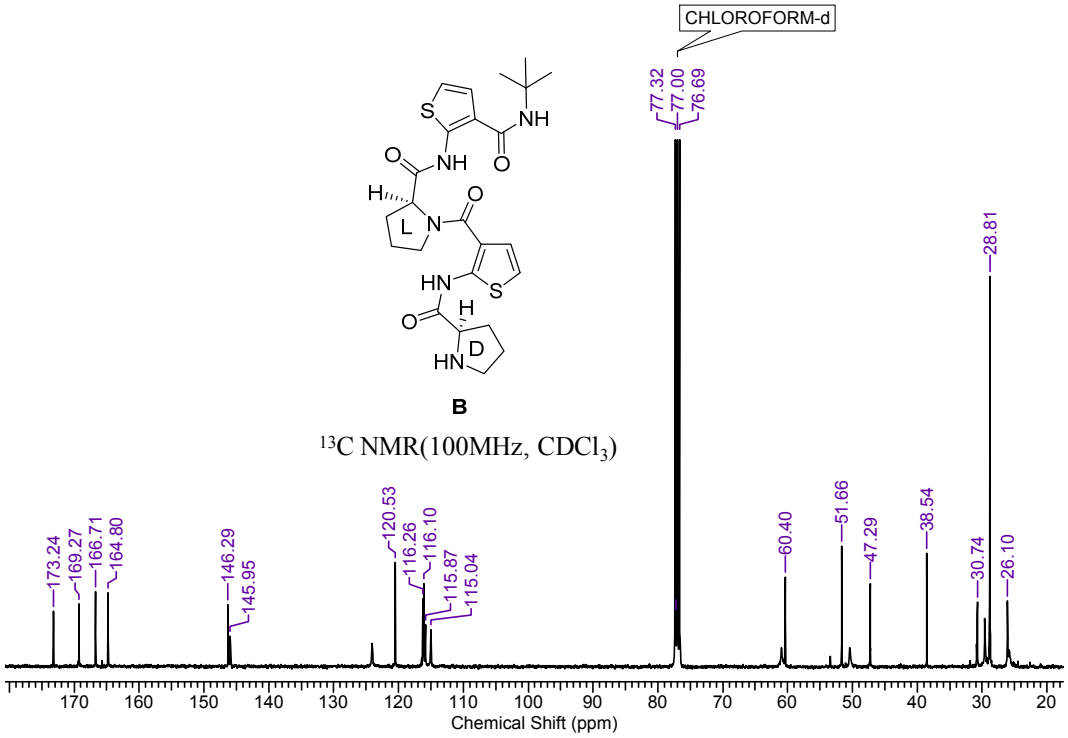

B

^{13}C NMR(100MHz, $CDCl_3$)

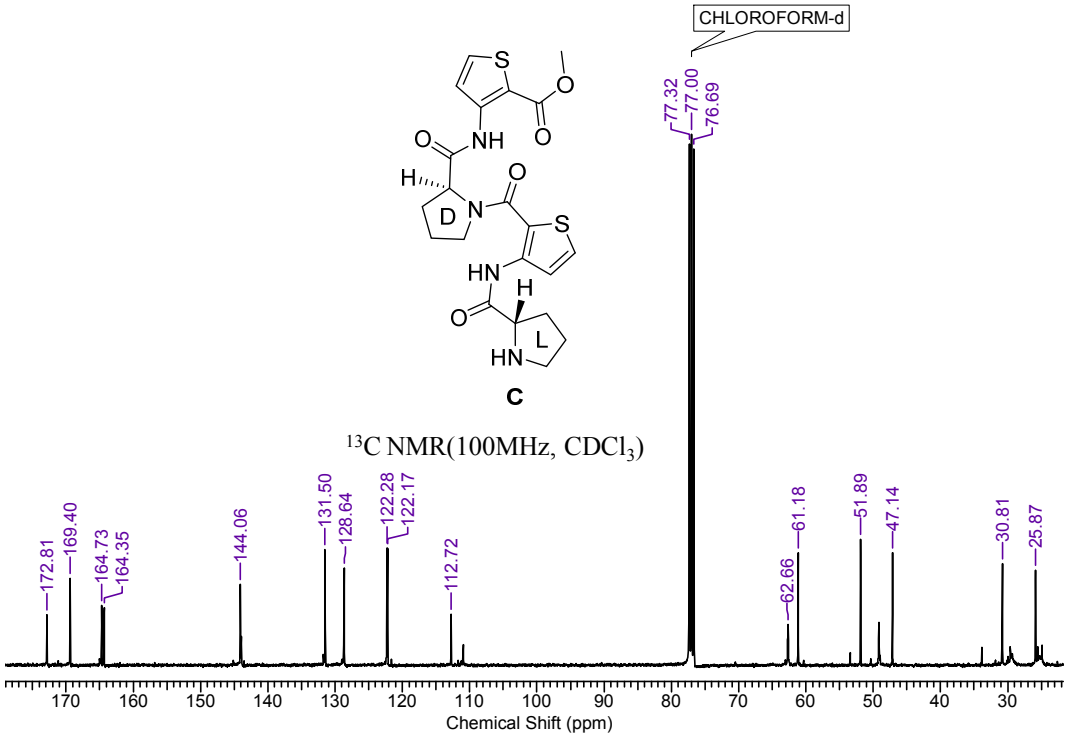

C

^{13}C NMR(100MHz, $CDCl_3$)

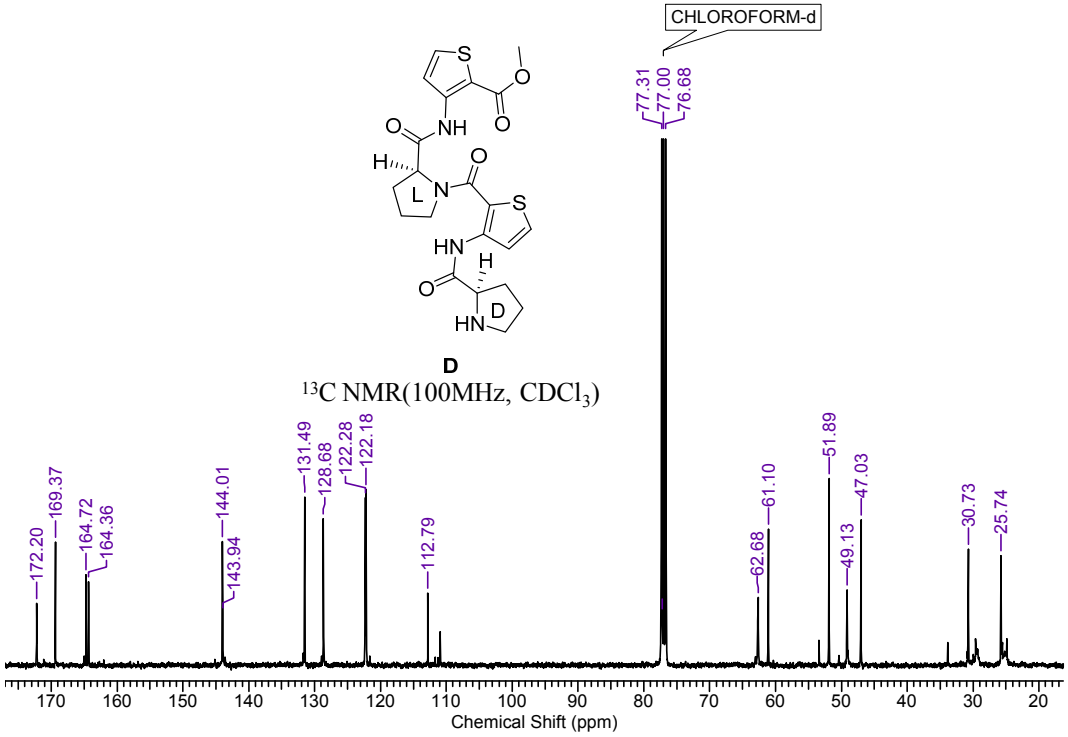

D

^{13}C NMR(100MHz, $CDCl_3$)

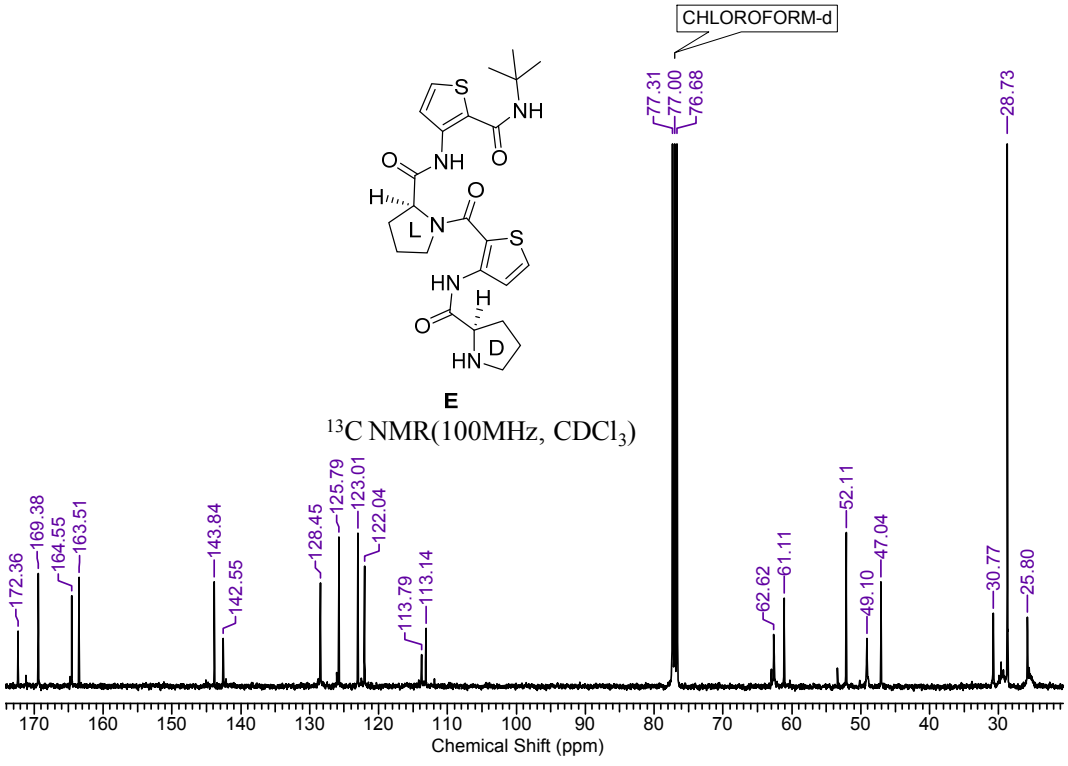

E

^{13}C NMR(100MHz, $CDCl_3$)

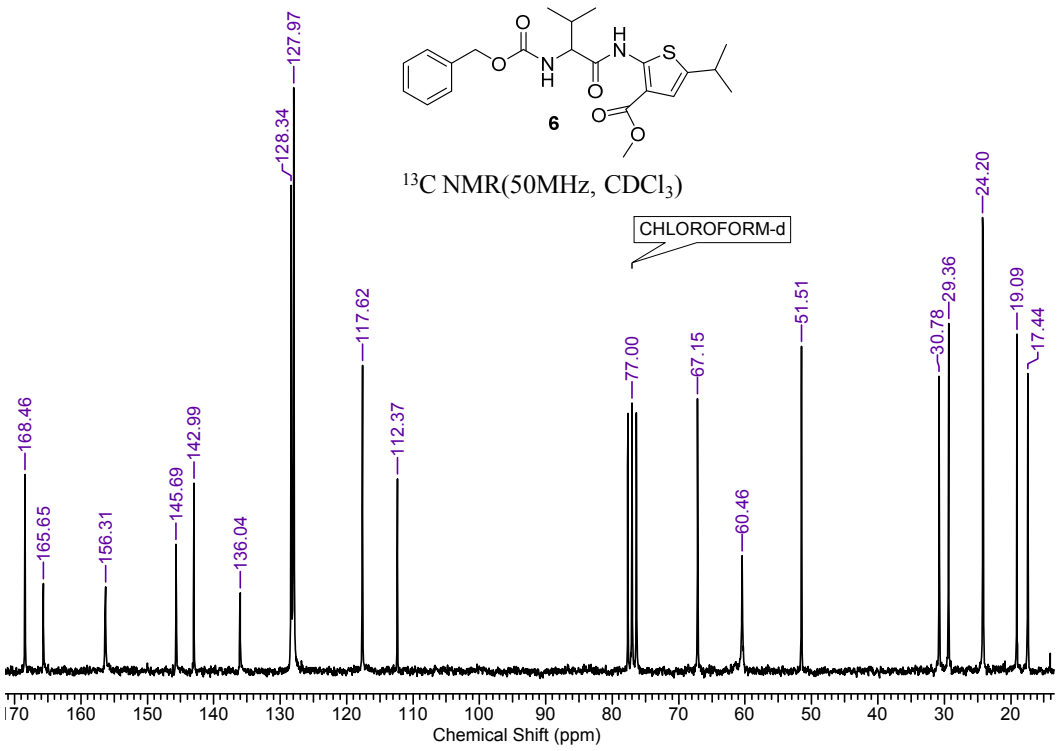
6
^{13}C NMR(50MHz, $CDCl_3$)
CHLOROFORM-d
168.46
165.65
156.31
145.69
142.99
136.04
128.34
127.97
117.62
112.37
77.00
67.15
60.46
51.51
30.78
29.36
24.20
19.09
17.44
Chemical Shift (ppm)

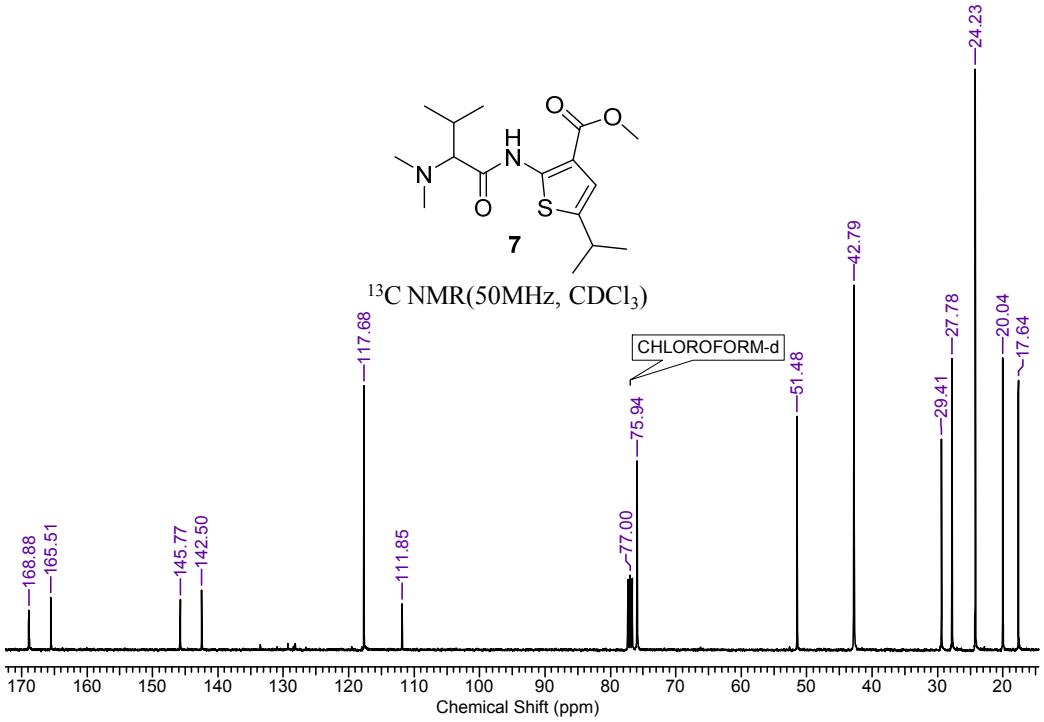
7
^{13}C NMR(50MHz, $CDCl_3$)
CHLOROFORM-d
168.88
165.51
145.77
142.50
117.68
111.85
77.00
75.94
51.48
42.79
29.41
27.78
24.23
20.04
17.64
Chemical Shift (ppm)

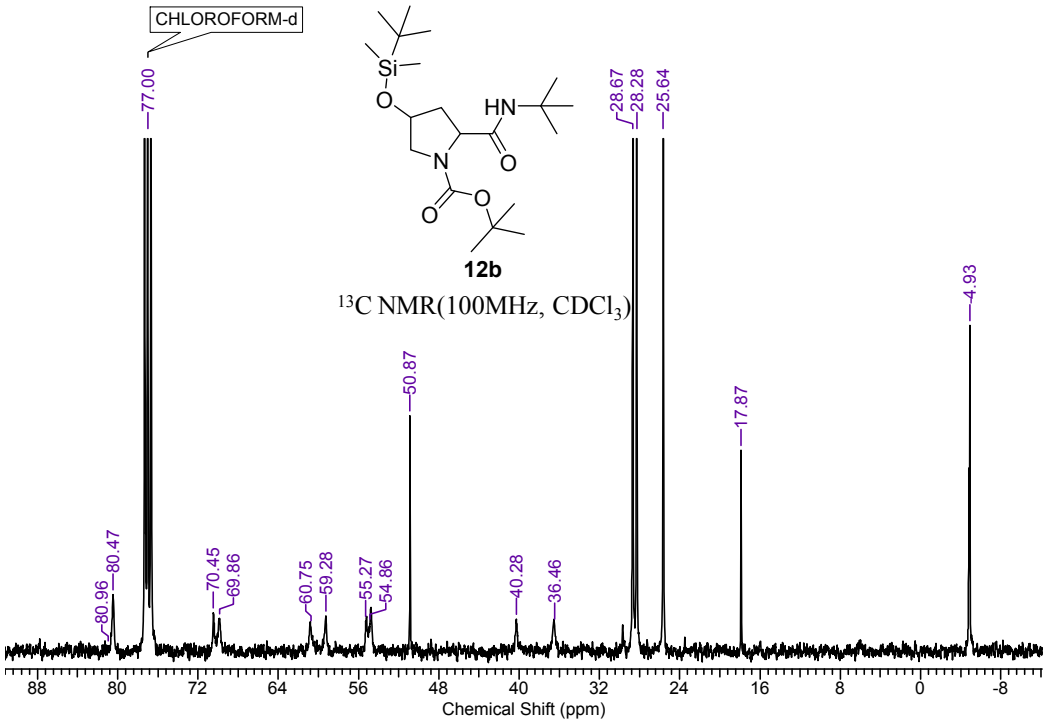

12b

^{13}C NMR(100MHz, $CDCl_3$)

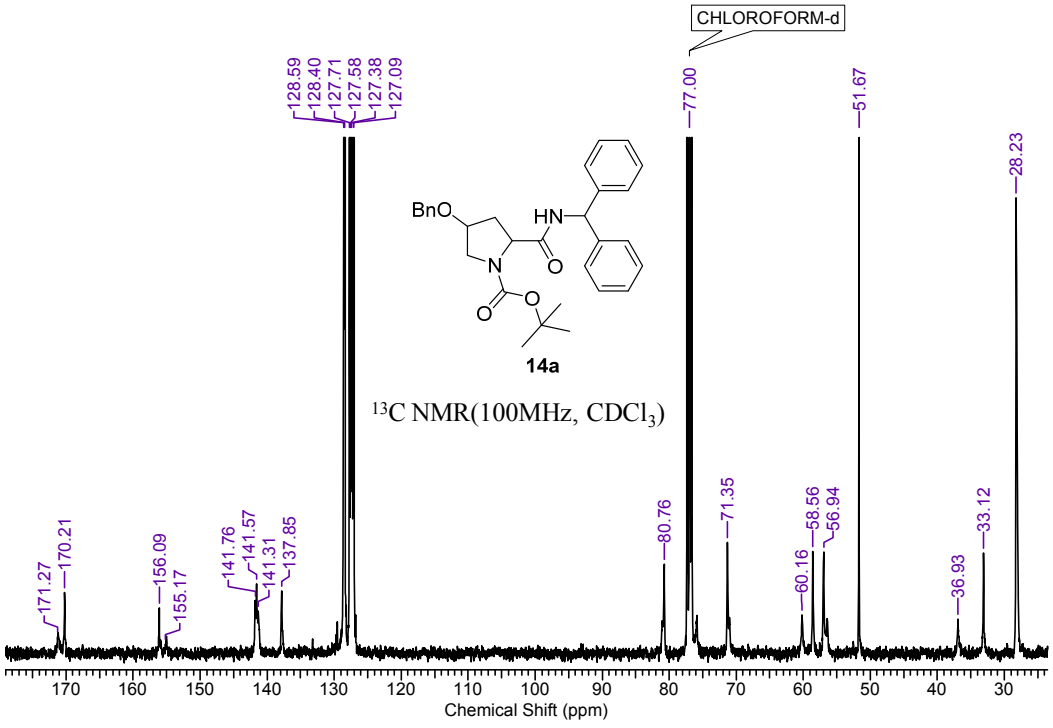

14a

^{13}C NMR(100MHz, $CDCl_3$)

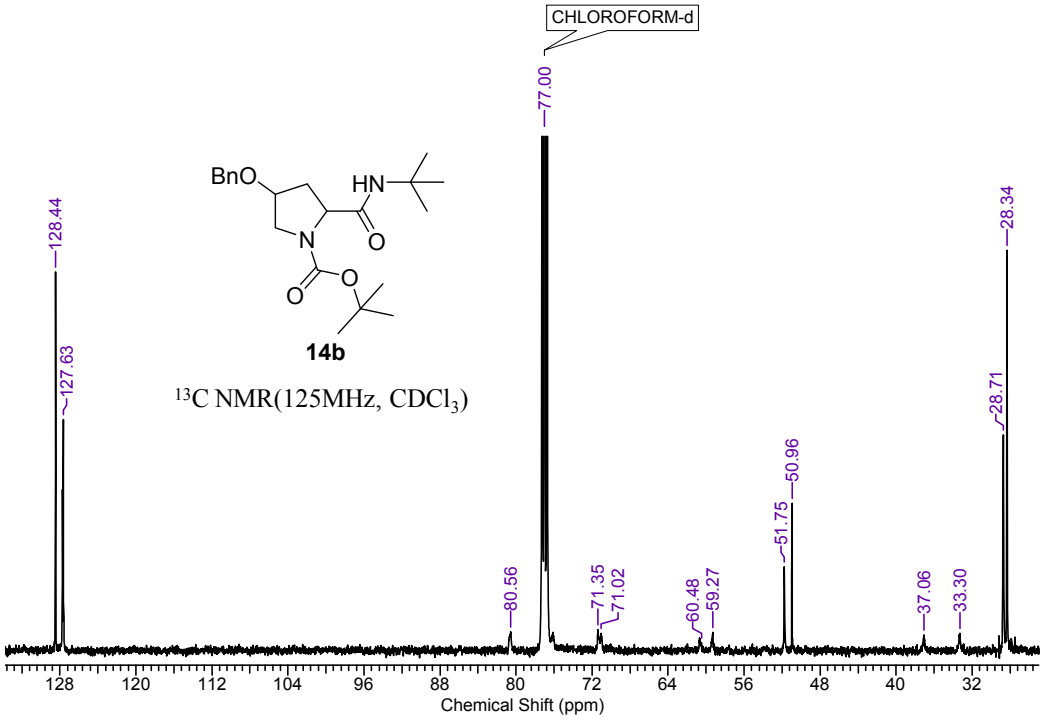
CHLOROFORM-d
77.00
BnO
HN
N
O
O
O
14b
13C NMR(125MHz, CDCl3)
128.44
127.63
80.56
71.35
71.02
60.48
59.27
51.75
50.96
37.06
33.30
28.71
28.34
128
120
112
104
96
88
80
72
64
56
48
40
32
Chemical Shift (ppm)

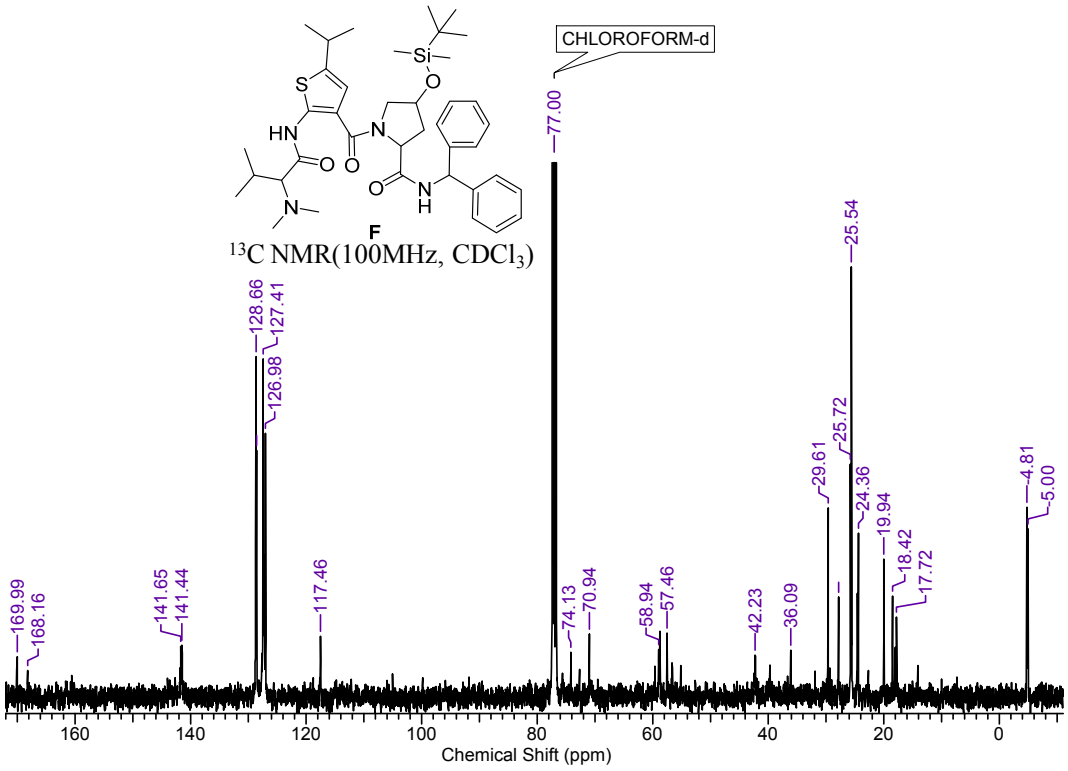
CHLOROFORM-d
77.00
Si
O
S
HN
N
O
O
O
N
H
F
13C NMR(100MHz, CDCl3)
128.66
127.41
126.98
169.99
168.16
141.65
141.44
117.46
74.13
70.94
58.94
57.46
42.23
36.09
29.61
25.72
25.54
24.36
19.94
18.42
17.72
4.81
5.00
160
140
120
100
80
60
40
20
0
Chemical Shift (ppm)

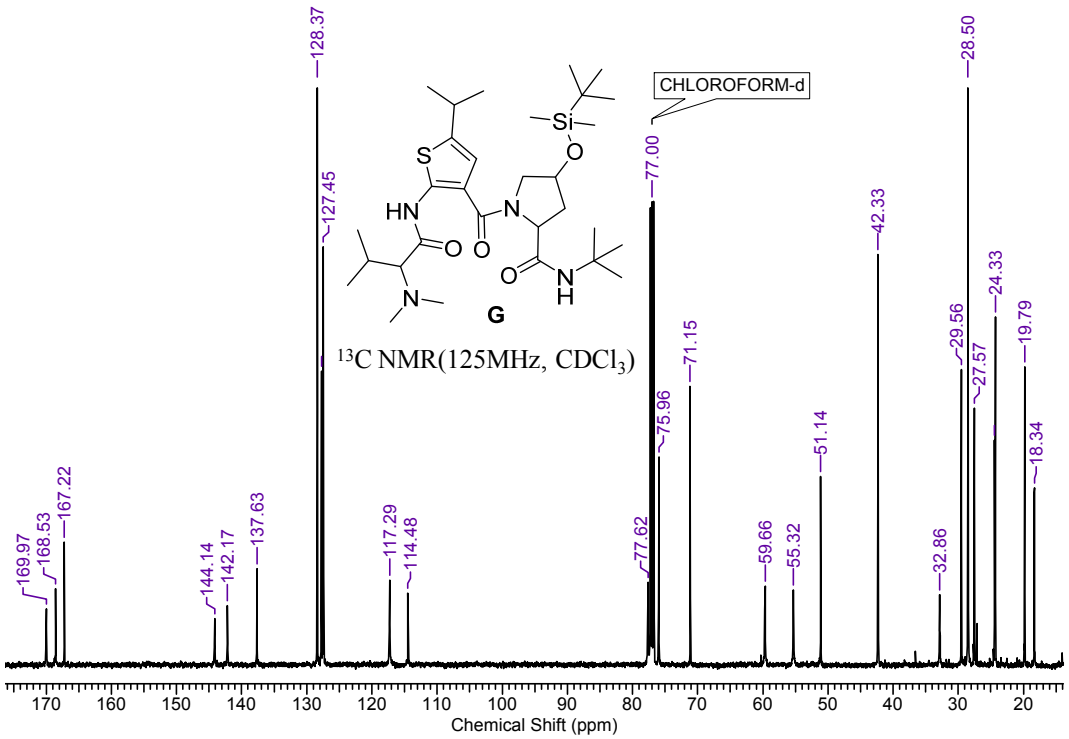
128.37
127.45
CHLOROFORM-d
77.00
28.50
42.33
24.33
29.56
27.57
19.79
71.15
76.96
51.14
18.34
169.97
168.53
167.22
144.14
142.17
137.63
117.29
114.48
77.62
59.66
55.32
32.86
G
13C NMR(125MHz, CDCl3)
Chemical Shift (ppm)

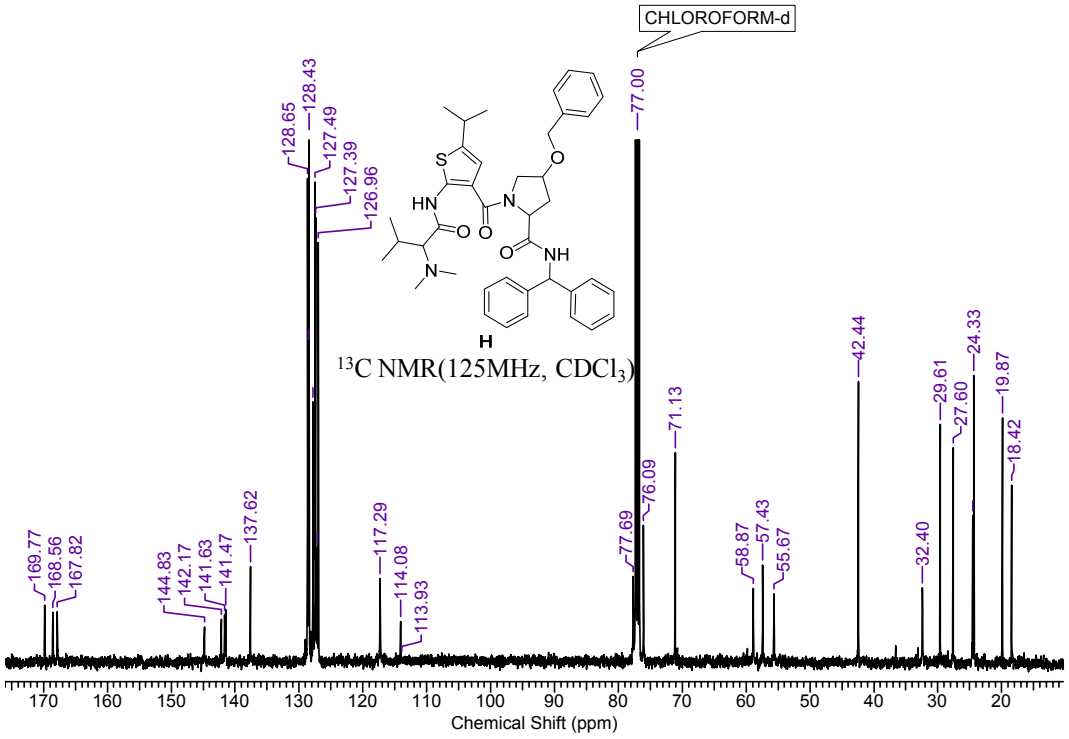
CHLOROFORM-d
128.65
128.43
127.49
127.39
126.96
77.00
42.44
24.33
29.61
27.60
19.87
71.13
18.42
76.09
169.77
168.56
167.82
144.83
142.17
141.63
141.47
137.62
117.29
114.08
113.93
77.69
58.87
57.43
55.67
32.40
H
13C NMR(125MHz, CDCl3)
Chemical Shift (ppm)

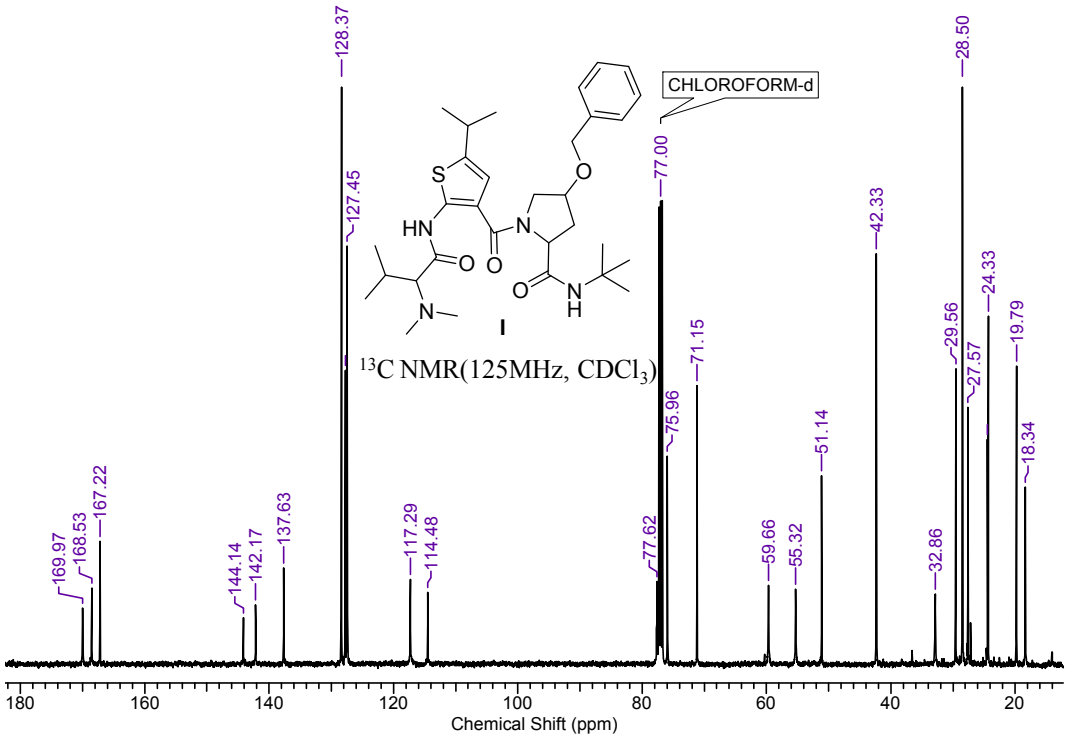

I

^{13}C NMR(125MHz, $CDCl_3$)

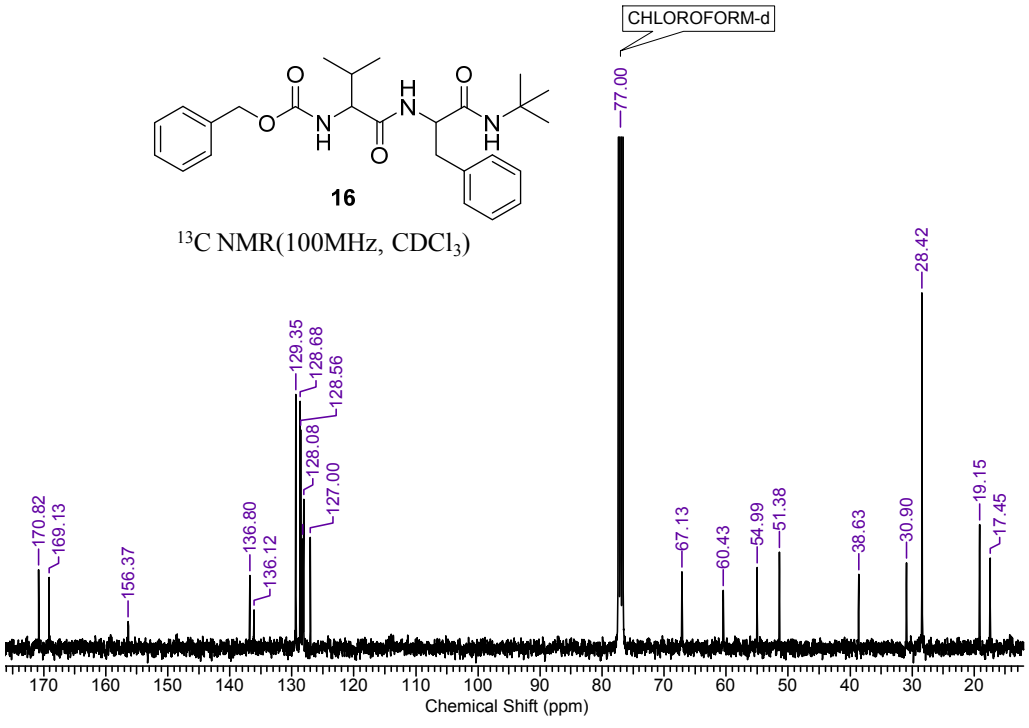

16

^{13}C NMR(100MHz, $CDCl_3$)

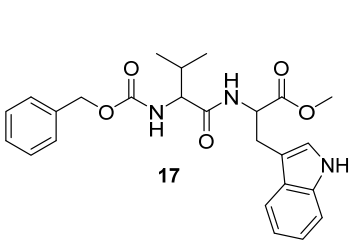

17

^{13}C NMR(100MHz, $CDCl_3$)

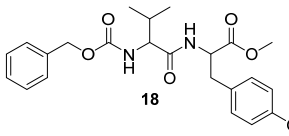

18

^{13}C NMR(50MHz, $CDCl_3$)

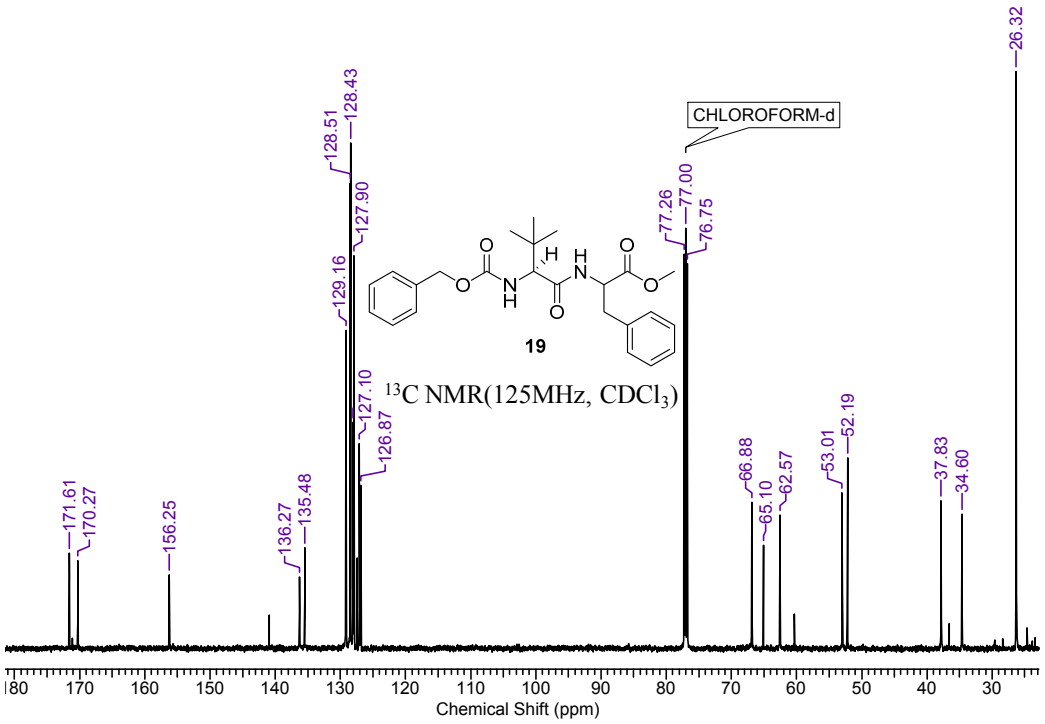
CHLOROFORM-d
19
^{13}C NMR(125MHz, CDCl$_3$)
Chemical Shift (ppm)

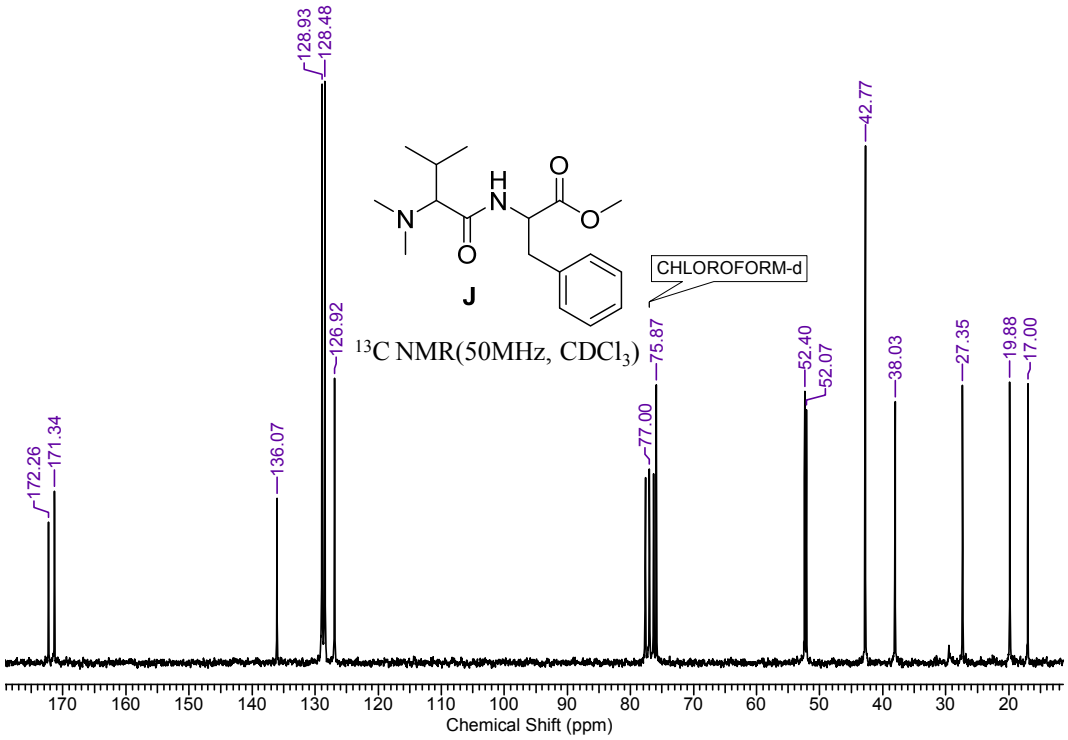
CHLOROFORM-d
J
^{13}C NMR(50MHz, CDCl$_3$)
Chemical Shift (ppm)

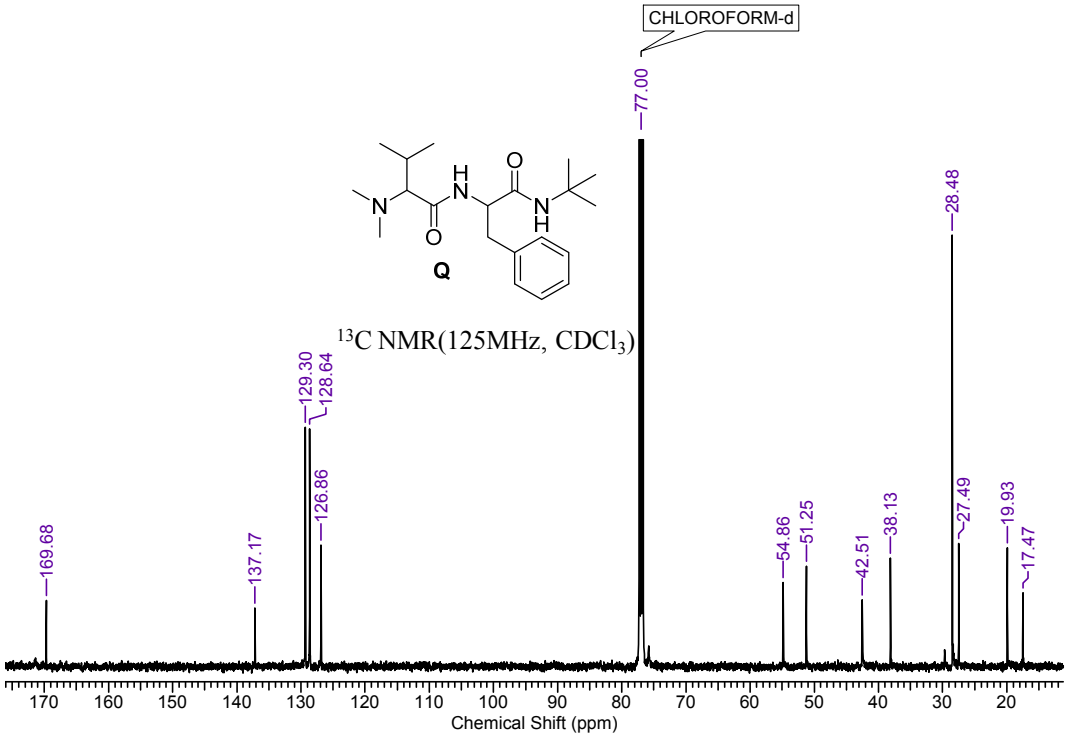
CHLOROFORM-d
77.00
28.48
Q
^{13}C NMR(125MHz, CDCl$_3$)
129.30
128.64
126.86
169.68
137.17
54.86
51.25
42.51
38.13
27.49
19.93
17.47
Chemical Shift (ppm)

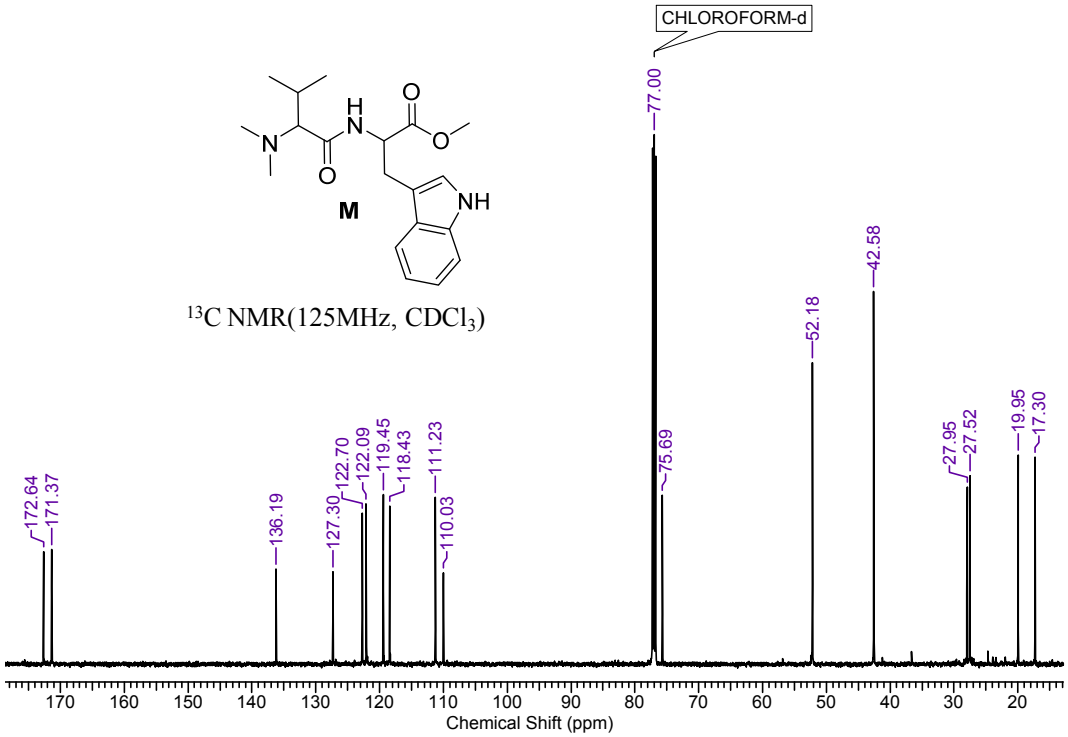
CHLOROFORM-d
77.00
M
^{13}C NMR(125MHz, CDCl$_3$)
42.58
52.18
75.69
172.64
171.37
136.19
127.30
122.70
122.09
119.45
118.43
111.23
110.03
27.95
27.52
19.95
17.30
Chemical Shift (ppm)

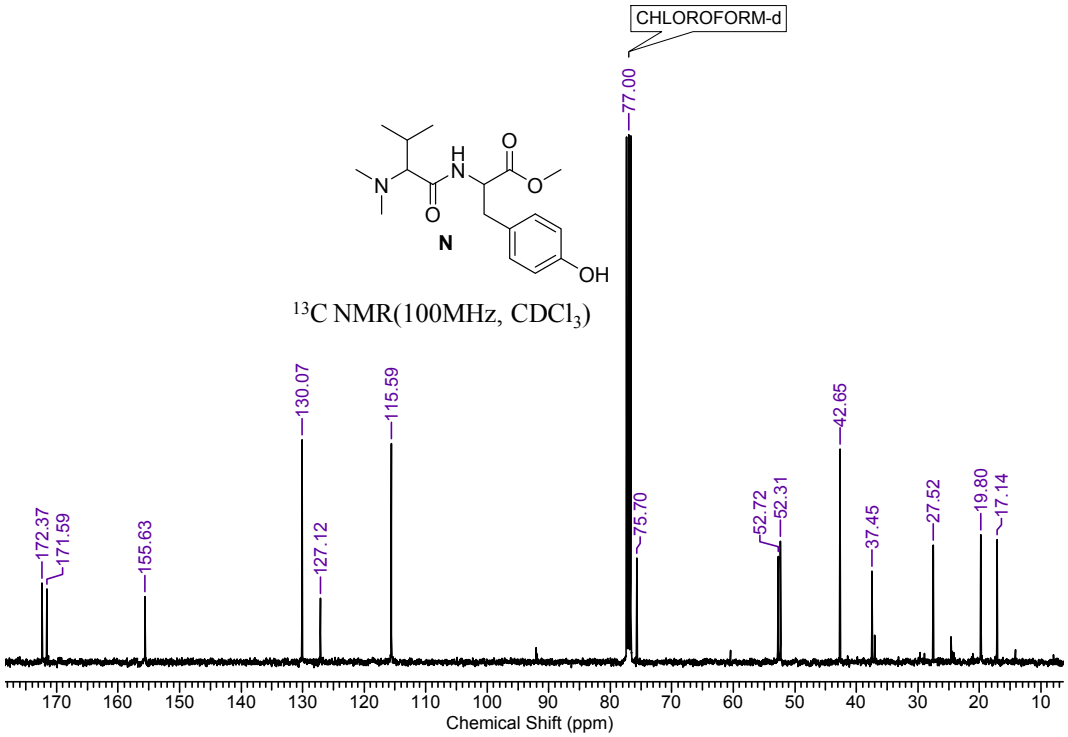
CHLOROFORM-d
77.00
N
OH
^{13}C NMR(100MHz, CDCl$_3$)
130.07
115.59
42.65
172.37
171.59
155.63
127.12
75.70
52.72
52.31
37.45
27.52
19.80
17.14
170 160 150 140 130 120 110 100 90 80 70 60 50 40 30 20 10
Chemical Shift (ppm)

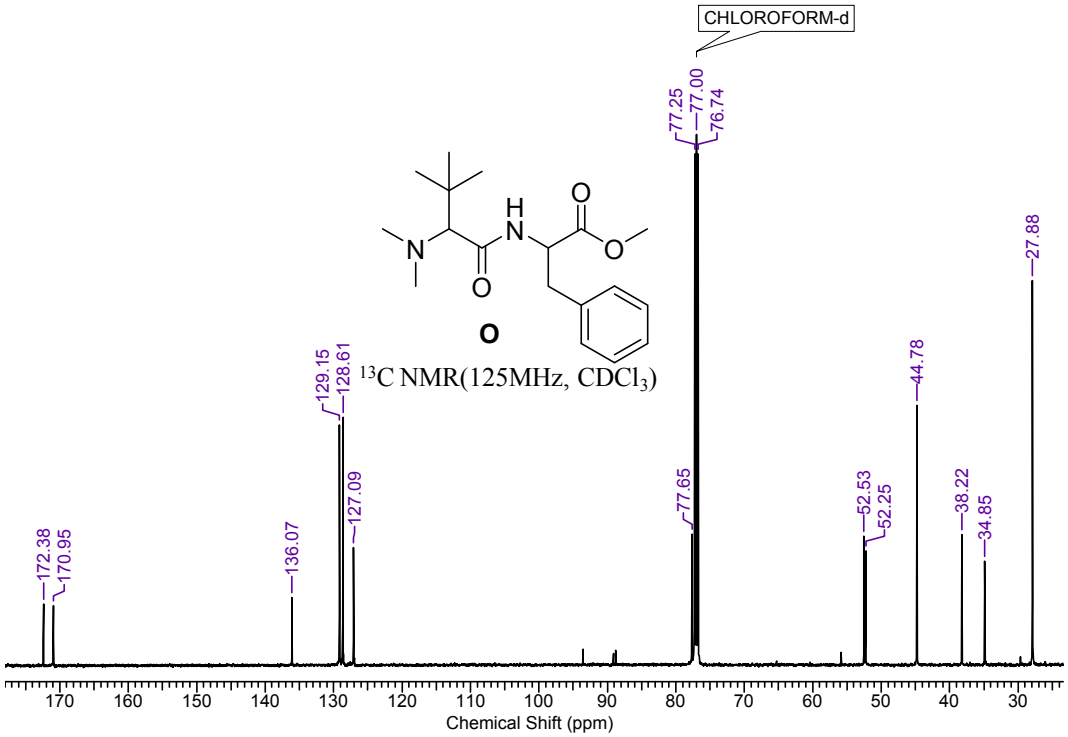
CHLOROFORM-d
77.25
77.00
76.74
O
^{13}C NMR(125MHz, CDCl$_3$)
129.15
128.61
44.78
27.88
127.09
77.65
52.53
52.25
38.22
34.85
172.38
170.95
136.07
170 160 150 140 130 120 110 100 90 80 70 60 50 40 30
Chemical Shift (ppm)

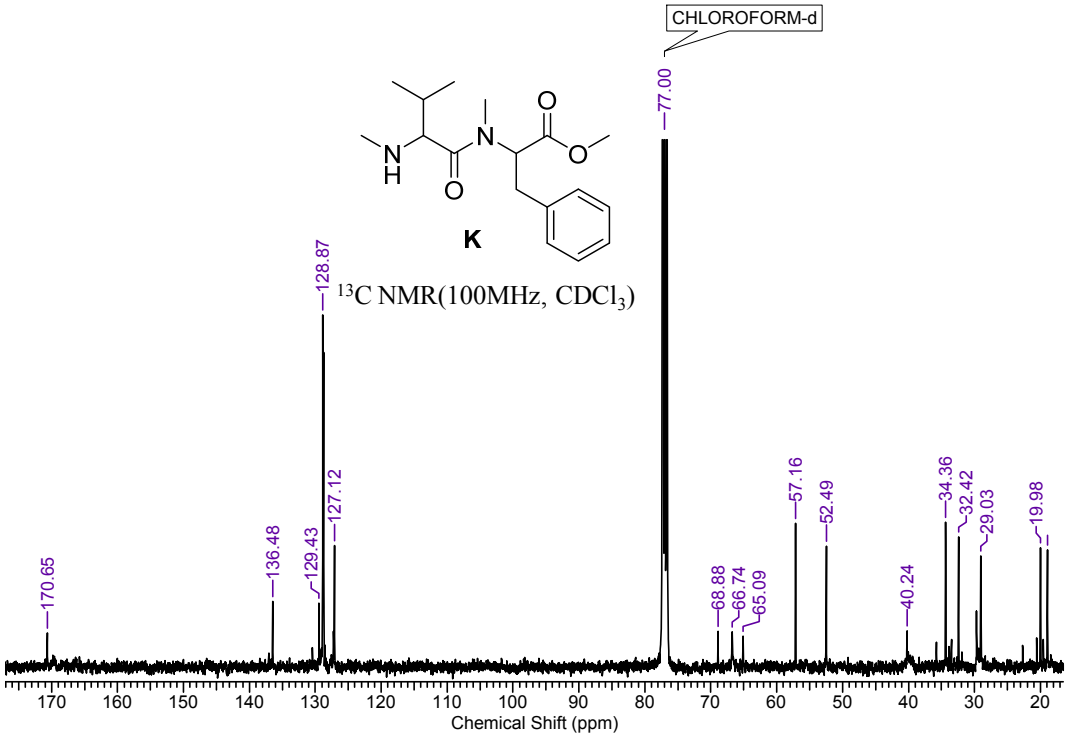
CHLOROFORM-d
77.00
K
128.87
^{13}C NMR(100MHz, $CDCl_3$)
170.65
136.48
129.43
127.12
68.88
66.74
65.09
57.16
52.49
40.24
34.36
32.42
29.03
19.98
Chemical Shift (ppm)

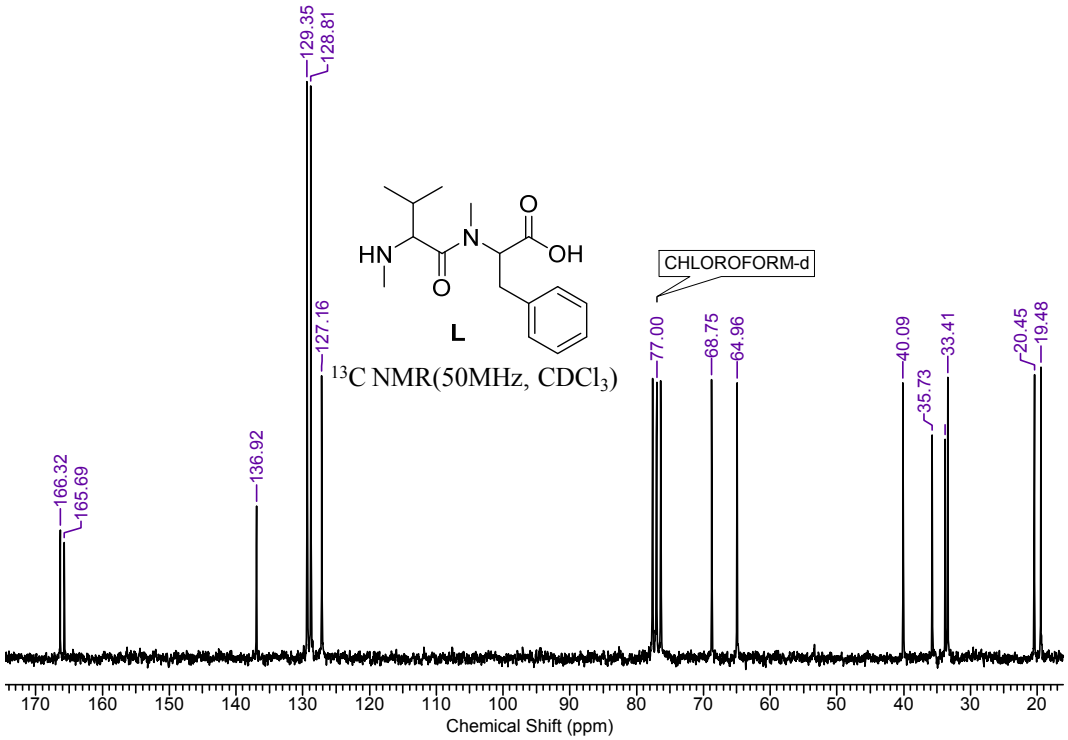
129.35
128.81
L
CHLOROFORM-d
127.16
77.00
68.75
64.96
40.09
35.73
33.41
20.45
19.48
^{13}C NMR(50MHz, $CDCl_3$)
166.32
165.69
136.92
Chemical Shift (ppm)

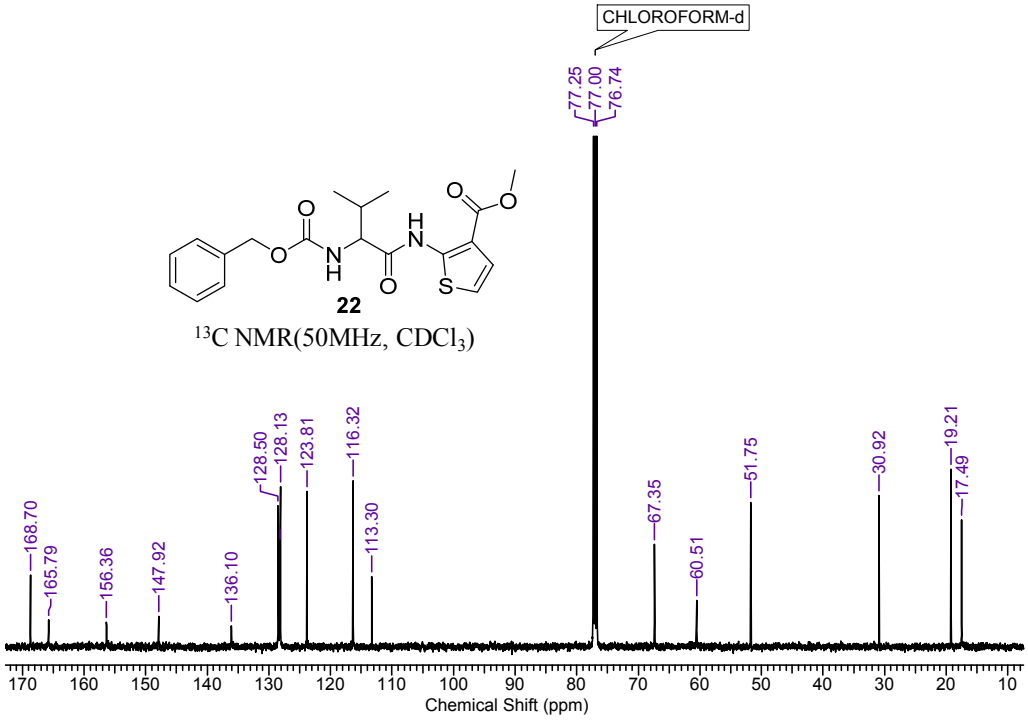

22

^{13}C NMR(50MHz, $CDCl_3$)

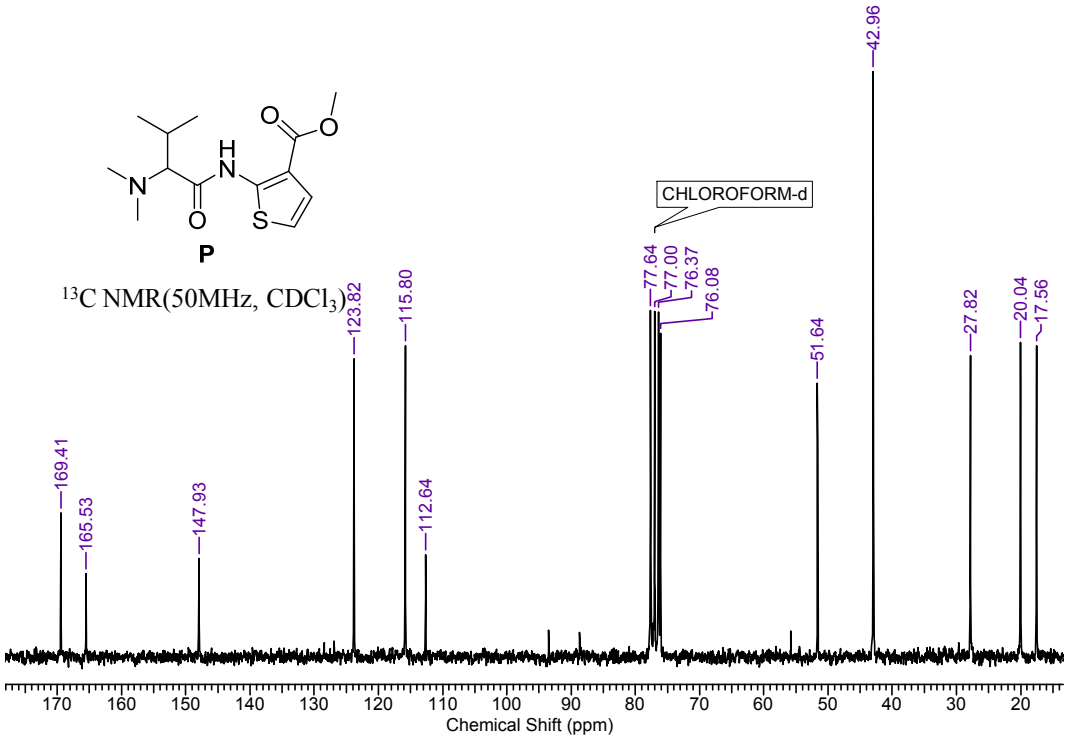

P

^{13}C NMR(50MHz, $CDCl_3$)

3.18 References and Notes

(1) (a) Vagner, J.; Qu, H.; Hruby, V. J. *Curr. Opin. Chem. Biol.* **2008,** *12*, 292. (b) Dormán, G.; Frank, R. *QSAR & Comb. Sci.* **2006,** *25*, 1007. (c) Ripka, A. S.; Rich, D. H. *Curr. Opin. Chem. Biol.* **1998**, *2*, 441. (d) Giannis, A.; Kolter, T. *Angew. Chem. Int. Ed.* **1993,** *32*, 1244. (d) Morgan, B. A.; Gainor, J. A. *Annu. Rep. Med. Chem.* **1989**, *24*, 243.

(2) (a) Welch, B. D.; VanDemark, A. P.; Heroux, A.; Hill, C. P.; Kay, M. S. *Proc*. *Nat*. *Acad Sci*. **2007**, *104*, 16828. (b) Walensky, L. D.; Kung, A. L.; Escher, I.; Malia, T. J.; Barbuto, S.; Wright, R. D.; Wagner, G.; Verdine, G. L.; Korsmeyer, S. J. *Science.* **2004**, *305*, 1466. (c) Gonnet, G.; Cohen, M.; Benner, S. *Science*. **1992**, *256,* 1443.

(3) Kharb, R.; Rana, M.; Sharma, P. C.; Yar, M. S. *J. Chem. Pharm. Res*. **2011**, *3*, 173.

(4) (a) Srinivas, N.; Jetter, P.; Ueberbacher, B. J.; Werneburg, M.; Zerbe, K.; Steinmann, J.; Van der Meijden, B.; Bernardini, F.; Lederer, A.; Dias, R. L. A.; Misson, P. E.; Henze, H.; Zumbrunn, J.; Gombert, F. O.; Obrecht, D.; Hunziker, P.; Schauer, S.; Ziegler, U.; Käch, A.; Eberl, L.; Riedel, K.; DeMarco, S. J.; Robinson, J. A. *Science*. **2010**, *327*, 1010. (b) Kruger, R. G.; Barkallah, S.; Frankel, B. A.; McCafferty, D. G. *Bioorg*. *Med*. *Chem*. **2004**, *12*, 3723. (c) Gabriel, G. J.; Som, A.; Madkour, A. E.; Eren, T.; Tew, G. N. *Mat*. *Sci*. *Eng*. *R*. *Rep*. **2007**, *57*, 28.

(5) (a) Liao, Y.-F.; Wang, B.-J.; Hsu, W.-M.; Lee, H.; Liao, C.-Y.; Wu, S.-Y.; Cheng, H.-T.; Hu, M.-K. *Mol*. *Pharmcol*. **2007**, *71*, 588. (b) Satyanarayanajois, S.; Villalba, S.; Jianchao, L.; Lin, G. M. *Chem*. *Biol*. *Drug. Des*. **2009**, *74*, 246. (c) Timmerman, P.; Barderas, R.; Desmet, J.; Altschuh, D.; Shochat, S.; Hollestelle, M. J.; Höppener, J. W. M.; Monasterio, A.; Casal, J. I.; Meloen, R. H. *J. Biol. Chem*. **2009**, *284*, 34126. (d) Lapis. K. *Magy. Onkol*. **2010**, *54*, 47. (e) Zobel, K.; Wang, L.; Varfolomeev, E.; Franklin, M. C.; Elliott, L. O.; Wallweber, H. J. A.; Okawa, D. C.; Flygare, J. A.; Vucic, D.; Fairbrother, W. J.; Deshayes, K. *ACS. Chem. Biol*. **2006**, *1*, 525.

(6) Georgi. H; Ivanka. S. *Sci. Pharm.*, **2011**, *79*, 259-264.

(7) (a) Murali. R.; Liu. Q.; Cheng. X.; Berezov. A.; Richter. M.; Furuchi. K.; Greene. M.I.; Zhang. H. *Cell. Mol. Biol*., **2003**, *49*, 209. (b) Dunehoo. A.L.; Anderson. M.; Majumdar. S.; Kobayashi. N.; Berkland. C.; Siahaan. T.J. *J. Pharm Sci.*, **2006**, *95*, 1856.

(8) Ettari, R.; Zappalà, M.; Micale, N.; Schirmeister, T.; Gelhaus, C.; Leippe, M.; Evers, A.; Grasso, S. *Eur. J. Med. Chem.* **2010**, *45*, 3228.

(9) Li, Q.; Fang, H.; Wang, X.; Hu, L.; Xu, W. *Eur. J. Med. Chem*. **2009**, *44*, 4819.

(10) Taka, N.; Matsuoka, H.; Sato, T.; Yoshino, H.; Imaoka, I.; Sato, H.; Kotake, K.; Kumagai, Y.; Kamei, K.; Ozaki, K.; Higashida, A.; Kuroki, T. *Bioorg. Med. Chem. Lett*. **2009**, *19*, 3426.

(11) Duggan, P. J.; Lewis, R. J.; Phei Lok, Y.; Lumsden, N. G.; Tuck, K. L.; Yang, A. *Bioorg. Med. Chem. Lett*. **2009**, *19*, 2763.

(12) S. K. Schwarcz, L. C. Hsu, E. Vittinghoff and M. H. Katz, *Am. J. Epidemiol.,* **2000**, *152*, 178.

(13) Gante, J. *Angew. Chem. Int. Ed.* **1994**, *33*, 1699.

(14) Bert, V.; Kenneth, W. K. *Nat. Med.* **2004**, *10*, 789.

(15) Jemal, A.; Bray, F.; Center, M. M.; Ferlay, J.; Ward, E.; Forman, D., *CA-Cancer J. Clin.* **2011**, *61*, 69.

(16) (a) Kakde. D.; Jain. D.; Shrivastava. V.; Kakde. R.; Patil. A. T. *J. App. Pharm. Sci.* **2011**, *9*, 1. (b) Enback. J.; Laakkonen, P. *Biochem. Soc. Trans.* **2007**, *35*, 780. (c) Dorsam, R. T.; Gutkind, J. S. *Nat. Rev. Cancer.* **2007**, *7*, 79. (d) Aina. O. H.; Sroka. T. C.; Chen, M. L; Lam, K. S. *Biopolymers.* **2002***, 66*, 184. (e) Zhang, X.-X.; Eden, H. S.; Chen, X. *J. Controlled. Release.* **2012,** *159,* 2.

(17) (a) Jordan, M. A.; Wilson, L. *Nat. Rev. Cancer.* **2004**, *4*, 253. (b) Verdier-Pinard, P.; Wang, F.; Burd, B.; Angeletti, R. H.; Horwitz, S. B.; Orr, G. A.

Biochemistry. **2003,** *42*, 12019. (c) Luduena, R. F. *Int. Rev. Cytology.* **1998**, *178*, 207.

(18) Gascoigne, K. E.; Taylor, S. S. *J. Cell. Sci.* **2009**, *122*, 2579.

(19) (a) Perez, E. A., *Mol. Cancer. The.* **2009**, *8*, 2086. (b) Orosz, F.; Horvath, I.; Ovadi, J. *Mini. Rev. Med. Chem*. **2006**, *6*, 1145. (c) Pieraccini, S.; Saladino, G.; Cappelletti, G.; Cartelli, D.; Francescato, P.; Speranza, G.; Manitto, P.; Sironi, M., *Nat. Chem.* **2009**, *1*, 642. (d) Dumontet, C.; Jordan, M. A. *Nat. Rev. Drug. Discov*. **2010**, *9*, 790. (e) Clardy, J.; Walsh, C. *Nature*. **2004**, *432,* 829.

(20) Sackett, D. L.; Sept, D. *Nat. Chem*. **2009**, *1*, 596.

(21) Zhou, L.; Giannakakou, P. *Curr. Med. Chem. Anticancer Agents.* **2005**, *5*, 65.

(22) Thundimadathil, J. *J. Amino Acids.* **2012**, *1*.

(23) (a) Miller. W. R.; Scott, W. N.; Morris, R. *Nature*, 1985, *313*, 231. (b) Engel, J. B.; Schally, A. V. *Nat. Clin. Pract. End. Met*. **2007**, *3*, 157. (c) Lee, T. H.; Lin, Y. H.; Seow, K. M.; Hwang, J. L.; Tzeng, C. R.; Yang, Y. S. *Fertility and Sterility*. **2008**, *90,* 113**.** (d) Debruyne, F.; Bhat, G.; Garnick, M. B. *Future Oncology* **2006,** *2*, 677. (e) Broqua, P.; Riviere, P. J. M.; Conn, P. M.; Rivier, J. E.; Aubert, M. L.; Junien, J. L. *J. Pharm. Exp. Ther*. **2002**, *301*, 95.

(24) (a) Strowski, M. Z.; Blake, A. D. *Mol. Cell. Endocrinol*. **2008**, *286,* 169. (b) Faiss, S.; Pape, U. F.; Böhmig, M.; Dörffel, Y.; Mansmann, U.; Golder, W.; Riecken, E. O.; Wiedenmann, B. *J. Clin. Oncol*. **2003**, *21*, 2689. (c) Rufini, V.; Calcagni, M. L.; Baum, R. P. *Semin. Nucl. Med*. **2006**, *36*, 228.

(25) (a) Kwekkeboom, D. J.; Teunissen, J. J.; Bakker, W. H.; Kooij, P. P.; de Herder, W. W.; Feelders, R. A.; Van Eijck, C. H.; Esser, J.-P.; Kam, B. L.; Krenning, E. P., *J. Clin. Oncol*. **2005**, *23*, 2754. (b) Esser, J. P.; Krenning, E. P.; Teunissen, J. J. M.; Kooij, P. P. M.; Gameren, A. L. H.; Bakker, W. H.; Kwekkeboom, D. J., *Eur. J. Nucl. Med. Mol. Imaging.* **2006,** *33*, 1346.

(26) (a) Henderson, R. A.; Mossman, S.; Nairn, N.; Cheever, M. A., *Vaccine.* **2005**, *23*, 2359. (b) Hareuveni, M.; Gautier, C.; Kieny, M. P.; Wreschner, D.; Chambon, P.; Lathe, R. *Proc. Nat. Acad. Sci.* **1990,** *87*, 9498. (c) Eisenbach, L.; Bar-Haim, E.; El-Shami, K. *Immunol. Lett.* **2000,** *74*, 27. (d) Oshima, M.; Deitiker, P.; Ashizawa, T.; Zouhair Atassi, M. *Autoimmunity.* **2002,** *35*, 183. (e) Ramanathan, R.; Lee, K.; McKolanis, J.; Hitbold, E.; Schraut, W.; Moser, A.; Warnick, E.; Whiteside, T.; Osborne, J.; Kim, H.; Day, R.; Troetschel, M.; Finn, O. *Cancer Immunol. Immunother.* **2005,** *54*, 254.

(27) (a) Akhtar, N. H.; Pail, O.; Saran, A.; Tyrell, L.; Tagawa, S. T. *Adv. Urol.* **2012**, *9*, 2012 (b) Ruoslahti, E.; Bhatia, S. N.; Sailor, M. J. *J. Cell. Biol.* **2010,** *188*, 759. (c) Gregorc, V.; De Braud, F. G.; De Pas, T. M.; Scalamogna, R.; Citterio, G.; Milani, A.; Boselli, S.; Catania, C.; Donadoni, G.; Rossoni, G.; Ghio, D.; Spitaleri, G.; Ammannati, C.; Colombi, S.; Caligaris-Cappio, F.; Lambiase, A.; Bordignon, C. *Clin. Cancer Res.* **2011,** *17*, 1964. (d) Sacchi, A.; Gasparri, A.; Gallo-Stampino, C.; Toma, S.; Curnis, F.; Corti, A. *Clin. Cancer. Res.* **2006,** *12*, 175. (e) Laakkonen, P.; Vuorinen, K. *Integr. Biol.* **2010,** *2*, 326.

(28) (a) Newman, D. J.; Cragg, G. M. *J. Nat. Prod.* **2004**, *67*, 1216. (b) Coleman, J. E.; Dilip de Silva, E.; Kong, F.; Andersen, R. J.; Allen, T. M. *Tetrahedron.* **1995,** *51*, 10653. (c) Zheng, L.-H.; Wang, Y.-J.; Sheng, J.; Wang, F.; Zheng, Y.; Lin, X.-K.; Sun, M. *Mar. Drugs.* **2011,** *9*, 1840. (d) Faulkner, D. J. *Nat. Prod. Rep*. **1995**, *12*, 223.

(29) (a) Oda, T.; Crane, Z. D.; Dicus, C. W.; Sufi, B. A.; Bates, R. B. *J. Mol. biol.* **2003**, *328*, 319. (b) Pettit, G. R.; Srirangam, J. K.; Herald, D. L.; Hamel, E. *J. Org. Chem.* **1994,** *59*, 6127.

(30) (a) Nieman, J. A.; Coleman, J. E.; Wallace, D. J.; Piers, E.; Lim, L. Y.; Roberge, M.; Andersen, R. J. *J. Nat. Prod.* **2002**, *66*, 183. (b) Krishnamurthy, G.; Cheng, W.; Lo, M.-C.; Aulabaugh, A.; Razinkov, V.; Ding, W.; Loganzo, F.; Zask, A.; Ellestad, G. *Biochemistry.* **2003,** *42*, 13484.

(31) (a) Sonnenschein, R. N.; Farias, J. J.; Tenney, K.; Mooberry, S. L.; Lobkovsky, E.; Clardy, J.; Crews, P. *Org. Lett.* **2004**, *6*, 779. (b) Chevallier, C.; Richardson, A. D.; Edler, M. C.; Hamel, E.; Harper, M. K.; Ireland, C. M. *Org. Lett.* **2003,** *5,* 3737.

(32) (a) Lo, M. C.; Aulabaugh, A.; Krishnamurthy, G.; Kaplan, J.; Zask, A.; Smith, R. P.; Ellestad, G. *J. Am. Chem. Soc.* **2004**, *126*, 9898. (b) Niu, C.; Smith, D.; Zask, A.; Loganzo, F.; Discafani, C.; Beyer, C.; Greenberger, L.; Ayral-Kaloustian, S. *Bioorg. Med. Chem. Lett.* **2004,** *14*, 4329.

(33) (a) Pettit, G. R.; Hogan, F.; Herald, D. L. *J. Org. Chem.* **2004,** *69*, 4019. (b) Coleman, J. E.; Patrick, B. O.; Andersen, R. J.; Rettig, S. J. *Acta Crystallogr. Sect. C.* **1996,** *52*, 1525.

(34) Mannhold, R.; Fulda, S.; Carosati, E. *Drug Discov. Today.* **2010**, *15*, 210.

(35) Horiuchi, T.; Chiba, J.; Uoto, K.; Soga, T. *Bioorg. Med. Chem. Lett.* **2009**, *19*, 305.

(36) Lee, C.-L.; Liao, Y.-C.; Hwang, T.-L.; Wu, C.-C.; Chang, F.-R.; Wu, Y.-C. *Bioorg. Med. Chem. Lett.* **2010**, *20*, 7354.

(37) Chatterjee, J.; Rechenmacher, F.; Kessler, H., *Angew. Chem. Int. Ed.* **2013**, *52*, 254.

(38) (a) Desjardins, A. E.; Proctor, R. H. *Int. J. Food Microbiol.* **2007**, *119*, 47. (b) Plattner, P. A.; Nager, U. *Helv. Chim. Acta.* **1948,** *31*, 665. (c) Dornetshuber, R.; Heffeter, P.; Kamyar, M.-R.; Peterbauer, T.; Berger, W.; Lemmens-Gruber, R. *Chem. Res. Toxicol.* **2007,** *20*, 465. (d) Hyun, U.; Lee, D. H.; Lee, C.; Shin, C.-G. *Toxicon.* **2009,** *53*, 723. (d) Hiraga, K.; Yamamoto, S.; Fukuda, H.; Hamanaka, N.; Oda, K. *Biochem. Biophy. Res. Commun.* **2005,** *328*, 1119. (e) Arceci, R. J.; Stieglitz, K.; Bierer, B. E. *Blood.* **1992**, *80*, 1528.

(39) (a) Dawson, S.; Malkinson, J. P.; Paumier, D.; Searcey, M. *Nat. Prod. Rep.* **2007**, *24*, 109. (b) Kong, D.; Park, E. J.; Stephen, A. G.; Calvani, M.; Cardellina, J. H.; Monks, A.; Fisher, R. J.; Shoemaker, R. H.; Melillo, G.

Cancer. Res. **2005,** *65*, 9047. (c) Zhang, Q.; Zhang, Z.-F.; Rao, J. Y.; Sato, J. D.; Brown, J.; Messadi, D. V.; Le, A. D. *Int. J. Cancer* **2004,** *111*, 849. (d) Tulla-Puche, J.; Marcucci, E.; Prats-Alfonso, E.; Bayó-Puxan, N. r.; Albericio, F. *J. Med. Chem.* **2009,** *52*, 834. (e) Kitagaki, J.; Yang, Y. *Biochem. Biophy. Res. Commun.* **2011,** *414*, 186.

(40) (a) Hitotsuyanagi, Y.; Lee, J.-E.; Kato, S.; Kim, I.-H.; Kohashi, H.; Fukaya, H.; Takeya, K. *Bioorg. Med. Chem.* **2011,** *19*, 2458. (b) Jolad, S. D.; Hoffman, J. J.; Torrance, S. J.; Wiedhopf, R. M.; Cole, J. R.; Arora, S. K.; Bates, R. B.; Gargiulo, R. L.; Kriek, G. R. *J. Am. Chem. Soc.* **1977,** *99*, 8040.

(41) (a) Liu, J.; Farmer Jr, J. D.; Lane, W. S.; Friedman, J.; Weissman, I.; Schreiber, S. L. *Cell.* **1991**, *66*, 807. (b) Mas-Moruno, C.; Rechenmacher, F.; Kessler, H. *Anti Cancer. Agents. Med. Chem*. **2010**, *10*, 753.

(42) Cerminara, I.; Chiummiento, L.; Funicello, M.; Guarnaccio, A.; Lupattelli, P. *Pharmaceuticals.* **2012**, *5*, 297.

(43) Hoogwater, D. A.; Peereboom, M. *Tetrahedron.* **1990**, *46*, 5325.

(44) (a) Loganzo, F.; Discafani, C. M.; Annable, T.; Beyer, C.; Musto, S.; Hari, M.; Tan, X.; Hardy, C.; Hernandez, R.; Baxter, M.; Singanallore, T.; Khafizova, G.; Poruchynsky, M. S.; Fojo, T.; Nieman, J. A.; Ayral-Kaloustian, S.; Zask, A.; Andersen, R. J.; Greenberger, L. M. *Cancer. Res.* **2003**, *63*, 1838. (b) Hall, D.; Minton, A. P. *Anal. Biochem.* **2005,** *345*, 198.

(45) Kamal, A.; Srikanth, Y. V. V.; Shaik, T. B.; Khan, M. N. A.; Ashraf, M.; Reddy, M. K.; Kumar, K. A.; Kalivendi, S. V. *Med. Chem. Comm.* **2011**, *2*, 819.